frontiers | Research Topics

Plant-bacteria association and symbiosis

Edited by
Carlos Henrique Meneses, Diogo Neves Proença,
Marcia Soares Vidal and German Andres Estrada-Bonilla

Published in
Frontiers in Plant Science

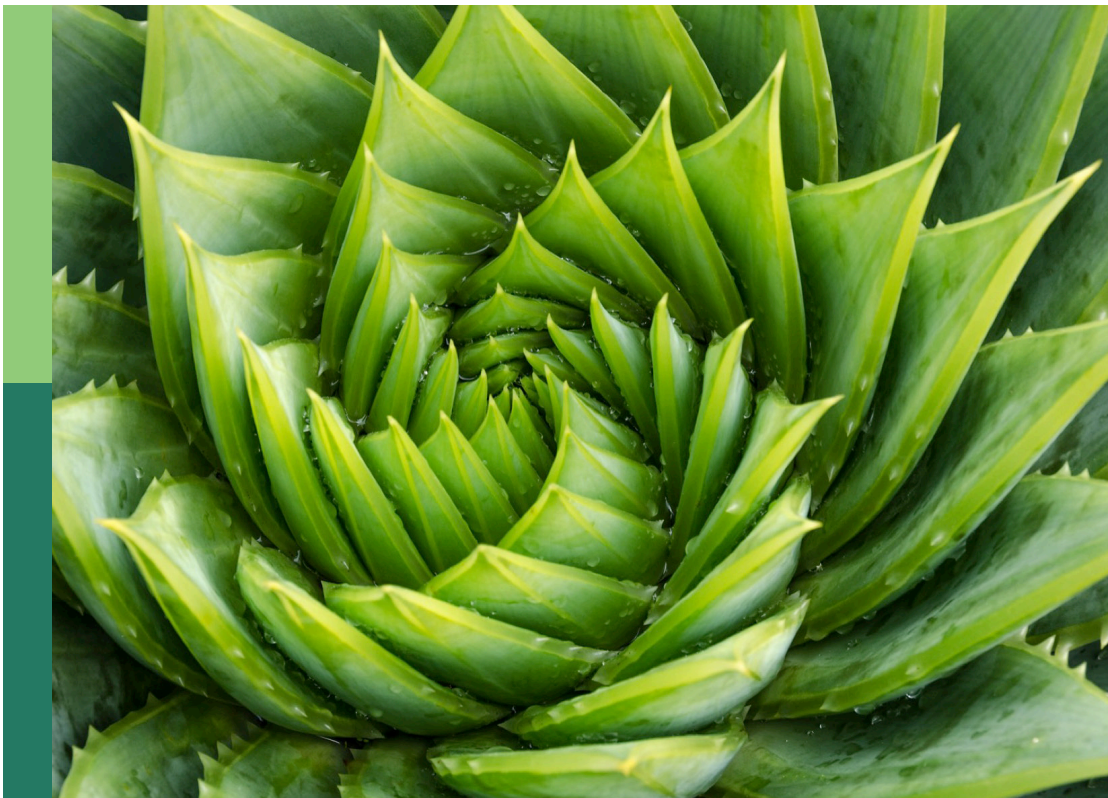

ISSN 1664-8714
ISBN 978-2-8325-4927-8
DOI 10.3389/978-2-8325-4927-8

About Frontiers

Frontiers is more than just an open access publisher of scholarly articles: it is a pioneering approach to the world of academia, radically improving the way scholarly research is managed. The grand vision of Frontiers is a world where all people have an equal opportunity to seek, share and generate knowledge. Frontiers provides immediate and permanent online open access to all its publications, but this alone is not enough to realize our grand goals.

Frontiers journal series

The Frontiers journal series is a multi-tier and interdisciplinary set of open-access, online journals, promising a paradigm shift from the current review, selection and dissemination processes in academic publishing. All Frontiers journals are driven by researchers for researchers; therefore, they constitute a service to the scholarly community. At the same time, the *Frontiers journal series* operates on a revolutionary invention, the tiered publishing system, initially addressing specific communities of scholars, and gradually climbing up to broader public understanding, thus serving the interests of the lay society, too.

Dedication to quality

Each Frontiers article is a landmark of the highest quality, thanks to genuinely collaborative interactions between authors and review editors, who include some of the world's best academicians. Research must be certified by peers before entering a stream of knowledge that may eventually reach the public - and shape society; therefore, Frontiers only applies the most rigorous and unbiased reviews. Frontiers revolutionizes research publishing by freely delivering the most outstanding research, evaluated with no bias from both the academic and social point of view. By applying the most advanced information technologies, Frontiers is catapulting scholarly publishing into a new generation.

What are Frontiers Research Topics?

Frontiers Research Topics are very popular trademarks of the *Frontiers journals series*: they are collections of at least ten articles, all centered on a particular subject. With their unique mix of varied contributions from Original Research to Review Articles, Frontiers Research Topics unify the most influential researchers, the latest key findings and historical advances in a hot research area.

Find out more on how to host your own Frontiers Research Topic or contribute to one as an author by contacting the Frontiers editorial office: frontiersin.org/about/contact

Plant-bacteria association and symbiosis

Topic editors

Carlos Henrique Meneses — State University of Paraíba, Brazil

Diogo Neves Proença — University of Coimbra, Portugal

Marcia Soares Vidal — Brazilian Agricultural Research Corporation (EMBRAPA), Brazil

German Andres Estrada-Bonilla — Corporación Colombiana de Investigación Agropecuaria (Agrosavia)-Tibaitatá, Colombia

Citation

Meneses, C. H., Proença, D. N., Vidal, M. S., Estrada-Bonilla, G. A., eds. (2024). *Plant-bacteria association and symbiosis*. Lausanne: Frontiers Media SA.

doi: 10.3389/978-2-8325-4927-8

Table of contents

frontiers | Frontiers in Plant Science

TYPE Editorial
PUBLISHED 10 May 2024
DOI 10.3389/fpls.2024.1423947

OPEN ACCESS

EDITED AND REVIEWED BY
Andrea Genre,
University of Turin, Italy

*CORRESPONDENCE
Carlos Henrique S. G. Meneses
carlos.meneses@servidor.uepb.edu.br
Diogo Neves Proença
diogo.proenca@uc.pt
German A. Estrada-Bonilla
gaestrada@agrosavia.co
Marcia Soares Vidal
marcia.vidal@embrapa.br

RECEIVED 26 April 2024
ACCEPTED 01 May 2024
PUBLISHED 10 May 2024

CITATION
Meneses CHSG, Proença DN, Estrada-Bonilla GA and Vidal MS (2024) Editorial: Plant-bacteria association and symbiosis.
Front. Plant Sci. 15:1423947.
doi: 10.3389/fpls.2024.1423947

Editorial: Plant-bacteria association and symbiosis

Carlos Henrique S. G. Meneses[1]*, Diogo Neves Proença[2]*, German A. Estrada-Bonilla[3]* and Marcia Soares Vidal[4]*

[1]Laboratory Plant Biotechnology, Graduate Program in Agricultural Sciences, Department of Biology, Center for Biological and Health Sciences, State University of Paraíba, Campina Grande, Brazil, [2]Department of Life Sciences, Centre for Mechanical Engineering, Materials and Processes (CEMMPRE), Advanced Production and Intelligent Systems (ARISE), University of Coimbra, Coimbra, Portugal, [3]Agricultural Microbiology Laboratory, Tibaitatá Research Center, Corporación Colombiana de Investigación Agropecuaria (AGROSAVIA), Mosquera, Colombia, [4]Laboratory of Genetics and Biochemistry, Empresa Brasileira de Pesquisa Agropecuária – EMBRAPA, Embrapa Agrobiologia, Rio de Janeiro, Seropédica, Brazil

KEYWORDS

plant-bacteria interactions, symbiosis, plant growth-promoting bacteria, endophytes, epiphytes

Editorial on the Research Topic
Plant-bacteria association and symbiosis

In the relentless pursuit of sustainable agricultural practices, society has pivoted its gaze towards alternatives to synthetic chemical fertilizers, recognizing the significant environmental impact they impose. Among the myriad of alternatives, the use of plant growth-promoting bacteria (PGPB) has emerged as a promising solution, encouraging potential to revolutionize plant nutrition in a manner that is both effective and environmentally sustainable. The interaction between plants and PGPB is a wonder of nature, encompassing a wide array of interactions that extend far beyond simple nutrient provision. These remarkable microorganisms, through their ability to harness unavailable nutrients and synthesize essential phytohormones, exert a profound influence on plant metabolism, enhancing growth and resilience even in challenging conditions.

At the heart of the challenge lies the enigmatic nature of plant-microbe interactions, fraught with complexities that confound even the most seasoned researchers. The quest to elucidate the dynamic interplay between plants and microorganisms across diverse environmental conditions remains a formidable task, yet one that is essential for unlocking the full potential of PGPB in sustainable agriculture. In their tireless quest for knowledge, researchers have harnessed the power of omics technologies to decipher the intricate network of biochemical, genetic, genomic, and molecular interactions that underpin the symbiotic relationship between plants and bacteria. However, despite the progress made, many mysteries remain unsolved, with intriguing discoveries awaiting exploration.

In our unwavering commitment to advancing crop improvement and fostering sustainable agriculture, we are proud to present a Research Topic dedicated to unraveling the mysteries of plant-bacteria relationships. The current Research Topic includes one review, one brief research report article and 10 original research studies focusing on (i) selection of efficient microbial strains and their characterization regarding their potential to alleviate abiotic stress; (ii) utilizing effective microbial species to enhance

soil nutrient availability for plants; (iii) exploring bacterial diversity, including both plant growth-promoting bacteria in cultivated plants and rhizospheric soil, and on (iv) describes the importance of a bacterial biopolymer in the plant intracellular colonization process.

The review presented by Choudhary et al. address the diversity of endophytic microorganisms and their significance in various industries, including agricultural, pharmaceuticals and biotechnology. Specifically, the authors highlight the importance of these endophytes in producing bioactive compounds with pharmaceutical and agricultural applications.

Regarding the first topic presented, da Silva et al. report on the responses of nitrogen fixation in bean nodules during drought, emphasizing the regulation of heat shock proteins and transcription factors. Meanwhile, Kim et al. demonstrate enhanced drought resistance in *Arabidopsis* and *Brassica* plants using the *Flavobacterium* sp. GJW24. Likewise, dos Santos et al. explore the molecular and biochemical responses of sesame to rhizobacteria inoculation under drought conditions. Finally, Teles et al. focus on the characterizing and evaluating halotolerant phosphate-solubilizing bacteria from the rhizosphere of *Salicornia fruticosa*. In the context of climate change, characterized by increasingly severe drought periods, these studies provide valuable insights for understanding and advancing agriculture under challenging conditions, including drought and salinity.

In the second topic of study, Tounsi-Hammami et al. optimize the growth of tomato seedlings by inoculation of indigenous mangrove bacteria and potentially reduce NPK fertilization. Results showed that applying bacterial inoculant with 50% NPK significantly increase plant growth, photosynthetic activity, and nutrient uptake. In another study, Rosman et al. new insights into on the relationship between plants, plant growth-promoting bacteria, and the environment. Furthermore, Nagah et al. demonstrate that endophytic bacteria isolated from medicinal plants enhance phosphorus acquisition, leading to improve vegetative growth and metabolic content in *Brassica napus* L. Lastly, Lu et al. evidence of increased phosphate uptake and alterations in bacterial communities in maize rhizosphere soil attributed to the presence of arbuscular mycorrhizal fungi. These studies contribute to the field plant-microbe-environment interactions, highlighting the significance of symbiotic relationships for crop growth and development.

In the third topic of research, Gätjens-Boniche et al. explore the connection between the microbiome of insect-induced galls in cassava and the genetic transformation of plant cells. Results indicate that microbiome enrichment and genetic transformation of plant cells contribute to gall development. Meanwhile, Shi et al. address the characteristics of the phyllosphere microbial community and its relationship to key aroma precursors during the tobacco maturation process. Both the study delves into various aspects of bacterial diversity, including their role in gall development in cassava and their influence on aroma precursor production during tobacco maturation.

Concluding the Research Topic, Baruah et al. present findings concerning the mobilization of poly-3-hydroxybutyrate and its significance in reducing protein aggregation in *Methylorubrum extorquens* DSM1306 under oxidative stress. The authors illustrate the pivotal role of biopolymer in initial stages of intracellular colonization.

In conclusion, the diverse range of research presented in this Research Topic underscores the pivotal role of plant-microbe interactions, especially the PGPB participation, in advancing sustainable agricultural practices. From elucidating the biochemical and molecular mechanisms underlying these interactions to exploring the potential of microbial inoculants in alleviating abiotic stresses and enhancing nutrient availability, each study contributes with valuable insights that pave the way for a greener and more resilient agricultural future. Additionally, the findings highlight the intricate dynamics between plants, microorganisms, and their environment, with the significance of symbiotic relationships in shaping crop growth and development under challenging conditions such as drought and salinity stresses. As we continue to unlock the secrets of sustainable agriculture, the synergistic partnership between plants and microorganisms emerges as a cornerstone for achieving a more sustainable and prosperous future for generations to come.

Author contributions

CM: Conceptualization, Writing – original draft, Writing – review & editing. DP: Conceptualization, Writing – original draft, Writing – review & editing. GE-B: Conceptualization, Writing – original draft, Writing – review & editing. MV: Conceptualization, Writing – original draft, Writing – review & editing.

Funding

The author(s) declare that no financial support was received for the research, authorship, and/or publication of this article.

Acknowledgments

CM (Process no 313075/2021-2) was a fellowships from CNPq (Brazil). This work was funded by national funds through Fundação para a Ciência e a Tecnologia (FCT), under the projects UID/EMS/00285/2020 and LA/P/0112/2020 (Portugal), and Ministerio de Agricultura y Desarrollo Rural" (grant no.1001774) (Colombia).

Conflict of interest

The authors declare that the research was conducted in the absence of any commercial or financial relationships that could be construed as a potential conflict of interest.

Publisher's note

frontiers | Frontiers in Plant Science

TYPE Original Research
PUBLISHED 22 June 2023
DOI 10.3389/fpls.2023.1206870

OPEN ACCESS

EDITED BY
Diogo Neves Proença,
University of Coimbra, Portugal

REVIEWED BY
Anyong Hu,
Nantong University, China
Simão Lindoso De Souza,
State University of Paraíba, Brazil

*CORRESPONDENCE
Fang Liu
liufang0019@ynu.edu.cn
Yunjian Xu
xuyunjian1992@ynu.edu.cn

†These authors have contributed equally to this work

RECEIVED 16 April 2023
ACCEPTED 31 May 2023
PUBLISHED 22 June 2023

CITATION
Lu Y, Yan Y, Qin J, Ou L, Yang X, Liu F and Xu Y (2023) Arbuscular mycorrhizal fungi enhance phosphate uptake and alter bacterial communities in maize rhizosphere soil.
Front. Plant Sci. 14:1206870.
doi: 10.3389/fpls.2023.1206870

Arbuscular mycorrhizal fungi enhance phosphate uptake and alter bacterial communities in maize rhizosphere soil

Yufan Lu[1†], Yixiu Yan[1†], Jie Qin[1], Luyan Ou[1], Xinyu Yang[1], Fang Liu[1*] and Yunjian Xu[2,3*]

[1]School of Agriculture, Yunnan University, Kunming, China, [2]Yunnan Key Laboratory of Plant Reproductive Adaptation and Evolutionary Ecology, Institute of Biodiversity, Yunnan University, Kunming, China, [3]School of Ecology and Environmental Science, Yunnan University, Kunming, Yunnan, China

Arbuscular mycorrhizal fungi (AMF) can symbiose with many plants and improve nutrient uptake for their host plant. Rhizosphere microorganisms have been pointed to play important roles in helping AMF to mobilize soil insoluble nutrients, especially phosphorus. Whether the change in phosphate transport under AMF colonization will affect rhizosphere microorganisms is still unknown. Here, we evaluated the links of interactions among AMF and the rhizosphere bacterial community of maize (*Zea mays* L.) by using a maize mycorrhizal defective mutant. Loss of mycorrhizal symbiosis function reduced the phosphorus concentration, biomass, and shoot length of maize colonized by AMF. Using 16S rRNA gene amplicon high-throughput sequencing, we found that the mutant material shifted the bacterial community in the rhizosphere under AMF colonization. Further functional prediction based on amplicon sequencing indicated that rhizosphere bacteria involved in sulfur reduction were recruited by the AMF colonized mutant but reduced in the AMF-colonized wild type. These bacteria harbored much abundance of sulfur metabolism-related genes and negatively correlated with biomass and phosphorus concentrations of maize. Collectively, this study shows that AMF symbiosis recruited rhizosphere bacterial communities to improve soil phosphate mobilization, which may also play a potential role in regulating sulfur uptake. This study provides a theoretical basis for improving crop adaptation to nutrient deficiency through soil microbial management practices.

KEYWORDS

mycorrhizal symbiosis, nutrient mobilization, plant growth promotion, plant-microbe interactions, sulfur metabolism

1 Introduction

Phosphorus (P) is an essential macronutrient for plant growth and development (Wang et al., 2021b). Plants can only acquire free inorganic phosphate (Pi) from the soil, whereas Pi concentration and mobility in the soil are limited; thus, plants often suffer from Pi starvation (Du et al., 2020; Wang et al., 2021b). As important soil microorganisms, arbuscular mycorrhizal fungi (AMF) can symbiose with most plants and improve their host plants' phosphorus status. When symbioses are formed, AMF provides Pi from soil to host plants through their hyphal networks (Smith and Read, 2008). However, the P in the soil mainly exists in organic matter and insoluble forms difficult for AMF to decompose directly (Tisserant et al., 2013; Zhang et al., 2022). AMF must depend on phosphate-solubilizing bacteria to complement their functional capabilities by mineralizing organic P resources (Falkowski et al., 2008; Zhang et al., 2022).

As an important mycorrhizal crop widely planted in the world, maize is sensitive to low Pi conditions (Liu et al., 2018; Ma et al., 2022). To improve the low Pi tolerance of maize, transgenic technology and the application of beneficial soil microbes (including AMF) have been used.

The rhizosphere inhabited by many microorganisms has been defined as the second plant genome (Kuzyakov and Razavi, 2019; Vetterlein et al., 2020). AMF symbiosis alters root exudates (Zhang et al., 2022; Xu et al., 2023a; Xu et al., 2023b), resulting in the rhizosphere microbiome being altered and stimulating soil nutrient turnover (Zhang et al., 2018a). AMF has been reported to influence the rhizosphere microbial composition involved in the decomposition of organic materials (Herman et al., 2012; Nuccio et al., 2013). Bacterial communities containing genes for alkaline phosphatases inhabiting on the AMF hyphal surface have been shown to enhance soil organic P mineralization (Zhang et al., 2018b). Jiang et al. (2021) show that AMF-carrying bacteria along their extraradical hyphae to organic P patches enhance organic P mineralization. Additionally, AMF also attracts some plant growth-promoting rhizobacteria that have potential functions in the mobilization of soil-insoluble nutrients, including P and sulfur (S) (Priyadharsini et al., 2016; Hestrin et al., 2019; Sun et al., 2020). There is an interaction between P and S absorption by plants (Mohamed et al., 2014; Sun et al., 2020). S starvation negatively impacts plant vitality when the P status is adequate (Sieh et al., 2013). Like P, inaccessible S in the soil also relies on interactions with AMF and associated microbes to promote their mobilization (Richardson et al., 2009). AMF has a crucial role in plant S metabolism *via* interaction with organo-sulfur mobilizing microbes (Narayan et al., 2022). Specific bacteria were attached to AMF symbiosis in agricultural soils, and some bacteria respond to the presence of specific AMF (Zhang et al., 2022), suggesting a high degree of specificity between bacteria and AMF. However, whether AMF recruits specific rhizobacteria to help maize cope with low Pi stress and whether these bacteria have an association with S metabolism is still largely unknown.

Increasingly, researchers believe that plant functional genes are important factors in regulating rhizosphere microbiota (Cordovez et al., 2019; Zhang et al., 2019). Plant functional genes can drive rhizosphere microbial community assembly by regulating root phenotypes, root exudates, and transporter activities (Zhalnina et al., 2018; Yu P. et al., 2021; Liu et al., 2022). Changes in the structure and function of rhizosphere microorganisms can also affect the expression of plant functional genes and take plants some growth advantages (Berendsen et al., 2018). Compared with NRT1.1B (encoding a nitrate transporter and sensor) mutant, there are more microorganisms involved in the nitrogen cycle in the rhizosphere of wild rice (Zhang et al., 2019). In another study, plants inoculated with synthetic microbial communities, nitrate transporter coding genes, and nitrate reductase coding genes are downregulated, whereas many phosphorus starvation genes, phosphate transport, and metabolism genes are activated by synthetic communities (SynComs) (Wang et al., 2021a). However, whether the mycorrhizal symbiosis-related genes in plants can regulate microbiota in the rhizospheres under AMF inoculation remains unknown. In this study, mycorrhizal defective mutant and wild-type (WT) maize plants were planted in soils inoculated with AMF. We examined the rhizosphere bacterial community by 16S rRNA amplicon sequencing and determined the soil bacteria changes affected by AMF symbiosis. This study provides a theoretical basis for improving crop fitness through rhizosphere microbial management practices.

2 Materials and methods

2.1 Greenhouse experiment

The wild type of maize B73 and the maize mycorrhizal defective mutant *Mut* were used in this study. Before planting, the seeds of maize were surface-sterilized with 75% ethyl alcohol and germinated for 2 days at 28°C after washing with ddH_2O. The soil used in this study was superficial soil (0–20 cm depth) collected from a maize field in Kunming, Yunnan Province, China (24°23′N, 102°10E) after maize was harvested. The soil type is red loam. Soil physicochemical properties were as follows: pH, 7.01; total nitrogen, 0.42 $g{\cdot}kg^{-1}$; total phosphorus, 1.59 $g{\cdot}kg^{-1}$; available phosphorus, 9.8 $mg\ kg^{-1}$; total potassium, 8.35 $g{\cdot}kg^{-1}$. Each pot (28 cm in height and 25 cm in diameter) contained 10 kg of soil. The experiments included AMF-inoculated and uninoculated treatments. The AMF inoculation was the mixed addition of *Diversispora epigaea*, *Claroideoglomus etunicatum*, *Claroideoglomus walkeri*, *Funneliformis mosseae*, and *Rhizophagus intraradices* inoculums. These inoculums were gifted by the National Engineering Lab of Crop Stress Resistance Breeding, Anhui Agricultural University, Anhui Province, China. There were 200 spores of each AMF species used to prepare the AMF mix, and a total of 1,000 AMF spores per pot were added. AMF uninoculated treatments were realized by applying benomyl. Benomyl has been shown to effectively reduce AM colonization with minimal direct effects on plants (Hetrick et al., 1990; Smith et al., 2000) and widely used in the investigation related to AM fungi (Wang et al., 2018; Li et al., 2019; Chen et al., 2020; Kang et al., 2020). Maize plants were grown at 28°C/25°C

under a 16-h-day/8-h-night cycle for 8 weeks at a greenhouse of Yunnan University in China. The plants were watered twice a week. Five replicates of each treatment were set.

2.2 Plant analyses

Plant samples were harvested to measure dry weight, shoot length phosphorus concentration, and mycorrhizal colonization rate. Maize plants were dried at 105°C for 30 min and then dried at 75°C to a constant weight to measure dry weight. Dried leaves were ground and sieved (0.25 mm) to detect the phosphorus concentration as follows: samples were firstly digested in H_2SO_4 with H_2O_2 as an additive, and then the total phosphorus concentration was determined by molybdenum blue colorimetry (Deng et al., 2020). Trypan blue staining was used to detect the mycorrhizal colonization rate (Liu et al., 2018) as follows: fresh root segments were soaked in 10% (v/v) KOH solution for 15 min, acidified in 2% HCl for 5 min, and then stained with 0.05% trypan blue solution for 12 h.

2.3 Rhizosphere soil and 16S rRNA gene sequencing

Amplicon sequencing was conducted on a total of 12 samples, including three groups (wild type, wild type inoculated with AMF, *Mut* inoculated with AMF) and four biological replicates of each group. Rhizosphere soil was collected as previously described (McPherson et al., 2018). Briefly, roots with attached soil (rhizosphere soil) were transported to 30 ml phosphate-buffered saline buffer (pH 7.5). The mixture was centrifuged and passed through an aseptic nylon mesh strainer (100 µm). The filtered liquid was then centrifuged, and the rhizosphere soil was collected. The rhizosphere soil was stored at −80°C for total DNA extraction. According to the manufacturer's instructions, the PowerSoil® DNA isolation kit was used to extract the total DNA of rhizosphere soils. 16S rRNA gene sequencing was performed by the company Sangon Biotech (Shanghai, China) using an Illumina MiSeq platform. The V3–V4 regions of the bacterial 16S rRNA gene were amplified with universal primers 341F: CCTACGGGNGGCWGCAG and 805R: GACTACHVGGGTATCTAATCC (Defez et al., 2017) for bacterial identification. The 16S amplicon analysis was performed as Xu et al. described (Xu et al., 2023b). In brief, the DADA2 method for amplicon sequence variant (ASV) inference was used to process the 16S rRNA gene amplicon data; relative abundances of each taxon in a sample were calculated by proportional normalization of each sample by its sequencing depth. The random forest analysis was conducted by the "randomForest" R package as Xu et al. described (Xu et al., 2023b).

2.4 Data analysis

All the raw sequence data for the rhizosphere bacterial community have been deposited in the National Center for Biotechnology Information (NCBI) Sequence Read Archive under accession number PRJNA871781. Statistics on sequencing data were calculated using the R statistical programming software. Other statistical analyses were made using SPSS (SPSS26, Inc., Chicago, IL, USA). Statistical tests used were detailed in each figure legend. Redundancy analysis (RDA) was used to visualize and quantify the correlations. RDA was performed using the RDA command of the vegan package of R (Version 3.6.0) (R Core Team, 2019). The correlation heat maps were constructed by the corrplot package (Wei and Simko, 2021) and the ggcorrplot package (Tian et al., 2021) in R.

3 Results

3.1 Mycorrhizal defect hinders maize growth and phosphate uptake under AMF colonization

To investigate the effect of mycorrhizal defective mutant *Mut* on AM symbiosis and maize growth, the wild type and *Mut* mutant were inoculated with AMF. Eight weeks later, maize plants showed distinguishable phosphorus (P) content and phenotypes. AMF inoculation significantly increased the leaf P concentrations of wild-type maize plants by 33.86% and 31.39% compared with non-inoculated wild type (CK) and AMF-inoculated *Mut* mutant, respectively (Figure 1A). In addition, compared with CK, AMF inoculation significantly increased the shoot dry weight and shoot length of wild-type plants, but the *Mut* mutant reduced these performances of plants from AM symbiosis (Figures 1B, C). Moreover, the mycorrhizal colonization rate of AMF-inoculated wild-type maize was 71.48% (Figure 1D), whereas it was only 58.20% in AMF-inoculated *Mut*. Above all, AMF inoculation improved maize growth and promoted P absorption for maize, but the mycorrhizal defect reduced the accumulation of phosphorus, plant biomass, and shoot length of maize colonized by AMF.

3.2 AM symbiosis has a distinct rhizosphere bacterial community

The difference of bacterial community structures in the rhizosphere of CK, AMF-colonized wild type, and AMF-colonized *Mut* was confirmed by non-metric multidimensional (NMDS). NMDS analyses showed that bacterial community structures in the rhizosphere of wild type under AMF colonization were distinguishable from those without AMF colonization (stress value = 0.0846, Figure S1A), indicating a significant effect of AMF colonization on soil microbiome assembly. Additionally, significant differences were also observed between the rhizosphere bacterial structures of AMF colonized wild-type vs. AMF colonized *Mut* mutant (stress value = 0.0607, Figure S1B), suggesting that the *Mut* mutant affects microbiome assembly in the rhizosphere of maize under AMF colonization.

10.3389/fpls.2023.1206870

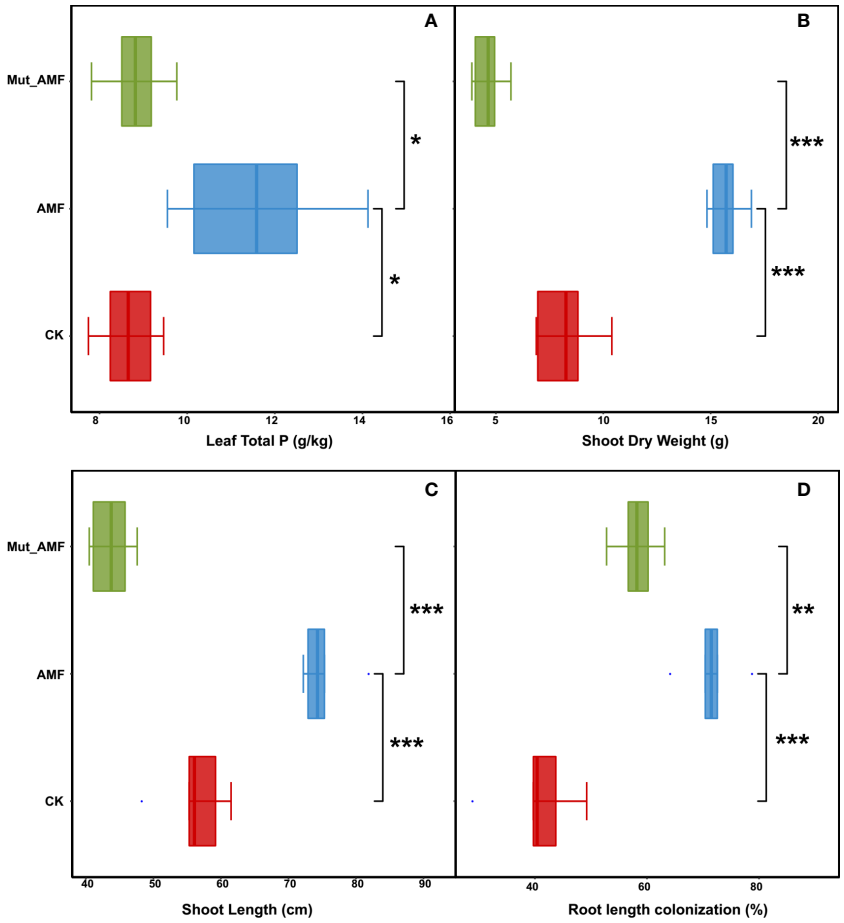

FIGURE 1
Arbuscular mycorrhizal fungal inoculation promotes maize growth and phosphate uptake. **(A)** Total P concentrations of plant. **(B)** Dry weight of shoot. **(C)** Shoot length. **(D)** Root length colonization rate. CK, wild-type maize without AMF (arbuscular mycorrhizal fungi) inoculation; AMF, wild-type maize inoculated with mix of *Diversispora epigaea*, *Claroideoglomus etunicatum*, *Claroideoglomus walkeri*, *Funneliformis mosseae*, and *Rhizophagus intraradices*. *Mut*, mycorrhizal defective mutant. The value of root length colonization rate was from three biological replicates with approximately 150 root segments per treatment. Bars are means ± SE and statistical differences were determined by two-sided t-test (***$p < 0.001$; **$p < 0.01$; *$p < 0.05$).

3.3 Rhizosphere bacteria act as biomarkers for AMF symbiosis

We further compared the relative abundance of rhizosphere bacteria between CK and AMF and between AMF-colonized wild-type and AMF-colonized *Mut*. Four genera of bacteria were enriched in the rhizosphere of maize colonized by AMF, namely, *Sphingomonas*, *Rhizobium*, *unclassified_Erythrobacteraceae*, and *unclassified_Nannocystineae* (Figure 2A). All four genera of bacteria belong to Proteobacteria. In the group of AMF-colonized wild type vs. AMF-colonized *Mut*, *Gp5* was significantly enriched, whereas *Streptophyta*, *Rhizobium*, and *unclassified_Erythrobacteraceae* were significantly depleted in the rhizosphere of AMF- colonized *Mut* (Figure 2B). *Gp5* belongs to Acidobacteria, and *Streptophyta* belongs to Cyanobacteria_Chloroplast. Figure 2 reveals that *Rhizobium* and *unclassified_Erythrobacteraceae* were enriched in the rhizosphere of AMF- colonized wild type but depleted in *Mut*.

We established a random forest to correlate AMF colonization with rhizosphere bacteria at the genus level. There were 15 genera identified as biomarker taxa in CK vs. AMF and AMF-colonized wild type vs. AMF-colonized *Mut*. Of these, eight genera showed higher relative abundance in AMF colonization compared to CK, namely, *Lysobacter*, *unclassified_Comamonadaceae*, *Terrimonas*, *unclassified_Anaerolineaceae*, *Parcubacteria_genera_incertae_sedis*, *unclassified_Sinobacteraceae*, *Sphingomonas*, and *unclassified_Erythrobacteraceae* (Figure 3A), whereas seven genera, namely, *unclassified_Bacteroidetes*, *Subdivision3_genera_incertae_sedis*, *unclassified_Sphingobacteriales*, *Gemmatimonas*, *Lacibacterium*, *unclassified_Chitinophagaceae*, and *Gp10*, were higher in CK. In AMF-colonized wild-type vs. AMF-colonized *Mut*, there were seven genera that were higher in wild type than *Mut*, namely, *unclassified_Sinobacteraceae*, *unclassified_Erythrobacteraceae*, *Devosia*, *unclassified_Comamonadaceae*, *unclassified_Alphaproteobacteria*, *unclassified_Rhizobiales*, and *unclassified_Deltaproteobacteria*, whereas eight genera with lower relative abundance were identified in AMF-colonized *Mut* compared with wild type (Figure 3B), namely, *unclassified_Burkholderiales*. *unclassified_Anaerolineaceae*, *WPS-1_genera_incertae_sedis*, *Photobacterium*, *unclassified_Betaproteobacteria*, *unclassified_Sphingobacteriales*, *Gp6*, and *unclassified_Chloroflexi*. Among these different bacteria members,

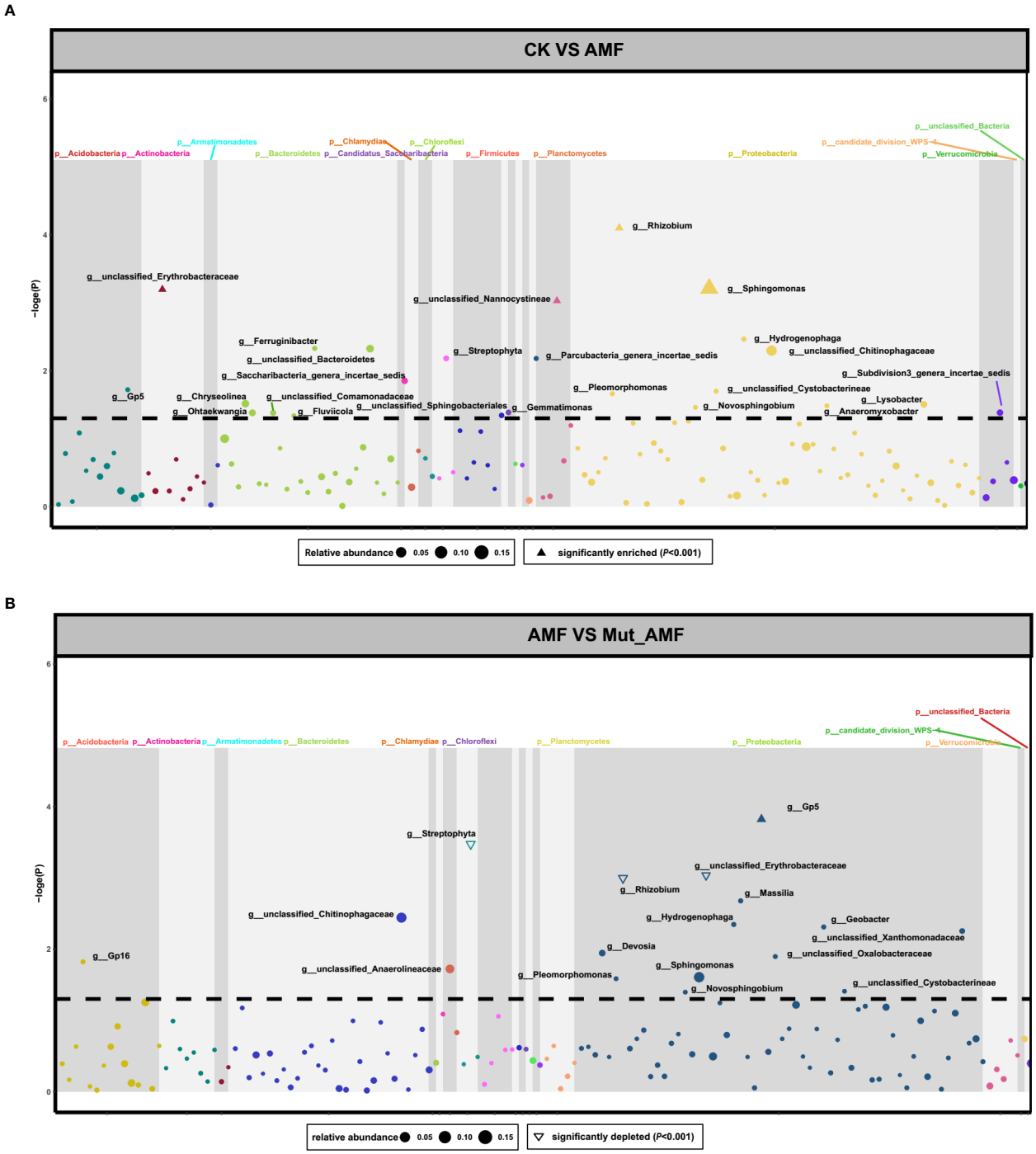

FIGURE 2
Changes of bacterial abundances in the rhizosphere of maize symbiosis with arbuscular mycorrhizal fungi. The dot represents the genera of bacteria. The Manhattan diagrams show changes of bacterial abundances in the rhizosphere of non-AMF (arbuscular mycorrhizal fungi) colonized (CK) vs. AMF colonized wild-type (AMF) **(A)**, and in the rhizosphere of AMF colonized wild-type vs. AMF colonized *Mut* mutant (Mut_AMF) **(B)**. The solid triangles represent significantly enriched bacteria. The hollow triangles represent significantly depleted bacteria, and the dot represents bacteria with no change. The dotted lines refer to the q value (-logP) of 0.05.

the genera of *unclassified_Erythrobacteraceae* showed higher relative abundance in the rhizosphere with AMF colonization compared with CK, whereas it was reduced in AMF-colonized *Mut*. LDA analysis further indicated that the significantly different genera *unclassified_Erythrobacteraceae* can serve as biomarker genera to distinguish whether maize is inoculated with AMF (Figure S2).

3.4 Potential functions of the rhizosphere bacterial community

The Functional Annotation of Procaryotic Taxa (FAPROTAX) analysis was further conducted to evaluate the different functions of bacterial communities in the rhizosphere of CK, AMF-colonized wild

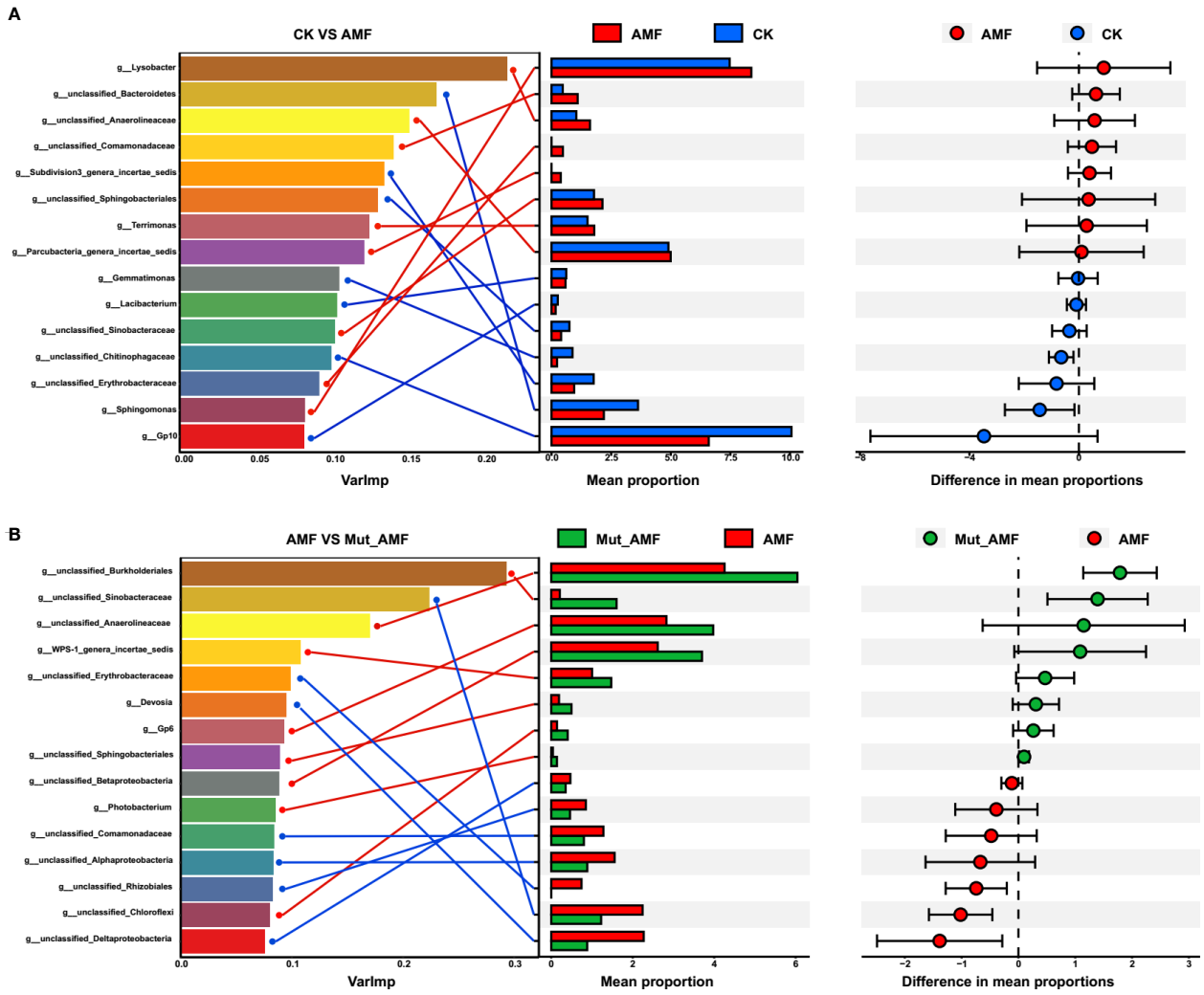

FIGURE 3
Analysis of biomarker bacterial genera by random forest modeling. The top 15 bacterial genera were identified by performing random forest classification of the relative abundance of the rhizosphere bacteria in non-AMF (arbuscular mycorrhizal fungi) colonized (CK) vs. AMF colonized wild-type (AMF) **(A)**, and in the rhizosphere of AMF colonized wild-type vs. AMF colonized *Mut* mutant (Mut_AMF) **(B)**. Biomarker taxa are ranked in descending order of importance to the accuracy of the model. Genus and its corresponding mean proportion were connected by lines.

type, and AMF-colonized *Mut* mutant. Compared with CK and AMF-colonized *Mut* mutants, the rhizosphere of the AMF-colonized wild type had relatively higher bacterial abundance with 14 functions (Figure S3). Among the 14 functions, three sulfate (S) metabolism-related functions (respiration_of_sulfur_compounds and sulfate_respiration) were included. To explore the mechanism of rhizosphere bacteria associated with AMF inoculation in S metabolism, the Kyoto Encyclopedia of Genes and Genomes (KEGG) pathways analysis was conducted. Hereby, four pathways related to three steps of S metabolism (sulfate reduction, sulfite reduction, and thiosulfate disproportionation) were identified, namely, sulfate reduction, sulfite reduction, thiosulfate disproportionation, and sulfur oxidation (Figures 4A, B). Sulfate reduction, sulfite reduction, and thiosulfate disproportionation belong to dissimilatory sulfur metabolism. Evidence for dissimilatory sulfur metabolism and sulfur oxidation was sought by whether the bacteria containing genes necessary to perform sulfate reduction, sulfite reduction, and thiosulfate disproportionation, including sulfate adenylyltransferase gene (*sat*), adenylylsulfate reductase alpha gene (*aprA*), dissimilatory sulfite reductase alpha and beta subunits gene (*dsrAB*), and anaerobic sulfite reductase gene (*asrC*) (Cai et al., 2021; Kieft et al., 2021; Yu X. et al., 2021). The *sat* and *aprA* genes are involved in sulfate reduction, *phsA* is involved in thiosulfate disproportionation, *dsrAB* is involved in sulfite reduction, and *asrC* is involved in sulfite reduction. The rhizosphere soil from CK and AMF-colonized *Mut* mutant contained a higher relative abundance of *sat*, *aprA*, *phsA*, and *dsrAB*. Conversely, a lower relative abundance of *asrC* in the rhizosphere samples was detected in CK and AMF-colonized *Mut* mutant compared with the AMF-colonized wild type.

3.5 Correlation of rhizosphere bacteria related to sulfur metabolism with maize plant performances

To further explore whether the bacteria associated with S metabolism correlate with maize growth, we first identified the

10.3389/fpls.2023.1206870

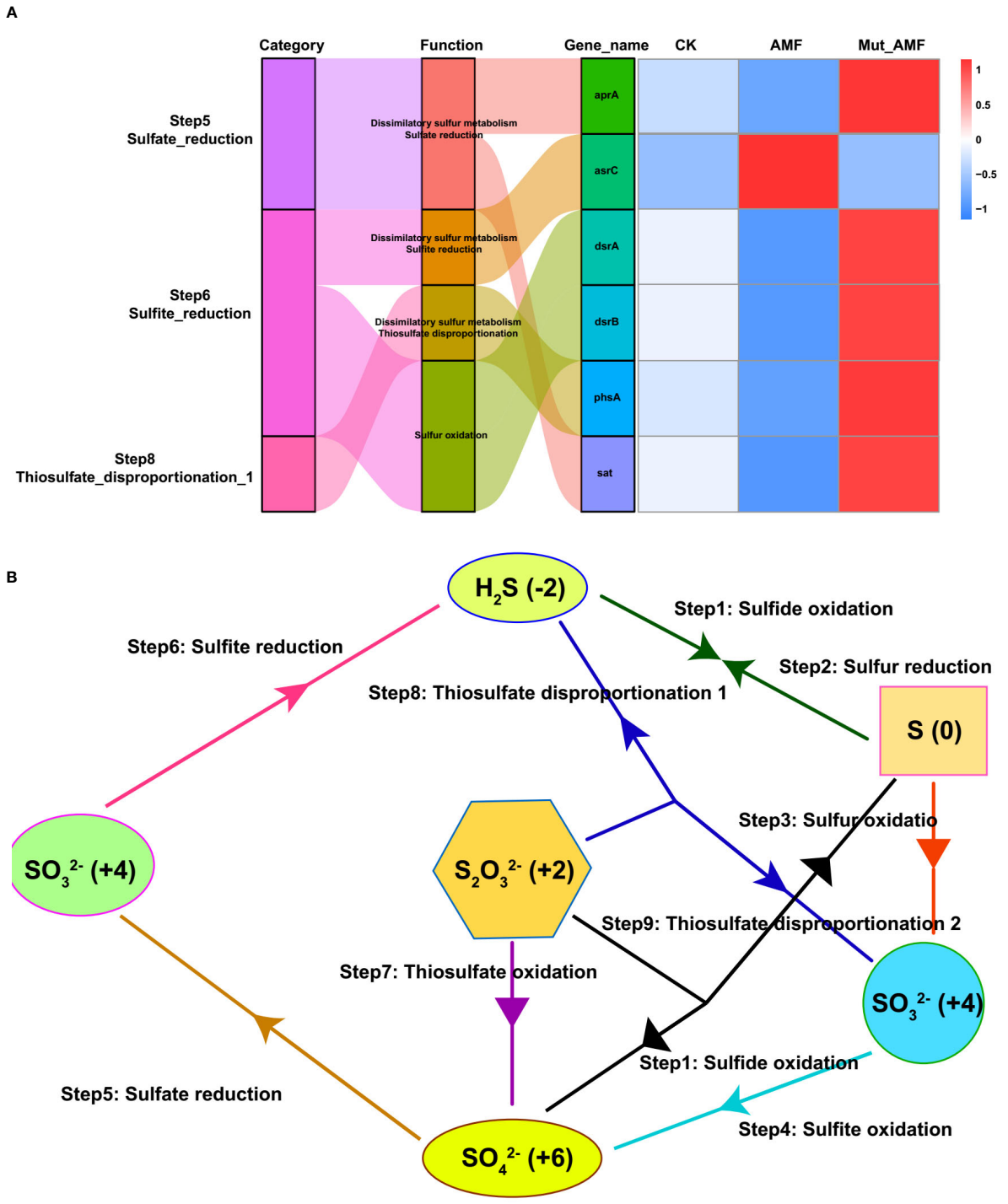

FIGURE 4
Sulfur metabolism-related genes in rhizosphere bacteria and their metabolic pathways. **(A)** Sankey diagram for sulfur metabolism pathway connected with related genes. The width of the flow is proportional to the number of bacterial genera. The right heatmap represents relative abundance of sulfur metabolism-related genes in the rhizosphere of non-AMF (arbuscular mycorrhizal fungi) colonized (CK), AMF colonized wild-type (AMF), and AMF colonized wild-type vs. AMF colonized *Mut* mutant (Mut_AMF). Relative abundance data were log2 transformed. **(B)** Sulfur metabolism.

bacterial genera that contained at least one of *sat*, *aprA*, *phsA*, *dsrA*, *dsrB*, or *asrC*. A total of 59 genera related to S metabolism were identified. Among them, the relative abundance of 34 bacterial genera was increased in the rhizosphere of the AMF-colonized wild type but decreased in the AMF-colonized *Mut* mutant. A relationship network between plant performances and the 34 bacterial genera was constructed. Almost all the 34 genera have a positive relationship with shoot length, shoot weight, leaf P concentration, and root length colonization (Figure 5A). Furthermore, significant correlations among all the 59 bacterial genera, S metabolism genes, and plant growth parameters were summed up as a heatmap (Figure 5B). The six S metabolism-related genes (*sat*, *aprA*, *phsA*, *dsrA*, *dsrB*, and *asrC*)

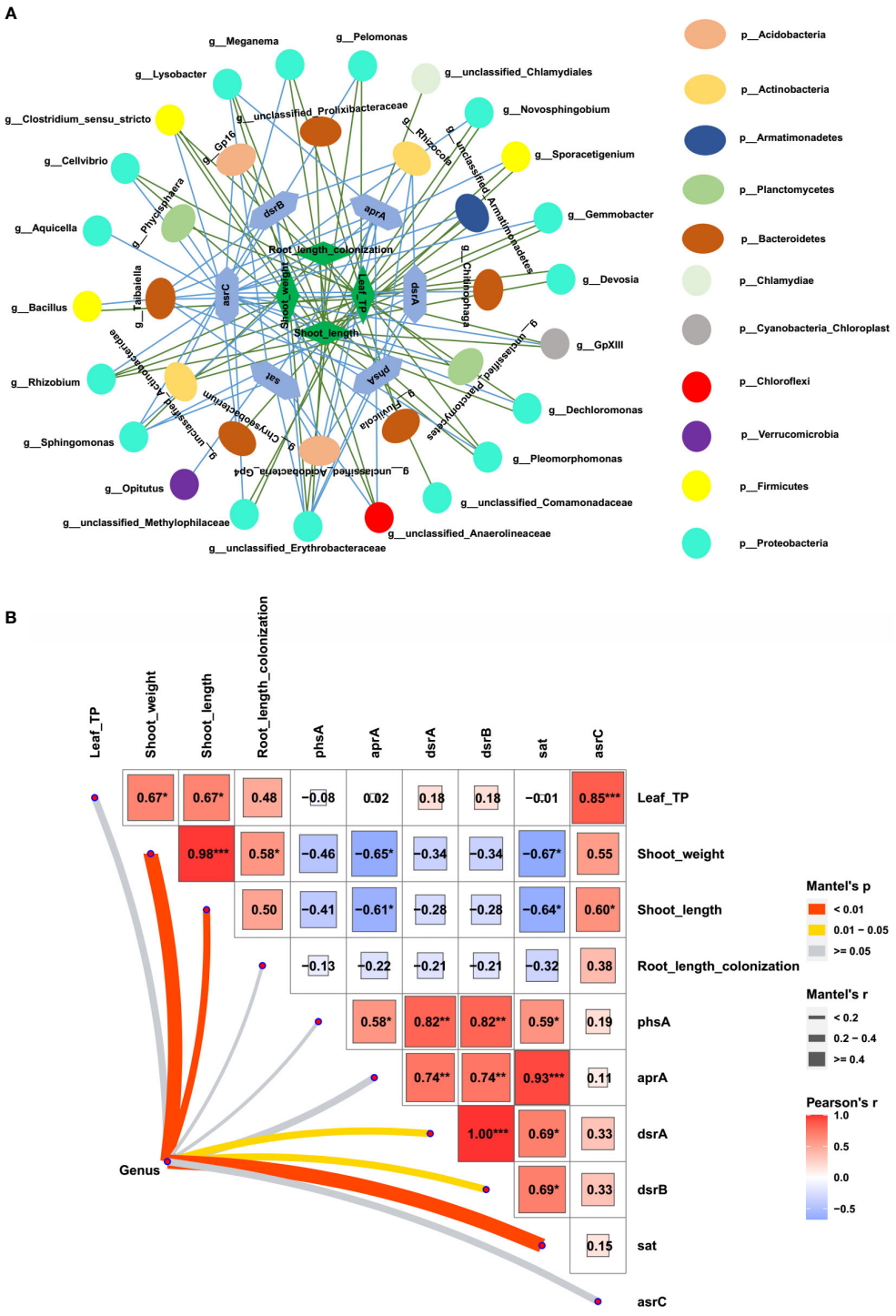

FIGURE 5
Correlation of sulfur metabolism- related rhizosphere bacterial genera and maize growth. **(A)** Network of sulfur metabolism- related rhizosphere bacterial genera, sulfur metabolism- related genes, and maize plant performances (shoot weight, shoot length, root length colonization, and shoot phosphorus concentration). **(B)** Correlation of sulfur metabolism- related rhizosphere bacterial genera with sulfur metabolism- related genes and maize performances.

showed a significant positive correlation with each other. Both *aprA* and *sat* showed a significant negative correlation with shoot length and shoot weight of maize, whereas *phsA*, *dsrA*, *dsrB*, and *asrC* tended to show a negative correlation with shoot length, shoot weight, leaf P concentration, and root length colonization. Most of the 59 genera had a significant relationship with shoot weight and shoot length.

4 Discussion

Symbiosis with AMF is important for the growth and development of maize (Liu et al., 2018; Ma et al., 2022). The beneficial effects of AMF symbiosis are often related to improving the host plant to obtain nutrients from the soil, especially P (Felföldi

et al., 2022). In our study, the contribution of *Mut* on P uptake through AMF symbiosis was confirmed. Statistically, the P concentration in maize plants was significantly increased post AMF inoculation, but it was reduced in the AMF- colonized *Mut* mutant compared with the wild type (Figure 1), suggesting that *Mut* plays roles in phosphate uptake for maize under AMF symbiosis.

Comparison between AMF- colonized and non-colonized rhizosphere samples (Figure 2A) indicated that AMF colonization affects the composition of the bacterial communities in the rhizosphere of maize. Emmett et al. also revealed a distinct bacterial community associated with *Glomus versiforme* by 16S rRNA gene sequencing (Emmett et al., 2021). However, the loss of the mycorrhizal symbiosis-related gene changed the bacterial community structure related to AMF symbiosis (Figure 2B). The changes of rhizosphere bacteria from the *Mut* mutant and wild type under AMF colonization showed that they had a preference for recruiting different soil bacterial communities. *Rhizobium* and *unclassified_Erythrobacteraceae* were depleted in the rhizosphere of AMF-colonized *Mut* but enriched in AMF-colonized wild type, which may be the specific microbial species greatly affected by the *Mut* with AM symbiosis. Rhizobia can symbiose with the roots of the host plant to improve host plant growth and yield (Yadav, 2021). Igiehon and Babalola (2021) showed that co-inoculation of soybean with rhizobium and AMF improved soybean yield under drought-stress conditions. The rhizobia has also been reported synergistically with AMF to promote root colonization, plant growth, and nitrogen acquisition (Liu et al., 2023; van der Heijden et al., 2023). The microbial species recruited in the mycorrhizal rhizosphere of maize were likely to help maize to obtain phosphate through the mycorrhizal pathway. AMF symbiosis changed exudates released into the rhizosphere soil to attract microorganisms, probably resulting in the directional enrichment of some special microorganisms (Jiang et al., 2021; Ma et al., 2022; Xu et al., 2023a; Xu et al., 2023b). The changes of rhizosphere bacteria in AMF-colonized *Mut* maize may result from the reduced AMF colonization rate, which might monitor changes of exudates in soil, and in turn, influence the recruitment of bacteria.

The changes of bacterial communities in the rhizosphere of the AMF-colonized *Mut* mutant suggested the key role of this maize gene in shaping soil bacterial communities under AMF colonization. Some plant genes have been revealed to affect rhizosphere microorganisms. For example, a rice nitrate transporter gene, NRT1.1B, has been reported to be associated with the recruitment of indica-enriched bacteria that could improve rice growth under organic nitrogen conditions using synthetic communities (Zhang et al., 2019); a salt-tolerant gene, *SST*, alleviates salt stress by regulating soil metabolites and microbiota in the rhizosphere of rice (Lian et al., 2020); and in soybean, transgenic *GsMYB10* shaped the rhizosphere microbial communities and harbored some beneficial microbes to resistant Al toxicity (Liu et al., 2023). In another way, the changes in soil microorganisms can also alter host gene expression (Stringlis et al., 2018; Rolfe et al., 2019). Rhizosphere microorganisms delay flowering by producing indole acetic acid (IAA) to downregulate genes that trigger flowering and stimulate further plant growth (Lu et al., 2018). The application of SynComs significantly upregulated many phosphate starvation responses (PSR) genes and downregulated nitrate transporter genes and nitrate reductase genes (Wang et al., 2021a). Therefore, it will be important to identify additional key genes in maize involved in AMF symbiosis or to screen the AMF-associated rhizosphere bacterial community as a potential molecular breeding target.

Cooperation between the host plant, AMF, and the soil bacteria is essential for plant growth in natural environments. Sulfur is an essential macro-element required for plant growth and is increasingly becoming limiting to crop yield (Narayan et al., 2022). Around 95% of sulfur is present in soil in organic form that cannot be directly utilized by plants, and plants rely on microorganisms in soil and rhizosphere to mobilize organic sulfur (Mahala et al., 2020). Many reports show that AMF symbiosis increases the sulfur content of plants (Narayan et al., 2022). For example, a study shows that AMF- colonized *Lolium perenne* increased cultivable sulfonate-mobilizing bacteria, helping in sulfur supply to the plant (Gahan and Schmalenberger, 2015). In this study, we found that AMF symbiosis reduced the proportion of rhizosphere bacteria related to sulfur reduction, including sulfate reduction, sulfite reduction, and thiosulfate disproportionation (Figure 4), which will increase inorganic sulfur content in the soil and promote plant to obtain sulfur. Dual inoculation with AMF and *Thiobacillus* has been revealed to improve the growth parameters and N, P, K, and S contents of onion and maize plants (Mohamed et al., 2014).

However, our study further found that bacteria associated with sulfur reduction were increased in the rhizosphere of *Mut* colonized by AMF (Figure 4), indicating that the sulfur reduction process is probably more efficient in AMF-colonized *Mut* root, which will reduce inorganic sulfur release from soil. There is an interaction between phosphorus and sulfur absorption by plants (Mohamed et al., 2014; Sun et al., 2020). AMF can affect the gene expression of plants in the process of sulfate transport, thus improving the nutritional status of plants. A sulfoquinovosyl diacylglycerol1 (SQD1) gene has been reported to affect Pi and S homeostasis (Sun et al., 2020). Mutation of *OsSQD1* increases the concentrations of sulfite but reduces the concentration of Pi in the Pi deficiency condition. The relative expression levels of Pi transporters *OsPT2*, *4*, *6*, and *8* were significantly lower in the *ossqd1* mutants. Another study has revealed that transcription factor *PHOSPHATE STARVATION RESPONSE 1* (*PHR1*, *At4g28610*), a key regulator of Pi starvation-responsive genes, also exerts a regulatory influence on the expression of sulfur transporter genes (*SULTR2.1* and *SULTR3.4*) and plays a key role in SO_4^{2-} shoot-to-root flux during Pi deficiency (Rouached et al., 2011). Above all, genes associated with sulfur or phosphorus uptake are probably responsible for phosphorus and sulfur homeostasis at the same time. Since the *Mut* mutant negatively regulates maize P uptake (Figure 1), we speculated that *Mut* may have a potential role in affecting the transport of sulfur, and the changes in P uptake altered the rhizosphere microbiota, which may affect the sulfur uptake.

Above all, this study suggested that maize plants coordinate soil bacterial communities to mobilize phosphate and sulfur from the soil under AMF colonization to promote plant growth. The interaction between the AMF, plant gene, and rhizosphere bacteria could pave the way for technologies to modulate the rhizosphere bacteria to increase crop productivity and sustainability.

Data availability statement

The datasets presented in this study can be found in online repositories. The names of the repository/repositories and accession number(s) can be found below: https://www.ncbi.nlm.nih.gov/, PRJNA871781.

Author contributions

FL and YX contributed to the study conception and design. Material preparation and data collection were performed by YL and YY. Data analysis was performed by YL, YY, JQ, LO and XY. FL, YX, YL, and YY discussed and wrote the manuscript. All authors contributed to the article and approved the submitted version.

Funding

This work was supported by the National Natural Science Foundation of China (31902104), Yunnan Fundamental Research Projects (202301AT070106), Scientific Research Fund Project of Yunnan Provincial Department of Education (2023Y0234), and the Graduate Student Research Innovation Project of Yunnan University (2021Y431, KC-22222188).

Conflict of interest

The authors declare that the research was conducted in the absence of any commercial or financial relationships that could be construed as a potential conflict of interest.

Publisher's note

Supplementary material

The Supplementary Material for this article can be found online at: https://www.frontiersin.org/articles/10.3389/fpls.2023.1206870/full#supplementary-material

SUPPLEMENTARY FIGURE 1
Non-metric Multidimensional Scaling plot (NMDS) showing beta diversity of rhizosphere bacterial communities in non-AMF (arbuscular mycorrhizal fungi) colonized (CK) wild-type vs. AMF colonized wild-type (AMF) **(A)**, and in AMF colonized wild-type vs. AMF colonized *Mut* mutant (Mut_AMF) **(B)**.

SUPPLEMENTARY FIGURE 2
Linear discriminant analysis Effect Size (LEfSe) identified the differentially abundant bacteria in the rhizosphere of non-AMF (arbuscular mycorrhizal fungi) colonized (CK) wild-type vs. AMF colonized wild-type (AMF) **(A)**, and AMF colonized wild-type vs. AMF colonized *Mut* mutant (Mut_AMF) **(B)**.

SUPPLEMENTARY FIGURE 3
Functional Annotation of Procaryotic Taxa (FAPROTAX) analysis showing functional prediction of bacteria in the rhizosphere of non-AMF (arbuscular mycorrhizal fungi) colonized (CK) wild-type vs. AMF colonized wild-type (AMF) **(A)**, and AMF colonized wild-type vs. AMF colonized *Mut* mutant (Mut_AMF) **(B)**.

References

Berendsen, R. L., Vismans, G., Yu, K., Song, Y., de Jonge, R., Burgman, W. P., et al. (2018). Disease-induced assemblage of a plant-beneficial bacterial consortium. *ISME J.* 12, 1496–1507. doi: 10.1038/s41396-018-0093-1

Cai, M. H., Luo, G., Li, J., Li, W. T., Li, Y., and Li, A. M. (2021). Substrate competition and microbial function in sulfate-reducing internal circulation anaerobic reactor in the presence of nitrate. *Chemosphere* 280, 130937. doi: 10.1016/j.chemosphere.2021.130937

Chen, E., Liao, H., Chen, B., and Peng, S. (2020). Arbuscular mycorrhizal fungi are a double-edged sword in plant invasion controlled by phosphorus concentration. *New Phytol.* 226, 295–300. doi: 10.1111/nph.16359

Cordovez, V., Dini-Andreote, F., Carrión, V. J., and Raaijmakers, J. M. (2019). Ecology and evolution of plant microbiomes. *Annu. Rev. Microbiol.* 73, 69–88. doi: 10.1146/annurev-micro-090817-062524

Defez, R., Andreozzi, A., and Bianco, C. (2017). The overproduction of indole-3-Acetic acid (IAA) in endophytes upregulates nitrogen fixation in both bacterial cultures and inoculated rice plants. *Microb. Ecol.* 74, 441–452. doi: 10.1007/s00248-017-0948-4

Deng, S., Lu, L., Li, J., Du, Z., Liu, T., Li, W., et al. (2020). Purple acid phosphatase 10c encodes a major acid phosphatase that regulates plant growth under phosphate-deficient conditions in rice. *J. Exp. Bot.* 71, 4321–4332. doi: 10.1093/jxb/eraa179

Du, E., Terrer, C., Pellegrini, A. F. A., Ahlström, A., van Lissa, C. J., Zhao, X., et al. (2020). Global patterns of terrestrial nitrogen and phosphorus limitation. *Nat. Geosci* 13, 221–226. doi: 10.1038/s41561-019-0530-4

Emmett, B. D., Lévesque-Tremblay, V., and Harrison, M. J. (2021). Conserved and reproducible bacterial communities associate with extraradical hyphae of arbuscular mycorrhizal fungi. *ISME J.* 15, 2276–2288. doi: 10.1038/s41396-021-00920-2

Falkowski, P. G., Fenchel, T., and Delong, E. F. (2008). The microbial engines that drive earth's biogeochemical cycles. *Science* 320, 1034–1039. doi: 10.1126/science.1153213

Felföldi, Z., Vidican, R., Stoian, V., Roman, I. A., Sestras, A. F., Rusu, T., et al. (2022). Arbuscular mycorrhizal fungi and fertilization influence yield, growth and root colonization of different tomato genotype. *Plants* 11, 1743. doi: 10.3390/plants11131743

Gahan, J., and Schmalenberger, A. (2015). Arbuscular mycorrhizal hyphae in grassland select for a diverse and abundant hyphospheric bacterial community involved in sulfonate desulfurization. *Appl. Soil Ecol.* 89, 113–121. doi: 10.1016/j.apsoil.2014.12.008

Herman, D. J., Firestone, M. K., Nuccio, E., and Hodge, A. (2012). Interactions between an arbuscular mycorrhizal fungus and a soil microbial community mediating litter decomposition. *FEMS Microbiol. Ecol.* 80, 236–247. doi: 10.1111/j.1574-6941.2011.01292.x

Hestrin, R., Hammer, E. C., Mueller, C. W., and Lehmann, J. (2019). Synergies between mycorrhizal fungi and soil microbial communities increase plant nitrogen acquisition. *Commun. Biol.* 2, 233. doi: 10.1038/s42003-019-0481-8

Hetrick, B. A. D., Wilson, G. W. T., and Todd, T. C. (1990). Differential responses of C3 and C4 grasses to mycorrhizal symbiosis, phosphorus fertilization, and soil microorganisms. *Can. J. Bot.* 68, 461–467. doi: 10.1139/b90-061

Igiehon, O. N., and Babalola, O. O. (2021). Rhizobium and mycorrhizal fungal species improved soybean yield under drought stress conditions. *Curr. Microbiol.* 78, 1615–1627. doi: 10.1007/s00284-021-02432-w

Jiang, F., Zhang, L., Zhou, J., George, T. S., and Feng, G. (2021). Arbuscular mycorrhizal fungi enhance mineralisation of organic phosphorus by carrying bacteria along their extraradical hyphae. *New Phytol.* 230, 304–315. doi: 10.1111/nph.17081

Kang, F., Yang, B., Wujisiguleng,, Yang, X., Wang, L., Guo, J., et al. (2020). Arbuscular mycorrhizal fungi alleviate the negative effect of nitrogen deposition on ecosystem functions in meadow grassland. *Land Degrad Dev.* 31, 748–759. doi: 10.1002/ldr.3491

Kieft, K., Zhou, Z., Anderson, R. E., Buchan, A., Campbell, B. J., Hallam, S. J., et al. (2021). Ecology of inorganic sulfur auxiliary metabolism in widespread bacteriophages. *Nat. Commun.* 12, 3503. doi: 10.1038/s41467-021-23698-5

Kuzyakov, Y., and Razavi, B. S. (2019). Rhizosphere size and shape: temporal dynamics and spatial stationarity. *Soil Biol. Biochem.* 135, 343–360. doi: 10.1016/j.soilbio.2019.05.011

Li, J., Meng, B., Chai, H., Yang, X., Song, W., Li, S., et al. (2019). Arbuscular mycorrhizal fungi alleviate drought stress in C3 (*Leymus chinensis*) and C4 (*Hemarthria altissima*) grasses *via* altering antioxidant enzyme activities and photosynthesis. *Front. Plant Sci.* 10, 499. doi: 10.3389/fpls.2019.00499

Lian, T., Huang, Y., Xie, X., Huo, X., Shahid, M. Q., Tian, L., et al. (2020). Rice SST variation shapes the rhizosphere bacterial community, conferring tolerance to salt stress through regulating soil metabolites. *mSystems* 5, e00721-20. doi: 10.1128/mSystems.00721-20

Liu, L., Cheng, L., Liu, K., Yu, T., Liu, Q., Gong, Z., et al. (2023). Transgenic soybean of *GsMYB10* shapes rhizosphere microbes to promote resistance to aluminum (Al) toxicity. *J. Hazard Mater* 455, 131621. doi: 10.1016/j.jhazmat.2023.131621

Liu, Y., Evans, S. E., Friesen, M. L., and Tiemann, L. K. (2022). Root exudates shift how n mineralization and n fixation contribute to the plant-available n supply in low fertility soils. *Soil Biol. Biochem.* 165, 108541. doi: 10.1016/j.soilbio.2021.108541

Liu, F., Xu, Y., Han, G., Wang, W., Li, X., and Cheng, B. (2018). Identification and functional characterization of a maize phosphate transporter induced by mycorrhiza formation. *Plant Cell Physiol.* 59, 1683–1694. doi: 10.1093/pcp/pcy094

Lu, T., Ke, M., Lavoie, M., Jin, Y., Fan, X., Zhang, Z., et al. (2018). Rhizosphere microorganisms can influence the timing of plant flowering. *Microbiome* 6, 231. doi: 10.1186/s40168-018-0615-0

Ma, J., Wang, W., Yang, J., Qin, S., Yang, Y., Sun, C., et al. (2022). Mycorrhizal symbiosis promotes the nutrient content accumulation and affects the root exudates in maize. *BMC Plant Biol.* 22, 64. doi: 10.1186/s12870-021-03370-2

Mahala, D. M., Maheshwari, H. S., Yadav, R. K., Prabina, B. J., Bharti, A., Reddy, K. K., et al. (2020). Microbial transformation of nutrients in soil: an overview. *In Rhizosphere microbes: Microorganisms sustainability* (Singapore) 23, 175–211. doi: 10.1007/978-981-15-9154-9_7

McPherson, M. R., Wang, P., Marsh, E. L., Mitchell, R. B., and Schachtman, D. P. (2018). Isolation and analysis of microbial communities in soil, rhizosphere, and roots in perennial grass experiments. *J. Vis. Exp.*, 57932. doi: 10.3791/57932

Mohamed, A. A., Eweda, W. E. E., Heggo, A. M., and Hassan, E. A. (2014). Effect of dual inoculation with arbuscular mycorrhizal fungi and sulphur-oxidising bacteria on onion (*Allium cepa* l.) and maize (*Zea mays* l.) grown in sandy soil under green house conditions. *Ann. Agric. Sci.* 59, 109–118. doi: 10.1016/j.aoas.2014.06.015

Narayan, O. P., Kumar, P., Yadav, B., Dua, M., and Johri, A. K. (2022). Sulfur nutrition and its role in plant growth and development. *Plant Signal Behav.* doi: 10.1080/15592324.2022.2030082

Nuccio, E. E., Hodge, A., Pett-Ridge, J., Herman, D. J., Weber, P. K., and Firestone, M. K. (2013). An arbuscular mycorrhizal fungus significantly modifies the soil bacterial community and nitrogen cycling during litter decomposition. *Environ. Microbiol.* 15, 1870–1881. doi: 10.1111/1462-2920.12081

Priyadharsini, P., Rojamala, K., Ravi, R. K., Muthuraja, R., Nagaraj, K., and Muthukumar, T. (2016). "Mycorrhizosphere: the extended rhizosphere and its significance," in *Plant-microbe interaction: an approach to sustainable agriculture*. Eds. D. Choudhary, A. Varma and N. Tuteja (Singapore: Springer), 97–124.

R Core Team (2019). *A language and environment for statistical computing* (Vienna: R Foundation for Statistical Computing).

Richardson, A. E., Barea, J. M., Mcneill, A. M., and Prigent-Combaret, C. (2009). Acquisition of phosphorus and nitrogen in the rhizosphere and plant growth promotion by microorganisms. *Plant Soil* 321, 305–339. doi: 10.1007/s11104-009-9895-2

Rolfe, S. A., Griffiths, J., and Ton, J. (2019). Crying out for help with root exudates: adaptive mechanisms by which stressed plants assemble health-promoting soil microbiomes. *Curr. Opin. Microbiol.* 49, 73–82. doi: 10.1016/j.mib.2019.10.003

Rouached, H., Secco, D., Arpat, B., and Poirier, Y. (2011). The transcription factor PHR1 plays a key role in the regulation of sulfate shoot-to-root flux upon phosphate starvation in arabidopsis. *BMC Plant Biol.* 11, 19. doi: 10.1186/1471-2229-11-19

Sieh, D., Watanabe, M., Devers, E. A., Brueckner, F., Hoefgen, R., and Krajinski, F. (2013). The arbuscular mycorrhizal symbiosis influences sulfur starvation responses of *Medicago truncatula*. *New Phytol.* 197, 606–616. doi: 10.1111/nph.12034

Smith, M. D., Hartnett, D. C., and Rice, C. W. (2000). Effects of long-term fungicide applications on microbial properties in tallgrass prairie soil. *Soil Biol. Biochem.* 32, 935–946. doi: 10.1016/S0038-0717(99)00223-0

Smith, S. E., and Read, D. J. (2008). *Mycorrhizal symbiosis* (London: Academic Press).

Stringlis, I. A., Yu, K., Feussner, K., de Jonge, R., Van Bentum, S., Van Verk, M. C., et al. (2018). MYB72-dependent coumarin exudation shapes root microbiome assembly to promote plant health. *PNAS* 115, E5213–E5222. doi: 10.1073/pnas.1722335115

Sun, Y., Jain, A., Xue, Y., Wang, X., Zhao, G., Liu, L., et al. (2020). OsSQD1 at the crossroads of phosphate and sulfur metabolism affects plant morphology and lipid composition in response to phosphate deprivation. *Plant Cell Environ.* 43, 1669–1690. doi: 10.1111/pce.13764

Tian, W., Xiang, X., and Wang, H. (2021). Differential impacts of water table and temperature on bacterial communities in pore water from a subalpine peatland, central China. *Front. Microbiol.* 12. doi: 10.3389/fmicb.2021.649981

Tisserant, E., Malbreil, M., Kuo, A., Kohler, A., Symeonidi, A., Balestrini, R., et al. (2013). Genome of an arbuscular mycorrhizal fungus provides insight into the oldest plant symbiosis. *PNAS* 110, 20117–20122. doi: 10.1073/pnas.1313452110

van der Heijden, M. G., de Bruin, S., Luckerhoff, L., van Logtestijn, R. S., and Schlaeppi, K. (2016). A widespread plant-fungal-bacterial symbiosis promotes plant biodiversity, plant nutrition and seedling recruitment. *ISME J.* 10, 389–399. doi: 10.1007/s10725-023-00966-6

Vetterlein, D., Carminati, A., Kögel-Knabner, I., Bienert, G. P., Smalla, K., Oburger, E., et al. (2020). Rhizosphere spatiotemporal organization–a key to rhizosphere functions. *Front. Agron.* 2. doi: 10.3389/fagro.2020.00008

Wang, Y., Chen, Y. F., and Wu, W. H. (2021b). Potassium and phosphorus transport and signaling in plants. *J. Integr. Plant Biol.* 63, 34–52. doi: 10.1111/jipb.13053

Wang, C., Li, Y., Li, M., Zhang, K., Ma, W., Zheng, L., et al. (2021a). Functional assembly of root-associated microbial consortia improves nutrient efficiency and yield in soybean. *J. Integr. Plant Biol.* 63, 1021–1035. doi: 10.1111/jipb.13073

Wang, X. X., Wang, X., Sun, Y., Cheng, Y., Liu, S., Chen, X., et al. (2018). Arbuscular mycorrhizal fungi negatively affect nitrogen acquisition and grain yield of maize in a n deficient soil. *Front. Microbiol.* 9. doi: 10.3389/fmicb.2018.00418

Wei, T., and Simko, V. (2021) *R package 'corrplot': visualization of a correlation matrix*. Available at: https://github.com/taiyun/corrplot.

Xu, Y., Chen, Z., Li, X., Tan, J., Liu, F., and Wu, J. (2023a). The mechanism of promoting rhizosphere nutrient turnover for arbuscular mycorrhizal fungi attributes to recruited functional bacterial assembly. *Mol. Ecol.* 32, 2335–2350. doi: 10.1111/mec.16880

Xu, Y., Chen, Z., Li, X., Tan, J., Liu, F., and Wu, J. (2023b). Mycorrhizal fungi alter root exudation to cultivate a beneficial microbiome for plant growth. *Funct. Ecol.* 37, 664–675. doi: 10.1111/1365-2435.14249

Yadav, A. N. (2021). Beneficial plant-microbe interactions for agricultural sustainability. *J. Appl. Biol. Biotech.* 9, 1–4. doi: 10.7324/JABB.2021.91ed

Yu, P., He, X., Baer, M., Beirinckx, S., Tian, T., Moya, Y. A. T., et al. (2021). Plant flavones enrich rhizosphere oxalobacteraceae to improve maize performance under nitrogen deprivation. *Nat. Plants* 7, 481–499. doi: 10.1038/s41477-021-00897-y

Yu, X., Zhou, J., Song, W., Xu, M., He, Q., Peng, Y., et al. (2021). SCycDB: a curated functional gene database for metagenomic profiling of sulphur cycling pathways. *Mol. Ecol. Resour.* 21, 924–940. doi: 10.1111/1755-0998.13306

Zhalnina, K., Louie, K. B., Hao, Z., Mansoori, N., da Rocha, U. N., Shi, S., et al. (2018). Dynamic root exudate chemistry and microbial substrate preferences drive patterns in rhizosphere microbial community assembly. *Nat. Microbiol.* 3, 470–480. doi: 10.1038/s41564-018-0129-3

Zhang, L., Feng, G., and Declerck, S. (2018a). Signal beyond nutrient, fructose, exuded by an arbuscular mycorrhizal fungus triggers phytate mineralization by a phosphate solubilizing bacterium. *ISME J.* 12, 2339–2351. doi: 10.1038/s41396-018-0171-4

Zhang, J., Liu, Y. X., Zhang, N., Hu, B., Jin, T., Xu, H., et al. (2019). NRT1.1B is associated with root microbiota composition and nitrogen use in field-grown rice. *Nat. Biotechnol.* 37, 676–684. doi: 10.1038/s41587-019-0104-4

Zhang, L., Shi, N., Fan, J., Wang, F., George, T. S., and Feng, G. (2018b). Arbuscular mycorrhizal fungi stimulate organic phosphate mobilization associated with changing bacterial community structure under field conditions. *Environ. Microbiol.* 20, 2639–2651. doi: 10.1111/1462-2920.14289

Zhang, L., Zhou, J., George, T. S., Limpens, E., and Feng, G. (2022). Arbuscular mycorrhizal fungi conducting the hyphosphere bacterial orchestra. *Trends Plant Sci.* 27, 402–411. doi: 10.1016/j.tplants.2021.10.008

frontiers | Frontiers in Plant Science

TYPE Review
PUBLISHED 10 July 2023
DOI 10.3389/fpls.2023.1193573

OPEN ACCESS

EDITED BY
Ricardo Aroca,
Spanish National Research Council (CSIC), Spain

REVIEWED BY
Parul Chaudhary,
Graphic Era Hill University, India
Shipra Pandey,
Indian Institute of Technology Bombay, India

*CORRESPONDENCE
Rakesh Kumar Verma
rkwat4@yahoo.com
Byong-Hun Jeon
bhjeon@hanyang.ac.kr
Rajarshi Kumar Gaur
gaurrajarshi@hotmail.com

RECEIVED 25 March 2023
ACCEPTED 31 May 2023
PUBLISHED 10 July 2023

CITATION
Choudhary N, Dhingra N, Gacem A, Yadav VK, Verma RK, Choudhary M, Bhardwaj U, Chundawat RS, Alqahtani MS, Gaur RK, Eltayeb LB, Al Abdulmonem W and Jeon B-H (2023) Towards further understanding the applications of endophytes: enriched source of bioactive compounds and bio factories for nanoparticles. *Front. Plant Sci.* 14:1193573. doi: 10.3389/fpls.2023.1193573

Towards further understanding the applications of endophytes: enriched source of bioactive compounds and bio factories for nanoparticles

Nisha Choudhary[1], Naveen Dhingra[2], Amel Gacem[3], Virendra Kumar Yadav[1,4], Rakesh Kumar Verma[1]*, Mahima Choudhary[1], Uma Bhardwaj[5], Rajendra Singh Chundawat[1], Mohammed S. Alqahtani[6,7], Rajarshi Kumar Gaur[8]*, Lienda Bashier Eltayeb[9], Waleed Al Abdulmonem[10] and Byong-Hun Jeon[11]*

[1]Dept of Biosciences, School of Liberal Arts and Sciences, Mody University of Science and Technology, Lakshmangarh, Sikar, Rajasthan, India, [2]Department of Agriculture, Medi-Caps University, Pigdamber Road, Rau, Indore, Madhya Pradesh, India, [3]Department of Physics, Faculty of Sciences, University 20 Août 1955, Skikda, Algeria, [4]Department of Life Sciences, Hemchandracharya North Gujarat University, Patan, Gujarat, India, [5]Department of Biotechnology, Noida International University, Noida, U.P., India, [6]Radiological Sciences Department, College of Applied Medical Sciences, King Khalid University, Abha, Saudi Arabia, [7]BioImaging Unit, Space Research Centre, University of Leicester, Leicester, United Kingdom, [8]Department of Biotechnology, Deen Dayal Upadhyaya (D.D.U.) Gorakhpur University, Gorakhpur, Uttar Pradesh, India, [9]Department of Medical Laboratory Sciences, College of Applied Medical Sciences, Prince Sattam Bin AbdulAziz University-Al-Kharj, Riyadh, Saudi Arabia, [10]Department of Pathology, College of Medicine, Qassim University, Buraidah, Saudi Arabia, [11]Department of Earth Resources and Environmental Engineering, Hanyang University, Seoul, Republic of Korea

The most significant issues that humans face today include a growing population, an altering climate, an growing reliance on pesticides, the appearance of novel infectious agents, and an accumulation of industrial waste. The production of agricultural goods has also been subject to a great number of significant shifts, often known as agricultural revolutions, which have been influenced by the progression of civilization, technology, and general human advancement. Sustainable measures that can be applied in agriculture, the environment, medicine, and industry are needed to lessen the harmful effects of the aforementioned problems. Endophytes, which might be bacterial or fungal, could be a successful solution. They protect plants and promote growth by producing phytohormones and by providing biotic and abiotic stress tolerance. Endophytes produce the diverse type of bioactive compounds such as alkaloids, saponins, flavonoids, tannins, terpenoids, quinones, chinones, phenolic acids etc. and are known for various therapeutic advantages such as anticancer, antitumor, antidiabetic, antifungal, antiviral, antimicrobial, antimalarial, antioxidant activity. Proteases, pectinases, amylases, cellulases, xylanases, laccases, lipases, and other types of enzymes that are vital for many different industries can also be produced by endophytes. Due to the presence of all these bioactive compounds

in endophytes, they have preferred sources for the green synthesis of nanoparticles. This review aims to comprehend the contributions and uses of endophytes in agriculture, medicinal, industrial sectors and bio-nanotechnology with their mechanism of action.

KEYWORDS

nano particle, plant growth promotion, larvicidal, bioactive component, endophytes

1 Introduction

According to the report published by the IPCC (2018), the probability of limiting the effects of global warming to 1.5°C is majorly determined by the cumulative emission of carbon dioxide (CO_2) and future non-CO_2 radiative forcing. The devastating impact of climate change can be observed in sustainable agriculture systems and overall agriculture productivity (Verma et al., 2022). Agricultural activities in the 21st century are largely depending on the extensive use of fertilizers, pesticides, fungicides etc. and also sometimes involve the over-irrigation and use of high-yielding crop varieties (Hegazy et al., 2017). Such practices have a negative impact on the environment and lead to low fertility of the soil by decreasing the symbiotic association of fungal and bacterial communities in the soil. Such practices also lead to groundwater pollution due to the leaching out of nitrogen and phosphorus from the soil into the groundwater (Rafi et al., 2019). In a similar vein, many biotic factors, such as bacteria, fungi, viruses, weeds, insects, and nematodes, are major constraints of stress that tend to increase the reactive oxygen species that affect the physiological and molecular functioning of plants and also lead to the decrease in crop productivity (Chaudhary et al., 2022). In addition, the increased temperatures, atmospheric CO_2 levels, and precipitation patterns also affect agricultural production and insect infestations (Skendžić et al., 2021). In order to reduce the negative impact of such practices and to maintain the fertility of the soil, various eco-friendly farming techniques are employed such as the inculcation of microorganisms as fertilizers encompassing nutrient mobilizing capacity (Gamez et al., 2019). The symbiotic relationship between plants and microorganisms exerts various benefits on plants such as an increase in height and weight, the high nutritional value of plants etc. It results in increasing crop yield, nutrient cycling and fertility of the soil (Card et al., 2021). A single plant is colonised by a large number of microbes, these microbes can be termed epiphytes and endophytes. Endophytes, symbiotic bacterial and fungal communities, are present in intercellular and intracellular spaces of plant parts, such as stems, roots, leaves, etc. (Oukala et al., 2021). Endophytes are also accommodated by weeds inflorescences, petioles, buds, and dead and hollow hyaline cells of plants, fruits and seeds (Lonkar and Bodade, 2021). Either the full or some part of the life cycle of endophyte microbes occur inside the host plant, without causing any negative impact on the plant (Joo et al., 2021). Endophytic associations are reported in various types of plants such as soybeans, chickpeas, cowpeas, sunflower, pearl millet, rice, maize, mustard, sugarcane, cotton, tomatoes, etc (Fadiji and Babalola, 2020). Endophytes are classified on the basis of their biological nature, mode of transmission, and diversity into two classes: transient endophytes and true endophytes (Sharma et al., 2021). In addition, on the basis of their association with host plants, endophytes are classified as obligate and facultative endophytes. Endophytes that spread among plants vertically and completely rely on plant metabolism for survival are referred to as "obligate endophytes," whereas endophytes that enter plants from neighbouring soil or environment and only partially rely on the host plant, completing only some part of the host plant's lifecycle, are referred as "facultative endophytes" (Khare et al., 2018). The endophytic world has gained popularity among researchers due to its significant contributions as it produces various types of bioactive compounds that play important roles in various industries such as agricultural, pharmaceutical, medical, and biotechnological industries (Figure 1) (Latz et al., 2018; Tiwari et al., 2023).

Endophytes have a significant impact on the health of their hosts, including their ability to absorb nutrients, produce phytohormones, and reduce the damage caused by pathogens through antibiosis, the generation of lytic enzymes, the activation of secondary metabolites, and the activation of hormones (Chaudhary et al., 2022). However, the complete elucidation of total metabolites produced by endophytes, their functions, protein-protein interactions, and the factors which influence the interaction between fungal, and bacterial endophytes with different plants is still in inferencing.

Nowadays, both fungal and bacterial endophytes are important in the industrial, pharmacological, and biotechnological sectors. This is because they produce different types of metabolites that are

Abbreviations: JA, Jasmonic Acid; OSMAC, approach; SPME GCMS, solid-phase microextraction-gas chromatography-mass spectroscopy; HPLCHRMS, highperformance liquid chromatography high-resolution mass spectroscopy; MALDIHRMS, matrix-associated laser desorption ionization-HRMS; IAA, indole-3-acetic acid; SAR, systemic acquired resistance; SA, salicylic acid; PR, Pathogenesis Related; HR, hypersensitivity reaction; ISR, induced system resistance; HMG-CoA reductase enzyme, hydroxyl methylglutaryl coenzyme A reductase; TMP, Tetramethylpyrazine; HupA, huperzine A; ChEI, cholinesterase inhibitor; TMP, Tetramethylpyrazine; DPT, Deoxypodophyllotoxin; ABA, Abscisic acid; ACC, 1-aminocyclopropane-1-carboxylic acid; VOCs, volatile organic compounds; PS, phosphate solubilization; NF, Nitrogen fixation; CE, Cyclopeptides echinocandins.

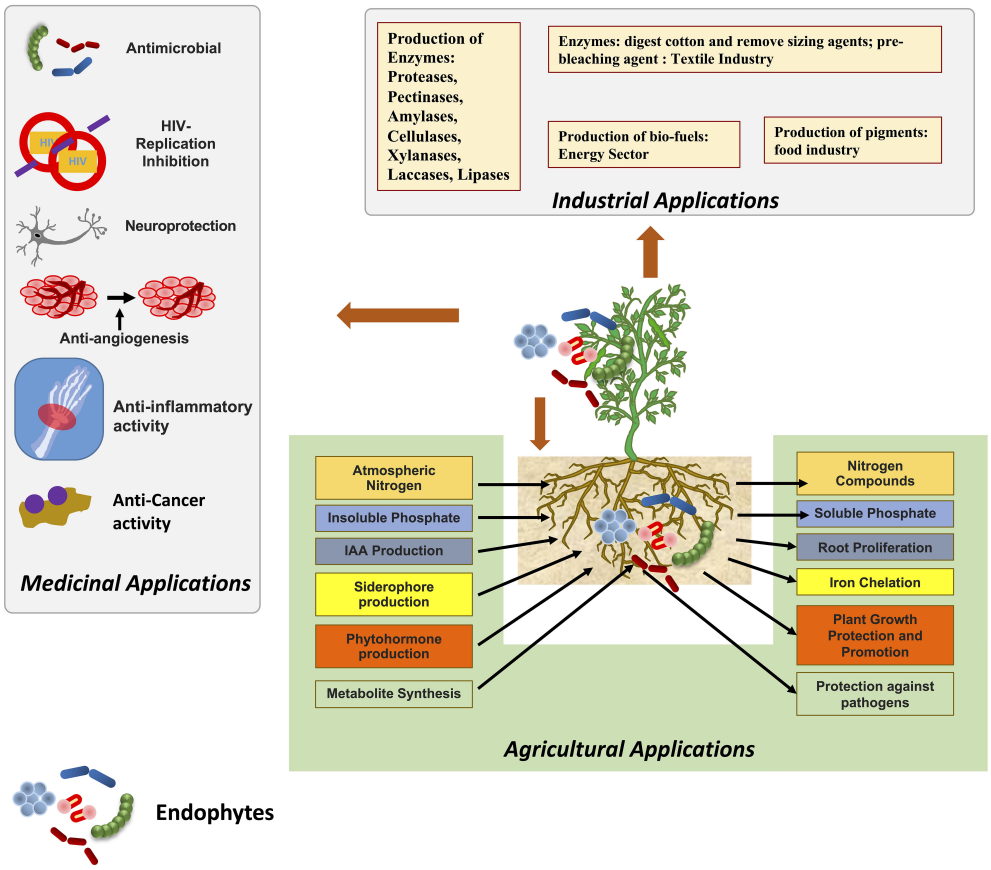

FIGURE 1
Endophytes and their applications in agriculture, industrial and medical fields.

used as antitumor, antiviral, and antimicrobial agents, plant growth promoters, bio-control agents, stress tolerance of plants, and immunosuppressants. They also produce different types of compounds that make them good antibiotic, anti-diabetic, and antioxidant agents (Gouda et al., 2016). Several researchers have demonstrated the potential of these endophytes in the synthesis of novel nanomaterials and the role of microbial endophytes in agriculture (Yadav et al., 2020), (Dhara et al., 2023).

In the present review, the authors have emphasized the importance of both fungal and bacterial endophytes in industries, pharmaceuticals and biotechnology. This study addressed recent research on endophytes in order to address a gap in the field and give a detailed application of the metabolites or bioactive components that have been isolated from endophytes and their potential application to bio-nanotechnology. In addition, this review has emphasised on the importance of endophytes-mediated synthesis of nanoparticles as well as their applicability in a variety of sectors.

2 Various approaches for screening bioactive compounds in endophytic culture

From the various pieces of literature, it has been proven that there are various approaches for the screening of bioactive compounds from the culture of endophytes like axenic culture, OSMAC approach, and elicitors (Gakuubi et al., 2021). All these three approaches play an important role in the activation of cryptic gene clusters in the endophyte's genome. In addition to this, there are several instrument-based approaches like solid-phase microextraction-gas chromatography-mass spectroscopy (SPME GCMS), high-performance liquid chromatography high-resolution mass spectroscopy (HPLC-HRMS) and matrix-associated laser desorption ionization-HRMS (MALDI-HRMS). SPGE-GC-MS helps in the screening of volatile compounds especially signalling compounds secreted by the endophytes. HPLC-HRMS helps in the screening for bioactive compounds mainly antimicrobial and anti-cancerous. MALDI-HRMS, the technique could help in the screening of the distribution and release of target compounds in host plants' apoplast (Mishra et al., 2022). Figure 2 is showing a schematic diagram for various approaches for screening bioactive compounds from endophytic culture.

3 The mechanism employed by endophytes in plant growth promotion and protection

Endophytes protect plants by employing two types of mechanisms: indirect and direct. In direct mechanism, endophytes

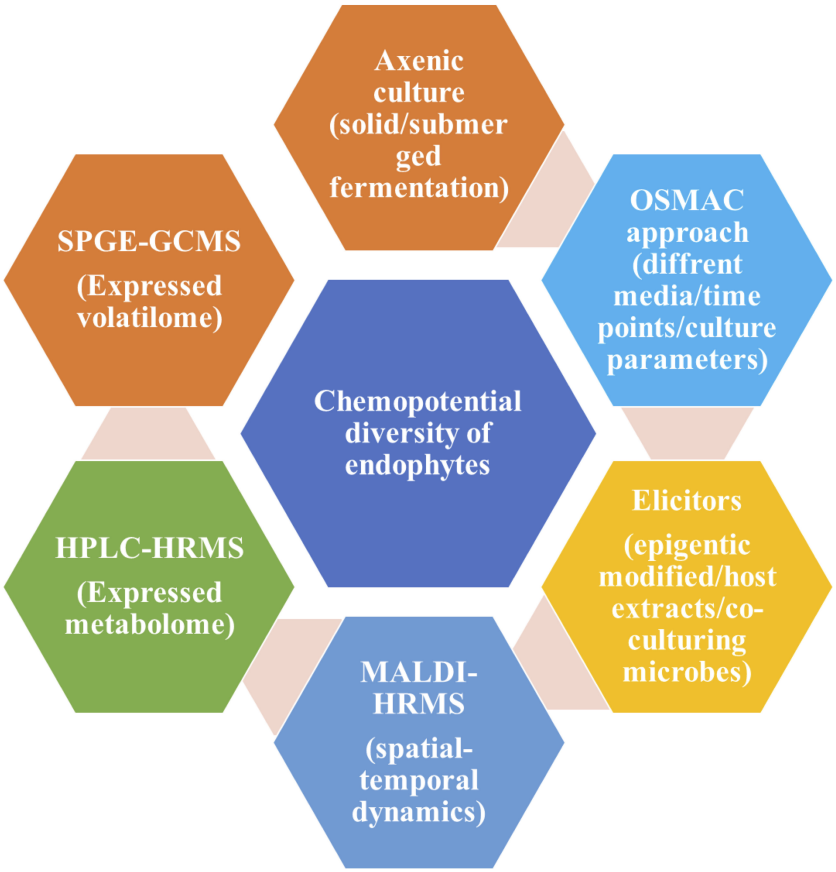

FIGURE 2
Schematic diagram for screening of various bioactive compounds from endophytic culture adopted from (Mishra et al., 2022).

directly promote plant cell elongation and proliferation by producing phytohormones, indole-3-acetic acid (IAA), siderophores, 1-aminocyclopropane-1-carboxylic acid, phosphate and potassium solubilization antibiosis, and by suppressing the pathogens, etc.

In addition, endophytes promote the capacity to convert atmospheric nitrogen into ammonia, which is required for the synthesis of proteins and nucleic acids and provides tolerance against salt and drought by synthesizing sugar molecules (Muthu Narayanan et al., 2022). Several studies have highlighted the role of endophytic fungi in mitigating biotic and abiotic stresses, making them an essential component of climate-smart and sustainable agriculture (Verma et al., 2022), (Tyagi et al., 2022). The endophytes are known to produce various types of siderophores such as carboxylate, catecholate, phenolates, and hydroxamates. These siderophores perform a variety of functions, including the biocontrol of phytopathogens by limiting the pathogens' ability to absorb iron, the reduction of heavy metal toxicity, and the induction of induced systemic resistance (ISR) (Chaudhary et al., 2022), (Gómez-Godínez et al., 2023). Several microbial species such as *Rhodococcus spp, Bacillus spp, Enterobacter spp*, Methylobacterium *spp, Pseudomonas fluorescens, Pseudomonas putida, Pantoea ananatis* and *Pantoea agglomerans*, etc. are positively shown to produce siderophores (Karuppiah et al., 2022; Singh et al., 2022). Endophytes emit different organic acids such as malic, gluconic, and citric acids that convert insoluble soil phosphate (apatite, fluorapatite and hydroxyapatite) into soluble orthophosphates by chelating cations attached to the phosphate (Fadiji and Babalola, 2020), (Yadav et al., 2018). Various bacterial and fungal endophytes have been reported to date for phosphate solubilisation activity, phosphate solubilisation, phytohormone production and nitrogen fixation activity (Supplementary Table 1). Endophytic associative nitrogen-fixing microbes are superior to rhizosphere microorganisms in terms of their ability to enable plant life to flourish in nitrogen-deficient soil and to support the overall health and growth of plants (Afzal et al., 2019). *Curvularia geniculata*, a dark septate root endophytic fungus isolated from the roots of *Parthenium hysterophorus*, is known to stimulate the growth of plants by solubilising phosphorus (P) and producing phytohormones (Mehta et al., 2019). Colonisation by the endophytic fungus *Serendipita indicia* enhances nutrient uptake and helps maintain ionic homeostasis by limiting the passage of sodium (Na^+) and potassium (K^+) ions in plants and enhancing gene transcription, both of which play important roles in Na+ and K^+ homeostasis (Tyagi et al., 2022). Endophytes like *Colletotrichum, Pseudomonas, Bacillus. Herbaspirillum, Alcaligenes, Streptomyces, Piriformospora indica, Sebacina vermifera*, and *Penicillium* have gained particular interest amongst others because of the propensity

to produce phytohormones such as auxins, gibberellins (GA), cytokinins and ethylene that favour improved plant development under harsh conditions (Burragoni and Jeon, 2021), (Omomowo et al., 2023). It has been found that the *pestalotiopsis microspore* produces pestalotin analogue, a metabolite with gibberellin activity that promotes faster germination (Li et al., 2018). Likewise, *Cladosporium sphaerospermum*, an endophyte of Glycine max, is responsible for the production of gibberellic acid, which is known to encourage the growth of rice and soybean plants (Omomowo et al., 2023).

The indirect mechanism adopted by endophytes promotes the plant growth by enhancing the plant defence system using various mechanisms like plant resistance induction, environmental stress tolerance, predation and hyperparasite, stimulation of secondary metabolites in plants etc (Tian et al., 2008). When a plant is under attack from a biotrophic pathogen, signalling molecules like salicylic acid (SA) and associated pathogenesis-related (PR) proteins act to induce "systemic acquired resistance" (SAR), which in turn triggers "local resistance" by producing a hypersensitivity reaction (HR) in the infected and surrounding areas of the plant (Muthu Narayanan et al., 2022). For instance, pre-treatment of *Pisum sativum* seeds with *Pseudomonas fluorescens* (OKC) and *Trichoderma asperellum* (T42) prevents powdery mildew disease by stimulating the defence response by upregulation of phytohormone, SA, and PR-1 protein (Patel and Saraf, 2017).

Induced system resistance (ISR) is the second defence mechanism plants use to fend against infections (Qin et al., 2021). By triggering the release and transport of signalling molecules like JA and associated PR proteins to the affected areas, it helps plants defend themselves against necrotrophic diseases. Neither the pathogenic virus nor its replication is directly hindered by the ISR approach. On the contrary, it reinforces the plants' inherent physical or chemical defences (Muthu Narayanan et al., 2022). For example, the modulation of signalling pathways by JA and its product JA-isoleucine (JA-Ile) hormone is often achieved by the utilisation of abscisic acid (ABA) or ethylene (necrotrophic pathogens defender) (Muthu Narayanan et al., 2022). ISR is induced by *Bacillus subtilis* PTA-271 and *Pseudomonas fluorescens* PTACT2 to prevent canker and grey mould disease caused by *Pseudomonas syringae* Pst DC3000 and *Botrytis cinerea*, respectively, in the Arabidopsis plants. Infected plant leaves provide evidence of their antagonistic impact through an increase in JA and ABA (Nguyen and Nguyen, 2020).

In antibiosis, various secondary metabolites such as lipopeptides antibiotics, amino acid-rich peptides (neomycin), and cyclic cationic lipopeptides are produced by different endophytes that serve as biocontrol agents as they exhibit antifungal, antibacterial, and nematocidal activities against phytopathogens (Muthu Narayanan et al., 2022). For instance, to protect the leaves of the *W. somnifera* plant from infection by *A. alternata*, endophytic bacteria like *B. amyloliquefaciens* and *P. fluorescens* enhance callose deposition in guard cells (Mishra et al., 2018). Epichloe is a monophyletic genus of filamentous fungi that develop everlasting symbioses with cool-season grasses (Card et al., 2021). Epichloe fungal endophytes not only boost plant immunity against chewing insects by creating protective alkaloids, but they also promote plant immunity by increasing endogenous defence responses mediated by the jasmonic acid (JA) pathway (Card et al., 2021). The foliar endophytic fungus *Colletotrichum tropicale* isolated from *T. cocoa* protects the cocoa tree from black pod disease caused by *Phytophthora* spp. by upregulating genes related to cellulose and lignin deposition and host cell wall hardening (Sadoral and Cumagun, 2021). *Bacillus atrophaeus* and *Bacillus mojavensis*, isolated from the *Glycyrrhiza uralensis* (Licorice) plant, have antifungal activity due to the presence of various compounds such as 1,2-bezenedicarboxyl acid, methyl ester, decanodioic acid, and bis (2-ethylhexyl) ester (Mohamad et al., 2018). The antibacterial activity of Aspergillus sp., endophyte, isolated from the *Bauhinia guianensis* plant has been reported due to the presence of fumigaclavine C and pseurtotin C (Wen et al., 2022). In another study, the protein bacillomycin D was produced by *B. amyloliquefaciens*, which was shown to have antagonistic action against the fungus *F. graminearum* (Gu et al., 2017).

4 Endophytic bioactive components of medicinal significance

The ecosystem is a treasure trove of medicinal plants that contain chemicals that have the potential to serve as a substitute for medications produced synthetically (Michel et al., 2020). The major problem with collecting these compounds from medicinal plants is that there aren't very many of them, while the demand is high. This leads to overexploitation, which in turn reduces plant population (Palanichamy et al., 2018). In order to fulfil the large-scale production of these compounds, alternative approaches like tissue culture, semi-synthesis, exploitation of endophytes for these compound syntheses, heterologous production, etc. are adopted (Sandargo et al., 2019). Endophytes present in plants are considered a treasure house of various bioactive compounds such as tannins, alkaloids, terpenoids, benzopyranones, quinones, polyketides, chinones, saponins, flavonoids, phenolic acids, steroids, xanthones etc. (Figure 3) (Kumari et al., 2020; Vaid et al., 2020). These bioactive compounds are known to have various uses in the medical sector.

Taxol (Paclitaxel) is a diterpene alkaloid which is produced in Taxus sp. by different endophytes such as- *Taxomyces andreanae, Fusarium solani, Metarhizium anisopliae* and many others which exhibit anticancer (antitumor) activity (Table 1). Taxol acts as a mitotic inhibitor and causing microtubules to break down at the time of cell division. Whereas other bioactive compounds such as- Brefeldin-A, Phomopsin-A/B/C, Cytosporone-B/C, Terpene, and cryptocandin produced in different plants *Quercus variabilis Blume, Excoecaria agallocha L., Allamanda cathartica L.* and *Tvipterigeum wilfordii Hook. f.* by different endophytes such as *Cladosporium* sp., *Phomopsis* sp., and *Cryptosporiopsis quercina* are known to have antimicrobial, antifungal, antibacterial and antimycotic activities respectively. Similarly, Lovastatin is produced in the *Solanum xanthocarpum* plant by *Phomopsis vexans* endophyte known to have blood cholesterol-lowering properties (Parthasarathy and Sathiyabama, 2015). Lovastatin inhibits the HMG-CoA reductase

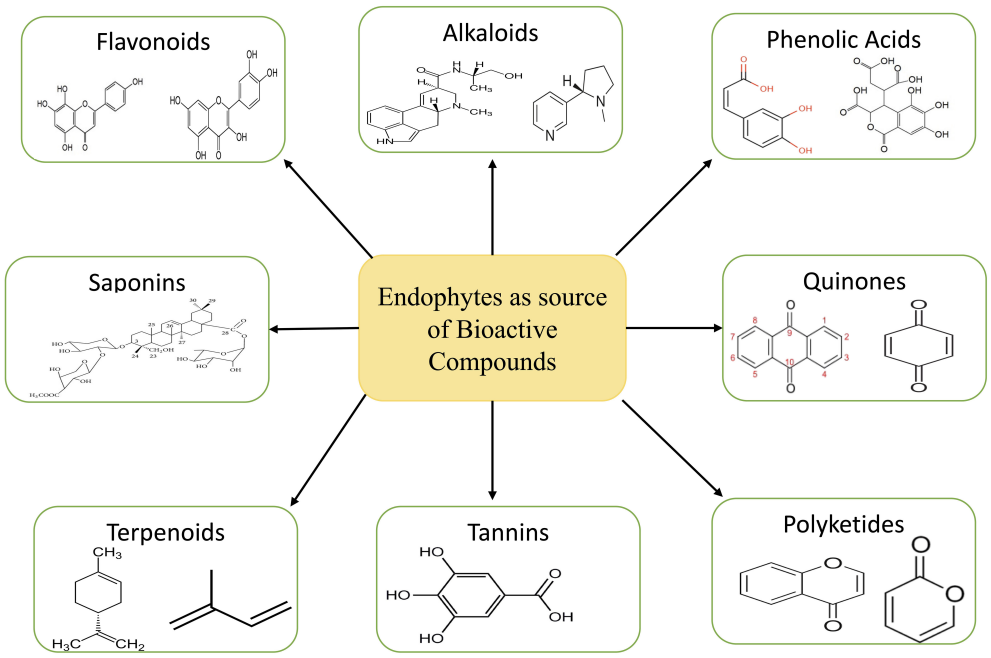

FIGURE 3
Bioactive compounds extracted from endophytes.

enzyme (hydroxyl methylglutaryl coenzyme A reductase), which plays an important role in the regulation of the rate-limiting step of cholesterol biosynthesis as this enzyme catalyses the conversion of HMG-CoA to mevalonate, in a competitive manner (Bhargavi et al., 2018). Ligustrazine which is also known as TMP (Tetra methylpyrazine) can stimulate neuronal differentiation by controlling Topoisomerase IIβ epigenetic activity (Lin et al., 2022). It safeguards against the oxygen-glucose deprivation-induced degeneration of neurons, encourages the migration of brain progenitor/precursor cells and also inhibits H_2O_2-induced apoptosis in bone marrow-derived mesenchymal stem cells by controlling the PI3K/Akt and ERK1/2 signalling pathways. 3-Nitropropionic acid and tenuazonic acid exhibit strong antitubercular effects on *M. tuberculosis* H37Ra by disrupting the isocitrate lyase enzyme pathways required for the metabolism and virulence of the pathogen (Adeleke and Babalola, 2021). HupA (huperzine A) acts as a cholinesterase inhibitor (ChEI) which function to decrease the breakdown of acetylcholine and is used in dementia and Alzheimer's treatment (Dou et al., 2018). Likewise; DPT (Deoxypodophyllotoxin) cyclolignan compound, isolated from various plants accompanied by endophytes (Table 1). The anti-cancer effect of DPT on colorectal cancer cells through induction of apoptosis, by destabilization of microtubules, activation of mitochondrial apoptotic pathway via regulation of B-cell lymphoma 2 (Bcl-2) family proteins, (decreasing Bcl-xL and increasing Bcl-2 associated X (BAX)) and suppression of tumorigenesis have been reported recently (Gamage et al., 2019). In addition, bilobalide, sesquiterpene tri-lactone, obtained from *Ginkgo biloba*, could be a potential therapeutic agent for brain ischemia and neurodegeneration due to its upregulation of mitochondrial DNA-encoded COX III subunit of cytochrome c oxidase and the ND1 subunit of NADH dehydrogenase genes. Both genes are involved in neuroprotection through the preservation of mitochondrial functions and hindrance in apoptosis. Nowadays the prodrug approach is often used to combat pharmacokinetic, pharmaceutical, and thermodynamic barriers that limit the inculcation of new drugs. The *influenza virus* is a deadly virus causing severe damage to human beings. Neuraminidase (NA) inhibitor drugs nowadays are used to treat influenza infections. But due to its antigenic drift and antigenic shift, the *influenza virus* is continuously evolving and may become resistant to previous drugs. Recently, cyclosporine A (CsA) and its analogues have been reported for antiviral activity against influenza A and B strains (Ma et al., 2016). Cyclosporine is a natural product and can be produced by endophytes (Supplementary Table 1). Likewise, *Human cytomegalovirus* (hCMV) encodes a 256 amino acid serine protease which is responsible for capsid assembly, an essential process for herpes virus production. Cytonic acids A and B, protease inhibitors, obtained from endophytic fungi *Cytonaema* sp., prevent the development of infectious herpes viruses by blocking the assembly (Tiwari et al., 2023).

5 Endophytes of agricultural significance

Endophytes exhibits numerous plant growth-promoting activities such as phosphate solubilization, siderophore production, IAA production, nitrogen fixation, ammonia production, etc. (Hashim et al., 2020; Zamin et al., 2020) *Piriformospora indica*, an endophytic basidiomycete fungus that colonises many plant roots, is

TABLE 1 Plant growth promotion activities of endophytes and their host plants.

Host Plant	Endophyte	Plant Growth Promotion Activity	References
Ephedra pachyclada	Fifteen Fugal endophyte species	Ammonia production, phosphate solubilization (PS), and IAA production	(Khalil et al., 2021)
Pulicaria incisa	Fifteen bacterial endophyte species	Ammonia production, phosphate solubilization, and IAA production	(Fouda et al., 2021)
Fagonia mollis Delile and Achillea fragrantissima	Thirteen bacterial endophyte species	Ammonia production, PS, and indole acetic acid production	(ALKahtani et al., 2020)
Piper nigrum	Twelve bacterial endophyte species	PS, IAA production, siderophore production	(Jasim et al., 2013)
Teucrium polium	Seven bacterial and five fungal endophyte species	Ammonia production and PS	(Hassan, 2017)
Salicornia europaea	Thirty-two bacterial endophyte species	PS, IAA production	(Zhao et al., 2016)
T. apollinea Moringa peregrina	Five bacterial endophyte species	Plant growth of soybean, IAA production	(Asaf et al., 2017)
Agave tequilana	Eleven bacterial endophyte species	N_2 fixation, IAA production and PS	(Martínez-Rodríguez et al., 2014)
Tephrosia apollinea	Thirteen bacterial endophytes	IAA production and gibberellins production	(Khan et al., 2014)
Cucumis sativus	*Paecilomyces formosus*	Gibberellins and IAA	(Khan et al., 2012)
Vigna unguiculata	*Azotobacter, Azospirillum, Rhizobium*	N_2 fixation and phytohormone production	(Arafa and El-Batanony, 2018)
Oryza sativa	*Sphingopyxis granuli* and *Pseudomonas aeruginosa*	Nitrogen metabolism	(Battu et al., 2017)
Cucumis sativus	*Phoma glomerata, Penicillium* sp.	Gibberellins and IAA	(Waqas et al., 2012)
Glycine max	*Streptomyces* sp. NEAU-S7GS2	Biocontrol and biofertilizer	(Liu et al., 2019)
Morus alba	*Bacillus subtilis 7PJ-16*	Antifungal, biofertilizer and biocontrol	(Xu et al., 2019)
Triticum aestivum L.	*Bacillus* sp. *strain WR11*	Abiotic stress alleviation	(Chen et al., 2020)
Glycine max	*Methylobacterium, Rhizobium*	Metabolite synthesis	(Hamayun et al., 2017)
Cajanus cajan (L.) Mill sp	*Fusarium* sp., *Neonectria* sp.	Cajaninstilbene acid	(Fuller et al., 2019)
Helianthus annuus L.	*Bacillus* sp., *Achromobacter* sp., *Alcaligenes* sp.	ABA, JA and phosphate solubilization	(Forchetti et al., 2007; Shahid et al., 2015)
Phragmites karka	*Mangrovibacter* sp. strain MP23	Uptake of nutrients, N_2 fixation (NF) and oxidative stress	(Behera et al., 2016)
Oryza sativa	*Azotobacter*	Siderophore production, NF and phosphate solubilization	(Banik et al., 2016)
Indigofera argentea	*Enterobacter* sp. SA187	Oxidative stress and antimicrobial compounds production	(Andrés-Barrao et al., 2017)
Glycine max	*Sphingomonas* sp. LK11	IAA production, phytoremediation and PS	(Asaf et al., 2018)
Ammodendron bifolium	*Bacillus mojavensis*, *Bacillus* sp.	IAA production, 1-aminocyclopropane-1-carboxylic acid deaminase activity, PS and NF	(Maheshwari et al., 2020)
Solanum lycopersicum	*Azospirillum, Pseudomonas*	PS and NF	(Bergna et al., 2018)
Oryza sativa L.	*Bacillus paralicheniformis*	NF	(Annapurna et al., 2018)
Pennisetum sinense Roxb	*Klebsiella variicola GN02*	NF	(Lin et al., 2019)
Pellaea calomelanos	*Pseudarthrobacter phenanthrenivorans MHSD1*	Siderophore production and NF	(Tshishonga and Serepa-Dlamini, 2020)
Orchid doritaenopsis	*Mycobacterium mya-zh01*	Seed germination	(Pan et al., 2020)

(Continued)

TABLE 1 Continued

Host Plant	Endophyte	Plant Growth Promotion Activity	References
Corchorus olitorius	*Micrococcus luteus*, *Kocuria* sp.	Siderophore production and IAA production	(Haidar et al., 2018)
Zygophyllum simplex	*Paenibacillus* sp. JZ16	Biotic and abiotic stress tolerance	(Eida et al., 2020)
Triticum aestivum	*Cladosporium herbarum*, *Azotobacter chroococcum and Bacillus circulans*	PS, NF and biocontrol agent	(Larran et al., 2016)
Vicia faba L., Secale cereale L., Zea mays L., Triticum aestivum L., Equisetum arvense L. and Arctium lappa L.	*Novosphingobium, Delftia, Achromobacter, Stenotrophomonas, Rhizobium, Brevundimonas, Variovorax, Comamonas, and Collimonas*	Siderophore production, IAA production, PS & NF	(Woźniak et al., 2019)
Nicotiana tabacum	*Pseudomonas* spp.	Trace metal tolerance, IAA production, NF, siderophore production, 1-aminocyclopropane-1-carboxylic acid deaminase activity and PS	(Ghanta et al., 2011)
Tephrosia apollinea	*Sphingomonas* sp.,	Drought tolerance	(Asaf et al., 2017; Asaf et al., 2018)
Urochloa ramosa	*Curtobacterium* sp., *Microbacterium* sp., *Methylobacterium* sp., *Bacillus amyloliquefaciens, Actinobacteria*	PS, biocontrol and auxin production	(Asaf et al., 2017; Asaf et al., 2018; Verma and White, 2018)
Avicennia marina	*Micrococcus yunnanensis*	Siderophore production, IAA production and ammonia production	(Soldan et al., 2019)
Lilium lancifolium	*Paenibacillus polymyxa*	Siderophore production, IAA production, ammonia production, 1-aminocyclopropane-1-carboxylic acid deaminase activity, PS, NF and biocontrol	(Khan et al., 2020)
Cool-season grasses of the sub-family *Pooideae*	Epichloe fungal endophytes	Increased the plant production of SA and enhanced the expression levels of plant genes of synthesis and response to the SA hormone	(Bubica Bustos et al., 2022)
Wheat plant (*T. aestivum*)	*Alternaria, Cladosporium, Penicillium, Cryptococcus spps*	Reduction in pathogen infection	(Rojas et al., 2020)
Apple orchid (*Malus domestica*)	*Penicillium, Fusarium, Chaetomium*	As a bio-control agents	(Liu et al., 2020)
Crucifers (*Brassica oleracea, B. rapa & Raphanus sativus*)	More than 15 fungal endophytes including *Trichoderma, Fusarium* etc	Antagonist effect (AGE) against the pathogenic fungi	(Chen et al., 2016)
Tea plant (*Camellia sinensis*)	*C. gleosporioides*	AGE against the pathogenic fungi	(Rabha et al., 2014)
Tomato plant (*Solanum lycopersicum*)	Species belonging to *Alternaria, Curvularia, Fusarium, Trichoderma* and many more	Antagonistic activities against the pathogenic nematodes	(Bogner et al., 2016)
Chrysanthemum (Dendrobium sp.)	Species of *Fusarium* md *Colletotrichum*	Increased IAA production and	(Shah et al., 2019)
Maize (Zea mays)	Around 8-9 fungal endophytes including *Acremonium, Cladosporium*,	Biological control against soybean pathogens	(de Souza Leite et al., 2013)
Onion (*Allium longicuspis*)	Alternaria, Fusarium and several species of Aspergillus	Protection against the pest *Thrips tabaci*	(Muvea et al., 2014)
Periwinkle (*Catharanthus roseus*)	*Macrophomina, Fusarium, Nigropspora* and *Colletotrichum*	Production of extracellular enzymes	(Ayob and Simarani, 2016), (Ayob and Simarani, 2016)
Neem (*Azadirachta indica*)	*Xylaria, Chloridium, Fusarium, Verticillium, Colletotrichum, Trichoderma, Curvularia*	Secretion of bioactive compounds	(Chutulo and Chalannavar, 2018)
Rapeseed (*Brassica napus*)	Botrytis, Rhizoctonia, Rhizopus, *C.gloesporioides*, Aspergillus, Phoma, Alaternaria, Penicillium	AGE against the pathogenic fungi	(Zhang et al., 2014)
Orchid (*Vanda cristata*)	*Fusarium sps*	PGR activities	(Liu-Xu et al., 2022)
Morchella tomentosa (leaves)	*Trichoderma longibrachiatum, Syncephalastrum racemosum*	Antagonistic effect (group of fungi) and ACA	(Ibrahim et al., 2017)
Euphorbia prostata	*Byssochlamys spectabilis Alternaria* sp.	ABA	(Khiralla et al., 2016)

(Continued)

TABLE 1 Continued

Host Plant	Endophyte	Plant Growth Promotion Activity	References
Vernonia amygdalina leaves	*Cladosporium cladosporioides 2*	ACA	(Khiralla et al., 2016)
Cephalotaxus hainanensis Li (all parts)	*Phomopsis quercella, Colletotrichum boninense, Neonectria macroconidialis, Xylaria* sp.	AMA	(Yang et al., 2015)
Bauhinia forficata	*Acremonium curvulum, Asp. ochraceus, Gibberella fujikuroi, Myrothecium verrucaria and Trichoderma piluliferum, Penicillium glabrum*	AMA	(Bezerra et al., 2015)

employed most often to promote the growth of plants (Burragoni and Jeon, 2021). Biopesticides and biofertilizers are becoming formulated with *Trichoderma species* like *T. hamatum, T. harzianum, T. polysporum*, and *T. virideare* because of their ability to colonise root tissues and interact with the host plant via molecular crosstalk, thereby improving nutrient and water uptake, inducing disease resistance, degrading toxic compounds, and ultimately promoting plant growth (Topolovec-Pintarić, 2019). Endophytes defend plants from environmental stresses such as salinity, drought, and others through a variety of mechanisms. One of these mechanisms is the increased production of abscisic acid (ABA), which in turn produces proteins that assist plants in reducing the amount of water lost through transpiration and oxidative stress (Sah et al., 2016). In addition, increased tryptophan production leads to the production of IAA, which is the plant growth hormone auxin and promotes plant growth and rooting (Khan et al., 2019). In a similar fashion, 1-Aminocyclopropane-1-carboxylase (ACC) deaminase hydrolyses the ACC and reduces the production of ethylene, which is responsible for the senescence of the plant, while promoting the production of ammonia and alpha ketobutyrate, which are potential plant growth promoters (Nascimento et al., 2018). Endophytes confer drought tolerance on their hosts by increasing tissue solute accumulation, decreasing water conduction through the leaf, lowering transpiration rates, or thickening the cuticle of the leaf and through osmoregulation for instance, *endophytic Neotyphodium* spp. improves grass plant drought tolerance (Chhipa and Deshmukh, 2019). Secretion of antioxidant metabolites such as ascorbate and glutathione by endophytes reduces host tissue reactive oxygen species and promotes salt stress tolerance (He et al., 2017). These mechanisms work together to improve plant growth under abiotic and biotic stress conditions by increasing root length and density, increasing nutrient supply to plants, suppressing phytopathogens (Supplementary Table 1), and improving relative water content, osmotic adjustment, and antioxidant property (Khan et al., 2019). Investigators have shown that fungal endophytes have an important role in the host plant, especially in Phyto-stimulation, phytoremediation, phyto-immobilization, phytotransformation and biological control. In addition to this such fungal endophytes produce secondary metabolites which play a role in the reduction of heavy metal toxicity (Radziemska et al., 2021), (Anamika et al., 2018). These boost the plant's antioxidative mechanism, leading to detoxification and allowing it to grow in polluted soil, thereby increasing the plant's resistance to heavy metals (Radziemska et al., 2021). Besides this, fungal endophytes have also several beneficial effect on the host plant which is shown below in Figure 4. Hydrophobic, organic molecules with a low molecular weight (300 Da) and a high vapour pressure (0.01 kPa at 20°C) are known as volatile organic compounds (VOCs). Most of these chemicals are derivatives of amino acids, benzenoid compounds, fatty acids, phenylpropanoids, or terpenoids (Kaddes et al., 2019). Endophytic bacteria and fungi produce volatile organic compounds (VOCs) that effectively prevent plant diseases caused by phytopathogens (Kaddes et al., 2019), (Etminani and Harighi, 2018; Etminani et al., 2022).

The endophytic fungus *Trichoderma harzianum*, isolated from the tomato plant *Solanum lycopersicum*, produces the volatile organic compound diterpene. This compound inhibits the growth of the phytopathogen *Botrytis cinerea* by inducing the expression of tomato defence genes related to salicylic acid (SA) (Faucon et al., 2017). Grapevine endophytic bacteria such as *Pantoea* sp. *Sa14*, *Pseudomonas* sp. *Sn48, Pseudomonas* sp. *Ou22*, *Pseudomonas* sp. *Ba35*, *Serratia* sp. *Ba10*, and *Enterobacter* sp. *Ou80* all produce volatile organic compounds (VOCs) that impede the growth of *Agrobacterium tumefaciens* in a number of ways, such as inhibiting the chemotaxis, motility, biofilm growth, and root attachment (Etminani and Harighi, 2018; Etminani et al., 2022) Antiherbivore defences in grasses are bolstered by the presence of the endophytic fungus Epichloe, both through alkaloid-dependent and-independent pathways (Bastias et al., 2017). Epichloe endophytes not only defend host plants against herbivores but also from several pathogens. For instance, the presence of an Epichloe endophyte within plants reduced the symptoms of plant diseases caused by the biotrophic fungal infections *Blumeria graminis, Claviceps purpurea, Ustilago bullata, and Laetisaria fuciformis* (Kou et al., 2021).

6 Endophytes of industrial significance

Bacterial and fungal endophytes are the greatest sources of enzyme production which can be used in several industries (Patel et al., 2017), (Hirata et al., 2018). Endophyte species produce several enzymes, including proteases, pectinases, amylases, cellulases, xylanases, laccases, lipases, and others, which are significant in many industrial industries (Table 2) (Zaferanloo et al., 2014). Additionally, some enzymes generated by endophytic species play crucial roles in a wide range of industries, including the production of biofuels in the energy sector, which is used as an alternative source of

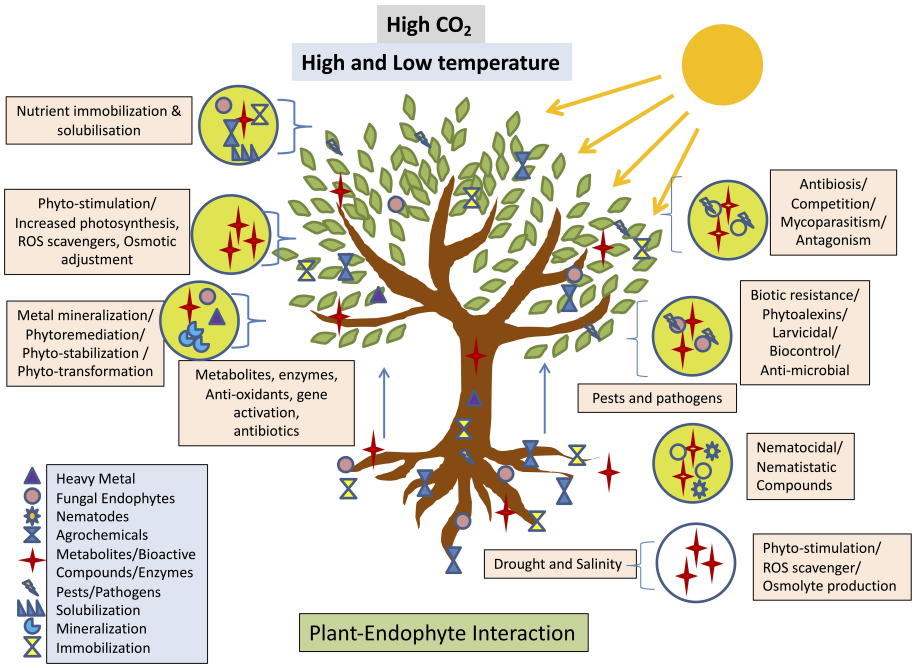

FIGURE 4
Interaction between fungal endophyte and plant expediates Phyto-stimulation conferring the stress response adopted from (Verma et al., 2022).

conventional fuel; the development of pigments for the food industry; the manufacturing of enzymes to degrade polyurethane; and many more (Mengistu, 2020; Singh et al., 2023). Endophytes Phomopsis, Cephalosporium, Microsphaeropsis, and Nigrospora were isolated from plants *Taxus chinensis* var. *mairei* Mast, *Cupressus torulosa D. Don, Keteleeria davidiana varchienpeii, Sabina chinensis* cv. *Kaizuca and Keteleeria evelyniana Mast*, are known to synthesize enzymes which aid in the extraction of biofuels (Tiwari et al., 2023). In place of toxic chemicals, the textile industry uses a combination of pectinase with amylase, lipase, cellulase, and hemicellulase to digest cotton and remove sizing agents. Pectinase has been investigated extensively in oil extraction from several sources, such as flaxseed, dates, and olives (Haile and Ayele, 2022). Currently, immobilised lipases are used in a wide range of commercial processes, including the manufacture of biosensors, biodiesel and cleansers as well as the organic synthesis of various substances, including cosmetics, meals, medications, fragrances, and tastes (Ismail and Baek, 2020). Xylanase is used as a pre-bleaching agent in the paper and pulp industries. It also has biotechnological applications in the biofuel, food, textile, and feed industries (Singh et al., 2019). Chemical, beverage, textile, food, biofuel, and paper sectors are just a few of the many that rely on the starch-digesting enzyme amylase. It is widely used in the pharmaceutical industry to hydrolyse starch to create various sugars including glucose and maltose, which have a variety of applications. The starch industry uses amylases most frequently to hydrolyze starch during the starch liquefaction process, which turns starch into fructose and glucose syrups (Mehta and Satyanarayana, 2016). Proteases are essential industrial enzymes with numerous uses in chemical and biological reactions. Proteases are also utilised in many other industries, including the production of detergents, the food industry, the tanning of leather, the manufacturing of paper, the recovery of silver from photographic films, the manufacturing of paper, bioremediation procedures and employed therapeutically to cure inflammation and dangerous lesions (Abdel Wahab and Ahmed, 2018; Othman et al., 2018). Cellulases are in great demand across many different industries, including the food and beverage industry, the paper and pulp businesses the manufacturing of textiles, the pharmaceutical field, the cleaning products industry, and the biofuels sector (Raghav et al., 2022). Cellulases are crucial in the selective processing of lignocellulosic biological materials (Payne et al., 2015; Jayasekara and Ratnayake, 2019). Lipopeptides are an important class of secondary metabolites produced by bacterial endophytes and consist of cyclic or linear peptides that are connected to lipophilic molecules. Antibiotic efficacy against numerous diseases places these lipopeptides among the most potent available compounds (Narayanan and Glick, 2022), (al Ayed et al., 2022). Endophytes producing lipopeptides were reported in the medicinal plant *Cordia dichotoma L.*, which is native to the Jammu region. These endophytes belonged to the genera Acidomonas, Alcaligenes, Bacillus, Pseudomonas, Peaenibacillus, Ralstonia, Streptococcus, Micrococcus, and Staphylococcus. Many of the lipopeptide-producing endophytes demonstrated antibacterial activity against a wide variety of bacteria, including *Salmonella typhi, Escherichia coli, Pseudomonas aeruginosa, Bacillus subtilis, Staphylococcus aureus, Klebsiella pneumoniae* (Sharma and Mallubhotla, 2022). *Aspergillus* sp. *A9, Aspergillus* sp. *A36, Penicillium* sp. *P5*, and *Penicillium* sp. *P15*, an endophytic fungus isolated from *M. guianensis*, was found to be an excellent producer of hydrolase enzymes. The lipase and protease produced by Penicillium P15 and *Penicillium* sp. *P5* were able to break down the S. aureus biofilm (Matias et al., 2021). Hydrolytic enzymes like peptidase, amylase, xylanase, and carboxylase are produced by endophytes, which lyse the rigid peptidoglycan or

TABLE 2 Industrial important endophytes and their sources (host).

Host Plant	Endophytes	Functionalities	References
Coffea Arabica L.	*Paenibacillus amylolyticus*	Pectinase	(Keggi and Doran-Peterson, 2019)
C. oblong-folius	*F. oxysporum PTM7*	Lipase	(Tuangporn, 2012)
Tithonia diversifolia	*C. kikuchii*	Lipase	(Costa-Silva et al., 2021)
Clerodendrum viscosum L.	*Phoma* sp.	Bio-pigment	(Srivastava et al., 2021)
Eucryphia cordifolia Cav.	*Gliocladium roseum*	Myco-diesel	(Strobel et al., 2004)
Ecuadorian Amazonian plant	*Pestalotiopsis microspora E2712A*	Polyurethanase	(Russell et al., 2011)
Zea mays	*Acremonio zeae*	Xylanase	(Bischoff et al., 2009)
M. peregrina	*A. terreus*	Xylanase	(Wu et al., 2022)
Catharanthus roseus	Colletotrichum sp., *Fusarium solani, Macrophomina phaseolina, Nigrospora sphaerica*	Amylase, cellulase, protease	(Ayob and Simarani, 2016)
E. longifolia	Preussia minima, Alternaria sp.	Amylase	(Zaferanloo et al., 2014)
A. altissima	F. proliferatum	Amylase	(Oukala et al., 2021).
Alpina calcarata (Haw) Roscoe	Cylindrocephalum sp.	Amylase	(Arawwawala et al., 2012)
Sporocarp	*Amanita muscaria, Boletus luridus, Hydnum rufescens, Lactariusa cerrimus, Piceirhiza bicolorata, Piloderma byssinum, P. fallax, Russulachloroides, Suillusluteus luteus*	Protease	(Devi et al., 2020)
Saraca asoca	Acremonium sp.	Protease	(Salvi et al., 2022)
D. hemprichi	*Penicillium* sp. *Morsy1*	Protease	(El-Gendy, 2010)
Eucalyptus	*Hormonema* sp., *Neofusicoccum luteum, N. australe, Ulocladium* sp.	Laccase	(Fillat et al., 2016)
Cajanus cajan L.	*M. verrucaria*	Laccase	(Sun et al., 2017)
Espeletia spp.	*P. glabrum*	Cellulase	(Cabezas et al., 2012)
Centella asiatica	*Penicillium* sp.	Cellulase	(Devi et al., 2012)
L. corticata	*Strain Tahrir-25*	Cellulase	(El-Bondkly and El-Gendy, 2012)
Opuntia ficus-indica Mill. (Cactaceae)	*Nigrosporasphaerica, Penicillium aurantiogriseum, Pestalotiopsis guepinii, Xylaria* sp. *1, Acrimonium terrícola, C. cladosporioides, Fusarium lateritium*	Cellulase, Protease, Xylanase	(Bezerra et al., 2012)
Opuntia ficus-indica Mill. (Cactaceae)	*Cladosporiums phaerospermum, Phoma tropica, Phomopsisarcheri, Tetraploa aristata, Xylaria* sp. *2*	Protease, Xylanase	(Bezerra et al., 2012)
Opuntia ficus-indica Mill. (Cactaceae)	*Aspergillus japonicus*	Cellulase, Pectinase, Protease, Xylanase	(Bezerra et al., 2012)
Cymbopogon citratus, Murraya koenigii	*Colletrotrichum, Fusarium, Phoma, Penicillium*	Asparaginase	(Chow and Ting, 2015)
Asclepias sinaica	*Alternaria alternate, Penicillium chrysogenum*	Amylase, Cellulase	(Fouda et al., 2019)
Drimys winteri	*Bjerkandera* sp.	Cellulase, Phenoloxidase	(Corrêa et al., 2014)
Glycine max (L.) Merril	*Rhizoctonia* sp., *Fusarium verticillioides*	Phytase	(Jain et al., 2014)
Osbeckia stellata, Camellia caduca, Schima khasiana	*Mortierella hyaline, Penicillium* sp.	Cellulase, Lipase, Protease, Xylanase	(Bhagobaty and Joshi, 2011a; Bhagobaty and Joshi, 2011b)
Osbeckia chinensis	*Paecilomyces variabilis*	Amylase, Lipase, Protease, Xylanase	(Corrêa et al., 2014)
From several plants	*Beauveria bassiana*	Chitinases, lipases and proteases	(Amobonye et al., 2020)

murein that protects bacterial cell walls (Muthu Narayanan et al., 2022). Endophytic hydrolytic enzymes have the ability to degrade the chitin cell walls that are present in pathogenic fungi, which in turn protects plants from becoming infected (Loc et al., 2020).

7 Role of endophytes in bio-nanotechnology

Nanotechnology and nanoparticles (NPs) have gained huge attention in the last decade due to their unique and remarkable properties like high surface area to volume ratio and high surface energies (Yadav et al., 2020). Due to these features, NPs are widely used in medicine, research, drug delivery, electronics and environmental clean-up (Modi et al., 2022). When it comes to drug delivery and medicine biocompatible and non-toxic nanomaterials are the first preference. So, biocompatible NPs could be easily synthesized by using fungal and bacterial endophytes. From the various pieces of literature, it has been revealed that numerous investigators have used both prokaryotic and eukaryotic endophytes for the synthesis of both metal NPs and metal oxide NPs (Ahmad and Kalra, 2020; Modi et al., 2022). All these methods mainly involve bottom-up approaches which involve exposure of metallic ions to the desired endophytes under desired conditions. Investigators have proven that the positively charged metal ions come closer to the negatively charged endophytic surfaces by electrostatic attraction. Further, these ions then get transported to the internal structure of the endophytes via ions channels where the metal ions get reduced to their zero-valent atomic states., which further then get aggregated to form NPs (Yadav et al., 2020), (Dhara et al., 2023). Figure 5 is showing basic steps involved in the green synthesis of NPs by using endophytic microorganisms.

Till date investigators have synthesized gold, silver, and copper metal NPs from the endophytes, which have been used in all the domains of science. In addition to this, investigators have reported the synthesis of zinc sulfide, copper oxide, cobalt oxide, nickel oxide, etc from endophytes isolated from terrestrial and marine regions. Fadiji and their colleagues showed the role of various NPs synthesized from the bacterial and fungal endophytes in sustainable agriculture by enhancing plant growth and improving disease resistance (Fadiji et al., 2022). Bogas and their team have shown that these endophytes could act as biofactories for nanoparticles. NPs synthesized from such endophytes have immense potential in healthcare applications (Bogas et al., 2022). In addition, Rathore and his colleagues have placed an emphasis on bacterial endophytes, discussing the recent biomedical scope of these organisms, as well as their synthesis, associated challenges, and importance in bio-nanotechnology (Rathore et al., 2022). Mishra and their groups have also emphasized the green synthesis of NPs by using fungal endophytes which have easy scale-up, downstream processing and eco-friendly nature (Misra et al., 2021). The majority of these NPs synthesized from the endophytes have a role as an antimicrobial agent or as an anti-cancer agent. The antimicrobial activity of endophyte-mediated synthesis NPs is shown in Figure 6 while Figure 7 is showing anticancer activity of the NPs synthesized from endophytes. Table 3 is showing a summarized form of various nanoparticle syntheses from endophytes, along with their applications.

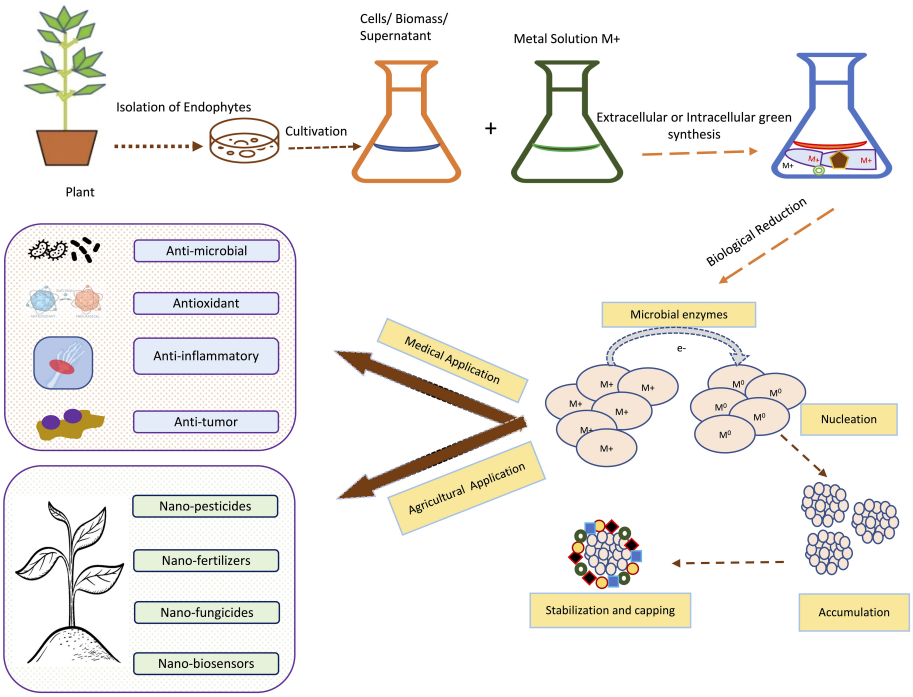

FIGURE 5
Schematic representation of the general steps for green synthesis of metal-based NPs using endophytic microorganisms isolated from tropical plant adopted from Bogas et al., (Bogas et al., 2022).

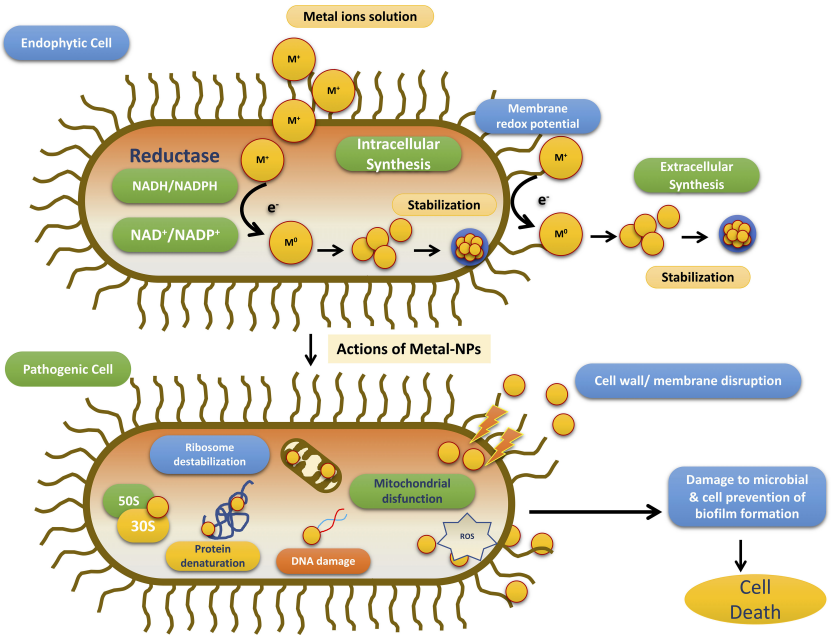

FIGURE 6
Schematic diagram for the steps involved in the antimicrobial activity of NPs synthesized by endophytes adopted from Bogas et al., (Bogas et al., 2022).

8 Conclusion

Endophytes are bacterial and fungal species beneficial to plants by fulfilling their requirements for growth and protection. Recent applications of endophytes in the agriculture sector not only accelerate plant growth by providing tolerance against various stresses but also reduces the use of numerous agrochemicals like chemical fertilizers and pesticides and this would make agriculture more sustainable and productive. In addition, the exploration of the insecticidal, antimicrobial, and pest-control activities of endophytes will make them good friends of farmers. Endophytes produce several bioactive compounds with huge industrial and medicinal applications as well as can be involved in the bio-transformation of hazardous chemicals like toxins, pollutants and heavy metals. Although

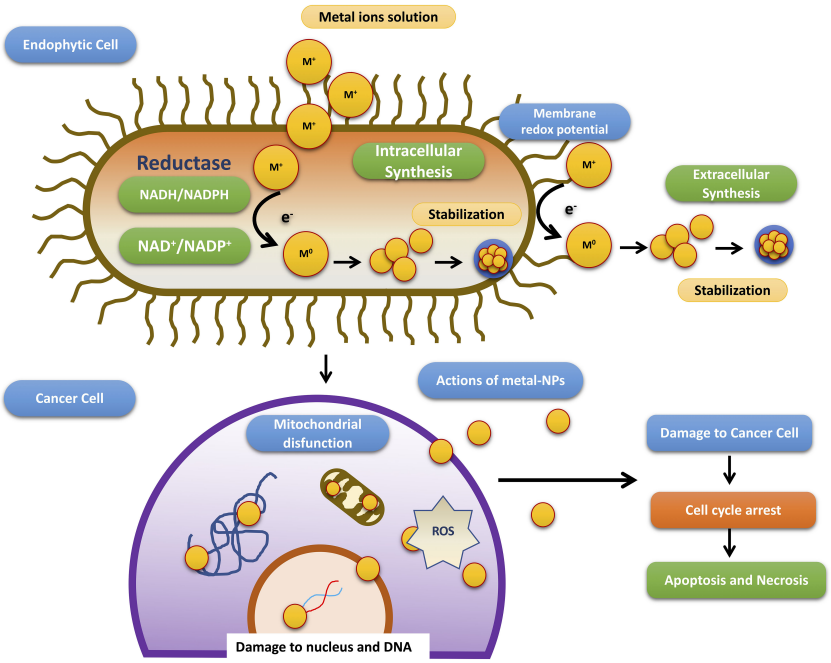

FIGURE 7
Schematic diagram representing steps involved in the anti-cancer activity of NPs synthesized by endophytes adopted from Bogas et al., (Bogas et al., 2022).

TABLE 3 Nanoparticles synthesis from endophytes, sources and their applications.

Nanoparticles	Plant & their parts	Endophytes	Applications	References
AgNPs (Silver nanoparticles)	Roots of tropical plants	Bacteria SYSU 333150, Isoptericola sp., *Streptomyces laurentii*	ABA, ACA	(Eid et al., 2020)
	Borszczowia aralocaspica Bunge (roots), *Raphanus sativus* & *Azadirachta indica* (leaves)	Endophytic strain SYSU 333150 Supernatant of fungi *Alternaria sp, Aspergillus* sp., *Chaetomium* sp., *Cladosporium* sp., *Colletotrichum* sp., *Curvularia* sp., *Guignardia* sp., *Penicillium* sp., *Pestalotia* sp., *Pestalotiopsis* sp., and *Phomopsis* sp.	ABA against *Staphylococcus warneri*	(Dong et al., 2017)
	Curcuma longa (turmeric)	*Penicillium Guignardia mangiferae A. terreus*	AMA against MDR *E. coli and S. aureus*, ACA AMA, against *S. aureus & B. subtilis*	(Singh et al., 2014) (Balakumaran et al., 2015) (Balakumaran et al., 2016)
	Calotropis procera (leaves extract)	Supernatant of *Penicillium* sp., *Alternaria* sp., *Aspergillus* sp. and *Cladosporium* sp.	Antibacterial activity against *E. coli* and *B. subtilis*	(Chowdhury et al., 2016)
	Rhizophora magle and *Laguncularia racemose*	*Aspergillus tubingensis* and *Bionectria ochroleuca*	Antimicrobial activity against *Pseudomonas aeruginosa*	(Rodrigues et al., 2013)
	Stypandra glauca	*Aspergillus niger*	Antibacterial activity against *E. coli* and *P. aeruginosa;*	(Hemashekhar et al., 2019) (Verma et al., 2009)
	Exserohilum rostrata	Cell-free extracts of *Ocimum tenuiflorum*	ABA, inhibit bacterial biofilm formation of *P. aeruginosa* and *S. aureus*	(Bagur et al., 2020)
	Tinospora cordifolia	*Penicillium* sp.	ACA	(Bagur et al., 2022)
	Bertholletia excelsa (Brazil nut) seeds	*Trichoderma* spp.	ABA	(Ramos et al., 2020)
AuNPs (Gold nanoparticles)	Enoki mushroom (*Flammulina velutipes*)-fruiting bodies	*A. terreus*	AMA, *against S. auresus & B. subtilis*, Methylene blue dye removal	(Balakumaran et al., 2016)
	Sargassum wightii (seaweed)	*C. cladosporioides* (marine endophytic fungi)	Antioxidant and AMA	(Manjunath et al., 2017)
	Commiphora wightii	*Cladosporium* sp.	ACA	(Munawer et al., 2020)
	Azadirachta indica	Cell extracts of *Aspergillus* sp.	Antimicrobial activity against *C. albicans, P. fluorescens* and *E. coli.*	(Hemashekhar et al., 2019), (Verma et al., 2009)
	Rauvolfia tetraphylla (roots)	Cell-free extracts of *Alternaria* sp.	Antibacterial activity against *E. coli, P. aeruginosa, K. pneumonia* and *S. aureusas* well as antioxidant and antimitotic activities	(Hemashekhar et al., 2019)
CuO NPs	*Aegle marmelosa* & *Origanum majorana*	*Aspergillus terreus* (biomass and supernatant)	ACA	(Mani et al., 2021)
	Calendula arvensis (leaves)	*Streptomyces capillispiralis* Ca-1 (marine actinomycetes), *Phaeoacremonium* sp.	AMA, biocontrol of plant pathogens	(Hassan et al., 2018)
ZnS quantum dots	*Nothapodytes foetida* (leaves)	*Aspergillus flavus*	Environmental and biomedical application	(Uddandarao and Mohan, 2016)
ZnS: Gd NPs	*N. foetida* (leaves)	*Aspergillus flavus*	Sensing; Fluorescence-Based Metal Detection	(Uddandarao et al., 2019)

(Continued)

TABLE 3 Continued

Nanoparticles	Plant & their parts	Endophytes	Applications	References
Co_3O_4 NPs	*Morus nigra*	*Asp terreus*	AO and AMA	(Mousa et al., 2021)
Fe_3O_4	*Origanum majorana*	*Asp terreus*	AO and AMA	(Mousa et al., 2021)
NiO NPs	*Origanum majorana*	*Asp terreus*	AO and AMA	(Mousa et al., 2021)
CoO NPs	*N. foetida* (leaves)	*Aspergillus nidulans*	Electrical applications	(Vijayanandan and Balakrishnan, 2018)
Micro and nano TiO_2	Roots of Sorghum bicolor	*Trichoderma citrinoviride*	ABA against *Pseudomonas aeruginosa*	(Arya et al., 2021)

the bio-transforming activities of endophytes is still in their infancy. Thus, future efforts should focus on the industrial and medicinal applications of the bio-transforming endophytes and strengthen their eco-friendly and cost-effective approaches in food safety and in the pharma sector. Endophytes exert various therapeutic activities such as anti-cancer, anti-diabetic, anti-inflammatory etc activities by their bioactive compounds. To date, there is no report on commercially available antibiotics derived from endophytes. Intensive research is required which emphasizes the development of new drugs or antibiotics from endophytes and their mechanism of action. The use of endophytic microbes is a relatively new area of study for the environmentally friendly synthesis of nanoparticles, especially when compared to saprophytic microorganisms. Endophyte-derived NPs have potential applications in medicine, including the elimination of multidrug-resistant bacteria, the transport of genetic elements in genetic engineering, and the detection of disease. At the interface of biology and nanotechnology, this area of study has the potential to usher in a plethora of novel nanomaterials. Incorporating metagenomics, metabolomics, and metabolic profiling approaches for elucidating the biosynthetic pathways adopted by endophytes and plants, as well as creating protein-protein interaction maps, and exploring endophytic nanoparticles, will greatly illuminate future applications of endophytes in agriculture, environment, medicine, and industry.

Author contributions

NC, ND, AG, RV and B-H J contributed in conceptualisation, supervision, review editing and writing, and VY, MC, UB, RG and RC reviewed the manuscript, involved in formal analysis, validation and review editing. MA, LE, WA and NC prepared the final draft. MA, LE, WA, RV and B-HJ contributed in visualisation, supervision, review editing and funding acquisition and RV, RG, B-HJ finalized and submitted the manuscript. All authors contributed to the article and approved the submitted version.

Funding

The authors extend their appreciation to the Deanship of Scientific Research at King Khalid University (KKU) for funding this research through the Research Group Program Under the Grant Number: (R.G.P.2/513/44). This work was supported by the Mid-Career Researcher Program (grant no. 2020R1A2C3004237) through the National Research Foundation of the Republic of Korea. The authors are also thankful to the Department of Biosciences; Mody University of Science and Technology, Lakshmangarh Sikar, Rajasthan (SM/2020-21/008 and SM/2022-23/008) for providing financial support.

Conflict of interest

The authors declare that the research was conducted in the absence of any commercial or financial relationships that could be construed as a potential conflict of interest.

Publisher's note

Supplementary Material

The Supplementary Material for this article can be found online at: https://www.frontiersin.org/articles/10.3389/fpls.2023.1193573/full#supplementary-material

References

Abdel Wahab, W. A., and Ahmed, S. A. (2018). Response surface methodology for production, characterization and application of solvent, salt and alkali-tolerant alkaline protease from isolated fungal strain aspergillus niger WA 2017. *Int. J. Biol. Macromol* 115, 447–458. doi: 10.1016/j.ijbiomac.2018.04.041

Adeleke, B. S., and Babalola, O. O. (2021). Pharmacological potential of fungal endophytes associated with medicinal plants: a review. *J. Fungi* 7, 1–16. doi: 10.3390/jof7020147

Afzal, I., Shinwari, Z. K., Sikandar, S., and Shahzad, S. (2019). Plant beneficial endophytic bacteria: mechanisms, diversity, host range and genetic determinants. *Microbiol. Res.* 221, 36–49. doi: 10.1016/j.micres.2019.02.001

Ahmad, W., and Kalra, D. (2020). Green synthesis, characterization and anti microbial activities of ZnO nanoparticles using euphorbia hirta leaf extract. *J. King Saud Univ Sci.* 32, 2358–2364. doi: 10.1016/j.jksus.2020.03.014

al Ayed, K., Ballantine, R. D., Hoekstra, M., Bann, S. J., Wesseling, C. M. J., Bakker, A. T., et al. (2022). Synthetic studies with the brevicidine and laterocidine lipopeptide antibiotics including analogues with enhanced properties and *in vivo* efficacy. *Chem. Sci.* 13, 3563–3570. doi: 10.1039/D2SC00143H

ALKahtani, M. D. F., Fouda, A., Attia, K. A., Al-Otaibi, F., Eid, A. M., El-Din Ewais, E., et al. (2020). Isolation and characterization of plant growth promoting endophytic bacteria from desert plants and their application as bioinoculants for sustainable agriculture. *Agronomy* 10. doi: 10.3390/agronomy10091325

Amobonye, A., Bhagwat, P., Pandey, A., Singh, S., and Pillai, S. (2020). Biotechnological potential of beauveria bassiana as a source of novel biocatalysts and metabolites. *Crit. Rev. Biotechnol.* 40, 1019–1034. doi: 10.1080/07388551.2020.1805403

Andrés-Barrao, C., Lafi, F. F., Alam, I., de Zélicourt, A., Eida, A. A., Bokhari, A., et al. (2017). Complete genome sequence analysis of enterobacter sp. SA187, a plant multi-stress tolerance promoting endophytic bacterium. *Front. Microbiol.* 8. doi: 10.3389/fmicb.2017.02023

Annapurna, K., Govindasamy, V., Sharma, M., Ghosh, A., and Chikara, S. K. (2018). Whole genome shotgun sequence of bacillus paralicheniformis strain KMS 80, a rhizobacterial endophyte isolated from rice (Oryza sativa l.). *3 Biotech.* 8, 223. doi: 10.1007/s13205-018-1242-y

Arafa, M. M., and El-Batanony, N. H. (2018). Growth, yield and chemical composition response of some legume crops to inoculation with non-rhizobial endophytic bacteria from melilotus indicus (L.). *All. Nodules*. 9, 353–358. doi: 10.21608/jpp.2018.35727

Arawwawala, L. D. A. M., Arambewela, L. S. R., and Ratnasooriya, W. D. (2012). Alpinia calcarata Roscoe: a potent anti inflammatory agent. *J. Ethnopharmacol* 139, 889–892. doi: 10.1016/j.jep.2011.12.036

Arya, S., Sonawane, H., Math, S., Tambade, P., Chaskar, M., and Shinde, D. (2021). Biogenic titanium nanoparticles (TiO2NPs) from tricoderma citrinoviride extract: synthesis, characterization and antibacterial activity against extremely drug-resistant pseudomonas aeruginosa. *Int. Nano Lett.* 11, 35–42. doi: 10.1007/s40089-020-00320-y

Asaf, S., Khan, A. L., Khan, M. A., Al-Harrasi, A., and Lee, I.-J. (2018). Complete genome sequencing and analysis of endophytic sphingomonas sp. LK11 and its potential in plant growth. *3 Biotech.* 8, 389. doi: 10.1007/s13205-018-1403-z

Asaf, S., Khan, M. A., Khan, A. L., Waqas, M., Shahzad, R., Kim, A.-Y., et al. (2017). Bacterial endophytes from arid land plants regulate endogenous hormone content and promote growth in crop plants: an example of sphingomonas sp. and serratia marcescens. *J. Plant Interact.* 12, 31–38. doi: 10.1080/17429145.2016.1274060

Ayob, F. W., and Simarani, K. (2016). Endophytic filamentous fungi from a catharanthus roseus: identification and its hydrolytic enzymes. *Saudi Pharm. J.* 24, 273–278. doi: 10.1016/j.jsps.2016.04.019

Bagur, H., Medidi, R. S., Somu, P., Choudhury, P. W. J., Karua, C. S., Guttula, P. K., et al. (2022). Endophyte fungal isolate mediated biogenic synthesis and evaluation of biomedical applications of silver nanoparticles. *Materials Technol.* 37, 167–178. doi: 10.1080/10667857.2020.1819089

Bagur, H., Poojari, C. C., Melappa, G., Rangappa, R., Chandrasekhar, N., and Somu, P. (2020). Biogenically synthesized silver nanoparticles using endophyte fungal extract of ocimum tenuiflorum and evaluation of biomedical properties. *J. Clust Sci.* 31, 1241–1255. doi: 10.1007/s10876-019-01731-4

Balakumaran, M. D., Ramachandran, R., Balashanmugam, P., Mukeshkumar, D. J., and Kalaichelvan, P. T. (2016). Mycosynthesis of silver and gold nanoparticles: optimization, characterization and antimicrobial activity against human pathogens. *Microbiol. Res.* 182, 8–20. doi: 10.1016/j.micres.2015.09.009

Balakumaran, M. D., Ramachandran, R., and Kalaichelvan, P. T. (2015). Exploitation of endophytic fungus, guignardia mangiferae for extracellular synthesis of silver nanoparticles and their *in vitro* biological activities. *Microbiol. Res.* 178, 9–17. doi: 10.1016/j.micres.2015.05.009

Banik, A., Mukhopadhaya, S. K., and Dangar, T. K. (2016). Characterization of N2-fixing plant growth promoting endophytic and epiphytic bacterial community of Indian cultivated and wild rice (Oryza spp.) genotypes. *Planta* 243, 799–812. doi: 10.1007/s00425-015-2444-8

Bastias, D. A., Martínez-Ghersa, M. A., Ballaré, C. L., and Gundel, P. E. (2017). Epichloe fungal endophytes and plant defenses: not just alkaloids. *Trends Plant Sci.* 22, 939–948. doi: 10.1016/j.tplants.2017.08.005

Battu, L., Reddy, M. M., Goud, B. S., Ulaganathan, K., and Kandasamy, U. (2017). Genome inside genome: NGS based identification and assembly of endophytic sphingopyxis granuli and pseudomonas aeruginosa genomes from rice genomic reads. *Genomics* 109, 141–146. doi: 10.1016/j.ygeno.2017.02.002

Behera, P., Vaishampayan, P., Singh, N. K., Mishra, S. R., Raina, V., Suar, M., et al. (2016). The draft genome sequence of mangrovibacter sp. strain MP23, an endophyte isolated from the roots of phragmites karka. *Genom Data* 9, 128–129. doi: 10.1016/j.gdata.2016.07.007

Bergna, A., Cernava, T., Rändler, M., Grosch, R., Zachow, C., and Berg, G. (2018). Tomato seeds preferably transmit plant beneficial endophytes. *Phytobiomes J.* 2, 183–193. doi: 10.1094/PBIOMES-06-18-0029-R

Bezerra, J. D. P., Nascimento, C. C. F., Barbosa, R., do, N., da Silva, D. C. V., Svedese, V. M., et al. (2015). Endophytic fungi from medicinal plant bauhinia forficata: diversity and biotechnological potential. *Braz. J. Microbiol.* 46, 49–57. doi: 10.1590/S1517-838246120130657

Bezerra, J. D. P., Santos, M. G. S., Svedese, V. M., Lima, D. M. M., Fernandes, M. J. S., Paiva, L. M., et al. (2012). Richness of endophytic fungi isolated from opuntia ficus-indica mill. (Cactaceae) and preliminary screening for enzyme production. *World J. Microbiol. Biotechnol.* 28, 1989–1995. doi: 10.1007/s11274-011-1001-2

Bhagobaty, R. K., and Joshi, S. R. (2011a). Fungal endophytes of five medicinal plants prevalent in the traditionally preserved 'Sacred forests' of meghalaya, India. *For. Sci. Technol.* 7, 151–154. doi: 10.1080/21580103.2011.621381

Bhagobaty, R. K., and Joshi, S. R. (2011b). Multi-loci molecular characterization of endophytic fungi isolated from five medicinal plants of meghalaya, India. *Mycobiology* 39, 71–78. doi: 10.4489/MYCO.2011.39.2.071

Bhargavi, S. D., Praveen, V. K., Anil Kumar, M., and Savitha, J. (2018). Comparative study on whole genome sequences of aspergillus terreus (Soil fungus) and diaporthe ampelina (Endophytic fungus) with reference to lovastatin production. *Curr. Microbiol.* 75, 84–91. doi: 10.1007/s00284-017-1353-4

Bischoff, K. M., Wicklow, D. T., Jordan, D. B., de Rezende, S. T., Liu, S., Hughes, S. R., et al. (2009). Extracellular hemicellulolytic enzymes from the maize endophyte acremonium zeae. *Curr. Microbiol.* 58, 499–503. doi: 10.1007/s00284-008-9353-z

Bogas, A. C., Henrique Rodrigues, S., Gonçalves, M. O., de Assis, M., Longo, E., and Paiva De Sousa, C. (2022). Endophytic microorganisms from the tropics as biofactories for the synthesis of metal-based nanoparticles: healthcare applications. *Front. Nanotechnology* 4. doi: 10.3389/fnano.2022.823236

Bogner, C. W., Kariuki, G. M., Elashry, A., Sichtermann, G., Buch, A.-K., Mishra, B., et al. (2016). Fungal root endophytes of tomato from Kenya and their nematode biocontrol potential. *Mycol Prog.* 15, 30. doi: 10.1007/s11557-016-1169-9

Bubica Bustos, L. M., Ueno, A. C., Biganzoli, F., Card, S. D., Mace, W. J., Martínez-Ghersa, M. A., et al. (2022). Can aphid herbivory induce intergenerational effects of endophyte-conferred resistance in grasses? *J. Chem. Ecol.* 48, 867–881. doi: 10.1007/s10886-022-01390-2

Burragoni, S. G., and Jeon, J. (2021). Applications of endophytic microbes in agriculture, biotechnology, medicine, and beyond. *Microbiol. Res.* 245, 126691. doi: 10.1016/j.micres.2020.126691

Cabezas, L., Calderon, C., Medina, L. M., Bahamon, I., Cardenas, M., Bernal, A. J., et al. (2012). Characterization of cellulases of fungal endophytes isolated from espeletia spp. *J. Microbiol.* 50, 1009–1013. doi: 10.1007/s12275-012-2130-5

Card, S. D., Bastías, D. A., and Caradus, J. R. (2021). Antagonism to plant pathogens by epichloë fungal endophytes–a review. *Plants* 10. doi: 10.3390/plants10101997

Chaudhary, P., Singh, S., Chaudhary, A., Sharma, A., and Kumar, G. (2022). Overview of biofertilizers in crop production and stress management for sustainable agriculture. *Front. Plant Sci.* 13. doi: 10.3389/fpls.2022.930340

Chen, J.-L., Sun, S.-Z., Miao, C.-P., Wu, K., Chen, Y.-W., Xu, L.-H., et al. (2016). Endophytic trichoderma gamsii YIM PH30019: a promising biocontrol agent with hyperosmolar, mycoparasitism, and antagonistic activities of induced volatile organic compounds on root-rot pathogenic fungi of panax notoginseng. *J. Ginseng Res.* 40, 315–324. doi: 10.1016/j.jgr.2015.09.006

Chen, C., Yue, Z., Chu, C., Ma, K., Li, L., and Sun, Z. (2020). Complete genome sequence of bacillus sp. strain WR11, an endophyte isolated from wheat root providing genomic insights into its plant growth-promoting effects. *Mol. Plant-Microbe Interactions®* 33, 876–879. doi: 10.1094/MPMI-02-20-0030-A

Chhipa, H., and Deshmukh, S. K. (2019). "Fungal endophytes: rising tools in sustainable agriculture production," in *Endophytes and secondary metabolites*. Ed. S. Jha (Cham: Springer International Publishing), 631–655. doi: 10.1007/978-3-319-90484-9_26

Chow, Y., and Ting, A. S. Y. (2015). Endophytic l-asparaginase-producing fungi from plants associated with anticancer properties. *J. Adv. Res.* 6, 869–876. doi: 10.1016/j.jare.2014.07.005

Chowdhury, D. R., Chatterjee, S. K., and Kanti Roy, S. (2016). Studies on endophytic fungi of calotropis procera (L.) R.Br. with a view to their antimicrobial and antioxidant actvities mediated by extracellular synthesised silver nanoparticles. *IOSR J. Pharm. Biol. Sci.* 11, 113–121. doi: 10.9790/3008-110502113121

Chutulo, E. C., and Chalannavar, R. K. (2018). Endophytic mycoflora and their bioactive compounds from azadirachta indica: a comprehensive review. *J. Fungi* 4. doi: 10.3390/jof4020042

Corrêa, R. C. G., Rhoden, S. A., Mota, T. R., Azevedo, J. L., Pamphile, J. A., de Souza, C. G. M., et al. (2014). Endophytic fungi: expanding the arsenal of industrial enzyme producers. *J. Ind. Microbiol. Biotechnol.* 41, 1467–1478. doi: 10.1007/s10295-014-1496-2

Costa-Silva, T. A., Carvalho, A. K. F., Souza, C. R. F., de Castro, H. F., Bachmann, L., Said, S., et al. (2021). Enhancement lipase activity via immobilization onto chitosan beads used as seed particles during fluidized bed drying: application in butyl butyrate production. *Appl. Catal A Gen.* 622, 118217. doi: 10.1016/j.apcata.2021.118217

de Souza Leite, T., Cnossen-Fassoni, A., Pereira, O. L., Mizubuti, E. S. G., de Araújo, E. F., and de Queiroz, M. V. (2013). Novel and highly diverse fungal endophytes in soybean revealed by the consortium of two different techniques. *J. Microbiol.* 51, 56–69. doi: 10.1007/s12275-013-2356-x

Devi, R., Kaur, T., Guleria, G., Rana, K. L., Kour, D., Yadav, N., et al. (2020). "Chapter 9 - fungal secondary metabolites and their biotechnological applications for human health," in *New and future developments in microbial biotechnology and bioengineering*. Eds. A. A. Rastegari, A. N. Yadav and N. Yadav (Elsevier), 147–161. doi: 10.1016/B978-0-12-820528-0.00010-7

Devi, N. N., Prabakaran, J. J., and Wahab, F. (2012). Phytochemical analysis and enzyme analysis of endophytic fungi from centella asiatica. *Asian Pac J. Trop. BioMed.* 2, S1280–S1284. doi: 10.1016/S2221-1691(12)60400-6

Dhara, M., Mahakud, D., and Naik, U. C. (2023). "17 - molecular mechanism for production of nanoparticles by endophytes," in *Endophytic association: what, why and how*. Eds. M. Shah and D. Deka (Academic Press), 353–367. doi: 10.1016/B978-0-323-91245-7.00018-3

Dong, Z.-Y., Narsing Rao, M. P., Xiao, M., Wang, H.-F., Hozzein, W. N., Chen, W., et al. (2017). Antibacterial activity of silver nanoparticles against staphylococcus warneri synthesized using endophytic bacteria by photo-irradiation. *Front. Microbiol.* 8. doi: 10.3389/fmicb.2017.01090

Dou, K.-X., Tan, M.-S., Tan, C.-C., Cao, X.-P., Hou, X.-H., Guo, Q.-H., et al. (2018). Comparative safety and effectiveness of cholinesterase inhibitors and memantine for alzheimer's disease: a network meta-analysis of 41 randomized controlled trials. *Alzheimers Res. Ther.* 10, 126. doi: 10.1186/s13195-018-0457-9

Eid, A. M., Fouda, A., Niedbała, G., Hassan, S. E. D., Salem, S. S., Abdo, A. M., et al. (2020). Endophytic streptomyces laurentii mediated green synthesis of Ag-NPs with antibacterial and anticancer properties for developing functional textile fabric properties. *Antibiotics* 9, 1–18. doi: 10.3390/antibiotics9100641

Eida, A. A., Bougouffa, S., Alam, I., Hirt, H., and Saad, M. M. (2020). Complete genome sequence of paenibacillus sp. JZ16, a plant growth promoting root endophytic bacterium of the desert halophyte zygophyllum simplex. *Curr. Microbiol.* 77, 1097–1103. doi: 10.1007/s00284-020-01908-5

El-Bondkly, A. M. A., and El-Gendy, M. M. A. (2012). Cellulase production from agricultural residues by recombinant fusant strain of a fungal endophyte of the marine sponge latrunculia corticata for production of ethanol. *Antonie Van Leeuwenhoek* 101, 331–346. doi: 10.1007/s10482-011-9639-1

El-Gendy, M. M. A. (2010). Keratinase production by endophytic penicillium spp. Morsy1 under solid-state fermentation using rice straw. *Appl. Biochem. Biotechnol.* 162, 780–794. doi: 10.1007/s12010-009-8802-x

Etminani, F., and Harighi, B. (2018). Isolation and identification of endophytic bacteria with plant growth promoting activity and biocontrol potential from wild pistachio trees. *Plant Pathol. J.* 34, 208–217. doi: 10.5423/PPJ.OA.07.2017.0158

Etminani, F., Harighi, B., and Mozafari, A. A. (2022). Effect of volatile compounds produced by endophytic bacteria on virulence traits of grapevine crown gall pathogen, agrobacterium tumefaciens. *Sci. Rep.* 12. doi: 10.1038/s41598-022-14864-w

Fadiji, A. E., and Babalola, O. O. (2020). Elucidating mechanisms of endophytes used in plant protection and other bioactivities with multifunctional prospects. *Front. Bioeng Biotechnol.* 8. doi: 10.3389/fbioe.2020.00467

Fadiji, A. E., Mortimer, P. E., Xu, J., Ebenso, E. E., and Babalola, O. O. (2022). Biosynthesis of nanoparticles using endophytes: a novel approach for enhancing plant growth and sustainable agriculture. *Sustainability (Switzerland)* 14. doi: 10.3390/su141710839

Faucon, M.-P., Houben, D., and Lambers, H. (2017). Plant functional traits: soil and ecosystem services. *Trends Plant Sci.* 22, 385–394. doi: 10.1016/j.tplants.2017.01.005

Fillat, Ú., Martín-Sampedro, R., Macaya-Sanz, D., Martín, J. A., Ibarra, D., Martínez, M. J., et al. (2016). Screening of eucalyptus wood endophytes for laccase activity. *Process Biochem.* 51, 589–598. doi: 10.1016/j.procbio.2016.02.006

Forchetti, G., Masciarelli, O., Alemano, S., Alvarez, D., and Abdala, G. (2007). Endophytic bacteria in sunflower (Helianthus annuus l.): isolation, characterization, and production of jasmonates and abscisic acid in culture medium. *Appl. Microbiol. Biotechnol.* 76, 1145–1152. doi: 10.1007/s00253-007-1077-7

Fouda, A., Eid, A. M., Elsaied, A., El-Belely, E. F., Barghoth, M. G., Azab, E., et al. (2021). Plant growth-promoting endophytic bacterial community inhabiting the leaves of pulicaria incisa (LAM.) DC inherent to arid regions. *Plants* 10, 1–22. doi: 10.3390/plants10010076

Fouda, A., Hassan, S. E. D., Eid, A. M., and El-Din Ewais, E. (2019). "The interaction between plants and bacterial endophytes under salinity stress," in *Endophytes and secondary metabolites*. Ed. S. Jha (Cham: Springer International Publishing), 591–607. doi: 10.1007/978-3-319-90484-9_15

Fuller, D. Q., Murphy, C., Kingwell-Banham, E., Castillo, C. C., and Naik, S. (2019). Cajanus cajan (L.) millsp. origins and domestication: the south and southeast Asian archaeobotanical evidence. *Genet. Resour Crop Evol.* 66, 1175–1188. doi: 10.1007/s10722-019-00774-w

Gakuubi, M. M., Munusamy, M., and Liang, Z. X. (2021). And ng, s Fungal endophytes: a promising frontier for discovery of novel bioactive compounds. *B. J. Fungi* 7. doi: 10.3390/jof7100786

Gamage, C. D. B., Park, S. Y., Yang, Y., Zhou, R., Taş, İ., Bae, W. K., et al. (2019). Deoxypodophyllotoxin exerts anti-cancer effects on colorectal cancer cells through induction of apoptosis and suppression of tumorigenesis. *Int. J. Mol. Sci.* 20. doi: 10.3390/ijms20112612

Gamez, R., Cardinale, M., Montes, M., Ramirez, S., Schnell, S., and Rodriguez, F. (2019). Screening, plant growth promotion and root colonization pattern of two rhizobacteria (Pseudomonas fluorescens Ps006 and bacillus amyloliquefaciens Bs006) on banana cv. williams (Musa acuminata colla). *Microbiol. Res.* 220, 12–20. doi: 10.1016/j.micres.2018.11.006

Ghanta, S., Bhattacharyya, D., Sinha, R., Banerjee, A., and Chattopadhyay, S. (2011). Nicotiana tabacum overexpressing γ-ECS exhibits biotic stress tolerance likely through NPR1-dependent salicylic acid-mediated pathway. *Planta* 233, 895–910. doi: 10.1007/s00425-011-1349-4

Gómez-Godínez, L. J., Aguirre-Noyola, J. L., Martínez-Romero, E., Arteaga-Garibay, R. I., Ireta-Moreno, J., and Ruvalcaba-Gómez, J. M. (2023). A look at plant-Growth-Promoting bacteria. *Plants* 12, 1668. doi: 10.3390/plants12081668

Gouda, S., Das, G., Sen, S. K., Shin, H. S., and Patra, J. K. (2016). Endophytes: a treasure house of bioactive compounds of medicinal importance. *Front. Microbiol.* 7. doi: 10.3389/fmicb.2016.01538

Gu, Q., Yang, Y., Yuan, Q., Shi, G., Wu, L., Lou, Z., et al. (2017). Bacillomycin d produced by bacillus amyloliquefaciens is involved in the antagonistic interaction with the plantpathogenic fungus fusarium graminearum. *Appl. Environ. Microbiol.* 83. doi: 10.1128/AEM.01075-17

Haidar, B., Ferdous, M., Fatema, B., Ferdous, A. S., Islam, M. R., and Khan, H. (2018). Population diversity of bacterial endophytes from jute (Corchorus olitorius) and evaluation of their potential role as bioinoculants. *Microbiol. Res.* 208, 43–53. doi: 10.1016/j.micres.2018.01.008

Haile, S., and Ayele, A. (2022). Pectinase from microorganisms and its industrial applications. *Sci. World J.* 2022. doi: 10.1155/2022/1881305

Hamayun, M., Hussain, A., Khan, S. A., Kim, H. Y., Khan, A. L., Waqas, M., et al. (2017). Gibberellins producing endophytic fungus porostereum spadiceum AGH786 rescues growth of salt affected soybean. *Front. Microbiol.* 8. doi: 10.3389/fmicb.2017.00686

Hashim, A. M., Alharbi, B. M., Abdulmajeed, A. M., Elkelish, A., Hassan, H. M., and Hozzein, W. N. (2020). Oxidative stress responses of some endemic plants to high altitudes by intensifying antioxidants and secondary metabolites content. *Plants* 9, 1–23. doi: 10.3390/plants9070869

Hassan, S. E.-D. (2017). Plant growth-promoting activities for bacterial and fungal endophytes isolated from medicinal plant of teucrium polium l. *J. Adv. Res.* 8, 687–695. doi: 10.1016/j.jare.2017.09.001

Hassan, S. E.-D., Salem, S. S., Fouda, A., Awad, M. A., El-Gamal, M. S., and Abdo, A. M. (2018). New approach for antimicrobial activity and bio-control of various pathogens by biosynthesized copper nanoparticles using endophytic actinomycetes. *J. Radiat. Res. Appl. Sci.* 11, 262–270. doi: 10.1016/j.jrras.2018.05.003

Hatamzadeh, S., Rahnama, K., Nasrollahnejad, S., Fotouhifar, K. B., Hemmati, K., White, J. F., et al. (2020). Isolation and identification of l-asparaginase-producing endophytic fungi from the asteraceae family plant species of Iran. *PeerJ* 2020. doi: 10.7717/peerj.8309

He, L., He, T., Farrar, S., Ji, L., Liu, T., and Ma, X. (2017). Antioxidants maintain cellular redox homeostasis by elimination of reactive oxygen species. *Cell. Physiol. Biochem.* 44, 532–553. doi: 10.1159/000485089

Hegazy, A. K., Emam, M. H., Lovett-Doust, L., Azab, E., and El-Khatib, A. A. (2017). Response of duckweed to lead exposure: phytomining, bioindicators and bioremediation. *Desalination Water Treat* 70, 227–234. doi: 10.5004/dwt.2017.20545

Hemashekhar, B., Chandrappa, C. P., Govindappa, M., and Chandrashekar, N. (2019). Endophytic fungus alternaria spp isolated from rauvolfia tetraphylla root arbitrate synthesis of gold nanoparticles and evaluation of their antibacterial, antioxidant and antimitotic activities. *Adv. Natural Sciences: Nanoscience Nanotechnology* 10, 035010. doi: 10.1088/2043-6254/ab38b0

Hirata, Y., Yamada, C., Ito, Y., Yamamoto, S., Nagase, H., Oh-hashi, K., et al. (2018). Novel oxindole derivatives prevent oxidative stress-induced cell death in mouse hippocampal HT22 cells. *Neuropharmacology* 135, 242–252. doi: 10.1016/j.neuropharm.2018.03.015

Ibrahim, M., Kaushik, N., Sowemimo, A., Chhipa, H., Koekemoer, T., van de Venter, M., et al. (2017). Antifungal and antiproliferative activities of endophytic fungi isolated from the leaves of markhamia tomentosa. *Pharm. Biol.* 55, 590–595. doi: 10.1080/13880209.2016.1263671

Ismail, A. R., and Baek, K.-H. (2020). Lipase immobilization with support materials, preparation techniques, and applications: present and future aspects. *Int. J. Biol. Macromol* 163, 1624–1639. doi: 10.1016/j.ijbiomac.2020.09.021

Jain, S., Vaishnav, A., Kasotia, A., Kumari, S., Gaur, R. K., and Choudhary, D. K. (2014). Rhizobacterium-mediated growth promotion and expression of stress enzymes in glycine max l. Merrill against fusarium wilt upon challenge inoculation. *World J. Microbiol. Biotechnol.* 30, 399–406. doi: 10.1007/s11274-013-1455-5

Jasim, B., John Jimtha, C., Jyothis, M., and Radhakrishnan, E. K. (2013). Plant growth promoting potential of endophytic bacteria isolated from piper nigrum. *Plant Growth Regul.* 71, 1–11. doi: 10.1007/s10725-013-9802-y

Jayasekara, S., and Ratnayake, R. (2019). "Microbial cellulases: an overview and applications," in *Cellulose*. Eds. A. R. Pascual and M. E. E. Martín (Rijeka: IntechOpen), 5. doi: 10.5772/intechopen.84531

Joo, H.-S., Deyrup, S. T., and Shim, S. H. (2021). Endophyte-produced antimicrobials: a review of potential lead compounds with a focus on quorum-sensing disruptors. *Phytochem. Rev.* 20, 543–568. doi: 10.1007/s11101-020-09711-7

Kaddes, A., Fauconnier, M. L., Sassi, K., Nasraoui, B., and Jijakli, M. H. (2019). Endophytic fungal volatile compounds as solution for sustainable agriculture. *Molecules* 24. doi: 10.3390/molecules24061065

Karuppiah, V., Natarajan, S., Gangatharan, M., Aldayel, M. F., Alsowayeh, N., and Thangavel, K. (2022). Development of siderophore-based rhizobacterial consortium for the mitigation of biotic and abiotic environmental stresses in tomatoes: an *in vitro* and in planta approach. *J. Appl. Microbiol. n/a*. 133, 3276–3287. doi: 10.1111/jam.15625

Keggi, C., and Doran-Peterson, J. (2019). Paenibacillus amylolyticus 27C64 has a diverse set of carbohydrate-active enzymes and complete pectin deconstruction system. *J. Ind. Microbiol. Biotechnol.* 46, 1–11. doi: 10.1007/s10295-018-2098-1

Khalil, A. M. A., Hassan, S. E. D., Alsharif, S. M., Eid, A. M., Ewais, E. E. D., Azab, E., et al. (2021). Isolation and characterization of fungal endophytes isolated from medicinal plant ephedra pachyclada as plant growth-promoting. *Biomolecules* 11, 1–18. doi: 10.3390/biom11020140

Khan, M. S., Gao, J., Chen, X., Zhang, M., Yang, F., Du, Y., et al. (2020). Isolation and characterization of plant growth-promoting endophytic bacteria paenibacillus polymyxa SK1 from lilium lancifolium. *BioMed. Res. Int.* 2020. doi: 10.1155/2020/8650957

Khan, A. L., Hamayun, M., Kang, S.-M., Kim, Y.-H., Jung, H.-Y., Lee, J.-H., et al. (2012). Endophytic fungal association via gibberellins and indole acetic acid can improve plant growth under abiotic stress: an example of paecilomyces formosus LHL10. *BMC Microbiol.* 12, 3. doi: 10.1186/1471-2180-12-3

Khan, I., Ullah, N., Zha, L., Bai, Y., Khan, A., Zhao, T., et al. (2019). Pathogens alteration of gut microbiota in inflammatory bowel disease (IBD): cause or consequence? *IBD Treat Targeting Gut Microbiome*. doi: 10.3390/pathogens8030126

Khan, A. L., Waqas, M., Kang, S.-M., Al-Harrasi, A., Hussain, J., Al-Rawahi, A., et al. (2014). Bacterial endophyte sphingomonas sp. LK11 produces gibberellins and IAA and promotes tomato plant growth. *J. Microbiol.* 52, 689–695. doi: 10.1007/s12275-014-4002-7

Khare, E., Mishra, J., and Arora, N. K. (2018). Multifaceted interactions between endophytes and plant: developments and prospects. *Front. Microbiol.* 9. doi: 10.3389/fmicb.2018.02732

Khiralla, A., Mohamed, I. E., Tzanova, T., Schohn, H., Slezack-Deschaumes, S., Hehn, A., et al. (2016). Endophytic fungi associated with Sudanese medicinal plants show cytotoxic and antibiotic potential. *FEMS Microbiol. Lett.* 363, fnw089. doi: 10.1093/femsle/fnw089

Kou, M. Z., Bastías, D. A., Christensen, M. J., Zhong, R., Nan, Z. B., and Zhang, X. X. (2021). The plant salicylic acid signalling pathway regulates the infection of a biotrophic pathogen in grasses associated with an epichloë endophyte. *J. Fungi* 7. doi: 10.3390/jof7080633

Kumari, P., Sharma, P., and Sharma, S. (2020). Synergism of rhizobium and rhizobacteria on growth, symbiotic parameters, soil quality and grain yield in summer mungbean (Vigna radiata l. wilczek). *Int. J. Curr. Microbiol. Appl. Sci.* 9, 136–151. doi: 10.20546/ijcmas.2020.903.017

Larran, S., Simón, M. R., Moreno, M., Siurana, M. P. S., and Perelló, A. (2016). Endophytes from wheat as biocontrol agents against tan spot disease. *Biol. Control* 92, 17–23. doi: 10.1016/j.biocontrol.2015.09.002

Latz, M. A. C., Jensen, B., Collinge, D. B., and Jørgensen, H. J. L. (2018). Endophytic fungi as biocontrol agents: elucidating mechanisms in disease suppression. *Plant Ecol. Divers.* 11, 555–567. doi: 10.1080/17550874.2018.1534146

Li, S.-J., Zhang, X., Wang, X.-H., and Zhao, C.-Q. (2018). Novel natural compounds from endophytic fungi with anticancer activity. *Eur. J. Med. Chem.* 156, 316–343. doi: 10.1016/j.ejmech.2018.07.015

Lin, B., Song, Z., Jia, Y., Zhang, Y., Wang, L., Fan, J., et al. (2019). Biological characteristics and genome-wide sequence analysis of endophytic nitrogen-fixing bacteria klebsiella variicola GN02. *Biotechnol. Biotechnol. Equip.* 33, 108–117. doi: 10.1080/13102818.2018.1555010

Lin, J., Wang, Q., Zhou, S., Xu, S., and Yao, K. (2022). Tetramethylpyrazine: a review on its mechanisms and functions. *Biomedicine Pharmacotherapy* 150, 113005. doi: 10.1016/j.biopha.2022.113005

Liu, J., Ridgway, H. J., and Jones, E. E. (2020). Apple endophyte community is shaped by tissue type, cultivar and site and has members with biocontrol potential against neonectria ditissima. *J. Appl. Microbiol.* 128, 1735–1753. doi: 10.1111/jam.14587

Liu, D., Yan, R., Fu, Y., Wang, X., Zhang, J., and Xiang, W. (2019). Antifungal, plant growth-promoting, and genomic properties of an endophytic actinobacterium streptomyces sp. NEAU-S7GS2. *Front. Microbiol.* 10. doi: 10.3389/fmicb.2019.02077

Liu-Xu, L., Vicedo, B., García-Agustín, P., and Llorens, E. (2022). Advances in endophytic fungi research: a data analysis of 25 years of achievements and challenges. *J. Plant Interact.* 17, 244–266. doi: 10.1080/17429145.2022.2032429

Loc, N. H., Huy, N. D., Quang, H. T., Lan, T. T., and Thu Ha, T. T. (2020). Characterisation and antifungal activity of extracellular chitinase from a biocontrol fungus, trichoderma asperellum PQ34. *Mycology* 11, 38–48. doi: 10.1080/21501203.2019.1703839

Lonkar, K., and Bodade, R. (2021). "Potential role of endophytes in weeds and herbicide tolerance in plants," in *Plant growth-promoting microbes for sustainable biotic and abiotic stress management*. Eds. H. I. Mohamed, H. E.-D. S. El-Beltagi and K. A. Abd-Elsalam (Cham: Springer International Publishing), 227–250. doi: 10.1007/978-3-030-66587-6_9

Ma, C., Li, F., Musharrafieh, R. G., and Wang, J. (2016). Discovery of cyclosporine a and its analogs as broad-spectrum anti-influenza drugs with a high *in vitro* genetic barrier of drug resistance. *Antiviral Res.* 133, 62–72. doi: 10.1016/j.antiviral.2016.07.019

Maheshwari, R., Bhutani, N., and Suneja, P. (2020). Isolation and characterization of ACC deaminase producing endophytic bacillus mojavensis PRN2 from pisum sativum. *Iran J. Biotechnol.* 18, 11–20. doi: 10.30498/IJB.2020.137279.2308

Mani, V. M., Kalaivani, S., Sabarathinam, S., Vasuki, M., Soundari, A. J. P. G., Ayyappa Das, M. P., et al. (2021). Copper oxide nanoparticles synthesized from an endophytic fungus aspergillus terreus: bioactivity and anti-cancer evaluations. *Environ. Res.* 201, 111502. doi: 10.1016/j.envres.2021.111502

Manjunath, M. H., Joshi, C. G., Danagoudar, A., Poyya, J., Kudva, A. K., and BL, D. (2017). Biogenic synthesis of gold nanoparticles by marine endophytic fungus-cladosporium cladosporioides isolated from seaweed and evaluation of their antioxidant and antimicrobial properties. *Process Biochem.* 63, 137–144. doi: 10.1016/j.procbio.2017.09.008

Martínez-Rodríguez, J. D. C., de la Mora-Amutio, M., Plascencia-Correa, L. A., Audelo-Regalado, E., Guardado, F. R., Hernández-Sánchez, E., et al. (2014) *Cultivable endophytic bacteria from leaf bases of agave tequilana and their role as plant growth promoters*. Available at: www.sbmicrobiologia.org.br.

Matias, R. R., Sepúlveda, A. M. G., Batista, B. N., de Lucena, J. M. V. M., and Albuquerque, P. M. (2021). Degradation of staphylococcus aureus biofilm using hydrolytic enzymes produced by Amazonian endophytic fungi. *Appl. Biochem. Biotechnol.* 193, 2145–2161. doi: 10.1007/s12010-021-03542-8

Mehta, D., and Satyanarayana, T. (2016). Bacterial and archaeal α-amylases: diversity and amelioration of the desirable characteristics for industrial applications. *Front. Microbiol.* 7. doi: 10.3389/fmicb.2016.01129

Mehta, P., Sharma, R., Putatunda, C., Walia, A., and Singh, B. P. (2019). "Endophytic fungi: role in phosphate solubilization," in *Advances in endophytic fungal research: present status and future challenges* (Cham: Springer International Publishing), 183–209. doi: 10.1007/978-3-030-03589-1_9

Mengistu, A. A. (2020). Endophytes: colonization, behaviour, and their role in defense mechanism. *Int. J. Microbiol.* 2020. doi: 10.1155/2020/6927219

Michel, J., Abd Rani, N. Z., and Husain, K. (2020). A review on the potential use of medicinal plants from asteraceae and lamiaceae plant family in cardiovascular diseases. *Front. Pharmacol.* 11. doi: 10.3389/fphar.2020.00852

Mishra, A., Pratap, S. S., Sahil, M., Pratap, S. S., Arpita, B., Nishtha, M., et al. (2018). Endophyte-mediated modulation of defense-related genes and systemic resistance in withania somnifera (L.) dunal under alternaria alternata stress. *Appl. Environ. Microbiol.* 84, e02845–e02817. doi: 10.1128/AEM.02845-17

Mishra, S., Priyanka, and Sharma, S. (2022). Metabolomic insights into endophyte-derived bioactive compounds. *Front. Microbiol.* 13. doi: 10.3389/fmicb.2022.835931

Misra, M., Sachan, A., and Sachan, S. G. (2021). "Chapter 15 - role of fungal endophytes in the green synthesis of nanoparticles and the mechanism," in *Fungi bio-prospects in sustainable agriculture, environment and nano-technology*. Eds. V. K. Sharma, M. P. Shah, S. Parmar and A. Kumar (Academic Press), 489–513. doi: 10.1016/B978-0-12-821734-4.00001-0

Modi, S., Inwati, G. K., Gacem, A., Saquib Abullais, S., Prajapati, R., Yadav, V. K., et al. (2022). Nanostructured antibiotics and their emerging medicinal applications: an overview of nanoantibiotics. *Antibiotics* 11, 708. doi: 10.3390/antibiotics11060708

Mohamad, O. A. A., Li, L., Ma, J. B., Hatab, S., Xu, L., Guo, J. W., et al. (2018). Evaluation of the antimicrobial activity of endophytic bacterial populations from Chinese traditional medicinal plant licorice and characterization of the bioactive secondary metabolites produced by bacillus atrophaeus against verticillium dahliae. *Front. Microbiol.* 9. doi: 10.3389/fmicb.2018.00924

Mousa, S. A., El-Sayed, E.-S. R., Mohamed, S. S., Abo El-Seoud, M. A., Elmehlawy, A. A., and Abdou, D. A. M. (2021). Novel mycosynthesis of Co3O4, CuO, Fe3O4, NiO, and ZnO nanoparticles by the endophytic aspergillus terreus and evaluation of their antioxidant and antimicrobial activities. *Appl. Microbiol. Biotechnol.* 105, 741–753. doi: 10.1007/s00253-020-11046-4

Munawer, U., Raghavendra, V. B., Ningaraju, S., Krishna, K. L., Ghosh, A. R., Melappa, G., et al. (2020). Biofabrication of gold nanoparticles mediated by the endophytic cladosporium species: photodegradation, *in vitro* anticancer activity and *in vivo* antitumor studies. *Int. J. Pharm.* 588, 119729. doi: 10.1016/j.ijpharm.2020.119729

Muthu Narayanan, M., Ahmad, N., Shivanand, P., and Metali, F. (2022). The role of endophytes in combating fungal- and bacterial-induced stress in plants. *Molecules* 27. doi: 10.3390/molecules27196549

Muvea, A. M., Meyhöfer, R., Subramanian, S., Poehling, H.-M., Ekesi, S., and Maniania, N. K. (2014). Colonization of onions by endophytic fungi and their impacts on the biology of thrips tabaci. *PloS One* 9, e108242-. doi: 10.1371/journal.pone.0108242

Narayanan, Z., and Glick, B. R. (2022). Secondary metabolites produced by plant growth-promoting bacterial endophytes. *Microorganisms* 10. doi: 10.3390/microorganisms10102008

Nascimento, F. X., Rossi, M. J., and Glick, B. R. (2018). Ethylene and 1-aminocyclopropane-1-carboxylate (ACC) in plant–bacterial interactions. *Front. Plant Sci.* 9. doi: 10.3389/fpls.2018.00114

Nguyen, N. T., and Nguyen, V. A. (2020). Synthesis, characterization, and photocatalytic activity of ZnO nanomaterials prepared by a green, nonchemical route. *J. Nanomater* 2020. doi: 10.1155/2020/1768371

Omomowo, I. O., Amao, J. A., Abubakar, A., Ogundola, A. F., Ezediuno, L. O., and Bamigboye, C. O. (2023). A review on the trends of endophytic fungi bioactivities. *Sci. Afr* 20, e01594. doi: 10.1016/j.sciaf.2023.e01594

Othman, A. M., Elsayed, M. A., Elshafei, A. M., and Hassan, M. M. (2018). Purification and biochemical characterization of two isolated laccase isoforms from agaricus bisporus CU13 and their potency in dye decolorization. *Int. J. Biol. Macromol* 113, 1142–1148. doi: 10.1016/j.ijbiomac.2018.03.043

Oukala, N., Pastor, V., and Aissat, K. (2021). Bacterial endophytes: the hidden actor in plant immune responses against biotic stress. *Plants* 10. doi: 10.3390/plants10051012

Palanichamy, P., Krishnamoorthy, G., Kannan, S., and Marudhamuthu, M. (2018). Bioactive potential of secondary metabolites derived from medicinal plant endophytes. *Egyptian J. Basic Appl. Sci.* 5, 303–312. doi: 10.1016/j.ejbas.2018.07.002

Pan, L., Chen, J., Ren, S., Shen, H., Rong, B., Liu, W., et al. (2020). Complete genome sequence of mycobacterium mya-zh01, an endophytic bacterium, promotes plant growth and seed germination isolated from flower stalk of doritaenopsis. *Arch. Microbiol.* 202, 1965–1976. doi: 10.1007/s00203-020-01924-w

Parthasarathy, R., and Sathiyabama, M. (2015). Lovastatin-producing endophytic fungus isolated from a medicinal plant solanum xanthocarpum. *Nat. Prod Res.* 29, 2282–2286. doi: 10.1080/14786419.2015.1016938

Patel, T., and Saraf, M. (2017). Biosynthesis of phytohormones from novel rhizobacterial isolates and their *in vitro* plant growth-promoting efficacy. *J. Plant Interact.* 12, 480–487. doi: 10.1080/17429145.2017.1392625

Patel, A. K., Singhania, R. R., and Pandey, A. (2017). "Chapter 2 - production, purification, and application of microbial enzymes," in *Biotechnology of microbial enzymes*. Ed. G. Brahmachari (Academic Press), 13–41. doi: 10.1016/B978-0-12-803725-6.00002-9

Payne, C. M., Knott, B. C., Mayes, H. B., Hansson, H., Himmel, M. E., Sandgren, M., et al. (2015). Fungal cellulases. *Chem. Rev.* 115, 1308–1448. doi: 10.1021/cr500351c

Qin, L., Tian, P., Cui, Q., Hu, S., Jian, W., Xie, C., et al. (2021). Bacillus circulans GN03 alters the microbiota, promotes cotton seedling growth and disease resistance, and increases the expression of phytohormone synthesis and disease resistance-related genes. *Front. Plant Sci.* 12. doi: 10.3389/fpls.2021.644597

Rabha, A. J., Naglot, A., Sharma, G. D., Gogoi, H. K., and Veer, V. (2014). *In vitro* evaluation of antagonism of endophytic colletotrichum gloeosporioides against potent fungal pathogens of camellia sinensis. *Indian J. Microbiol.* 54, 302–309. doi: 10.1007/s12088-014-0458-8

Radziemska, M., Gusiatin, Z. M., Cydzik-Kwiatkowska, A., Cerdà, A., Pecina, V., Bęś, A., et al. (2021). Insight into metal immobilization and microbial community structure in soil from a steel disposal dump phytostabilized with composted, pyrolyzed or gasified wastes. *Chemosphere* 272, 129576. doi: 10.1016/j.chemosphere.2021.129576

Rafi, M. M., Krishnaveni, M. S., and Charyulu, P. B. B. N. (2019). "Chapter 17 - phosphate-solubilizing microorganisms and their emerging role in sustainable agriculture," in *Recent developments in applied microbiology and biochemistry*. Ed. V. Buddolla (Academic Press), 223–233. doi: 10.1016/B978-0-12-816328-3.00017-9

Raghav, D., Jyoti, A., Siddiqui, A. J., and Saxena, J. (2022). Plant-associated endophytic fungi as potential bio-factories for extracellular enzymes: progress, challenges and strain improvement with precision approaches. *J. Appl. Microbiol.* 133, 287–310. doi: 10.1111/jam.15574

Ramos, M. M., dos S. Morais, E., da S. Sena, I., Lima, A. L., de Oliveira, F. R., de Freitas, C. M., et al. (2020). Silver nanoparticle from whole cells of the fungi trichoderma spp. isolated from Brazilian Amazon. *Biotechnol. Lett.* 42, 833–843. doi: 10.1007/s10529-020-02819-y

Rathore, S., Ujjainwal, M., Kaushik, A., and Bala, J. (2022). "Bacterial endophytes and bio-nanotechnology," in *Bacterial endophytes for sustainable agriculture and environmental management*. Eds. A. K. Singh, V. Tripathi, A. K. Shukla and P. Kumar (Singapore: Springer Singapore), 201–212. doi: 10.1007/978-981-16-4497-9_10

Rodrigues, A. G., Ping, L. Y., Marcato, P. D., Alves, O. L., Silva, M. C. P., Ruiz, R. C., et al. (2013). Biogenic antimicrobial silver nanoparticles produced by fungi. *Appl. Microbiol. Biotechnol.* 97, 775–782. doi: 10.1007/s00253-012-4209-7

Rojas, E. C., Jensen, B., Jørgensen, H. J. L., Latz, M. A. C., Esteban, P., Ding, Y., et al. (2020). Selection of fungal endophytes with biocontrol potential against fusarium head blight in wheat. *Biol. Control* 144, 104222. doi: 10.1016/j.biocontrol.2020.104222

Russell, J. R., Jeffrey, H., Pria, A., Kaury, K., Sandoval., A. G., Dantzler., K. W., et al. (2011). Biodegradation of polyester polyurethane by endophytic fungi. *Appl. Environ. Microbiol.* 77, 6076–6084. doi: 10.1128/AEM.00521-11

Sadoral, J. P., and Cumagun, C. J. R. (2021). Observations on the potential of an endophytic fungus associated with cacao leaves against phytophthora palmivora. *Microbiol. Res. (Pavia)* 12, 528–538. doi: 10.3390/microbiolres12030037

Sah, S. K., Reddy, K. R., and Li, J. (2016). Abscisic acid and abiotic stress tolerance in crop plants. *Front. Plant Sci.* 7. doi: 10.3389/fpls.2016.00571

Salvi, S., Varghese, R., Digholkar, G., Deshpande, A., Malvankar, C., Pawar, A., et al. (2022). Saraca asoca: a scoping review on the phytoconstituents, bioactives and their therapeutic effects. *German J. Pharm. Biomaterials* 1, 03–13. doi: 10.5530/gjpb.2022.3.11

Sandargo, B., Chepkirui, C., Cheng, T., Chaverra-Muñoz, L., Thongbai, B., Stadler, M., et al. (2019). Biological and chemical diversity go hand in hand: basidiomycota as source of new pharmaceuticals and agrochemicals. *Biotechnol. Adv.* 37, 107344. doi: 10.1016/j.biotechadv.2019.01.011

Shah, S., Shrestha, R., Maharjan, S., Selosse, M. A., and Pant, B. (2019). Isolation and characterization of plant growth-promoting endophytic fungi from the roots of dendrobium moniliforme. *Plants* 8. doi: 10.3390/plants8010005

Shahid, M., Hameed, S., Tariq, M., Zafar, M., Ali, A., and Ahmad, N. (2015). Characterization of mineral phosphate-solubilizing bacteria for enhanced sunflower growth and yield-attributing traits. *Ann. Microbiol.* 65, 1525–1536. doi: 10.1007/s13213-014-0991-z

Sharma, M., and Mallubhotla, S. (2022). Diversity, antimicrobial activity, and antibiotic susceptibility pattern of endophytic bacteria sourced from cordia dichotoma l. *Front. Microbiol.* 13. doi: 10.3389/fmicb.2022.879386

Sharma, H., Rai, A. K., Dahiya, D., Chettri, R., and Nigam, P. S. (2021). Exploring endophytes for *in vitro* synthesis of bioactive compounds similar to metabolites produced *in vivo* by host plants. *AIMS Microbiol.* 7, 175–199. doi: 10.3934/MICROBIOL.2021012

Singh, D., Rathod, V., Ninganagouda, S., Hiremath, J., Singh, A. K., and Mathew, J. (2014). Optimization and characterization of silver nanoparticle by endophytic fungi *Penicillium* sp. isolated from *Curcuma longa* (Turmeric) and application studies against MDR *E. coli* and *S. aureus*. *Bioinorg Chem. Appl.* 2014, 408021. doi: 10.1155/2014/408021

Singh, S., Sidhu, G. K., Kumar, V., Dhanjal, D. S., Datta, S., and Singh, J. (2019). "Fungal xylanases: sources, types, and biotechnological applications," in *Recent advancement in white biotechnology through fungi: volume 1: diversity and enzymes perspectives*. Eds. A. N. Yadav, S. Mishra, S. Singh and A. Gupta (Cham: Springer International Publishing), 405–428. doi: 10.1007/978-3-030-10480-1_12

Singh, D., Yadav, V. K., Ali, D., Soni, S., Kumar, G., Dawane, V., et al. (2022). Isolation and characterization of siderophores producing chemolithotrophic bacteria from the coal samples of the aluminum industry. *Geomicrobiol J.* 40(4), 307–314. doi: 10.1080/01490451.2022.2128114

Singh, A., Yadav, V. K., Chundawat, R. S., Soltane, R., Awwad, N. S., Ibrahium, H. A., et al. (2023). Enhancing plant growth promoting rhizobacterial activities through consortium exposure: a review. *Front. Bioeng Biotechnol.* 11. doi: 10.3389/fbioe.2023.1099999

Skendžić, S., Zovko, M., Živković, I. P., Lešić, V., and Lemić, D. (2021). The impact of climate change on agricultural insect pests. *Insects* 12. doi: 10.3390/insects12050440

Soldan, R., Mapelli, F., Crotti, E., Schnell, S., Daffonchio, D., Marasco, R., et al. (2019). Bacterial endophytes of mangrove propagules elicit early establishment of the natural host and promote growth of cereal crops under salt stress. *Microbiol. Res.*, 223–225. doi: 10.1016/j.micres.2019.03.008

Srivastava, M., Maurya, P., Jyotshna, and Shanker, K. (2021). Clerodendrum viscosum: a critical review on phytochemistry, pharmacology, quality assurance, and safety data. *Medicinal Chem. Res.* 30, 2145–2167. doi: 10.1007/s00044-021-02804-8

Strobel, G., Daisy, B., Castillo, U., and Harper, J. (2004). Natural products from endophytic microorganisms. *J. Nat. Prod* 67, 257–268. doi: 10.1021/np030397v

Sun, J., Guo, N., Niu, L. L., Wang, Q. F., Zang, Y. P., Zu, Y. G., et al. (2017). Production of laccase by a new myrothecium verrucaria MD-R-16 isolated from pigeon pea [Cajanus cajan (L.) millsp.] and its application on dye decolorization. *Molecules* 22. doi: 10.3390/molecules22040673

Tian, P., Nan, Z., Li, C., and Spangenberg, G. (2008). Effect of the endophyte neotyphodium lolii on susceptibility and host physiological response of perennial ryegrass to fungal pathogens. *Eur. J. Plant Pathol.* 122, 593–602. doi: 10.1007/s10658-008-9329-7

Tiwari, P., Kang, S., and Bae, H. (2023). Plant-endophyte associations: rich yet under-explored sources of novel bioactive molecules and applications. *Microbiol. Res.* 266, 127241. doi: 10.1016/j.micres.2022.127241

Topolovec-Pintarić, S. (2019). "Trichoderm : Invisible Partner for Visible Impact on Agriculture," in *Trichoderma - The Most Widely Used Fungicide* (London, UK: IntechOpen). doi: 10.5772/intechopen.83363

Tshishonga, K., and Serepa-Dlamini, M. H. (2020). Draft genome sequence of pseudarthrobacter phenanthrenivorans strain MHSD1, a bacterial endophyte isolated from the medicinal plant pellaea calomelanos. *Evolutionary Bioinf.* 16, 1176934320913257. doi: 10.1177/1176934320913257

Tuangporn, P. (2012). An extracellular lipase from the endophytic fungi fusarium oxysporum isolated from the Thai medicinal plant, croton oblongifolius roxb. *Afr J. Microbiol. Res.* 6, 2622–2638. doi: 10.5897/ajmr11.965

Tyagi, J., Chaudhary, P., Jyotsana, Bhagwati, U., Bhandari, G., and Chaudhary, A. (2022). "Chapter 17 impact of endophytic fungi in biotic stress management," in *From chemicals to biologicals*. Eds. R. Soni, D. C. Suyal and R. Goel, 447–462. doi: 10.1515/9783110771558-017

Uddandarao, P., Balakrishnan, R. M., Ashok, A., Swarup, S., and Sinha, P. (2019). Bioinspired ZnS: gd nanoparticles synthesized from an endophytic fungi aspergillus flavus for fluorescence-based metal detection. *Biomimetics* 4. doi: 10.3390/biomimetics4010011

Uddandarao, P., and Mohan, R. B. (2016). ZnS semiconductor quantum dots production by an endophytic fungus aspergillus flavus. *Materials Sci. Engineering: B* 207, 26–32. doi: 10.1016/j.mseb.2016.01.013

Vaid, S. K., Srivastava, P. C., Pachauri, S. P., Sharma, A., Rawat, D., Shankhadhar, S. C., et al. (2020). Effective zinc mobilization to rice grains using rhizobacterial consortium. *Isr. J. Plant Sci.* 67, 145–157. doi: 10.1163/22238980-20201085

Verma, V. C., Kharwar, R. N., and Gange, A. C. (2009). Biosynthesis of antimicrobial silver nanoparticles by the endophytic fungus aspergillus clavatus. *Nanomedicine* 5, 33–40. doi: 10.2217/nnm.09.77

Verma, A., Shameem, N., Jatav, H. S., Sathyanarayana, E., Parray, J. A., Poczai, P., et al. (2022). Fungal endophytes to combat biotic and abiotic stresses for climate-smart and sustainable agriculture. *Front. Plant Sci.* 13. doi: 10.3389/fpls.2022.953836

Verma, S. K., and White, J. F. (2018). Indigenous endophytic seed bacteria promote seedling development and defend against fungal disease in browntop millet (Urochloa ramosa l.). *J. Appl. Microbiol.* 124, 764–778. doi: 10.1111/jam.13673

Vijayanandan, A. S., and Balakrishnan, R. M. (2018). Biosynthesis of cobalt oxide nanoparticles using endophytic fungus aspergillus nidulans. *J. Environ. Manage* 218, 442–450. doi: 10.1016/j.jenvman.2018.04.032

Waqas, M., Khan, A. L., Kamran, M., Hamayun, M., Kang, S. M., Kim, Y. H., et al. (2012). Endophytic fungi produce gibberellins and indoleacetic acid and promotes host-plant growth during stress. *Molecules* 17, 10754–10773. doi: 10.3390/molecules170910754

Wen, J., Okyere, S. K., Wang, S., Wang, J., Xie, L., Ran, Y., et al. (2022). Endophytic fungi: an effective alternative source of plant-derived bioactive compounds for pharmacological studies. *J. Fungi* 8. doi: 10.3390/jof8020205

Woźniak, M., Gałązka, A., Tyśkiewicz, R., and Jaroszuk-ściseł, J. (2019). Endophytic bacteria potentially promote plant growth by synthesizing different metabolites and their phenotypic/physiological profiles in the biolog gen iii microplate™ test. *Int. J. Mol. Sci.* 20. doi: 10.3390/ijms20215283

Wu, Y., Shu, T., Li, P., Wang, Z., Wang, H., Pan, F., et al. (2022). A novel endo-β-1,4-xylanase xyl-1 from aspergillus terreus HG-52 for high-efficiency ramie degumming. *J. Natural Fibers* 19, 13890–13900. doi: 10.1080/15440478.2022.2111390

Xu, W., Ren, H., Ou, T., Lei, T., Wei, J., Huang, C., et al. (2019). Genomic and functional characterization of the endophytic bacillus subtilis 7PJ-16 strain, a potential biocontrol agent of mulberry fruit sclerotiniose. *Microb. Ecol.* 77, 651–663. doi: 10.1007/s00248-018-1247-4

Yadav, V. K., Khan, S. H., Malik, P., Thappa, A., Suriyaprabha, R., Ravi, R. K., et al. (2020). "Microbial synthesis of nanoparticles and their applications for wastewater treatment," in *Microbial biotechnology: basic research and applications* (Springer), 147–187.

Yadav, A. N., Kumar, V., Dhaliwal, H. S., Prasad, R., and Saxena, A. K. (2018). "Chapter 15 - microbiome in crops: diversity, distribution, and potential role in crop improvement," in *Crop improvement through microbial biotechnology*. Eds. R. Prasad, S. S. Gill and N. Tuteja (Elsevier), 305–332. doi: 10.1016/B978-0-444-63987-5.00015-3

Yang, H. R., Hu, X. P., Jiang, C. J., Qi, J., Wu, Y. C., Li, W., et al. (2015). Diversity and antimicrobial activity of endophytic fungi isolated from cephalotaxus hainanensis Li, a well-known medicinal plant in China. *Lett. Appl. Microbiol.* 61, 484–490. doi: 10.1111/lam.12483

Zaferanloo, B., Bhattacharjee, S., Ghorbani, M. M., Mahon, P. J., and Palombo, E. A. (2014). Amylase production by preussia minima, a fungus of endophytic origin: optimization of fermentation conditions and analysis of fungal secretome by LC-MS. *BMC Microbiol.* 14, 55. doi: 10.1186/1471-2180-14-55

Zamin, M., Fahad, S., Khattak, A. M., Adnan, M., Wahid, F., Raza, A., et al. (2020). Developing the first halophytic turfgrasses for the urban landscape from native Arabian desert grass. *Environ. Sci. pollut. Res.* 27, 39702–39716. doi: 10.1007/s11356-019-06218-3

Zhang, Q., Zhang, J., Yang, L., Zhang, L., Jiang, D., Chen, W., et al. (2014). Diversity and biocontrol potential of endophytic fungi in brassica napus. *Biol. Control* 72, 98–108. doi: 10.1016/j.biocontrol.2014.02.018

Zhao, S., Zhou, N., Zhao, Z.-Y., Zhang, K., Wu, G.-H., and Tian, C.-Y. (2016). Isolation of endophytic plant growth-promoting bacteria associated with the halophyte salicornia europaea and evaluation of their promoting activity under salt stress. *Curr. Microbiol.* 73, 574–581. doi: 10.1007/s00284-016-1096-7

frontiers | Frontiers in Plant Science

TYPE Brief Research Report
PUBLISHED 13 October 2023
DOI 10.3389/fpls.2023.1257137

OPEN ACCESS

EDITED BY
Diogo Neves Proença,
University of Coimbra, Portugal

REVIEWED BY
Raul Riesco Jarrin,
University of Salamanca, Spain
Sangeeta Paul,
Indian Agricultural Research Institute (ICAR), India
Eduardo Valencia-Cantero,
Michoacana University of San Nicolás de Hidalgo, Mexico

*CORRESPONDENCE
Jae-Hoon Lee
jhlee72@pusan.ac.kr

†These authors have contributed equally to this work

RECEIVED 12 July 2023
ACCEPTED 06 September 2023
PUBLISHED 13 October 2023

CITATION
Kim H, Woo O-G, Kim JB, Yoon S-Y, Kim J-S, Sul WJ, Hwang J-Y and Lee J-H (2023) *Flavobacterium* sp. strain GJW24 ameliorates drought resistance in *Arabidopsis* and *Brassica*. *Front. Plant Sci.* 14:1257137. doi: 10.3389/fpls.2023.1257137

Flavobacterium sp. strain GJW24 ameliorates drought resistance in *Arabidopsis* and *Brassica*

Hani Kim[1†], Og-Geum Woo[1†], Ji Bin Kim[1], So-Young Yoon[2], Jong-Shik Kim[3], Woo Jun Sul[4], Jee-Yeon Hwang[2] and Jae-Hoon Lee[1*]

[1]Department of Biology Education, Pusan National University, Busan, Republic of Korea, [2]Department of Pharmacology and Neuroscience, Creighton University School of Medicine, Omaha, NE, United States, [3]Marine Industry Research Institute for East Sea Rim, Uljin, Republic of Korea, [4]Department of Systems Biotechnology, Chung-Ang University, Anseong, Republic of Korea

Candidate strains that contribute to drought resistance in plants have been previously screened using approximately 500 plant growth-promoting rhizobacteria (PGPR) obtained from Gotjawal, South Korea, to further understand PGPR associated with plant drought tolerance. In this study, a selected PGPR candidate, *Flavobacterium* sp. strain GJW24, was employed to enhance plant drought tolerance. GJW24 application to *Arabidopsis* increased its survival rate under drought stress and enhanced stomatal closure. Furthermore, GJW24 promoted *Arabidopsis* survival under salt stress, which is highly associated with drought stress. GJW24 ameliorated the drought/salt tolerance of *Brassica* as well as *Arabidopsis*, indicating that the drought-resistance characteristics of GJW24 could be applied to various plant species. Transcriptome sequencing revealed that GJW24 upregulated a large portion of drought- and drought-related stress-inducible genes in *Arabidopsis*. Moreover, Gene Ontology analysis revealed that GJW24-upregulated genes were highly related to the categories involved in root system architecture and development, which are connected to amelioration of plant drought resistance. The hyper-induction of many drought/salt-responsive genes by GJW24 in *Arabidopsis* and *Brassica* demonstrated that the drought/salt stress tolerance conferred by GJW24 might be achieved, at least in part, through regulating the expression of the corresponding genes. This study suggests that GJW24 can be utilized as a microbial agent to offset the detrimental effects of drought stress in plants.

KEYWORDS

GJW24, *Flavobacterium*, plant growth-promoting rhizobacteria, drought tolerance, salt stress tolerance

Introduction

Various abiotic stresses including heat, cold, UV, drought, high salt, and heavy metals, adversely affect plant productivity (Zhu, 2002). However, plants have developed regulatory mechanisms via plant-microbe interactions as a strategy to overcome these stresses. Plant growth-promoting rhizobacteria (PGPR), which are indigenous to the plant rhizosphere, can play a positive role in plant growth via diverse mechanisms, including enhancement of abiotic stress tolerance (Vejan et al., 2016). When plants face abiotic stresses, PGPR provides plants with adaptation mechanisms such as the regulation of hormones such as indole-3-acetic acid (IAA), cytokinin (CK), gibberellic acid (GA), and abscisic acid (ABA); the production of 1-aminocyclopropane 1-carboxylic acid (ACC) deaminase; the production of antioxidants; the secretion of osmolytes; and the secretion of microbial exopolysaccharide (EPS) (Ma et al., 2020). Although a diverse range of bacteria belonging to *Pseudomonas* and *Bacillus* have been reported as PGPR, the study on PGPR responsible for abiotic stress tolerance in other groups has been relatively poor (Beneduzi et al., 2012).

Drought is one of the abiotic stresses determining plant productivity. It has several adverse effects during plant life cycle, such as the inhibition of photosynthesis, alteration of the respiration rate, disruption of metabolic processes, and improper ion uptake (Hussain et al., 2018). Therefore, to offset these adverse effects, studies on useful PGPR involved in improving plant drought tolerance have been rapidly conducted in recent years. Many studies have revealed that various PGPR ameliorate drought stress resistance in diverse plant species. IAA and GA from several PGPR promote nutrient acquisition and growth of plants, enabling plant survival under drought/salt stress conditions (Ma et al., 2020; Uzma et al., 2022). The treatment of CK-producing *Bacillus subtilis* has been shown to improve drought resistance in *Platycladus orientalis* (Liu et al., 2013). These PGPR-produced phytohormones regulate the formation of root hairs and lateral roots, leading to increased uptake of water and nutrients. PGPR, such as *Bacillus licheniformis* Rt4M10, *Phyllobacterium brassicacearum* STM196, and *Azospirillum brasilense* Sp 245, increase ABA content in plants, consequently ameliorating drought tolerance (Bresson et al., 2013; Cohen et al., 2015). Abiotic stress-induced ethylene inhibits plant growth; however, ACC deaminase (an ACC-degrading enzyme)-producing PGPR can mitigate the adverse effects of abiotic stressors and positively regulate plant growth (Lephatsi et al., 2021). Several reports have demonstrated that ACC deaminase-producing microbes confers enhanced tolerance to drought/salt stress in diverse plant species (Forni et al., 2017). Abiotic stress triggers the production of reactive oxygen species, which are highly toxic to macromolecules and lipids and result in oxidative damage in plant cells (You and Chan, 2015). Some PGPR are involved in regulating the activities of antioxidant enzymes and their gene expression, which mitigates the deleterious effects of abiotic stressors, including drought (Bharti et al., 2016; Batool et al., 2020). Plants utilize compatible osmolytes as osmoprotectants to stabilize macromolecules and membrane structure under drought/salt stress. PGPR-produced EPS is able to help keep the water potential of the rhizosphere high by binding soil particles, thereby ameliorating plant abiotic stress tolerance (Naseem et al., 2018). The existence of PGPR, which produces these osmolytes and EPS, has been widely reported, with a focus on its effect on enhancing resistance to drought/salt stress (Naseem et al., 2018; Khan and Bano, 2019; Ma et al., 2020). Collectively, these studies show that various PGPR strains play crucial roles in ameliorating plant drought stress resistance via diverse mechanisms.

In this research, we show that *Flavobacterium* sp. strain GJW24 improved drought and drought-related salt stress resistance in *Arabidopsis* and *Brassica* plants. The abiotic stress resistance phenotype conferred by GJW24 increases the possibility that GJW24 can be utilized as a biological material to positively regulate plant growth and yield under such unfavorable environments.

Materials and methods

Plant materials and culture conditions

Arabidopsis (*A. thaliana*) ecotype Col-0 and cabbage (*Brassica campestris* L. ssp. pekinensis, cultivar; 'Chun Yeon Gold') were used as the wild types in this study. The surfaces of the plant seeds were sterilized, and the seeds were grown on 1× MS plate supplemented with 0.8% bacto agar and 1% sucrose (pH 5.8). The seeds were kept for 7 d in a growth chamber at 23°C under a 16 h light/8 h dark cycle. Then, the resulting seedlings were moved to into a pot filled with horticultural soil mix (cocopeat 51.5%, peat moss 10%, vermiculite 13%, perlite 15%, zeolite10%, humic acid 0.1%, fertilizer 0.4%) and kept in a growth chamber at 23°C under a 16 h light/8 h dark cycle for further analysis.

Bacterial growth conditions and plant inoculation

The *Flavobacterium* sp. strain GJW24 was obtained from Gotjawal soil, Jeju Island, South Korea (Kim et al., 2018). GJW24 was incubated on R2A plates overnight at 28°C. The resulting microbes were adjusted to an OD_{600} of 0.02~0.03 using MS solution. Next, one milliliter of the bacterial suspension was added to the region around the growth areas of *Arabidopsis* and *Brassica*.

Assay for drought/salt stress resistance in *Arabidopsis*

Assays for drought and salt stress resistance in *Arabidopsis* were performed using the MS liquid (mock) or GJW24-treated plants. For the drought tolerance assay, 8-day-old plants were exposed to mock or GJW24. Seven days after treatment, they were exposed to water deficiency (drought stress) for 14 d, followed by re-watering for 4 d. The assays were conducted with four biological replicates. For each assay, at least ten plants were used for mock or GJW24

treatment. The assay for salt stress resistance was conducted by supplying 50 mL of water or 150 mM NaCl solution to the soil 7 d after mock or GJW24 treatment, three times for 6 d at 3-d intervals. Survival rates were monitored 3 d after the last day of NaCl treatment. The assays were conducted with six biological replicates. In four combinations of GJW24 and salt stress treatments for each assay, at least eight plants were used for each combination.

Assay for drought/salt stress resistance in *Brassica*

For the drought tolerance assay for *Brassica*, 8-day-old *Brassica* plants were exposed to MS liquid (mock) or GJW24. Seven days after treatment, the plants were exposed to water deficiency (drought stress) for 10 d, followed by re-watering for 6 d. The assays were conducted with four biological replicates. For each assay, at least six plants were used for mock or GJW24 treatment. The assay for salt stress resistance was performed by supplying 50 mL of water or 150 mM NaCl solution to the soil 7 d after mock or GJW24 treatment, eight times at 3-d intervals. Survival rates were monitored 1 d after the last day of NaCl treatment. For each assay, at least eleven plants were used for mock or GJW24 treatment.

Measurement of stomatal aperture

Eight-day-old *Arabidopsis* plants were exposed to mock or GJW24. Seven days after treatment, detached leaves from mock- or GJW24-treated plants were floated in stomatal opening solution containing 10 mM MES-KOH (pH 6.15), 50 mM KCl and 10 mM $CaCl_2$ for 2.5 h in the light (Lee et al., 2013). Then, the samples were additionally incubated in the same buffer with 0 or 20 μM ABA for 2.5 h in the light. The stomatal apertures from the abaxial part of the treated leaves were measured using a microscope (DM750, Leica) and the ImageJ program, as described by Kim et al. (2020).

Measurement of chlorophyll concentration

The total chlorophyll contents of the mock- or GJW24-treated samples under salt stress were quantified as described by Woo et al. (2020). The extracts were prepared using 80% acetone, and were then maintained in the dark for 30 min. The assays were conducted with six biological replicates. The chlorophyll content was quantified using the supernatants from centrifugation, and determined as described by Woo et al. (2020).

RNA isolation and RT-qPCR analysis

Total RNA was extracted using TRIzol reagent (Ambion). From one microgram of total RNA, complementary DNA (cDNA) was synthesized using RevertAid™ reverse transcriptase (Fermentas). Quantitative real-time PCR (qRT-PCR) was performed as described by Woo et al. (2020). The qRT-PCR was performed using the Solg™ 2 × real-time PCR Smart Mix (SolGent) and analyzed with the Rotor-Gene Q system (Qiagen). The transcript amounts of each gene were monitored using the comparative cycle threshold (CT) method, which was normalized against the transcripts from the reference genes; *Arabidopsis ACTIN2* or *Brassica ACT7* (Schmittgen and Livak, 2008). The DNA sequences for RT-qPCR analysis are listed in Table S1. The qRT-PCR analyses were performed with at least six biological replicates.

Transcriptome sequencing analysis

For transcriptome sequencing analysis, eight-day-old *Arabidopsis* plants were exposed to mock or GJW24. Total RNAs were independently extracted from the entire *Arabidopsis* plants (8 plants for each treatment) with three biological replicates 7 d after mock or GJW24 treatment. The replicates were not pooled per treatment. The analysis was done by MacroGen Inc. (Korea). To evaluate total RNA integrity, samples were run on a TapeStation RNA Screentape (Agilent Technologies). The RNA library was generated using RNA with RNA integrity number higher than 7.0. A total RNA library (0.5 μg) for each sample was produced using the Illumina TruSeq Stranded Total RNA Library Prep Plant Kit (Illumina, Inc.). After removing the total ribosomal RNA, the messenger RNA was fragmented using divalent cations at elevated temperatures. The resulting fragmented mRNAs were converted into first-strand cDNA with random primers and SuperScript II reverse transcriptase (Invitrogen). After second-strand cDNA synthesis using DNA Polymerase I, RNase H and dUTP, the resulting cDNA fragments go through an end repair process, the addition of a single 'A' base, and then ligation of the adapters. After purification, the products were enriched using PCR to construct the final cDNA library. Libraries were quantified using KAPA Library Quantification kits for Illumina Sequencing platforms (Kapa Biosystems) and qualified using a TapeStation D1000 ScreenTape (Agilent Technologies). Paired-end (2×100 bp) sequencing of indexed libraries was conducted using an Illumina NovaSeq system (Illumina, Inc.), by MacroGen Inc. (Korea). After removing adapter sequences and trimming bases with poor base quality using Trimmomatic v0.38, the cleaned reads were aligned to TAIR 10.1 with HISAT v2.1.0 (Kim et al., 2015), based on the HISAT and Bowtie2 implementations. The reference genome sequence and the gene annotation data were retrieved from NCBI Genome assembly and NCBI RefSeq database, respectively. Aligned data were sorted and indexed with SAMtools v 1.9, and the transcripts were assembled and quantified with StringTie v2.1.3b (Pertea et al., 2015; Pertea et al., 2016). Gene-level and transcript-level quantification were calculated with raw read count, FPKM and TPM.

Differential gene expression analysis

Among total 38,338 genes, 21,834 genes with non-zero counts in all replicates at least one period group were retrieved during the

QC step. The fold change and the statistical significance of DEGs was investigated by exactTest using edgeR (Robinson et al., 2010). Among the 21,834 genes analyzed, the expression of the transcript that satisfied with FC ≥ 2 and $p < 0.05$ at all comparisons was considered as significantly up-regulated genes. All p-values are adjusted using Benjamini-Hochberg algorithm to control false discovery rate. To investigate characteristic biological attributes of the genes upregulated by GJW24 treatment, Gene Ontology (GO) analysis was performed with the functional annotation tool on DAVID (https://david.ncifcrf.gov/tools.jsp), and the GJW24-upregulated genes were assigned to different categories for biological processes (BPs) and molecular functions (MFs). The inducibility of GJW24-upregulated genes under drought stress were checked using the database from the Arabidopsis eFP Browser (Winter et al., 2007).

Phylogenetic analysis

To generate a phylogenetic tree based on the 16s rRNA sequences, the 16s rRNA sequences of 17 *Flavobacterium* type strains, which exhibited the highest similarity to that of GJW24 based on a BLAST search, and 9 type strains from other genera in the family *Flavobacteriaceae* were obtained from 'The List of Prokaryotic names with Standing in Nomenclature' (LPSN) (https://lpsn.dsmz.de/text/approved-lists). The 16s rRNA sequences were aligned with ClustalW running in the MEGA11 program (Tamura et al., 2021). A rooted phylogenetic tree was generated with the MEGA11 using the maximum-likelihood method. The bootstrap method was performed to assess statistical significance of the tree using 1000 replicates.

Results and discussion

Identification of a *Flavobacterium* involved in drought tolerance process in *Arabidopsis*

Approximately 500 soil microbes, which included a unique microbial community, have previously been obtained from Gotjawal, Jeju Island (Kim et al., 2018; Woo et al., 2020). Through a preliminary screening process to select PGPR involved in drought stress resistance in *Arabidopsis*, several microbes whose applications resulted in the upregulation of drought resistance marker genes in *Arabidopsis* were identified (Woo et al., 2020). The 16S rRNA gene of the selected candidate exhibited the highest similarity to those of diverse *Flavobacterium* strains based on a BLAST search, showing that it belongs to the genus *Flavobacterium*. Therefore, the strain was named *Flavobacterium* sp. strain GJW24. The 16S rRNA gene sequence of GJW24 has been uploaded in GenBank under accession number OR272272. To examine how closely related GJW24 is to other *Flavobacterium* strains that have already been characterized, the 16s rRNA sequences of type strains from diverse *Flavobacteria* and other genera in the family *Flavobacteriaceae* were obtained from LPSN, and a phylogenetic tree based on the 16s rRNA sequences of GJW24 and the selected type strains was generated (Figure 1). Although the *Flavobacterium* genus has been reported as a PGPR group, studies on its biological contribution to the drought stress response in plants are highly limited (Gontia-Mishra et al., 2016; Kim et al., 2020); therefore, the biological function of GJW24 was further analyzed in this study.

Improved drought/salt stress resistance in *Arabidopsis* and *Brassica* following GJW24 application

To examine the potential functional role of GJW24 in the drought stress response, a phenotypic analysis of drought resistance in *Arabidopsis* was performed in the presence and absence of GJW24. The survival rate of GJW24-treated plants under drought condition was more than 2.5-fold higher than that of the mock-treated plants (Figure 2A). Given that tolerance against drought stress is largely achieved through the modulation of the stomatal aperture in plants, the effect of GJW24 on stomatal aperture regulation was further monitored. Although the difference of the stomatal apertures between mock-treated and GJW24-treated plants was not detected in the absence of ABA, the stomatal closure of GJW24-treated plants was significantly enhanced compared to mock-treated plants in the presence of ABA, indicating that GJW24 is involved in the promotion of ABA-mediated stomatal closure (Figure 2B). ABA is a crucial phytohormone that mediates drought tolerance by promoting stomatal closure and modulating drought-responsive genes (Takahashi et al., 2020). Thus, the enhancement of ABA-dependent stomatal closure in *Arabidopsis* by GJW24 (Figure 2B) shows that the regulation of the ABA signal transduction pathway is involved in the GJW24-mediated drought tolerance process. Collectively, these findings indicate that GJW24 improves tolerance against drought stress and that this process may be accomplished by minimizing water loss from transpiration, which results, at least in part, from the promotion of ABA-mediated stomatal closure. As salt stress increases endogenous ABA levels in plants, the plant salt stress response has been reported to largely overlap with the ABA-mediated drought stress response (Shinozaki and Yamaguchi-Shinozaki, 2007). Therefore, to confirm the GJW24-induced improvement in drought tolerance, the effect of GJW24 on salt stress resistance was examined. Similar to drought stress, the survival rate and chlorophyll content of GJW24-treated plants were approximately two- and three-fold higher than those of mock-treated ones under salt stress, respectively (Figure 2C), indicating that GJW24 application enhanced salt stress tolerance. To determine whether the GJW24-induced drought/salt stress resistance in *Arabidopsis* could be applied to other plants, the effect of GJW24 on abiotic stress resistance in *Brassica*, a crop most closely related to *Arabidopsis*, was investigated (Lagercrantz et al., 1996; Woo et al., 2020). Similar to its effect on *Arabidopsis*, GJW24 improved drought/salt stress tolerance in *Brassica*. Under drought and salt stress, the survival rate of GJW24-treated *Brassica* plants was more than three- and two-fold higher than that of mock-treated plants, respectively (Figures 2D, E). GJW24-induced improved drought/salt stress tolerance in *Arabidopsis* and

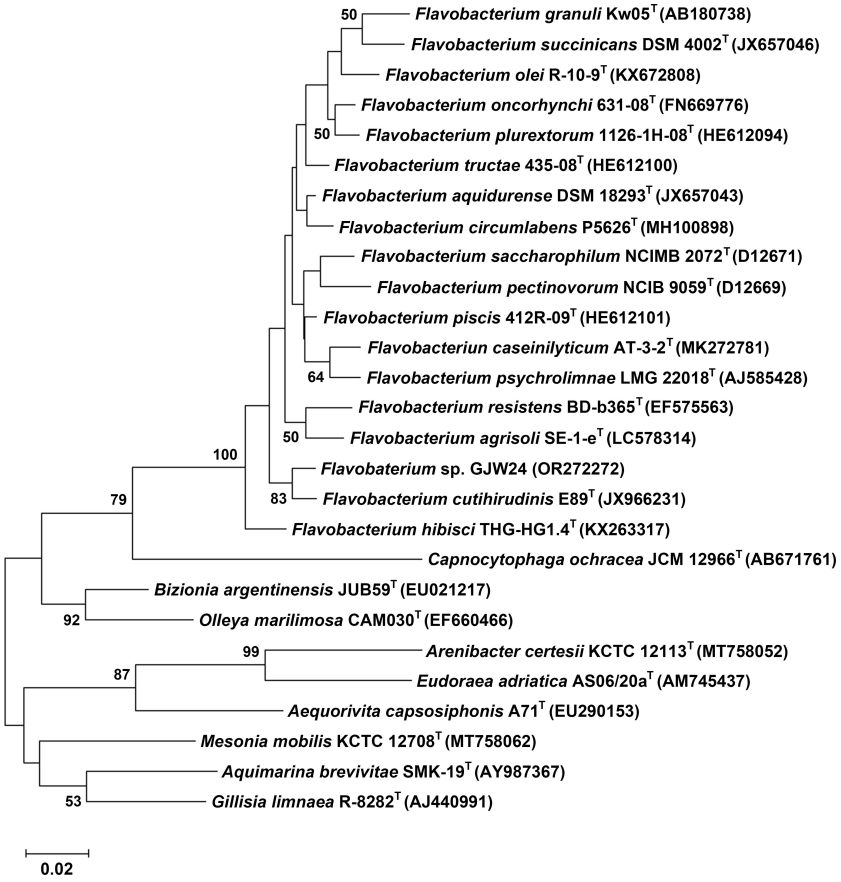

FIGURE 1
A phylogenetic tree among *Flavobacterium* sp. strain GJW24, diverse *Flavobacterium* type strains, and type strains from other genera in the family *Flavobacteriaceae*, based on their 16S rRNA gene sequences. The 16s rRNA sequences were obtained from LPSN and aligned with ClustalW running in the MEGA11 program. A rooted phylogenetic tree was generated with the MEGA11 using the maximum-likelihood method. The bootstrap method was performed to assess statistical significance of the tree using 1000 replicates. Bootstrap values (>50%) are indicated at the nodes.

Brassica increases the possibility that GJW24 may be utilized as a biological resource to facilitate plant growth under drought/salt stress condition.

GJW24 increases upregulation of a large portion of drought/salt/osmotic stress –inducible genes

To understand the action mechanism of GJW24 in drought/salt stress resistance in *Arabidopsis*, transcriptome sequencing analysis of *Arabidopsis* was performed in the presence and absence of GJW24. Among the 21,834 genes analyzed, the expression of 251 showed at least a two-fold increase in the GJW24-treated samples compared to the mock-treated samples (Tables 1, S2). To investigate characteristic biological attributes of the genes upregulated by GJW24 treatment, Gene Ontology (GO) analysis was done with the functional annotation tool on DAVID (https://david.ncifcrf.gov/tools.jsp), and the GJW24-upregulated genes were assigned to different categories for biological processes (BPs) (Figure 3A and Table S3) and molecular functions (MFs) (Figure 3B and Table S4). For BP, the genes were highly related to categories involved in root system architecture and development. Furthermore, GO terms related to 'response to stress' were notably enriched. To investigate whether the GJW24-conferred drought resistance phenotype in *Arabidopsis* is functionally associated with the altered expression patterns observed in GJW24-treated plants, the inducibility of GJW24-upregulated genes under drought stress was monitored using the database from the Arabidopsis eFP Browser (Winter et al., 2007). Based on information from the Arabidopsis eFP Browser, for each gene, the expression values from drought-treated samples (approximately 10% fresh weight loss) at various time points (0.25, 0.5, 1, 3, 6, 12 or 24 h) were divided by the values from untreated samples at the same time points. The maximum fold increase for each gene was then retrieved. Of the total 251 GJW24-specific genes, 100 (39.8%) exhibited increased expression patterns by more than twofold by drought stress, indicating that the application of GJW24 upregulated several drought-inducible genes (Tables 1, S2). Given that drought stress responses in plants largely overlaps with the responses to salt and osmotic stressors (Zhu, 2002), the inducibility of the GJW24-upregulated genes to salt and osmotic stress was also

10.3389/fpls.2023.1257137

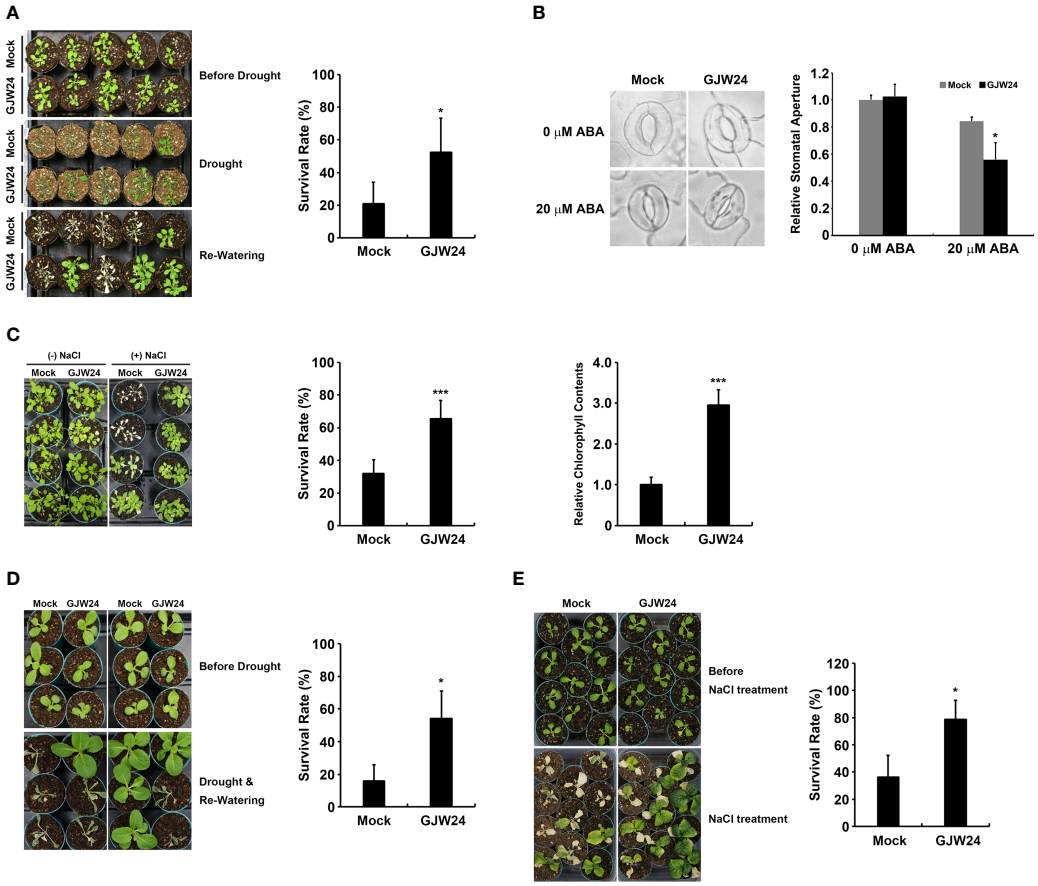

FIGURE 2
Phenotypic analysis of *Arabidopsis* and *Brassica* plants in response to drought and salt stressors in the presence and absence of GJW24. **(A)** Increased drought tolerance of *Arabidopsis*. Eight-day-old *Arabidopsis* plants were treated with mock or GJW24 and watered regularly for 1 week. The resulting plants were exposed to dehydration stress for 14 d, followed by re-watering for 4 (d) Error bars indicate the standard deviation (SD) of four biologically independent experiments. A Student's t-test was conducted to identify statistically significant differences; *P < 0.05. **(B)** Stomatal movements of *Arabidopsis* with or without GJW24, in the absence or presence of ABA. Eight-day-old *Arabidopsis* plants were treated with mock or GJW24. Seven days after treatment, detached leaves from mock- or GJW24-treated plants were prepared to measure the stomatal apertures in the absence or presence of ABA. Error bars indicate the SD of three biologically independent experiments (at least 40 stomata for each biological sample); *P < 0.05. **(C)** Enhanced salt resistance in *Arabidopsis* following GJW24 application. Eight-day-old plants were treated with mock or GJW24. Salt stress resistance was observed by introducing 50 mL of water or 150 mM NaCl solution to the soil 7 d after GJW24 treatment, three times for 6 d at 3-d intervals. The survival rates (n = 6) and the chlorophyll contents (n = 6) under salt stress were determined 3 and 4 d after the final salt treatment, respectively; ***P < 0.001. **(D)** Improved drought resistance in *Brassica* following GJW24 application. Eight-day-old *Brassica* plants were treated with mock or GJW24 and watered regularly for 1 week. The resulting plants were subjected to dehydration stress for 10 d, followed by re-watering for 6 (d) Error bars indicate the SD of four biologically independent experiments; *P < 0.05. **(E)** Enhanced salt tolerance in *Brassica* following GJW24 application. Ten-day-old *Brassica* plants were treated with mock or GJW24. Salt stress tolerance was observed by introducing 50 mL of water or 150 mM NaCl solution to the soil 7 d after mock or GJW24 treatment, eight times at 3-d intervals. The survival rates under salt stress were determined 1 d after the final salt treatment (n = 6); ***P < 0.001.

TABLE 1 Changes in expression patterns of abiotic stress-inducible genes following GJW24 application.

		Upregulated genes by GJW24 treatment[a]
Total number of genes		251
The number of genes induced by drought stress	More than two times[b]	100 (39.8%)
	More than five times[b]	36 (14.3%)
	More than ten times[b]	18 (7.1%)
The number of genes induced by salt stress	More than two times[b]	115 (45.8)
	More than five times[b]	53 (21.1%)

(Continued)

TABLE 1 Continued

		Upregulated genes by GJW24 treatment[a]
	More than ten times[b]	23 (9.1%)
The number of genes induced by osmotic stress	More than two times[b]	110 (43.8%)
	More than five times[b]	52 (20.7%)
	More than ten times[b]	30 (12.0%)

[a]Genes with increased expression rates by more than twofold in GJW24-treated samples compared to mock-treated samples.
[b]Increased gene expression rates following abiotic stress based on information from Arabidopsis eFP Browser. Detailed information is provided in Table S2.

investigated based on information from the Arabidopsis eFP Browser. For each gene, the expression values from 150 mM NaCl-treated samples (salt) at various time points (0.5, 1, 3, 6, 12 or 24 h) or 300 mM mannitol-treated samples (osmotic) at various time points (0.5, 1, 3, 6, 12 or 24 h) were divided by the values from untreated samples at the same time points. The maximum fold increase for each gene was then obtained. Similar to drought-inducible genes, 115 (45.8%) and 110 (43.8%) of the total 251 GJW24-specific genes exhibited upregulated expression of more than twofold by salt and osmotic stress, respectively (Tables 1, S2). Moreover, 47.9% (70 genes) of the 146 genes induced by drought, salt, or osmotic stress among the GJW24-upregulated genes were commonly upregulated by these three stressors (Figure 3C). Collectively, these findings indicate that GJW24 upregulated a large portion of drought- and drought-related stress-inducible genes in *Arabidopsis*. Previous researches have shown that drought resistance traits are functionally associated with the upregulation of drought-inducible genes in plants (Kim et al., 2020; Woo et al., 2020); therefore, GJW24-induced enhanced drought/salt stress tolerance may result from the overall enhancement of the upregulation of genes induced by drought and drought-related stressors. The GO analysis results revealed that the GJW24-upregulated genes were highly assigned to the categories related to root development. Several PGPR have been demonstrated to modify root system architecture and modulate root development (Vacheron et al., 2013; Zamioudis et al., 2013; Zhou et al., 2016), which supports our suggestion that GJW24 can play a role as a PGPR. Furthermore, many reports indicate that several PGPR involved in root development and growth contribute to enhanced plant drought stress tolerance (Cohen et al., 2015; Vurukonda et al., 2016; Jochum et al., 2019; Woo et al., 2020; Zia et al., 2021), showing that the GJW24-induced improvement of drought resistance may be associated with its possible role in root system architecture and development for efficient water uptake.

GJW24-mediated expression pattern of several drought- and drought-related stress-responsive genes in *Arabidopsis* and *Brassica*

The GJW24 treatment led to an overall enhancement of the upregulation of drought stress-inducible genes (Table 1). To confirm the list of GJW24-upregulated genes based on the information from the transcriptome sequencing analysis and their drought responsiveness using the Arabidopsis eFP Browser, several genes whose expression was increased by more than two folds by both GJW24 and drought stress were retrieved from Table S2, and their expression patterns were validated using qPCR (Figure 4A). The four selected genes, *MYB74*, *CRK36*, *SQP2*, and *YSL7*, showed similar GJW24- and drought-inducible patterns to those shown in the transcriptome sequencing analysis and the Arabidopsis eFP Browser database, supporting the reliability of the gene expression profiling results related to both GJW24- and drought-inducible genes (Figure 4A). Furthermore, GJW24 enhanced the upregulation of the selected genes under drought stress (Figure 4A). The expression levels of *PERK13*, *SLAH1*, *PGL4*, *YUC9*, and *ACS4*, which were selected from the list of GJW24- and salt-up-regulated genes, were also increased by GJW24 under salt stress (Figure 4B). Next, to determine whether the GJW24-induced drought- and salt-stress resistant phenotypes in *Brassica* were functionally connected to the expression of the corresponding stress-responsive genes, the expression patterns of drought- or salt-inducible genes in *Brassica* were examined with or without GJW24 treatment under stress conditions. GJW24 increased the expression of selected drought– (*BrEXLB1*, *BrDREB2A*, *BrTIFY3a*, *BraCSD3* and *Bra009300*) and salt–inducible genes (*BrRD29B*, *Bra034402*, *BrSR3*, *BrLAS* and *Bra005748*) in *Brassica* plants, similar to *Arabidopsis* (Figures 4C, D) (Yadav et al., 2015; Saha et al., 2016; Li et al., 2018; Yoon et al., 2018; Alam et al., 2019; Jin et al., 2019; Verma et al., 2019; Muthusamy et al., 2020). Collectively, these gene expression results indicate that GJW24 was involved in the upregulation of various drought- and salt-inducible genes in *Brassica* and *Arabidopsis*, suggesting that the modulation of drought and salt stress resistance by GJW24 may be achieved, at least in part, by regulating the expression of genes associated with drought and salt resistance in both plant species.

Conclusion

Compared to chemical fertilizers or pesticides, which cause environmental pollution, the use of environmentally friendly PGPR may contribute to improved plant growth in a more desirable manner. Here, GJW24 was selected from Gotjawal soil as a useful PGPR that increased the drought resistance of *Arabidopsis* and *Brassica*. Although the potential value of GJW24 as a biological agent in agriculture has been demonstrated in this study, the

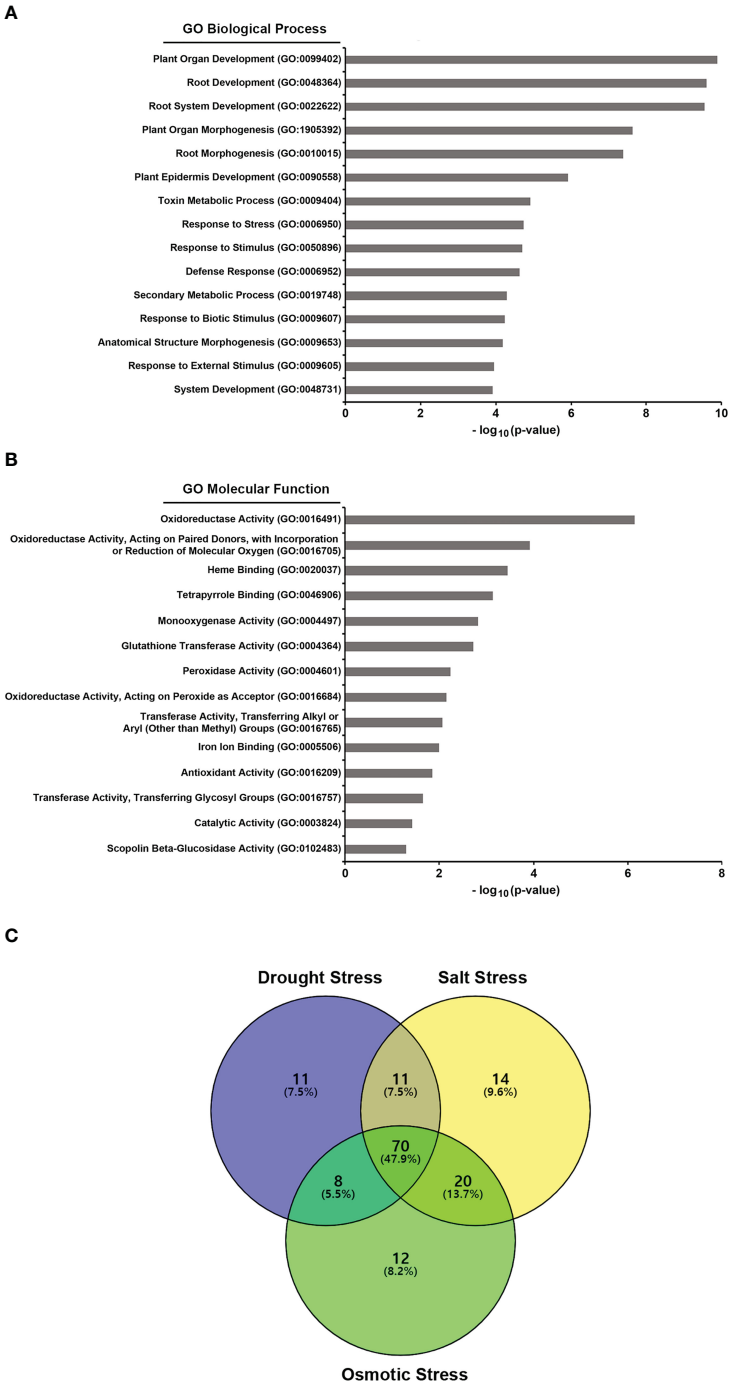

FIGURE 3
Gene ontology (GO) analysis of the GJW24-upregulated genes and Venn diagram of the genes induced by drought and drought-related stressors among the GJW24-upregulated genes. **(A, B)** GO analysis of biological processes **(A)** and molecular functions **(B)** for GJW24-upregulated genes. GO terms were identified by the functional annotation tool on DAVID. **(C)** Three-set Venn diagram of the overlap of drought stress-, salt stress- and osmotic stress-inducible genes in the GJW24-upregulated gene expression datasets. Among 251 genes that showed increased gene expression by at least twofold in the GJW24-treated samples, drought stress- (100 genes), salt stress- (115 genes), and osmotic stress-inducible genes (110 genes), which exhibited more than two-fold increases by each stressor (based on Arabidopsis eFP Browser) were retrieved and used generate Venn diagram. Courtesy: Oliveros, J.C. (2007-2015) Venny. An interactive tool for comparing lists with Venn diagrams: http://bioinfogp.cnb.csic.es/tools/venny/index.html.

detailed mechanism by which GJW24 enhances plant drought tolerance still requires further investigation. Given that various secondary metabolites and phytohormones (IAA, cytokinin, ABA, and GA) produced by PGPR have been reported to aid the adaptation of plants to abiotic stress conditions (Ma et al., 2020), predicting the list of secondary metabolites and phytohormones that GJW24 can produce from the whole genome sequencing of GJW24 may be useful for a better understanding of the function of

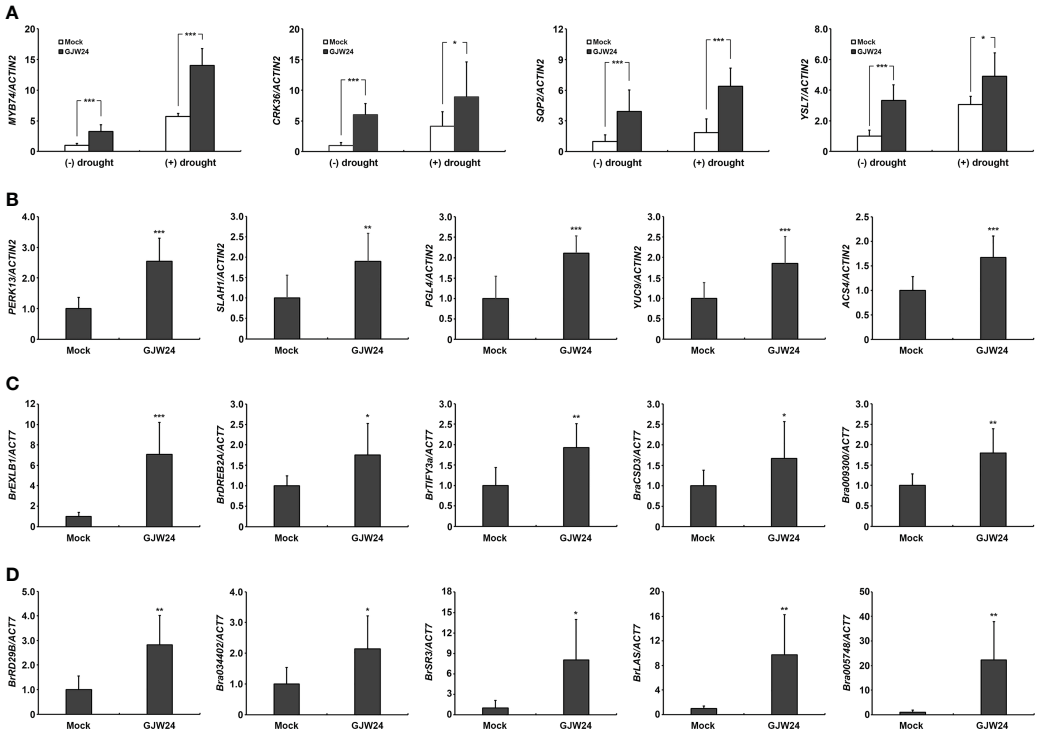

FIGURE 4
Induction of several drought- and salt-inducible genes in response to GJW24 treatment in *Arabidopsis* and *Brassica*. **(A)** Validation of the GJW24- and drought-upregulated genes from transcriptome sequencing analysis and Arabidopsis eFP Browser. Eight-day-old *Arabidopsis* seedlings were exposed to mock or GJW24. After 7 d, they were taken out of the pots in which they were growing. After checking the fresh weight, they were placed on filter paper until approximately 20% of their total fresh weight was lost or maintained without dehydration. The average expression value of each gene from mock-treated samples without drought stress was set to 1.0. Values indicate means ± SD ($n \geq 6$). A Student's t-test was conducted to identify statistically significant differences; *P < 0.05; ***P < 0.001. **(B)** Upregulation of various salt-inducible genes in *Arabidopsis* by GJW24 treatment under salt stress. Eight-day-old *Arabidopsis* seedlings were exposed to mock or GJW24. The salt stress resistance assay was conducted by adding 50 mL of 200 mM NaCl solution or water to the soil 7 d after mock or GJW24 treatment, twice at 3-d intervals for 3 (d) The samples were obtained 3 d after the last day of NaCl treatment. The average expression value of each gene from mock-treated samples was set to 1.0. Values indicate means ± SD ($n \geq 6$); **P < 0.01; ***P < 0.001. **(C)** Upregulation of various drought-inducible genes in *Brassica* by GJW24 treatment under drought stress. Eight-day-old *Brassica* seedlings were treated with mock or GJW24. After 7 d, they were taken out of the pots in which they were growing. After checking the fresh weight, they were placed on filter paper until approximately 20% of their total fresh weight was lost. Values indicate means ± SD ($n \geq 6$); *P < 0.05; **P < 0.01; ***P < 0.001. **(D)** Upregulation of various salt-inducible genes in *Brassica* by GJW24 treatment under salt stress. Eight-day-old *Brassica* seedlings were treated with mock or GJW24. The salt stress resistance assay was conducted by adding 50 mL of water or 300 mM NaCl solution to the soil 7 d after mock or GJW24 treatment, twice at a 3-day interval for 3 (d) The samples were obtained 3 d after the last day of NaCl treatment. Values indicate means ± SD ($n \geq 6$); *P < 0.05; **P < 0.01.

GJW24. The finding that several auxin- and ABA-responsive genes are included in the list of GJW24-upregulated *Arabidopsis* genes increases the possibility that GJW24 may utilize the regulation of plant hormone signaling as a strategy to confer drought tolerance in plants (Table S2).

Data availability statement

The data presented in this study are deposited in the NCBI repository (https://www.ncbi.nlm.nih.gov/), accession number OR272272.

Author contributions

HK: Conceptualization, Data curation, Funding acquisition, Investigation, Validation, Writing – review & editing, Formal Analysis. O-GW: Data curation, Formal Analysis, Investigation, Validation, Writing – review & editing, Writing – original draft. JBK: Data curation, Formal Analysis, Investigation, Validation, Writing – review & editing. S-YY: Data curation, Validation, Writing – review & editing. J-SK: Writing – review & editing, Resources. WJS: Writing – review & editing, Data curation, Formal Analysis. J-YH: Data curation, Formal Analysis, Writing – review & editing. J-HL: Data curation, Writing – review & editing, Conceptualization, Funding acquisition, Investigation, Project administration, Supervision, Validation, Writing – original draft.

Funding

The authors declare financial support was received for the research, authorship, and/or publication of this article. This research was supported by the Basic Science Research Program through the National Research Foundation of Korea (NRF),

funded by the Ministry of Education (NRF- 2020R1A6 A3A01100030 to HK and NRF-2021R1F1A1045505 to J-HL), by the LB692 Nebraska Biomedical Research Development Fund (to J-YH), and by the Strategic Initiative for Microbiomes in Agriculture and Food, Ministry of Agriculture, Food and Rural Affairs, Republic of Korea (916007021HD040 to J-HL).

Conflict of interest

The authors declare that the research was conducted in the absence of any commercial or financial relationships that could be construed as a potential conflict of interest.

Publisher's note

Supplementary material

The Supplementary Material for this article can be found online at: https://www.frontiersin.org/articles/10.3389/fpls.2023.1257137/full#supplementary-material

References

Alam, I., Cui, D. L., Batool, K., Yang, Y. Q., and Lu, Y. H. (2019). Comprehensive genomic survey, characterization and expression analysis of the HECT gene family in *Brassica rapa* L. and *Brassica oleracea* L. *Genes (Basel)* 10, 400. doi: 10.3390/genes10050400

Batool, T., Ali, S., Seleiman, M. F., Naveed, N. H., Ali, A., Ahmed, K., et al. (2020). Plant growth promoting rhizobacteria alleviates drought stress in potato in response to suppressive oxidative stress and antioxidant enzymes activities. *Sci. Rep.* 10, 16975. doi: 10.1038/s41598-020-73489-z

Beneduzi, A., Ambrosini, A., and Passaglia, L. M. (2012). Plant growth-promoting rhizobacteria (PGPR): Their potential as antagonists and biocontrol agents. *Genet. Mol. Biol.* 35, 1044–1051. doi: 10.1590/S1415-47572012000600020

Bharti, N., Pandey, S. S., Barnawal, D., Patel, V. K., and Kalra, A. (2016). Plant growth promoting rhizobacteria *Dietzia natronolimnaea* modulates the expression of stress responsive genes providing protection of wheat from salinity stress. *Sci. Rep.* 6, 34768. doi: 10.1038/srep34768

Bresson, J., Varoquaux, F., Bontpart, T., Touraine, B., and Vile, D. (2013). The PGPR strain *Phyllobacterium brassicacearum* STM196 induces a reproductive delay and physiological changes that result in improved drought tolerance in *Arabidopsis*. *New Phytol.* 200, 558–569. doi: 10.1111/nph.12383

Cohen, A. C., Bottini, R., Pontin, M., Berli, F. J., Moreno, D., Boccanlandro, H., et al. (2015). *Azospirillum brasilense* ameliorates the response of *Arabidopsis thaliana* to drought mainly via enhancement of ABA levels. *Physiol. Plant* 153, 79–90. doi: 10.1111/ppl.12221

Forni, C., Duca, D., and Glick, B. R. (2017). Mechanisms of plant response to salt and drought stress and their alteration by rhizobacteria. *Plant Soil* 410, 335–356. doi: 10.1007/s11104-016-3007-x

Gontia-Mishra, I., Sapre, S., Sharma, A., and Tiwari, S. (2016). Amelioration of drought tolerance in wheat by the interaction of plant growth-promoting rhizobacteria. *Plant Biol. (Stuttg)* 18, 992–1000. doi: 10.1111/plb.12505

Hussain, H. A., Hussain, S., Khaliq, A., Ashraf, U., Anjum, S. A., Men, S., et al. (2018). Chilling and drought stresses in crop plants: Implications, cross talk, and potential management opportunities. *Front. Plant Sci.* 9, 393. doi: 10.3389/fpls.2018.00393

Jin, L., Ouyang, N., Huang, Y., Liu, C., and Ruan, Y. (2019). Genome-wide analysis of sulfotransferase genes and their responses to abiotic stresses in Chinese cabbage (*Brassica rapa L.*). *PloS One* 14, e0221422. doi: 10.1371/journal.pone.0221422

Jochum, M. D., McWilliams, K. L., Borrego, E. J., Kolomiets, M. V., Niu, G., Pierson, E. A., et al. (2019). Bioprospecting plant growth-promoting rhizobacteria that mitigate drought stress in grasses. *Front. Microbiol.* 10, 2106. doi: 10.3389/fmicb.2019.02106

Khan, N., and Bano, A. (2019). Exopolysaccharide producing rhizobacteria and their impact on growth and drought tolerance of wheat grown under rainfed conditions. *PLoS One* 14, e0222302. doi: 10.1371/journal.pone.0222302

Kim, J. S., Kim, D. S., Lee, K. C., Lee, J. S., King, G. M., and Kang, S. (2018). Microbial community structure and functional potential of lava-formed Gotjawal soils in Jeju, Korea. *PLoS One* 13, e0204761. doi: 10.1371/journal.pone.0204761

Kim, D., Langmead, B., and Salzberg, S. L. (2015). HISAT: a fast spliced aligner with low memory requirements. *Nat. Methods* 12, 357–360. doi: 10.1038/nmeth.3317

Kim, J. E., Woo, O. G., Bae, Y., Keum, H. L., Chung, S., Sul, W. J., et al. (2020). Enhanced drought and salt stress tolerance in *Arabidopsis* by *Flavobacterium crocinum* HYN0056^{T}. *J. Plant Biol.* 63, 63–71. doi: 10.1007/s12374-020-09236-8

Lagercrantz, U., Putterill, J., Coupland, G., and Lydiate, D. (1996). Comparative mapping in *Arabidopsis* and *Brassica*, fine scale genome collinearity and congruence of genes controlling flowering time. *Plant J.* 9, 13–20. doi: 10.1046/j.1365-313X.1996.09010013.x

Lee, S. C., Lim, C. W., Lan, W., He, K., and Luan, S. (2013). ABA signaling in guard cells entails a dynamic protein-protein interaction relay from the PYL-RCAR family receptors to ion channels. *Mol. Plant* 6, 528–538. doi: 10.1093/mp/sss078

Lephatsi, M. M., Meyer, V., Piater, L. A., Dubery, I. A., and Tugizimana, F. (2021). Plant responses to abiotic stresses and rhizobacterial biostimulants: metabolomics and epigenetics perspectives. *Metabolites* 11, 457. doi: 10.3390/metabo11070457

Li, P., Zhang, B., Su, T., Li, P., Xin, X., Wang, W., et al. (2018). *BrLAS*, a GRAS transcription factor from *Brassica rapa*, is involved in drought stress tolerance in transgenic *Arabidopsis*. *Front. Plant Sci.* 9, 1792. doi: 10.3389/fpls.2018.01792

Liu, F., Xing, S., Ma, H., Du, Z., and Ma, B. (2013). Cytokinin-producing, plant growth-promoting rhizobacteria that confer resistance to drought stress in *Platycladus orientalis* container seedlings. *Appl. Microbiol. Biotechnol.* 97, 9155–9164. doi: 10.1007/s00253-013-5193-2

Ma, Y., Dias, M. C., and Freitas, H. (2020). Drought and salinity stress responses and microbe-induced tolerance in plants. *Front. Plant Sci.* 11, 591911. doi: 10.3389/fpls.2020.591911

Muthusamy, M., Kim, J. Y., Yoon, E. K., Kim, J. A., and Lee, S. I. (2020). *BrEXLB1*, a *Brassica rapa* Expansin-Like B1 gene is associated with root development, drought stress response, and seed germination. *Genes (Basel)* 11, 404. doi: 10.3390/genes11040404

Naseem, H., Ahsan, M., Shahid, M. A., and Khan, N. (2018). Exopolysaccharides producing rhizobacteria and their role in plant growth and drought tolerance. *J. Basic Microbiol.* 58, 1009–1022. doi: 10.1002/jobm.201800309

Pertea, M., Kim, D., Pertea, G. M., Leek, J. T., and Salzberg, S. L. (2016). Transcript-level expression analysis of RNA-seq experiments with HISAT, StringTie and Ballgown. *Nat. Protoc.* 11, 1650–1667. doi: 10.1038/nprot.2016.095

Pertea, M., Pertea, G. M., Antonescu, C. M., Chang, T. C., Mendell, J. T., and Salzberg, S. L. (2015). StringTie enables improved reconstruction of a transcriptome from RNA-seq reads. *Nat. Biotechnol.* 33, 290–295. doi: 10.1038/nbt.3122

Robinson, M. D., McCarthy, D. J., and Smyth, G. K. (2010). edgeR: a Bioconductor package for differential expression analysis of digital gene expression data. *Bioinformatics* 26, 139–140. doi: 10.1093/bioinformatics/btp616

Saha, G., Park, J. I., Kayum, M. A., and Nou, I. S. (2016). A genome-wide analysis reveals stress and hormone responsive patterns of TIFY family genes in *Brassica rapa*. *Front. Plant Sci.* 7, 936. doi: 10.3389/fpls.2016.00936

Schmittgen, T. D., and Livak, K. J. (2008). Analyzing real-time PCR data by the comparative C(T) method. *Nat. Protoc.* 3, 1101–1108. doi: 10.1038/nprot.2008.73

Shinozaki, K., and Yamaguchi-Shinozaki, K. (2007). Gene networks involved in drought stress response and tolerance. *J. Exp. Bot.* 58, 221–227. doi: 10.1093/jxb/erl164

Takahashi, F., Kuromori, T., Urano, K., Yamaguchi-Shinozaki, K., and Shinozaki, K. (2020). Drought stress responses and resistance in plants: From cellular responses to long-distance intercellular communication. *Front. Plant Sci.* 11, 556972. doi: 10.3389/fpls.2020.556972

Tamura, K., Stecher, G., and Kumar, S. (2021). MEGA11: molecular evolutionary genetics analysis version 11. *Mol. Biol. Evol.* 38, 3022–3027. doi: 10.1093/molbev/msab120

Uzma, M., Iqbal, A., and Hasnain, S. (2022). Drought tolerance induction and growth promotion by indole acetic acid producing Pseudomonas *aeruginosa* in *Vigna radiata*. *PLoS One* 17, e0262932. doi: 10.1371/journal.pone.0262932

Vacheron, J., Desbrosses, G., Bouffaud, M. L., Touraine, B., Moënne-Loccoz, Y., Muller, D., et al. (2013). Plant growth-promoting rhizobacteria and root system functioning. *Front. Plant Sci.* 4, 356. doi: 10.3389/fpls.2013.00356

Vejan, P., Abdullah, R., Khadiran, T., Ismail, S., and Nasrulhaq Boyce, A. (2016). Role of plant growth promoting rhizobacteria in agricultural sustainability-a review. *Molecules* 21, 573. doi: 10.3390/molecules21050573

Verma, D., Lakhanpal, N., and Singh, K. (2019). Genome-wide identification and characterization of abiotic-stress responsive *SOD* (*superoxide dismutase*) gene family in *Brassica juncea* and *B. rapa*. *BMC Genomics* 20, 227. doi: 10.1186/s12864-019-5593-5

Vurukonda, S. S., Vardharajula, S., Shrivastava, M., and SkZ, A. (2016). Enhancement of drought stress tolerance in crops by plant growth promoting rhizobacteria. *Microbiol. Res.* 184, 13–24. doi: 10.1016/j.micres.2015.12.003

Winter, D., Vinegar, B., Nahal, H., Ammar, R., Wilson, G. V., and Provart, N. J. (2007). An "Electronic Fluorescent Pictograph" browser for exploring and analyzing large-scale biological data sets. *PLoS One* 2, e718. doi: 10.1371/journal.pone.0000718

Woo, O. G., Kim, H., Kim, J. S., Keum, H. L., Lee, K. C., Sul, W. J., et al. (2020). *Bacillus subtilis* strain GOT9 confers enhanced tolerance to drought and salt stresses in *Arabidopsis thaliana* and *Brassica campestris*. *Plant Physiol. Biochem.* 148, 359–367. doi: 10.1016/j.plaphy.2020.01.032

Yadav, D., Ahmed, I., and Kirti, P. B. (2015). Genome-wide identification and expression profiling of annexins in *Brassica rapa* and their phylogenetic sequence comparison with *B. juncea* and *A. thaliana* annexins. *Plant Gene* 4, 109–124. doi: 10.1016/j.plgene.2015.10.001

Yoon, E. K., Krishnamurthy, P., Kim, J. A., Jeong, M. J., and Lee, S. I. (2018). Genome-wide characterization of *Brassica rapa* genes encoding serine/arginine-rich proteins: expression and alternative splicing events by abiotic stresses. *J. Plant Biol.* 61, 198–209. doi: 10.1007/s12374-017-0391-6

You, J., and Chan, Z. (2015). ROS regulation during abiotic stress responses in crop plants. *Front. Plant Sci.* 6, 1092. doi: 10.3389/fpls.2015.01092

Zamioudis, C., Mastranesti, P., Dhonukshe, P., Blilou, I., and Pieterse, C. M. (2013). Unraveling root developmental programs initiated by beneficial *Pseudomonas* spp. bacteria. *Plant Physiol.* 162, 304–318. doi: 10.1104/pp.112.212597

Zhou, C., Ma, Z., Zhu, L., Xiao, X., Xie, Y., Zhu, J., et al. (2016). Rhizobacterial strain *Bacillus megaterium* BOFC15 induces cellular polyamine changes that improve plant growth and drought resistance. *Int. J. Mol. Sci.* 17, 976. doi: 10.3390/ijms17060976

Zhu, J. K. (2002). Salt and drought stress signal transduction in plants. *Annu. Rev. Plant Biol.* 53, 247–273. doi: 10.1146/annurev.arplant.53.091401.143329

Zia, R., Nawaz, M. S., Siddique, M. J., Hakim, S., and Imran, A. (2021). Plant survival under drought stress: Implications, adaptive responses, and integrated rhizosphere management strategy for stress mitigation. *Microbiol. Res.* 242, 126626. doi: 10.1016/j.micres.2020.126626

frontiers | Frontiers in Plant Science

TYPE Original Research
PUBLISHED 29 November 2023
DOI 10.3389/fpls.2023.1237966

OPEN ACCESS

EDITED BY
Carlos Henrique Meneses,
State University of Paraíba, Brazil

REVIEWED BY
Katia Scortecci,
Federal University of Rio Grande do Norte, Brazil
Jean Luiz Simoes-Araujo,
Brazilian Agricultural Research Corporation (EMBRAPA), Brazil
David Johnston-Monje,
University of the Valley, Colombia

*CORRESPONDENCE
Omar Gätjens-Boniche
ogatjens@itcr.ac.cr

RECEIVED 10 June 2023
ACCEPTED 18 October 2023
PUBLISHED 29 November 2023

CITATION
Gätjens-Boniche O, Jiménez-Madrigal JP, Whetten RW, Valenzuela-Diaz S, Alemán-Gutiérrez A, Hanson PE and Pinto-Tomás AA (2023) Microbiome and plant cell transformation trigger insect gall induction in cassava. *Front. Plant Sci.* 14:1237966. doi: 10.3389/fpls.2023.1237966

Microbiome and plant cell transformation trigger insect gall induction in cassava

Omar Gätjens-Boniche [1]*, Jose Pablo Jiménez-Madrigal [1], Ross W. Whetten [2], Sandro Valenzuela-Diaz [3], Alvaro Alemán-Gutiérrez [1,4], Paul E. Hanson [5] and Adrián A. Pinto-Tomás [6]

[1]Laboratorio de Biología Molecular, Escuela de Ciencias Naturales y Exactas, Campus Tecnológico Local San Carlos, Instituto Tecnológico de Costa Rica, Alajuela, Costa Rica, [2]Department of Forestry and Environmental Resources, North Carolina State University, Raleigh, NC, United States, [3]Human Microbiome Research Program, Faculty of Medicine, The Helsinki University, Helsinki, Finland, [4]Laboratorio de Genómica y Biodiversidad, Facultad de Ciencias, Universidad del Bío-Bío, Chillán, Chile, [5]Escuela de Biología, Universidad de Costa Rica, San Pedro, San José, Costa Rica, [6]Center for Research in Microscopic Structures and Department of Biochemistry, School of Medicine, University of Costa Rica, San José, Costa Rica

Several specialised insects can manipulate normal plant development to induce a highly organised structure known as a gall, which represents one of the most complex interactions between insects and plants. Thus far, the mechanism for insect-induced plant galls has remained elusive. To study the induction mechanism of insect galls, we selected the gall induced by *Iatrophobia brasiliensis* (Diptera: Cecidomyiidae) in cassava (Euphorbiaceae: *Manihot esculenta* Crantz) as our model. PCR-based molecular markers and deep metagenomic sequencing data were employed to analyse the gall microbiome and to test the hypothesis that gall cells are genetically transformed by insect vectored bacteria. A shotgun sequencing discrimination approach was implemented to selectively discriminate between foreign DNA and the reference host plant genome. Several known candidate insertion sequences were identified, the most significant being DNA sequences found in bacterial genes related to the transcription regulatory factor CadR, cadmium-transporting ATPase encoded by the *cadA* gene, nitrate transport permease protein (*nrtB* gene), and arsenical pump ATPase (*arsA* gene). In addition, a DNA fragment associated with ubiquitin-like gene *E2* was identified as a potential accessory genetic element involved in gall induction mechanism. Furthermore, our results suggest that the increased quality and rapid development of gall tissue are mostly driven by microbiome enrichment and the acquisition of critical endophytes. An initial gall-like structure was experimentally obtained in *M. esculenta* cultured tissues through inoculation assays using a *Rhodococcus* bacterial strain that originated from the inducing insect, which we related to the gall induction process. We provide evidence that the modification of the endophytic microbiome and the genetic transformation of plant cells in *M. esculenta* are

two essential requirements for insect-induced gall formation. Based on these findings and having observed the same potential DNA marker in galls from other plant species (ubiquitin-like gene *E2*), we speculate that bacterially mediated genetic transformation of plant cells may represent a more widespread gall induction mechanism found in nature.

KEYWORDS

***Iatrophobia brasiliensis*, *Manihot esculenta*, plant galls, metagenomics, induction mechanism, genetic transformation, endophytes**

Introduction

Insect galls are abnormal structures developed by the presence and stimuli of insects in the host plant. Insect-induced plant galls are specialised plant tissues with an organised arrangement of cells and predetermined growth. The size, structure, and metabolism of galls are under the control of gall-forming insects and host plant species (Rohfritsch and Shorthouse, 1982; Leitch, 1994; Raman, 2011).

Insect gall tissues exhibit biochemical and cytological modifications that provide them with a higher nutritional quality than the surrounding plant tissue, thus facilitating a continuous source of food and additional benefits to the inducing insect (Koyama et al., 2004; Nabity et al., 2013; Ferreira et al., 2017). Most galls contain highly specialised tissue known as nutritive tissue, characterised by high concentrations of sugar (Nogueira et al., 2018), lipids, proteins, nitrogen, and a variety of other compounds (Shorthouse and Rohfritsch, 1992; Huang et al., 2015; Isaias et al., 2018).

The ability to induce galls in plants has emerged several times among and within insect orders, with representatives of gall-inducing species currently known in Diptera, Hymenoptera, Hemiptera, Coleoptera, Lepidoptera, and Thysanoptera (Mani, 1992; Espírito-Santo and Fernandes, 2007). In each order, the ability to form such structures appears to have an independent origin (Nyman and Julkunen, 2000; Ronquist et al., 2015).

In addition to insects, plant galls can be induced by mites and nematodes (Favery et al., 2016; de Lillo et al., 2018; Harris and Pitzschke, 2020; Olmo et al., 2020; Desnitskiy et al., 2023). Some fungi and bacteria species and even some viruses can also induce primary gall-like growths or, simply, neoplasm formation with low levels of cell differentiation (Ananthakrishnan, 1998; Raman, 2011; Gätjens-Boniche, 2019; Harris and Pitzschke, 2020). Examples of gall-like growths induced by microorganisms include *Agrobacterium tumefaciens* (crown gall), *Rhodococcus fascians*, *Pseudomonas savastanoi*, *Xanthomonas citri*, *Pantoea agglomerans*, *Taphrina betulina* (witches broom), and *Ustilago esculenta* (Swarup et al., 1991; Jump and Woodward, 1994; Chalupowicz et al., 2009; You et al., 2011; Dolzblasz et al., 2018; Harris and Pitzschke, 2020). Of these, *A. tumefaciens* is the best studied, as its habit of genetically transforming plant cells has found extensive use in plant biotechnology (Kavipriya et al., 2019; Song et al., 2019; Lian et al., 2022). Because *A. tumefaciens*-mediated genetic transformation of plant cells is the most understood mechanism of plant gall formation (Chou et al., 2022; Hopp et al., 2022; Azizi-Dargahlou and Pouresmaeil, 2023), this constitutes the best referenced system to propose alternative induction mechanisms in which complex gall formation caused by insects such as cynips (Hymenoptera) and cecidomyiids (Diptera) (Sinnott, 1960; Raman, 2011) is also the result of a based plant cell genetic transformation.

A large number of endosymbiotic bacteria in different insect groups, including gall-inducing insects, have been reported in several studies (Campbell et al., 2015; El-Sayed and Ibrahim, 2015; Gutzwiller et al., 2015; Michell and Nyman, 2021; Yang et al., 2021; Coolen et al., 2022; Yang et al., 2022). Insect-associated microorganisms could be important mediators of interactions between insects and plants (Hammer and Bowers, 2015; Sugio et al., 2015; Wielkopolan and Jakubowska, 2021; Coolen et al., 2022). Symbiotic relationships between inducing insects and microorganisms have been hypothesised to be involved in plant gall development (Hansen and Moran, 2014; Tooker and Helms, 2014; Gätjens-Boniche, 2019; Klimov et al., 2022). Delivery of bacteria under natural or artificial conditions by insect vectors has been reported in many insect–plant interactions (Zeidan and Czosnek, 1994; Galambos et al., 2021; Wielkopolan and Jakubowska, 2021; Ratcliffe et al., 2022). Insect-vectored bacteria in plants have been described in well-known systems such as the Huanglongbing (HLB) disease of citrus caused by the phytopathogenic bacterium Candidatus *Liberibacter asiaticus* (CLas), which is transmitted by the psyllid *Diaphorina citri*. Likewise, acquisition and effective delivery of *A. tumefaciens* by the whitefly *Bemisia tabaci* was demonstrated by Zeidan and Czosnek (1994).

It has been hypothesised that phytohormone elicitor molecules delivered by the insect inducer (Rohfritsch and Shorthouse, 1982; Tooker and Helms, 2014; Ponce et al., 2021) or indirectly by an associated microorganism (Giron et al., 2013; Bartlett and Connor, 2014; Giron et al., 2016), and effector proteins secreted by the gall-inducing insect (Zhao et al., 2015; Cambier et al., 2019; Zhao et al., 2019; Korgaonkar et al., 2021) may be the main triggering stimuli responsible for the gall induction process.

Cassava (*Manihot esculenta* Crantz) is a widely cultivated crop in Africa, Asia, and Central and South America that provides an important food source for millions of people worldwide. Cassava plants can be grown yearlong in the tropics. Moreover, it can be

easily propagated in greenhouse and *in vitro* conditions. Owing to its versatility and potential, plant breeding programmes and international consortiums have invested significant resources in understanding cassava genetics. This has led to the creation of genetic linkage maps and chromosome-scale genome assembly (Wang et al., 2014; ICGMC (International Cassava Genetic Map Consortium), 2015; Lyons et al., 2022). Cassava plants are subject to gall formation, particularly cylindrical galls induced by the Cecidomyiidae, *Iatrophobia brasiliensis* (Montaldo, 1977; Rivera Hernández, 2011). However, detailed studies are lacking on the induction and formation processes of this gall.

Here, we tested the hypothesis proposed by Gätjens-Boniche (2019), who postulated that characteristic hyperplasia in the initial phase of gall induction can be triggered by the insertion of exogenous genetic elements into the genome of plant cells through an endosymbiotic bacterium originating from the inducing insect. To test this hypothesis, we employed a combination of genetic marker analyses, metagenomic analyses, and experimental gall induction in cassava plants. Taken together, our findings provide support for the role of microorganisms and genetic transformation in gall induction mechanisms.

Materials and methods

Galling insect model

We chose the cylindrical gall induced in Euphorbiaceae *M. esculenta* Crantz (cassava) (Figure 1A) by the Cecidomyiidae *I. brasiliensis* (Montaldo, 1977; Rivera Hernández, 2011) as our biological model (Figure 1B). The cassava genome has been well documented (Wang et al., 2014; ICGMC (International Cassava Genetic Map Consortium), 2015; Lyons et al., 2022), allowing the identification of potential alterations or insertions from exogenous sources.

Additionally, six prosoplasmic gall morphotypes (greater structural complexity) and two kataplasmic galls (low structural complexity) were selected to validate the general induction hypothesis (Figure 1D). For details, see Supplementary Text.

Samples were obtained from several plant specimens collected in the Guanacaste Conservation Area, Guanacaste, Costa Rica, as well as around the Santa Clara community, San Carlos, Alajuela, Costa Rica. A voucher specimen of each host plant species and galls was deposited at the Cecidiarium (specialised gall herbarium), established at the Instituto Tecnológico de Costa Rica.

Microdissection of salivary glands from *Iatrophobia brasiliensis* larvae

Larval salivary glands from *I. brasiliensis* were extracted by microdissection in a biosafety flow-hood (High Ten, Model 3BH-24), under sterile conditions (Figure S1). Larvae were surface decontaminated according to the protocol established by Zahner et al. (2008) with some modifications. Consecutive rinses were done for 2 min in 3% sodium hypochlorite and then 70% ethanol, followed by a rinse in sterile nuclease-free water. All dissected salivary glands were collected and employed in the DNA extraction. All life stages were surface cleaned.

Isolation and characterisation of endosymbiotic insect bacteria

Two colony-forming units (CFUs) were preliminarily isolated from the larval head of *I. brasiliensis* under sterile conditions. The dissected larvae were in instars one or two. The larvae were extracted live from the inner chamber of the gall, and only active larvae were collected. Different parts of the larva, such as the head and segments of the digestive system, were placed in YEB 1× culture medium (Piñol et al., 1996) to obtain a primary bacterial culture. Serial dilutions were made from the original culture to obtain single colonies (CFUs). The cells were recovered and maintained in YEB 1× solid and liquid suspension to 4–8°C and in glycerol (20% w/v) at −80°C. Each of the CFUs was named isolated symbiotic bacteria (ISB).

ISB 2 formed short rods and macroscopically coccoid-like elements and produced round, entire, convex, orange/pinkish colonies with smooth matte surfaces on YEB 1× Bacto agar medium after 4–5 days of incubation at 26°C. The bacterium showed features of a pinkish, flat, circular, slightly irregular border, variable length with curved shapes in some of them, and a mucous texture; it was a Gram-positive bacillus (Figure S2).

Molecular characterisation of bacteria was done through 16S sequencing using the procedures described by Rainey et al. (1996) and Hanshew et al. (2013), with some modifications. Taxonomic identification of the endosymbiotic bacteria was done using Kraken2 (Wood et al., 2019), the same for the endophytic bacteria, as described later. Details of the analytical pipeline are described below. Bacterial strains were identified by 16S gene sequencing before each inoculation assay to induce gall formation in the selected cassava tissues. We prepared templates for PCR either by total DNA extraction or by lysis of CFU bacteria growing in a solid culture medium. Bacterial cells were diluted in Elution Buffer (10 mM Tris, pH 8.0) (Qiagen, Hilden, Germany). Samples were lysed by vortexing and heating at 95°C for 5 min. The filtrate was then centrifuged at 8,000 *g* for 5 min.

Isolation of culturable microorganisms associated with plant gall tissue

We isolated CFUs that potentially represent endophytic bacterial strains and one fungal growth from surface-sterilised internal sections of *M. esculenta* gall tissue sections. Seven were selected for high-throughput sequencing (HTS). Each of these CFUs was named an isolate of endophytic bacteria (IEB).

Surface tissue was sterilised following the methodology described for DNA purification. CFUs grown directly from gall slice explants were carefully collected by a sterile bacteriological

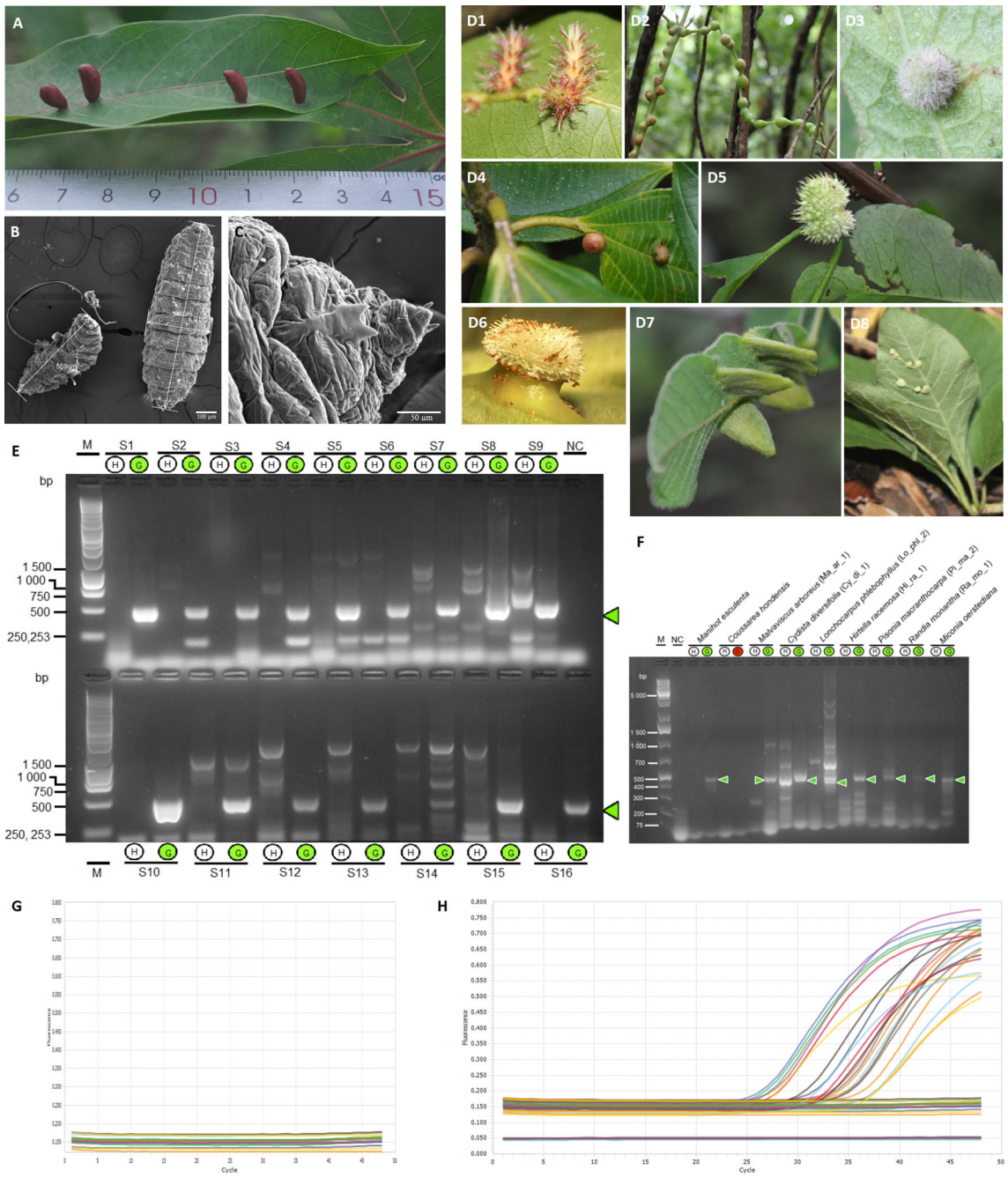

FIGURE 1
Identification of a potential universal marker in different gall systems. **(A)** Gall induced by the Cecidomyiidae *Iatrophobia brasiliensis* in *Manihot esculenta* (Montaldo, 1977). **(B)** Scanning electron micrograph of *I. brasiliensis* larva. **(C)** Scanning electron micrograph of the ventral area near the head of *I. brasiliensis* larva. **(D1)** Gall induced in *Hirtella racemosa* Lam. (Chrysobalanaceae), morphotype Hi_ra_1, by an unidentified Cecidomyiidae. **(D2)** Gall induced in *Cydista diversifolia* (Kunth) Miers (Bignoniaceae), morphotype Cy_di_1 by an unidentified Cecidomyiidae. **(D3)** Gall induced in *Malvaviscus arboreus* Dill. ex Cav. (Malvaceae), morphotype Ma_ar_1, by an unidentified Cecidomyiidae. **(D4)** Gall induced in *Miconia oerstediana* (Melastomataceae) by an unidentified Cecidomyiidae. **(D5)** Gall in *Pisonia macranthocarpa* (Donn. Sm.) Donn. Sm. (Nyctaginaceae), morphotype Pi_ma_4, induced by an unknown insect species. **(D6)** Gall in *Coussarea hondensis* (Standl.) C.M. Taylor & W.C. Burger (Rubiaceae) induced by an unknown insect. **(D7)** Gall induced in *Lonchocarpus phlebophyllus* Standl & Steyerm. (Fabaceae), morphotype Lo_phl_1, induced by a Psyllidae. **(D8)** Gall induced in *Randia monantha* Benth. (Rubiaceae), morphotype Ra_mo_1, induced by an unknown insect species. **(D2–D8)** Gätjens-Boniche et al. (2021). **(E)** Agarose gel electrophoresis of DNA fragments (specific gall fragment marker, SGF) amplified by PCR, comparing healthy leaf tissue DNA samples **(H)** and gall tissue DNA samples **(G)**. Lane M, molecular weight marker (1 kb ladder); line NC, negative control (reagents only); lines S1–S16, samples of healthy leaf and gall tissues growing in the same plant organ (pair-compared). **(F)** Gel electrophoresis of PCR products using primers for the specific gall fragment marker (SGF) in gall morphotypes of different host plant species. Lane M, molecular weight marker (Gene Ruler 1 KB Plus); line NC, negative control (reagents only); lines 3–20, samples of healthy leaf and gall tissues of different plants growing in the same plant organ (pair-compared). The green circle indicates a positive sample for the specific gall fragment amplification **(E, F)**. **(G, H)** Real-time PCR by Taq Man Probe showing the detection of the specific gall fragment from gall DNA samples of *Manihot esculenta* (amplification plot H) and from healthy leaf samples (amplification plot G). Each trace shows the ΔRn (normalised net fluorescence signal of the PCR product) plotted against the number of PCR cycles.

loop in a sterile biosafety chamber. Primary cultured bacteria were diluted in liquid medium YEB 1× (Piñol et al., 1996) until CFUs were obtained on solid medium. This process was repeated two to three times. Bacteria in cultured media were grown for 3–4 days at 26°C. Subsequently, bacterial cells were recovered and maintained in YEB 1× solid medium and suspended in liquid medium YEB 1× at 4–8°C and in glycerol (20% w/v) at −80°C.

DNA purification

Isolation of total genomic DNA from plant tissues

All tissues were sampled from plants morphologically identifiable as *M. esculenta*. Healthy leaf tissue from *M. esculenta* was checked in a stereoscope to avoid visible microgalls or some other type of foliar damage or disturbance. Prior to DNA extraction, the galls were dissected by carefully splitting them in half without damaging the larva present in the internal chamber, which was removed from the tissue. Healthy leaves and galls were washed with alkaline liquid soap and Triton X-100 detergent (dissolved in sterile water). The plant material was vortexed three times with 70% ethanol (v/v) and sterile water. Subsequently, the leaves and galls were surface sterilised according to the methodology suggested by Meyer and Hoy (2008) and Mueller et al. (2004), with some modifications. Plant materials were immersed for less than 30 s in sodium hypochlorite sequential solutions (3% NaOCl, 6% NaOCl, and 3% NaOCl) and rinsed with sterile water. The sterilisation process was conducted in a biosafety flow-hood (High Ten, Model 3BH-24). After cleaning and sterilisation, all samples were immediately stored at −80°C until DNA extraction.

Genomic DNA extraction was performed according to the methodology established by Dellaporta et al. (1983), with modifications and following column precipitation steps as described by the Dneasy Power Plant Pro Kit protocol (Mobio/QIAGEN, Carlsbad, CA, USA). The phenolic separation solution (PSS) in the Dneasy Power Plant Pro Kit was used during maceration to avoid DNA methylation. Total genomic DNA was extracted from both healthy leaf and gall tissues (different morphotypes). In the case of galls, DNA samples were collected from individual and pooled galls growing on the same leaf.

Genomic DNA isolation from salivary glands of inducing insects, *Iatrophobia brasiliensis*

Larval samples for DNA extraction were collected by dissecting galls from *M. esculenta*. Pools of 10 larvae of *I. brasiliensis* were decontaminated by being exposed to 3% NaOCl for 3–4 min, followed by successive 70% alcohol and water rinses under a biosafety flow-hood (High Ten, Model 3BH-24). Genomic DNA purification from the salivary glands of the insect larvae was performed using the Power Soil DNA Isolation Kit (Mobio/QIAGEN, Carlsbad, CA, USA) with the additional steps, mainly K proteinase (100 mg/mL) treatment and incubation at 65°C for 1 h. Furthermore, salivary gland DNA samples were extracted three times with phenol-chloroform isoamyl alcohol (PCI).

DNA isolation from endophyte and putative insect endosymbiotic bacteria

Total genomic DNA from endosymbiotic bacteria isolated from *I. brasiliensis* insects was extracted using a Dneasy Blood and Tissue Kit (Qiagen, Hilden, Germany). The same DNA extraction protocol was used for endophytic bacteria strains grown from surface-sterilised internal sections of *M. esculenta* gall tissue sections. Plasmid DNA from the isolated bacteria strains was carried out by alkaline lysis, as described by Li et al. (1995) with some modifications. The integrity and yield of bacterial genomic DNA and wild-type plasmids were checked by 0.8% agarose gel electrophoresis.

For all genomic DNA samples (plant, insect, and bacteria), quality was assessed by 260/280 and 260/230 ratios measured on a NanoDrop 8000 Spectrophotometer (Thermo Scientific, Wilmington, DE, USA).

Modified RAPD methodology for discovering gall-associated molecular markers

Samples of healthy leaf and gall tissues growing in the same plant organ were compared to detect differentially amplified DNA fragments in the DNA of the gall and not present in the same healthy tissue. The theoretical approach of this methodology is shown in Figure S3A. Assays were made under standard RAPD methodology conditions with the commercial random primers OPC-06, OPI-04, OPA-03, OPD-18, OPD-03, OPE-06, OPA-17, and OPB-04 (Operon Technologies, Alameda, California, USA). In these analyses, a modified methodological approach was also carried out by simultaneously using a combination of two non-random primers of conserved sequences from *A. tumefaciens* genes along with a non-standard RAPD thermal profile. Primers from conserved *A. tumefaciens* genes were used because the genetic transformation of plant cells mediated by this bacterium is the best-studied genetic transformation in a plant system. Decamer primers derived from conserved sequences of the Isopentyl Transferase Gene (ipt) and from the iaaM gene (Tryptophan 2-monooxygenase) harboured in the transfer DNA of the Ti plasmid of *Agrobacterium* species generated the highest number of differentially amplified fragments in previous RAPD assays. Primers were designed from the alignment of conserved regions in different species that harbour these genes using DNA Star Lasergene 99 (Madison, Wisconsin, USA) and BioEdit version 4.8.10.1 (Hall, 1999). Nucleotide sequences for these genes were obtained from the National Center for Biotechnology Information (www.ncbi.nlm.nih.gov/pubmed/). Accessions for the iaaM genes were M91609, Z18270, X77327, U04358, and L33867, and for the ipt genes, they were X77327, X53945, X17428, M91610, and Z46375. RAPD reactions were performed on 200-µL sterile, pyrogen-safe, thin-walled plastic tubes for PCR RNase-DNase (Axygen, CA, USA), using 0.5 units of Dream Taq (Fermentas Life Sciences, Lithuania), PCR 1× (750 mM Tris-HCl [pH 8.8], 0.2 mM dNTPs, 1.5 mM $MgCl_2$, 0.5 µM of each primer, and 10 ng of

DNA), adjusted to a final volume of 25 µl with nuclease-free sterile water (Promega Corporation, Madison, Wisconsin, USA). The primer set used was ipt forward, 5′-CGGTGAACGA-3′ and iaaM reverse, 5′-TCCAATTTCT-3′. DNA was initially denatured for 3.5 min at 95°C, followed by 15 cycles of 95°C for 30 s, 34.5°C for 30 s, and 72°C for 2 min. This was followed by 35 cycles of 30 s denaturation at 95°C, 30 s annealing at 46°C, and 2 min elongation at 72°C, with a final elongation step of 72°C for 7 min. Reactions were carried out in a thermocycler PTC-200 DNA Engine (MJ-Research, Waltham, Massachusetts, USA). Samples of healthy and gall tissues growing in the same plant were compared in pairs. Each primer set and RAPD condition was carefully tested more than three times using 20 to 30 samples. Reactions were performed in a flow-hood (High Ten, Model 3BH-24).

RAPD products were analysed by 1%–1.5% agarose gel electrophoresis with 0.5 × TBE and 1× Gel Red at 75 V (Electrophoresis chamber and Power Pac 300 Bio-Rad, Hercules, California, USA). Amplicons were separated in a MultiNA automated system for DNA and RNA microchip analysis (MultiNA-Shimadzu, Tokyo, Japan). PCR products were cleaned using Promega Wizard SV gel and the PCR clean-up system, as per the manufacturer's directions (Promega, Madison, WI).

The DNA gall fragments differentially amplified from the insect gall tissue of cassava by modified RAPD methodology were sequenced at the Centro de Investigaciones en Biología Celular y Molecular, Universidad de Costa Rica, San José, Costa Rica. Sequencing reactions were performed using dideoxynucleotide chain termination with the BigDye™ Terminator Kit (Applied Biosystems, USA) and 5 pmol of each ipt forward and iaaM reverse sequencing primers and analysed with an ABI Prism® 3700 Automated Sequencer (Applied Biosystems, USA). Sequenced fragments were aligned using DNA Star Lasergene 99 (Madison, Wisconsin, USA) and BioEdit version 4.8.10.1 (Hall, 1999).

PCR amplification and sequencing for the specific gall marker

The DNA gall fragments differentially amplified from gall samples were used as templates to design a potential gall molecular marker based on our RAPD results. Primers were designed using Primer3 v.4.1.0 (Koressaar and Remm, 2007; Untergrasser et al., 2012). The primer sequences were 5′-CTT GAC ATG TTC TGG AGC GG-3′ for the forward primer (Primer_Gall-Forward) and 5′-AAC GAG CGT GGT ACT GTG AT-3′ for the reverse primer (Primer_Gall-Reverse) (Invitrogen, Carlsbad, CA, USA). The expected amplicon size was 471 bp. Primers were tested with DNA samples from both healthy and gall tissues from *M. esculenta* plants and other gall morphotypes, as well as with DNA extracted from insect salivary glands. Subsequently, the target gene was amplified in the isolated wild-type plasmids from two putative insect endosymbiotic bacteria of the genus *Rhodococcus* and *Pseudomonas* and in wild-type plasmids of all endophytic bacteria isolated from the cassava gall tissue. PCR was carried out with 1× PCR buffer (750 mM Tris-HCl [pH 8.8], 200 mM $(NH_4)_2SO_4$, and 0.1% Tween 20), 1.5 mM $MgCl_2$, 0.2 mM dNTPs, 2 U Taq Polymerase (Thermo Fisher Scientific, Wilmington, DE, USA), 0.5 µM forward and reverse primers (Invitrogen, Carlsbad, CA, USA), 10 ng of sample DNA, and H_2O (Promega Corporation, Madison, Wisconsin, USA) for a final reaction volume of 25 µL. Amplification was performed in a thermal cycler PTC-200 DNA Engine (MJ-Research, Waltham, Massachusetts, USA) using the following cycling conditions: initial denaturation at 95°C for 3,5 min.; 40 cycles of 95°C for 30 s, 62°C for 45 s, and 72°C for 1 min; and final extension at 72°C for 5 min. The transition temperature between each step was 1°C/s. The assays were repeated multiple times for 170 galls and healthy tissue samples. Three samples with varying amounts of salivary glands were used in total, as were two bacterial plasmid samples. PCR reactions for these samples were repeated at least six times.

The PCR products were separated on a 1.5% agarose gel with 1 × TAE and 1× Gel Red at 75 V (Electrophoresis chamber and Power Pac 300 Bio-Rad, Hercules, California, USA). The expected amplicons were excised from the gel and purified using the QIAquick Gel Extraction Kit, following the manufacturer's directions (QIAGEN, Hilden, Germany). Samples were sequenced using the Sanger method through a Macrogen service provider (Macrogen Inc., Seoul, Korea). Samples were purified and prepared for sequencing according to the methodology established by Macrogen. Sequencing of nonspecific amplified fragments for PCR was attempted; however, good quality and long base sequences could not be obtained, except for two of the samples. Sequenced fragments were aligned using DNA Star Lasergene 99 (Madison, Wisconsin, USA) and BioEdit version 4.8.10.1 (Hall, 1999).

All amplified fragments were aligned to the SGF consensus sequence using BioEdit version 4.8.10.1 (Hall, 1999) and Jalview version 2-a, 2.11.1.5 (Waterhouse et al., 2009). For salivary gland amplified fragments, an overlap of bases was frequent in several of the sequenced PCR fragments, which could show variants of the target DNA sequence in this insect tissue. A similar trend was observed in one of the colonies from endosymbiont *Rhodococcus* isolated from the inducer insect when their wild-type plasmids were analysed and linked to the DNA amplification profile, which could indicate polymorphic variants of their wild-type plasmids.

Both DNA fragments amplified from gall samples (RAPD modified technique) and the SGF were analysed using BLAST [National Center for Biotechnology Information (NCBI) (www.ncbi.nlm.nih.gov/pubmed/), Integrated Microbial Genomes & Microbiomes (IMG/M) system (https://img.jgi.doe.gov)].

Detection of the specific gall fragment by real-time qPCR

A real-time PCR marker was designed and tested in healthy and gall tissue using a TaqMan probe with homology to the consensus of differentially amplified DNA from galls. TaqMan-based qPCR was carried out in a 20-µL reaction mixture containing Go Taq Master Mix 2X (Promega, USA) and 1µL of 20X TaqMan®Gene Expression Primer/Probe Mix (Applied Biosystem, CA, USA).

Primers and the TaqMan probe were designed and synthesised from the specific gall fragment target with 0.5 µM of each primer (AI7ZYBP_Forward: 5′-TGTTCGCTGCACAGAGTTCT-3′ and AI7ZYBP_Reverse: 5′-GGCTTGAGTGCTTCGATTTCG-3′), 0.25 µM of the MGB probe, labelled with FAM reporter dye at the 5′ and non-fluorescence Quencher TAMRA at the 3′ end (AI7ZYBP_M_TCTGCCACCGGACCCT_NFQ), and 2.5µL of 5 ng/µL of extracted DNA. qPCR cycling conditions included initial denaturation at 95°C for 3 min and 35 cycles of denaturation at 95°C for 30 s and primer annealing and extension steps together at 60°C for 60 s. Three replicates of the negative template control consisting of nuclease-free water for molecular biology grade reactions were included in each amplification assay. Assays were performed on a LightCycler 96 Real-Time PCR System (Roche Diagnostics, Risch-Rotkreuz, Switzerland). We tested over 30 healthy tissue and gall samples and obtained an amplification average of 90% for the PCR marker or amplification signal in the case of qPCR. The assays were repeated more than six times for the same healthy leaf and gall samples.

Bioinformatic analysis

Library preparation and sequencing

Short-read libraries were prepared using Illumina's DNA TruSeq Nano Library preparation kit, following the manufacturer's instructions. For the leaf and gall genomic DNA samples, 150-bp single-ended (SE) libraries were prepared and sequenced on the Illumina HiSeq2500 platform using the SBS sequencing kit version 4. For the bacterial isolates' genomic DNA samples, 250-bp paired-ended (PE) libraries were prepared and sequenced in the Illumina MiSeq platform using Reagent kit version 2. Both library preparation and next-generation sequencing were performed by the NC State University Genomic Sciences Laboratory (Raleigh, NC, USA). Raw data can be retrieved from the Short Read Archive (SRA) under the Bioproject accession number: PRJNA905450.

No sequencing was performed for any endosymbiotic or endophytic bacteria wild-type plasmids due to the stability and integrity of the plasmid DNA during the fragmentation procedure.

Host discriminant genomic analysis

The aim of this analysis was to identify potential genes or insertion sequences from bacteria in the cassava genomic DNA samples (genotype Valencia); these sequences were believed to induce gall formation in otherwise healthy plants. To do so, a stepwise filtering strategy was implemented. First, sequence read quality was assessed with FastQC (Andrews, 2010); when needed, index, adapters, and low-quality sequences were eliminated. After quality control, reads from both healthy and gall tissues were mapped against the cassava reference genome CV AM560-2 (Phytozome genome ID: 520; Bredeson et al., 2016) using BBmap, part of the BBTools suite (Bushnell, 2015), with the semiperfect mode option. Unmapped reads from healthy leaf tissue and leaf galls were compared against each other, and the shared reads were filtered using BBduk, part of the BBTools suite. The remaining gall reads, unmapped to the reference genome and unmatched to healthy leaves according to defined parameters, were *de novo* assembled into contigs using SPAdes (Prjibelski et al., 2020). A MegaBlast of the selected contigs was performed, setting the minimum length to 200 bp and the percentage of homology to ≥95%. The resulting contigs, the product of gall exclusive reads, were then mapped against the cassava reference genome using the Burrows–Wheeler Aligner (BWA-MEM) (Li and Durbin, 2009). Alignments with low mapping quality (≥20) were filtered using SAMtools (Li et al., 2009). Contigs with matching sequences in either their 5′, 3′, or both ends but non-matching sequences in their core, based on the CIGAR string, were selected as potential foreign DNA insertion sites. Reads were mapped back to the gall hybrid/fusion contigs containing potential foreign DNA insertion sites to assess coverage. Contigs with less than three cover reads were discarded, except for three of them that showed significant annotations with known gene sequences.

We also analysed the putative gall insertion sequence marker (named gall fragment) experimentally in plasmids isolated from all seven isolated endophytic bacteria and the two bacteria isolated from the larval insect head of *I. brasiliensis* and *in silico* by bioinformatic tools in the assembled genomes of the same sequenced bacteria species. In particular, for the *in silico* analysis, isPCR and the primer sequences designed for the gall fragment marker did not show any amplification from the cassava reference genome, nor did it produce amplification products for the insect endosymbiotic bacteria genomes.

Metagenomic sequence analysis and taxonomic profile assignment

Shotgun metagenomic sequencing approach was used to analyse the microbiome associated with cassava galls and healthy leaf tissues. Taxonomic profiles were performed using Kraken2 (Wood et al., 2019) and its standard database, which includes bacteria, archaea, viruses, and eukaryotic genomes (https://benlangmead.github.io/aws-indexes/k2). Analyses were applied to reads data (QC filtered reads) from the sequenced gall and healthy tissue samples with an abundance filter of 10K reads.

Taxonomic profiles were also carried out to identify unique reads in the gall tissue following the host discriminant genomic analysis (HDGA) methodological approach to determine their taxonomic origin. Reads were mapped against the cassava genome, retaining only unmapped reads. We then clustered the sequences to obtain unique reads by sample only. This finding was further confirmed by contrasting the resulting taxonomic profiles of healthy samples with gall samples.

After a detailed analysis of the taxonomic profiles was carried out to identify the likely contaminants introduced during processing or due to any potential contaminant event during the final stage of DNA purification of cassava healthy leaves and gall samples, five bacteria taxa were removed as possible external contamination in all sequenced samples.

Bacteria endophytic condition determination by synteny analysis

We applied synteny bioinformatic analysis to confirm whether isolated bacteria from both gall tissue and the inducing insect were components of the endophytic microbiome in this structure. To carry out this analysis, exclusive gall reads and bacteria samples were *de novo* assembled using SPAdes (Bankevich et al., 2012) in their metagenome mode for gall reads and isolate mode for bacteria samples. To confirm synteny, contigs from both sides were compared using BLAST+ (Camacho et al., 2009).

Genome annotation and functional analyses

To analyse potential differences in terms of function in bacterial groups (endophytic vs. endosymbiont), an enrichment analysis was performed using the Gene Ontology (GO) terms included in the TopGO R package (Alexa, 2022) and a cluster of gene ontology approach (COG) (Galperin et al., 2019). To carry out the analysis, bacterial genomes previously assembled were annotated using prokka (Seemann, 2014). To obtain their corresponding GO and COG terms, the proteins were further annotated using eggnog (Huerta-Cepas et al., 2019). To obtain the raw counts of genes, original assembly reads were mapped back to the annotated genes using BWA MEM (Li, 2013) and filtered with SAMtools (Li et al., 2009), including flags 0 × 8 for non-paired reads and 0 × 2 for properly paired reads. Then, raw counts were obtained using the HTSeq-count from the HTSeq framework (Anders et al., 2015). Finally, differential abundance analysis was performed on shared genes using DESeq2 (Love et al., 2014), allowing their differentiation in abundance post-analysis of their GO terms.

Ab initio predictions

Ab initio prediction was performed on the differentially amplified fragments from *M. esculenta* gall tissues (consensus DNA sequence) and on amplified fragments from purified plasmids of the endophytes IEB 1-2, IEB 3-1, and IEB 5-1, as well as purified plasmids from ISB 1 and ISB 2 isolated from the larval head of the inducing insect. These fragments were amplified with specific gall primers as previously described in the PCR methodology section. *Ab initio* prediction was also carried out on the hybrid sequence fasta files. Gene predictions and their functions were performed using the pipelines of Rapid Prokaryotic Genome Annotation (Prokka) (Seemann, 2014) on the web server Galaxy (www.usegalaxy.org). The pipeline of Prokka uses Prodigal and UniProt for the prediction of coding regions and functional similarity, respectively.

Identification of gene segments

The identification of conserved genetic regions in all target sequences obtained by PCR and in the possible hybrid sequences of interest, obtained by high-throughput sequencing, was performed using the PipMaker program (http://pipmaker.bx.psu.edu/cgi-bin/pipmaker?advanced) to produce local alignments of the genetic sequences using BlastZ (Schwartz et al., 2003), and dot plots of the gap-free segments of the alignments were generated as unbroken diagonal lines, indicating a high degree of identity across the genetic sequences (Schwartz et al., 2000).

Inoculation assays for primary gall induction

Two bacteria grown in solid and liquid YEB 1× culture medium (Piñol et al., 1996) were used to inoculate emerging leaves from apical buds and young leaves of *M. esculenta* (Cassava). Bacterial strains isolated from the larval head of *I. brasiliensis*, subsequently identified as *Rhodococcus* (related to *Rhodococcus* sp. P-2 and *Rhodococcus erythropolis* species, according to the taxonomic profile), were cultured in YEB 1× solid medium and cultured at 26 ± 1°C in a shaker to 110 rpm (Hotech® model 721-2T, Hotech Instruments Corp., New Taipei City, Taiwan) for 3–4 days in the dark. Subsequently, a single clone was used to inoculate 5 mL of YEB 1× liquid medium. After culturing under shaking conditions at 26 ± 1°C for 2–3 days in the dark, a small bacterial suspension was transferred to 10 mL of YEB 1× liquid medium and transferred once again under a sterile biosafety flow-hood to YEB 1× solid medium and cultured for 2–3 days under the above conditions. Then, a single clone was used to inoculate 100 mL of YEB 1× liquid medium to the same preconditions. The endophytic bacterium *Pantoea ananatis*, one of the endophytic bacteria isolated from gall tissue, was used as a control bacterium. The management and culture of this bacterium were carried out under the same conditions described above.

In vitro micropropagated *M. esculenta* plants were used for bacterial inoculation assays under sterile conditions. Apical bud and leaf sections of 0.5–1.0 cm were used for inoculation. Explants were maintained first in solid MS medium for different periods of time. Prior to plant material co-cultivation with bacterial cultures, all explants were treated with slight mechanical abrasion using wet filter paper impregnated with ground glass. Just before inoculation, bacterial biomass was measured with a Lambda 25 spectrophotometer (Perkin Elmer-Applied Biosystems, Foster City, California, USA) and set to a OD_{600} value of 0.5–1.0. Then, *in vitro* plant material was submerged into bacteria cultured in YEB 1× liquid medium and shaken in the dark at 28 ± 1°C, for 16–24 h. Inoculated explants were placed in sterile glass Erlenmeyer flasks and washed three times with sterile water. Excess water was removed, and explants were grown separately on MS solid (agar 5.7 g/L) or liquid medium without plant growth regulators. Half of the cultures were supplemented with 3 mg L^{-1} Kathon (only in solid medium), a bacteriostatic reagent used to inhibit bacterial growth in the cultured medium, under white, fluorescent light with an irradiance of 27 µmol m^{-2} s^{-1} at 28 ± 1°C and 110 rpm in a shaker for the liquid medium (Hotech® model 721-2T, Hotech Instruments Corp., New Taipei City, Taiwan). Both types of explants not co-cultured with the bacteria but treated with mechanical abrasion were employed as controls. Thirty to fifty explants were used in each experiment, which was repeated five times in solid medium and two times in liquid medium. Kathon reagent was used only in the first assay carried out in a solid medium.

Inoculation of plants grown in soil under controlled greenhouse conditions was also attempted. The experimental conditions and bacterial growth were carried out using the same methodology. Groups of 50 plants per treatment grown in pots with soil were used to manually inoculate one to two new emerging leaves. Before bacterial inoculation, the leaf surface was carefully cleaned with 70% ethanol. Then, the emerging leaves were treated with a slight mechanical abrasion using a sterilised YEB 1× liquid medium containing ground glass, followed by rubbing the leaf surface by hand using clean latex gloves. After this, sterilised cotton impregnated with liquid medium containing the bacterial growth was placed and fixed on the prepared leaf surface for 1–2 days. The inoculated leaf area was covered with sterile gauze and sterile insulating plastic. This inoculation test was repeated three times.

A randomised block design was followed in this assay. However, because of the viability decline observed in cassava leaves under the established experimental conditions, only presence–absence results for gall-like structure and abnormal tissue development were displayed graphically. Infostat software version 2020p (http://www.infostat.com.ar) was employed to graph the results obtained from the experiments (Di Rienzo et al., 2020). Daily evaluations were performed in all treatments for 6 weeks. Data are shown as the mean and standard error (±SE) of tissue response due to inoculation with the bacteria. Taxonomic identification of the alleged endosymbiotic bacteria strain from the inducing insect (*Rhodococcus*, isolation ISB 2), used in these gall induction assays, was determined before each test by 16S gene sequencing and then confirmed by a taxonomic profile using genomic bioinformatics tools, as also performed for endophytic bacteria.

Sample preparation for scanning electron microscopy and transmission electron microscopy

Samples of healthy leaves and galls of different sizes from *M. esculenta* plants, as well as the larvae of the inducing insect, were prepared as described by Sánchez et al. (2006), with the modification of fragmentation in liquid nitrogen and dehydration by passage through a gradient of acetone solutions. Sample preparation was performed at the Center for Research in Microscopic Structures, University of Costa Rica, San José, Costa Rica. Samples were observed using a scanning electron microscope (Hitachi S-3700, Tokyo, Japan) with an acceleration voltage of 15 kV.

For transmission electron microscopy (TEM) analyses, samples were fixed with a modified Karnowsky solution, then post-fixed with 2% osmium tetroxide for 1 h, submitted to contrast, and dehydrated in a gradient of acetone solutions (i.e., 30%, 50%, 70%, 90%, and 100%). After washing with 100% acetone, the samples were submitted to pre-infiltration with 1:1 Spurr resin/100% acetone for 5 h with shaking. The subsequent filtration of the samples was performed with pure resin for 12 h. The samples were then shaped and polymerised at 70°C for 3 days. The blocks were then cut into 70-nm-thick sections on an ultramicrotome (Leica Power Tome PC, Leica Microsystems GmbH, Wetzlar, Germany) with a diamond blade (45°), mounted on uncoated 200-mesh copper grids, and stained with uranyl acetate and lead citrate. TEM observations were performed using a Hitachi model HT-7700 microscope (Tokyo, Japan) operating at 100 kV.

Results and discussion

Characterising a potential gall molecular marker

To assess our hypothesis, DNA samples from healthy leaf and gall tissues from the same plant were purified (Figures 1A, D1–D8). Samples were collected from healthy leaves of *M. esculenta* and galls induced by Cecidomyiidae *I. brasiliensis* (Figures 1B, C), and these were carefully cleaned and sterilised to guarantee total epidermis disinfection, including the inner gall chamber.

Possible exogenous DNA, or a DNA insertion sequence present only in gall cells but not in the healthy plant tissue of *M. esculenta* plants, was initially explored using specific PCR primers as a potential gall marker. The primer pair was designed based on the consensus DNA sequence resulting from the alignment of differentially amplified fragments obtained through a previously carried out modified RAPD assay.

A high number of RAPD assays were performed using different random primers; however, decamer primers derived from conserved sequences of the ipt and iAAM genes harboured in the transfer DNA of the Ti plasmid of *Agrobacterium* species and other related bacteria generated the highest number of differentially amplified fragments from gall samples. The quality of purified DNA, as well as the modified RAPD amplification conditions and thermal conditions, allowed us to obtain high reproducibility and reliability in the DNA profiles at different concentrations of analysed DNA. Analytical detections of the RAPD amplicons by gel electrophoresis and the Microchip Electrophoresis System for DNA/RNA (MultiNA) showed differentially amplified fragments of several sizes in all gall samples tested, often from 100 to 4,500 base pairs (bp) (Figures S3B, C). Using these approaches, we isolated and obtained the nucleotide sequences of four samples from the most common differentially amplified fragments derived from gall genomic DNA. Three of these sequences were identical, showing the same nucleotide sequence as the fragment of approximately 500 bp (Supplementary Data 1). The consensus DNA sequence obtained was used as a template to design and test specific PCR primers. For further information, see Supplementary Text.

The gall DNA fragment differentially amplified from gall samples (which we call a specific gall fragment, SGF) was isolated and sequenced. The expected PCR fragment was specifically amplified only in gall samples from *M. esculenta* (Figure 1E), total DNA from the inducing-insect salivary glands, and in the isolated wild-type plasmids from two putative insect endosymbiotic bacteria of the genera *Rhodococcus* (ISB 2 bacterial isolate) and *Pseudomonas* (ISB 1 bacterial isolate) (Figures 2A, S4). Moreover, PCR products with sizes between 350 and 600 bp were also amplified from wild-type plasmids of all endophytic bacteria isolated from cassava gall tissue (Figures 2A, S4). Additionally, specific gall PCR fragments showing a size similar to that expected

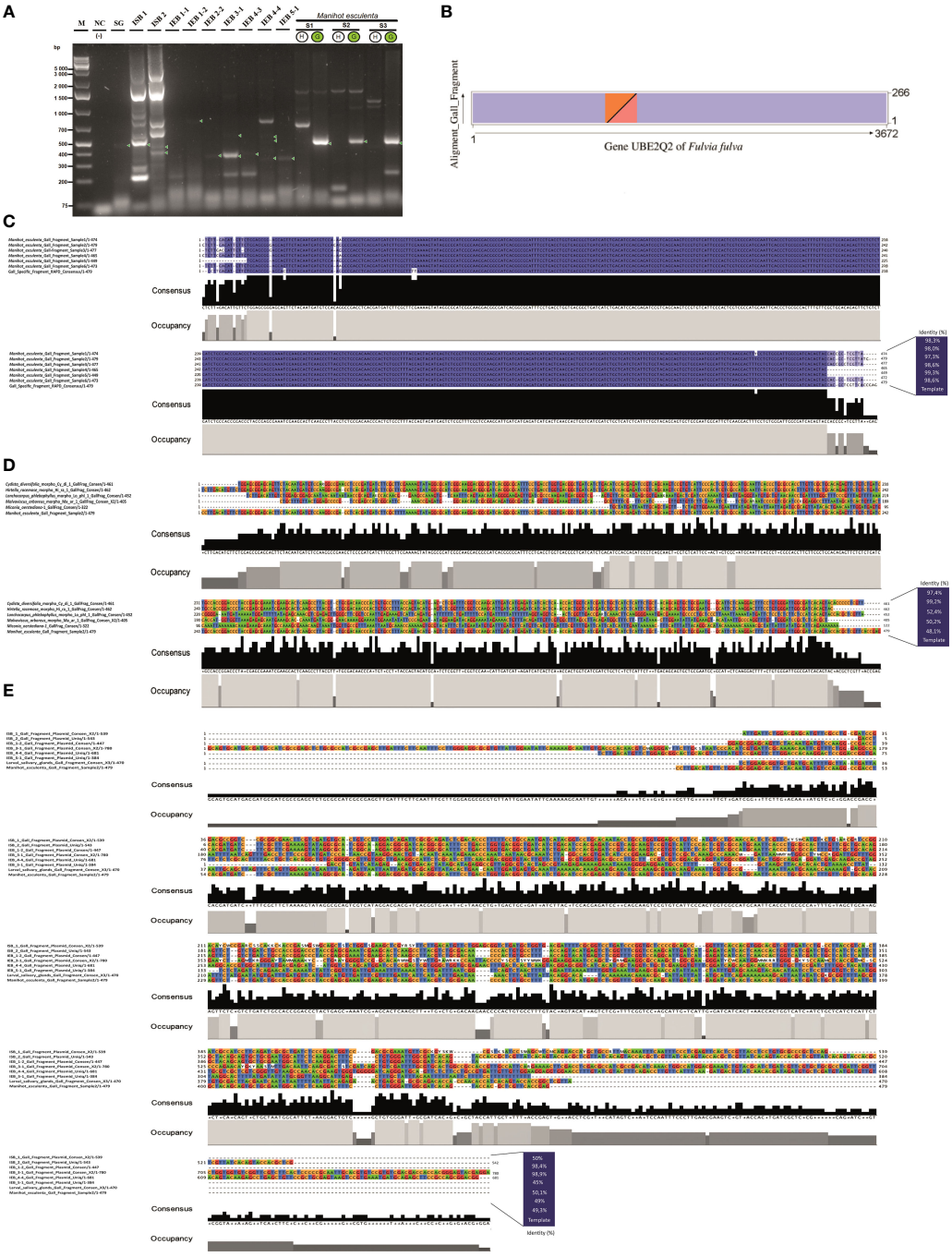

FIGURE 2
Genetic characterisation of the specific gall fragment marker. **(A)** Gel electrophoresis of PCR products using primers for the specific gall fragment marker (SGF) from purified wild-type plasmids of two putative endosymbiotic bacteria, *Pseudomonas* and *Rhodococcus*, isolated from the larval head of the inducing insect *Iatrophobia brasiliensis* (isolates ISB 1 and ISB 2), as well as from purified wild-type plasmids of seven possible endophytic bacteria isolates selected from the cassava plant gall tissue (IEB). PCR amplicons are also shown for the inducing insect salivary gland sample (SG). Samples of DNA purified from healthy leaf and gall cassava tissues were used as positive reaction controls (lines S1–S3). Lane M, molecular weight marker (Gene Ruler 1 KB Plus); line NC, negative control (reagents only). Green circles indicate positive samples for the specific gall fragment amplification (S1–S3). **(B)** Dot plot representation of the aligned and annotated specific gall fragment sequence showing overlapping regions with the *UBE2Q2* gene of *Fulvia fulva*. The overlapping region between the sequences is shown as coloured triangles in each of the represented axes. **(C)** Alignments of specific gall fragments amplified and sequenced from six gall samples compared to the 479 consensus bp DNA reference sequence. **(D)** Alignments among the 479 consensus DNA sequences of the specific gall fragment from cassava and five sequenced gall morphotypes of different host plant species. **(E)** Alignment of sequenced PCR amplicons performed using specific gall fragment primers over purified wild-type plasmids of two alleged endosymbiotic bacteria isolated from the larval head of the inducing insect *I. brasiliensis* (colony-forming units ISB 1 and ISB 2) and from purified wild-type plasmids of seven possible endophytic bacteria isolations selected from the cassava plant gall tissue (colony-forming units IEB), as well as from PCR sequenced fragments from the inducing insect salivary gland (SG). The consensus sequence of the specific gall fragments (SGF) of cassava was used as a template sequence. Grey bar plots show the occupancy within each sequence position, and the black bar shows the base consensus within each sequence position in the resulting alignment.

from cassava galls were selectively amplified from gall morphotype samples of eight different host plant species (Figure 1F). Many of these fragments were sequenced and then aligned to the consensus sequence of the differentially amplified fragment from the cassava gall. The aligned sequences showed high identity with the reference DNA fragment in all *M. esculenta* gall samples (99%–100%) (Figure 2C) and with the two IEB isolates 1-2 isolated from inner plant gall tissue (98.9%) and ISB 2 isolated from the larval insect head (98.4%) (Figure 2E). Furthermore, samples of other galls from *Cydista diversifolia* (97.4%) and *Hirtella racemosa* (99%) also showed high identity (Figure 2D), but a less conspicuous homology (between 48% and 53%) was detected from galls on *Lonchocarpus phlebophyllus*, *Malvaviscus arboreus*, and *Miconia oerstediana* (Figure 2D). This, in turn, suggests a diversification of the coding genetic element under different selection pressures for functional adaptation. Moreover, a repeatedly amplified DNA fragment from the salivary glands of a similar size to that expected showed an identity mean value comparable to the previous reference (49.3%), which could suggest that other bacteria in the salivary glands or an insect homologous gene might harbour a similar DNA sequence (Figure 2E).

A real-time PCR marker by the TaqMan probe was designed and tested following a similar approach used for end-point PCR assays with corresponding modifications. The results showed amplification signals only in the gall tissue (Figures 1G, H) and in plasmids purified from the isolated colonies of the insect endosymbiotic bacteria *Pseudomonas* sp. and *Rhodococcus* sp. (results not shown).

The differentially amplified gall DNA fragment from gall samples (SGF) did not show statistically significant similarity with any other reported gene according to the Basic Local Alignment Search Tool [BLAST, NCBI Genbank database, and Integrated Microbial Genomes & Microbiomes (IMG/M) system, https://img.jgi.doe.gov] and annotation analysis. Nevertheless, several results showed partial pairings with low to medium and often discontinuous length coverage with some ubiquitin-like genes, more specifically, the ubiquitin-like gene *E2*, a component of the ubiquitin-proteosome system (UPS), which has frequently been reported in different fungus species. This fragment showed partial homology to the Ubiquitin-conjugating enzyme E2 Q2 of the fungus *Fulvia fulva*, which was among the most significant (E-value = 6.37e−29, identity = 71.8%, 266 bp of length, accession number CP090172) (Figure 2B). However, we predicted that it was different enough to represent a new ubiquitin-like regulatory genetic element associated with the manipulation of the ubiquitin–proteasome system, used indirectly by the inducing insect via the bacteria to manipulate and redirect plant development during gall formation.

The ubiquitin gene family encodes peptides involved in protein–protein signalling and destination as a component of the basic cellular regulation machinery. These types of proteins regulate gene expression at the transcriptional (Adams and Spoel, 2018) and post-translational levels (Xu and Xue, 2019; Liu et al., 2020). The ubiquitin gene family has been reported as an essential part of molecular cell manipulation mechanisms in different pathogen and endosymbiotic–host interactions (Janjusevic et al., 2006; Vierstra, 2009; Park et al., 2012; Singer et al., 2013; Banfield, 2015; Kud et al., 2019). Ubiquitin-like genes from bacterial secreted effector molecules with structural and/or functional similarity to UPS pathway components mimic and modify the host UPS system (Ramachandran et al., 2021), allowing the hijacking of the cellular machinery, as has been previously reported in the crown gall system induced by *A. tumefaciens* (Magori and Citovsky, 2012; Lacroix and Citovsky, 2015). The UPS system is considered the major protein turnover pathway found across all domains of life and is especially important in regulating almost all plant development signalling pathways, including hormone-mediated plant growth and development, as well as plant responses to stress (Santner and Estelle, 2010; Sadanandom et al., 2013; Shu and Yang, 2017; Adams and Spoel, 2018; Xu and Xue, 2019). Although less is known about UPS manipulation in galling insects, there is emerging evidence that plant development can be manipulated through the UPS system by effector molecules in the salivary glands of the gall inducer (Zhao et al., 2015).

Genetic insertion events inferred from bioinformatic analysis provide evidence for plant cell transformation

Through a discrimination approach using shotgun metagenomic sequencing, we showed the presence of potential foreign-exclusive DNA within plant gall tissue. We named this methodological approach host discriminant genomic analysis (HDGA) (Figure S5). HTS data from healthy leaves and gall tissue (16× sequencing depth) were processed to separate, assemble, and analyse the DNA sequence reads different from the referenced host plant genome of *M. esculenta*. On average, 4.6% of the raw reads from both healthy leaf and gall tissues did not map to the reference genome. Furthermore, of those unmapped reads, 12.4% were unique to the gall tissue samples. *De novo* assembly of these specific reads produced 17,148 contigs. Eight of these assembled contigs produced fragments with sizes between 2,000 and 2,501 bases, 306 between 1,000 and 2,000 bases, 2,161 contigs of 500–1,000 bases, 14,664 fragments between 200 and 500 bases, and 8 fragments smaller than 200 bases (Supplementary Data 2). Using this approach, reads that did not map to the cassava reference nor were they shared between healthy and gall tissue, represent potential foreign DNA from endophytic organisms unique to galls, such as bacteria or fungi, or possible foreign DNA integrated into the genome of gall cells (see Figure S5 for the general pipeline-flow diagram approach). The resulting assemblies were compared against the reference *M. esculenta* genome to identify possible hybrid/fusion fragments, which must harbour homologous sequences with the host plant, along with external sequences without any homology to the host reference genome. When the assembled contigs were filtered once again following this approach, 407 contigs were retained, 59 of which had 300–571 bases, and 348 had 229–300 bases (Supplementary Data 3). Our analysis found 130 of the reported hybrid/fusion contigs with coverage from 10 to 30 reads. A total of 124 showed coverage ranging from six to nine. Only 74 displayed five to four reads, and 63 had three reads. Moreover, seven contigs showed the largest number of reads, with more than 95 (Supplementary Data 3). These hybrid sequences represent potential insertion regions for foreign DNA integrated into the

10.3389/fpls.2023.1237966

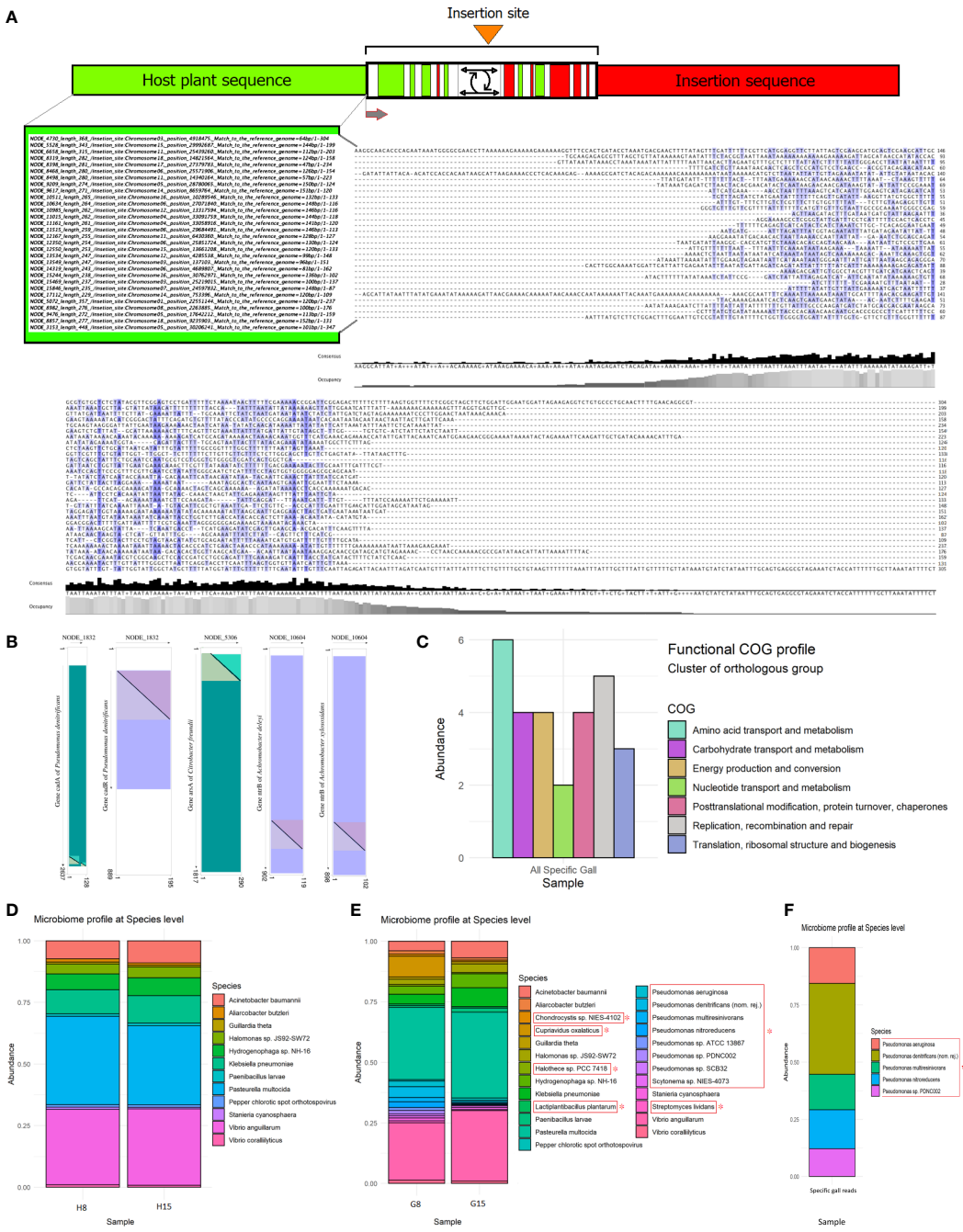

FIGURE 3
Bioinformatic analysis expands the catalogue of gall-specific sequences. **(A)** Theoretical diagram of the insertion regions according to the methodological approach applied. Position of the insertion sites into each host chromosome in the *Manihot esculenta* reference genome is shown on the left in a selected subgroup of hybrid contigs, mostly in forward orientation. Only the alignment framework of unmatched sequences to the cassava reference genome from hybrid/fusion contigs is shown on the right. Grey bar plots show the occupancy within each sequence position, and the black bar shows the base consensus within each sequence position in the resulting alignment scheme. **(B)** Dot plot representation of the aligned and annotated hybrid contigs region of unmatched sequences to the cassava reference genome, showing candidate insertion sequences in several of the hybrid contigs assembled, harbouring known DNA sequences revealing partial significant identity matches and covering with reported genes. Overlapping regions between the contigs and the annotated genes are shown as coloured triangles in each of the represented axes. Purple colour in the referenced gene represents forward strain orientation, and the blue-green colour (viridian) represents reverse strain orientation. **(C)** COG function classification histogram. Count of genes belonging to the COG categories related to exclusive gall reads involved in essential metabolic pathways and biological functions. **(D, E)** Microbiome profile of healthy plant tissue and gall tissue samples. Relative abundance of microorganism taxa identified in the microbiome of healthy leaves and gall samples of cassava. Taxonomic profiles were carried out to a 10K filter using raw reads generated by the shotgun sequencing approach. Each bar represents the organism taxon detected in one sample. The profile showed a similar abundance between both healthy samples **(D)**, but a different relative abundance of microorganisms between gall samples. **(E)** Asterisks indicate enriched or exclusive microorganism species present only in gall tissue according to the taxonomic profile carried out, comparing sequenced heathy leaf samples with gall samples. The most common core endophyte taxa between leaf and gall tissues are also shown. **(F)** Taxonomic identity profile (10K) associated with some of the selected gall-specific reads. Gall-specific reads were bioinformatically filtered from the sequenced gall samples, which mismatched with the cassava reference genome and filtered against shared reads from healthy tissue samples.

genome of gall cells in the sample of mixed galls used for library preparation. Thirty hybrid contigs showing the highest alignment parameters when compared with the cassava reference genome, mainly mapped to the forward strand of this reference genome, are shown in Figure 3A. The estimated insertion position within the assigned chromosomes in the host *M. esculenta* genome is also shown, evidencing multiple possible insertion sites in the genome of plant cells (see Supplementary Data 3 for all candidate hybrid assemblies).

Structural variations, such as repeated sequences, including retrotransposons (Bartlett et al., 2014), inversions, in tandem sequences (Gang et al., 2019), deletions, duplications, and other

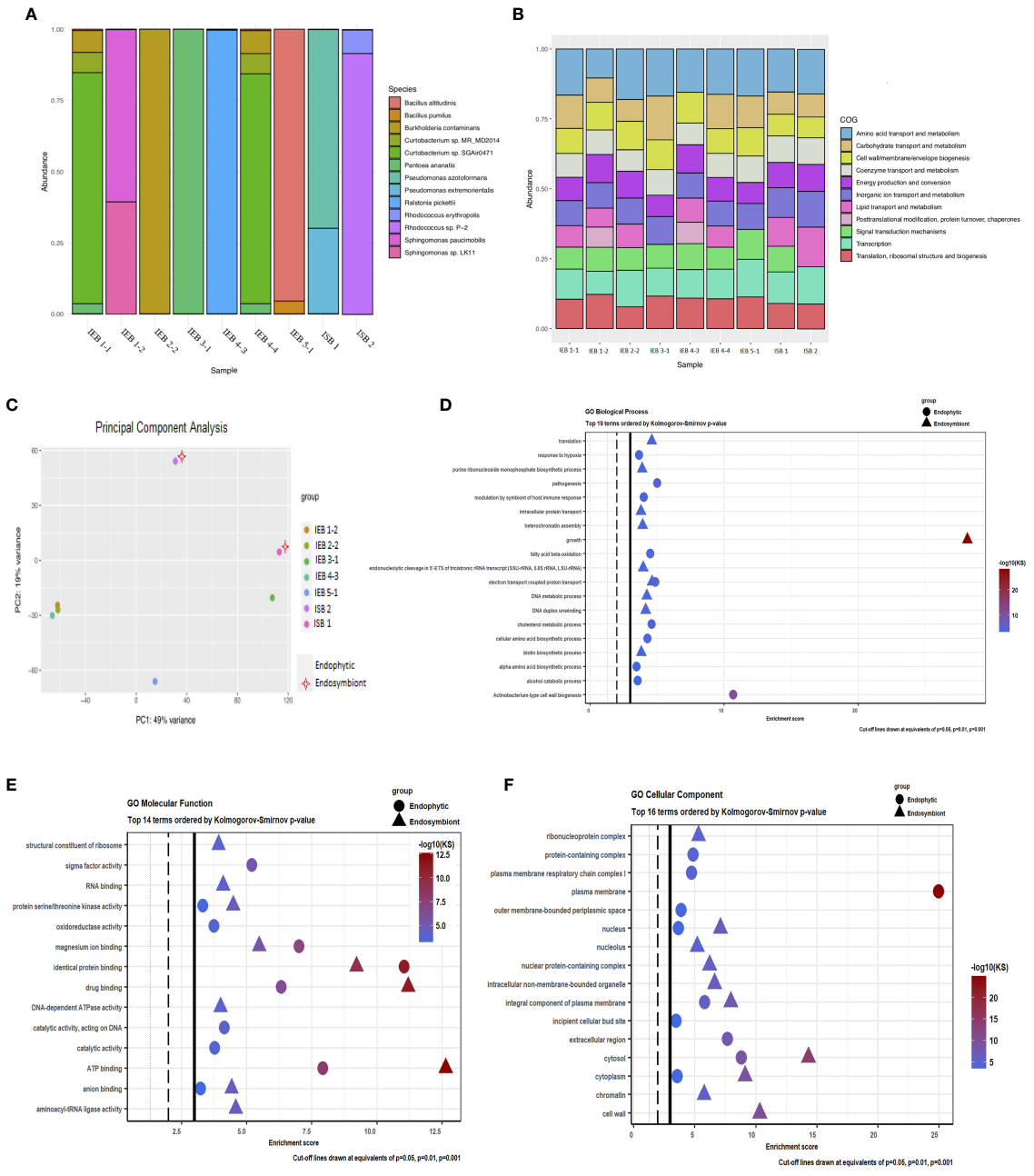

FIGURE 4
Microbiome taxonomic profile and functional analysis of gall endophytes and putative endosymbionts of the inducing insect. **(A)** Relative abundance of bacterial taxa identified in each of the samples of colony-forming units (CFUs) obtained from gall tissue of *Manihot esculenta* and from the larva head of the inducing insect *Iatrophobia brasiliensis*. The figure displays the most abundant taxa individually, with the remainder grouped together. Each bar represents the bacterial taxa detected in one sample. Each CFU from the insect head was called an isolated symbiotic bacteria (ISB). Each of the CFUs isolated and grown from internal sections of sterilised gall epidermis tissue was called an isolated endophytic bacteria (IEB).
(B) Distribution of COG functional categories for CFU isolates from gall tissue and from the larval head of the inducing insect. **(C)** Genetic identity comparison of sequenced bacterial isolates classified up to genus by principal component analysis. **(D–F)** Functional analysis showing the top Gene Ontology enriched pathways of endophytic and alleged endosymbiont bacteria genomes. A high score indicates a high degree of enrichment.

complex rearrangements, including vector backbone or chromosome sequences carried over together with insertion sequences, may occur around or near the insertion point regions bordering the exogenous DNA and in the host plant DNA. A similar phenomenon has been reported in the flanking regions of the T-DNA insertion fragment harboured in the Ti plasmid of *A. tumefaciens* (Krizkova and Hrouda, 1998; Brunaud et al., 2002; Bartlett et al., 2014; Kleinboelting et al., 2015). They could also occur due to the activity of transposable elements (Wicker et al., 2016), such as *Mariner*-like elements in the genomes of seven species of *Rhus* gall aphids (Ahmad et al., 2021). The integration sites within plant genomes seem to be largely randomly distributed under non-selective conditions (Kim and Gelvin, 2007). Small areas of microhomology in insertion sites between T-DNA and neighbouring plant genomic DNA have also been reported (Brunaud et al., 2002; Kleinboelting et al., 2015). The analyses of microhomology indicate that this type of sequence could be, most of the time, a prerequisite for integration events (Gorbunova and Levy, 1999). Furthermore, a depth analysis of the host plant flanking sequences revealed a high proportion of the characterised T-DNAs inserted into or close to repetitive elements in transgenic barley lines without causing negative effects on transgene expression (Bartlett et al., 2014).

Because each insertion process is a single event that potentially generates a structurally hypervariable region in the DNA around the specific insertion site, finding a consensus sequence or motif around these sites is a challenge (Figure 3A). Those regions containing hypervariable sequences around the integration sites could certainly limit the assembly of reads towards the exogenous DNA sequence, thus restricting the length in hybrid/fusion contigs reported in this survey. Likewise, the extension of read assemblies towards the plant genome orientation in the hybrid contigs is also restricted because all common reads between the sequenced genomes of healthy plants and galls were filtered out, primarily with the reference cassava genome and then by pairing against themselves. The alignment quality with regard to the reference cassava genome, filtering stringency, and the read coverage obtained in our analysis provide evidence in support of the hypothesis that genetic material is inserted into the genomes of plant gall cells (Figure 3A, Supplementary Data 3). Technical artifacts, such as sequencing errors, formation of chimeric DNA during library preparation, and nonspecific assemblies, are unlikely to account for all our observations of putative hybrid/fusion fragments, nor is the presence of hypothetical orthologues of genes from an endophytic microorganism in the plant genome.

BLAST and annotation analysis of the unmatched sequences in some hybrid contigs not associated with the *M. esculenta* reference genome did not show a high identity frequency with reported DNA sequences, while others showed low identity and coverage. However, following our methodological approach, we located known candidate insertion sequences in several assembled hybrid contigs. Some of these candidates harbour DNA sequences revealing partially significant identity matches and cover with reported genes (Figure 3B, Supplementary Data 4). Among the outstanding associated genes, transcription regulatory factor CadR and CadA (Cd^{2+} transporting ATPase enzyme) were found in the hybrid contig NODE_1832_length_571_cov_2.279352_0 (E-value = 8E−89, identity = 96%, 194 bp of length, accession number CP043626 and E-value = 6E−33, identity = 81%, 127 bp of length, accession CP043626, respectively) (Supplementary Data 4, Figure 3B), located at the distal end to the possible insertion site in the region not associated with the cassava reference genome, which showed identity with *Pseudomonas* species, such as *Pseudomonas nitroreducens* strain HBP1, *Pseudomonas denitrificans* strain BG1, and *Pseudomonas multiresinovorans* strain populi, which will be reported later as exclusive or enriched components of the gall microbiome (Figures 3D, E). Likewise, significant putative insertion sequences associated with the *arsA* gene (arsenical pump ATPase), NODE_5306_length_349_cov_1.058824_1 (E-value = 9E−112, identity = 100%, 215 bp of length, accession number CP070545), GTP-binding protein encoded by the *obg* gene, NODE_9526_length_272_cov_0.441026_16 (E-value = 1E−12, identity = 76%, 107 bp of length, accession AP018162), nitrate transport permease protein encoded by the *nrtB* gene, NODE_10604_length_264_cov_0.786096_0 (E-value = 4E−46, identity = 92%, 118 bp of length, accession CP065997), assimilatory nitrite reductase enzyme encoded by the *nasE* gene involved in biological nitrate assimilation, NODE_10604_length_264_cov_0.786096_0 (E-value = 2E−44, identity = 91%, 118 bp of length, accession LT976871), and bicarbonate transport system permease protein encoded by the *cmpB* gene, NODE_10604_length_264_cov_0.786096_0 (E-value = 3E−35, identity = 85%, 118 bp of length, accession LR594671) were also found (Figure 3B, Supplementary Data 4). Interestingly, despite its similarity to reported genes in bacteria, all of them are essential for rapid plant growth, maintenance, and survival under unfavourable conditions and are also associated with gene regulation mechanisms (Supplementary Data 4).

Additionally, the association among the 17,148 gall-specific contigs as potential components of an integrated DNA fragment in the gall cells could be inferred based on their annotated function. However, for many hypothetical proteins, a function could not be assigned (Supplementary Data 5). The presence of different transcriptional, post-translational, and cell cycle regulatory factors, as well as exogenous polymerases, transposases (transposase A), or the integration host factor subunit alpha of bacteriophage lambda (which plays a crucial role in the insertion process of lambda DNA into the *Escherichia coli* chromosome), among others, within the gall-specific contigs, provide indirect evidence and are particularly revealing.

Functional Cluster of Orthologous Group (COG) profile analysis, using gall exclusive contigs, showed that the COG categories of amino acid transport and metabolism, carbohydrate transport and metabolism, energy production and conversion, nucleotide transport and metabolism, posttranslational modification, the translation of the ribosomal structure and biogenesis, and DNA replication, recombination, and repair were the main functional categories represented. Although a relatively small number of contigs were used due to bioinformatic processing, these results could indicate that functions related to growth, transport of plant metabolites to inner gall tissues, replication, and expression of nucleic acids, in addition to gene regulation at

different levels, might be promoted or increased by the exogenous DNA detected in gall cells (Figure 3C).

Metagenomes reveal an enriched microbial community in galls

We used HTS to analyse the metagenomes of two gall samples, each consisting of a pool of galls and two healthy tissue samples. The average percentage of assigned reads to any species-level taxon for healthy tissue samples was 4.64%, whereas 4.77% was the average for gall samples, according to reference databases. We showed only the significant microorganisms found at a filter resolution of 10K. The resulting taxonomic profile showed a common microbiome between gall and healthy tissue samples, including a core community dominated by 12 taxa, 9 of which were bacteria, namely, *Acinetobacter baumannii*, *Aliarcobacter butzleri*, *Halomonas* sp. JS92–SW72, *Hydrogenophaga* sp. NH–16, *Klebsiella pneumoniae*, *Paenibacillus larvae*, *Pasteurella multocida*, *Vibrio anguillarum*, and *Vibrio coralliilyticus*, in addition to two cyanobacteria, *Guillardia theta* and *Stanieria cyanosphaera*, and the Pepper chlorotic spot orthotospovirus (Figures 3D, E). Furthermore, an exclusive or enriched microbial community was detected in samples of gall tissues. The taxonomic composition included a community dominated by eight species belonging to the genus *Pseudomonas*, two species of cyanobacteria (*Chondrocystis* sp. and *Halothece* sp. PCC 7418), and three other bacteria species, *Cupriavidus oxalaticus*, *Lactiplantibacillus plantarum*, and *Streptomyces lividans* (filamentous bacterium) (Figure 3E). A brief overview of the relevant functional characteristics reported for these microorganisms and their possible role in gall development and maintenance can be found in the Supplementary Text section.

From the sequencing data exclusive to gall tissue, up to 69.2% of the reads were unassigned to any taxon. These may correspond to microorganisms not included in the available databases at the time of our analysis, or even indicate the possibility of new species as part of this unique microbial community. Nevertheless, a significant amount of exclusive gall reads was associated with several of the same *Pseudomonas* species reported as exclusive or enriched by metagenomic analysis in gall tissue (Figures 3E, F).

Isolation and genomic analysis of putative gall-inducing symbionts and gall endophytes

Two isolates (CFUs) from the original culture grown from the larval head of the inducing insect, *I. brasiliensis*, as well as seven endophytic bacteria isolates selected from cassava gall tissue, were sequenced using high-throughput platforms. Taxonomic profile analysis applied to all isolates revealed that four corresponded to a single species (IEB 2-2 = *Burkholderia contaminans*, IEB 3-1 = *P. ananatis*, IEB 4-3 = *Ralstonia pickettii*, and IEB 5-1 = *Bacillus altitudinis*). Moreover, three isolates showed association with two bacteria species of the same genus (IEB 1-2 = *Sphingomonas* sp. LK11 and *Sphingomonas paucimobilis*), and the two isolates from the original culture grown from the inducer insect, isolate ISB 1, which was *Pseudomonas azotoformans* and *Pseudomonas extremorientalis*, and isolate ISB 2, which was *Rhodococcus* sp. P-2 (which could not be classified to the species level, major component) and *R. erythropolis*. Likewise, isolates IEB 1-1 and IEB 4-4 were assigned to the same bacteria species: *Burkholderia contaminans*, *Curtobacterium* sp. MR_MD2014, *Curtobacterium* sp. SGAir0471, and *P. ananatis* (Figure 4A). However, none of the bacteria isolated from either the gall or the inducing insect larva were precisely detected in the resulting taxonomic profiles belonging to the sequenced samples of healthy plants and gall tissues (Figures 3D, E). Nevertheless, through synteny comparison analysis using specific gall contigs as target sequences compared to each of the sequenced bacterial genomes, the endophytic condition was determined only for the bacteria species isolated from gall tissue, not for those from the inducing insect (Figure S6). Thus, these endophytes might be a marginal component of the gall microbiome, but many of them could also be exclusive components of the microbial community within gall tissues. None of the gall-specific fragment consensus sequences (obtained experimentally) shared homology or aligned with any of the bacterial genomes. The isolation, identification, and subsequent characterisation of microbiome components are difficult tasks due to their low abundance in tissue. This is especially true when using whole-host genome sequencing techniques. However, this barrier may often be overcome using different culture media for growth.

Interestingly, Yang et al. (2021) reported the same bacterial genera sequenced in this study (both gall and inducing insect), except for *R. pickettii*, in their bacterial community of *Lithosaphonecrus arcoverticus* (Hymenoptera: Cynipidae) and in their gall (galled twigs) in *Lithocarpus glaber* (Fagaceae). *Pseudomonas* and *Sphingomonas* have also been identified as members of a common core bacterial community in willow-galling sawflies (Michell and Nyman, 2021). Moreover, *R. erythropolis*, *P. ananatis*, and *Pseudomonas* spp. were recently identified from the bacterial communities by Yang et al. (2022) as predominant species in chestnut tree galls induced by *Dryocosmus kuriphilus*. These bacteria were also identified as components of the microbial communities of the inducing insect and in *Torymus sinensis*, a host-specific parasitoid of *D. kuriphilus*.

Microbial genome comparison by COG functional categories is shown in the COG profile for each isolated CFU (Figure 4B). Also, genetic identity comparison by principal component analysis of sequenced bacterial isolates is shown in Figure 4C. Gene Ontology enrichment analysis of endophytic bacteria genomes showed that the most relevant enriched terms were those related to *Actinobacterium*-type cell wall biogenesis in the category of biological processes and plasma membrane in the category of cellular components. Of the 14 most significant molecular functions identified, sigma factor activity, magnesium ion binding, identical protein binding, drug binding, and ATP binding were the most significantly enriched. Moreover, growth factors for biological processes, in addition to the nucleus, intracellular non-membrane-bounded organelle, nuclear protein-containing complex, integral components of the plasma membrane, cytosol, cytoplasm, and cell wall of GO cellular component, were significantly increased in putative larval endosymbiotic bacteria.

Similarly, magnesium ion binding, identical protein binding, drug binding, and ATP binding were the most significant molecular functions in the enrichment values for these bacteria (Figures 4D–F). Significant discrete GO terms from endophytic bacteria and possible insect endosymbiotic bacteria are shown in Supplementary Data 6. Thus, functional analyses carried out on the endophytic bacteria and on the presumed endosymbiotic bacteria isolated and sequenced from the gall tissue and insect head, respectively, as well as functions associated with the exclusive or enriched microbial community identified in cassava galls by metagenomic analysis (Figure 3E), suggest that the microbial community may play an important role in gall induction, growth, and maintenance. The inferred metabolic pathways and biological functions show that several endophytic bacterial species have a range of different potential functions, including biodegradation of phenolic and potentially harmful metabolic compounds, nutrient supplementation, synthesis of plant hormones, and secondary metabolite degradation. Moreover, this endophytic bacterial community has the potential to synthesise essential amino acids and vitamins, and some of them could be involved in nitrogen and phosphate metabolism, suggesting that these bacterial species could contribute significantly to the nutritional quality of gall tissue. Hence, from an ecological, evolutionary, and functional point of view, our data show that some components of this microbiome can play important roles, both in the host plant itself and in galls. Furthermore, we argue that an unrevealed, induced microbial community that seems to be evident in our findings might have a critical impact on insect gall induction and maintenance despite their low abundance in the gall tissue.

Artificial gall induction by potential bacterial symbionts

An initial gall-like structure was obtained using the *Rhodococcus* bacterial strain, which was related to the gall induction process (Figures 5A, I–P). Putative insect endosymbiotic bacterial lines isolated from the inducing insect (larva head), initially classified as *Rhodococcus* sp. by sequencing the 16S gene and then identified as the genus *Rhodococcus* based on the taxonomic profile (related to *Rhodococcus* sp. P-2 and *R. erythropolis*), were used in these assays. The endophytic bacterium *P. ananatis* isolated from gall tissue was used as a control bacterium.

Plant tissue culture inoculation assays on *M. esculenta* were carried out under controlled laboratory conditions. Most of the gall-like structures were formed in leaves and leaf sections of *M. esculenta* rather than in micro-stakes with apical shoots (apical buds with small leaf primordia), where their formation was the lowest in the first 2 weeks. However, a greater increase in tissue necrosis was observed after 2 weeks of culture (Figure 5A). Moreover, since the culture medium used was not optimised for the propagation and maintenance of leaves, it was not possible to maintain the structure for more than 4–5 weeks. Necrosis and early fall of the inoculated leaves did not allow long-term monitoring of *in vitro* materials (with a few exceptions), an effect also observed in inoculated greenhouse plants.

The inoculation of plants grown in soil under greenhouse conditions was also attempted. However, except for the rare event of neoplasm formation over the inoculated leaf primordia, no gall-like structures were clearly observed (results not shown). This could be the consequence of an increased level of control by the plant in its growth process or unaccounted for environmental factors. Moreover, strong tissue chlorosis was observed after the first week, when the bacteria *P. ananatis* was used in the assay (control inoculation bacterium), observing broad bacterial growth on the tissues without tissue folding or gall-like structures (Figure 5C). Likewise, no significant tissue folding or gall-like structure was observed in the control material treated only with mechanical abrasion using the ground glass (Figure 5B). The different success rates of inducing gall-like structures in the *in vitro* assays and under controlled greenhouse conditions indicate that specific inoculation conditions have yet to be optimised.

After inoculation and incubation with cassava explants, bacterial colonies on plant tissue were frequently observed and were usually associated with invaginations and folds of the leaf blade. However, these leaf deformations and invaginations were not frequently associated with macroscopically visible bacterial growth (Figures 5I, K, L, N, P). Furthermore, a few showed differentiated neoplastic tissue that visually differed from the surrounding tissue (Figures 5l, N, P). An increased tissue reaction was observed when a high bacterial density grew over the plant tissues. This increased reaction induced a higher rate of deformation and invagination of the leaf blade, which usually triggered an earlier necrosis condition in the explants (Figure 5A, images not shown), probably generated by the hypersensitive reaction of the plant tissue. Initial gall formation induced under natural field conditions on young leaf primordia and on medium-mature young leaves is showed in Figures 5D–H.

The ability to induce abnormal gall-like growth has also been reported in *Rhodoccocus fascians* (Stes et al., 2011; Dolzblasz et al., 2018; Harris and Pitzschke, 2020). The development of plant growth is closely related to a linear virulence plasmid harbouring an array of cytokinin genes encoded by the fasciation (fas) operon in most pathogenic isolates (Francis et al., 2012; Creason et al., 2014; Radhika et al., 2015; Jameson et al., 2019). Furthermore, despite the absence of authentic leafy galls in Pistachio Bushy Top Syndrome (PBTS), synergistic coinfection has been reported between *Rhodococcus corynebacterioides* and *R. fascians* by Vereecke et al. (2020).

Bacterial strains belonging to the genus *Rhodococcus* (Figure 4A), isolated from the inducing insect (ISB 2 isolate) and used in gall induction assays, were not detected with certainty at the species level in the sequenced samples of galls and healthy plant tissues when metagenomic analysis was applied (Figures 3D–F). Therefore, we suggest three possible explanations for our findings. The first scenario proposes that the bacterial lines used in our gall induction assays were not conclusively detected because the bacteria had a lower relative abundance within the gall tissue. Thus, the target bacterial DNA would not have a representative fraction in the gall samples purified

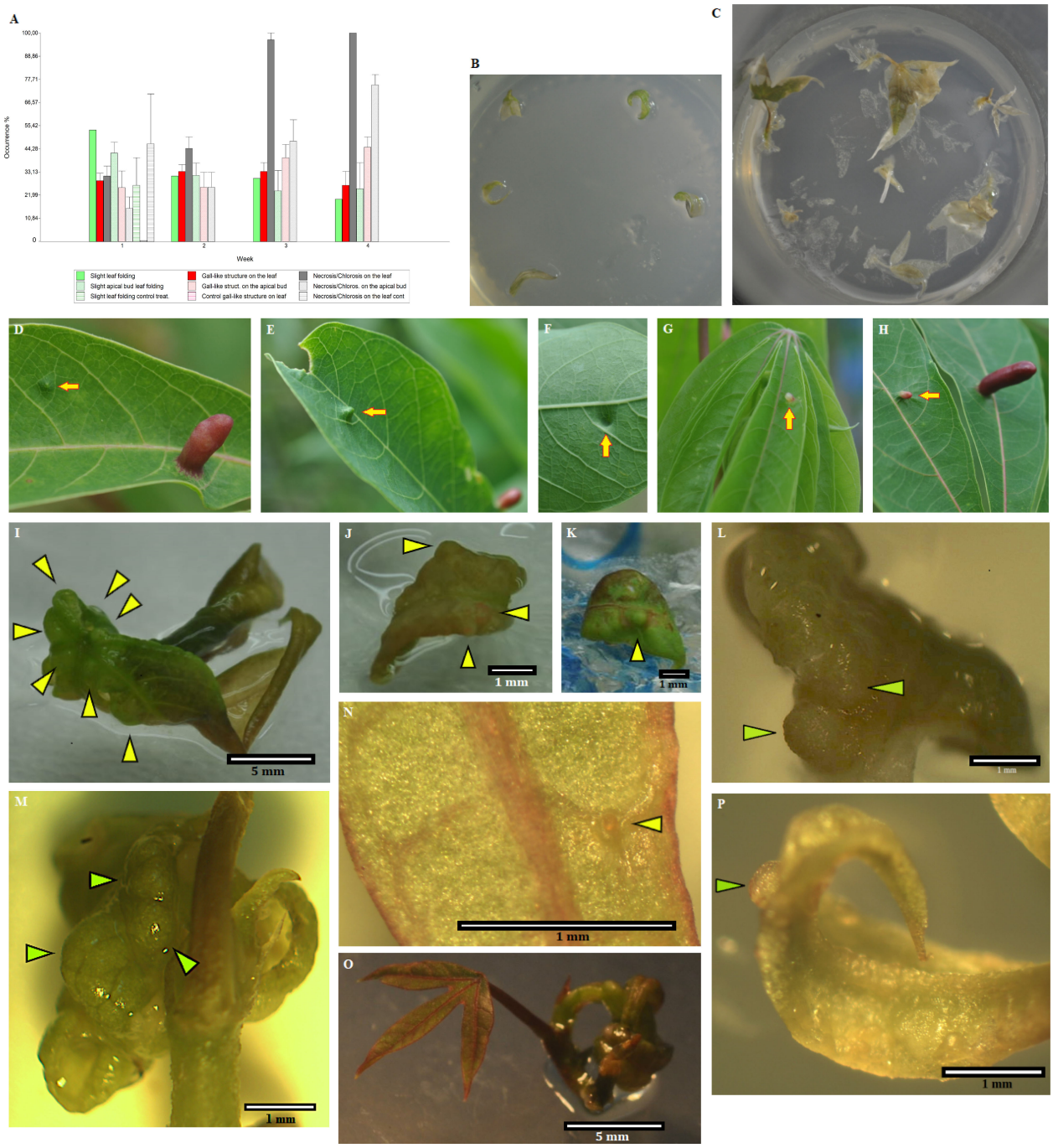

FIGURE 5
Bioassays show that potential insect endosymbiotic bacteria of the genus *Rhodococcus* induce gall-like structures in *Manihot esculenta* plants. **(A)** Graph of primary gall induction on leaves and micro-stakes with apical buds. Data for bacterial inoculation control are not shown due to the tissue damage caused since the first week of data collection. **(B)** Control inoculation, with only slight mechanical abrasion (without bacteria inoculation) in solid medium. **(C)** Leaf and apical buds control culture, inoculated with *Pantoea ananatis* (IEB 3-1) control bacterium. **(D–F, H)** Initial gall formation induced under natural field conditions on medium-mature young leaves. **(G)** Gall induced under natural field conditions on young leaf primordia. **(I–L)** Gall-like structure induced on leaves by inoculation with the isolated *Rhodococcus* strain (1–2 weeks of culture). The solid medium was supplemented with 3 mg L^{-1} Kathon, a bacteriostatic reagent used to inhibit bacterial growth in the culture medium. **(M–P)** Gall-like structure induced on apical buds by inoculation with the isolated *Rhodococcus* strain (**M**, 4 weeks of culture; **N–P**, 3 weeks of culture). Green or yellowish arrows show the formation of gall-like structures. Data are shown as the mean (± SE) of tissue response due to inoculation with the bacteria.

for sequencing. An additional explanation could be that the putative bacterium is involved in the gall induction process, but it is not a component of the gall cell endophytic microbiome, according to our results, thus performing its action externally to the plant cell. Furthermore, the bacterium could exert its action at the initial stage of gall induction. Third, another taxonomically related bacterium sharing a similar molecular mechanism might also induce the formation of this structure in its initial stage.

Detection of the specific gall marker fragment in sequenced plant material and sequenced bacterial isolates

The non-detection of the differentially amplified gall fragment (specific gall fragment experimentally obtained) in the sequenced *M. esculenta* gall genome and specifically in the sequenced *Rhodococcus* spp., which we argue is related to the gall induction process, could be explained by the sequencing of large low-copy-number wild-type plasmids harbouring large duplications, making it nearly impossible to correctly determine a plasmid genome sequence using a short-read sequencing platform, such as Illumina HiSeq and MiSeq (Smalla et al., 2015; Orlek et al., 2017). Moreover, large wild-type plasmids are difficult to reconstruct from whole-genome sequencing data; this arduous task usually requires a hybrid assembly approach that combines the long reads with the accuracy of short-read sequencing (Berbers et al., 2020). Consequently, localising genes in specific plasmids may be difficult (Orlek et al., 2017). Hence, based on our findings, no direct evidence that the specific gall fragment could be part of an insertion sequence was obtained, and we therefore argue otherwise that this specific gall fragment would be an accessory genetic component of the bacteria transformation machinery, harbouring a transformation plasmid, but this would not be part of the insertion sequence integrated into the genome of the plant cell, analogous to the configuration of the Ti plasmid in *A. tumefaciens* strains (Suzuki et al., 2015; Shao et al., 2018; Chou et al., 2022). Therefore, its specific detection in the DNA extracted from gall tissue by PCR-based methodologies could be the consequence of the transferred endophytic form of *Rhodococcus* spp. by the inducing insect, or another bacterium sharing the same genetic element, in which genomic and plasmid DNA are co-precipitated along with host plant DNA. Moreover, *in silico* PCR analysis of the specific gall fragment did not produce any amplicon from the cassava reference genome (results not shown), thus demonstrating that this DNA fragment is not a component of the host plant genome. However, further research on this specific topic should be carried out to provide more evidence.

Conclusion

We provide evidence suggesting an insect-induced gall formation mechanism mediated by genetic transformation events in host plant cells. Our data allude to a potential mobile genetic element harboured in *Rhodococcus* spp. bacteria isolated from the inducing insect that could be involved in the induction mechanism. Moreover, gall induction and growth could also be associated with a change in the microbiome composition in plant tissue. It is possible that the inducing insect injects components of the gall-specific endophytic community during female oviposition and larval feeding. Genetic transformation and microbiome modification of gall tissue in *M. esculenta* could be a more widely distributed induction mechanism in nature. This was supported by the detection of a potential accessory genetic component of the transformation machinery (ubiquitin-like gene *E2*) or with a similar identity in other insect galls in other plant species, and even detected in wild-type plasmids purified from endophytic bacteria species isolated from the same cassava gall tissue. While our results provide greater insight into plant–bacteria–insect interactions, further research is needed to fully understand the complex mechanisms of gall induction and formation. Moreover, the insertion of genetic elements from a putative bacterium could function as a switch in the molecular interaction between the inducing insect and the host plant.

Data availability statement

The datasets presented in this study can be found in online repositories. The names of the repository/repositories and accession number(s) can be found in the article/Supplementary Material.

Ethics statement

The manuscript presents research on animals that do not require ethical approval for their study.

Author contributions

OG-B: conceived the survey; substantial contribution to the concept and design of the bioinformatic approach; performed most of the molecular biology experiments; contribution to data analysis and interpretation; contribution to the data collection, registration, and processing; obtained and provided financial support; and wrote the article. JJ-M: substantial contribution to the concept, design, and analysis of the bioinformatic approach; participated in writing the manuscript. RW: contribution to the design and analysis of the bioinformatic approach; and critical revision of the manuscript. PH: contribution to the concept and design of the study; contribution to critical revision; and addition of intellectual content. SV-D: contribution to bioinformatic analysis and interpretation; contribution to critical revision and adding intellectual content; and contribution to manuscript preparation. AA-G: contribution to data analysis and interpretation; and contribution to manuscript preparation. AP-T: contribution to critical revision; adding intellectual content; and contribution to manuscript preparation. All authors contributed to the article and approved the submitted version.

Funding

The author(s) declare that no financial support was received for the research, authorship, and/or publication of this article. This research received no external funding. The postgraduate system at University of Costa Rica covered the Article Processing Fee as a Ph.D. student support.

Acknowledgments

We are grateful to Dr. Pedro León-Azofeifa, Dr. Federico Albertassi, and Dr. Jorge Lobo for their constructive comments on this research, and we would like to kindly thank Dr. Cecilia Díaz for the discussion of ideas, critical revision, and adding intellectual content. We would like to thank Dr. Julin Weing for the larva head microdissection. We appreciate the support and collaboration provided by the staff of the Biotechnology Laboratory (Escuela de Agronomía, Campus San Carlos del Instituto Tecnológico de Costa Rica), as well as Miguel Pacheco for Gram-staining bacteria. We thank the biologist Alonso Quesada at the Herbario Museo Nacional, Costa Rica, and Dr. Mario Blanco Coto at the Herbario Escuela de Biologia, UCR, for their help with the taxonomic identification of some host plant materials used in this work. We also appreciate the technical cooperation of Luis Benavides. Finally, we appreciate the initial logistic and material support given by Dr. Pedro León-Azofeifa in his laboratory at Centro de Investigaciones en Biología Celular y Molecular, Universidad de Costa Rica.

Conflict of interest

The authors declare that the research was conducted in the absence of any commercial or financial relationships that could be construed as a potential conflict of interest.

Publisher's note

All claims expressed in this article are solely those of the authors and do not necessarily represent those of their affiliated organizations, or those of the publisher, the editors and the reviewers. Any product that may be evaluated in this article, or claim that may be made by its manufacturer, is not guaranteed or endorsed by the publisher.

Supplementary material

The Supplementary Material for this article can be found online at: https://www.frontiersin.org/articles/10.3389/fpls.2023.1237966/full#supplementary-material

References

Adams, E., and Spoel, S. H. (2018). The ubiquitin-proteasome system as a transcriptional regulator of plant immunity. *J. Exp. Bot.* 69 (19), 4529–4537. doi: 10.1093/jxb/ery216

Ahmad, A., Wallau, G. L., and Ren, Z. (2021). Characterization of Mariner transposons in seven species of *Rhus* gall aphids. *Sci. Rep.* 11, 16349. doi: 10.1038/s41598-021-95843-5

Alexa, A. (2022). *Rahnenfuhrer J. topGO: Enrichment analysis for gene ontology (2.46. 0) [Computer software]. Bioconductor version: release (3.14).*

Ananthakrishnan, T. (1998). Insect gall systems: patterns, processes and adaptive diversity. *Curr. Sci.* 75 (7), 672–676.

Anders, S., Pyl, P. T., and Huber, W. (2015). HTSeq-a Python framework to work with high-throughput sequencing data. *Bioinformatics* 31 (2), 166–169. doi: 10.1093/bioinformatics/btu638

Andrews, S. (2010). *FastQC: a quality control tool for high throughput sequence data.*

Azizi-Dargahlou, S., and Pouresmaeil, M. (2023). *Agrobacterium tumefaciens*-mediated plant Transformation: a review. *Mol. Biotechnol.* 1–18. doi: 10.1007/s12033-023-00788-x

Banfield, M. J. (2015). Perturbation of host ubiquitin systems by plant pathogen/pest effector proteins. *Cell Microbiol.* 17, 18–25. doi: 10.1111/cmi.12385

Bankevich, A., Nurk, S., Antipov, D., Gurevich, A. A., Dvorkin, M., Kulikov, A. S., et al. (2012). SPAdes: a new genome assembly algorithm and its applications to single-cell sequencing. *J. Comput. Biol.* 19 (5), 455–477. doi: 10.1089/cmb.2012.0021

Bartlett, J. G., Smedley, M. A., and Harwood, W. A. (2014). Analysis of t-DNA/host-plant DNA junction sequences in single-copy transgenic barley lines. *Biology* 3 (1), 39–55. doi: 10.3390/biology3010039

Bartlett, L., and Connor, E. F. (2014). Exogenous phytohormones and the induction of plant galls by insects. *Arthropod-Plant Interact.* 8 (4), 339–348. doi: 10.1007/s11829-014-9309-0

Berbers, B., Saltykova, A., Garcia-Graells, C., Philipp, P., Arella, F., Marchal, K., et al. (2020). Combining short and long read sequencing to characterize antimicrobial resistance genes on plasmids applied to an unauthorized genetically modified *Bacillus*. *Sci. Rep.* 10, 4310. doi: 10.1038/s41598-020-61158-0

Bredeson, J. V., Lyons, J. B., Prochnik, S. E., Wu, G. A., Ha, C. M., Edsinger-Gonzales, E., et al. (2016). Sequencing wild and cultivated cassava and related species reveals extensive interspecific hybridization and genetic diversity. *Nat. Biotechnol.* 34, 562–570. doi: 10.1038/nbt.3535

Brunaud, V., Balzergue, S., Dubreucq, B., Aubourg, S., Samson, F., Chauvin, S., et al. (2002). T-DNA integration into the *Arabidopsis* genome depends on sequences of pre-insertion sites. *EMBO Rep.* 3, 1152–1157. doi: 10.1093/embo-reports/kvf237

Bushnell, B. (2015). *BBMap short-read aligner, and other bioinformatics tools.* (Berkeley: University of California).

Camacho, C., Coulouris, G., Avagyan, V., Ma, N., Papadopoulos, J., Bealer, K., et al. (2009). BLAST+: architecture and applications. *BMC Bioinf.* 15 (10), 421. doi: 10.1186/1471-2105-10-421

Cambier, S., Ginis, O., Moreau, S. J. M., Gayral, P., Hearn, J., Stone, G. N., et al. (2019). Gall wasp transcriptomes unravel potential effectors involved in molecular dialogues with oak and rose. *Front. Physiol.* 10. doi: 10.3389/fphys.2019.00926

Campbell, M. A., Van Leuven, J. T., Meister, R. C., Carey, K. M., Simon, C., and McCutcheon, J. P. (2015). Genome expansion via lineage splitting and genome reduction in the cicada endosymbiont *Hodgkinia*. *Proc. Natl. Acad. Sci. United States America* 112 (33), 10192–10199. doi: 10.1073/pnas.1421386112

Chalupowicz, L., Barash, I., Panijel, M., Sessa, G., and Manulis-Sasson, S. (2009). Regulatory interactions between quorum-sensing, auxin, cytokinin, and the hrp regulon in relation to gall formation and epiphytic fitness of Pantoea agglomerans pv. *gypsophilae*. *Mol. Plant–Microbe Interact.* 22, 849–856. doi: 10.1094/MPMI-22-7-0849

Chou, L., Lin, Y. C., Haryono, M., Santos, M. N., Cho, S. T., Weisberg, A. J., et al. (2022). Modular evolution of secretion systems and virulence plasmids in a bacterial species complex. *BMC Biol.* 20, 16. doi: 10.1186/s12915-021-01221-y

Coolen, S., Magda, R. D., and Welte, C. U. (2022). The secret life of insect-associated microbes and how they shape insect-plant interactions. *FEMS Microbiol. Ecol.* 98 (9), fiac083. doi: 10.1093/femsec/fiac083

Creason, A. L., Vandeputte, O. M., Savory, E. A., Davis, E. W. II, Putnam, M. L., Hu, E., et al. (2014). Analysis of genome sequences from plant pathogenic *Rhodococcus* reveals genetic novelties in virulence loci. *PloS One* 9, e101996. doi: 10.1371/journal.pone.0101996

de Lillo, E., Pozzebon, A., Valenzano, D., and Duso, C. (2018). An intimate relationship between eriophyoid mites and their host plants - A review. *Front. Plant Sci.* 9. doi: 10.3389/fpls.2018.01786

Dellaporta, S. L., Wood, J., and Hicks, J. B. (1983). A plant DNA minipreparation: version II. *Plant Mol. Biology Rep.* 1 (14), 19–21. doi: 10.1007/BF02712670

Desnitskiy, A. G., Chetverikov, P. E., Ivanova, L. A., Kuzmin, I. V., Ozman-Sullivan, S. K., and Sukhareva, S. I. (2023). Molecular aspects of gall formation induced by mites and insects. *Life* 13 (6), 1347. doi: 10.3390/life13061347

Di Rienzo, J. A., Casanoves, F., Balzarini, M. G., Gonzalez, L., Tablada, M., and Robledo, C. W. (2020). *InfoStat versión* (FCA, Universidad Nacional de Córdoba, Argentina: Centro de Transferencia InfoStat).

Dolzblasz, A., Banasiak, A., and Vereecke, D. (2018). Neovascularization during leafy gall formation on *Arabidopsis thaliana* upon *Rhodococcus fascians* infection. *Planta* 247 (1), 215–228. doi: 10.1007/s00425-017-2778-5

El-Sayed, W. S., and Ibrahim, R. A. (2015). Diversity and phylogenetic analysis of endosymbiotic bacteria of the date palm root borer *Oryctes agamemnon* (Coleoptera: Scarabaeidae). *BMC Microbiol.* 15 (1), 88. doi: 10.1186/s12866-015-0422-8

Espírito-Santo, M. M., and Fernandes, G. W. (2007). How many species of gall-inducing insects are there on earth, and where are they? *Ann. Entomological Soc. America* 100 (2), 95–99. doi: 10.1603/0013-8746(2007)100[95:HMSOGI]2.0.CO;2

Favery, B., Quentin, M., Jaubert-Possamai, S., and Abad, P. (2016). Gall-forming root-knot nematodes hijack key plant cellular functions to induce multinucleate and hypertrophied feeding cells. *J. Insect Physiol.* 84, 60–69. doi: 10.1016/j.jinsphys.2015.07.013

Ferreira, B. G., Álvarez, R., Avritzer, S. C., and Isaias, R. M. S. (2017). Revisiting the histological patterns of storage tissues: beyond the limits of gall-inducing taxa. *Botany* 95 (2), 173–184. doi: 10.1139/cjb-2016-018

Francis, I., De Keyser, A., De Backer, P., Simón-Mateo, S., Kalkus, K., Pertry, I., et al. (2012). pFiD188, the linear virulence plasmid of *Rhodococcus fascians* strain D188. Mol. *Plant-Microbe Interact.* 25, 637–647. doi: 10.1094/MPMI-08-11-0215

Galambos, N., Compant, S., Wäckers, F., Sessitsch, A., Anfora, G., Mazzoni, V., et al. (2021). Beneficial insects deliver plant growth-promoting bacterial endophytes between tomato plants. *Microorganisms* 9 (6), 1294. doi: 10.3390/microorganisms9061294

Galperin, M. Y., Kristensen, D. M., Makarova, K. S., Wolf, Y. I., and Koonin, E. V. (2019). Microbial Genome analysis: COG approach. *Briefings Bioinf.* 20 (4), 1063–1070. doi: 10.1093/bib/bbx117

Gang, H., Liu, G., Zhang, M., Zhao, Y., Jiang, J., and Chen, S. (2019). Comprehensive characterization of T-DNA integration induced chromosomal rearrangement in a birch T-DNA mutant. *BMC Genomics* 20, 311. doi: 10.1186/s12864-019-5636-y

Gätjens-Boniche, O. (2019). The mechanism of plant gall induction by insects: revealing clues, facts, and consequences in a cross-kingdom complex interaction. *Rev. Biología Trop.* 67 (6), 1359–1382. doi: 10.15517/rbt.v67i6.33984

Gätjens-Boniche, O., Sánchez-Valverde, M., Trejos-Araya, C., Espinoza-Obando, R., Pinto-Tomás, A., and Hanson, P. E. (2021). Plant galls recorded from Guanacaste Conservation Area-Costa Rica as an integrated concept of a biological database. *Biota Neotropica* 21 (3). doi: 10.1590/1676-0611-bn-2020-1153

Giron, D., Frago, E., Glevarec, G., Pieterse, C. M. J., and Dicke, M. (2013). Cytokinins as key regulators in plant–microbe–insect interactions: connecting plant growth and defense. *Funct. Ecol.* 27, 599–609. doi: 10.1111/1365-2435.12042

Giron, D., Huguet, E., Stone, G. N., and Body, M. (2016). Insect-induced effects on plants and possible effectors used by galling and leaf-mining insects to manipulate their host-plant. *J. Insect Physiol.* 84, 70–89. doi: 10.1016/j.jinsphys.2015.12.009

Gorbunova, V. V., and Levy, A. A. (1999). How plants make ends meet: DNA double-strand break repair. *Trends Plant Sci.* 4, 263–269. doi: 10.1016/S1360-1385(99)01430-2

Gutzwiller, F., Dedeine, F., Káiser, W., and Giron, D. (2015). Correlation between the green-island phenotype and *Wolbachia* infections during the evolutionary diversification of Gracillariidae leaf-mining moths. *Ecol. Evol.* 5 (18), 4049–4062. doi: 10.1002/ece3.1580

Hall, T. A. (1999). BioEdit: a user-friendly biological sequence alignment editor and analysis program for Windows 95/98/NT. *Nucleic Acids Symp. Ser.* 41, 95–98.

Hammer, T. J., and Bowers, M. D. (2015). Gut microbes may facilitate insect herbivory of chemically defended plants. *Oecologia* 179 (1), 1–14. doi: 10.1007/s00442-015-3327-1

Hansen, A. K., and Moran, N. A. (2014). The impact of microbial symbionts on host plant utilization by herbivorous insects. *Mol. Ecol.* 23 (6), 1473–1496. doi: 10.1111/mec.12421

Hanshew, A. S., Mason, C. J., Raffa, K. F., and Currie, C. R. (2013). Minimization of chloroplast contamination in 16S rRNA gene pyrosequencing of insect herbivore bacterial communities. *J. Microbiological Methods* 95 (2), 149–155. doi: 10.1016/j.mimet.2013.08.007

Harris, M. O., and Pitzschke, A. (2020). Plants make galls to accommodate foreigners: some are friends, most are foes. *New Phytol.* 225, 1852–1872. doi: 10.1111/nph.16340

Hopp, H. E., Spangenberg, G., and Herrera-Estrella, L. (2022). Editorial: plant transformation. *Front. Plant Sci.* 13. doi: 10.3389/fpls.2022.876671

Huang, M. Y., Huang, W. D., Chou, H. M., Chen, C. C., Chen, P. J., Chang, Y. T., et al. (2015). Structural, biochemical, and physiological characterization of photosynthesis in leaf-derived cup-shaped galls on *Litsea acuminata*. *BMC Plant Biol.* 15 (1), 61. doi: 10.1186/s12870-015-0446-0

Huerta-Cepas, J., Szklarczyk, D., Heller, D., Hernández-Plaza, A., Forslund, S. K., Cook, H., et al. (2019). eggNOG 5.0: a hierarchical, functionally andphylogenetically annotated orthology resource basedon 5090 organisms and 2502 viruses. *Nucleic Acids Res.* 8, 47 (Database issue), D309–D314. doi: 10.1093/nar/gky1085

ICGMC (International Cassava Genetic Map Consortium) (2015). High-resolution linkage map and chromosome-scale genome assembly for cassava (*Manihot esculenta* Crantz) from 10 populations. *G3 (Bethesda)* 5 (1), 133–144. doi: 10.1534/g3.114.015008

Isaias, R. M. S., Ferreira, B. G., Alvarenga, D. R., Barbosa, L. R., Salminen, J. P., and Steinbauer, M. J. (2018). Functional compartmentalisation of nutrients and phenolics in the tissues of galls induced by *Leptocybe invasa* (Hymenoptera: Eulophidae) on *Eucalyptus camaldulensis* (Myrtaceae). *Austral. Entomology* 57 (2), 238–246. doi: 10.1111/aen.12336

Jameson, P. E., Dhandapani, P., Song, J., Zatloukal, M., Strnad, M., Remus-Emsermann, M. N. P., et al. (2019). The cytokinin complex associated with *Rhodococcus fascians*: which compounds are critical for virulence? *Front. Plant Sci.* 10. doi: 10.3389/fpls.2019.00674

Janjusevic, R., Abramovitch, R. B., Martin, G. B., and Stebbins, C. E. (2006). A bacterial inhibitor of host programmed cell death defenses is an E3 ubiquitin ligase. *Science* 311, 222–226. doi: 10.1126/science.1120131

Jump, B. A., and Woodward, S. (1994). Histology of witches' brooms on *Betula pubescens*. *Eur. J. For. Pathol.* 24, 229–237. doi: 10.1111/j.1439-0329.1994.tb00989.x

Kavipriya, C., Yuvaraja, A., Senthil, K., and Menaka, C. (2019). Genetic transformation methods for crop improvement- A brief review. *Agric. Rev.* 40 (4), 281–288. doi: 10.18805/ag.R-1904

Kim, S., and Gelvin, S. (2007). Genome-wide analysis of Agrobacterium T-DNA integration sites in the Arabidopsis genome generated under non-selective conditions. *Plant J.* 51, 779–791. doi: 10.1111/j.1365-313X.2007.03183.x

Kleinboelting, N., Huep, G., Appelhagen, I., Viehoever, P., Li, Y., and Weisshaar, B. (2015). The structural features of thousands of t-DNA insertion sites are consistent with a double-strand break repair-based insertion mechanism. *Mol. Plant* 8 (11), 1651–1664. doi: 10.1016/j.molp.2015.08.011

Klimov, P. B., Chetverikov, P. E., Dodueva, I. E., Vishnyakov, A. E., Bolton, S. J., Paponova, S. S., et al. (2022). Symbiotic bacteria of the gall-inducing mite *Fragariocoptes setiger* (Eriophyoidea) and phylogenomic resolution of the eriophyoid position among Acari. *Sci. Rep.* 12 (1), 3811. doi: 10.1038/s41598-022-07535-3

Koressaar, T., and Remm, M. (2007). Enhancements and modifications of primer design program Primer3. *Bioinformatics* 23 (10), 1289–1291. doi: 10.1093/bioinformatics/btm091

Korgaonkar, A., Han, C., Lemire, A. L., Siwanowicz, I., Bennouna, D., Kopec, R. E., et al. (2021). A novel family of secreted insect proteins linked to plant gall development. *Curr. Biol.* 31, 1–14. doi: 10.1016/j.cub.2021.01.104

Koyama, Y., Yao, I., and Akimoto, S. I. (2004). Aphid galls accumulate high concentrations of amino acids: a support for the nutrition hypothesis for gall formation. *Entomol. Exp. Appl.* 113 (1), 35–44. doi: 10.1111/j.0013-8703.2004.00207.x

Krizkova, L., and Hrouda, M. (1998). Direct repeats of T-DNA integrated in tobacco chromosome: characterization of junction regions. *Plant J.* 16, 673–680. doi: 10.1046/j.1365-313x.1998.00330.x

Kud, J., Wang, W., Gross, R., Fan, Y., Huang, L., Yuan, Y., et al. (2019). The potato cyst nematode effector RHA1B is a ubiquitin ligase and uses two distinct mechanisms to suppress plant immune signaling. *PloS Pathog.* 15, e1007720. doi: 10.1371/journal.ppat.1007720

Lacroix, B., and Citovsky, V. (2015). Nopaline-type Ti plasmid of *Agrobacterium* encodes a VirF-like functional F-box protein. *Sci. Rep.* 5, 16610. doi: 10.1038/srep16610

Leitch, I. J. (1994). "Induction and development of the bean gall caused by *Pontania proxima*," in *Plant Galls: Organisms, Interactions, Populations. The Systematics Association (Systematics Association Special Vol. 49)*. Ed. M. Williams (London, United Kingdom: Clarendon Press, Oxford), 283–283.

Li, H. (2013). Aligning sequence reads, clone sequences and assembly contigs with BWA-MEM. *arXiv [Preprint] arXiv:1303.3997*.

Li, H., and Durbin, R. (2009). Fast and accurate short read alignment with Burrows-Wheeler transform. *Bioinformatics* 25, 1754–1760. doi: 10.1093/bioinformatics/btp324

Li, H., Handsaker, B., Wysoker, A., Fennell, T., Ruan, J., Homer, N., et al. (2009). The sequence alignment/map format and SAMtools. *Bioinformatics* 25 (16), 2078–2079. doi: 10.1093/bioinformatics/btp352

Li, X. Q., Stahl, R., and Brown, G. (1995). Rapid micropreps and minipreps of Ti plasmid and binary vector from *Agrobacterium tumefaciens*. *Transgenic Res.* 4, 349–351. doi: 10.1007/BF01972532

Lian, Z., Nguyen, C. D., Liu, L., Wang, G., Chen, J., Wang, S., et al. (2022). Application of developmental regulators to improve in planta or in *vitro* transformation in plants. *Plant Biotechnol. J.* 20 (8), 1622–1635. doi: 10.1111/pbi.13837

Liu, W., Tang, X., Qi, X., Fu, X., Ghimire, S., Ma, R., et al. (2020). The ubiquitin conjugating enzyme: an important ubiquitin transfer platform in ubiquitin-proteasome system. *Int. J. Mol. Sci.* 21 (8), 2894. doi: 10.3390/ijms21082894

Love, M. I., Huber, W., and Anders, S. (2014). Moderated estimation of fold change and dispersion for RNA-seq data with DESeq2. *Genome Biol.* 15, 550. doi: 10.1186/s13059-014-0550-8

Lyons, J. B., Bredeson, J. V., Mansfeld, B. N., Bauchet, G. J., Berry, J., Boyher, A., et al. (2022). Current status and impending progress for cassava structural genomics. *Plant Mol. Biol.* 109, 177–191. doi: 10.1007/s11103-020-01104-w

Magori, S., and Citovsky, V. (2012). The role of the ubiquitin-proteasome system in *Agrobacterium tumefaciens*-mediated genetic transformation of plants. *Plant Physiol.* 160 (1), 65–71. doi: 10.1104/pp.112.200949

Mani, M. S. (1992). "Introduction to cecidology," in *Biology of Insect- Induced Galls*. Eds. J. D. Shorthouse and O. Rohfritsch (New York, USA: Oxford University Press), 1–7.

Meyer, J. M., and Hoy, M. A. (2008). Removal of fungal contaminants and their DNA from the surface of *Diaphorina citri* (Hemiptera: Psyllidae) prior to a molecular survey of endosymbionts. *Fla. Entomol.* 91 (4), 702–705.

Michell, C. T., and Nyman, T. (2021). Microbiomes of willow-galling sawflies: effects of host plant, gall type, and phylogeny on community structure and function. *Genome* 64 (6), 615–626. doi: 10.1139/gen-2020-0018

Montaldo, A. (1977). *Cultivo de Raíces y Tubérculos Tropicales* (Lima, Perú: Instituto Interamericano de Ciencias Agrícolas de la OEA).

Mueller, G. M., Bills, G. F., Foster, M. S., and Burlington, M. A. (2004). *Biodiversity of Fungi: Inventory and Monitoring Methods* (Elsevier Academic Press). doi: 10.1016/B978-0-12-509551-8.X5000-4

Nabity, P. D., Haus, M. J., Berenbaum, M. R., and Delucia, E. H. (2013). Leaf-galling *Phylloxera* on grapes reprograms host metabolism and morphology. *Proc. Natl. Acad. Sci.* 110 (41), 16663–16668. doi: 10.1073/pnas.1220219110

Nogueira, R. M., Costa, E. C., Silva, J. S., and Isaias, R. M. (2018). Structural and histochemical profile of *Lopesia* sp. Rübsaamen 1908 pinnula galls on *Mimosa tenuiflora* (Willd.) Poir. in a Caatinga environment. *Hoehnea* 45 (2), 314–322. doi: 10.1590/2236-8906-80/201

Nyman, T., and Julkunen, T. (2000). Manipulation of phenolic chemistry of willows by gall–inducing sawflies. *Proc. Natl. Acad. Sci. United States America* 97, 13184–13187. doi: 10.1073/pnas.230294097

Olmo, R., Cabrera, J., Díaz-Manzano, F. E., Ruiz-Ferrer, V., Barcala, M., Ishida, T., et al. (2020). Root-knot nematodes induce gall formation by recruiting developmental pathways of post-embryonic organogenesis and regeneration to promote transient pluripotency. *New Phytol.* 227 (1), 200–215. doi: 10.1111/nph.16521

Orlek, A., Stoesser, N., Anjum, M. F., Doumith, M., Ellington, M. J., Peto, T., et al. (2017). Plasmid classification in an era of whole-genome sequencing: application in studies of antibiotic resistance epidemiology. *Front. Microbiol.* 8. doi: 10.3389/fmicb.2017.00182

Park, C., Chen, S., Shirsekar, G., Zhou, B., Khang, C. H., Songkumarn, P., et al. (2012). The *Magnaporthe oryzae* effector AvrPiz-t targets the RING E3 ubiquitin ligase APIP6 to suppress pathogen-associated molecular pattern–triggered immunity in rice. *Plant Cell* 24 (11), 4748–4762. doi: 10.1105/tpc.112.105429

Piñol, M., Palazón, J., Cusidó, R., and Serrano, M. (1996). Effects of Ri T–DNA *Agrobacterium* rhizogenes on growth and Hyoscyamine production in *Datura stramonium* roots cultures. *Botánica Acta* 109, 133–138. doi: 10.1111/j.1438-8677.1996.tb00553.x

Ponce, G. E., Fuse, M., Chan, A., and Connor, E. F. (2021). The localization of phytohormones within the gall-inducing insect *Eurosta solidaginis* (Diptera: Tephritidae). *Arthropod-Plant Interact.* 15 (3), 375–385. doi: 10.1007/s11829-021-09817-5

Prjibelski, A., Antipov, D., Meleshko, D., Lapidus, A., and Korobeynikov, A. (2020). Using SPAdes *de novo* assembler. *Curr. Protoc. Bioinf.* 70 (1), e102. doi: 10.1002/cpbi.102

Radhika, V., Ueda, N., Tsuboi, Y., Kojima, M., Kikuchi, J., Kudo, T., et al. (2015). Methylated cytokinins from the phytopathogen *Rhodococcus fascians* mimic plant hormone activity. *Plant Physiol.* 169, 1118–1126. doi: 10.1104/pp.15

Rainey, F. A., Ward-Rainey, N., Kroppenstedt, R. M., and Stackebrandt, E. (1996). The genus Nocardiopsis represents a phylogenetically coherent taxon and a distinct actinomycete lineage: proposal of Nocardiopsiaceae fam. nov. *Int. J. Syst. Bacteriol.* 46, 1088–1092. doi: 10.1099/00207713-46-4-1088

Ramachandran, P., Joshi, B. J., Maupin-Furlow, J. A., and Uthandi, S. (2021). Bacterial effectors mimicking ubiquitin-proteasome pathway tweak plant immunity. *Microbiological Res.* 250, 126810. doi: 10.1016/j.micres.2021.126810

Raman, A. (2011). Morphogenesis of insect-induced plant galls: fact and questions. Flora-Morphology, Distribution. *Funct. Ecol. Plants* 206 (6), 517–533. doi: 10.1016/j.flora.2010.08.004

Ratcliffe, N. A., Furtado Pacheco, J. P., Dyson, P., Castro, H. C., Gonzalez, M. S., Azambuja, P., et al. (2022). Overview of paratransgenesis as a strategy to control pathogen transmission by insect vectors. *Parasites Vectors* 15 (1), 112. doi: 10.1186/s13071-021-05132-3

Rivera Hernández, J. F. (2011). La mosca de las agallas (*Jatrophobia brasiliensis*) en el cultivo de yuca. *Rev. la Universidad la Salle* 56, 277–288.

Rohfritsch, O., and Shorthouse, J. D. (1982). "Insect galls," in *Molecular Biology of Plant Tumors*. Eds. G. Kahl and J. S. Schell (New York, USA: Academic Press), 131–152.

Ronquist, F., Nieves-Aldrey, J. L., Buffington, M. L., Liu, Z., Liljeblad, J., and Nylander, J. A. (2015). Phylogeny, evolution and classification of gall wasps: the plot thickens. *PloS One* 10 (5), e0123301. doi: 10.1371/journal.pone.0123301

Sadanandom, A., Bailey, M., Ewan, R., Lee, J., and Nelis, S. (2013). The ubiquitin-proteasome system: central modifier of plant signaling. *New Phytol.* 196, 13–28. doi: 10.1111/j.1469-8137.2012.04266.x

Sánchez, E., Quesada, T., and Espinoza, A. M. (2006). Ultrastructure of the wild rice *Oryza grandiglumis* (Gramineae) in Costa Rica. *Rev. Biol. Trop.* 54, 377–385. doi: 10.15517/rbt.v54i2.13878

Santner, A., and Estelle, M. (2010). The ubiquitin-proteasome system regulates plant hormone signaling. *Plant J.* 61, 1029–1040. doi: 10.1111/j.1365-313X.2010.04112.x

Schwartz, S., Elnitski, L., Li, M., Weirauch, M., Riemer, C., Smit, A., et al. (2003). MultiPipMaker and supporting tools: alignments and analysis of multiple genomic DNA sequences. *Nucleic Acids Res.* 31 (13), 3518–3524. doi: 10.1093/nar/gkg579

Schwartz, S., Zhang, Z., Frazer, K. A., Smit, A., Riemer, C., Bouck, J., et al. (2000). PipMaker-a web server for aligning two genomic DNA sequences. *Genome Res.* 10 (4), 577–586. doi: 10.1101/gr.10.4.577

Seemann, T. (2014). Prokka: rapid prokaryotic genome annotation. *Bioinformatics* 30 (14), 2068–2069. doi: 10.1093/bioinformatics/btu153

Shao, S., Zhang, X., van Heusden, G. P. H., and Hooykaas, P. J. J. (2018). Complete sequence of the tumor-inducing plasmid pTiChry5 from the hypervirulent *Agrobacterium tumefaciens* strain Chry5. *Plasmid* 96–97, 1–6. doi: 10.1016/j.plasmid.2018.02.001

Shorthouse, J. D., and Rohfritsch, O. (1992). *Biology of the Insect-Induced Galls* (New York, USA: Oxford University Press).

Shu, K., and Yang, W. (2017). E3 ubiquitin ligases: ubiquitous actors in plant development and abiotic stress responses. *Plant Cell Physiol.* 58, 1461–1476. doi: 10.1093/pcp/pcx071

Singer, A. U., Schulze, S., Skarina, T., Xu, X., Cui, H., Eschen-Lippold, L., et al. (2013). A pathogen type III effector with a novel E3 ubiquitin ligase architecture. *PloS Patholog.* 9 (1), e1003121. doi: 10.1371/annotation/8c6eaae4-72a7-460a-8b1a-f855731f3706

Sinnott, E. W. (1960). *Plant Morphogenesis* (New York: McGraw-Hill).

Smalla, K., Jechalke, S., and Top, E. M. (2015). Plasmid detection, characterization, and ecology. *Microbiol. Spectr.* 3 (1). doi: 10.1128/microbiolspec.PLAS-0038-2014

Song, G. Q., Prieto, H., and Orbovic, V. (2019). *Agrobacterium*-mediated transformation of tree fruit crops: Methods, progress, and challenges. *Front. Plant Sci.* 10. doi: 10.3389/fpls.2019.00226

Stes, E., Vandeputte, O. M., El Jaziri, M., Holsters, M., and Vereecke, D. (2011). A successful bacterial coup d'état: how *Rhodococcus fascians* redirects plant development. *Annu. Rev. Phytopathol.* 49, 69–86. doi: 10.1146/annurev-phyto-072910-095217

Sugio, A., Dubreuil, G., Giron, D., and Simon, G. C. (2015). Plant-insect interactions under bacterial influence: ecological implications and underlying mechanisms. *J. Exp. Bot.* 66 (2), 467–478. doi: 10.1093/jxb/eru435

Suzuki, K., Moriguchi, K., and Yamamoto, S. (2015). Horizontal DNA transfer from bacteria to eukaryotes and a lesson from experimental transfers. *Res. Microbiol.* 166 (10), 753–763. doi: 10.1016/j.resmic.2015.08.001

Swarup, S., De Feyter, R., Brlansky, R. H., and Gabriel, D. W. (1991). A pathogenicity locus from *Xanthomonas citri* enables strains from several pathovars of *X. campestris* to elicit cankerlike lesions on citrus. *Phytopathology* 81, 802–809. doi: 10.1094/Phyto-81-802

Tooker, J. F., and Helms, A. M. (2014). Phytohormone dynamics associated with gall insects, and their potential role in the evolution of the gall-inducing habit. *J. Chem. Ecol.* 40 (7), 742–753. doi: 10.1007/s10886-014-0457-6

Untergrasser, A., Cutcutache, I., Koressaar, T., Ye, J., Faircloth, B. C., Remm, M., et al. (2012). Primer3-new capabilities and interfaces. *Nucleic Acids Res.* 40 (15), e115. doi: 10.1093/nar/gks596

Vereecke, D., Zhang, Y., Francis, I. M., Lambert, P. Q., Venneman, J., Stamler, R. A., et al. (2020). Functional genomics insights into the pathogenicity, habitat fitness, and mechanisms modifying plant development of *Rhodococcus* sp. PBTS1 and PBTS2. *Front. Microbiol.* 11. doi: 10.3389/fmicb.2020.00014

Vierstra, R. D. (2009). The ubiquitin-26S proteasome system at the nexus of plant biology. *Nat. Rev. Mol. Cell Biol.* 10, 385–397. doi: 10.1038/nrm2688

Wang, W., Feng, B., Xiao, J., Xia, Z., Zhou, X., Li, P., et al. (2014). Cassava genome from a wild ancestor to cultivated varieties. *Nat. Commun.* 5, 5110. doi: 10.1038/ncomms6110

Waterhouse, A. M., Procter, J. B., Martin, D. M. A., Clamp, M., and Barton, G. J. (2009). Jalview Version 2-a multiple sequence alignment editor and analysis workbench. *Bioinformatics* 25, 1189–1191. doi: 10.1093/bioinformatics/btp033

Wicker, T., Yu, Y., Haberer, G., Mayer, K. F., Marri, P. R., Rounsley, S., et al. (2016). DNA transposon activity is associated with increased mutation rates in genes of rice and other grasses. *Nat. Commun.* 7, 12790. doi: 10.1038/ncomms12790

Wielkopolan, B., and Jakubowska, M. (2021). Beetles as plant pathogen vectors. *Front. Plant Sci.* 12. doi: 10.3389/fpls.2021.748093

Wood, D. E., Lu, J., and Langmead, B. (2019). Improved metagenomic analysis with Kraken 2. *Genome Biol.* 20, 257. doi: 10.1186/s13059-019-1891-0

Xu, F.-Q., and Xue, H.-W. (2019). The ubiquitin-proteasome system in plant responses to environments. *Plant Cell Environ.* 42, 2931–2944. doi: 10.1111/pce.13633

Yang, X. M., Hui, Y., Zhao, L. Q., Zhu, D. H., Zeng, Y., and Yang, X. H. (2021). Comparison of auxin and cytokinins concentrations, and the structure of bacterial community between host twigs and *Lithosaphonecrus arcoverticus* galls. *Insects* 12 (11), 982. doi: 10.3390/insects12110982

Yang, X., Hui, Y., Zhu, D., Zeng, Y., Zhao, L., Yang, X., et al. (2022). The diversity of bacteria associated with the invasive gall wasp *Dryocosmus kuriphilus*, its galls and a specialist parasitoid on chestnuts. *Insects* 13 (1), 86. doi: 10.3390/insects13010086

You, W., Liu, Q., Zou, K., Yu, X., Cui, H., and Ye, Z. (2011). Morphological and molecular differences in two strains of *Ustilago esculenta*. *Curr. Microbiol.* 62 (1), 44–54. doi: 10.1007/s00284-010-9673-7

Zahner, V., Lucarotti, C. J., and McIntosh, D. (2008). Application of 16S rDNA-DGGE and plate culture to characterization of bacterial communities associated with the sawfly, Acantholyda erythrocephala (Hymenoptera, Pamphiliidae). *Curr. Microbiol.* 57 (6), 564–569. doi: 10.1007/s00284-008-9243-4

Zeidan, M., and Czosnek, H. (1994). Acquisition and transmission of *Agrobacterium* by the whitefly *Bemisia tabaci*. *Mol. Plant-Microbe Interact.* 7 (6), 792–798. doi: 10.1094/mpmi-7-0792

Zhao, C., Escalante, L. N., Chen, H., Benatti, T. R., Qu, J., Chellapilla, S., et al. (2015). A massive expansion of effector genes underlies gall-formation in the wheat pest *Mayetiola destructor*. *Curr. Biol.* 25 (5), 613–620. doi: 10.1016/j.cub.2014.12.057

Zhao, C., Rispe, C., and Nabity, P. D. (2019). Secretory RING finger proteins function as effectors in a grapevine galling insect. *BMC Genomics* 20, 923. doi: 10.1186/s12864-019-6313-x

frontiers | Frontiers in Plant Science

TYPE Original Research
PUBLISHED 15 January 2024
DOI 10.3389/fpls.2023.1324056

OPEN ACCESS

EDITED BY
Carlos Henrique Meneses,
State University of Paraíba, Brazil

REVIEWED BY
Juan Ignacio Vilchez Morillas,
Universidade Nova de Lisboa, Portugal
Beckley Ikhajiagbe,
University of Benin, Nigeria

*CORRESPONDENCE
I. S. Coelho
irenecoelho@ufrrj.br

RECEIVED 18 October 2023
ACCEPTED 20 December 2023
PUBLISHED 15 January 2024

CITATION
Teles EAP, Xavier JF, Arcênio FS, Amaya RL, Gonçalves JVS, Rouws LFM, Zonta E and Coelho IS (2024) Characterization and evaluation of potential halotolerant phosphate solubilizing bacteria from *Salicornia fruticosa* rhizosphere. *Front. Plant Sci.* 14:1324056. doi: 10.3389/fpls.2023.1324056

Characterization and evaluation of potential halotolerant phosphate solubilizing bacteria from *Salicornia fruticosa* rhizosphere

E. A. P. Teles[1], J. F. Xavier[1], F. S. Arcênio[1], R. L. Amaya[1], J. V. S. Gonçalves[1], L. F. M. Rouws[2], E. Zonta[3] and I. S. Coelho[1*]

[1]Laboratory of Molecular Genetics of Microorganisms, Department of Veterinary Microbiology and Immunology, Veterinary Institute, Federal Rural University of Rio de Janeiro, Seropedica, Brazil, [2]Embrapa Agrobiologia, Seropedica, Brazil, [3]Laboratory of Soil-Plant Relationship, Department of Soils, Institute of Agronomy, UFRRJ, Seropedica, Brazil

Soil salinization is a significant abiotic factor threatening agricultural production, while the low availability of phosphorus (P) in plants is another worldwide limitation. Approximately 95–99% of the P in soil is unavailable to plants. Phosphate-solubilizing bacteria (PSB) transform insoluble phosphates into soluble forms that plants can utilize. The application of PSB can replace or partially reduce the use of P fertilizers. Therefore, selecting bacteria with high solubilization capacity from extreme environments, such as saline soils, becomes crucial. This study aimed to identify twenty-nine bacterial strains from the rhizosphere of *Salicornia fruticosa* by sequencing the 16S rDNA gene, evaluate their development in increasing concentrations of NaCl, classify them according to their salinity response, and determine their P solubilization capability. The bacteria were cultivated in nutrient agar medium with NaCl concentrations ranging from 0.5% to 30%. The phosphate solubilization capacity of the bacteria was evaluated in angar and broth National Botanical Research Institute (NBRIP) media supplemented with calcium phosphate ($CaHPO_4$) and aluminum phosphate ($AlPO_4$), and increased with 3% NaCl. All bacterial strains were classified as halotolerant and identified to the genera *Bacillus*, *Enterobacter*, *Halomonas*, *Kushneria*, *Oceanobacillus*, *Pantoea*, *Pseudomonas*, and *Staphylococcus*, with only one isolate was not identified. The isolates with the highest ability to solubilize phosphorus from $CaHPO_4$ in the liquid medium were *Kushneria* sp. (SS102) and *Enterobacter* sp. (SS186), with 989.53 and 956.37 $mg{\cdot}Kg^{-1}$ P content and final pH of 4.1 and 3.9, respectively. For the solubilization of $AlPO_4$, the most effective isolates were *Bacillus* sp. (SS89) and *Oceanobacillus* sp. (SS94), which raised soluble P by 61.10 and 45.82 $mg{\cdot}Kg^{-1}$ and final pH of 2.9 and 3.6, respectively. These bacteria demonstrated promising results in *in vitro* P

solubilization and can present potential for the development of bioinput. Further analyses, involving different phosphate sources and the composition of produced organic acids, will be conducted to contribute to a comprehensive understanding of their applications in sustainable agriculture.

KEYWORDS

salinity, tolerance, phosphorus, rhizobacteria, soil

1 Introduction

Soil salinization is one of the main abiotic factors that threaten agricultural production (Gamalero et al., 2020; Sagar et al., 2022). Saline soils naturally occur in arid and semi-arid climatic regions under limited drainage conditions, associated with the presence of a high water table, and in coastal regions (Pedrotti et al., 2015; Gamalero et al., 2020; Sagar et al., 2022). This process is aggravated by climate change, which causes increases in global temperature, rainfall regimes, and sea level (Ullah et al., 2021). Anthropogenic actions also cause the accumulation of salts in the soil, and it can occur in agricultural areas owing to incorrect management of irrigation water, use of low-quality water, poor drainage, and poor soil and fertilizer management (Pedrotti et al., 2015; Gamalero et al., 2020; Sagar et al., 2022). The occurrence of salinized arable land increases annually. It is estimated that more than 3.0% of the surface soils and 6% of the subsoils are salinized owing to natural or anthropogenic processes (Food and Agriculture Organization, 2021). Salinization has accelerated in coastal agricultural lands, with salinity increasing from 1 to 33% over the last 25 years (Ullah et al., 2021).

Most plant species cannot tolerate high salinity (Etesami and Beattie, 2018; Ondrasek et al., 2022). The harmful effects caused by excess salt in plants are related to osmotic and ionic stress, which globally affect the plant and impair its water balance and nutrition, leading to a reduction in the photosynthetic rate and the generation of reactive oxygen species that cause molecular damage (Hashem et al., 2016; Bulgari et al., 2019). Thus, soil salinization severely affects crop productivity and limits agricultural use in affected areas. However, some plant species, called halophyte plants, have adapted to environments with high salinity (Etesami and Beattie, 2018). These adaptations can be morphological, physiological, or biochemical but can also be related to symbiotic interactions with plant growth-promoting bacteria (PGPB) (Etesami and Beattie, 2018; Egamberdieva et al., 2022). Plants of the genus *Salicornia* are halophytes that develop in coastal regions and have ecological importance and commercial value, as they develop in areas where most plants cannot develop and produce a large amount of biomass that can be used for the production of vegetable salt (Furtado et al., 2019). Some studies have reported PGPB isolated from the rhizosphere of *Salicornia* spp., such as *Klebsiella pneumoniae* from *Salicornia bigelovii* (Rueda-Puente et al., 2003), *Pseudomonas pseudoalcaligenes* from *Salicornia europea* (Ozawa et al., 2007) and *Brachybacterium sausashtrense* and *Pseudomonas* spp. from *Salicornia brachiata* (Jha et al., 2012).

Another limiting factor in agricultural production worldwide is the low availability of phosphorus (P) in plants. Plants absorb P in the form of monobasic (H_2PO_4) and dibasic (HPO_4^{2-}) ions (Gomes et al., 2010). However, approximately 95–99% of the P in soil is unavailable to plants. It is associated with the mineral fraction, mainly calcium in calcareous soils, iron and aluminum in acidic soils, and organic compounds in soils rich in organic matter (Gomes et al., 2010; Rasul et al., 2019). In acidic soils, the most common forms are aluminum phosphates variscite ($AlPO_4 \bullet 2H_2O$), followed by strengite ($FePO_4 \bullet 2H_2O$) (Bashan et al., 2013). In alkaline soils with high availability of Ca^+, phosphate is associated with calcium (P-Ca), which are, in decreasing order of solubility, dihydrated dicalcium phosphate (brushite) $CaHPO_4 \bullet 2H_2O$ > anhydrous dicalcium phosphate (monetite) $CaHPO_4$ > octacalcium phosphate $Ca_8H_2(PO_4)_6 \bullet 5H_2O$ > tricalcium phosphate $Ca_3(PO_4)_2$ > hydroxyapatite $Ca_5(PO_4)_3OH$ > fluorapatite $Ca_5(PO_4)_3F$ (Bashan et al., 2013). It is estimated that more than 40% of agricultural land has limited productivity due to P deficiency (Balemi and Negisho, 2012). In recent years, the use of phosphate fertilizers to maintain agricultural production has increased. For example, in Brazil, the total annual use of phosphate fertilizers has increased from an annual average of 0.04 T in 1960 to 2.2 T in 2016 (Withers et al., 2018). However, P added to the soil is quickly immobilized and becomes inaccessible to plants, resulting in the low utilization of phosphate fertilizer. In addition, the application and accumulation of phosphate fertilizers promote the eutrophication of water bodies and contamination by metals in the soil, causing damage to plants, animals, and humans (Katherine, 2010; Azzi et al., 2017). Additionally, the high salinity may induce competition between $H_2PO_4^-$ and Cl^- ions (Maksimovic and Žarko, 2012). Therefore, the consequences of saline stress can lead to even greater difficulties in phosphorus uptake by plants. Moreover, plants under salt stress are most affected in crucial systems for nutrient absorption, cellular membrane stability, and transport pathways, and this also affects the absorption of phosphorus by the plant (Muhammed et al., 1987; Cruz et al., 2018; Roy and Chowdhury, 2021).

Phosphate-solubilizing microorganisms play a crucial role in the dynamics of P cycling in the soil (Alori et al., 2017, Zhu et al., 2018). These microorganisms can act as plant growth promoters by making P available to plants (Oliveira et al., 2009). The mobilization of P by microorganisms occurs through a variety of mechanisms such as a) acidification of the medium by the extrusion of H^+ and/or organic acids, b) metal complexation, c) metal reduction, d) extrusion of phosphatases, and e) indirect dissolution of phosphate through the stimulation of acid production by plants (Bashan et al., 2013; Krishnaraj and Dahale, 2014). Various studies have sought to isolate and identify phosphate-solubilizing bacteria as bioprospecting strains with the potential to develop sustainable alternatives for P management in agriculturalOliveira et al., 2009; Zhu et al., 2011; Jiang et al., 2018; Suleman et al., 2018; Chen and Liu, 2019; Wan et al., 2020; Jiang et al., 2022). Many soil microorganisms can mobilize P; however, their transformation capacity may be associated with ecological conditions.

Environmental stressors lead to a decrease in various microbial activities, such as respiration, nitrogen mineralization, and the functioning of various enzymes (Zhu et al., 2011; Singh, 2016). An increase in salinity can profoundly impact the efficacy of phosphate-solubilizing microorganisms due to the inhibition of certain enzyme activities (Sritongon et al., 2022). For instance, the activities of enzymes such as dehydrogenases, which play a crucial role in acid synthesis, and phosphatases, involved in the mineralization of organic phosphorus, can be inhibited (Silva et al., 2007; Suleman et al., 2018). As a result, the overall performance of microorganisms in phosphate solubilization can be severely compromised. Silva et al. (2007) reported that continuous soil irrigation with reject water from a salt mine decreased the activity of several enzymes, including dehydrogenases and phosphatases. On the other hand, Sritongon et al. (2022) observed high enzymatic activity in the rhizosphere soils of *O. sativa* grown in saline fields.

The prospecting of phosphate-solubilizing bacteria (PST) as an environmentally friendly alternative to improve phosphorus uptake by plants is promising. However, these bacteria may experience a reduction in their solubilization activity due to an increase in salinity. Therefore, studies aiming to bioprospect microorganisms that are tolerant to higher salt concentrations and possess attributes for plant growth are promising. Gil et al. (2023) isolated and identified bacteria from hypersaline and hypergypsic soils that exhibit traits promoting plant growth. They were capable of increasing root size under osmotic stress in *Medicago* sp. plants. In light of these considerations, this study aimed to identify and evaluate the tolerance of bacteria isolated from the rhizosphere of *Salicornia fruticosa* to increasing amounts of salt (NaCl) and their ability to solubilize calcium ($CaHPO_4$) and aluminum phosphate ($AlPO_4$).

2 Materials and methods

2.1 Origin of the isolates

The bacterial strains characterized in this study were isolated from the rhizosphere of *S. fruticosa* in two different saline environments: hypersaline plains (Rio de Janeiro, RJ) (23°00′10″ S, 43°34′30″ W) and a deactivated salt mine (São Pedro da Aldeia, RJ) (22°49′59″ S, 42°05′15″ W) by Xavier (2021). The bacteria were isolated in Nutrient Agar medium supplemented with 5%, 10%, 15%, and 20% NaCl. The bacteria, identified with the 'SS' acronym representing 'saline soils' from where they were isolated, have been stored in agar stock at -20°C in the Molecular Genetics Laboratory of Microorganisms at the Federal Rural University of Rio de Janeiro.

2.2 DNA extraction, amplification, and sequencing of the 16S rDNA gene

DNA was extracted as described by Tito et al. (2015). The 16S rDNA gene was amplified using the polymerase chain reaction (PCR) technique, using primers 338F 5'- AGAGTTTGATCCTGGCTCAG-3' and 1378R 5'-CGGTGTGTACAAGGCCCGGGAACG-3'. PCR assays were performed in 25 µL volumes containing the following reagents: reaction buffer (1X), 1 U of Taq DNA polymerase, 2.5 mM of $MgCl_2$, 0.2 mM of dNTP, and 0.4 µM of each primer. The reaction was performed in a thermocycler (Bio-Rad, Hercules, CA, USA), with an initial step of denaturation at 94°C for 5 min; followed by 35 cycles of denaturation at 94°C for 30 s, annealing at 56°C for 40 s; extension at 72°C for 1 min and 30 s; and a final extension step at 72°C for 7 min (Weisburg et al., 1991). The PCR products were separated using electrophoresis on a 1.5% agarose gel, stained with SYBR Green I (Life Technologies, Carlsbad, CA, EUA), and visualized under ultraviolet light using an L-PIX EX photodocumentation system (Loccus Biotechnology, Cotia, SP, Brazil).

The PCR products were purified using Exo-Sap (USB Corporation, Cleveland, Ohio, USA), as recommended by the manufacturer. The purified PCR products were sequenced using BigDye™ Terminator v3.1 Cycle Sequencing Kit. The reaction was performed in a thermocycler (Bio-Rad, Hercules, CA, USA), with initial denaturation at 94°C for 1 min; followed by 35 cycles of denaturation at 94°C for 15 s, annealing at 56°C for 15 s; and extension at 72°C for 4 min. Samples were purified by precipitation using 3M sodium acetate, 125 mM EDTA, and 70% ethanol. Sequencing of the samples was performed using the 3500 Genetic Analyzer equipment (Applied Biosystems®).

The sequences were edited using BioNumerics software (v. 7.6) and compared with the sequences deposited in the NCBI database using the BLASTn algorithm (Altschul et al., 1997). Sequence alignment was performed using the ClustalW algorithm (Thompson et al., 1994) in MEGAX software (v.11.0.8). Phylogenetic relationships were determined using the neighbor joining (NJ) algorithm and p-distance model. The strength of each branch was determined using a nonparametric bootstrap test with 1000 repetitions (Felsenstein, 1985). A sequence derived from *Arthrobacter oryzae* (NR 041545.1) was used as the external group.

2.3 Salinity test and classification of bacterial isolates

Bacterial isolates were seeded onto nutrient agar (meat extract 1.0 $g.L^{-1}$; yeast extract 2.0 $g.L^{-1}$; peptone 5.0 $g.L^{-1}$; sodium chloride

5.0 $g.L^{-1}$; agar 15. 0 $g.L^{-1}$) with increasing concentrations of NaCl (0.5%, 1%, 1,5%, 2%, 2,5%, 3%, 5%, 10%, 15%, 20%, 25%, and 30%). Plates containing the cultures were placed in an incubator at 30°C and analyzed over 10 days after inoculation. The growth interval was determined based on the NaCl concentration at which the isolate grew. The bacteria were inoculated into the medium in triplicates.

The isolates were classified according to their growth intervals at different NaCl concentrations: non-halophilic (0.5% to 3% NaCl), halotolerant (0.5 to > 5% NaCl), and halophilic (5% to 25%). The classification range was adapted from Oren (2013) and Daoud and Ben Ali (2020).

2.4 Evaluation of phosphorus-solubilizing ability in solid medium

The bacterial isolates were inoculated into test tubes containing 5 mL of DYGS medium and incubated for 24 h at 150 rpm. Subsequently, the optical density (OD) of each culture was adjusted to 0.9–1.0 by spectrophotometry at 600 nm. An aliquot of 7 µL of the cultures was inoculated onto 6 mm paper discs arranged on modified National Botanical Research Institute's phosphate (NBRIP) medium (glucose 10 gL^{-1}; $MgCl_2.6H_2O$ 5 gL^{-1}; $MgSO_4.7H_2O$, 0.25 gL^{-1}; KCl, 0.2 gL^{-1} and $(NH_4)_2SO_4$, 0.1 g L^{-1}; plus 3% NaCl and containing 5gL^{-1} of $CaHPO_4$ or $AlPO_4$ as a phosphate source. The bacteria were inoculated into the medium in triplicates. The solubilization halo formed around the colonies was determined on the seventeenth day after inoculation. The solubilization index (SI) was calculated using the following formula:

$$SI = \frac{halo\ \ diameter\ \ (mm)}{colony\ \ diameter\ \ (mm)}$$

The bacterial isolates were classified according to their solubilization capacity as low (SI<2), medium (2≤SI<4), and high (SI≥4) (Berraquero et al., 1976).

2.5 Evaluation of phosphorus-solubilizing ability in liquid medium

The bacterial isolates were cultured and their optical densities were adjusted as previously described. The NBRIP liquid culture medium was supplemented with 3% NaCl containing $CaHPO_4$ or $AlPO_4$ and the pH was adjusted to 7.0. The isolates were inoculated into the medium in triplicates. Three hundred microliters of each culture was inoculated into 50 mL falcon tubes containing 35 mL of NBRIP medium and cultivated under agitation at 150 rpm for 14 days. The concentration of soluble phosphate was determined on the day of inoculation (day 0) and at the end of the incubation period (final 14 days). For this, a 10 mL aliquot of each sample was transferred to a 15 mL falcon tube and centrifuged at 6000 rpm for 10 min. The supernatant was filtered with the aid of a syringe filter with a 0.22-µm membrane. The filtrate was used to determine the soluble phosphate content with adapted methods described by Teixeira et al. (2017), and the final pH of the medium after cultivation. For quantification, the filtrates were diluted 1:150 (*v/v*) or 1:200 (*v/v*) for $CaHPO_4$ and 1:50 for $AlPO_4$ using deionized water. Quantification is based on the formation of a blue-colored molybdic phosphorus complex obtained after the reduction of molybdate with ascorbic acid and measured by spectrophotometry at 660 nm. A phosphate standard curve was constructed using anhydrous KH_2PO_4. Available P values were determined according to the equation:

$$P = \frac{L - b}{a} * d$$

In which:

P – concentration of available phosphorus, in mg kg^{-1}.

L – sample absorbance reading.

a – angular coefficient of the standard curve (intercept).

b – linear coefficient of the standard curve.

d – dilution factor of the filtrate.

3 Results

3.1 Identification of bacteria and classification according to salinity

Among the 29 bacterial strains, 19 belonged to the phylum Proteobacteria and 10 belonged to the phylum Firmicutes. Bacteria in Proteobacteria belonged to the genera *Enterobacter*, *Halomonas*, *Kushneria*, *Pantoea*, and *Pseudomonas*. Isolate (SS145) grouped

TABLE 1 Identification of isolates, collection area, percentage of salt in the isolation medium, growth range, classification according to salinity, solubilization index (SI) in solid culture medium with $CaHPO_4$, and quantification of solubilized P and final pH value in liquid culture medium containing $CaHPO_4$ and $AlPO_4$.

Isolate ID	Genus	Collection area	%NaCl in the isolation medium	Growth interval	Classification according to salinity	SI	$CaHPO_4$		$AlPO_4$	
							P (mg kg^{-1})	pH	P (mg kg^{-1})	pH
SS85	*Bacillus* sp./CP049019.1	Deactivated salt mine	5%	0.5% - 10%	Halotolerant	Medium	474.798	4.2	2.50	2.8
SS89	*Bacillus* sp./CP049019.1	Deactivated salt mine	5%	0.5% - 10%	Halotolerant	Low	210.651	4.5	61.10	4.3

(Continued)

TABLE 1 Continued

Isolate ID	Genus	Collection area	%NaCl in the isolation medium	Growth interval	Classification according to salinity	SI	$CaHPO_4$		$AlPO_4$	
							P (mg kg^{-1})	pH	P (mg kg^{-1})	pH
SS231	*Bacillus* sp./CP115738.1	Hypersaline plains	5%	0,5% - 5%	Halotolerant	Medium	500.476	4.5	1.84	2.9
SS294	*Bacillus* sp./KX456341.1	Hypersaline plains	5%	0,5% - 10%	Halotolerant	Medium	351.641	4.7	8.02	3.8
SS186	*Enterobacter* sp./KR189294.1	Hypersaline plains	5%	0,5% - 15%	Halotolerant	Medium	956.372	3.9	12.36	4.7
SS97	*Enterobacter* sp./MK872311.1	Deactivated salt mine	15%	0,5% - 15%	Halotolerant	Medium	327.984	4.8	5.29	5.0
SS164	*Enterobacter* sp./MT613378.1	Hypersaline plains	5%	0,5% - 5%	Halotolerant	Medium	648.122	4.2	7.01	4.7
SS148	*Halomonas* sp./KP715923.1	Hypersaline plains	15%	0,5% - 15%	Halotolerant	Low	553.733	4.1	3.27	3.5
SS149	*Halomonas* sp./KY436502.1	Hypersaline plains	15%	0,5% - 15%	Halotolerant	Medium	213.861	4.7	7.91	3.2
SS157	*Halomonas* sp./MT760104.1	Hypersaline plains	5%	0,5% - 15%	Halotolerant	Low	401.450	4.5	9.75	3.6
SS151	*Kushneria* sp./AB970650.1	Hypersaline plains	15%	0,5% - 15%	Halotolerant	Low	266.286	4.4	9.75	3.8
SS162	*Kushneria* sp./KF560351.1	Hypersaline plains	5%	0,5% - 10%	Halotolerant	Medium	587.732	4.3	5.41	3.7
SS104	*Kushneria* sp./LR655847.1	Deactivated salt mine	20%	0,5% - 20%	Halotolerant	Low	345.340	4.3	2.50	3.8
SS99	*Kushneria* sp./ NR_044001.1	Deactivated salt mine	15%	0,5% - 20%	Halotolerant	Medium	274.251	5.0	13.02	4.0
SS102	*Kushneria* sp./ NR_044001.1	Deactivated salt mine	20%	0,5% - 20%	Halotolerant	Medium	989.539	4.1	10.88	3.0
SS88	*Oceanobacillus* sp./MH118526.1	Deactivated salt mine	5%	0,5% - 10%	Halotolerant	Medium	310.390	4.1	4.22	3.4
SS94	*Oceanobacillus* sp./MH118526.1	Deactivated salt mine	5%	0,5% - 20%	Halotolerant	Low	218.141	5.1	45.83	3.6
SS150	*Pantoea* sp./MH915636.1	Hypersaline plains	15%	0,5% - 20%	Halotolerant	Medium	436.044	4.6	23.89	3.5
SS141	*Pseudomonas* sp./KY072850.1	Deactivated salt mine	5%	0,5% - 10%	Halotolerant	Low	410.010	4.7	6.30	3.2
SS183	*Pseudomonas* sp./MN625859.1	Hypersaline plains	5%	0,5% - 15%	Halotolerant	Low	376.486	4.2	21.28	3.0
SS134	*Pseudomonas* sp./OP737584.1	Deactivated salt mine	15%	0,5% - 15%	Halotolerant	Medium	485.616	3.9	9.21	4.8
SS140	*Pseudomonas* sp./OP737584.1	Deactivated salt mine	5%	0,5% - 15%	Halotolerant	Low	365.430	4.4	8.98	4.6
SS161	*Pseudomonas* sp./OP737584.1	Hypersaline plains	5%	0,5% - 5%	Halotolerant	Medium	292.796	4.7	3.39	4.6
SS197	*Pseudomonas* sp./OP737601.1	Hypersaline plains	5%	0,5% - 5%	Halotolerant	Medium	687.589	5.0	4.22	3.4

(Continued)

TABLE 1 Continued

Isolate ID	Genus	Collection area	%NaCl in the isolation medium	Growth interval	Classification according to salinity	SI	$CaHPO_4$		$AlPO_4$	
							P (mg kg^{-1})	pH	P (mg kg^{-1})	pH
SS96	*Staphylococcus* sp./LC511705.1	Deactivated salt mine	15%	0,5% - 15%	Halotolerant	Medium	344.270	4.7	7.55	3.6
SS101	*Staphylococcus* sp./MT353655.1	Deactivated salt mine	15%	0,5% - 15%	Halotolerant	Low	466.358	4.8	11.12	4.8
SS100	*Staphylococcus* sp./MT550814.1	Deactivated salt mine	15%	0,5% - 15%	Halotolerant	Low	532.573	4.7	14.68	4.3
SS308	*Straphylococcus* sp./MT550814.1	Hypersaline plains	5%	0,5% - 15%	Halotolerant	Medium	240.490	4.6	12.60	3.7
SS145	Uncultured bacterium/ HQ143327.1	Hypersaline plains	15%	0,5% - 10%	Halotolerant	Low	783.286	5.6	1.84	4.3

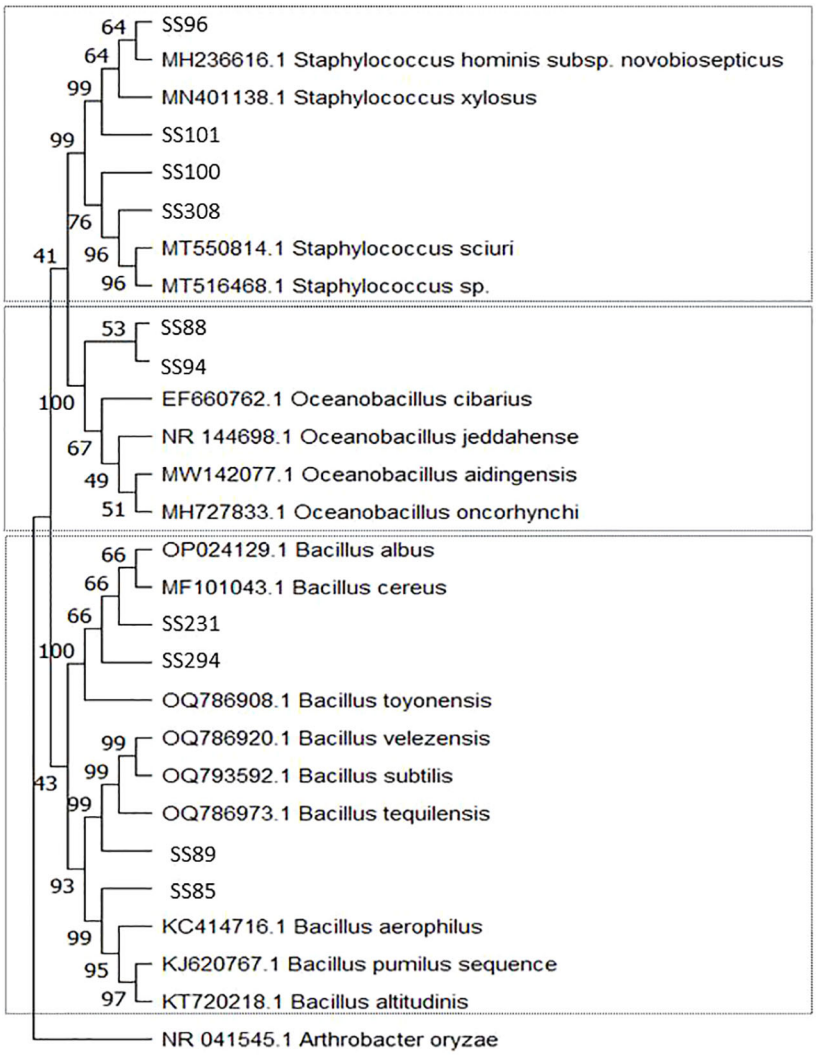

FIGURE 1
Phylogenetic tree constructed by the Neighbor-Joining method and Tajima-Nei model based on the 16S rDNA gene sequences of Proteobacteria phylum bacteria isolated from the rhizosphere of *Salicornia fruticosa*. The numbers at the nodes indicate the bootstrap values from 1,000 replicas.

with isolates from the phylum Proteobacteria but was not associated with any clade (Table 1, Figure 1). Isolates from the phylum Firmicutes belonged to the genera *Bacillus*, *Oceanobacillus*, and *Staphylococcus* (Table 1, Figure 2).

All isolates grown in both media containing 0.5% and above 5% NaCl, than were classified as halotolerant (Table 1) (Oren, 2008; Daoud and Ben Ali, 2020). Two isolates of *Pseudomonas* spp., one of *Enterobacter* sp., and one of *Bacillus* sp. developed at a maximum concentration of 5% NaCl. Three isolates of *Bacillus* spp., one of *Kushneria* sp., one of *Pseudomonas* sp., one of *Oceanobacillus* sp., and isolate (SS145) grew in 10% NaCl. Four isolates of *Staphylococcus* spp., three of *Halomonas* spp., three of *Pseudomonas* spp., two of *Enterobacter* spp., one of *Bacillus* sp., and one of *Kushneria* sp. accounted for growth up to 15% NaCl. Finally, three isolates of *Kushneria* spp., one of *Pantoea* sp., and one of *Oceanobacillus* sp. were grown in media containing up to 20% NaCl.

3.2 Phosphate solubilization in solid medium

All isolates grew in a solid culture medium containing dibasic calcium phosphate ($CaHPO_4$) as a phosphate source (Figure 3). Ten isolates (31.0%) showed a low solubilization and 18 (58.6%) showed a medium SI (Table 1). Despite colony development, halo formation

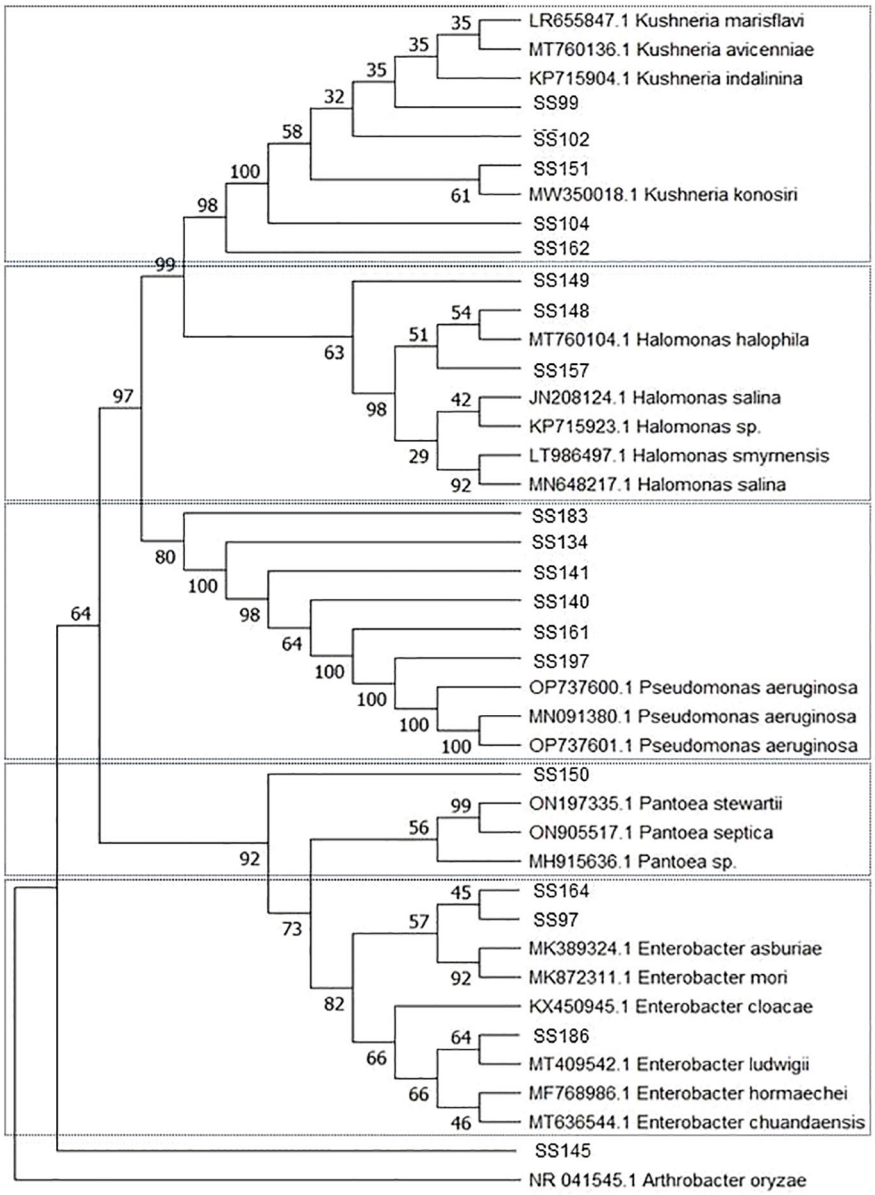

FIGURE 2
Phylogenetic tree constructed by the Neighbor-Joining method and Tajima-Nei model based on the 16S rDNA gene sequences of Firmicutes phylum bacteria isolated from the rhizosphere of *Salicornia fruticosa*. The numbers at the nodes indicate the bootstrap values from 1,000 replicas.

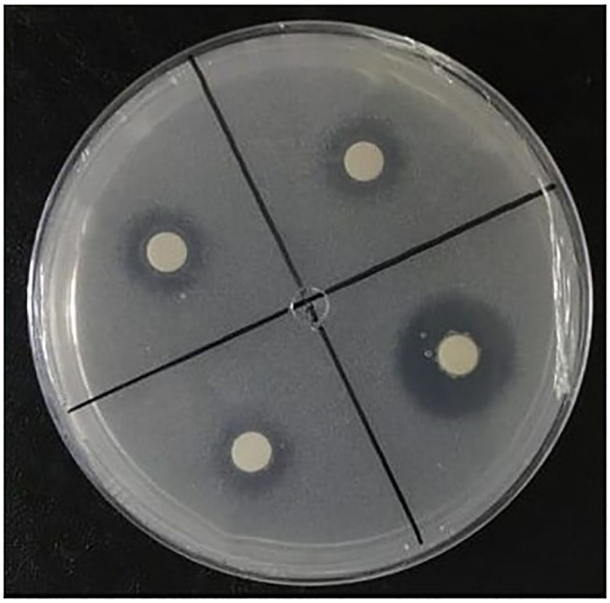

FIGURE 3
NBRIP medium containing $CaHPO_4$ inoculated with bacteria, displaying solubilization halos.

was not observed in the isolates of *Pseudomonas* sp. (SS140) and *Halomonas* sp. (SS157). The isolates also grew in a culture medium containing aluminum phosphate ($AlPO_4$) as a P source, but no halo formation was observed.

3.3 Phosphate solubilization in liquid medium

The solubilization of the two sources of phosphorus, $CaHPO_4$ and $AlPO_4$, by the bacterial isolates was accompanied by a reduction in pH. The content of P solubilized from $CaHPO_4$ varied from 210.65 to 989.54 mg·Kg^{-1} and the pH of the culture media at the end of cultivation varied from 5.4 to 3.9 (Table 1, Figure 4). The *Kushneria* sp. (SS102) demonstrated the highest $CaHPO_4$ solubilization, reaching 989.54 mg•Kg^{-1}, resulting in a final pH of 4.1. An increase in available P was also observed in media containing $AlPO_4$, varying from 1.84 to 61.10 mg·Kg^{-1}. The decrease in pH in media containing $AlPO_4$ was higher than that in media containing $CaHPO_4$, varying from 5.0 to 2.8 (Table 1, Figure 4). The *Bacillus* sp. (SS89) and *Oceanobacillus* sp. (SS94) isolates showed the highest soluble P contents for $AlPO_4$, 61.10 and 45.83 mg·Kg^{-1}, with a final pH of 2.9 and 3.6.

4 Discussion

The inoculation of cultivated plants with PGPB is considered a promising practice for promoting the development of agriculture under adverse conditions, such as saline soils (Gamalero et al., 2020). The main objective of this study was to evaluate the efficiency of halotolerant bacterial isolates from the rhizosphere of the halophyte *S. fruticosa* in the inorganic phosphates solubilization in solid and liquid culture media. The isolation and identification of bacteria associated with halophyte plants with growth-promoting attributes can contribute to the identification of strains with the potential for the development of bioinputs (Oliveira et al., 2009).

The isolates analyzed in this study came from media containing 5–20% NaCl and were all classified as halotolerant, exhibiting growth both at a concentration of 0.5% and above 5% NaCl (Oren, 2013; Daoud and Ben Ali, 2020). The salt content in saline soils is quite variable because of the influence of environmental factors, such as rain and tidal variations, which provide microhabitats with different salt concentrations (Quesada et al., 1982; Ventosa et al., 2008). Heterogeneity in the habitat can favor the selection of halotolerant microorganisms, as they are capable of adapting to fluctuating saline conditions in these environments, which gives them an advantage over specialized microorganisms, such as halophiles. The variation in salt content may explain why halotolerant bacteria were predominant among the evaluated bacteria. Halotolerant bacteria may offer increased benefits in agriculture owing to their superior adaptability to variations in salinity compared with halophilic bacteria.

The selection of phosphate-solubilizing bacteria in solid culture media has served as a universal indicator of phosphate solubilization for over half a century because it is a simple and inexpensive technique (Bashan et al., 2013). This method is based on the formation of a translucent halo around colonies. Halo formation occurs due to the dissolution of insoluble phosphate (Katznelson et al., 1962). The exudation of organic acids is one of the main mechanisms by which bacteria mobilize mineral phosphates (Alori et al., 2017). These acids can form metallic complexes or chelates with Ca, Al, and Fe^{+3} ions associated with phosphates without leading to the formation of translucent halos in the culture media (Merbach et al., 2009; Bashan et al., 2013). Therefore, plate tests must be complemented using quantitative tests in a liquid culture medium. Among the isolates studied, 27 showed solubilization activity of $CaHPO_4$ from the formation of translucent halos (Table 1, Figure 3). No solubilization halos were observed in media containing $AlPO_4$ despite colony development.

All isolates showed variations in the amount of available P and a reduction in pH in the liquid medium tests with $CaHPO_4$ and $AlPO_4$ (Table 1, Figure 3). Thus, solid culture media may be more suitable for the isolation of phosphate-solubilizing bacteria, as the ability to develop colonies in media containing insoluble P sources may indicate solubilization capacity even in the absence of halo formation. The levels of P mobilized from $CaHPO_4$ were higher than those mobilized from $AlPO_4$. The solubility of P-Ca was strongly influenced by pH, increasing rapidly with a decrease in pH from 6.5. However, the solubility of P–Al increases because of acids at pH levels below 3, which is rarely observed in soils (Fankem et al., 2008). Wan et al. (2020) observed similar results in tests carried out with 18 phosphate-solubilizing bacteria isolated from soil at the Laiyang Experimental Station, Shandong, China, which were able to solubilize from 47.08 to 250.77 mg L^{-1} of P from $Ca_3(PO_4)_2$ and from 14.99 to 81.99 mg L^{-1} from $AlPO_4$. Fankem et al. (2008) tested strains of *P. fluorescens* to solubilize different inorganic phosphate sources: $Ca_3(PO_4)_2$, $AlPO_4$, and $FePO_4$. Solubilization of Ca-P was possible by simply acidifying the

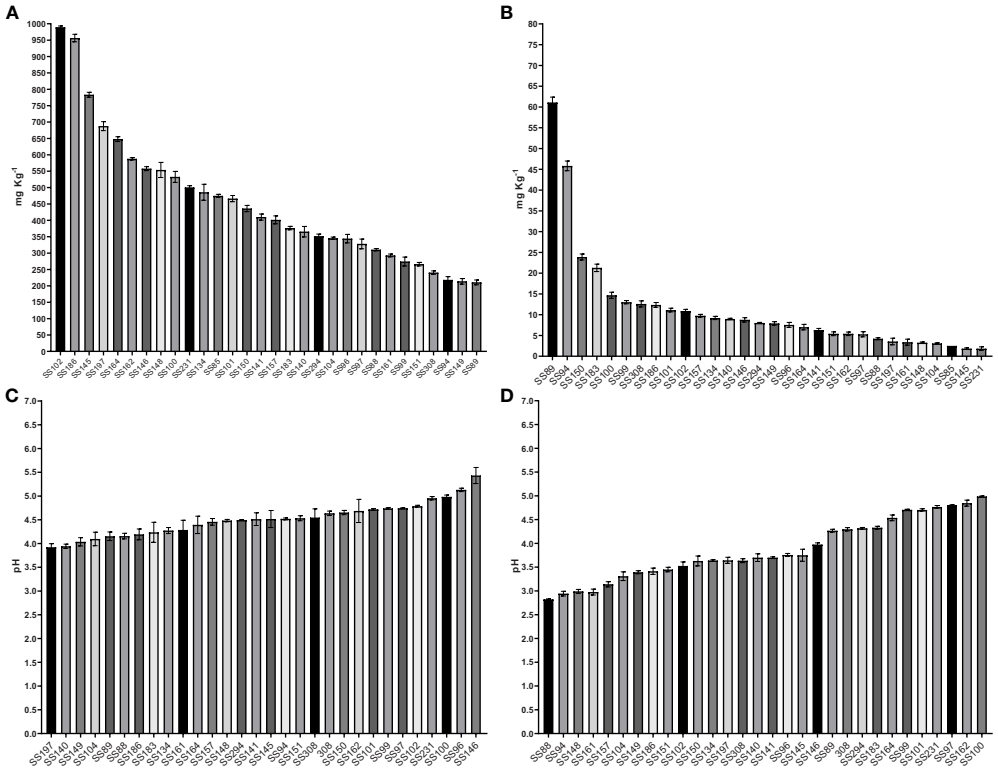

FIGURE 4
The P solubilizing levels, in mg Kg^{-1}, of bacteria in liquid NBRIP medium containing $CaHPO_4$ **(A)**, $AlPO_4$ **(B)**, and final pH on medium containing $CaHPO_4$ **(C)** and $AlPO_4$ **(D)**. The results are the mean value of three replicates, error bars represent standard error.

medium. In addition, the authors analyzed the action of different organic acids produced by bacteria on $Ca_3(PO_4)_2$ at pH 7 and 4 and found that acidity contributed to the solubilization of Ca-P by carboxylic acids. In contrast, the solubilization of $AlPO_4$ and $FePO_4$ seems to be related to the stability constants of the bond between the Fe or Al complex and different organic acids exuded by the bacteria (Fankem et al., 2008). Merbach et al. (2009) observed the production of various organic acids by bacteria capable of solubilizing different sources of mineral phosphate. These authors pointed out that bacterial strains that were more efficient in mobilizing P from calcium phosphate produced large amounts of citrate and tartarate, and to a lesser extent, malate. Furthermore, strains that solubilize iron and aluminum phosphates have tartarate and malate as their most important carboxylates, respectively (Merbach et al., 2009).

In our analyses, *Kushneria* sp. (SS102), *Enterobacter* sp. (SS186), and isolate (SS145) solubilized the highest amount of P from $CaHPO_4$, with 989.53, 956.37, and 783.82 mg·Kg^{-1}, respectively. The solubilization of phosphate from $AlPO_4$ was more pronounced for the isolates *Bacillus* sp. (SS89) and *Oceanobacillus* sp. (SS94), which increased the soluble P to 61.10 and 45.82 mg·Kg^{-1}, respectively. These two isolates showed relatively low calcium phosphate solubilization capacity compared to the others, at 210.65 and 218.14 mg·Kg^{-1} of P. Similar results were observed by Wan et al. (2020) for a strain of *Bacillus* sp., which solubilized about 60 mg·Kg^{-1} of P from calcium phosphate but showed considerably high capacity for iron and aluminum phosphate, at 30 mg·Kg^{-1} and 50 mg·Kg^{-1}, respectively. The isolates *Pantoea* sp. (SS150) and *Pseudomonas* sp. (SS183) also showed superior aluminum phosphate solubilization activity to the others, raising the soluble P in the medium to 23.99 and 21.7 mg·Kg^{-1}, respectively. They showed intermediate values for calcium phosphate, at 436.04 and 376.49 mg·Kg^{-1} of soluble P. In acidic soils, there is an increases the relative distributions of cations as H^+ and Al^{3+}, which may lead to negative effects such as the depletion of nutrients and the high solubility of Al, Fe, and Mn, causing toxicity in plants (Tian and Niu, 2015). Furthermore, soil acidification reduces P availability for plant due to fixation with acidic cations such as Al and Fe (Gomes et al., 2010; Xiao et al., 2013; Qaswar et al., 2020). Therefore, the exploration of PSB capable of solubilizing aluminum phosphate can be particularly promising for Brazilian soils.

5 Conclusion

Bacteria isolated from the rhizosphere of *S. fruticosa* were classified as halotolerant. Some isolates demonstrated promising results in *in vitro* P solubilization and hold potential for the development of bioinputs or for the bioprocessing of rock phosphates. Analyses involving higher salt concentrations, different phosphate sources and the composition of produced organic acids will be conducted to contribute to a comprehensive understanding of their applications in sustainable agriculture.

Data availability statement

The original contributions presented in the study are included in the article/supplementary material, further inquiries can be directed to the corresponding author.

Author contributions

TE: Conceptualization, Data curation, Formal analysis, Investigation, Methodology, Project administration, Supervision, Visualization, Writing – original draft, Writing – review & editing. XJ: Conceptualization, Data curation, Methodology, Writing – review & editing. AF: Investigation, Methodology, Writing – review & editing. GJ: Investigation, Methodology, Writing – review & editing. AR: Investigation, Methodology, Writing – review & editing. RL: Conceptualization, Project administration, Resources, Writing – review & editing. ZE: Conceptualization, Data curation, Formal analysis, Funding acquisition, Methodology, Resources, Supervision, Writing – review & editing. CI: Conceptualization, Data curation, Formal analysis, Funding acquisition, Project administration, Resources, Supervision, Validation, Visualization, Writing – review & editing.

Funding

The author(s) declare financial support was received for the research, authorship, and/or publication of this article. The following research funding agencies provided financial support: CNPq (National Council for Scientifc and Technological Development), CAPES (Coordination for the Improvement of Higher Education Personnel), and FAPERJ (Fundação Carlos Chagas Filho de Amparo à Pesquisa do Estado do Rio de Janeiro).

Acknowledgments

We thank the Federal Rural University of Rio de Janeiro and the Graduate Program in Agronomy - Soil Sciences for their technical and theoretical support throughout the research development.

Conflict of interest

The authors declare that the research was conducted in the absence of any commercial or financial relationships that could be construed as a potential conflict of interest.

Publisher's note

References

Alori, E. T., Glick, B. R., and Babalola, O. O. (2017). Microbial phosphorus solubilization and its potential for use in sustainable agriculture. *Front. Microbiol.* 8. doi: 10.3389/fmicb.2017.00971

Altschul, S. F., Madden, T. L., Schäffer, A. A., Zhang, J., Zhang, Z., Miller, W., et al. (1997). Gapped BLAST and PSI-BLAST: a new generation of protein database search programs. *Nucleic Acids Res.* 25, 3389–3402. doi: 10.1093/nar/25.17.3389

Azzi, V., Kanso, A., Kazpard, V., Kobeissi, A., Lartiges, B., and El Samrani, A. (2017). Lactuca sativa growth in compacted and non-compacted semi-arid alkaline soil under phosphate fertilizer treatment and cadmium contamination. *Soil Tillage Res.* 165, 1–10. doi: 10.1016/j.still.2016.07.014

Balemi, T., and Negisho, K. (2012). Management of soil phosphorus and plant adaptation mechanisms to phosphorus stress for sustainable crop production: a review. *J. Soil Sci. Plant Nutr.* 12, 547–562. doi: 10.4067/S0718-95162012005000015

Bashan, Y., Kamnev, A. A., and de-Bashan, L. E. (2013). Tricalcium phosphate is inappropriate as a universal selection factor for isolating and testing phosphate-solubilizing bacteria that enhance plant growth: a proposal for an alternative procedure. *Biol. Fertil. Soils* 49, 465–479. doi: 10.1007/s00374-012-0737-7

Berraquero, F. R., Baya, A., and Cormenzana, A. R. (1976). Establecimiento de índices para el estudio de la solubilización de fosfatos por bacterias del suelo. *Ars. Pharm.* 17, 399–406. doi: 10.30827/ars

Bulgari, R., Franzoni, G., and Ferrante, A. (2019). Biostimulants application in horticultural crops under abiotic stress conditions. *Agronomy* 9, 306. doi: 10.3390/agronomy9060306

Chen, Q., and Liu, S. (2019). Identification and characterization of the phosphate-solubilizing bacterium *pantoea* sp. S32 in reclamation soil in Shanxi, China. *Front. Microbiol.* 10. doi: 10.3389/fmicb.2019.02171

Cruz, J. L., Coelho, E. F., Coelho Filho, M. A., and Santos, A.A.d. (2018). Salinity reduces nutrients absorption and efficiency of their utilization in cassava plants. *Cienc. Rural* 48, 11. doi: 10.1590/0103-8478cr20180351

Daoud, L., and Ben Ali, M. (2020). "Halophilic microorganisms: Interesting group of extremophiles with important applications in biotechnology and environment," in *Physiological and biotechnological aspects of extremophiles* Elsevier Cambridge, UK: Academic Press), 51–64. doi: 10.1016/B978-0-12-818322-9.00005-8

Egamberdieva, D., Alimov, J., Shurigin, V., Alaylar, B., Wirth, S., and Bellingrath-Kimura, S. D. (2022). Diversity and plant growth-promoting ability of endophytic, halotolerant bacteria associated with *tetragonia tetragonioides* (Pall.) kuntze. *Plants* 11, 49. doi: 10.3390/plants11010049

Etesami, H., and Beattie, G. A. (2018). Mining halophytes for plant growth-promoting halotolerant bacteria to enhance the salinity tolerance of non-halophytic crops. *Front. Microbiol.* 9. doi: 10.3389/fmicb.2018.00148

Fankem, H., Ngo, L., Deubel, A., Quinn, J., Merbach, W., Etoa, F.-X., et al. (2008). Solubilization of inorganic phosphates and plant growth promotion by strains of *Pseudomonas fluorescens* isolated from acidic soils of Cameroon. *Afr. J. Microbiol. Res.* 2, 171–178. doi: 10.5897/AJMR.9000660

Felsenstein, J. (1985). Confidence limits on phylogenies: an approach using the bootstrap. *Evolution* 39, 783–791. doi: 10.1111/j.1558-5646.1985.tb00420.x

Food and Agriculture Organization (2021) *Global Map of Salt-affected Soils*. Available at: https://www.fao.org/soils-portal/data-hub/soil-maps-and-databases/global-map-of-salt-affected-soils/en/#:~:text=With%20the%20current%20information%20from%20118%20countries%20covering,saline%2C%2010%25%20are%20sodic%20and%205%25%20are%20saline-sodic (Accessed 10, 2023).

Furtado, B. U., Gołębiewski, M., Skorupa, M., Hulisz, P., and Hrynkiewicz, K. (2019). Bacterial and fungal endophytic microbiomes of *salicornia europaea*. *Appl. Environ. Microbiol.* 85, 13. doi: 10.1128/AEM.00305-19

Gamalero, E., Bona, E., Todeschini, V., and Lingua, G. (2020). Saline and arid soils: impact on bacteria, plants, and their interaction. *Biol. (Basel)* 9, 116. doi: 10.3390/biology9060116

Gil, T., Teixeira, R., Sousa, A., d'Oliveira Palmeiro, M. A., Cruz Coimbra de Matos, A., Niza Costa, M., et al. (2023). Isolation and characterization of culturable

osmotolerant microbiota in hypersaline and hypergypsic soils as new treatment for osmotic stress in plants. *Soil Syst.* 7, 86. doi: 10.3390/soilsystems7040086

Gomes, E. A., Souza, F.A.d.e, Sousa, S.M.d.e, Vasconcelos, M.J.V.d.e, Marriel, I. E., and Silva, U.C.d.a (2010). *Prospecção de Comunidades Microbianas do Solo Ativasno Aproveitamento Agrícolade Fontes de Fósforo de Baixa Solubilidade* Vol. 107 (Embrapa Milho e Sorgo. Documentos), 1-34. Available at: https://www.embrapa.br/busca-de-publicacoes/-/publicacao/883157/prospeccao-de-comunidades-microbianas-do-solo-ativas-no-aproveitamento-agricola-de-fontes-de-fosforo-de-baixa-solubilidade.

Hashem, A., Abd Allah, E. F., Alqarawi, A. A., Al-Huqail, A. A., and Shah, M. A. (2016). Induction of Osmoregulation and Modulation of Salt Stress in *Acacia gerrardii* Benth. by Arbuscular Mycorrhizal Fungi and *Bacillus subtilis* (BERA 71). *BioMed. Res. Int.* 2016, 6294098. doi: 10.1155/2016/6294098

Jha, B., Gontia, I., and Hartmann, A. (2012). The roots of the halophyte Salicornia brachiata are a source of new halotolerant diazotrophic bacteria with plant growth-promoting potential. *Plant Soil* 356, 265–277. doi: 10.1007/s11104-011-0877-9

Jiang, H., Qi, P., Wang, T., Wang, M., Chen, M., Chen, N., et al. (2018). Isolation and characterization of halotolerant phosphate-solubilizing microorganisms from saline soils. *3 Biotech.* 8, 461. doi: 10.1007/s13205-018-1485-7

Jiang, Y., Zhao, X., Zhou, Y., and Ding, C. (2022). Effect of the phosphate solubilization and mineralization synergistic mechanism of Ochrobactrum sp. on the remediation of lead. *Environ. Sci. pollut. Res. Int.* 29, 58037–58052. doi: 10.1007/s11356-022-19960-y

Katherine, K. (2010). *Environmental impacts of agricultural technologies* Vol. 65 (Evans School Policy Analysis & Research (EPAR). EPAR Brief), 1–18. Available at: https://www.researchgate.net/publication/254452871_Environmental_Impacts_of_Agricultural_Technologies_EPAR_Brief_No_65

Katznelson, H., Peterson, E. A., and Rouatt, J. W. (1962). Phosphate-dissolving microorganisms on seed and in the root zone of plants. *Can. J. Bot.* 40, 1181–1186. doi: 10.1139/b62-108

Krishnaraj, P. U., and Dahale, S. (2014). Mineral phosphate solubilization: concepts and prospects in sustainable agriculture. *PINSA* 80, 389. doi: 10.16943/ptinsa/2014/v80i2/55116

Maksimovic, I., and Žarko, I. (2012). *Effects of salinity on vegetable growth and nutrients uptake. Irrigation systems and practices in challenging environments*. Ed. T. S. Lee (London, UK: InTech), 169-190. doi: 10.5772/29976

Merbach, W., Fankem, H., and Deubel, A. (2009). "Influence of rhizosphere bacteria of African oil palm (Elaeis guineensis) on calcium, iron, and aluminum phosphate in *vitro* mobilization," in *International symposium "Root Research and Applications* (Vienna, AT), 2–4. Available at: http://asrr.boku.ac.at/fileadmin/files/RRcd/session03/poster/042.

Muhammed, S., Akbar, M., and Neue, H. U. (1987). Effect of Na/Ca and Na/K ratios in saline culture solution on the growth and mineral nutrition of rice (Oryza sativa L.). *Plant Soil* 104 (1), 57–62. doi: 10.1007/BF02370625

Oliveira, C. A., Alves, V. M. C., Marriel, I. E., Gomes, E. A., Scotti, M. R., Carneiro, N. P., et al. (2009). Phosphate solubilizing microorganisms isolated from rhizosphere of maize cultivated in an oxisol of the Brazilian Cerrado Biome. *Soil Biol. Biochem.* 41, 1782–1787. doi: 10.1016/j.soilbio.2008.01.012

Ondrasek, G., Rathod, S., Manohara, K. K., Gireesh, C., Anantha, M. S., Sakhare, A. S., et al. (2022). Salt stress in plants and mitigation approaches. *Plants* 11. doi: 10.3390/plants11060717

Oren, A. (2008). Microbial life at high salt concentrations: phylogenetic and metabolic diversity. *Saline Syst.* 4, 2. doi: 10.1186/1746-1448-4-2

Oren, A. (2013). Life at high salt concentrations, intracellular KCl concentrations, and acidic proteomes. *Front. Microbiol.* 4. doi: 10.3389/fmicb.2013.00315

Ozawa, T., Wu, J., and Fujii, S. (2007). Effect of inoculation with a strain of *Pseudomonas pseudoalcaligenes* isolated from the endorhizosphere of *Salicornia europea* on salt tolerance of the glasswort. *Soil Sci. Plant Nutr.* 53, 12–16. doi: 10.1111/j.1747-0765.2007.00098.x

Pedrotti, A., Chagas, R. M., Ramos, V. C., Prata, A. P. M., Lucas, A. A. T., and Santos, P. B. S. (2015). Causas e conseqüências do processo de salinização dos solos. *Rev. Eletrônica em Gestão Educação e Tecnologia Ambiental* 19, 1308–1324. doi: 105902/2236117016544

Qaswar, M., Dongchu, L., Jing, H., Tianfu, H., Ahmed, W., Abbas, M., et al. (2020). Interaction of liming and long-term fertilization increased crop yield and phosphorus use efficiency (PUE) through mediating exchangeable cations in acidic soil under wheat-maize cropping system. *Sci. Rep.* 10, 19828. doi: 10.1038/s41598-020-76892-8

Quesada, E., Ventosa, A., Rodriguez-Valera, F., and Ramos-Cormenzana, A. (1982). Types and properties of some bacteria isolated from hypersaline soils. *J. Appl. Bacteriology* 53, 155–161. doi: 10.1111/j.1365-2672.1982.tb04671.x

Rasul, M., Yasmin, S., Suleman, M., Zaheer, A., Reitz, T., Tarkka, M. T., et al. (2019). Glucose dehydrogenase gene containing phosphobacteria for biofortification of Phosphorus with growth promotion of rice. *Microbiol. Res.* 223–225, 1–12. doi: 10.1016/j.micres.2019.03.004

Roy, S., and Chowdhury, N. (2021). "Salt stress in plants and amelioration strategies: A critical review" in *Abiotic stress in plants*. Eds. S. Fahad, S. Saud, Y. Chen, C. Wu and D. Wang (London, UK: InTech), 1-32. doi: 10.5772/intechopen.93552

Rueda-Puente, E., Castellanos, T., Troyo-Dieguez, E., Diaz de Leon-Alvarez, J. L., and Murillo-Amador, B. (2003). Effects of a Nitrogen-Fixing Indigenous Bacterium (*Klebsiella pneumoniae*) on the Growth and Development of the Halophyte *Salicornia bigelovii* as a New Crop for Saline Environments. *J. Agro. Crop Sci.* 189, 323–332. doi: 10.1046/j.1439-037X.2003.00051.x

Sagar, A., Rai, S., Ilyas, N., Sayyed, R. Z., Al-Turki, A. I., El Enshasy, H. A., et al. (2022). Halotolerant rhizobacteria for salinity-stress mitigation: diversity, mechanisms and molecular approaches. *Sustainability* 14, 490. doi: 10.3390/su14010490

Silva, C. D. S., Vieira, R., and Porto, E. (2007). "Efeito da salinidade sobre a atividade enzimática em solos de região semi-árida do Brasil" in *CONGRESSO VIRTUAL IBEROAMERICANO SOBRE GESTION DE CALIDAD EN LABORATORIOS, 4., 2007, Madrid* (Madrid: IBEROLAB), 2007. Comunicaciones...

Singh, K. (2016). Microbial and enzyme activities of saline and sodic soils. *Land Degrad. Dev.* 27, 706–718. doi: 10.1002/ldr.2385

Sritongon, N., Sarin, P., Theerakulpisut, P., and Riddech, N. (2022). The effect of salinity on soil chemical characteristics, enzyme activity and bacterial community composition in rice rhizospheres in Northeastern Thailand. *Sci. Rep.* 12, 20360. doi: 10.1038/s41598-022-24902-2

Suleman, M., Yasmin, S., Rasul, M., Yahya, M., Atta, B. M., and Mirza, M. S. (2018). Phosphate solubilizing bacteria with glucose dehydrogenase gene for phosphorus uptake and beneficial effects on wheat. *PloS One* 13, e0204408. doi: 10.1371/journal.pone.0204408

Teixeira, P. C., Donagemma, G. K., Fontana, A., and Teixeira, W. G. (2017). Manual de métodos de análise de solo. *Brasília DF: Embrapa.* 3, 204–208.

Thompson, J. D., Higgins, D. G., and Gibson, T. J. (1994). CLUSTAL W: improving the sensitivity of progressive multiple sequence alignment through sequence weighting, position-specific gap penalties and weight matrix choice. *Nucleic Acids Res.* 22, 4673–4680. doi: 10.1093/nar/22.22.4673

Tian, D., and Niu, S. (2015). A global analysis of soil acidification caused by nitrogen addition. *Environ. Res. Lett.* 10, 24019. doi: 10.1088/1748-9326/10/2/024019

Tito, T. M., Rodrigues, N. D. M. B., Coelho, S. M. O., Souza, M. M. S., Zonta, E., and Coelho, I. S. (2015). Choice of DNA extraction protocols from Gram negative and positive bacteria and directly from the soil. *Afr. J. Microbiol. Res.* 9, 863–871. doi: 10.5897/AJMR2014.7259

Ullah, A., Bano, A., and Khan, N. (2021). Climate change and salinity effects on crops and chemical communication between plants and plant growth-promoting microorganisms under stress. *Front. Sustain. Food Syst.* 5. doi: 10.3389/fsufs.2021.618092

Ventosa, A., Mellado, E., Sanchez-Porro, C., and Marquez, M. C. (2008). "Halophilic and Halotolerant Micro-Organisms from Soils," in *Microbiology of extreme soils Soil Biology*. Eds. P. Dion and C. S. Nautiyal (Berlin, Heidelberg: Springer Berlin Heidelberg), 87–115.

Wan, W., Qin, Y., Wu, H., Zuo, W., He, H., Tan, J., et al. (2020). Isolation and characterization of phosphorus solubilizing bacteria with multiple phosphorus sources utilizing capability and their potential for lead immobilization in soil. *Front. Microbiol.* 11. doi: 10.3389/fmicb.2020.00752

Weisburg, W. G., Barns, S. M., Pelletier, D. A., and Lane, D. J. (1991). 16S ribosomal DNA amplification for phylogenetic study. *J. bacteriology* 173, 697–703. doi: 10.1128/jb.173.2.697-703.1991

Withers, P. J. A., Rodrigues, M., Soltangheisi, A., de Carvalho, T. S., Guilherme, L. R. G., Benites, V., et al. (2018). Transitions to sustainable management of phosphorus in Brazilian agriculture. *Sci. Rep.* 8, 2537. doi: 10.1038/s41598-018-20887-z

Xavier, J. F. (2021). *Isolamento e Caracterização de Bactérias Associadas À Rizosfera de Plantas Halófitas. [Dissertation]* ([Seropédica (RJ)]: Rural Federal University of Rio de Janeiro).

Xiao, C., Chi, R., and Hu, L. (2013). Solubilization of aluminum phosphate by specific Penicillium spp. *J. Cent. South Univ.* 20, 2109–2114. doi: 10.1007/s11771-013-1714-5

Zhu, F., Qu, L., Hong, X., and Sun, X. (2011). Isolation and characterization of a phosphate-solubilizing halophilic bacterium kushneria sp. YCWA18 from daqiao saltern on the coast of yellow sea of China. *Evid. Based Complement. Alternat. Med.* 2011, 615032. doi: 10.1155/2011/615032

Zhu, J., Li, M., and Whelan, M. (2018). Phosphorus activators contribute to legacy phosphorus availability in agricultural soils: A review. *Sci. Total Environ.* 612, 522–537. doi: 10.1016/j.scitotenv.2017.08.095

frontiers | Frontiers in Plant Science

TYPE Original Research
PUBLISHED 18 January 2024
DOI 10.3389/fpls.2023.1324643

OPEN ACCESS

EDITED BY
Diogo Neves Proença,
University of Coimbra, Portugal

REVIEWED BY
Mostafa Mohamed El-Sheekh,
Tanta University, Egypt
Mohammed Ali Abd Elhammed Abd Allah,
Desert Research Center, Egypt
Ana Garofolo,
Embrapa Agrobiologia, Brazil

*CORRESPONDENCE
Liziane Maria de Lima
liziane.lima@embrapa.br

RECEIVED 19 October 2023
ACCEPTED 27 December 2023
PUBLISHED 18 January 2024

CITATION
dos Santos AR, da Rocha GMG, Machado AP, Fernandes-Junior PI, Arriel NHC, Gondim TMdS and de Lima LM (2024) Molecular and biochemical responses of sesame (*Sesame indicum* L.) to rhizobacteria inoculation under water deficit. *Front. Plant Sci.* 14:1324643. doi: 10.3389/fpls.2023.1324643

Molecular and biochemical responses of sesame (*Sesame indicum* L.) to rhizobacteria inoculation under water deficit

Anderson Reges dos Santos[1], Geisenilma Maria Gonçalves da Rocha[2], Alexandre Paulo Machado[3], Paulo Ivan Fernandes-Junior[4], Nair Helena Castro Arriel[5], Tarcisio Marcos de Souza Gondim[5] and Liziane Maria de Lima[5]*

[1]Master's Degree in Agricultural Sciences, State University of Paraiba (UEPB), Campina Grande, PB, Brazil, [2]Postdoc, Embrapa Algodão, Campina Grande, PB, Brazil, [3]Department of Basic Health Sciences, Federal University of Mato Grosso, Cuibá, MT, Brazil, [4]Embrapa Semiárido, Petrolina, PE, Brazil, [5]Embrapa Algodão, Campina Grande, PB, Brazil

Introduction: Water scarcity is a challenge for sesame cultivation under rainfed conditions. In this scenario, a potential strategy to alleviate the water deficit is the application of plant growth-promoting bacteria. The objective of this study was to analyze the interaction of rhizobacteria with sesame cultivation under water deficit conditions.

Methods: An experiment was conducted in pots in a greenhouse using the BRS Morena sesame cultivar. The experimental design was completely randomized in a factorial scheme: 2 (irrigation regimes - daily irrigation and water deficit by suspending irrigation until 90% stomatal closure) x 6 (treatments with nitrogen or inoculants), with 5 replications. The types of fertilization were characterized by the addition of nitrogen (ammonium sulfate; 21% N), inoculants based on Bacillus spp. (pant001, ESA 13, and ESA 402), Agrobacterium sp. (ESA 441), and without nitrogen (control). On the fifth day after the suspension of irrigation, plant material was collected for gene expression analysis (DREB1 and HDZ7), activities of antioxidant enzymes (superoxide dismutase and catalase), relative proline content, and photosynthetic pigments. At the end of the crop cycle (about 85 days), production characteristics (root dry matter, aboveground dry matter, number of capsules, and thousand seed weight), as well as leaf nitrogen (N) and phosphorus (P) content, were evaluated.

Results and Discussion: There was a positive effect on both production and biochemical characteristics (proline, superoxide dismutase, catalase, and photosynthetic pigments). Regarding gene expression, most of the inoculated treatments exhibited increased expression of the DREB1 and HDZ7 genes. These biological indicators demonstrate the potential of rhizobacteria for application in sesame cultivation, providing nutritional supply and reducing the effects of water deficit.

KEYWORDS

diazotrophic bacteria, symbiosis, antioxidant enzymes, *DREB1* and *HDZ7* genes, drought

1 Introduction

Sesame (*Sesamum indicum* L.) is an oilseed crop that has numerous nutritional benefits for humans and animals. Its seeds are rich in oil, proteins, carbohydrates, minerals, and various antioxidants (Dossou et al., 2023). The main antioxidants in sesame in terms of value and level are lignans; among lignans, sesamin and sesamolin are the main compounds due to their health-promoting properties (Abe-Kanoh et al., 2019; Majdalawieh et al., 2020).

Worldwide, the culture of sesame has great socioeconomic importance, the most recent data on seed production points to a production of 6.4 million tons, occupying 13 million hectares in 2021 (FAOSTAT, 2021).

Among various abiotic stresses, water deficit is one of the most detrimental and leads to significant reductions in crop yield (Wang et al., 2019). To mitigate the negative effects of drought, plants exhibit several physiological mechanisms that stem from the induction of various genes (Mehmood et al., 2022), antioxidant defense systems (Santos et al., 2022), and the accumulation of osmoprotectants (Lima et al., 2023), among other factors.

Understanding the physiological and molecular mechanisms induced by drought is a fundamental step toward the development of high-yielding and drought-tolerant crop varieties. Several crops such as maize (Sah et al., 2020), sugarcane (Pereira et al., 2022), and soybean (Dong et al., 2019) have long-standing research results reporting gene expression patterns under water stress conditions. Sesame genotypes tolerant to water deficit were also evaluated, and 61 candidate genes that confer greater tolerance to drought were identified. These genes may constitute useful resources for improving drought tolerance (Dossa et al., 2017).

Drought tolerance is a complex trait involving multiple genes associated with cellular signaling pathways that induce various physiological, morphological, and molecular responses. The membranes of plant cells perceive stress signals and trigger various self-activated and hormone-dependent signaling mechanisms, such as abscisic acid, for instance (Mahmood et al., 2019; Wang et al., 2022). Environmental signals related to drought are initially detected by specific receptors, which, upon activation, initiate metabolic pathways for intercellular signal transfer and activate transcription factors (TFs) for the expression of specific gene sets (Guttikonda et al., 2014). Transcription factors are among the most important gene families in the transcriptional regulation of responses to water stress (Dossa et al., 2016a; Dossa et al., 2016b; Baghery et al., 2022).

The homeodomain-leucine zipper (HD-Zip) gene family is involved in various stress-related processes in many plant species (Zhang et al., 2022) and plays a crucial role in protecting plants against biotic and abiotic stresses (Gao et al., 2015). HD-Zip is a well-characterized family of transcription factors found in several plant species. HD-Zip is associated with various regulatory processes in plant growth and development and responses to various external environmental signals; it is expressed in different plant tissues and organs and at various developmental stages (Wang et al., 2013; Capella et al., 2015; Ding et al., 2017).

Others genes are induced by drought. Transcription factors Dehydration-Responsive Element Binding (DREB1 and DREB2), belonging to the APETALA 2/Ethylene-Responsive Element Binding Protein (AP2/EREBP) group, bind to the dehydration-responsive element (DRE) cis-element in the promoter region of stress-inducible genes and regulate their expression in response to different abiotic stresses. The DREB subfamily plays a particularly important role in regulating plant responses to stress conditions (Dossa et al., 2016a; Zhang and Xia, 2023).

Recent studies have revealed that the application of plant growth-promoting bacteria (PGPB), like to the genera *Bacillus* spp. and *Bradyrhizobium* spp., can be used as a strategy to mitigate water stress (Brito et al., 2019; Lastochkina et al., 2019). The interaction between plants and microorganisms can also enhance the plant's tolerance to water deficit, as already assessed in crops such as maize (Kavamura et al., 2013; Santos et al., 2020), sorghum (Santana et al., 2020), wheat (Gontia-Mishra et al., 2016), foxtail millet (Niu et al., 2018), tomato (Gowtham et al., 2020), and more recently in sesame (Lima et al., 2023). Inoculation with these bacteria can result in physiological changes such as the regulation of the antioxidant system (Barbosa et al., 2018; Andrade et al., 2021), stomatal closure regulation by altering abscisic acid levels (Chieb and Gachomo, 2023), and production of osmoregulators like trehalose and proline (Barbosa et al., 2018). For sesame cultivation, a pioneering study demonstrating PGPB as tools to reduce the effects of water stress was recently published by our research group (Lima et al., 2023). However, the mechanisms triggered by these bacteria in sesame remain unknown.

In the present study, the objective was to analyze the molecular response mechanisms to drought through the expression of the *DREB1* and *HDZ7* genes, along with the analysis of physiological and biochemical parameters, in the BRS Morena sesame cultivar inoculated with plant growth-promoting rhizobacteria and drought tolerance-promoting rhizobacteria.

2 Material and methods

2.1 Preparation of inoculants

The *Bacillus* spp. ESA 13 (Fernandes-Júnior et al., 2015), ESA 402 (Antunes et al., 2019), and *Agrobacterium* sp. ESA 441 (Silva et al., 2018) strains were deposited in the "Collection of Microorganisms of Agricultural Interest of Embrapa Semiárido" (Embrapa Semiárido, Petrolina-PE, Brazil). They were inoculated on solid Luria Bertani (LB) medium and incubated for 24 hours at 28 °C. Subsequently, they were subcultured in liquid LB medium and incubated at 28 °C, 180 rpm, for 72 hours until reaching the exponential phase of bacterial growth (1.0 x 10^9 CFU ml^{-1}) (Vincent, 1970). The inoculant containing the pant001 strain (Carvalho et al., 2023) (*Bacillus subtilis* - Panta Premium) was provided by the Geoclean company. Then the bacteria subcultured in liquid medium were used directly for seed inoculation.

10.3389/fpls.2023.1324643

2.2 Experiment procedure

The experiment was conducted in a greenhouse at Embrapa Algodão, Campina Grande, PB (latitude 07°13' 30" S; longitude 35° 54'17" W; altitude 546 m). The sesame cultivar BRS Morena was used in pots with a capacity of 20 liters, filled with sandy-clay soil. A soil sample was analyzed for physical and chemical characteristics (Teixeira et al., 2017), and based on the results, fertilization was carried out according to the crop's demands (Gomes and Coutinho, 1998). Nitrogen was omitted in the treatments inoculated with bacteria and in the absolute control.

The experimental design was completely randomized in a factorial scheme of 2 (water regimes) x 6 (nitrogen treatments or inoculation), having a total of 12 treatments, with 5 replicates (Table 1). The water regimes were characterized as follows: 1) maintaining soil moisture with daily irrigation up to field capacity, and 2) inducing water deficit from the 30th day after emergence (DAE) by suspending irrigation for five days when plants with wilting symptoms exhibited 90% stomatal closure. The duration of irrigation suspension was determined using an Infra Red Gas Analyzer (IRGA, model LCpro-SD). After the stress period, the plants were rehydrated, and water supply was resumed. The nitrogen treatment involved the application of ammonium sulfate, divided into two applications. The first application was made 15 days after emergence, and the second application was done 20 days after the first. The absolute control treatment did not receive any inoculation or nitrogen fertilization. The inoculated treatments included the application of inoculants containing one of the strains: pant001, ESA 13, ESA 402, or ESA 441.

Phosphorus and potassium fertilization followed the recommendation of Gomes and Coutinho (1998), using triple superphosphate containing in its composition 20% P_2O_5 and potassium chloride containing 60% K_2O (Table 1).

The sesame seeds were disinfected with 70% ethanol for 15 seconds, 1% sodium hypochlorite for 1 minute, and rinsed 10 times with sterile distilled water (Hungria and Araujo, 1994). The disinfected seeds were placed in Petri dishes and microbiolized by immersion in the inoculants for 30 minutes. Ten seeds were sown per pot, and at 10 DAE of the seedlings, thinning was carried out, leaving only two plants per pot.

2.3 Vegetative development and productivity

The following growth characteristics were evaluated at the end of the phenological cycle (85 DAE): plant height (cm), measured from the base to the tip of the main stem of the plant; stem diameter; number of capsules per plant; mass of aboveground dry matter (g) and root dry matter (g), determined by drying the material in a forced-air circulation oven at 65 °C for approximately 96 hours until a constant mass was achieved, followed by weighing on a precision scale; and mass of 1000 seeds.

2.4 Analysis of nitrogen and phosphorus in the aboveground part

Initially, leaves from the plants at the end of the cycle were collected, placed in paper bags, and kept in a forced-air circulation oven for 72 hours at 65°C. After drying, the leaves were ground into a fine powder consistency using a knife mill.

For nitrogen analysis, a cold pre-digestion was performed at room temperature for 12 hours following the Kjeldahl method (Bezerra Neto and Barreto, 2011). Approximately 2 mg of dried plant material, 50 mg of sodium sulfate, 0.5 mg of copper sulfate, and 5 ml of sulfuric acid were used. Then, the solution was heated in a digestion block at 350 °C until all organic matter was dissolved, resulting in a clear solution. Subsequently, a 1 ml aliquot of the digested extract was added to a volumetric flask (50 ml) containing 40 ml of deionized water, 1 ml of sodium hydroxide, 1 ml of sodium silicate, and 2 ml of Nessler's reagent. The volume was completed to 50 ml with deionized water. The reading was carried out in a spectrophotometer at 410 nm, and the accumulated nitrogen in the

TABLE 1 Treatments generated by the combination of factors (irrigation x sources of N) using BRS Morena sesame inoculated with rhizobacteria under water restriction.

No.	Treatments with irrigation	Concentration	No.	Treatments without irrigation	Concentration
1	Ammonium sulfate; phosphorus; potassium	24 g; 20 g; 7 g (per pot^{-1})	7	Ammonium sulfate; phosphorus; potassium	24 g; 20 g; 7 g (per pot^{-1})
2	Without N and without inoculation; phosphorus; potassium	(-); 20 g; 7 g (per pot^{-1})	8	Without N and without inoculation; phosphorus; potassium	(-); 20 g; 7 g (per pot^{-1})
3	pant001; phosphorus; potassium	1.0 x 10^9 CFU ml^{-1}; 20 g; 7 g (per pot^{-1})	9	pant001; phosphorus; potassium	1.0 x 10^9 CFU ml^{-1}; 20 g; 7 g (per pot^{-1})
4	ESA 13; phosphorus; potassium	1.0 x 10^9 CFU ml^{-1}; 20 g; 7 g (per pot^{-1})	10	ESA 13; phosphorus; potassium	1.0 x 10^9 CFU ml^{-1}; 20 g; 7 g (per pot^{-1})
5	ESA 402; phosphorus; potassium	1.0 x 10^9 CFU ml^{-1}; 20 g; 7 g (per pot^{-1})	11	ESA 402; phosphorus; potassium	1.0 x 10^9 CFU ml^{-1}; 20 g; 7 g (per pot^{-1})
6	ESA 441; phosphorus; potassium	1.0 x 10^9 CFU ml^{-1}; 20 g; 7 g (per pot^{-1})	12	ESA 441; phosphorus; potassium	1.0 x 10^9 CFU ml^{-1}; 20 g; 7 g (per pot^{-1})

aboveground part was calculated according to Alcantara et al. (2014).

For phosphorus analysis, a solution containing 2 mg of dried plant material, 50 mg of sodium sulfate, 0.5 mg of copper sulfate, and 5 ml of sulfuric acid was prepared for cold pre-digestion at room temperature for 12 hours. Then, the solution was heated in a digestion block at 350 °C until all organic matter was dissolved, resulting in a clear solution. A 5 ml aliquot of the digested extract was added to a volumetric flask (50 ml) containing 10 ml of diluted molybdate solution and 40 mg of ascorbic acid and stirred until the mixture was homogeneous. The reading was carried out in a spectrophotometer at 660 nm. The phosphorus content in the samples was obtained from the relationship between absorbance value and concentration (Nogueira and Souza, 2005).

2.5 Enzymatic analyses and free proline content

A sample of two mature leaves from each plant was collected on the fifth day of water restriction (near 90% stomatal closure), immediately immersed in liquid N_2, and stored at -80°C for subsequent protein extraction. For protein extraction, 0.2 g of the leaves were ground in liquid N_2, and 3 ml of 0.1 M potassium phosphate buffer, pH 7.0, containing 100 mM EDTA, 1 mM L-ascorbic acid, and 4% polyvinylpyrrolidone (PVP) were added. Protein quantification was performed using the Bradford method (1976) on a spectrophotometer at 595 nm. The protein extract was stored at -20°C for enzymatic analyzes.

The activity of superoxide dismutase (SOD) was determined using the Giannopolitis and Ries method (1977) with 40 µl of leaf protein extract, 1.5 ml of 100 mM potassium phosphate buffer, pH 7.8, containing 1 mM EDTA, 13 mM methionine, 75 mM p-nitrotriazolium blue (NBT), and 460 µl of 1 mM riboflavin. The activity was determined using a spectrophotometer at 560 nm.

The catalase activity (CAT) was determined according to Azevedo et al. (1998). A 100 µl aliquot of leaf protein extract was mixed with 2.9 ml of 100 mM potassium phosphate buffer, pH 7.0, containing 40 mM H_2O_2. The reading was performed using a spectrophotometer at 240 nm.

The free proline content was determined using the methodology described by Bates et al. (1973). The reading was performed on a spectrophotometer at 520 nm.

2.6 Photosynthetic pigments

The levels of chlorophyll a, b, and total (a+b), as well as carotenoids, were determined using the 80% acetone extraction method (Lichtenthaler, 1987). The entire procedure was carried out in the presence of green light to prevent chlorophyll degradation. A 200 mg sample of plant tissue was ground in liquid N_2 and then solubilized in 10 ml of 80% acetone. Subsequently, the solution was filtered through qualitative filter paper, and the following absorbances were determined: 470; 646.8; 663.2; and 710 nm.

2.7 Analysis of *HDZ7* and *DREB1* gene expression by RT-qPCR

For gene expression analyses, leaves were collected on the fifth day of water restriction (near 90% stomatal closure), immersed in liquid N_2, and stored at -80°C. Total RNA was extracted using the Invisorb Spin Plant RNA Mini kit (Invitec). RNA integrity was assessed by 0.8% agarose gel electrophoresis, and concentration and purity were determined by spectrophotometry. A 1 µg aliquot of RNA was treated with DNase I, and cDNA synthesis was performed using the ImProm-II™ Reverse Transcription System kit (Promega). All procedures followed the manufacturers' recommendations.

Real-time quantitative analyses were conducted on the QuantStudio™ 5 Real-Time PCR System thermocycler (ThermoFisher) to amplify fragments of approximately 180 bp at an annealing temperature of 60°C. For each reaction, 6 µl of GoTaq® qPCR Master Mix (Promega), 0.4 µl of each primer (10 µM) (Table 2), 1.0 µl of cDNA (diluted 1:20, v/v), and water were used to achieve a final volume of 12 µl. The amplification conditions were as follows: 95°C for 10 minutes and 40 cycles of 95°C for 15 seconds, 60°C for 1 minute, and finally 72°C for 15 seconds. The graphs, melt curves, and Cqs were automatically generated by the QuantStudio™ 5 Real-Time PCR System thermocycler (ThermoFisher) based on the ΔΔCq normalization method (Livak and Schmittgen, 2001). Relative quantification was used for pattern analysis. Reactions with the constitutive actin gene were performed as an endogenous control.

2.8 Statistical analysis

The collected data was analyzed using the statistical software SISVAR version 5.6 (Ferreira, 2014), subjected to analysis of variance, and means were compared using the Tukey test ($P \leq 0.05$).

3 Results

3.1 Vegetative growth and grain production

Regarding the dry aboveground biomass, under water stress, plants inoculated with pant001 showed the highest average compared to the other treatments, followed by plants with nitrogen (WN) and

TABLE 2 Genes and sequences of the oligonucleotides used in quantitative analyses.

Gene	Sequence 5′→3′	Reference
HDZ7	F- TCTAAGCAAATCGAGCAAGAG R- TCTGTCTACCTGGGTGAGC	Mehmood et al. (2022)
DREB1	F- AGGGAGCCCAACAAGA R- TTAGCATTCGCAGACG	Dossa et al. (2016a)
ACTINA	F- CTGTCAACAGAATTGGGTG R- GCAACTGGGATGATATGG	Wei et al. (2015)

10.3389/fpls.2023.1324643

inoculated with ESA 402 (Figure 1A). About the dry root mass production, a significant effect was observed in the ESA 402 treatment (Figure 1B). For the number of capsules, the pant001 treatment under water stress obtained a higher average with a 21% increase compared to the irrigated treatment (Figure 1C). When analyzing the mass of a thousand seeds, it was observed that the pant001 and ESA 441 treatments under water stress had the highest averages compared to the non-inoculated treatments (Figure 1D).

3.2 Analysis of nitrogen and phosphorus in plant tissue

When analyzing the nitrogen content in leaves at the end of the experiment, the nitrogen-fertilized treatment, in both water conditions, had higher averages. Another treatment that showed a significant increase in nitrogen content was pant001 under water stress, compared to the irrigated condition, with an increase of 34% (Figure 2A). Regarding phosphorus content, the treatments with pant001, ESA 13, ESA 402, and nitrogen showed statistical differences when comparing the water conditions. Non-irrigated plants inoculated with pant001 had a higher concentration (0.45 dag kg^{-1}), an increase of 75%, compared to their irrigated treatment (Figure 2B).

3.3 Proline content and antioxidant activities

In the analysis of free proline, an increase in the concentration of this amino acid was observed in all treatments under water deficit conditions, differing statistically from the irrigated condition. Stressed plants treated with pant001, as well as those fertilized with nitrogen, had a higher concentration of proline, corresponding to an increase of 63% and 67%, respectively, when compared to plants without nitrogen (NN) under water stress (Figure 3A).

The analysis of SOD activity revealed a higher concentration in treatments under water stress, implying a physiological adjustment of the plants to water deficit, with significant differences between these water conditions. Plants inoculated with ESA 441 under water stress had higher SOD activity, with an increase of 50% when compared to the irrigated condition (Figure 3B). CAT activity, under water stress, differed statistically from the irrigated condition in treatments with pant001 and NN (Figure 3C).

3.4 Photosynthetic pigments

Despite the water restriction, treatments with pant001, ESA 441, WN, and NN showed a positive interaction, increasing the concentration of chlorophyll a, b, and total chlorophyll (Figures 4A–C, respectively). Under irrigated conditions, the best treatment for both forms of chlorophyll, as well as total chlorophyll, was with ESA 402, with an increase of approximately 55% compared to the treatment without nitrogen.

Regarding the concentration of carotenoids (Figure 4D), it was observed that most of the plants under water deficit increased the production of this pigment, with a significant difference between the water conditions. The treatment with pant001 showed the highest average increase when compared to the other non-irrigated treatments.

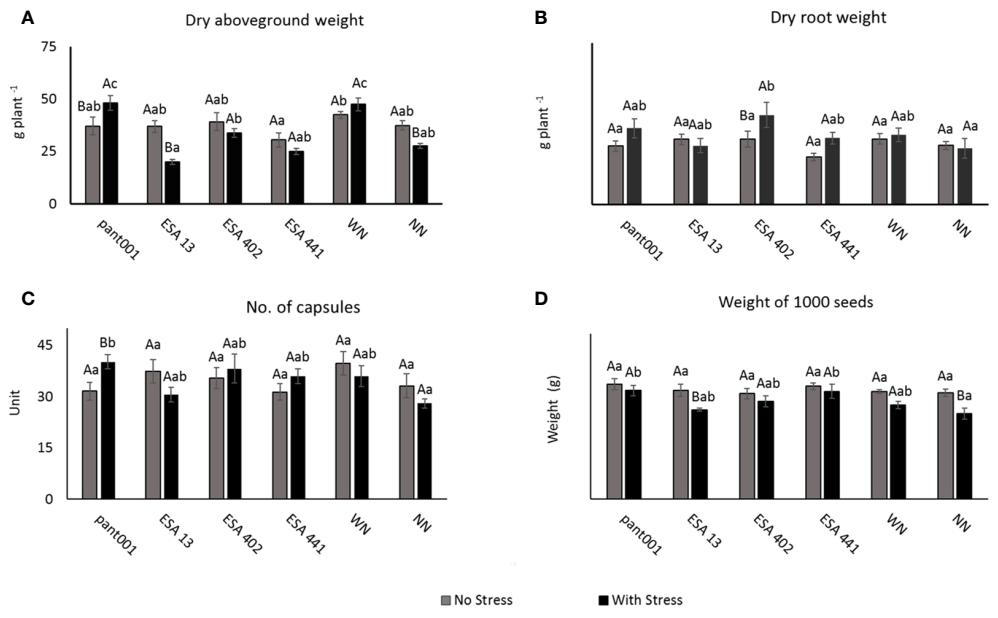

FIGURE 1
(A) Dry aboveground biomass; **(B)** Dry root weight; **(C)** Number of capsules; **(D)** Weight of a thousand sesame seeds of BRS Morena sesame inoculated with rhizobacteria under water restriction. Lowercase letters compare the treatments; uppercase letters compare the water regimes within each treatment. With nitrogen - WN; Without nitrogen – NN; No stress - daily irrigation; With stress - suspension of irrigation for five days, with stomatal closure near 90%. Tukey at 5% probability.

10.3389/fpls.2023.1324643

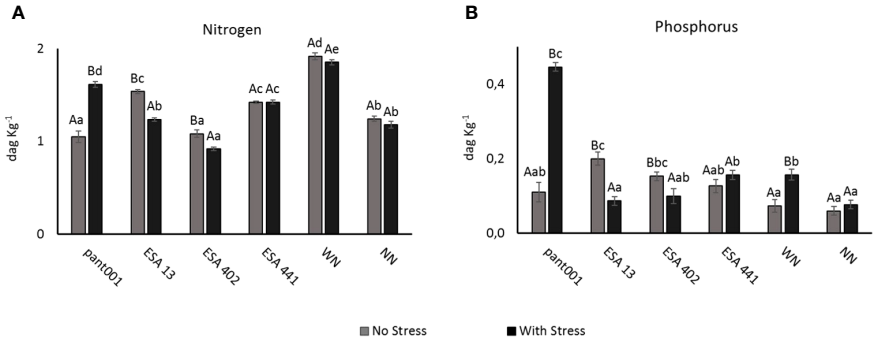

FIGURE 2
Accumulation of nitrogen **(A)** and phosphorus **(B)** in leaves of BRS Morena sesame inoculated with rhizobacteria under water restriction. Lowercase letters compare the treatments; uppercase letters compare the water regimes within each treatment. With nitrogen - WN; Without nitrogen – NN; No stress - daily irrigation; With stress - suspension of irrigation for five days, with stomatal closure near 90%. Tukey at 5% probability.

3.5 Expression of *HDZ7* and *DREB1* Genes

The *HDZ7* gene was significantly expressed in all stressed plants (Figures 5A, B). Plants WN had higher expression, being seven times higher than nitrogen-free plants. The treatments with ESA 402 and ESA 13 were also highlighted.

All plants under water deficit conditions showed an induction of the *DREB1* gene expression. Plants inoculated with ESA 402 exhibited higher expression, being eight times higher than the non-irrigated treatment without nitrogen. The nitrogen treatment under water deficit conditions showed a six-fold higher expression compared to the treatment NN under water deficit (Figures 5A, C).

4 Discussion

Most of the plants inoculated with the strains of rhizobacteria evaluated increased root production even under water deficit conditions (Figure 1). Similar responses have been reported in other crops such as maize (Kavamura et al., 2013), sorghum (Santana et al., 2020), cowpea (Abiala et al., 2023), and spinach (Jabborova et al., 2023). Many rhizospheric microorganisms are efficient in producing phytohormones such as abscisic acid, gibberellins, cytokinins, but mainly auxins, which promote root growth, branching, and hair formation (Araújo and Hungria, 1999). Among the rhizobacteria evaluated in this study, the production of

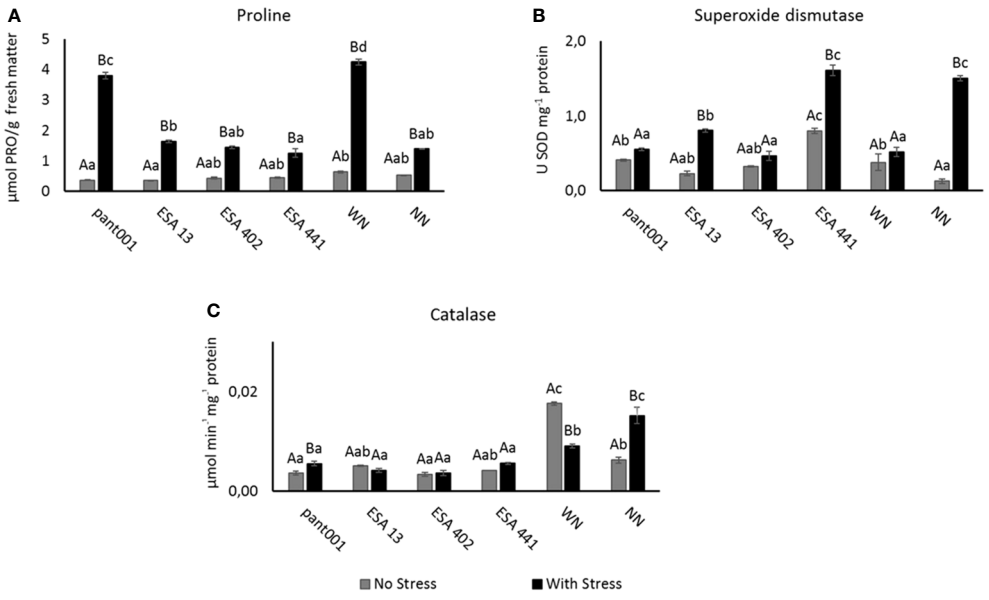

FIGURE 3
Analysis of sesame plants inoculated with rhizobacteria and under water restriction: **(A)** Concentration of free proline; **(B)** superoxide dismutase - SOD; **(C)** catalase - CAT. Lowercase letters compare the treatments; uppercase letters compare the water regimes within each treatment. With nitrogen - WN; Without nitrogen – NN; No stress - daily irrigation; With stress - suspension of irrigation for five days, with stomatal closure near 90%. Tukey at 5% probability.

10.3389/fpls.2023.1324643

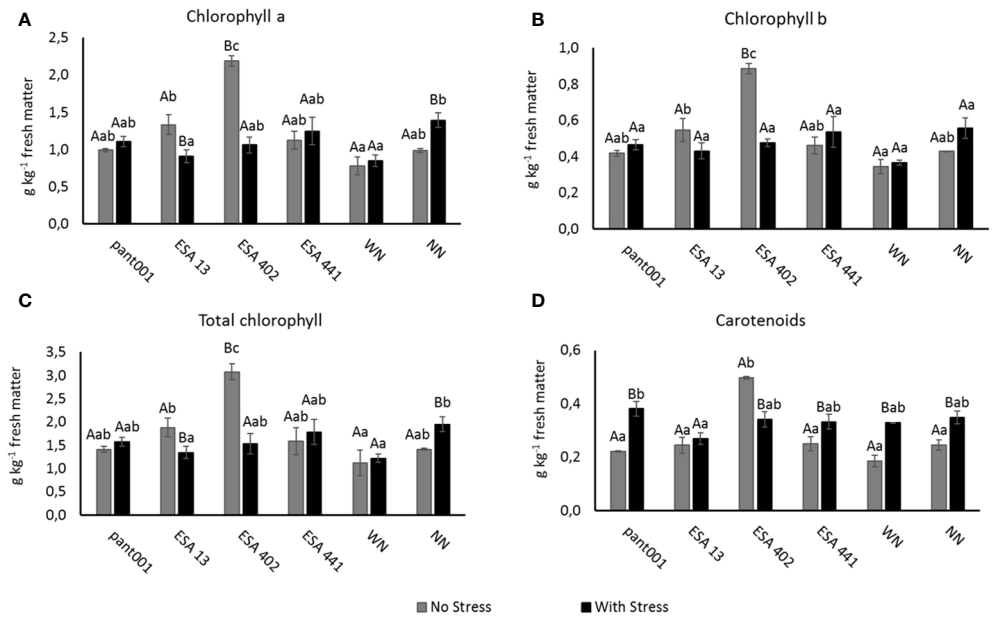

FIGURE 4
Analysis of photosynthetic pigments in sesame plants BRS Morena, inoculated with rhizobacteria and under water restriction: **(A)** chlorophyll a; **(B)** chlorophyll b; **(C)** total chlorophyll; **(D)** carotenoids. Lowercase letters compare the treatments; uppercase letters compare the water regimes within each treatment. With nitrogen - WN; without nitrogen - NN; No stress - daily irrigation; With stress - suspension of irrigation for five days, with stomatal closure near 90%. (Tukey at 5% probability).

varying amounts of auxins *in vitro* has already been demonstrated for the strains ESA 13 (Fernandes-Júnior et al., 2015), ESA 402 (Antunes et al., 2019), and ESA 441 (Silva et al., 2018). These factors are likely involved in inducing the increase in the root system of BRS Morena sesame observed in this study. Increased root volume is desirable under water deficit conditions as it allows for greater soil exploration and water absorption. Therefore, the inoculation of bacterial strains that stimulate root growth under water deficit conditions is desirable, and strains with this characteristic are potential inoculants.

The treatments with different inoculants showed an increase in phosphorus content (Figure 2B). Walia et al. (2014), in a study with tomatoes using biofertilizers containing *B. subtilis*, observed a 57% increase in phosphorus content. According to these authors, *B.*

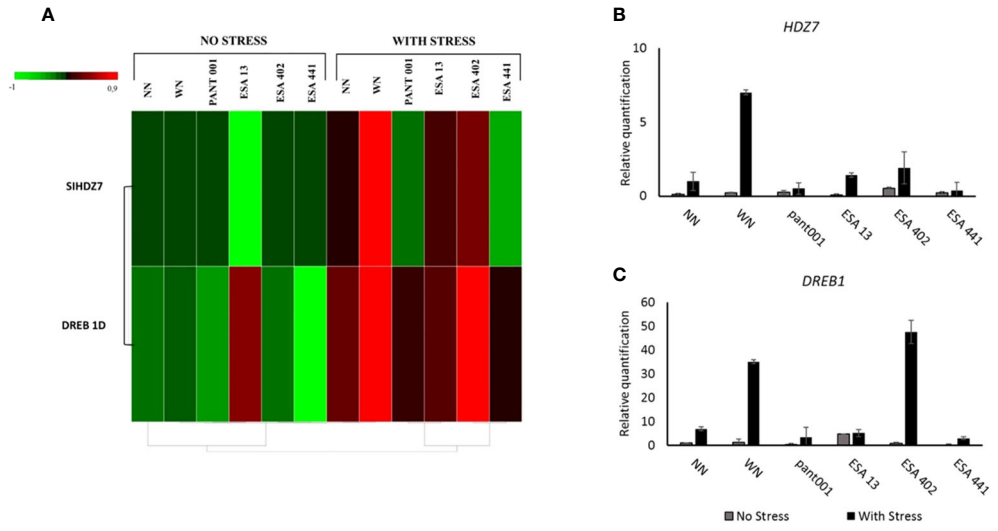

FIGURE 5
Analysis of the expression profile of the *HDZ7* and *DREB1* genes in the leaf tissues on the 5th day of water deficit (90% stomatal closure) in BRS Morena sesame plants inoculated with rhizobacteria. **(A)** Gene expression heatmap highlighting the difference in expression for plants without water stress versus plants under water deficit; Quantitative expression of the HDZ7 **(B)** and DREB1 **(C)** genes. With nitrogen - WN; without nitrogen – NN; No stress - daily irrigation; With stress - suspension of irrigation for five days, with stomatal closure near 90%. Tukey at 5% probability.

subtilis has a high capacity to improve plant growth and yield by enhancing the root's ability to mobilize and absorb nutrients and substances for the overall reproductive fitness of the plants.

The total free proline content in sesame plants on the 5th day of water deficit showed a significant increase in all treatments (Figure 3A). This elevated proline content suggests that the plants were under stress and were able to promote osmotic adjustment. Proline is known to play a role in stabilizing proteins, membranes, and cellular structures in plants subjected to stress and may be a factor that restricts the level of Reactive Oxygen Species (ROS). Zhou et al. (2022) investigated sweet potato plants under water stress and found proline accumulation associated with positive regulation of SOD and CAT activities. These characteristics help plants cope with drought (Ebrahimi et al., 2016; Cruz et al., 2022). Like other abiotic stresses, drought results in the accumulation of ROS, primarily in chloroplasts and to some extent in mitochondria. This leads to oxidative stress associated with superoxide anion radical (O_2^-) reactions. Oxidative stress can be detoxified by various antioxidants that alleviate oxidative damage and thus confer drought resistance. For example, the activation of the enzymes superoxide dismutase and catalase serves this function (Santos et al., 2022; Lima et al., 2023).

The increase in catalase activity (Figure 3C) highlights the importance of antioxidants as a defense mechanism in response to worsening water deficit, preventing oxidative stress (Nikolaeva et al., 2017). According to the results of this research, there may have been the activation of defense systems in sesame, as the enzymes of the plant's antioxidative mechanism are present in different cellular compartments and effectively contribute to the control of ROS, ensuring redox homeostasis in the system. Among these enzymes, catalase stands out, as it converts H_2O_2 to H_2O and O_2 without the need for a reducing agent to remove H_2O_2, which can favor greater efficiency in the removal of high concentrations of H_2O_2 under severe stress (Sharma et al., 2012).

During the research, the increase in SOD activity observed in sesame plants inoculated with growth-promoting bacteria, especially ESA 441 (Figure 3B), under water stress conditions is consistent with findings reported by Gholinezhad et al. (2020) in sesame associated with mycorrhizal inoculation under water restriction. These observations can be explained by the fact that plants can overcome the adverse effects of drought through various physiological responses, such as the increase in the activities of antioxidant enzymes to eliminate ROS.

The inoculation with pant001 significantly increased the chlorophyll content in sesame leaves (Figure 4), which may be related to the *B. subtilis* capacity to make nitrogen available to plants, a relatively unexplored aspect. In line with this hypothesis, this study observed that pant001 promoted a considerably high increase in nitrogen content (Figure 2A). According to López et al. (2014), the chlorophyll content in leaves is directly related to the nitrogen concentration in the plant. Lima et al. (2023) obtained similar results regarding chlorophyll content with the use of *Bacillus* in sesame cultivation. Inoculation with *B. subtilis* also increased chlorophyll a and total chlorophyll concentrations by 30% and 24% in sugarcane plants grown under normal water conditions and by 25% and 29% in plants stressed by drought, respectively (Fonseca et al., 2022). Satapute et al. (2012) and Hashem et al. (2019) suggested that *B. subtilis* can be exploited as a soil inoculant and used to provide nitrogen to soils. Chlorophylls are responsible for absorbing and converting light radiation into energy (ATP and NADPH) in the biological cycle of plants (Larcher, 2000). Therefore, the higher concentration of these pigments in plants subjected to water deficit represents greater stress tolerance capacity due to the intrinsic relationship between chlorophylls, photosynthetic potential, and productivity (O'Neill et al., 2006). Thus, it is expected that inoculation with bacilli can lead to good results in sesame crop productivity since the production of assimilates will be higher.

With the complete sequencing of the sesame genome, many transcription factors involved in responses to biotic and abiotic stresses have been identified, including DREB (Dossa et al., 2016a) and HDZ7, proteins that play crucial roles in gene expression regulation in plants (Mehmood et al., 2022).

In this study, the *DREB* gene profile was analyzed in the BRS Morena sesame genotype. As shown in Figure 5, transcript expression was higher in treatments subjected to water stress, which is consistent with findings in the literature reporting the involvement of this gene in plant responses to water stress situations (Guttikonda et al., 2014; Dossa et al., 2016a). According to Zhang and Xia (2023), *DREB* plays a crucial role in plant responses to water deficit. When plants are exposed to water scarcity, *DREB* is activated and binds to specific DNA sequences called Dehydration-Responsive Elements (DRE) to control the expression of genes involved in drought tolerance, activating defense responses so that plants implement a series of mechanisms to cope with water stress. Through the regulation of target genes, *DREB* activates the synthesis of cellular protection proteins, including antioxidant enzymes, membrane-stabilizing proteins, and osmotic regulators (Dossa et al., 2016a). Therefore, the increase in SOD activity (Figure 3B) as a plant antioxidant response to the imposed stress may be related to the increased expression of *DREB*.

Moreover, *HDZ7* demonstrated responsivity in most treatments subjected to water deficit in BRS Morena (Figure 5). According to the literature, *HDZ7* plays an important role in responding to abiotic stresses, primarily regulating genes related to responses to water deficit, salinity, temperature, light, and other stresses. These target genes may be related to the synthesis of protective proteins, osmotic adjustment, water transport, and other physiological processes that help plants tolerate water stress (Gong et al., 2019; Wei et al., 2019; Baek et al., 2023). Therefore, the BRS Morena sesame genotype, under conditions of water deficit, activates a defense system that includes the increased expression of at least two genes responsive to this condition, *DREB* and *HDZ7*, which in turn activate other defense responses in plants, as observed in this study.

Moreover, it has been observed that *HDZ7* plays a relevant role in root system growth and development. It regulates root architecture, including length, branching, and distribution of root hairs, which can promote the ability of plants to absorb nutrients and water (Wang et al., 2022). The increase in the mass of dry roots in sesame plants subjected to water deficit (Figure 1B) may be related to the considerable increase in the expression of *HDZ7* observed in this study. Plants likely benefited from the positive influence of rhizobacteria, as the

inoculated treatments promoted an increase in the mass of dry roots. The HD-Zip gene family may become a valuable tool for improving stress tolerance in molecular breeding methods (Wang et al., 2022).

5 Conclusion

In this study, it was reported that rhizobacteria can improve the tolerance of sesame plants to water deficit. The results revealed that inoculation positively altered nutritional, biochemical, and vegetative growth parameters of plants subjected to water deficit and plants under normal hydration conditions.

Another noteworthy observation pertained to the defense against ROS, with treatments under water stress showing an increase in both SOD activity and the content of free proline. Some inoculated treatments favored the increase in photosynthetic pigments during water stress. These cascade effects may have potentiated root development. In another line of defense, the *DREB1* and *HDZ7* genes had their expression increased, improving the performance of sesame plants. These results have positive implications for sesame cultivation, especially when grown during periods of reduced water availability, and indicate that the inoculation of rhizobacteria could be an option to mitigate the negative effects of drought using new microbial inoculants.

Data availability statement

The original contributions presented in the study are included in the article/supplementary materials, further inquiries can be directed to the corresponding author.

Author contributions

AS: Formal Analysis, Investigation, Writing – original draft. GR: Formal Analysis, Investigation, Validation, Writing – review & editing. AM: Writing – review & editing, Visualization. PF: Visualization, Methodology, Writing – review & editing. NA: Writing – review & editing, Funding acquisition. TG: Writing – review & editing, Conceptualization, Data curation, Methodology. LL: Conceptualization, Funding acquisition, Project administration, Validation, Writing – original draft.

Funding

The author(s) declare financial support was received for the research, authorship, and/or publication of this article. This research received financial support from Agricultural Research Corporation (Embrapa, SEG 20.18.01.021.00.00) and Graduate Development Program (PDPG) - Strategic Partnerships in States III, Notice No. 38/2022, Paraiba State Research Foundation (FAPESQ), Grant Agreement No. 397/2023.

Conflict of interest

The authors declare that the research was conducted in the absence of any commercial or financial relationships that could be construed as a potential conflict of interest.

The reviewer AG declared a shared affiliation with the authors GR, PF-J, NA, TG, and LL to the handling editor at the time of review.

Publisher's note

References

Abe-Kanoh, N., Kunimoto, Y., Takemoto, D., Ono, Y., Shibata, H., Ohnishi, K., et al. (2019). Sesamin catechol glucuronides exert anti-inflammatory effects by suppressing interferon β and inducible nitric oxide synthase expression through deconjugation in macrophage-like J774.1 cells. *J. Agric. Food Chem.* 10, 7640–7649. doi: 10.1021/acs.jafc.8b07227

Abiala, M., Sadhukhan, A., Muthuvel, J., Shekhawat, R. S., Yadav, P., and Sahoo, L. (2023). Rhizosphere *Priestia* species altered cowpea root transcriptome and enhanced growth under drought and nutrient deficiency. *Plants* 257, 1–20. doi: 10.1007/S00425-022-04047-2

Alcantara, R. M. C. M., Xavier, G. R., Rumjanek, N. G., Rocha, M. M., and Carvalho, J. S. (2014). Eficiência simbiótica de progenitores de cultivares brasileiras de feijão-caupi. *Rev. Sci. Agron.* 45, 1–9. doi: 10.1590/S1806-66902014000100001

Andrade, W. L., de Melo, A. S., de Melo, Y. L., da Silva Sá, F.V., Rocha, M. M., da Oliveira, A. P. S., et al. (2021). *Bradyrhizobium* inoculation plus foliar application of salicylic acid mitigates water deficit effects on cowpea. *J. Plant Growth Regul.* 40, 656–667. doi: 10.1007/s00344-020-10130-3

Antunes, G. D. R., Santana, S. R. A., Escobar, I. E. C., Brasil, M. D. S., Araújo, G. G. L. D., Voltolini, T. V., et al. (2019). Associative diazotrophic bacteria from forage grasses in the Brazilian semi-arid region are effective plant growth promoters. *Crop Pasture Sci.* 70, 899–907. doi: 10.1071/CP19076

Araújo, F. F., and Hungria, M. (1999). Nodulação e rendimento de soja co-infectada com *Bacillus subtilis* e *Bradyrhizobium japonicum*/*Bradyrhizobium elkanii*. Pesq. *Agropec. Bras. 34* 9, 1633–1643. doi: 10.1590/S0100-204X1999000900014

Azevedo, R. A., Alas, R. M., Smith, R. J., and Lea, P. J. (1998). Response of antioxidante enzymes to transfer from elevated carbondioxide to air and ozone fumigation, in leaves and roots of wild type and catalase- deficient mutant of barley. *Plant Physiol.* 104, 280–292. doi: 10.1034/j.1399-3054.1998.1040217.x

Baek, W., Bae, Y., Lim, C. W., and Lee, S. C. (2023). Pepper homeobox abscisic acid signalling-related transcription factor 1, CaHAT1, plays a positive role in drought response. *Plant Cell Environ.* 46, 2061–2077. doi: 10.1111/pce.14597

Baghery, M. A., Kazemitabar, S. K., Dehestani, A., and Mehrabanjoubani, P. (2022). Insight into gene regulatory networks involved in sesame (*Sesamum indicum* L.) drought response. *Biologia* 77, 1181–1196. doi: 10.1007/s11756-022-01009-7

Barbosa, D. D., Brito, S. L., Fernandes Junior, P. I., Fernandes, P. D., and Lima, L. M. (2018). Can *Bradyrhizobium* strains inoculation reduce water deficit effects on peanuts? *World J. Microbiol. Biotechnol.* 34, 1–11. doi: 10.1007/s11274-018-2474-z

Bates, L., Waldren, R. P., and Teare, I. D. (1973). Rapid determination of free proline for water-stress studies. *Plant Soil.* 39, 205–207. doi: 10.1007/BF00018060

Bezerra Neto, E., and Barreto, L. P. (2011). *Análises químicas e bioquímicas em plantas* (Recife: Imprensa Universitária da UFRPE).

Bradford, M. M. (1976). A rapid and sensitive method for the quantitation of microgram quantities of protein utilizing the principle of protein-dye binding. *Anal. Biochem.* 7, 248–254. doi: 10.1006/abio.1976.9999

Brito, S. L., Santos, A. B., Barbosa, D. D., Fernandes, P. D., Fernandes Junior, P. I., and Lima, L. M. (2019). *Bradyrhizobium* spp. as attenuators of water deficit stress in runner peanut genotypes based on physiological and gene expression responses. *Genet. Mol. Res.* 18, 1–12. doi: 10.4238/gmr18379

Capella, M., Ribone, P. A., Arce, A. L., and Chan, R. L. (2015). *Arabidopsis thaliana* homeobox 1 (AtHB1), a homedomain-leucine zipper I (HD-Zip I) transcription factor, is regulated by phytochrome-interacting factor 1 to promote hypocotyl elongation. *New Phytologist.* 207, 669–682. doi: 10.1111/nph.13401

Carvalho, M. A. C., Sá, M. E., Campos, D. T. S., MaChado, A. P., and Chagas Junior, A. F. (2023). *Bacillus subtilis* UFMT-Pant001 as a plant growth promoter in soybean in a greenhouse. *Afr. J. Agric. Res.* 19, 161–169. doi: 10.55905/oelv21n6-101

Chieb, M., and Gachomo, E. W. (2023). The role of plant growth promoting rhizobacteria in plant drought stress responses. *BMC Plant Biol.* 23, 407. doi: 10.1186/s12870-023-04403-8

Cruz, C., Cardoso, P., Santos, J., Matos, D., and Figueira, E. (2022). Bioprospecting soil bacteria from arid zones to increase plant tolerance to drought: growth and biochemical status of maize inoculated with plant growth-promoting bacteria isolated from sal island cape verde. *Plants* 11, 2912. doi: 10.3390/plants11212912

Ding, Z., Fu, L., and Yan, Y. (2017). Genome-wide characterization and expression profiling of HD-Zip gene family related to abiotic stress in cassava. *PloS One* 2, 1–20. doi: 10.1371/journal.pone.0173043

Dong, S., Jiang, Y., Dong, Y., Wang, L., Wang, W., Ma, Z., et al. (2019). A study on soybean responses to drought stress and rehydration. *Saudi J. Biol. Sci.* 26, 2006–2017. doi: 10.1016/j.sjbs.2019.08.005

Dossa, K., Li, D., Wang, L., Zheng, X., Liu, A., Yu, J., et al. (2017). Transcriptomic, biochemical and physio-anatomical investigations shed more light on responses to drought stress in two contrasting sesame genotypes. *Sci. Rep.* 7, 8755. doi: 10.1038/s41598-017-09397-6

Dossa, K., Niang, M., Assogbadjo, A. E., Cissé, N., and Diouf, D. (2016b). Whole genome homology-based identification of candidate genes for drought tolerance in sesame (*Sesamum indicum* L.). *Afric. J. Biotec.* 15, 1464–1475. doi: 10.5897/AJB2016.15420

Dossa, K., Wei, X., Li, D., Fonceka, D., Zhang, Y., Wang, L., et al. (2016a). Insight into the AP2/ERF transcription factor superfamily in sesame and expression profiling of DREB subfamily under drought stress. *BMC Plant Biol.* 16, 171. doi: 10.1186/s12870-016-0859-4

Dossou, S. S. K., Xu, F., Dossa, K., Zhou, R., Zhao, Y.-z., and Wang, D.-h. (2023). Antioxidant lignans sesamin and sesamolin in sesame (*Sesamum indicum* L.): A comprehensive review and future prospects. *J. Integ. Agric.* 22, 14–30. doi: 10.1016/j.jia.2022.08.097

Ebrahimi, M., Zamani, G. R., and Alizadeh, Z. (2016). Antioxidant activity: a strategy for alleviating the effects of drought on *Calendula officinalis* L. *Eur. J. Med. Plants.* 15, 1–14. doi: 10.9734/EJMP/2016/27035

FAOSTAT (2021)Crops and livestock products. In: *Food and Agriculture Organization of the United Nations*. Available at: https://www.fao.org/faostat/en/#data/QCL (Accessed November 28, 2023).

Fernandes-Júnior, P. I., Aidar, S. T., Morgante, C. V., Gava, C. A. T., Zilli, J. É., Souza, L. S. B., et al. (2015). The resurrection plant *Tripogon Spicatus* (Poaceae) harbors a diversity of plant growth promoting bacteria in Northeastern Brazilian Caatinga. *Rev. Bras. Ciênc. Solo* 39, 993–1002. doi: 10.1590/01000683rbcs20140646

Ferreira, D. F. (2014). Sisvar: a Guide for its Bootstrap procedures in multiple comparisons. *Ciênc. Agrotec.* 38, 109–112. doi: 10.1590/S1413-70542014000200001

Fonseca, M. C., Bossolani, J. W., Oliveira, S. L., Moretti, L. G., Portugal, J. R., Scudeletti, D., et al. (2022). *Bacillus subtilis* inoculation improves nutrient uptake and physiological activity in sugarcane under drought stress. *Microorganisms* 10, 809. doi: 10.3390/microorganisms10040809

Gao, Y., Gao, S., Xiong, C., Yu, G., Chang, J., Ye, Z., et al. (2015). Comprehensive analysis and expression profile of the homeodomain leucine zipper IV transcription factor family in tomato. *Plant Physiol. Biochem.* 96, 141–153. doi: 10.1016/j.plaphy.2015.07.025

Gholinezhad, E., Darvishzadeh, R., Moghaddam, S. S., and Popović-Djordjević, J. (2020). Effect of mycorrhizal inoculation in reducing water stress in sesame (*Sesamum indicum* L.): The assessment of agrobiochemical traits and enzymatic antioxidant activity. *Agric. Water Manage.* 238, 106234. doi: 10.1016/j.agwat.2020.106234

Giannopolitis, C. N., and Ries, S. K. (1977). Superoxide desmutases occurrence in higher plants. *Plant Physiol.* 59, 14–309. doi: 10.1104/pp.59.2.309

Gomes, R. V., and Coutinho, J. L. B. (1998). "Gergelim," in *Recomendações de adubação para o Estado de Pernambuco (2ª aproximação), 2.ed*. Eds. F. J. A. Cavalcanti, J. C. P. Santos, J. R. Pereira, J. P. Leite, M. C. L. Silva, F. J. Freire, et al (Recife: IPA), 144.

Gong, S., Ding, Y., Hu, S., Ding, L., Chen, Z., and Zhu, C. (2019). The role of HD-Zip class I transcription factors in plant response to abiotic stresses. *Physiol. Plant* 167, 516–525. doi: 10.1111/ppl.12965

Gontia-Mishra, I., Sapre, S., Sharma, A., and Tiwari, S. (2016). Amelioration of drought tolerance in wheat by the interaction of plant growth-promoting rhizobacteria. *Plant Biol. J.* 18, 992–1000. doi: 10.1111/plb.12505

Gowtham, H. G., Brijesh Singh, S., Murali, M., Shilpa, N., Prasad, M., Aiyaz, M., et al. (2020). Induction of drought tolerance in tomato upon the application of ACC deaminase producing plant growth promoting rhizobacterium *Bacillus subtilis* Rhizo SF 48. *Microbiol. Res.* 234, 126422. doi: 10.1016/j.micres.2020.126422

Guttikonda, S. K., Valliyodan, B., Neelakandan, A. K., Tran, L. S. P., Kumar, R., Quach, T. N., et al. (2014). Overexpression of AtDREB1D transcription factor improves drought tolerance in soybean. *Mol. Biol. Rep.* 41, 7995–8008. doi: 10.1007/s11033-014-3695-3

Hashem, A., Tabassum, B., and Abdallah., E. F. (2019). *Bacillus subtilis*: A plant-growth promoting rhizobacterium that also impacts biotic stress. *Saudi J. Biologic. Sci.* 26, 1291–1297. doi: 10.1016/j.sjbs.2019.05.004

Hungria, M., and Araujo, R. S. (1994). *Manual de mètodos empregados em estudos de microbiologia agrícola* (Brasília, DF: Embrapa-Serviço de Produção e Informação).

Jabborova, D., Ziyadullaeva, N., Enakiev, Y., Narimanov, A., Dave, A., Sulaymanov, K., et al. (2023). Growth of spinach as influenced by biochar and *Bacillus endophyticus* IGPEB 33 in drought condition. *Pak. J. Bot.* 55, 53–59. doi: 10.30848/PJB2023-SI(6

Kavamura, V. N., Santos, S. N., Silva, J. L., Parma, M. M., Ávila, L. A., Visconti, A., et al. (2013). Screening of Brazilian cacti rhizobacteria for plant growth promotion under drought. *Microbiol. Res.* 168, 183–191. doi: 10.1016/j.micres.2012.12.002

Larcher, W. (2000). Ecofisiologia vegetal. São Paulo: Rimas Artes.

Lastochkina, O., Islam, M. T., Rahman, M. M., Pandey, P., Boehme, M. H., and Haesaert, G. (2019). *Bacillus subtilis*-mediated abiotic stress tolerance in plants. *Bacilli Agrobiotechnol.: Phytostimulation Biocontrol.* 2, 97–133. doi: 10.1007/978-3-030-15175-1_6

Lichtenthaler, H. K. (1987). Chlorophylls and carotenoids: Pigments of photosynthetic biomembranes. *Meth. Enzymol.* 148, 350–382. doi: 10.1016/0076-6879(87)48036-1

Lima, G. B. P., Gomes, E. F., Rocha, G. M. G., Silva, F. A., Fernandes, P. D., MaChado, A. P., et al. (2023). Bacilli rhizobacteria as biostimulants of growth and production of sesame cultivars under water deficit. *Plants* 12, 1337. doi: 10.3390/plants12061337

Livak, K. J., and Schmittgen, T. D. (2001). Analysis of relative gene expression data using real-time quantitative PCR and the 2(-Delta Delta C(T)) method. *Methods* 25, 402–408. doi: 10.1006/meth.2001.1262

López, D. B. S., Hoyos, A. M. G., Perdomo, F. A. R., and Buitrago, R. R. B. (2014). Efecto de rizobacterias promotoras de crecimiento vegetal solubilizadoras de fosfato en *Lactuca sativa* cultivar White Boston. *Rev. Colomb. Biotec.* 16, 122–128. doi: 10.15446/rev.colomb.biote.v16n2.41077

Mahmood, T., Khalid, S., Abdullah, M., Ahmed, Z., Shah, M., K., N., et al. (2019). Insights into drought stress signaling in plants and the molecular genetic basis of cotton drought tolerance. *Cells* 9, 105. doi: 10.3390/cells9010105

Majdalawieh, A. F., Dalibalta, S., and Yousef, S. M. (2020). Effects of sesamin on fatty acid and cholesterol metabolism, macrophage cholesterol homeostasis and serum lipid profile: A comprehensive review. *Eur. J. Pharmacol.* 885, 173417. doi: 10.1016/j.ejphar.2020.173417

Mehmood, M., Khan, M. J., Akhtar, N., Mughal, F., Shah, S. T. A., Hyder, M. Z., et al. (2022). Systematic analysis of HD-ZIP transcription factors in sesame genome and gene expression profiling of SiHD-ZIP class I entailing drought stress responses at early seedling stage. *Mol. Biol. Rep.* 49, 2059–2071. doi: 10.1007/s11033-021-07024-2

Nikolaeva, M. K., Maevskaya, S. N., and Voronin, P. Y. (2017). Photosynthetic CO_2 /H_2O gas exchange and dynamics of carbohydrates content in maize leaves under drought. *Russ. J. Plant Physiol.* 64, 536–542. doi: 10.1134/S1021443717030116

Niu, J., Zhang, S., Liu, S., Ma, H., Chen, J., Shen, Q., et al. (2018). The compensation effects of physiology and yield in cotton after drought stress. *J. Plant Physiol.* 224-225, 30–48. doi: 10.1016/j.jplph.2018.03.001

Nogueira, A. R., and Souza, G. B. (2005). *Manual de laboratórios: Solo, Água, Nutrição vegetal* (São Carlos – SP. Ed. Embrapa: Nutrição Animal e Alimentos).

O'Neill, P. M., Shanahan, J. F., and Schepers, J. S. (2006). Use of chlorophyll fluorescence assessments to differentiate corn hybrid response to variable water conditions. *Crop Sci.* 46, 681–687. doi: 10.2135/cropsci2005.06-0170

Pereira, L. B., Gambarini, V. M. O., Menezes, A. B., Ottoboni, L. M. M., and Vicentini, R. (2022). Influence of sugarcane variety on rhizosphere microbiota under irrigated and water-limiting conditions. *Curr. Microbiol.* 79, 246. doi: 10.1007/s00284-022-02946-x

Sah, R. P., Chakraborty, M., Prasad, K., Pandit, M., Tudu, V. K., Chakravarty, M. K., et al. (2020). Impact of water deficit stress in maize: Phenology and yield components. *Sci. Rep.* 10, 2944. doi: 10.1038/s41598-020-59689-7

Santana, S. R. A., Voltolini, T. V., Antunes, G. R., Silva, V. M., Simões, W. L., and Morgante, C. V. (2020). Inoculation of plant growth-promoting bacteria attenuates the negative effects of drought on sorghum. *Arch. Microbiol.* 202, 1015–1024. doi: 10.1007/s00203-020-01810-5

Santos, R. M., Diaz, P. A. E., Lobo, L. L. B., and Rigobelo, E. C. (2020). Use of plant growth-promoting rhizobacteria in maize and sugarcane: characteristics and applications. *Front. Sustain. Food Syst.* 4. doi: 10.3389/fsufs.2020.00136

Santos, A. R., Melo, Y. L., Oliveira, L. F., Cavalcante, I. E., Ferraz, R. L. S., Silva Sá, F. V., et al. (2022). Exogenous silicon and proline modulate osmoprotection and antioxidant activity in cowpea under drought stress. *J. Soil Sci. Plant Nutr.* 22, 1692–1699. doi: 10.1007/s42729-022-00764-5

Satapute, P. P., Olekar, H. S., Shetti, A. A., Kulkarni, A. G., Hiremath, G. B., Patagundi, B. I., et al. (2012). Isolation and characterization of nitrogen fixing *Bacillus subtilis* strain as-4 from agricultural soil. *Int. J. Recent Sci. Res.* 3, 762–765.

Sharma, P., Jha, A. B., Dubey, R. S., and Pessarakli, M. (2012). Reactive oxygen species, oxidative damage, and antioxidative defense mechanism in plants under stressful conditions. *J. Bot.* 12, 1–26. doi: 10.1155/2012/217037

Silva, J. F., Silva, T. R., Escobar, I. E. C., Fraiz, A. C. R., Santos, J. W. M., Nascimento, T. R., et al. (2018). Screening of plant growth promotion ability among bacteria isolated from field-grown sorghum under different managements in Brazilian drylands. *World J. Microbiol. Biotechnol.* 34, 186. doi: 10.1007/s12275-014-3019-2

Teixeira, P. C., Donagemma, G. K., Fontana, A., and Geraldes, W. (2017). *Manual de métodos de análise de solo. 3. Ed* (Brasília: Embrapa).

Vincent, J. M. (1970). *A manual for the practical study of root-nodule bacteria* (Oxford: Blackwell Science Publication).

Walia, A., Mehta, P., Chauhan, A., and Shirkot, C. K. (2014). Effect of *Bacillus subtilis* strain CKT1 as inoculum on growth of tomato seedlings under net house conditions. *Proc. Natl. Acad. Sci. India Sect. B Biol. Sci.* 84, 145–155. doi: 10.1007/s40011-013-0189-3

Wang, D., Gong, Y., Li, Y., and Nie, S. (2022). Genome-wide analysis of the homeodomain-leucine zipper family in *Lotus japonicus* and the overexpression of LjHDZ7 in *Arabidopsis* for salt tolerance. *Front. Plant Sci.* 13. doi: 10.3389/fpls.2022.955199

Wang, H., Li, G. B., Zhang, D. Y., Lin, J., Sheng, B. L., Han, J. L., et al. (2013). [Biological functions of HD-Zip transcription factors]. *Yi Chuan.* 35, 1179–1188. doi: 10.3724/sp.j.1005.2013.01179

Wang, B., Liu, C., Zhang, D., He, C., and Li, Z. (2019). Effects of maize organ-specific drought stress response on yields from transcriptome analysis. *BMC Plant Biol.* 19, 335–343. doi: 10.1186/s12870-019-1941-5

Wei, X., Liu, K., Zhang, Y., Feng, Q., Wang, L., Zhao, Y., et al. (2015). Genetic discovery for oil production and quality in sesame. *Nat. Commun.* 6, 8609. doi: 10.1038/ncomms9609

Wei, M., Liu, A., Zhang, Y., Zhou, Y., Li, D., Dossa, K., et al. (2019). Genome-wide characterization and expression analysis of the HD-Zip gene family in response to drought and salinity stresses in sesame. *BMC Genom.* 20, 748. doi: 10.1186/s12864-019-6091-5

Zhang, Q., Chen, T., Wang, X., Wang, J., Gu, K., Yu, J., et al. (2022). Genome-wide identification and expression analyses of homeodomain-leucine zipper family genes reveal their involvement in stress response in apple (*Malus × domestica*). *Hortic. Plant J.* 8, 261–278. doi: 10.1016/j.ijbiomac.2023.125231

Zhang, Y., and Xia, P. (2023). The DREB transcription factor, a biomacromolecule, responds to abiotic stress by regulating the expression of stress-related genes. *Int. J. Biol. Macromol.* 243, 125231. doi: 10.1016/j.ijbiomac.2023.125231

Zhou, Y., Zhai, H., Xing, S., Wei, Z., He, S., Zhang, H., et al. (2022). A novel small open reading frame gene, IbEGF, enhances drought tolerance in transgenic sweet potato. *Front. Plant Sci.* 13. doi: 10.3389/fpls.2022.965069

frontiers | Frontiers in Plant Science

TYPE Original Research
PUBLISHED 26 January 2024
DOI 10.3389/fpls.2024.1345379

OPEN ACCESS

EDITED BY
Andrea Genre,
University of Turin, Italy

REVIEWED BY
Gayacharan,
Indian Council of Agricultural Research (ICAR), India
Rodrigo Vassoler Serrato,
Federal University of Paraná, Brazil

*CORRESPONDENCE
Jean Luiz Simões-Araújo
jean.araujo@embrapa.br

RECEIVED 27 November 2023
ACCEPTED 05 January 2024
PUBLISHED 26 January 2024

CITATION
da Silva HAP, Caetano VS, Pessôa DDV, Pacheco RS, Meneses CHSG and Simões-Araújo JL (2024) Unraveling the drought-responsive transcriptomes in nodules of two common bean genotypes during biological nitrogen fixation. *Front. Plant Sci.* 15:1345379. doi: 10.3389/fpls.2024.1345379

Unraveling the drought-responsive transcriptomes in nodules of two common bean genotypes during biological nitrogen fixation

Helder Anderson Pinto da Silva[1], Vanessa Santana Caetano[1], Daniella Duarte Villarinho Pessôa[1], Rafael Sanches Pacheco[2], Carlos Henrique S. G. Meneses[3] and Jean Luiz Simões-Araújo[1,2,4]*

[1]Programa de Pós-Graduação em Biotecnologia Vegetal, Centro de Ciências da Saúde (CCS), Universidade Federal do Rio de Janeiro (UFRJ), Rio de Janeiro, Brazil, [2]Programa de Pós-graduação em Fitossanidade e Biotecnologia Aplicada, Universidade Federal Rural do Rio de Janeiro (UFRRJ), Seropédica, RJ, Brazil, [3]Departamento de Biologia, Centro de Ciências Biológicas e da Saúde, Universidade Estadual da Paraíba, Campina Grande, Brazil, [4]Centro Nacional de Pesquisa de Agrobiologia, CNPAB – Embrapa, Laboratório de Genética e Bioquímica, Seropédica, RJ, Brazil

Common bean (*Phaseolus vulgaris*) can efficiently fix atmospheric nitrogen when associated with Rhizobia. However, drought stress impairs plant metabolic processes, especially the biological nitrogen fixation (BNF). Here, we assessed transcriptional responses in nodules of two common bean genotypes to drought stress under BNF reliance. The RNA-Seq analysis yielded a total of 81,489,262 and 72,497,478 high quality reads for Negro Argel and BAT 477 genotypes, respectively. The reads were mapped to the *Phaseolus vulgaris* reference genome and expression analysis identified 145 and 1451 differentially expressed genes (DEGs) for Negro Argel and BAT 477 genotypes, respectively. Although BAT 477 had more DEGs, both genotypes shared certain drought-responsive genes, including an up-regulated heat shock protein (HSP) and a down-regulated peroxidase, indicating shared pathways activated during drought in nodule tissue. Functional analysis using MapMan software highlighted the up-regulation of genes involved in abiotic stress responses, such as HSPs and specific transcription factors (TFs), in both genotypes. There was a significant down-regulation in metabolic pathways related to antioxidant protection, hormone signaling, metabolism, and transcriptional regulation. To validate these findings, we conducted RT-qPCR experiments for ten DEGs in nodules from both genotypes, for which the expression profile was confirmed, thus reinforcing their functional relevance in the nodule responses to drought stress during BNF. BAT 477 genotype exhibited more pronounced response to drought, characterized by a high number of DEGs. The strong down-regulation of DEGs leads to transcriptional disturbances in several pathways related to stress acclimation such as hormone and antioxidant metabolism. Additionally, we identified several genes that are known to play key roles in enhancing drought tolerance, such as HSPs and crucial TFs. Our results provide new insights into the

10.3389/fpls.2024.1345379

transcriptional responses in root-nodules, an underexplored tissue of plants mainly under drought conditions. This research paves the way for potential improvements in plant-bacteria interactions, contributing to common bean adaptations in the face of challenging environmental conditions.

KEYWORDS

symbiotic nitrogen assimilation, water deficit, genetic transcript profile, RT-qPCR, candidate genes

1 Introduction

Common bean (*Phaseolus vulgaris* L.) is among of the major food crops for direct human consumption, representing the main dietary protein source in developing countries worldwide (Chavez-Mendoza and Sanchez, 2017; Losa et al., 2022). This leguminous species has the ability to symbiotically fix atmospheric nitrogen (N_2) in association with a specific group of soil diazotrophic bacteria known as rhizobia. In this symbiosis, the rhizobia invade the root tissues and, after a complex molecular dialogue with the host plant, form specialized structures called root-nodules (Cooper, 2007; Ferguson et al., 2010). These symbiotic structures are essential for providing rhizobia with a carbon source and establishing an optimal cellular environment. Within the nodule, rhizobia use the host plant's energy to convert N_2 into ammonium (NH_4^+) through the action of the bacterial enzyme nitrogenase. This NH_4^+ is subsequently absorbed and utilized by the host plant, constituting a fundamental process known as biological nitrogen fixation (BNF) (Masson-Boivin and Sachs, 2018). The BNF has been considered an environmentally friendly technology for plant nitrogen nutrition, sustaining plant growth and development in nitrogen-poor soils. In this case the plants are inoculated with *Rhizobium* strains reducing the use of mineral fertilizers which contributes to satisfactory yield at a low cost (Yoseph and Shanko, 2017). However, seed inoculation technology in the common bean crop has not yet reached its full potential (Hungria and Franco, 1993). These constraints are mainly a result of low nodulation effectiveness in this promiscuous-nodulating host plant, as well as the high susceptibility of symbiosis to abiotic stresses (Hungria and Vargas, 2000; Ramos et al., 2003).

Drought is known as a significant environmental factor that is expected to have an increasingly substantial impact on agricultural regions due to climate change (Feller and Vaseva, 2014; Fahad et al., 2017). It is estimated to affect more than 60% of common bean production worldwide (Beebe et al., 2008; Heinemann et al., 2017). Furthermore, despite the identification of different common bean genotypes that exhibit superior performance under drought conditions (Darkwa et al., 2016; Ribeiro et al., 2019), drought stress significantly impairs BNF in this leguminous species. When common bean plants inoculated with rhizobia are subjected to drought conditions nodule metabolism are disrupted, leading to adverse effects on nitrogenase activity, nitrogen accumulation, and crop yield potential (Mnasri et al., 2007; Devi et al., 2013; Polania et al., 2016), and the impacts on nodule structure and N_2 fixation, vary among genotypes (Ramos et al., 2003; Devi et al., 2013; Polania et al., 2016). Recent advances on understanding of how drought affects common bean growth have been predominantly based on above-ground traits evaluation (Mukeshimana et al., 2014; Hoyos-Villegas et al., 2017; Wu et al., 2017). In addition, although root-nodules have been used as important sensors of drought-stress in leguminous species grown under symbiosis, the responses of this organ and their drought adaptive mechanisms remain poorly characterized (Kunert et al., 2016). It is known that in peanut nodules under drought-stress conditions nitrogenase activity decreases (Furlan et al., 2014) and amide metabolism is impaired (Furlan et al., 2017). In soybean, drought-stressed nodules exhibit lower water potential (Gil-Quintana et al., 2015) and undergoes to premature senescence (Cilliers et al., 2018) compromising the BNF activity and nitrogen accumulation. Most recently, it has been demonstrated that changes in nitrogenase activity as well as in global gene expression have occurred not only in nodules from *Medicago truncatula* and *Lotus japonicum* in response to drought, but also in their symbiotic partners *Sinorhizobium meliloti* and *Mesorhizobium loti*, which adjust their gene expression in response to water shortage (Sańko-Sawczenko et al., 2019).

The RNA-Sequencing (RNA-Seq) technology has revolutionized the field of plant functional genomics and has accelerated our understanding of gene expression profiles associated with biologically significant traits, including plant-microbe interactions (Kamfwa et al., 2017; Sańko-Sawczenko et al., 2019), plant responses to pathogens (Padder et al., 2016) and abiotic stress responses (Hiz et al., 2014; Recchia et al., 2018). In addition, a comprehensive high-resolution RNA-Seq atlas has been established for agriculturally important leguminous species such as soybean (Severin et al., 2010; Sreedasyam et al., 2023) and common bean (O'Rourke et al., 2014b). While significant strides have been made in common bean research utilizing RNA-Seq technology (Kamfwa et al., 2017; Recchia et al., 2018; Pereira et al., 2020; Subramani et al., 2023; Zheng et al., 2023) and the release of its genome draft to the public (Schmutz et al., 2014), the application of RNA-Seq to investigate biological nitrogen fixation (BNF) in common beans is limited. Furthermore, a comprehensive

exploration of the nodule transcriptome under adverse conditions during BNF in this species has not been undertaken. Therefore, a thorough examination of how drought stress influences the nodule transcriptional profile in common beans could reveal pivotal stress-related genes affecting BNF performance, offering valuable insights into nodule functionality under challenging conditions.

In this study, we conducted an analysis of the nodule transcriptome using RNA-Seq for a highly efficient genotype for BNF, Negro Argel (Hungria and Neves, 1987), and a well-known drought-tolerant common bean genotype, BAT 477 (Beebe et al., 2013; Arruda et al., 2018), under limited water conditions. Our RNA-Seq profiling showed the up-regulation of several stress-related genes, including those associated with embryogenesis abundance (LEA), heat shock proteins (HSP), and 9-cis epoxycarotenoid dioxygenase (*NCED9*), all of which were previously identified as drought-responsive genes. Additionally, set enrichment analysis (SE) of gene ontology (GO) terms highlighted a significant down-regulation in various metabolic pathways, with a particular focus on the antioxidant metabolism within the nodules. Furthermore, we observed the regulation of specific classes of transcription factors (TFs), notably WRKY, MYB, and AP2/ERF, and several receptor-like kinases such as LyM, LRR, WAK, and LRK in response to drought stress in common bean nodules. These findings provide valuable insights into the transcriptional responses and the key pathways affected by drought stress in common bean root nodules. They contribute to a better understanding of how common bean plants adapt to growth conditions that involve BNF under drought stress.

2 Materials and methods

2.1 Plant material, growth conditions and drought-stress treatment

The two common bean genotypes Negro Argel and BAT 477 were previously selected in a greenhouse experiment in which they differ in their BNF performance when grown under symbiosis with *Rhizobium* strains and water restriction (da Silva et al., 2012a). Next, to dissect the transcriptional responses of root-nodules to drought-stress, a greenhouse experiment was carried out at Centro Nacional de Pesquisa de Agrobiologia (Embrapa - Seropédica, Rio de Janeiro State, Brazil) followed by root-nodules RNA-profiling using Illumina RNA-Seq technology. Seeds of Negro Argel and BAT 477, the former a high efficient for BNF and the latter a known drought-tolerant genotype (Hungria and Neves, 1987; Beebe et al., 2013), were surface disinfected for 5 min in 0.1% (w/v) sodium hypochlorite, sown into 1 L plastic pots containing a 2:1 (v/v) sand/vermiculite mixture and inoculated (1 mL/seed) with a mix (1:1) of the two *Rhizobium* strains broadly used as commercial inoculants in Brazil: *Rhizobium tropici* CIAT 899 (BR 322 syn SEMIA 4077), a broad host-range rhizobial strain isolated from tropical acid soils (Martínez-Romero et al., 1991); and *Rhizobium freirei* PR-F81 (syn SEMIA 4080), isolated from soil of Southern Brazil (Hungria et al., 2000), which were previously grown in yeast malt (YM) liquid medium (Fred and Waksman, 1928) over 3 days at 30°C 120 rpm.

The experiment included two water availability conditions: well-watered and drought-stress. The plants were grown in a greenhouse exposed to natural light, with daily temperatures ranging from 20-32°C and humidity fluctuating between 40% and 90%. These conditions are typical of tropical regions where common beans are commonly cultivated. Norris nutritive solution (Norris and T'mannetje, 1964) lacking nitrogen, was supplied for plant once a week until the start of drought-stress treatment. To monitor the greenhouse environment, temperature and relative humidity were measured using a Datalogger DHT-2230 device (Perceptec) (data not shown).

Throughout the experiment, we monitored soil moisture (W) using a gravimetric method for each pot, following the procedure described by Casagrande et al. (2001). The plants in the well-watered treatment were consistently kept at optimal W levels, which were approximately 80% of the field capacity, throughout the entire experiment. For the plants in the drought-stressed treatment, they were also maintained at around 80% of field capacity until 25 days after plant emergence (DAE), at which point irrigation was suspended. Well-watered (WW) and drought-stressed (DS) plants were sampled when the soil water content for the latter group reached around 5–10% to field capacity. At sampling, leaves from WW and DS plants were collected to determine the leaf relative water content (RWC) following the procedure described by Chartzoulakis et al. (1997).

For molecular analyses, nodules from WW and DS plants were separated from roots, immediately frozen in liquid nitrogen and stored at -80°C until total RNA extraction. For each treatment, a total of twelve plants from different pots were harvested and subdivided into three biological replicates, corresponding to four plants by group. Furthermore, after water deprivation a portion of 25 DAE WW and DS plants were rehydrated to a high moisture level, maintained under greenhouse conditions for 10 days (recovery period) and harvested to determined nodules' dry weight (NDW), shoot dry weight (SDW) and shoot total nitrogen content (STNC). Some of these plants were also used to collect the whole nodulated-roots for nitrogenase activity (N2ase) analyses.

2.2 Evaluation of nodules' dry weight, shoot dry weight, shoot total nitrogen content and nitrogenase activity (N2ase)

To evaluate the extent of the injury caused by the drought stress on BNF performance after recovery period, the well-watered and the rehydrated plants were harvested to assess the shoot and nodules' dry weights (SDW and NDW, respectively), shoot total nitrogen content (STNC) determined by Kjeldahl method (Kjeldahl, 1883) and the N2ase in nodules by acetylene reduction assay (ARA) method (Vance et al., 1979). For N2ase analyses, intact nodulated roots from three plants were incubated into 10% C2H2 atmosphere for 10 minutes at room temperature and then the C_2H_4 content was determined by using a gas chromatography (Perkin Elmer Auto System) with flame ionization. The N2ase analyses was expressed as mmol. L^{-1}. h^{-1}. g. $nodule^{-1}$.

2.3 Statistical analyses

The drought-stress experiment was performed in a completely randomized design and the results were presented as means with standard deviation (SD) of five independent samples by treatment (WW and DS plants) for RWC, W, SDW, NDW, STNC and N2ase analyses. Data were analyzed by Student's t-test ($p < 0.05$) on the Sisvar software (version 4.2), by Ferreira (2011). For RT-qPCR data, significant differences were determined by estimation of the standard error (SE) and also using the REST software version 2.0.7 ($p < 0.05$) which performs a Pair Wise Fixed Reallocation Randomization Test (bootstrap = 2,000 permutation as default) to obtain p values (Pfaffl et al., 2002 - http://www.gene-quantification.info).

2.4 Root-nodules Transcriptome analysis by RNA-Seq using Illumina HiSeq 2000 platform

2.4.1 RNA isolation and sample preparation

Total RNA was extracted from nodules of WW and DS plants using the Tris-SDS method (Ragueh et al., 1989). The nodules were ground to a fine powder in liquid nitrogen using a pestle and mortar, and 300 mg from those samples were used. The RNA was precipitated overnight at 4°C in 2.5 M LiCl, dissolved in 100 µL of nuclease free water and stored at -80°C until molecular analyses. The integrity of total RNA was examined by 2% (w/v) agarose gel electrophoresis looking for distinct ethidium bromide-stained rRNA bands followed by quantification using the Thermo Scientific NanoDrop ND-1000 spectrophotometer (NanoDrop Technologies, Wilmington, DE, USA). Contaminating DNA was removed from RNA using DNase I (Epicentre Biotechnologies, Madison, WI, USA) and the RNA was quantified again using Qubit® 2.0 Fluorometer (Invitrogen, Waltham, MA, USA) for more accurate quantification after DNase I treatment to ensure adequate total RNA for downstream analyses.

2.4.2 cDNA library construction and RNA-Seq profiling of common bean root-nodules

To prepare the cDNA libraries for Negro Argel and BAT 477 well-watered (WW) and drought-stressed (DS) plants, the total RNA from root-nodules was processed using a TruSeqTM RNA Sample Preparation Kit according to manufacturer instructions (Illumina, San Diego, CA, United States of America). Next, these samples were submitted to high-throughput parallel sequencing using the Illumina HiSeq 2000 Platform by a commercial service provider (Fasteris, Plan-les-Ouates, Switzerland). In our analyses, a total of eight cDNA libraries, encompassing two independent biological replicates by treatment, were sequenced to generate about 153 million of 100 bp (base pair) single-end (SE) reads and perform RNA-Seq profiling.

2.4.3 Mapping of short reads and assessment of differential gene expression

The FASTQ files for the eight cDNA library containing the raw sequences from the Illumina HiSeq 2000 Platform were analyzed using publicly available tools. In this case, the output data was filtered using FastQC (Andrews, 2010) and the high-quality reads obtained were trimmed using FASTX-Toolkit. Only those reads with quality above 20 ($Q > 20$) were used. After trimming the resulting high-quality reads were aligned against the detailed *Phaseolus vulgaris* reference genome v1.0 (Schmutz et al., 2014) using a series of programs, including Bowtie v1.0 (Langmead et al., 2009) and TopHat2 v2.1 for read mapping (Kim et al., 2013). Then, the mapped reads counting was performed using HT-Seq-count version 0.5.3p9 (Anders et al., 2014). The differential expression (DE) was estimated and tested by using three different statistical algorithms: CuffDiff (Trapnell et al., 2012), DESeq1 (Anders and Huber, 2010) and edgeR (Robinson et al., 2010), a software package in R-Bioconductor 2.15. Transcripts with adjusted p-value ≤ 0.05 and estimated $|\log2\ (FC)| \geq 2$ (up-regulated) or $|\log2\ (FC)| \leq 2$ (down-regulated) detected by the three software were considered as differentially expressed genes (DEGs) and selected for functional annotation and downstream analyses. The RNA-Seq experiment workflow as well as the bioinformatics pipeline used in our analyses are depicted in Supplementary Figure S1.

2.4.4 Functional annotation of differentially expressed genes

To understand the molecular responses of root-nodules to drought-stress as well as the differences between the two common bean genotypes, we submitted the common bean DEGs to BLASTn analysis (Altschul et al., 1990) against the *Phaseolus vulgaris* reference genome v1.0, available in the Phytozome v12.1 data base (Goodstein et al., 2012) and recovery the functional annotations. In addition, the genes and pathways showing the most relevant responses of common bean nodules to drought-stress were identified by set enrichment analysis (SEA) of GO terms using the AgriGO software v2.0 available at http://bioinfo.cau.edu.cn/agriGO/ (Tian et al., 2017). Based on SEA analysis, a hypergeometric test (p-values ≤ 0.005; FDR ≤ 0.05) was applied to identify which biological processes (BP) and molecular functions (MF) were overrepresented in our list of DEGs. In addition, functional analyses were performed to obtain a representative overview of the pathways affected by drought-stress in common bean nodules mapping the DEGs into *Phaseolus vulgaris* v1.0 genome (Schmutz et al., 2014) available in the MapMan software v3.6 (Thimm et al., 2004). MapMan is a user-driven tool that displays large genomic datasets onto diagrams of different metabolic pathways and biological processes. Next, based in the functional categories potentially involved in the nodule responses to drought, ten DEGs were selected for validation using reverse transcription-quantitative PCR (RT-qPCR).

2.5 RT-qPCR analyses for validation of RNA-Seq data

2.5.1 Primer design

To validate our RNA-Seq profiling experiment, reverse transcription quantitative PCR (RT-qPCR) analyses were carried out for ten DEGs identified in common bean nodules, five up-regulated and five down-regulated. Hence, specific primers for these genes were designed using the Primer3Plus Software (Untergasser et al., 2007), and the following criteria were set out: primer length of 19-22 nucleotides; annealing temperature between 58-62°C; GC content of 50-80% and product size ranging from 100-180 base pairs. Primers' parameters were further checked and adjusted using Oligo Explorer 1.2 software (Gene Link - http://www.genelink.com/tools/gl-oe.asp).

2.5.2 First-strand cDNA synthesis

Total RNA samples from nodules of Negro Argel and BAT477 common bean genotypes, previously treated with DNase I, were used for first-strand cDNA synthesis. The presence of contaminant DNA was checked by endpoint PCR and no genomic DNA was detected in any sample tested in this work (data not shown). First-strand cDNAs syntheses were performed using 4 µg of DNase I treated total RNA, 1 µL oligo (dT) primer (1 µg/µL) and SuperScript III Reverse Transcriptase™ Kit (Invitrogen, Waltham, MA, USA) following the manufacturer's instructions. The cDNA was diluted 1:50 in nuclease free water and then used for qPCR analyses.

2.5.3 RT-qPCR experiment and data analysis

Quantitative PCR was performed on the 7500 Fast Real Timer PCR System using the SYBR Green PCR Master Mix (Applied Biosystems, Carlsbad, CA, USA). The reactions consisted of 7.5 µL of SYBR Green PCR Master Mix, 10 µM of forward and reverse primers for both target (Table 1) and reference genes (Supplementary Table S1), and 7.5 µL of 1:50 diluted fist-strand cDNA template in a total volume of 16 µL. Cycling was performed using the default conditions of the 7500 Software v2.0.5: 2 min at

TABLE 1 Description of genes and primers used in the RT-qPCR and comparison of RT-qPCR and RNA-Seq experiments results.

Gene Abbreviation	*Phaseolus vulgaris* locus (Accession Number)	Gene description	Primers' sequence (5'-3')	Eff ± SD**	qPCR	Log2FC N. Argel	Log2FC BAT 477
Up-Regulated DEGs							
PvBdzp-Receptor	Phvul.001G205900.v1.0 (XM_007163034.1)	Benzodiazepine receptor-related (ABA Hormone)	TCCTCTTGTGTTCGCTGTTG GGCAAGGCTTTATCAGACCA	1.886 ± 0.004	Confirmed	Non Detected on RNA-Seq	**3.7**
PvRPK-LRR	Phvul.005G007100.v1.0 (XM_007148637.1)	RPK-LRR-disease-resistance-protein	GGACTTGTCGTGGAACAGGT TTCATCTCGGGAAACGGGT	1.889 ± 0.007	Confirmed	Non Detected on RNA-Seq	**4.2**
PvUSP	Phvul.001G206900.v1.0 (XM_007163045.1)	Universal Stress Protein	AGTGGAAGTGGTGGAAGGTG TGCAGTGTGCATGGTGAGCA	1.892 ± 0.003	Confirmed	Non Detected on RNA-Seq	**3.0**
PvMYB41	Phvul.005G109100.v1.0 (XM_007149846.1)	MYB transcriptional factor family	AACAAGTGGTCGGCAATAGC GAGCGTGTGTAACAGGGTCA	1.894 ± 0.004	Confirmed	Non Detected on RNA-Seq	**4.2**
PvWRKY56	Phvul.008G058000.v1.0 (XM_007139715.1)	WRKY transcriptional factor family	GAGCAAGGGCTACGTGACTC CACCTTTCCTTTTCTCCTGGT	1.876 ± 0.004	Confirmed	Non Detected on RNA-Seq	**5.8**
Down-Regulated DEGs							
PvRCI3	Phvul.009G038500.v1.0 (XM_007136296.1)	Rare Cold Inducible Gene 3	GCAGCAAGAGACAGTGTGGA CATTGAAGGTTGGAGGTGGT	1.883 ± 0.007	Confirmed	Non Detected on RNA-Seq	**-3.3**
PvPer22	Phvul.006G129400.v1.0 (XM_007147434.1)	Peroxidase 22	TGCGACGATAGTGAGTGAGC CCAGCCAGAACTGAAGAGAC	1.939 ± 0.098	Confirmed	Non Detected on RNA-Seq	**-4.4**
PvWRKY51	Phvul.009G138900.v1.0 (XM_007137526.1)	WRKY transcriptional factor family	CATCGGAGAAAGCAACCTC TTGACTCACTTCTGCCTTCC	1.875 ± 0.005	Confirmed	Non Detected on RNA-Seq	**-4.7**
PvDRFP	Phvul.004G114700.v1.0 (XM_007152199.1)	Disease resistance family protein	GCAACTCGTTCTCCAAATCC AATGGTCCAACAGTCGGGTA	1.895 ± 0.002	Confirmed	Non Detected on RNA-Seq	**-6.5**
PvAP2-ERF034	Phvul.008G141000.v1.0 (XM_007140714.1)	AP2 Ethylene-responsive transcription factor ERF034	CTTCTCCTCCTCCACATCCA CTTGGTGCATGAGTTTGAGC	1.884 ± 0.005	Confirmed	Non Detected on RNA-Seq	**-3.9**

95°C, followed by 40 cycles of 20 s at 95°C and 30 s at 60°C. Three technical replicates and non-template controls were used, as well as three independent biological samples for each experimental condition (biological replicates) were analyzed. Each primer sets' efficiencies and the optimal quantification cycle threshold (Cq values) were estimated by Miner Software (Zhao and Fernald, 2005).

Prior to target genes' analyses, the expression stability for three candidate reference genes (*PvEf1-Alpha*, *PvAct* and *PvIDE*) was determined. The Cq values for these genes across all sample set were converted by the qBase Software v1.3.5 (Hellemans et al., 2007) into non-normalized relative quantities, and corrected by PCR efficiency as described by Hellemans et al. (2007). These quantities were imported independently into geNorm v3.5 (Vandesompele et al., 2002) and NormFinder (Andersen et al., 2004) analysis tools, which were used according to their manuals to determine the expression stability of the candidate reference genes. These data were analyzed in both programs and the two more stable genes (*PvEF1-Apha* and *PvAct*) were used for data normalization of target genes in the qBase Software analyses.

For the relative quantification (RQ) of target genes the Cq values and PCR efficiencies estimated by Miner Software were imported into the qBase Software, which estimates the RQ using the classical $2^{-\Delta\Delta Ct}$ method (Livak and Schmittgen, 2001); and relative to the calibrator sample (control plant); however, it accounts for multiple stably expressed reference genes to improve normalization (Hellemans et al., 2007). Significant differences were determined by REST software version 2.0.7 ($p < 0.05$) (Pfaffl et al., 2002) as described as previously described.

3 Results

3.1 Negro Argel and BAT 477 genotypes showed different BNF performance under drought-stress conditions

Previously, we performed a screening experiment to select common bean genotypes which can be able to maintain their BNF capacity when submitted to drought stress. In these analyses Negro Argel and BAT 477, the former a highly efficient for BNF and the latter a known drought-tolerant genotype, respectively (Hungria and Neves, 1987; Beebe et al., 2013), showed different BNF performances when grown under water limited conditions. While Negro Argel seems to be not affected by drought, BAT 477 decreased their BNF performance in these conditions. Our findings suggested that different mechanisms to cope with drought occur in Negro Argel and BAT 477 when grown under symbiosis (unpublished data). These two genotypes were then selected to perform a new greenhouse experiment to investigate the nodule transcriptional changes in response to drought-stress. In our analyses, the shoot total nitrogen content (STNC) and shoot dry weight (SDW), which were used as phenotypic markers for BNF performance under drought stress, showed divergent patterns between the two genotypes. The STNC as well as SDW were significantly decreased in BAT 477 genotype; on the other hand, for Negro Argel these phenotypic markers remained unaffected by drought (Table 2). Negro Argel plants was less affected by drought (Supplementary Figure S2) It is noteworthy to mention that all phenotypic parameters evaluated were at least two-fold higher for this genotype when compared to BAT 477 genotype. Interestingly, despite the two genotypes being in the same gravimetric soil moisture (*w*) under stress (Figure 1B), BAT 477 plants began to wilt after stress treatment (Supplementary Figure S2) and a decline in the leaf relative water content (RWC) was observed (Figure 1A). Meanwhile, the Negro Argel genotype exhibited no symptoms of drought stress ten days after plant rehydration (recovery) (Supplementary Figure S1). Our analyses revealed a significant decrease in N2ase analyses in BAT 477, whereas its activity was only slightly affected and not statistically significant ($p > 0.05$) in Negro Argel (Figure 1C). Collectively, these results confirm the distinct biological nitrogen fixation (BNF) performances of BAT 477 and Negro Argel genotypes when grown under symbiosis with Rhizobium strains and subjected to drought stress conditions, as previously observed by our group.

3.2 Summary of RNA-Seq data analyses

The RNA-Sequencing output yielded about 153 million raw reads (81,499,516 for Negro Argel and 72,504,111 for BAT 477) for the eight RNS-Seq libraries. Each library represented at least 14 million reads, ranging from 14,425,608 for Negro Argel DS R1 to 29,183,581 for Negro Argel WW R1 samples (Table 3), a tag density sufficient for quantitative analysis of gene expression (Vargas et al., 2014; Guo et al., 2015). After stringent quality assessment and data filtering, a total of 81,489,262 and 72,497,478 high-quality reads ($Q > 20$) were obtained for N. Argel and BAT 477 genotypes, respectively. In addition, the clean reads accounted for more than

TABLE 2 Shoot total nitrogen content (STNC) and shoot dry weight (SDW) of common bean plants ten days after rehydration (recovery).

Genotype	Water availability regimen	STNC (mg.planta^{-1})	STNC variation (%)	SDW (g.planta^{-1})	SDW variation (%)
Negro Argel	Well-watered plants	14.87a	-13.58	0.93a	+4.3
	Drought-stressed plants	12.85a		0.97a	
BAT 477	Well-watered plants	37.13a	-34.34	1.88a	-24.47
	Drought-stressed plants	24.38b		1.42b	

The variation (%) of these parameters in drought-stressed plants related to control (well-watered plants) was estimated and the difference for BNF performance under drought conditions for Negro Argel and BAT 477 genotypes was confirmed. For all analyses, values followed by the same letter indicate that the differences were not statistically significant within each genotype by Fisher test ($p<0.05$). Standard deviation bars are shown for five biological replicates (two plants by replica).

10.3389/fpls.2024.1345379

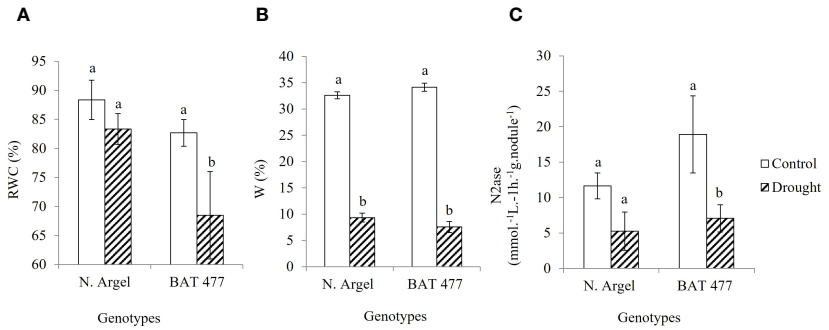

FIGURE 1
Comparison of BNF performance in Negro Argel and BAT 477 plants submitted to drought-stress. Evaluation of physiological status of common bean plants using the leaf relative water content (RWC) **(A)** and gravimetric soil moisture (*w*) **(B)**. BNF activity in drought-stressed common bean nodules estimated by acetylene reduction assay (ARA) for N. Argel and BAT 477 genotypes ten days after rehydration (recovery). Nitrogenase (N_2ase) analyses is shown as mmol.L^{-1}.h^{-1}.g.nodule^{-1} **(C)**. For all analyses, different letters indicate statistical differences between well-watered and drought-stressed plants within each genotype by Fisher test ($p<0.05$). Standard deviation bars are shown for five biological replicates (two plants by replica).

99.98% of the total reads for both genotypes which indicates few biases in our RNA-Seq analyses (Table 3). These reads were then mapped to the *P. vulgaris* reference genome v1.0 (Schmutz et al., 2014) and a high number of unique mapped reads was observed for both Negro Argel and BAT 477 libraries which corresponded to about 85% of the total high-quality reads obtained.

3.3 Overview of the differentially expressed genes in response to drought-stress

To characterize the transcriptional responses of common bean nodules to drought, we performed RNA-profiling and the DEGs were identified by implementing three different statistical algorithms (CuffDiff, DESeq1 and edgeR). Only those genes concomitantly detected in all three algorithms were considered as responsive to drought and selected for further investigations. In our analyses, 145 and 1451 genes were differentially expressed (adjusted p-value ≤ 0.05, |log2 FC| ≥ 2.0) in Negro Argel and BAT 477, respectively. Among them, 47 (32.4%) were up-regulated whereas 98 (67.6%) were down-regulated in Negro Argel. For BAT 477 genotype, 325 genes (22.4%) were up-regulated and 1126 (77.6%) were down-regulated in nodules in response to drought. Interestingly, for both genotypes, edgeR algorithm identified the highest number of DEGs followed by CuffDiff and DESeq1. The number of DEGs identified by each algorithm as well as a pairwise comparison with the number of shared DEGs among them is summarized in Figure 2 and Supplementary Figure S3.

3.4 Functional categorization of drought-regulated genes in common bean root-nodules

3.4.1 Top 10 drought-responsive DEGs identified in each genotype

To investigate how genes are strongly regulated by drought in common root-nodules, we examined the top 10 up- and down-

TABLE 3 Common bean RNA-Seq experiment statistics.

Sample	Total number of reads	Reads after trimmer (Q20)	Trimmed reads	Unique aligned reads (%)
N. Argel Control R1	29,183,581	29,179,782	3,799	82.5
N. Argel Control R2	19,231,955	19,230,007	1,948	84.9
N. Argel Drought R1	14,427,803	14,425,608	2,195	83.8
N. Argel Drought R2	18,656,177	18,653,865	2,312	84.5
Total	81,499,516	81,489,262	10,254	
BAT 477 Control R1	21,104,767	21,102,985	1,782	85.5
BAT 477 Control R2	15,141,812	15,140,588	1,224	84.6
BAT 477 Drought R1	17,922,096	17,920,130	1,996	84.2
BAT 477 Drought R2	18,335,436	18,333,775	1,661	86.3
Total	72,504,111	72,497,478	6,663	

Summary of RNA-Seq data output from Illumina HiSeq 2000 platform, statistical analysis of reads number and mapping of the reads onto the common bean (*Phaseolus vulgaris* L.) reference genome.

10.3389/fpls.2024.1345379

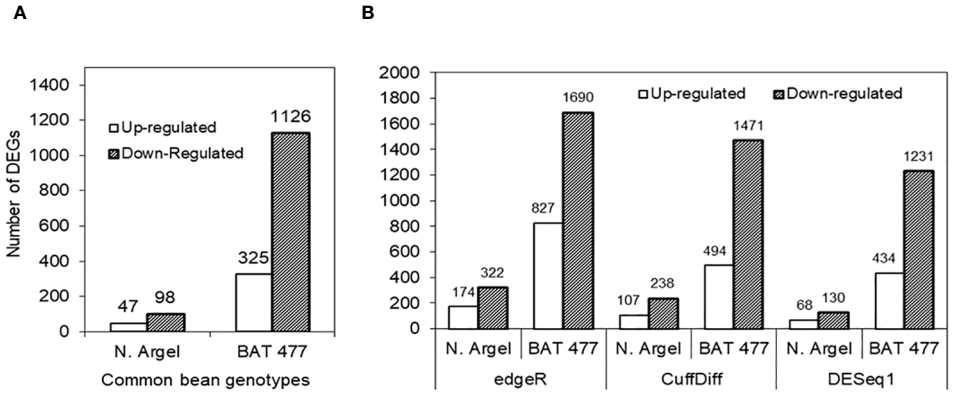

FIGURE 2
Number of differentially expressed genes (DEGs) in nodules from Negro Argel and BAT 477 common bean genotypes submitted to drought-stress. DEGs concomitantly identified by RNA-Seq in the three different statistical algorithms used for differential expression analysis: edgeR, CuffDiff and DESeq1 **(A)**, and up and down-regulated genes detected by each algorithm **(B)**.

regulated genes (up and down-DEGs, respectively) for each genotype (Tables 4, 5), as well as the shared DEGs between them (Supplementary Figure S4). In the case of the Negro Argel genotype, a hypothetical protein (Phvul.008G186200.v1.0) and a heat shock protein from the hsp20/alpha crystallin family (Phvul.010G155300.v1.0) were among the most strongly induced genes in nodules in response to drought (Table 4). Additionally, two heat shock proteins (HSP 70 and cytosolic sHSP class II), transcriptional factors (MYB and homeobox associated leucine zipper protein), and a seed maturation protein were detected among the top 10 up-DEGs. Interestingly, another hypothetical protein (Phvul_007G069800.v1.0), similar to RD29B, a protein responsive to desiccation in *Arabidopsis thaliana*, was also found in our analyses. On the other hand, genes related to glycoside hydrolase family 17 (Phvul.001G128500.v1.0) and silicon efflux transporter (Phvul.004G111900.v1.0) were the most strongly down-regulated genes in common bean nodules in response to drought. Moreover, genes belonging to important functional classes were also identified among the top 10 down-regulated DEGs, such as lipid transfer protein, cell wall associated kinase-like protein, RNA-binding and disease resistance family proteins, and a peroxidase family protein (Table 4).

In our analyses, a late embryogenesis abundant (LEA) protein (Phvul.007G225200.v1.0) was the most highly expressed DEG in BAT 477 nodules (Table 5). Moreover, another LEA protein, genes related to HSPs, seed maturation, two synthases (galactinol synthase, chalcone and stilbene synthase), and a caa3_CtaG domain-containing hypothetical protein were found among the top 10 up-DEGs. As for the down-regulated genes in BAT 477, we found a glycoside hydrolase family 17 protein (Phvul.001G128500.v1.0) as the most strongly down-regulated gene in nodules. Additionally, similar to the Negro Argel

TABLE 4 Top 10 highest and lowest expressed genes in drought-stressed common bean (*P. vulgaris* L.) nodules, Negro Argel genotype, identified in RNA-Seq experiment.

ID *P. vulgaris*	ID *M. truncatula*	E-value	Description	Log2FC
Top 10 highest expressed genes				
Phvul.008G186200.v1.0	Medtr5g067740.1	2E-57	hypothetical protein	5.9
Phvul.010G155300.v1.0	Medtr4g010320.1	1E-121	hsp20/alpha crystallin family protein	5.8
Phvul.006G116000.v1.0	Medtr8g026960.1	1E-116	homeobox associated leucine zipper protein	5.3
Phvul.001G223700.v1.0	Medtr7g111850.1	0.0	galactinol synthase	4.9
Phvul.003G154800.v1.0	Medtr4g130540.1	0.0	heat shock 70 kDa protein	4.9
Phvul.009G131000.v1.0	Medtr3g088675.1	0.0	chalcone and stilbene synthase family protein	4.6
Phvul.006G192900.v1.0	Medtr2g011660.1	1E-147	myb transcription factor	4.6
Phvul.009G080200.v1.0	Medtr3g104780.1	1E-98	cytosolic class II small heat-shock protein	4.6
Phvul.007G069800.v1.0	Medtr1g100627.1	9E-63	hypothetical protein	4.3
Phvul.001G142000.v1.0	Medtr7g093170.1	7E-53	seed maturation protein	4.2

(Continued)

10.3389/fpls.2024.1345379

TABLE 4 Continued

ID *P. vulgaris*	ID *M. truncatula*	E-value	Description	Log2FC
Top 10 lowest expressed genes				
Phvul.001G128500.v1.0	Medtr4g076570.1	3E-67	glycoside hydrolase family 17 protein	-6.1
Phvul.004G111900.v1.0	Medtr6g045483.3	0	silicon efflux transporter	-5.3
Phvul.003G218900.v1.0	Medtr4g101280.1	5E-81	Lipid transfer protein	-4.2
Phvul.007G030800.v1.0	Medtr1g110180.1	0.0	wall associated kinase-like protein	-3.8
Phvul.005G140100.v1.0	Medtr4g062170.1	0.0	3-ketoacyl-CoA synthase-like protein	-3.8
Phvul.003G078000.v1.0	Medtr2g023010.1	1E-24	down-regulated protein in the presence of paraquat	-3.7
Phvul.003G278400.v1.0	Medtr8g072260.1	0.0	cytochrome P450 family ABA 8'-hydroxylase	-3.7
Phvul.010G122000.v1.0	Medtr7g117495.2	3E-70	RNA-binding (RRM/RBD/RNP motif) family protein	-3.6
Phvul.007G254300.v1.0	Medtr1g078490.1	0.0	disease resistance protein (CC-NBS-LRR class) family protein	-3.6
Phvul.006G075700.v1.0	Medtr3g467600.1	0.0	peroxidase family protein	-3.5

Common bean plants were submitted to 4 days of drought stress. Gene expression is shown as log2 fold-change (Log2FC) between control and drought-stressed plants. Bold/underlined Common bean IDs indicate common genes shared with BAT 477 genotype within the top 10 up and down expressed genes.

TABLE 5 Top 10 highest and lowest expressed genes in drought-stressed common bean (*P. vulgaris* L.) nodules, BAT 477 identified in RNA-Seq experiment.

ID *P. vulgaris*	ID *M. truncatula*	E-value	Description	Log2FC
Top 10 highest expressed genes				
Phvul.007G225200.v1.0	Medtr1g061730.1	1E-64	late embryogenesis abundant protein, putative	9.8
Phvul.008G186200.v1.0	Medtr5g067740.1	2E-57	hypothetical protein	8.3
Phvul.008G228100.v1.0	Medtr5g081530.1	3E-95	17.6 kDa class I heat shock protein	8.1
Phvul.010G155300.v1.0	Medtr4g010320.1	1E-121	hsp20/alpha crystallin family protein	8.0
Phvul.009G131000.v1.0	Medtr3g088675.1	0.0	chalcone and stilbene synthase family protein	7.9
Phvul.001G223700.v1.0	Medtr7g111850.1	0.0	galactinol synthase	7.8
Phvul.003G096700.v1.0	Medtr4g120040.1	4E-40	late embryogenesis abundant protein	7.8
Phvul.002G231400.v1.0	Medtr6g061850.1	1E-137	17.6 kDa class I heat shock protein	7.3
Phvul.001G142000.v1.0	Medtr7g093170.1	7E-53	seed maturation protein	7.3
Phvul.007G113700.v1.0	Medtr1g076910.1	1E-130	22.0 kDa class IV heat shock protein	7.3
Top 10 lowest expressed genes				
Phvul.001G128500.v1.0	Medtr4g076570.1	3E-67	glycoside hydrolase family 17 protein	-9.5
Phvul.008G086800.v1.0	Medtr7g072510.1	0.0	class III peroxidase	-8.86
Phvul.003G169100.v1.0	Medtr4g115360.2	7E-69	lipid transfer protein	-8.54
Phvul.006G075700.v1.0	Medtr3g467600.1	0.0	peroxidase family protein	-8.29
Phvul.011G105900.v1.0	Medtr4g046713.1	0.0	peroxidase family protein	-8.17
Phvul.003G218800.v1.0	Medtr4g101330.1	4E-75	Lipid transfer protein	-7.89
Phvul.001G050300.v1.0	Medtr1g012710.1	5E-71	protease inhibitor/seed storage/LTP family protein	-7.89
Phvul.011G047400.v1.0	Medtr4g069170.1	4E-28	lipid transfer protein	-7.79
Phvul.010G122000.v1.0	Medtr7g117495.2	3E-70	RNA-binding (RRM/RBD/RNP motif) family protein	-7.64
Phvul.005G111700.v1.0	Medtr2g089120.1	0.0	sesquiterpene synthase	-7.6

Common bean plants were submitted to 4 days of drought stress. Gene expression is shown as log2 fold-change (Log2FC) between control and drought-stressed plants. Bold/underlined Common bean IDs indicate common genes shared with BAT 477 genotype within the top 10 up and down expressed genes.

10.3389/fpls.2024.1345379

genotype, three peroxidases and three lipid transfer proteins were down-regulated in BAT 477. Moreover, a protease inhibitor/seed storage/LTP family protein, a gene related to sesquiterpene synthase, and an RNA-binding family protein were also down-regulated (Tables 4, 5).

To compare the molecular responses of Negro Argel and BAT 477 nodules under drought, we determined the common shared up- and down-regulated DEGs between these two genotypes based on the top 10 up- and down-regulated gene lists (Supplementary Figure S4). We found five common up-regulated genes: caa3_CtaG domain-containing hypothetical protein (Phvul.008G186200.v1.0), hsp20/alpha crystallin family protein (Phvul.010G155300.v1.0), chalcone and stilbene synthase family protein (Phvul.009G131000.v1.0), galactinol synthase (Phvul.001G223700.v1.0), and seed maturation protein (Phvul.001G142000.v1.0). There were also three common down-regulated genes: glycoside hydrolase family 17 protein (Phvul.001G128500.v1.0), peroxidase family protein (Phvul.006G075700.v1.0), and RNA-binding (RRM/RBD/RNP motif) family protein (Phvul.010G122000.v1.0). Interestingly, in both cases, the Log2FC in response to drought was more pronounced in BAT 477 nodules when compared to the Negro Argel genotype, showing higher values for |Log2FC| (Supplementary Figure S4).

3.4.2 AgriGO search for enrichment analysis

In addition to BLASTn functional annotation, a set enrichment analysis (SEA) was performed using the AgriGO software to determine which genes and pathways were the most relevant responses of common bean nodules to drought stress, and an overview of the main pathways affected during these responses, summarized for the three main gene ontology categories: "Biological Process", "Cellular Component" and "Molecular Function", are shown in Figure 3. In the "Biological Process (BP)" category, the SEA results showed significant enrichment for BAT 477 up-regulated DEGs (up-DEGs) associated with the "lipid metabolic process" (GO:0006629). This enrichment included specific terms such as "fatty acid metabolic process" (GO:0006631) and "fatty acid biosynthetic process" (GO:0006633) as significant GO terms (Supplementary Figure S5). However, there was no statistical significance found for Negro Argel genotype up-DEGs. Furthermore, we evaluated the down-regulated DEGs (down-DEGs), which accounted for 77.6% and 67.6% of BAT 477 and Negro Argel DEGs, respectively (Figure 2). Both genotypes showed enrichment in GO terms such as "cell wall organization or biogenesis" (GO:0071554) and "response to chemical stimulus" (GO:0042221). Notably, the "response to oxidative stress" (GO:0042221) term was highly significant for Negro Argel. Additionally, BAT 477 had additional enriched GO terms, including "carbohydrate metabolic process" (GO:0005975), "oxidation reduction" (GO:0055114), "phosphorus metabolic process" (GO:0006793), and "macromolecule modification" (GO:0043412). These results suggest a higher metabolic activity in BAT 477 nodules when compared to the Negro Argel genotype. For a detailed overview of the more significant GO terms in the BP category found in SEA analyses for BAT 477 and Negro Argel DEGs, refer to Supplementary Figures S6 and S7, respectively.

In the "Molecular Function" (MF) category, the up-regulated DEGs were primarily associated with "transferase activity" (GO:0016746) in BAT 477 genotype (Supplementary Figure S8). However, for the Negro Argel genotype, similar to the BP category, no significant GO terms were found. On the other hand, when analyzing the down-regulated DEGs, significant GO terms were enriched for both genotypes. These included the terms "antioxidant

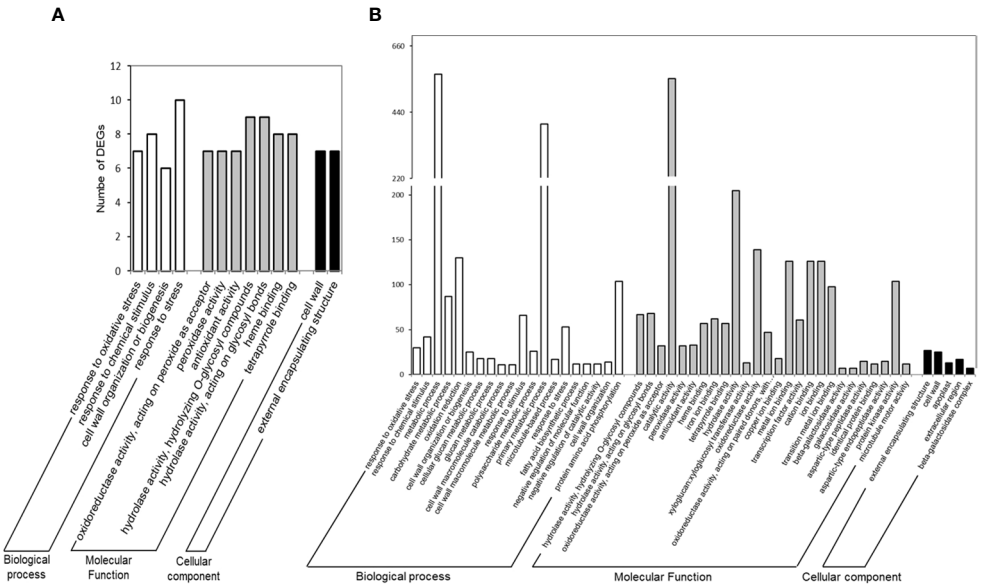

FIGURE 3
Functional annotation of differentially expressed genes (DEGs) in Negro Argel **(A)** and BAT 477 **(B)** drought-stressed nodules. Gene ontology (GO) categorization was performed after SEA analysis using AgriGO Software v2.0. Results are summarized for the three main GO categories: Biological Process, Molecular Function, and Cellular Component.

10.3389/fpls.2024.1345379

activity" (GO:0016209), which encompasses "peroxidase activity" (GO:0004601), "hydrolase activity" (GO:0016787), and "heme binding" (GO:0020037) in AgriGO SEA analyses (Supplementary Figures S9A and S9B for BAT 477 and Negro Argel, respectively). Furthermore, additional GO terms specifically enriched in BAT 477 included "protein kinase activity" (GO:0004672) and "transcription factor activity" (GO:0003700). These terms include genes involved in cell signaling and gene expression regulation (Supplementary Figure S9A). These findings highlight the differential responses of these two genotypes to drought stress in terms of molecular functions.

3.4.3 Main metabolic pathways modulated by drought-stress in nodules

In addition to the AgriGO SEA analysis, we performed an analysis using MapMan Software to gain a comprehensive overview of the main pathways affected in nodules under drought stress. Similar to the AgriGO SEA analysis, we found that DEGs from different metabolic pathways were affected in drought-stressed nodules for both genotypes (Supplementary Figures S10, S11). These pathways included those related to heat shock proteins and abiotic stress responses, which are directly involved in responding to abiotic stress. Furthermore, we observed dynamic regulation in pathways associated with cell wall metabolism, cell signaling, and transcription factor activities, among other effects.

For a more detailed perspective, we used the MapMan "biotic stress" (Figure 4) and "regulation overview" (Supplementary Figures S10, S11) files for mapping the DEGs. Our results indicated that abiotic stress-related genes were induced in Negro Argel and BAT 477 genotypes. Furthermore, both genotypes exhibited several up-regulated DEGs in the "heat shock proteins" and "abiotic stress" categories Interestingly, only down-regulated DEGs were mapped to "peroxidases" within the antioxidant metabolism-related category and "auxins" in the hormone signaling and metabolism pathway. A great number of DEGs in hormone signaling and metabolism, cell wall metabolism, cell signaling, transcription factors (TFs), and proteolysis (in the case of BAT 477) were down-regulated. Additionally, PR-proteins, which play a role in plant-pathogen interactions, displayed dynamic regulation in BAT 477 drought-stressed nodules, with some DEGs being up-regulated and others down-regulated (Figure 4B), whereas only one PR-protein was mapped to this category in Negro Argel (Figure 4A).

To gain insight into the intricate regulation of common bean nodule responses to drought stress, we utilized the "regulation overview" map file in MapMan functional analyses. While some DEGs in categories like TFs and receptor kinases were up-regulated in drought-stressed common bean nodules (Supplementary Figures S10, S11), the prevailing trend for both BAT 477 and Negro Argel genotypes was down-regulation across several processes. Transcriptional repression was observed in genes related to receptor kinases, G-proteins, calcium signaling, transcription factors, protein modification and degradation, the ascorbate-glutathione cycle, and genes involved in regulation mediated by the phytohormones auxin, gibberellic acid, and jasmonate. Interestingly, these responses were more pronounced in BAT 477, and in certain instances, some processes were observed exclusively in this genotype, such as the regulation pathways related to ABA, jasmonate, and gibberellic acid (Supplementary Figures S10, S11).

For a more focused discussion, we emphasize on key gene categories potentially involved in plant responses to abiotic stresses based on the AgriGO SEA and MapMan analyses, as well as processes related to nodule responses under drought stress. We examined both down- and up-regulated DEGs in the following categories: "heat shock proteins," "cell signaling," "transcription factors," "hormone metabolism and signaling," and "antioxidant activity." These selected categories, with

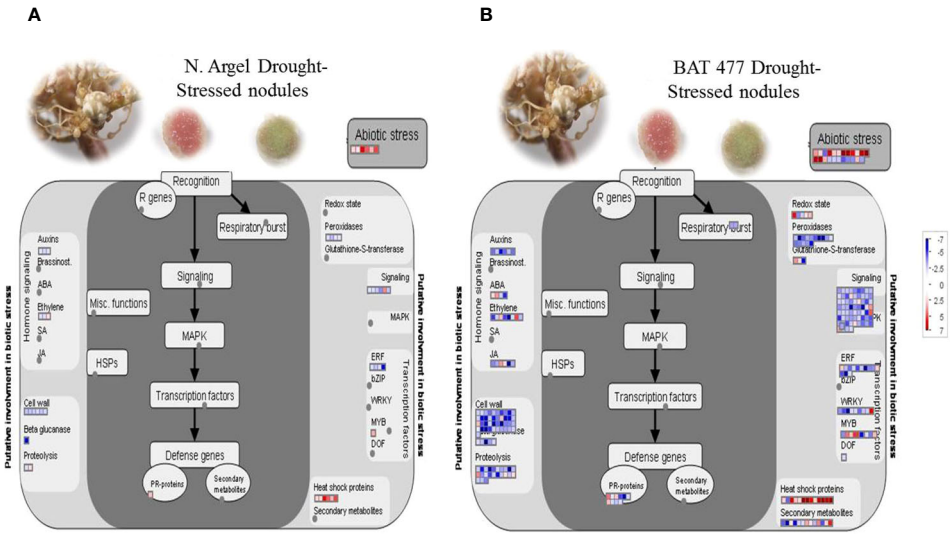

FIGURE 4
MapMan "biotic stress" overview of differentially expressed genes (DEGs) in root nodules in response to drought stress. Results for Negro Argel **(A)** and BAT 477 **(B)** genotypes inoculated with *Rhizobium tropici* BR520 and BR534 strains and submitted to four days of drought stress are shown. Blue stands for down-regulated and red stands for up-regulated genes. Only DEGs are shown, with adjusted p-value ≤ 0.05, |log2FC| ≥ 2.0 differences from control.

the exception of hormone metabolism, showed significant enrichment in our AgriGO SEA analysis (see AgriGO results).

3.4.5 Heat shock proteins and abiotic stress responses

In our MapMan analysis, we identified thirteen DEGs within the "heat shock proteins" (HSPs) category for BAT 477 and five DEGs for the Negro Argel genotype (Figure 4; Supplementary Tables S2, S3). Additionally, some genes related to the "abiotic stress responses" category, which includes HSPs, were found in BAT 477 DEGs. Unlike HSPs, DEGs related to cold, drought, salt, and light responses were generally down-regulated in nodules in response to drought in BAT 477. Notably, a gene related to cold stress, COLD-REGULATED 413-PLASMA MEMBRANE 2 (COR413-PM2), was up-regulated in BAT 477 nodules, indicating potential crosstalk between cold and drought stress responses (Supplementary Table S2). We also identified a universal stress protein (USP) in the BAT 477 DEGs.

3.4.6 Cell signaling

We identified DEGs related to cell signaling. In the case of BAT 477, we found sixty-nine DEGs that were mapped to this category. These included three genes involved in signaling related to sugar and nutrient physiology, 41 receptor kinases of LRR and DUF26 types, along with other kinases. Additionally, there were eleven genes associated with calcium signaling and eight DEGs related to G-protein signaling, among other signaling processes (Supplementary Table S2). Notably, many of the DEGs in this category showed down-regulation in their Log2FC values. In contrast, for Negro Argel, only five DEGs related to receptor kinases and one DEG involved in calcium signaling were identified (Supplementary Table S3). Once again, a significant proportion of these DEGs in the signaling category exhibited down-regulation.

3.4.7 Transcription factors

Transcriptional regulation plays a crucial role in plant responses to environmental constraints. In our analysis, we observed the regulation of several classes of transcription factors (TFs) in response to drought stress in both BAT 477 and Negro Argel genotypes (Supplementary Tables S2, S3). For BAT 477, the major classes of TFs regulated by drought included MYB, WRKY, and AP2-EREBP (APETALA2/Ethylene-responsive element binding protein) TFs. Notably, a majority of the WRKY and AP2-EREBP genes were down-regulated, while among the nine MYB TFs, five were up-regulated in response to drought. In the case of Negro Argel, we identified five TFs that were mapped (Supplementary Table S3). Among these, one MYB TF was up-regulated, while four AP2-EREBP (APETALA2/Ethylene-responsive element binding protein) TFs were down-regulated in nodules in response to drought.

3.4.8 Hormone metabolism and signaling

While our AgriGO analyses did not reveal gene ontology terms related to hormones, we identified several DEGs associated with hormone metabolism and signaling in both the "biotic stress" and "regulation overview" MapMan files (Supplementary Tables S2, S3). For BAT 477, we found twenty-four genes linked to abscisic acid (ABA), auxin, ethylene, and jasmonate phytohormones that were regulated by drought. Among these DEGs, only five genes were up-regulated: two genes regulated by ABA, one involved in ethylene synthesis/degradation, and two involved in jasmonate synthesis/degradation. The majority of DEGs related to hormone metabolism and signaling were down-regulated. In the case of Negro Argel, we identified three down-regulated genes related to auxin metabolism and signaling, and two genes associated with ethylene metabolism. Additionally, one gene activated by ethylene (MBF1C-MULTIPROTEIN BRIDGING FACTOR 1C) was up-regulated in response to drought stress in nodules.

3.4.9 Antioxidant activity

Regarding antioxidant metabolism in nodules under drought stress, we observed a significant decrease in the expression of peroxidase genes for both BAT 477 and Negro Argel genotypes (Supplementary Tables S2, S3). Additionally, for BAT 477, the regulation of other classes of genes related to antioxidant metabolism, including glutathione S-transferase, thioredoxin, ascorbate-glutathione, and glutaredoxin, was affected. Interestingly, two DEGs associated with the ascorbate-glutathione cycle were down-regulated, indicating a reduction in antioxidant protection at the transcriptional level.

3.5 Validation of transcriptome data and evaluation of the expression profile of genes related to drought stress responses in common bean nodules

To validate our RNA-Seq results, we selected 10 DEGs (5 up-regulated and 5 down-regulated) based on the main pathways affected by drought stress as identified in the AgriGO analysis (see Figure 3 and Supplementary Figures S5–S9) and MapMan analysis (Figure 4; Supplementary Figures S10–S11). Before conducting RT-qPCR analysis of these DEGs, we assessed the expression stability of three candidate reference genes (*PvEf1-Alpha*, *PvAct*, and *PvIDE*). This was done using two different algorithms, geNorm and NormFinder Software. Both algorithms identified *PvEf1-Alpha* and *PvAct* as the most suitable reference genes for normalizing the qPCR data under our experimental conditions (Supplementary Table S1; Supplementary Figure S12). In the RT-qPCR experiments (Table 1), we observed that *PvPer22*, *PvRCI3*, *PvWRKY51*, and *PvAp2-ERF034* were down-regulated in both genotypes, whereas *PvDRFP* was down-regulated only in the BAT 477 genotype. On the other hand, *PvBdzp*-Receptor, *PvMYB41*, *PvWRKY56*, *PvRPK-LRR*, and PvUSP were up-regulated in response to drought in both genotypes (Figure 5). Notably, in the BAT 477 drought stress samples, Cq was not detected for the genes *PvPer22*, *PvWRKY51*, *PvDRFP*, and *PvAp2-ERF034*. The expression profiles of genes related to nitrogen metabolism and assimilation in common bean nodules were also different for the two genotypes under stress. PvUriII, involved in the ureide biosynthetic pathway, was severely down-regulated in BAT 477 and almost unaffected in N. Argel. On the other hand, PvGS(n-1), an enzyme responsible for the assimilation of NH4+ into organic nitrogen, was significantly induced under stress for both genotypes (Figure 6). Furthermore, similar to the RNA-Seq transcriptome

10.3389/fpls.2024.1345379

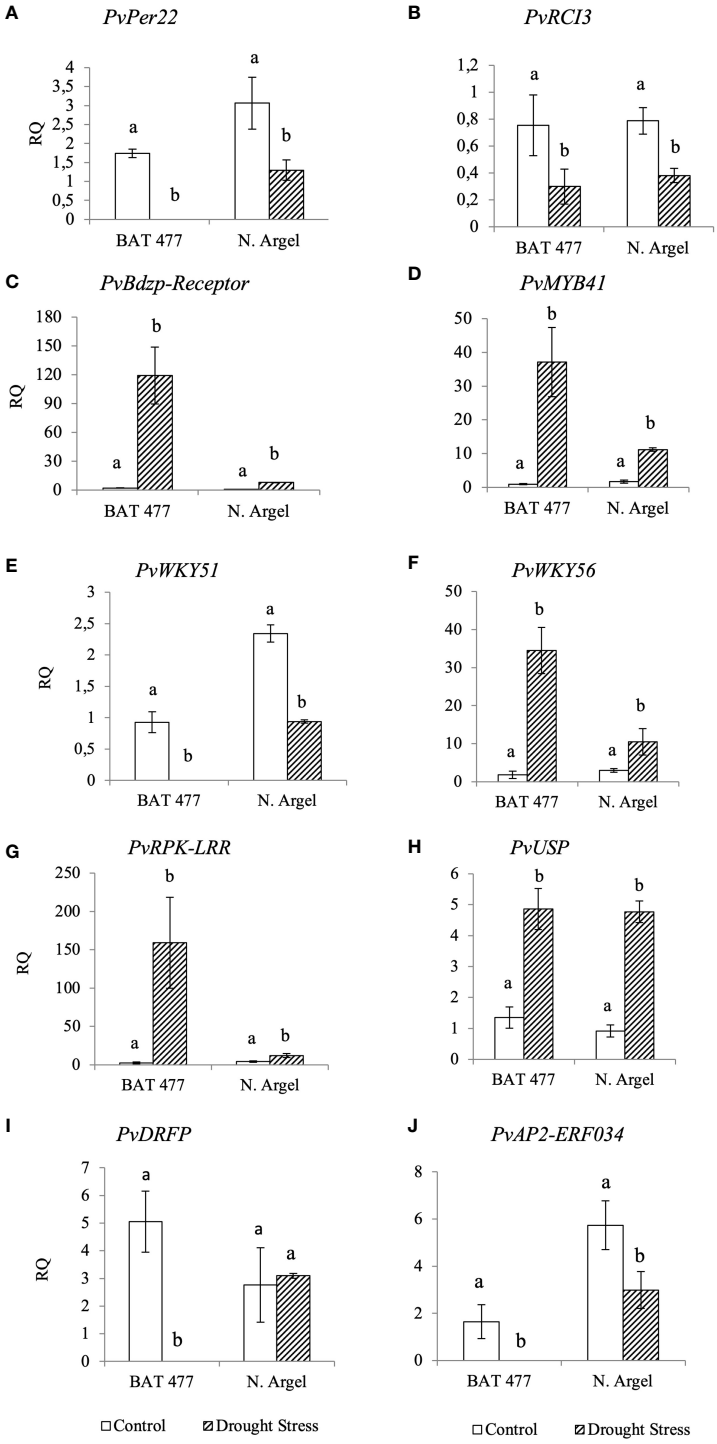

FIGURE 5
Expression profiles of differentially expressed genes (DEGs) by RT-PCR for RNA-Seq transcriptome validation. The expression profile of ten DEGs identified in RNA-Seq analyses was confirmed by RT-qPCR using cDNA from BAT 477 and Negro Argel control and drought-stressed nodules. The reference genes *PvEf1-Aplha* and *PvAct* were previously evaluated on geNorm and NormFinder algorithms (Supplementary Figure S7) and used for data normalization. For the genes *PvPer22*, *PvWRKY51*, *PvDRFP* and *PvAP2-ERF034*, the Cqs were not detected for "BAT 477 drought stress" samples. **(A)** *Per22*: Peroxidase 22; **(B)** *RCI3*: Rare Cold Inducible 3 gene; **(C)** *PvBdzp-Receptor*: Benzodiazepine receptor-related; **(D)** *PvMYB41*; **(E)** *PvWRKY51* and *PvWKY56* **(F)**: *WRKY* transcription factors, **(G)** *PvRPK-LRR:* RPK-LRR-disease- resistance-protein, **(H)** Universal stress protein; **(I)** *PvDRFP:* Disease resistance family protein, **(J)** *PvAP2-ERF034:* AP2 Ethylene-responsive transcription factor ERF034. Standard deviation (SD) bars are shown for biological replicates. Values followed by different letters indicate significant differences ($p<0.05$) between control and drought-stressed nodules by genotype as estimated by REST Software analysis. RQ, Relative quantification.

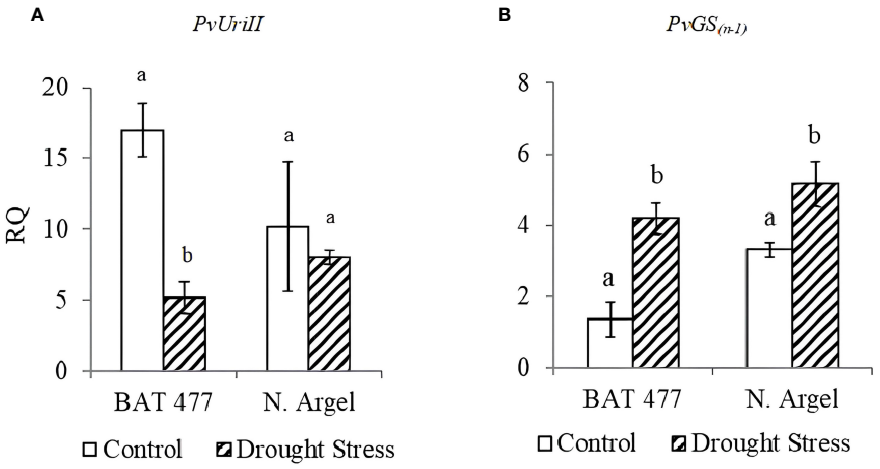

FIGURE 6
Expression profiles of two genes related to nitrogen metabolism and assimilation in common bean nodules upon aging senescence. *PvUrilI*: Uricase II, involved in ureides biosynthetic pathway **(A)**; *PvGS(n-1):* Glutamine synthetase gamma-subunit, an enzyme responsible for the assimilation of NH_4^+ into organic nitrogen **(B)**; Standard deviation (SD) bars are shown for biological replicates. Values followed by different letters indicate significant differences between control and drought-stressed nodules by genotype as estimated by the REST software version 2.0.7 ($p<0.05$). RQ, Relative quantification.

analysis, the relative quantification (RQ) values were higher for BAT 477 (up-regulated DEGs) or lower (down-regulated DEGs) compared to Negro Argel. This indicates a significant impact of drought stress in the BAT 477 genotype. Overall, these results are consistent with the RNA-Seq analysis, providing strong validation for our nodule transcriptome data, confirming the up- and down-regulated genes in both genotypes.

4 Discussion

The development of next-generation sequencing (NGS) technology has provided unprecedented opportunity and a powerful tool for gene expression profiling in plants (O'Rourke et al., 2014a; Schmutz et al., 2014). To our knowledge, previous studies using RNA-Seq technology concerning to BNF in common bean are scarce (O'Rourke et al., 2014b; Kamfwa et al., 2017) mainly those focused on transcriptional responses in root-nodules tissue. Hence, in the present study, we used the Illumina HiSeq 2000 platform to examine BNF under abiotic stress conditions. We focused on understanding the transcriptional changes in nodules from two common bean genotypes in response to drought. For this purpose, the plants were inoculated with a mixture of *Rhizobium tropici* strains and submitted to four days of drought stress by suspension of irrigation.

In our conditions, the BNF activity was severely affected by drought in BAT 477 genotype showing a significant decreasing in N2ase analyses as well as STNC and SDW, which were evaluated ten days after plants rehydration (Figure 1C and Table 2). On the other hand, Negro Argel was not significantly affected in any of these parameters which suggest a lower susceptibility to drought during symbiosis in this genotype. Hence, the STNC, SDW and N2ase analyses phenotypic markers allowed evaluate the BNF performance of the two genotypes after stress and the contrasting susceptibility of Negro Argel (tolerant) and BAT 477 (susceptible) to drought stress under BNF conditions was confirmed. Summerfield et al. (1985) observed that the drought-tolerant cultivar, such as Negro Argel, showed greater maintenance of leaf area under water deficit, resulting in greater productivity. This trait can be important for BNF drought tolerant as well. Pimentel and Cruz Perez (2000), in order to establish parameters for drought tolerance evaluation in common bean genotypes showed that the SDW, along with leaf water potential (Ψf) and leaf area, is a suitable marker of the effect of drought. Interestingly, although BAT 477 has been considered a drought-tolerant genotype under N fertilized field conditions (Sponchiado et al., 1989; Guimarães, 1996), in our conditions BAT 477 plants began to wilt after drought with a 68.5% RWC value (Figure 1A). On the other hand, Negro Argel genotype showed no symptoms of drought stress (Supplementary Figure 1), showing the RWC unaltered (Figure 1A), despite the low value of substrate humidity measured by gravimetric soil moisture (w) was very similar for both genotypes (Figure 1B). Similar results have been reported by Gomes et al., 2000 in which Negro Argel genotype presented lower reductions in stem biomass at the end of growth cycle, in leaf area duration, and in grain yield, demonstrating a higher drought tolerance. Taken together, these results suggest that Negro Argel drought tolerance under BFN conditions differ from BAT 477 genotype by using a different mechanism to overcome the drought even under similar conditions of irrigation.

The drought tolerance observed in BAT 477 under field conditions is mainly attributed to its extensive and deep root system when growing in soils with insufficient water or nutrient supplies (Sponchiado et al., 1989). However, in our experimental setup, the effectiveness of this mechanism is constrained by the substrate volume explored by the root system. Some studies have suggested that common beans growing under conditions of nitrogen (N_2) fixation exhibit greater drought tolerance than those supplied with sufficient levels of nitrogen fertilizer (NH_4NO_3) (Lodeiro et al., 2000).

Nevertheless, the understanding of the effects of BNF on drought tolerance in common beans remains unclear and depends on various factors, including genotype (Ramos et al., 2003; Devi et al., 2013) and the specific symbiotic combination (Tajini et al., 2012; Hungria and Kaschuk, 2013).

In the present study, an RNA-Seq nodule transcriptome analysis was carried out using Illumina High-Seq 2000 platform. Comparative transcriptional level analysis of drought-stressed and control plants using three different statistical algorithms (CuffDiff, DESeq1 and edgeR) revealed a higher number of down-regulated DEGs in susceptible genotype (BAT 477) when compared to the drought tolerant one (Negro Argel) (Figure 2; Supplementary Figure S3). Overall, there was much more genes responsive to drought in BAT 477 suggesting a pronounced effect of drought stress for this genotype. In agreement with our results, a higher number of DEGs as well as down-regulated genes was observed for a drought-sensitive genotype of common bean (Wu et al., 2014). Moreover, in a salt tolerant common bean genotype a great number of down-regulated genes in roots and leaves submitted to salt stress was found (Hiz et al., 2014). Although a remarkable difference in DEGs number among the two contrasting genotypes has been observed, some common up- and down-regulated genes were found within the top 10 DEGs including one small heat shock protein (up-regulated) and one peroxidase family protein (down-regulated) (Supplementary Figure S4) suggesting the recruitment of shared pathways in drought stress responses.

Throughout BNF, nodule oxygen (O_2) permeability regulated by the O_2 diffusion barrier (ODB) is among the main processes limiting nodule performance (Arrese-Igor et al., 2011). Under drought stress, a decline in the permeability to O_2 diffusion leading to a reduction in nodule respiration and therefore a lower production of energy via ATP synthase has been described (Serraj and Sinclair, 1996). Interestingly, in our analysis a hypothetical protein containing cytochrome c oxidase assembly factor CtaG domain (GeneBank: XP_007141322.1) was highly induced in both genotypes (Supplementary Figure 2). Since BNF is an energy demanding process, a high rate of oxygen respiration is necessary to supply this requirement. Cytochrome C oxidase shows high affinity to O_2, and its induction in nodules may be contributing to maintain respiration rate at low O_2 levels and consequently nodule performance under drought stress.

Several BAT 477-Negro Argel shared up-regulated genes were identified in the top 10 DEGs. Among them, galactinol synthase (GenBank: XP_007163306.1) plays a crucial role in the biosynthesis of raffinose family oligosaccharides (RFOs), functioning as osmoprotectants with potential stress mitigation properties (Santos et al., 2015). Additionally, a chalcone/stilbene synthase (CSH) family protein (GenBank: XP_007137487.1) was found, which serves as a key enzyme in the flavonoid/isoflavonoid biosynthesis pathway. This enzyme is induced in plants under various stress conditions such as UV light exposure and bacterial or fungal infections. The expression of CHS leads to the accumulation of flavonoids and isoflavonoids, contributing to the plant's defense mechanism, particularly through the salicylic acid defense pathway (Dao et al., 2011).

Drought tolerance is a complex trait that involves several molecular, biochemical, and physiological mechanisms to avoid or tolerate periods of drought stress (Todaka et al., 2015). The MapMan analysis of DEGs provided a comprehensive overview of the key pathways influenced by drought stress in nodules (Figure 4 and Supplementary Figures S10 and S11), aligning with the enriched Gene Ontology (GO) terms identified in AgriGO SEA (Supplementary Figures S8 and S9). Collectively, our results imply comparable responses to drought stress between the two genotypes. Nonetheless, BAT 477 exhibited a higher number of genes in all drought-affected pathways (Figure 4B), likely linked to its heightened susceptibility to drought, as evidenced in analyses of shoot dry weight (SDW), total nitrogen content (STNC), and nitrogenase activity (N2ase) (Figure 1). Furthermore, BAT 477 displayed exclusive regulation of certain pathways, including "ABA and jasmonate hormone signaling," "redox state," "glutathione-S-transferase," and "secondary metabolism".

As sessile organisms, cell signaling and transcriptional regulation of gene expression is a crucial trait in plant responses to environmental constraints (Li et al., 2014). Moreover, signal-transduction genes are important at the different stages of *Rhizobium* and leguminous symbiosis as well as the maintenance of nodule metabolism during BNF (Carvalho et al., 2013). In our analysis, several signaling-related genes were responsive to drought in nodules for the two genotypes (Supplementary Tables S2, S3). These DEGs included signaling genes related to sugar and nutrient physiology processes, receptors kinases such as LRR and DUF 26 types, G proteins and calcium signaling transduction related-genes. Plant membrane receptors and sensor proteins play important roles in various signaling pathways, conveying information to their cytoplasmic target proteins via catalytic processes, such as phosphorylation. Moreover, it has been hypothesized that these signaling proteins are involved in the initial process of water status perception outside the cell which includes calcium signaling and receptors-like kinases (Maathuis, 2014). In Arabidopsis, the RLK receptors family includes more than 600 members, with the leucine rich-repeat (LRR)-RLKs constituting the largest subgroup (Gish and Clark, 2011). Interestingly, for Negro Argel genotype the number of genes in this category was very limited when compared to BAT 477 (Supplementary Tables S2, S3). Moreover, the majority of signaling genes were down-regulated in both genotypes and a further characterization of them, and the integrated investigation of the changes in nodule metabolism mediated by differential gene expression, could give insights on the signal transduction pathways to reprogramming nodule metabolism in response to drought.

Several transcription factors play important roles in translating stress signals into changes in gene expression (Li et al., 2014). In our analysis, some classes of TFs were regulated by drought in both genotypes (Supplementary Tables S2, S3) and the major TFs identified were MYB, WRKY and AP2-EREBP/AP2-ERF. These TFs have been reported to be involved in abiotic stress responses in different species (Oh et al., 2011; Niu et al., 2012; Wu et al., 2014). Similar results were found by Hiz et al. (2014) which used RNA-Seq approach to investigate the transcriptional responses to salt stress in leaves and roots of common bean plants in which AP2-EREBP, WRKY and MYB were identified among the most abundant differentially expressed TF families. Recently, WRKY and MYB genes were overrepresented in the common bean transcriptome

analysis for drought-responsive genes discovery (Wu et al., 2014). As one of the largest TF groups in plants, the MYB family has been shown to be essential for the responses to abiotic stresses (Chen et al., 2014; Li et al., 2014). In *Arabidopsis* MYB60, a regulator of stomata movement was down-regulated by drought stress, and its overexpression resulted in hypersensitivity to water deficit (Oh et al., 2011). On the other hand, the biosynthesis of cuticular wax activated by MYB96 is required for the drought tolerance of plants (Seo et al., 2009; Seo et al., 2011) and the gene AtMYB41 is induced by drought and may function as a transcription factor in modulating cell expansion and cuticle deposition during drought stress (Cominelli et al., 2008). These results showed the dynamic regulation of this TF family on drought stress responses in plants. Additionally, other two important TF families were found in our DEGs. The AP2/ERF family proteins are plant-specific transcription factors involved in plant abiotic stress responses (Mizoi et al., 2012) and the majority of these TFs was down-regulated in our data set. Similar to AP2/ERF genes, WRKY-type transcription factors are involved in multiple aspects of plant growth, development, and stress responses (Chen et al., 2012). Moreover, a single WRKY gene can be simultaneously regulated by several stress factors (Wei et al., 2008; Niu et al., 2012), showing its diverse regulatory function on transcriptional reprograming during plant stress responses. In wheat, the genes *TaWRKY2* was regulated by drought, salt, and ABA meanwhile *TaWRKY19* was regulated by cold, drought, salt, and ABA treatments (Niu et al., 2012). *TcWRKY53* is also simultaneously induced by cold, salt and PEG treatments (Wei et al., 2008). Some works have reported WRKY proteins as key components of ABA (Shang et al., 2010) and ROS signaling (Davletova et al., 2005), which are among the major events triggered in the plant cells when submitted to stresses (Cruz de Carvalho, 2008). In *Arabidopsis*, the heterologous expression of two wheat WRKY genes (*TaWRKY2* and *TaWRKY19)* conferred tolerance to multiples abiotic stresses by up-regulation of downstream genes responsive to stress (Niu et al., 2012).

In addition to signal transduction and transcription factors related-genes, we found in our DEGs some transcripts involved in plant hormone signaling and metabolism, such as abscisic acid, auxin, ethylene and jasmonate (Supplementary Tables S2, S3). Ethylene is known as a senescence inducer and stress-related phytohormone. In agreement with this assumption, in our analysis the gene 1-aminocyclopropane-1-carboxylate oxidase (Phvul.008G214200.1), which is involved in the key step of ethylene biosynthetic pathway, was up-regulated in nodules of BAT 477, but not in Negro Argel genotype, in response to drought. On the other hand, the majority of genes, involved in ethylene signaling and metabolism as well as other phytohormones, were down-regulated and this response in nodules needs further investigation.

Some environmental conditions, such as drought or salinity, are responsible for nodule senescence and also cause an O_2 content imbalance, which is necessary to ensure a successful BNF activity (Puppo et al., 2005). Moreover, the oxidative stress in plants negatively affects the cell membrane, nucleic acids, and proteins structures, leading to metabolic disturbances (Cruz de Carvalho, 2008). Although some works have described an increase in antioxidant responses under drought (Naya et al., 2007). A remarkable down-regulation in antioxidant metabolism related-genes was observed, mainly for BAT 477 genotype (Supplementary Tables S2, S3; Figure 6) and included gene related to ascorbate-glutathione cycle, which is the major antioxidant cytosolic mechanism operating in the nodule (Becana et al., 2010), suggesting a decreasing on antioxidant protection at transcriptional level. In agreement with these findings, some studies reported that severe drought stress decreased antioxidant activity in nodules (Gogorcena et al., 1995; Porcel et al., 2003), which could partially explain the results observed for BAT 477, the susceptible genotype.

Heat shock proteins (HSPs) play a fundamental role in protecting plants against stress by re-establishing normal protein conformation and thus cellular homeostasis (Wang et al., 2004). In our results, the induction of HSP-encoding genes suggests an acclimation response of nodules to maintain its metabolism (Figure 4; Supplementary Tables S2, S3). In cowpea, a high tolerant leguminous species, the induction of HSPs has been reported in nodules under drought and heat stresses (Simoes-Araujo et al., 2008; da Silva et al., 2012b). Moreover, the induction of HSPs was correlated to heat tolerance in different genotypes of common bean (Simões-Araújo et al., 2003). Interestingly, a COLD-REGULATED 413-PLASMA MEMBRANE 2 gene (COR413-PM2) was up-regulated in BAT 477 nodules suggesting a crosstalk among cold and drought responses (Figure 6B; Supplementary Table S2). The COR413-PM2 is a stress-regulated multispanning transmembrane family protein restrict to the plant kingdom which is correlated with the development of freezing tolerance in cereals and Arabidopsis and several members of those family are also regulated by drought stress, light, and abscisic acid (Breton et al., 2003).

In this study, 10 DEGs were selected for RNA-Seq validation by RT-qPCR and our results showed that the expression profile of DEGs was very similar to RNA-Seq results (Figure 5). In some cases, such as *PvPer22*, *PvWRKY51*, *DRFP* and *PvAP2-ERF034*, the transcripts abundance of these genes was undetectable for BAT 477 drought stressed samples which suggests a strong down-regulation for this genotype. The evaluated DEGs corresponded to different functional categories such as antioxidant metabolism (e.g PvPer22), transcription factors (e.g *PvWRKY51*) and cell signalling (e.g *PvRPK-LRR*) which confirmed the MapMan and AgriGO results.

5 Conclusion

In this study, we conducted a comprehensive analysis of the common bean nodule transcriptome under drought stress using Illumina sequencing technology. To the best of our knowledge, this work represents the first systematic investigation of common bean nodule gene expression during biological nitrogen fixation under adverse conditions. Our comparative expression analysis, employing three statistical algorithms (CuffDiff, DESeq1, and edgeR), in conjunction with AgriGO and MapMan analysis, revealed a notable down-regulation of numerous metabolic pathways in common bean nodules in response to drought stress. These affected pathways encompassed antioxidant metabolism and genes related to protein kinases. Intriguingly, some gene categories, including heat shock proteins (HSPs) and specific transcription

factors (TFs), were up-regulated by drought stress. While a substantial number of TFs were down-regulated, our study identified three classes of TFs (MYB, WRKY, and AP2/ERF) that were up-regulated and are well-known for their roles in plant responses to various stresses. Their involvement in nodules' responses to drought remains a subject of ongoing research. A detailed characterization of these TFs could be a promising starting point for biotechnological strategies aimed at enhancing drought tolerance in common beans and other leguminous species. Our findings suggest that, under drought stress, common bean nodules activate genes related to abiotic stress, such as HSPs and LEA protein genes, as well as specific some transcription factors. However, the majority of DEGs are repressed, indicating a down-regulation of various metabolic processes at the transcriptional level, including antioxidant activity, the transcriptional regulation of downstream genes, and events mediated by hormones. Our results shed light on the transcriptional changes occurring in common bean nodules under drought stress. This information may serve as a foundation for the development of new strategies to enhance drought tolerance in common bean when grown under biological nitrogen fixation reliance.

Data availability statement

The datasets presented in this study can be found in online repositories. The names of the repository/repositories and accession number(s) can be found in the article/Supplementary Material.

Author contributions

Hd: Writing – review & editing, Data curation, Investigation, Methodology, Software, Writing – original draft. VC: Investigation, Methodology, Writing – review & editing. DP: Investigation, Methodology, Writing – review & editing. RP: Data curation, Writing – review & editing. CM: Writing – review & editing. JS: Writing – review & editing, Conceptualization, Funding acquisition, Project administration, Supervision.

Funding

The author(s) declare financial support was received for the research, authorship, and/or publication of this article. This work was supported by the Centro Nacional de Pesquisa de Agrobiologia (Embrapa Agrobiologia), Conselho Nacional de Desenvolvimento Científico e Tecnológico (CNPq), Coordenação de Aperfeiçoamento de Pessoal do Ensino Superior (CAPES), and Paraiba State University (PRPGP Grant #01/2024) partially financed this study.

Acknowledgments

We are grateful to thank Dr[a]. Janaína Cavalcante, Dr. José Ivo Baldani, Dr. Marcio Alves-Ferreira, Dr. Luc Rouws and Dr. Jerri Édson Zilli for helpful discussions and suggestions to improve the manuscript. Carlos Henrique Salvino Gadelha Meneses (Process n° 313075/2021-2) and Jean Luiz Simões-Araújo (Process n° 307253/2022-8) were supported by fellowships from CNPq.

Conflict of interest

The authors declare that the research was conducted in the absence of any commercial or financial relationships that could be construed as a potential conflict of interest.

Publisher's note

Supplementary material

The Supplementary Material for this article can be found online at: https://www.frontiersin.org/articles/10.3389/fpls.2024.1345379/full#supplementary-material

SUPPLEMENTARY FIGURE 1
RNA-Seq experiment workflow and bioinformatics pipeline. Common bean plants submitted to drought-stress were collected ① and root-nodules' total RNA samples from well-watered (WW) and drought-stressed (DS) plants were used send to RNA-Seq profiling ②. After Illumina HiSeq 2000 RNA-sequencing, the bioinformatics pipeline consisted in filter the low-quality reads (Q<20) followed by trimming using the FASTX-Toolkit ③. The high-quality reads (Q≥20) were then mapped against the *P. vulgaris* L. reference genome using the Bowtie and TopHat2 software ④. A table of normalized of read counts was obtained using HT-Seq-count software ⑤, and the differentially expressed genes (DEGs) were tested using three independent algorithms: DESeq1, edgeR and CuffDiff ⑥. Only those genes concomitantly detected in the three algorithms were considered differentially expressed. In these analyses, a list of 1451 differentially expressed genes (DEGs) was obtained from Negro Argel and BAT 477 drought-stressed nodules (output data) and used for functional annotation and further downstream analyses (Gene Ontology, MapMan etc).

SUPPLEMENTARY FIGURE 2
Negro Argel and BAT 477 common bean genotypes submitted to four days after drought stress drought stress.

SUPPLEMENTARY FIGURE 3
Identification of differentially expressed genes (DEGs) using three independent statistical algorithms. Venn diagram showing the number of DEGs concomitantly identified by CuffDiff, DESeq1 and edgeR algorithms (bold values) for BAT 477 and N. Argel genotypes. A pairwise comparison for DEGs shared between two algorithms as well as the number of DEGs specifically identified by each algorithm can be visualized. Additionally, the total number of DEGs by algorithm is indicated in parentheses.

SUPPLEMENTARY FIGURE 4
Common recruitment of drought-regulated genes in nodules of the two common bean genotypes. BAT 477 and Negro Argel shared genes from the top10 highest and lowest differentially expressed genes (DEGs) in nodules submitted to drought stress are shown.

SUPPLEMENTARY FIGURE 5
Functional annotation of differentially expressed up-regulated genes (up-regulated DEGs) in BAT 477 drought-stressed nodules. Gene ontology (GO) categorization was performed after SEA analysis using **AgriGO** Software v2.0 and the results are summarized for in the Biological Process GO category.

SUPPLEMENTARY FIGURE 6
Functional annotation of differentially expressed down-regulated genes (up-regulated DEGs) in BAT 477 drought-stressed nodules. Gene ontology (GO) categorization was performed after SEA analysis using **AgriGO** Software v2.0 and the results are summarized for in the Biological Process GO category.

SUPPLEMENTARY FIGURE 7
Functional annotation of differentially expressed up-regulated genes (up-regulated DEGs) in BAT 477 drought-stressed nodules. Gene ontology (GO) categorization was performed after SEA analysis using **AgriGO** Software v2.0 and the results are summarized for Biological Process GO category.

SUPPLEMENTARY FIGURE 8
Functional annotation of differentially expressed up-regulated genes (up-regulated DEGs) in BAT 477 drought-stressed nodules. Gene ontology (GO) categorization was performed after SEA analysis using **AgriGO** Software v2.0 and the results are summarized for Molecular Function GO category.

SUPPLEMENTARY FIGURE 9
Functional annotation of differentially expressed down-regulated genes (down-regulated DEGs) in BAT 477 (a) and Negro Argel (b) drought-stressed nodules. Gene ontology (GO) categorization was performed after SEA analysis using **AgriGO** Software v2.0 and the results are summarized for Molecular Function GO category.

SUPPLEMENTARY FIGURE 10
BAT 477 nodules regulation overview under drought stress.

SUPPLEMENTARY FIGURE 11
N. Argel nodules regulation overview under drought stress.

SUPPLEMENTARY FIGURE 12
Evaluation of expression stability candidate reference genes in common bean nodules. Three common bean candidate reference genes (*PvIDE*, *PvEf1-Alpha* and *PvAct*) were evaluated by two different algorithms (geNorm and NormFinder softwares) and used for qPCR data normalization.

SUPPLEMENTARY TABLE 1
Description of candidate reference genes and their primer sequences. Prior to DEGs validation experiments, the expression stability of three candidate reference genes was evaluated using geNorm and NormFinder algorithms in common bean (P. vulgaris L.) nodules submitted to drought stress.

References

Altschul, S. F., Gish, W., Miller, W., Myers, E. W., and Lipman, D. J. (1990). Basic local alignment search tool. *J. Mol. Biol.* 5, 403–410. doi: 10.1016/S0022-2836(05)80360-2

Anders, S., and Huber, W. (2010). Differential expression analysis for sequence count data. *Genome Biol.* 11, R106. doi: 10.1186/gb-2010-11-10-r106

Anders, S., Pyl, P. T., and Huber, W. (2014). HTSeq—a Python framework to work with high-throughput sequencing data. *Bioinformatics* 31, 166–169. doi: 10.1093/bioinformatics/btu638

Andersen, C. L., Jensen, J. L., and Ørntoft, T. F. (2004). Normalization of real-time quantitative reverse transcription-PCR data: a model-based variance estimation approach to identify genes suited for normalization, applied to bladder and colon cancer data sets. *Cancer Res.* 64, 5245–5250. doi: 10.1158/0008-5472.CAN-04-0496

Andrews, S. (2010) *FastQC a Quality Control Tool for High Throughput Sequence Data*. Available at: https://www.bioinformatics.babraham.ac.uk/projects/fastqc/ (Accessed March 15, 2023).

Arrese-Igor, C., Gonzalez, E. M., Marino, D., Ladrera, R., Larrainzar, E., and Gil-Quintana, E. (2011). Physiological response of legume nodules to drought. *Plant Stress* 5, 24–31.

Arruda, I. M., Moda-Cirino, V., Koltun, A., Dos Santos, O. J. A. P., Moreira, R. S., Moreira, A. F. P., et al. (2018). Physiological, biochemical and morphoagronomic characterization of drought-tolerant and drought-sensitive bean genotypes under water stress. *Physiol. Mol. Biol. Plants* 24, 1059–1067. doi: 10.1007/s12298-018-0555-y

Becana, M., Matamoros, M. A., Udvardi, M., and Dalton, D. A. (2010). Recent insights into antioxidant defenses of legume root nodules. *New Phytol.* 188, 960–976. doi: 10.1111/j.1469-8137.2010.03512.x

Beebe, S. E., Rao, I. M., Blair, M. W., and Acosta-Gallegos, J. A. (2013). Phenotyping common beans for adaptation to drought. *Front. Physiol.* 6. doi: 10.3389/fphys.2013.00035

Beebe, S. E., Rao, I. M., Cajiao, I., and Grajales, M. (2008). Selection for drought resistance in common bean also improves yield in phosphorus limited and favorable environments. *Crop Sci.* 48, 582–592. doi: 10.2135/cropsci2007.07.0404

Breton, G., Danyluk, J., Charron, J. B., and Sarhan, F. (2003). Expression profiling and bioinformatic analyses of a novel stress-regulated multispanning transmembrane protein family from cereals and *Arabidopsis*. *Plant Physiol.* 132, 64–74. doi: 10.1104/pp.102.015255

Carvalho, G. A. B., Batista, J. S. S., Marcelino-Guimarães, F. C., do Nascimento, L. C., and Hungria, M. (2013). Transcriptional analysis of genes involved in nodulation in soybean roots inoculated with *Bradyrhizobium japonicum* strain CPAC 15. *BMC Genomics* 153. doi: 10.1186/1471-2164-14-153

Casagrande, E. C., Farias, J. R. B., Neumaier, N., Oya, T., Pedroso, J., Martins, P. K., et al. (2001). Expressão gênica diferencial durante déficit hídrico em soja. *Rev. Bras. Fisiol. Vegetal* 13, 168–184. doi: 10.1590/S0103-31312001000200006

Chartzoulakis, K., Therios, I., and Noitsakis, B. (1997). The effect of soil water deficit on internal water relations of kiwifruit. In Proceeds of the Third International Symposium on Kiwifruit. *Acta Hortic.* 444, 305–310. doi: 10.17660/ActaHortic.1997.444.47

Chavez-Mendoza, C., and Sanchez, E. (2017). Bioactive compounds from mexican varieties of the common bean (*Phaseolus vulgaris*): Implications for health. *Molecules* 22, 1360. doi: 10.3390/molecules22081360

Chen, L., Yu, S., Li, S., Zhang, L., Zou, C., and Yu, D. (2012). The Role of WRKY transcription factors in plant abiotic stresses. *Biochim. Biophys. Acta Gene Regul. Mech.* 1819, 120–128. doi: 10.1016/j.bbagrm.2011.09.002

Chen, N., Yang, Q., Pan, L., Chi, X., Chen, M., Hu, D., et al. (2014). Identification of 30 MYB transcription factor genes and analysis of their expression during abiotic stress in peanut (*Arachis hypogaea* L.). *Gene* 533, 332–345. doi: 10.1016/j.gene.2013.08.092

Cilliers, M., van Wyk, S. G., van Heerden, P. D. R., Kunert, K. J., and Vorster, B. J. (2018). Identification and changes of the drought-induced cysteine protease transcriptome in soybean (*Glycine max*) root nodules. *J. Exp. Environ. Bot.* 148, 59–69. doi: 10.1016/j.envexpbot.2017.12.005

Cominelli, E., Sala, T., Calvi, D., Gusmaroli, G., and Tonelli, C. (2008). Over-expression of the *Arabidopsis* AtMYB41 gene alters cell expansion and leaf surface permeability. *Plant J.* 53, 53–64. doi: 10.1111/j.1365-313X.2007.03310.x

Cooper, J. E. (2007). Early interactions between legumes and rhizobia: disclosing complexity in a molecular dialogue. *J. Appl. Microbiol.* 103, 1355–1365. doi: 10.1111/j.1365-2672.2007.03366.x

Cruz de Carvalho, M. ,. H. (2008). Drought stress and reactive oxygen species: Production, scavenging and signaling. *Plant Signal Behav.* 3, 156–165. doi: 10.4161/psb.3.3.5536

Dao, T. T., Linthorst, H. J., and Verpoorte, R. (2011). Chalcone synthase and its functions in plant resistance. *Phytochem. Rev.* 10, 397–412. doi: 10.1007/s11101-011-9211-7

Darkwa, K., Ambachew, D., Mohammed, H., Asfaw, A., and Blair, M. W. (2016). Evaluation of common bean (*Phaseolus vulgaris* L.) genotypes for drought stress adaptation in Ethiopia. *Crop J.* 4, 367–376. doi: 10.1016/j.cj.2016.06.007

da Silva, H. A. P., Caetano, V. S., Bezerra, A. C. M., Vidal, M. S., and Simões-Araújo, J. L. (2012b). *Efeito do déficit hídrico sobre a fixação biológica de N_2 em cultivares de feijão comum* (Seropédica, RJ: Embrapa Agrobiologia, 2012 (Boletim de Pesquisa e Desenvolimento).

da Silva, H. A. P., Galisa, P. S., Oliveira, R. S. S., Vidal, M. S., and Simões-Araújo, J. L. (2012a). Expressão gênica induzida por estresses abióticos em nódulos de feijão-caupi. *Pesquisa Agropecuária Bras.* 47, 797–807. doi: 10.1590/S0100-204X2012000600010

Davletova, S., Rizhsky, L., Liang, H., Shengqiang, Z., Oliver, D. J., Coutu, J., et al. (2005). Cytosolic ascorbate peroxidase 1 is a central component of the reactive oxygen gene network of *Arabidopsis*. *Plant Cell* 17, 268–281. doi: 10.1105/tpc.104.026971.1

Devi, M. J., Sinclair, T. R., Beebe, S. E., and Rao, I. M. (2013). Comparison of common bean (*Phaseolus vulgaris* L.) genotypes for nitrogen fixation tolerance to soil drying. *Plant Soil* 364, 29–37. doi: 10.1007/s11104-012-1330-4

Fahad, S., Bajwa, A. A., Nazir, U., Anjum, S. A., Farooq, A., Zohaib, A., et al. (2017). Crop production under drought and heat stress: plant responses and management options. *Front. Plant Sci.* 8. doi: 10.3389/fpls.2017.01147

Feller, U., and Vaseva, I. I. (2014). Extreme climatic events: impacts of drought and high temperature on physiological processes in agronomically important plants. *Front. Environ. Sci.* 2. doi: 10.3389/fenvs.2014.00039

Ferguson, B. J., Indrasumunar, A., Hayashi, S., Lin, M.-H., Lin, Y.-H., Reid, D. E., et al. (2010). Molecular analysis of legume nodule development and autoregulation. *J. Integr. Plant Biol.* 52, 61–76. doi: 10.1111/j.1744-7909.2010.00899.x

Ferreira, D. F. (2011). SISVAR: A computer statistical analysis system. *Ciec. e Agrotecnol.* 35, 1039–1042. doi: 10.1590/S1413-70542011000600001

Fred, E. B., and Waksman, S. A. (1928). *Yeast Extract – Mannitol Agar for Laboratory Manual of General Microbiology* (New York: McGraw Hil).

Furlan, A. L., Bianucci, E., Castro, S., and Dietz, K. J. (2017). Metabolic features involved in drought stress tolerance mechanisms in peanut nodules and their contribution to biological nitrogen fixation. *Plant Sci.* 263, 12–22. doi: 10.1016/j.plantsci.2017.06.009

Furlan, A., Bianucci, E., Tordable, M. C., Castro, S., and Dietz, K. J. (2014). Antioxidant enzyme activities and gene expression patterns in peanut nodules during a drought and rehydration cycle. *Funct. Plant Biol.* 41, 704–713. doi: 10.1071/FP13311

Gil-Quintana, E., Lyon, D., Staudinger, C., Wienkoop, S., and González, E. M. (2015). *Medicago truncatula* and *Glycine max*: different drought tolerance and similar local response of the root nodule proteome. *J. Proteome Res.* 14, 5240–5251. doi: 10.1021/acs.jproteome.5b00617

Gish, L. A., and Clark, S. E. (2011). The RLK/Pelle family of kinases. *Plant J.* 66, 117–127. doi: 10.1111/j.1365-313X.2011.04518.x

Gogorcena, Y., Iturbe-Ormaetxe, I., Escuredo, P. R., and Becana, M. (1995). Antioxidant defenses against activated oxygen in pea nodules subjected to water stress. *Plant Physiol.* 108, 753–759. doi: 10.1104/pp.108.2.753

Gomes, A. A., Araújo, A. P., Rossiello, R., and Pimentel, C. (2000). Acumulação de biomassa, características fisiológicas e rendimento de grãos em cultivares de feijoeiro irrigado e sob sequeiro. *Pesquis. Agropecuária Bras.* 35, 1927–1937. doi: 10.1590/S0100-204X2000001000003

Goodstein, D. M., Shu, S., Howson, R., Neupane, R., Hayes, R. D., Fazo, J., et al. (2012). Phytozome: a comparative platform for green plant genomics. *Nucleic Acids Res.* 40 (Database issue), D1178–D1186. doi: 10.1093/nar/gkr944

Guimarães, C. M. (1996). "Relações hídricas," in *cultura do feijoeiro comum no Brasil*. Eds. R. S. Araújo, C. A. Rava, L. F. Stone and M. Zimmermann (Piracicaba: Potafos), 139–168.

Guo, F., Yu, H., Xu, Q., and Deng, X. (2015). Transcriptomic analysis of differentially expressed genes in an orange-pericarp mutant and wild type in pummelo (*Citrus grandis*). *BMC Plant Biol.* 15, 44. doi: 10.1186/s12870-015-0435-3

Heinemann, A. B., Ramirez-Villegas, J., Stone, L. F., and Didonet, A. D. (2017). Climate change determined drought stress profiles in rainfed common bean production systems in Brazil. *Agric. For. Meteorol.* 246, 64–77. doi: 10.1016/j.agrformet.2017.06.005

Hellemans, J., Mortier, G., De Paepe, A., Speleman, F., and Vandesompele, J. (2007). qBase relative quantification framework and software for management and automated analysis of real-time quantitative PCR data. *Genome Biol.* R19. doi: 10.1186/gb-2007-8-2-r19

Hiz, M. C., Canher, B., Niron, H., and Turet, M. (2014). Transcriptome analysis of salt tolerant common bean (*Phaseolus vulgaris* L.) under saline conditions. *PloS One* 9, e92598. doi: 10.1371/journal.pone.0092598

Hoyos-Villegas, V., Song, Q., and Kelly, J. D. (2017). Genome-wide association analysis for drought tolerance and associated traits in common bean. *Plant Genome* 10. doi: 10.3835/plantgenome2015.12.0122

Hungria, M., Andrade, D. S., Chueire, L. M. O., Probanza, A., Guttierrez-Manero, J., and Megías, M. (2000). Isolation and characterization of new efficient and competitive bean (Phaseolus vulgaris L.) rhizobia strains. *Soil Biol. Biochem.* 32, 1515–1528. doi: 10.1016/S0038-0717(00)00063-8

Hungria, M., and Franco, A. A. (1993). Effects of high temperature on nodulation and nitrogen fixation by *Phaseolus vulgaris* L. *Plant Soil* 149, 95–102. doi: 10.1007/BF00010766

Hungria, M., and Kaschuk, G. (2013). Regulation of N_2 Fixation and NO_3–/NH_4+ assimilation in nodulated and n-fertilized *Phaseolus vulgaris* L. exposed to high temperature stress". *Environ. Exp. Bot.* 98, 32–39. doi: 10.1016/j.envexpbot.2013.10.010

Hungria, M., and Neves, M. C. P. (1987). Cultivar and Rhizobium strain effect on nitrogen fixation and transport in *Phaseolus vulgaris* L. *Plant Soil* 103, 111–121. doi: 10.1007/BF02370675

Hungria, M., and Vargas, M. A. T. (2000). Environmental factors affecting N_2 fixation in grain legumes in the tropics, with an emphasis on Brazil. *Field Crops Res.* 65, 151–164. doi: 10.1016/S0378-4290(99)00084-2

Kamfwa, K., Zhao, D., Kelly, J. D., and Cichy, K. A. (2017). Transcriptome analysis of two recombinant inbred lines of common bean contrasting for symbiotic nitrogen fixation. *PloS One* 12, e0172141. doi: 10.1371/journal.pone.0172141

Kim, D., Pertea, G., Trapnell, C., Pimentel, H., Kelley, R., and Salzberg., S. L. (2013). TopHat2: accurate alignment of transcriptomes in the presence of insertions, deletions, and gene fusions. *Genome Biol.* 14, R36. doi: 10.1186/gb-2013-14-4-r36

Kjeldahl, J. (1883). Neue methode zur bestimmung des stickstoffs in organischen körpern. *New Method Determination Nitrogen Org Substances Z. Für Analytische Chem.* 22, 366–383. doi: 10.1007/BF01338151

Kunert, K. J., Vorster, B. J., Fenta, B. A., Kibido, T., Dionisio, G., and Foyer, C. H. (2016). Drought stress responses in soybean roots and nodules. *Front. Plant Sci. 12* 7. doi: 10.3389/fpls.2016.01015

Langmead, B., Trapnell, C., Pop, M., and Salzberg, S. L. (2009). Ultrafast and memory-efficient alignment of short DNA sequences to the human genome. *Genome Biol.* 10, R25. doi: 10.1186/gb-2009-10-3-r25

Li, C., Ng, C. K.-Y., and Liu-Min, F. (2014). MYB transcription factors, active players in abiotic stress signaling. *Environ. Exp. Bot.* 114, 80–91. doi: 10.1016/j.envexpbot.2014.06.014

Livak, K. J., and Schmittgen, T. D. (2001). Analysis of relative gene expression data using real-time quantitative PCR and the $2^{-\Delta\Delta C}{}_T$ Method. *Methods* 25, 402–408. doi: 10.1006/meth.2001.1262

Lodeiro, A. R., González, P., Hernández, A., Balagué, L. J., and Favelukes, G. (2000). Comparison of drought tolerance in nitrogen-fixing and inorganic nitrogen-grown common beans. *Plant Sci.* 154, 31–41. doi: 10.1016/S0168-9452(99)00246-0

Losa, A., Vorster, J., Cominelli, E., Sparvoli, F., Paolo, D., Sala, T., et al. (2022). Drought and heat affect common bean minerals and human diet—What we know and where to go. *Food Energy Secur.* 11, e351. doi: 10.1002/fes3.351

Maathuis, F. J. M. (2014). Sodium in plants: perception, signalling, and regulation of sodium fluxes. *J. Exp. Bot.* 65, 849–858. doi: 10.1093/jxb/ert326

Martínez-Romero, E., Segovia, E., Mercante, F. M., Franco, A. A., Graham, P. H., and Pardo, M. A. (1991). *Rhizobium tropici*, a novel species nodulating *Phaseolus vulgaris* L. beans and Leucaena sp. trees. *Inter. J. Syst. Bacteriol.* 41, 417–426. doi: 10.1099/00207713-41-3-417

Masson-Boivin, C., and Sachs, J. L. (2018). Symbiotic nitrogen fixation by rhizobia-the roots of a success story. *Curr. Opin. Plant Biol.* 44, 7–15. doi: 10.1016/j.pbi.2017.12.001

Mizoi, J., Shinozaki, K., and Yamaguchi-Shinozaki, K. (2012). AP2/ERF family transcription factors in plant abiotic stress responses. *Biochim. Biophys. Acta (BBA) Gene Regul. Mech.* 1819, 86–96. doi: 10.1016/j.bbagrm.2011.08.004

Mnasri, B., Aouani, M. E., and Mhamdi, R. (2007). Nodulation and growth of common bean (*Phaseolus Vulgaris*) under water deficiency. *Soil Biol. Biochem.* 39, 1744–1750. doi: 10.1016/j.soilbio.2007.01.030

Mukeshimana, G., Butare, L., Cregan, P. B., Blair, M. W., and Kelly, J. D. (2014). Quantitative trait loci associated with drought tolerance in common bean. *Crop Sci.* 54, 923–938. doi: 10.2135/cropsci2013.06.0427

Naya, L., Ladrera, R., Ramos, J., González, E. M., Arrese-Igor, C., Minchin, F. R., et al. (2007). The response of carbon metabolism and antioxidant defenses of alfalfa nodules to drought stress and to the subsequent recovery of plants. *Plant Physiol.* 144, 1104–1114. doi: 10.1104/pp.107.099648

Niu, C.-F., Wei, W., Zhou, Q.-Y., Tian, A.-G., Hao, Y.-J., Zhang, W.-K., et al. (2012). Wheat WRKY genes TaWRKY2 and TaWRKY19 regulate abiotic stress tolerance in transgenic *Arabidopsis* plants. *Plant Cell Environ.* 35, 1156–1170. doi: 10.1111/j.1365-3040.2012.02480.x

Norris, O. D., and T'mannetje, L. (1964). The symbiotic specialization of African Trifolium spp. in relation to their taxonomy and their agronomic use. *East Afr. Agric. For. J.* 29, 214–235. doi: 10.1080/00128325.1964.11661928

O'Rourke, J. A., Bolon, Y. T., Bucciarelli, B., and Vance, C. P. (2014a). Legume genomics: understanding biology through DNA and RNA sequencing. *Ann. Bot.* 113, 1107–1120. doi: 10.1093/aob/mcu072

O'Rourke, J. A., Iniguez, L. P., Fu, F., Bucciarelli, B., Miller, S. S., Jackson, S. A., et al. (2014b). An RNA-Seq based gene expression atlas of the common bean. *BMC Genomics* 15, 866. doi: 10.1186/1471-2164-15-866

Oh, J. E., Kwon, Y., Kim, J. H., Noh, H., Hong, S. W., and Lee, H. (2011). A dual role for MYB60 in stomatal regulation and root growth of *Arabidopsis thaliana* under drought stress. *Plant Mol. Biol.* 77, 91–103. doi: 10.1007/s11103-011-9796-7

Padder, B. A., Kamfwa, K., Awale, H. E., and Kelly, J. D. (2016). Transcriptome profiling of the *Phaseolus vulgaris - Colletotrichum lindemuthianum* Pathosystem. *PloS One* 11, e0165823. doi: 10.1371/journal.pone.0165823

Pereira, W. J., Melo, A. T. O., Coelho, A. S. G., Rodrigues, F. A., Mamidi, S., Alencar, S. A., et al. (2020). Genome-wide analysis of the transcriptional response to drought stress in root and leaf of common bean. *Genet. Mol. Biol. Mar.* 16, e20180259. doi: 10.1590/1678-4685-GMB-2018-0259

Pfaffl, M. W., Horgan, G. W., and Dempfle, L. (2002). Relative Expression Software Tool (REST) for group-wise comparison and statistical analysis of relative expression results in Real-Time PCR. *Nucleic Acids Res.* 30, e36. doi: 10.1093/nar/30.9.e36

Pimentel, C., and Cruz Perez, A. J. L. (2000). Estabelecimento de parâmetros para avaliação de tolerância à seca, em genótipos de feijoeiro. *Pesquisa Agropecuária Bras.* 35, 31–39. doi: 10.1590/S0100-204X2000000100005

Polania, J., Poschenrieder, C., Rao, I., and Beebe, S. (2016). Estimation of phenotypic variability in symbiotic nitrogen fixation ability of common bean under drought stress using ^{15}N natural abundance in grain. *Europ. J. Agron.* 79, 66–73. doi: 10.1016/j.eja.2016.05.014

Porcel, R., Barea, J. M., and Ruiz-Lozano, J. M. (2003). Antioxidant activities in mycorrhizal soybean plants under drought stress and their possible relationship to the process of nodule senescence. *New Phytol.* 157, 135–143. doi: 10.1046/j.1469-8137.2003.00658.x

Puppo, A., Groten, K., Bastian, F., Carzaniga, R., Soussi, M., Lucas, M. M., et al. (2005). Legume nodule senescence: roles for redox and hormone signalling in the orchestration of the natural aging process. *New Phytol.* 165, 683–701. doi: 10.1111/j.1469-8137.2004.01285.x

Ragueh, F., Lescure, N., Roby, D., and Marco, Y. (1989). Gene Expression in *Nicotiana tabacum* in response to compatible and incompatible isolates of *Pseudomonas solanacearum*. *Physiol. Mol. Plant Pathol.* 35, 23–33. doi: 10.1016/0885-5765(89)90004-0

Ramos, M. L. G., Parsons, R., Spront, J. I., and James., E. K. (2003). Effect of water stress on nitrogen fixation and nodule structure of common bean. *Pesquisa Agropecuária Bras.* 38 (3), 339–347. doi: 10.1590/S0100-204X2003000300002

Recchia, G. H., Konzen, E. R., Cassieri, F., Caldas, D. G. G., and Tsai, S. M. (2018). Arbuscular mycorrhizal symbiosis leads to differential regulation of drought-responsive genes in tissue-specific root cells of common bean. *Front. Microbiol.* 9. doi: 10.3389/fmicb.2018.01339

Ribeiro, T., Da Silva, D. A., Esteves, J. A. D. F., Azevedo, C. V. G., Gonçalves, J. G. R., Carbonell, S. A. M., et al. (2019). Evaluation of common bean genotypes for drought tolerance. *Bragantia* 78, 1–11. doi: 10.1590/1678-4499.2018002

Robinson, M. D., McCarthy, D. J., and Smyth, G. K. (2010). edgeR: a Bioconductor package for differential expression analysis of digital gene expression data. *Bioinformatics* 26, 139–140. doi: 10.1093/bioinformatics/btp616

Sańko-Sawczenko, I., Łotocka, B., Mielecki, J., Rekosz-Burlaga, H., and Czarnocka, W. (2019). Transcriptomic changes in *Medicago truncatula* and *Lotus japonicus* root nodules during drought stress. *Int. J. Mol. Sci.* 20, 1204. doi: 10.3390/ijms20051204

Santos, T. B., de Lima, R. B., Nagashima, G. T., Petkowicz, C. L., Carpentieri-Pípolo, V., Pereira, L. F., et al. (2015). Galactinol synthase transcriptional profile in two genotypes of *Coffea canephora* with contrasting tolerance to drought. *Genet. Mol. Biol.* 38, 182–190. doi: 10.1590/S1415-475738220140171

Schmutz, J., McClean, P. E., Mamidi, S., Wu, G. A., Cannon, S. B., Grimwood, J., et al. (2014). A reference genome for common bean and genome-wide analysis of dual domestications. *Nat. Genet.* 46, 707–713. doi: 10.1038/ng.3008

Seo, P. J., Lee, S. B., Suh, M. C., Park, M.-J., Go, Y. S., and Park, C.-M. (2011). The MYB96 transcription factor regulates cuticular wax biosynthesis under drought conditions in *Arabidopsis*. *Plant Cell* 23, 1138–1152. doi: 10.1105/tpc.111.083485

Seo, P. J., Xiang, F., Qiao, M., Park, J.-Y., Lee, Y. N., Kim, S.-G., et al. (2009). The MYB96 transcription factor mediates abscisic acid signaling during drought stress response in *Arabidopsis*. *Plant Physiol.* 151, 275–289. doi: 10.1104/pp.109.144220

Serraj, R., and Sinclair, T. R. (1996). Processes contributing to N_2-fixation intensitivity to drought in the soybean cultivar jackson. *Crop Sci.* 36, 961–968. doi: 10.2135/cropsci1996.0011183X003600040024x

Severin, A. J., Woody, J. L., Bolon, Y.-T., Joseph, B., Diers, B. W., Farmer, A. D., et al. (2010). RNA-Seq atlas of *Glycine max*: a guide to the soybean transcriptome. *BMC Plant Biol.* 10, 160. doi: 10.1186/1471-2229-10-160

Shang, Y., Yan, L., Liu, Z.-Q., Cao, Z., Mei, C., Wu, Q.X.F.-Q., et al. (2010). The Mg-chelatase H subunit of *Arabidopsis antagonizes* a group of WRKY transcription repressors to relieve ABA-responsive genes of inhibition. *Plant Cell* 22, 1909–1935. doi: 10.1105/tpc.110.073874

Simoes-Araujo, J. L., Alves-Ferreira, M., Rumjanek, N. G., and Margis-Pinheiro, M. (2008). VuNIP1 (NOD26-Like) and VuHSP17.7 gene expression are regulated in response to heat stress in cowpea nodule. *Environ. Exp. Bot.* 63, 256–265. doi: 10.1016/j.envexpbot.2007.10.027

Simões-Araújo, J. L., Rumjanek, N. G., and Margis-Pinheiro, M. (2003). Small heat shock proteins genes are differentially expressed in distinct varieties of common bean. *Braz. J. Plant Physiol.* 15, 33–41. doi: 10.1590/S1677-04202003000100005

Sponchiado, B. N., White, J. W., Castillo, J. A., and Jones, P. G. (1989). Root growth of four common bean cultivars in relation to drought tolerance in environments with contrasting soil types. *Exp. Agric.* 25, 249. doi: 10.1017/S0014479700016756

Sreedasyam, A., Plott, C., Hossain, M., Lovell, J. T., Grimwood, J., Jenkins, J. W., et al. (2023). JGI Plant Gene Atlas: an updateable transcriptome resource to improve functional gene descriptions across the plant kingdom. *Nucleic Acids Res.* 51, 8383–8401. doi: 10.1093/nar/gkad616

Subramani, M., Urrea, C. A., Habib, R., Bhide, K., Thimmapuram, J., and Kalavacharla, V. (2023). Comparative transcriptome analysis of tolerant and sensitive genotypes of common bean (*Phaseolus vulgaris* L.) in response to terminal drought stress. *Plants (Basel)* 3, 210. doi: 10.3390/plants12010210

Summerfield, R. J., Pate, J. S., Roberts, E. H., and Wien, H. C. (1985). ""The physiology of cowpeas"," in *Cowpea Research, Production and Utilization*. Eds. S. R. Singh and K. O. Rachie (New York: John Wiley), 66–101.

Tajini, F., Trabelsi, M., and Drevon, J. J. (2012). Comparison between the reference *Rhizobium tropici* CIAT899 and the native *Rhizobium etli* 12a3 for some nitrogen fixation parameters in common bean (*Phaseolus vulgaris* L.) under water stress. *Afr. J. Microbiol. Res.* 6, 4058–4067. doi: 10.5897/AJMR12.566

Thimm, O., Bläsing, O., Gibon, Y., Nagel, A., Meyer, S., Krüger, P., et al. (2004). Mapman: a user-driven tool to display genomics data sets onto diagrams of metabolic pathways and other biological processes. *Plant J.* 37, 914–939. doi: 10.1111/j.1365-313X.2004.02016.x

Tian, T., Liu., Y., Yan, H., You, Q., Yi, X., Du, Z., et al. (2017). agriGO v2.0: a GO analysis toolkit for the agricultural community 2007 update. *Nucleic Acids Res.* 3, W122–W129. doi: 10.1093/nar/gkx382

Todaka, D., Shinozaki, K., and Yamaguchi-Shinozaki., K. (2015). Recent advances in the dissection of drought-stress regulatory networks and strategies for development of drought-tolerant transgenic rice plants. *Front. Plant Sci.* 6. doi: 10.3389/fpls.2015.00084

Trapnell, C., Roberts, A., Goff, L., Pertea, G., Kim, D., Kelley, D. R., et al. (2012). Differential gene and transcript expression analysis of RNA-seq experiments with TopHat and Cufflinks. *Nat. Protoc.* 7, 562–578. doi: 10.1038/nprot.2012.016

Untergasser, A., Nijveen, H., Rao, X., Bisseling, T., Geurts, R., and Leunissen, J. A. M. (2007). Primer3Plus, an enhanced web interface to Primer3. *Nucleic Acids Res.* 35, W71–W74. doi: 10.1093/nar/gkm306

Vance, C. P., Heichel, G. H., Barnes, D. K., Bryan, J. W., and Johnson, L. E. (1979). Nitrogen fixation, nodule development, and vegetative regrowth of alfalfa (*Medicago sativa* L.) following harvest. *Plant Physiol.* 64, 1–8. doi: 10.1104/pp.64.1.1

Vandesompele, J., De Preter, K., Pattyn, F., Poppe, B., Roy, N. V., De Paepe, A., et al. (2002). Accurate normalization of real-time quantitative RT-PCR data by geometric averaging of multiple internal control genes. *Genome Biol.* 3, research0034.1. doi: 10.1186/gb-2002-3-7-research0034

Vargas, L., Brígida, A. B. S., Mota Filho, J. P., de Carvalho, T. G., Rojas, C., Vaneechoutte, D., et al. (2014). Drought tolerance conferred to sugarcane by association with *Gluconacetobacter dazotrophicus*: a transcriptomic view of hormone pathways. *PloS One* 9, e114744. doi: 10.1371/journal.pone.0114744

Wang, W., Vinocur, B., Shoseyov, O., and Altman, A. (2004). Role of plant heat-shock proteins and molecular chaperones in the abiotic stress response. *Trends Plant Sci.* 9, 244–252. doi: 10.1016/j.tplants.2004.03.006

Wei, W., Zhang, Y., Han, L., Guan, Z., and Chai., T. (2008). A Novel WRKY transcriptional factor from *Thlaspi caerulescens* negatively regulates the osmotic stress tolerance of transgenic tobacco. *Plant Cell Rep.* 27, 795–803. doi: 10.1007/s00299-007-0499-0

Wu, J., Wang, L., Li, L., and Wang, S. (2014). *De novo* assembly of the common bean transcriptome using short reads for the discovery of drought-responsive genes. *PloS One* 9, e109262. doi: 10.1371/journal.pone.0109262

Wu, J., Wang, L., and Wang, S. (2017). MicroRNAs associated with drought response in the pulse crop common bean (*Phaseolus vulgaris* L.). *Gene* 628, 78–86. doi: 10.1016/j.gene.2017.07.038

Yoseph, T., and Shanko, S. (2017). Growth, symbiotic and yield response of N-fertilized and Rhizobium inoculated common bean (*Phaseolus vulgaris* L.). *Afr. J. Plant Sci.* 11, 197–202. doi: 10.5897/AJPS2017.1528

Zhao, S., and Fernald, R. D. (2005). Comprehensive algorithm for quantitative real-time polymerase chain reaction. *J. Comput. Biol.* 12, 1047–1064. doi: 10.1089/cmb.2005.12.1047

Zheng, S., Zhou, D., Liu, T., Wang, T., Zhai, X., Xing, G., et al. (2023). Comparative transcriptome analysis of two varieties of common bean (*Phaseolus vulgaris* L.) to identify candidate drought resistance genes. *Biotechnol. Biotechnol. Equip.* 37, 1. doi: 10.1080/13102818.2023.2238847

frontiers | Frontiers in Plant Science

TYPE Original Research
PUBLISHED 02 February 2024
DOI 10.3389/fpls.2024.1302705

OPEN ACCESS

EDITED BY
Marcia Soares Vidal,
Brazilian Agricultural Research Corporation (EMBRAPA), Brazil

REVIEWED BY
Raul Riesco Jarrin,
University of Salamanca, Spain
Shaikhul Islam,
Bangladesh Wheat and Maize Research Institute (BWMRI), Bangladesh
Chang Fu Tian,
China Agricultural University, China
Anindya Kundu,
National Institute of Agricultural Botany (NIAB), United Kingdom

*CORRESPONDENCE
Anna Maria Pirttilä
am.pirttila@oulu.fi

†PRESENT ADDRESS
Roosa Haajanen,
Blueprint Genetics,
A Quest Diagnostics Company, Espoo, Finland

RECEIVED 26 September 2023
ACCEPTED 15 January 2024
PUBLISHED 02 February 2024

CITATION
Baruah N, Haajanen R, Rahman MT, Pirttilä AM and Koskimäki JJ (2024) Biosynthesis of polyhydroxybutyrate by *Methylorubrum extorquens* DSM13060 is essential for intracellular colonization in plant endosymbiosis. *Front. Plant Sci.* 15:1302705. doi: 10.3389/fpls.2024.1302705

Biosynthesis of polyhydroxybutyrate by *Methylorubrum extorquens* DSM13060 is essential for intracellular colonization in plant endosymbiosis

Namrata Baruah[1], Roosa Haajanen[1†], Mohammad Tanvir Rahman[2], Anna Maria Pirttilä[1*] and Janne J. Koskimäki[1]

[1]Ecology and Genetics Research Unit, University of Oulu, Oulu, Finland, [2]Disease Networks, Faculty of Biochemistry and Molecular Medicine, University of Oulu, Oulu, Finland

Methylorubrum extorquens DSM13060 is an endosymbiont that lives in the cells of shoot tip meristems. The bacterium is methylotrophic and consumes plant-derived methanol for the production of polyhydroxybutyrate (PHB). The PHB provides protection against oxidative stress for both host and endosymbiont cells through its fragments, methyl-esterified 3-hydroxybutyrate (ME-3HB) oligomers. We evaluated the role of the genes involved in the production of ME-3HB oligomers in the host colonization by the endosymbiont *M. extorquens* DSM13060 through targeted genetic mutations. The strains with deletions in PHB synthase (*phaC*), PHB depolymerase (*phaZ1*), and a transcription factor (*phaR*) showed altered PHB granule characteristics, as *ΔphaC* had a significantly low number of granules, *ΔphaR* had a significantly increased number of granules, and *ΔphaZ1* had significantly large PHB granules in the bacterial cells. When the deletion strains were exposed to oxidative stress, the *ΔphaC* strain was sensitive to 10 mM HO· and 20 mM H_2O_2. The colonization of the host, Scots pine (*Pinus sylvestris* L.), by the deletion strains varied greatly. The deletion strain *ΔphaR* colonized the host mainly intercellularly, whereas the *ΔphaZ1* strain was a slightly poorer colonizer than the control. The deletion strain *ΔphaC* lacked the colonization potential, living mainly on the surfaces of the epidermis of pine roots and shoots in contrast to the control, which intracellularly colonized all pine tissues within the study period. In earlier studies, deletions within the PHB metabolic pathway have had a minor effect on plant colonization by rhizobia. We have previously shown the association between ME-3HB oligomers, produced by PhaC and PhaZ1, and the ability to alleviate host-generated oxidative stress during plant infection by the endosymbiont *M. extorquens* DSM13060. Our current results show that the

10.3389/fpls.2024.1302705

low capacity for PHB synthesis leads to poor tolerance of oxidative stress and loss of colonization potential by the endosymbiont. Altogether, our findings demonstrate that the metabolism of PHB in *M. extorquens* DSM13060 is an important trait in the non-rhizobial endosymbiosis.

KEYWORDS

endophytes, endosymbiosis, intracellular, plant-microbe interaction, mutualism, oxidative stress, infection, colonization

Introduction

Plants carry communities of microbes inside all of their tissues, endophytes, which often have various positive effects on their hosts. Most endophytes, bacteria and fungi, promote plant growth and protect the host against pathogens and abiotic stress. The endophytes typically enter the plant from the rhizosphere from the points of lateral root emergence, cracks or wounds, or through stomata in stem and leaf surfaces (Hardoim et al., 2015). The majority of endophytes colonize in the intercellular spaces of roots (James et al., 1994; Ryan et al., 2008; Izumi, 2011; Hardoim et al., 2015), and a small group of endophytes can breach through the endodermis to the vascular tissues, from where they enter the shoots in the xylem transpiration flow (Compant et al., 2005). The endophytic bacteria are rarely observed inside cells, and when present, they usually colonize dead plant cells, or alternatively, the intracellular infection induces plant cell death (James and Olivares, 1998; White et al., 2014).

We have earlier identified an endophyte that intracellularly colonizes meristematic tissues of Scots pine trees (*Pinus sylvestris* L.) (Pirttilä et al., 2000; Koskimäki et al., 2015; Koskimäki et al., 2016). A specific feature of the facultative endosymbiont, *Methylorubrum extorquens* DSM13060, is the accumulation of bacterial cells near the plant nuclei (Koskimäki et al., 2015). *M. extorquens* DSM13060 significantly improves the growth and affects the stress tolerance of the host (Pohjanen et al., 2014; Koskimäki et al., 2022). The endosymbiont produces compounds that alleviate oxidative stress in both plant and bacterial cells, methyl-esterified 3-hydroxybutyrate oligomers (ME-3HB). These compounds are the break-down products of polyhydroxybutyrate (PHB), which the endosymbiont synthesizes from methanol produced by the plant (Koskimäki et al., 2016; Müller-Santos et al., 2021).

Besides the crucial role in global CO_2 fixation, plants participate in the carbon budget by emissions of methanol. The methanol is produced in plant tissue from pectin by the methyl esterase enzyme, and nonenzymatically, from the methoxyl groups of pectin and lignin. Plants lack mechanisms for detoxifying methanol, which is mainly emitted through stomata (Nemecek-Marshall et al., 1995). Methylotrophs, such as *M. extorquens* DSM13060, living inside and on the plant tissues, consume the plant-produced methanol and transform it to non-toxic forms, such as PHB (Fall, 1996; Sy et al., 2005; Knief et al., 2008; Hardoim et al., 2015).

The ME-3HB oligomers produced by the endosymbiont *M. extorquens* DSM13060 from plant-derived methanol have potent antioxidative activity against hydroxyl radicals. They are the result of the action by the PhaZ1 depolymerase, which degrades PHB, as well as the PHB synthase PhaC, which synthesizes PHB (Koskimäki et al., 2016). The degradation and biosynthesis of PHB is coordinated by the transcription factor, PhaR, which is a master regulator of PHB metabolism (Nishihata et al., 2018). The oxidative burst induced in the plant tissues during microbial infection creates hydroxyl radicals (Mucha et al., 2012; Koskimäki et al., 2016). When pine seedlings are infected by *M. extorquens* DSM13060, the hydroxyl radicals accumulate at the infection site, and activation of the genes *phaC* and *phaZ1* along with degradation of PHB granules take place to suppress the oxidative stress by the ME-3HB oligomers (Koskimäki et al., 2016).

As *M. extorquens* DSM13060 is an endosymbiont that penetrates the host cells, and the ME-3HB oligomers have an antioxidative role in the infection of plant tissues (Koskimäki et al., 2016), we hypothesized that the capacity for PHB synthesis and degradation is crucial for colonization of the plant host. Therefore, we examined the importance of the enzymes involved in PHB metabolism in *M. extorquens* DSM13060 for plant colonization through targeted single gene mutations.

Materials and methods

Bacterial strains and cultivation

Methylorubrum extorquens DSM13060 [Genbank: AGJK00000000] was originally discovered from bud tissues of mature Scots pine in Oulu, Finland (65°0′ N; 25°30′ E) (Pirttilä et al., 2000; Koskimäki et al., 2015). The derivate fluorescent *M. extorquens* 13061 (Pohjanen et al., 2014) with two successive chromosomal GFP coding genes under constitutive promoter was used as the parent strain for generation of gene in-frame deletion mutants (Xi et al., 1999). Strains

Abbreviations: CLSM, confocal laser scanning microscopy; ddPCR, droplet digital PCR; dpi, days-post-inoculation; hpi, hours-post-induction of stress; ME-3HB, methyl-esterified hydroxybutyrate; MeOH, methanol; PHB, polyhydroxybutyrate; TEM, transmission electron microscopy; w, weight, v, volume.

10.3389/fpls.2024.1302705

and plasmids used are described in Table 1. For isolation of genomic DNA, mutant construction, and inoculum preparation, *M. extorquens* 13061 and constructed mutants were grown by shaking at 28°C in ammonium mineral salts (AMS) medium (ATCC medium 784) supplemented with 1% (v/v) methanol (MeOH), 1% (w/v) sodium succinate, and appropriate antibiotics when required (Kanamycin 50 µg/ml). The AMS medium contained 0.66 g/l $(NH_4)_2SO_4$, 1.0 g/l $MgSO_4$-$7H_2O$, and 0.015 g/l $CaCl_2$-$2H_2O$. In addition, after sterilization, 1.0 ml/l of AMS trace elements solution, 1 ml/l of stock A, and 20 ml/l of 1.0 M phosphate buffer were added. The AMS stock A contained 5.0 g/l Fe-NaEDTA and 2.0 g $NaMoO_4$*$2H_2O$. The AMS trace elements solution contained 0.5 g/l $FeSO_4$*$7H_2O$, 0.4 g/l $ZnSO_4$*$7H_2O$, 0.02 g/l $MnSO_4$*H_2O, 0.015 g/l H_3BO_3, 0.01 g/l $NiCl_2$*$6H_2O$, 0.25 g/l EDTA, 0.05 g/l $CoCl_2$*$6H_2O$, and 0.005 g/l of $CuCl_2$*$2H_2O$. The 1 M phosphate buffer consisted of 113.0 g/l K_2HPO_4 and 47.0 g/l KH_2PO_4.

Escherichia coli strains DH5α and SM10*λpir*, used for the mutant construction, were grown in Luria-Bertani (LB) medium (1% tryptone, 0.5% yeast-extract, 1% NaCl) at 37°C, supplemented either with 100 µg/ml ampicillin or with 10 µg/ml tetracycline.

TABLE 1 The strains and vectors used for the study.

Strains or plasmids	Description	Reference or source
Escherichia coli		
DH5α	*endA1 gyrSA96 hrdR17 (rK-mK-) supE44 recA1*; general host strain used for the transformation and propagation of plasmids	(Boyer and Roulland-dussoix, 1969)
SM10 λ pir	Donor strain (mobilizing strain) carrying the transfer genes of the broad host range IncP type plasmid RP4 integrated into its chromosome. Useful for mobilizing mobRP4 plasmids, Km^r	BCCM ref. LMBP 3889
HB101-pRK2013	*E. coli* HB101 carrying a self-transmissible plasmid pRK2013 containing the broad host-range transfer system of RK2, Km^r	(Figurski and Helinski, 1979)
Methylorubrum extorquens		
DSM13060	Wild type; a plant growth-promoting conifer endophyte	(Pirttilä et al., 2000)
13061	DSM13060 containing mTn5*gusA-pgfp21*-Km^r cassette (pFAJ1820)	(Pohjanen et al., 2014)
Plasmids		
pJET 1.2	Cloning vector for amplified PCR products; Ap^r	Thermo Fisher Scientific
pT18mobsacB	Broad host-range cloning vector maintained in Gram-negative bacteria offering sucrose counter-selection allelic exchange, Tc^r	(Wei et al., 2013)
pCM433	Broad host-range cloning vector maintained in Gram-negative bacteria offering bacteria allelic exchange, Chl^r and Ap^r	(Marx, 2008)

Seed sterilization, plant growth conditions, and bacterial inoculation

Seeds of Scots pine were prepared by heat treatment for 72 h at 55°C in the dark, followed by incubation in sterile water overnight at room temperature and surface sterilization with 3% calcium hypochlorite (w/v) for 20 min. Once the seeds were surface sterilized, they were rinsed three times with sterile water and grown on moist sterile vermiculite in glass jars. Germination took place after 7-10 days at 24± 3°C at 16/8 h photoperiod. For the inoculation, the bacteria were grown in AMS supplemented with 1% MeOH, and 1% sodium succinate, for 3-4 days. The bacterial cultures were diluted with sterile water to the density of 2.5×10^8 CFU/ml, and 100 µl of the inoculum was pipetted onto each germinated pine seedling.

Isolation of genomic DNA

Bacterial cells were cultured and grown to the late logarithmic phase (optical density at 600 nm (OD_{600}) 0.8 – 1.0) and harvested by centrifugation at 6000×g for 5 minutes at 4° C. The bacterial pellet was ground in liquid nitrogen with mortar and pestle, and the genomic DNA was isolated using DNeasy Plant Mini kit according to the manufacturer's instructions (Qiagen). The quality and concentration of DNA were analyzed by NanoDrop ND-1000 spectrophotometer (NanoDrop Technologies) and Qubit 2.0 fluorometer with dsDNA HS assay kit (Invitrogen).

Construction of the *ΔphaR*, *ΔphaC*, and *ΔphaZ1* deletion strains

The genomic data were retrieved from the JGI genome portal (https://img.jgi.doe.gov/) and used to design primers specific for the genes *phaR*, *phaC*, and *phaZ1* (IMG gene accessions 2507326187, 2507325801, 2507328730 respectively; and primer sequences are listed in Table 2). *M. extorquens* 13061 was used for generation of targeted deletion mutants *ΔphaR*, *ΔphaC*, and *ΔphaZ1* according to the method described earlier (Schäfer et al., 1994). Briefly, 0.5 kb regions upstream (AB) and downstream (CD) of the target genes were amplified using primers with restriction sites at overlap sequences specified in Table 2. Upstream and downstream regions were joined (AB+CD) by overlap extension PCR (OE-PCR) using Phusion High-Fidelity DNA polymerase (Thermo Scientific). The amplified constructs were verified on agarose gel, purified, and cloned into the pJET 1.2 vector (CloneJET PCR Cloning Kit, Thermo Scientific). The plasmids were then electroporated (Gene Pulser Electroporation system, BioRad) into *E. coli* DH5α. Transformants were selected on LB agar plates supplemented with ampicillin (100 µg/ml) and incubated overnight at 37°C. The colonies were screened by colony PCR (DreamTaq polymerase, Thermo Scientific) specific for the deletion (Tables 2, 3), and the constructs were confirmed by Sanger sequencing (Eurofins Genomics).

TABLE 2 The primers designed for constructing the mutants.

Deleted gene	Sequence	Primer name, Restriction site
phaR	TATTGAATTCTGCCAGCGATGTGAAGAAC	phaR-F, *EcoRI*
phaR	AATAAAGCTTAAGATCACCTCGTCCACGTC	phaR-R, *HindIII*
phaC	TATTACGCGTTTGGACTCGTTGCGGTTG	phaC-F, *MluI*
phaC	TATTGAGCTCACCCAGCAGGTAGGGAATG	phaC-R, *SacI*
phaZ1	TATTACGCGTTCGACGGGGAAGAACCAG	phaZ1-F, *MluI*
phaZ1	TATTGAGCTCAATCGCGGCCACTTCTTC	phaZ1-R, *SacI*

Restriction sites are underlined and sequences for overlap extension are italicized.

The plasmid DNA was isolated using GeneJet plasmid miniprep kit (Thermo Scientific). The deletion constructs were restricted from the pJET 1.2 plasmids and cloned into the suicide vector, either pT18mobsacB (*ΔphaR*), or pCM433 (*ΔphaC*, *ΔphaZ1*). Transformation of the suicide vector(s) was carried out in *E. coli* SM10*λpir* by electroporation. The transformants were grown on LB agar containing either tetracyclin (10 µg/ml) or ampicillin (100 µg/ml) in the presence of 2% X-gal and IPTG (in the case of pT18mobsacB). The positive colonies were selected by blue-white screening and confirmed by colony-PCR (sequences listed in Table 3).

Transposon mutagenesis and mutant screening

Conjugations of the deletion constructs *ΔphaR* and *ΔphaC* (pT18mobsacB) in *E. coli* SM10*λpir* were performed by triparental mating using the *E. coli* HB101::pRK2013 as a helper strain, and *M. extorquens* 13061 as a recipient, as described before (Heinze et al., 2018). For the *ΔphaZ1* construct in pCM433 plasmid, the conjugation was performed by biparental mating without the helper strain, as previously described (Choi et al., 2006; Marx, 2008). The individual cultures were grown until the OD_{600} of 0.8–1.0 was reached. The donor, recipient, and helper strains were mixed by resuspending after centrifugation at 3000×g, 4°C for 5 min. The mixed pellet was suspended in 1 ml of AMS supplemented with 1% MeOH, and 200 µl of the cell suspension was transferred on 0.22 µm filter discs and incubated on AMS agar supplemented with 1% MeOH for 48-72 hours at 28°C for conjugation. Dilutions were made thereafter by suspending the filters in liquid AMS plates supplemented with 1% MeOH, 1% sodium succinate, tetracycline (30 µg/ml) and rifampicin (50 µg/ml) for 48 hours at 28°C. Counter selections were made using 10% sucrose for lacZ selection. Correct transformants were identified by colony-PCR (Table 3).

TABLE 3 The primers specific for the vectors used.

Plasmid	Sequences	Primer name
pJET1.2	CGACTCACTATAGGGAGAGCGGC	pJET1.2-F
pJET1.2	AAGAACATCGATTTTCCATGGCAG	pJET1.2-R
pT18mobsacB	TGTAAAACGACGGCCAGT	pT18mobsacB-F
pT18mobsacB	AACAGCTATGACATGA	pT18mobsacB-R
pCM433	TGTAAAACGACGGCCAGT	M13 (-21) F
pCM433	CAGGAAACAGCTATGAC	M13 R

Bacterial growth curves

The *M. extorquens* 13061 and the deletion mutants *ΔphaR*, *ΔphaC*, and *ΔphaZ1* were grown in 30 ml of AMS liquid medium supplemented with 1% MeOH and 1% sodium succinate for 48-72 hours with shaking at 28°C until the cultures reached OD_{600} of 0.8-1.0. Precultures of each strain were adjusted to equal cell densities (10^8 CFU/ml), and the OD_{600} was measured after 12 h, 24 h, 48 h, 72 h, and 96 h. The total number of viable cells were determined as colony-forming-units (CFU/ml) by plating dilution series on AMS with 1% MeOH and 1% sodium succinate and counting the colonies after 72 h. A minimum of two biological replicates with three technical repeats were measured for each time point.

In vitro stress assays

In the heat shock stress assays, bacterial strains were grown in AMS supplemented with 1% MeOH, and 1% sodium succinate, reaching the logarithmic phase at 28°C for 2-3 days. The cultures were then transferred to an incubator for heat shock at 55°C for up to 60 mins under shaking at 150 rpm. The sampling was done at 0, 30, and 60 min, where 100 µl of the culture was harvested and serially diluted by 10-fold to count the CFU/ml. For the UV irradiation assay, the strains were transferred to UV radiation at 4.8 joules/m^2 under a wavelength of 254 nm for 45 s. At 0 s (before UV irradiation) and at 45 s, 100 µl of the samples were harvested and plated on AMS with 1% MeOH, and 1% sodium succinate in 10-fold dilutions for the CFU counting. The hydroxyl radical-induced stress assays were performed for the deletion and control strains as described before (Koskimäki et al., 2016). Hydroxyl radicals (HO·) were generated by Fenton reaction using H_2O_2 and ferric iron (Fe^{3+}) in a modified M9 minimal salts medium. The concentration of H_2O_2 was adjusted to 10 mM, 15 mM, and 20 mM, which was supplemented with and without $FeCl_3$ at 0.26 mM, 0.39 mM, and 0.52 mM, respectively, to produce a stable flux of hydroxyl radicals (Moore et al., 2006). The assay was performed in 24-well culture plates in three

biological replicates. The bacteria were cultured up to the late exponential phase and their final cell density was adjusted to OD_{600} of 0.8-1.0 equal to 10^8 CFU/ml in each sample. The assay reactions were adjusted to a total volume of 2 ml and incubated at 28°C with orbital shaking at 150 rpm for 1 and 3 h. Five 10-fold serial dilutions (from 10^{-1} to 10^{-5} cells) were made per treatment, and 4-µl samples of each strain were pipetted on AMS with 1% MeOH, and 1% sodium succinate agar plates at every sampling interval. Up to five separate treatments were pipetted per Petri plate, including control without stress, control with H_2O_2 stress, with or without $FeCl_3$, and the deletion strains with H_2O_2 stress, with, or without $FeCl_3$. The culture plates were digitally imaged and analyzed after 24 and 48 h. All treatments were pipetted in triplicates and the experiment was repeated twice.

Droplet digital PCR (ddPCR)

Samples from HO· growth stress on *M. extorquens* 13061 and the deletion strain *ΔphaZ1* were taken at 0 h, 1 h, and 3 h post-induction of stress (hpi). Cells in each sample were harvested by centrifugation at 5,000×g for 5 min at 4°C, treated with 10 volumes (v/v) of RNA shield stabilizing solution (Zymo Research), and incubated at 4°C overnight. RNA was extracted by *Quick*-RNA miniprep kit (Zymo Research), and the genomic DNA was removed with DNase I (Thermo Fisher Scientific). The quantity and quality of the total RNA was analyzed by NanoDrop ND-1000 spectrophotometer (Thermo Fisher Scientific) and agarose gel electrophoresis.

Complementary DNA (cDNA) was synthesized from 1 µg of total RNA with random hexamer primers using SuperScript III First-Strand Synthesis System (Thermo Fisher Scientific). The gene expression was analyzed with primers specific for *phaZ1* and *phaZ2*, designed by GenScript Real-time PCR primer designing software (Primer3, V2.0) (Table 4). The specificity of the primers was confirmed by melting curve analysis using the LightCycler 480 Real-Time PCR System (Roche Diagnostics), as previously (Koskimäki et al., 2016). Each 20-µl ddPCR reaction mixture consisted of 2×QX200 ddPCR EvaGreen supermix (Bio-Rad), 250 nM forward and reverse primers, and the cDNA sample (3 µl; 1:50 dilution). The reaction mixtures were loaded into a DG8 cartridge (Bio-Rad) with 70 µl of Droplet Generation Oil (Bio-Rad) to generate thousands of droplets using the QX200 Droplet Generator (Bio-Rad). Droplets of 40 µl from each well were transferred to a ddPCR 96-well PCR plate (Bio-Rad). PCR reactions were performed in a T100 Thermal Cycler (Bio-Rad) following the program: initial heating at 95°C for 5 min, 40 cycles of denaturation at 95°C for 30 s and annealing at 58°C for 1 min, followed by 4°C for 5 min, and final denaturation at 90°C for 5 min. The endpoint data collected using a Bio-Rad QX200 droplet reader was analyzed using the Bio-Rad QuantaSoft program. Fluorescence measurements were recorded in the appropriate channel in the reader. The reader counted the number of droplets containing the target sequence (positive) and droplets without the target (negative). Each positive droplet was assigned a value of one and negative droplets were assigned a value of zero. A Poisson correction was applied by the QuantaSoft program so that the mean number of target sequences per partition could be estimated. The results from samples with unusually low amplitude shifts (relative to other samples) were discarded and necessary repetitions were made. The experiment contained three biological replicates, and controls were analyzed with technical repeats.

TABLE 4 The primers used for the Droplet Digital PCR.

Gene	Sequence	Primer name
phaZ1	AGAGGGTGGTCTGGGAAC	ddPCR_PhaZ1-Fw
phaZ1	CGGTGATGAAGACCTGATGG	ddPCR_PhaZ1-Rv
phaZ2	ATCGAGACCTTCTACGACGA	ddPCR_phaZ2-Fw
phaZ2	CCTTCCACCGTCATCAGG	ddPCR_phaZ2-Rv

Transmission electron microscopy (TEM)

Bacterial strains were grown at 28°C for 4-5 days with shaking in M9 minimal salts medium (Obruca et al., 2010; Koskimäki et al., 2016) supplemented 0.5% sodium succinate and 1% MeOH until OD_{600} ≥1.0. The bacterial cultures were then centrifuged at 5000×g for 3 min and washed once with 1×PBS (pH 7.4). The pelleted cells were first fixed in 1% glutaraldehyde and 4% formaldehyde in 0.1M phosphate buffer, and then post-fixed with 1% osmium tetroxide in acetone and embedded in Epon LX112 (Ladd Research Industries Inc.). Thin sections were cut with an ultramicrotome (Leica UC6), stained with uranyl acetate and lead citrate, and examined with a Tecnai G2 Spirit 120 kV transmission electron microscope. Images were captured by a Quemesa CCD camera (Olympus Soft Imaging Solutions GMBH).

A total of five biological replicates of *ΔphaR, ΔphaC*, and *ΔphaZ1* and the control *M. extorquens* 13061 were analyzed for cell number, PHB granule distribution, and the granular area. The components were measured in the imaging and processing platform ImageJ (Lam et al., 2021). The number of cells per biological replicate and their PHB granule distribution was measured with the automatic cell counter plugin. The area of the PHB granules was measured with the manual exclusion of background coupled with appropriate settings of scale length and width to ensure an unbiased universal approach.

Confocal laser scanning microscopy (CLSM)

The seedlings were analyzed at 60 and 120 dpi (days-post-inoculation). A total of 10-12 seedlings/sampling interval/strain was analyzed. The experiment consisted of 3 biological replicates conducted over the period of a year. Roots and shoots were cut into 2-3 mm pieces and fixed in 4% paraformaldehyde (w/v), 0.1% glutaraldehyde (v/v), 20% glycerol (v/v), and 0.1 M sodium phosphate buffer (pH 7.4) at 4°C under vacuum. The root

samples were fixed for 4 h and the shoots were fixed for 8 h, followed by overnight incubation at 4°C. The fixed tissues were cut into 30-40 µm sections with a cryomicrotome (Reichert-Jung 2800 Frigocut with 2040 microtome) and mounted on microscopy slides with Vectashield antifade mounting medium with DAPI (Vector Laboratories). The pine tissue sections were studied with CLSM (LSM 5 Pascal; Carl Zeiss) using Plan-Neofluor 40×/1.3 and Plan-Apochromat 63×/1.4 oil objectives. The GFP fluorophore was excited at a wavelength of 488 nm by an argon ion laser, and emissions were detected using a 505-530 nm band-pass filter. The background autofluorescence of the plant tissues was detected using a 670 nm long-pass filter. The projections of the channels were analyzed and merged using the Zeiss LSM Image Browser (ver. 4.2.0.121) and Zeiss ZEN ver. 2.5 software (Blue edition; Carl Zeiss Microscopy GmbH). Representatives from 50-60 CLSM images were selected for each strain for the figure panels.

Light microscopy for hydroxyl radical detection

At 60 dpi, the roots of seedlings inoculated with water or *M. extorquens* DSM13060 were cut into segments of 3 mm and fixed with Metacarn (60% methanol (v/v), 30% chloroform (v/v), 10% glacial acetic acid (v/v)) for 15 h at +4°C. For detection of potential sites of hydroxyl radical production in the pine tissue, a double staining of the Fenton reagents, H_2O_2 and iron (Fe^{2+} or Fe^{3+}) was performed (Liu et al., 2007; Mucha et al., 2012). The root tissues were re-hydrated through an ethanol-water series, after which the samples were washed two times in sterile distilled water. Then, the root tissues were incubated in 7% (w/v) potassium ferrocyanide for 24 h for Fe^{3+} detection. Alternatively, for the detection of Fe^{2+}, the samples were treated with 7% (w/v) potassium ferricyanide in aqueous 3% (v/v) HCl for 48 h. For the detection of H_2O_2, the samples were incubated for 75 min in 1 mg/ml 3,3'-diaminobenzidine (pH 3.8). The root samples were then dissected to sections of 20-25 µm thickness using the cryomicrotome and mounted on microscopy slides. The samples were examined with a light microscope (LSM 5 Pascal) and Plan-Apochromat 63x/1.4 and Plan-Neofluor 40x/1.3 objectives.

Statistical analyses

The data from the analysis of the PHB granules was collected in Excel and statistically analyzed using the Student's *t*-tests at the significance level of $p<0.05$. The normal distribution of ddPCR data was determined using the Shapiro-Wilk's test for normality, and equality of variances was analyzed by the Levene's test. For data that was not normally distributed, the Kruskal-Wallis test was used. For all normally distributed datasets with equal variances, a one-way analysis of variance (ANOVA) was performed. For the datasets that showed statistical significance, Tukey's test was performed. The box plot for ddPCR data was constructed in RStudio, version 2022.07.2 using packages ggpubr and ggplot2.

Results

Characterization of the deletion strains *in vitro*

Cell and PHB granule morphology

Transmission Electron Microscopy (TEM) was performed to evaluate the characteristics of PHB granules in the deletion strains. The strains were grown in the presence of minimal requirements of nitrogen and high carbon content to facilitating maximal PHB granule growth, and they showed differences in their pigmentation and turbidity (Supplementary Figure 1). Whereas the control and *ΔphaR* grew normally with a pink coloration of the cells, *ΔphaC* showed an opaque color with clumps formed in the growth medium, and *ΔphaZ1* grew with a more intense pink shade and higher turbidity (Supplementary Figure 1).

The control *M. extorquens* 13061 showed normal PHB granule size and distribution, having approximately two granules in each rod-shaped cell, and an even distribution of granules to daughter cells (Figures 1A–C; 2A, B). The *ΔphaC* had an abnormal cell shape, being typically elongated (Figures 1D–F). The number of granules was significantly lower than in the control and most cells lacked granules (Figures 1E, F; 2A). The size of the granule, when present, was also significantly smaller than in the control (Figure 2B), and the granules were unevenly transferred to the daughter cells (Figure 1F). A dark-stained mediation element (Tian et al., 2005a; Tian et al., 2005b) resembling polyphosphate granules (Quelas et al., 2013) was present in the polar segment of the *ΔphaC* cells (Figure 1E). In *ΔphaR*, the cells had an irregular shape accompanied by a significantly increased number of granules (4-6 granules/cell) (Figures 1G–I; 2A, B). The volume of the granules was significantly smaller than in the control strain (Figure 2B), and the granules were unevenly distributed within the cytoplasm and to the daughter cells during cell division (Figure 1I). The cells of *ΔphaZ1* carried significantly larger granules compared to the control (Figures 1J–L; 2B). Typically, there were 2-3 granules per cell (Figures 1K; 2A).

Bacterial growth curves and stress tolerance

The stress tolerance of the deletion strains *ΔphaR*, *ΔphaC*, and *ΔphaZ1* was tested based on their growth curves in normal growth conditions and under elevated temperature and UV irradiation. In the normal growth conditions, the deletion strains followed a similar growth pattern as the control (Supplementary Figure 2A). When a heat shock was applied, no difference in growth between the control and the deletion strains was seen. However, after 60 min of the heat shock, *ΔphaR*, *ΔphaZ1*, and the control ceased their growth, whereas *ΔphaC* survived with a few colonies growing (Supplementary Figure 2B). When the UV stress was applied, the strains showed decreased growth 45 s after UV irradiation with no significant differences between strains (Supplementary Figure 2C). When the hypersensitivity of the deletion strains to oxidative stress was investigated, the growth of *ΔphaR* and *ΔphaZ1* was unaffected in the presence of H_2O_2 and HO·, similar to the control. However, *ΔphaC* showed sensitivity to H_2O_2 at 20 mM, and to HO· already at 10 mM concentration (Figure 3).

10.3389/fpls.2024.1302705

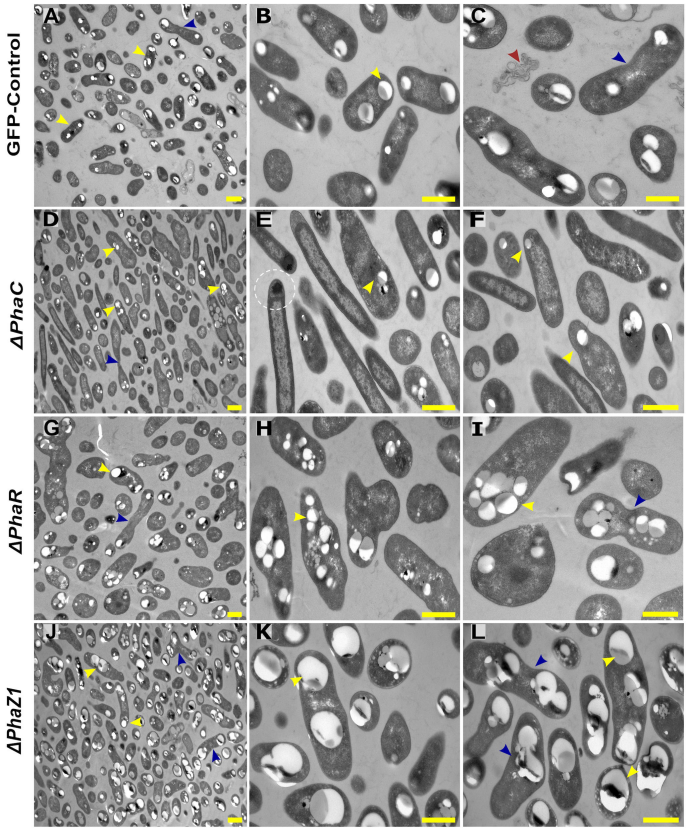

FIGURE 1
TEM images of PHB granules in the deletion mutant strains, *ΔphaC*, *ΔphaR*, *ΔphaZ1*, and control. **(A)** Cells of the control with a yellow arrowhead pointing the PHB granules, **(B, C)** 5× magnification of the control. The blue arrow shows a dividing cell, and the red arrow shows dead cellular accumulates. **(D)** *ΔphaC*, where the cells are irregularly shaped with a low number of small granules (yellow arrowhead) or the absence of granules. **(E, F)** A magnification showing mediation elements (circled), a single granule at the polar end of the cell (yellow arrowhead). **(G)** In *ΔphaR*, cells were irregular with numerous PHB granules per cell. **(H, I)** A magnification, where multiple granules are being distributed to the daughter cells (blue arrowhead). **(J)** *ΔphaZ1* cells had an increase in the volume of the granules. **(K, L)** A magnification showing enlarged masses of PHB granules (yellow arrowhead). The division of granules (blue arrowhead) was non-uniform. Scale bars, 1 µm.

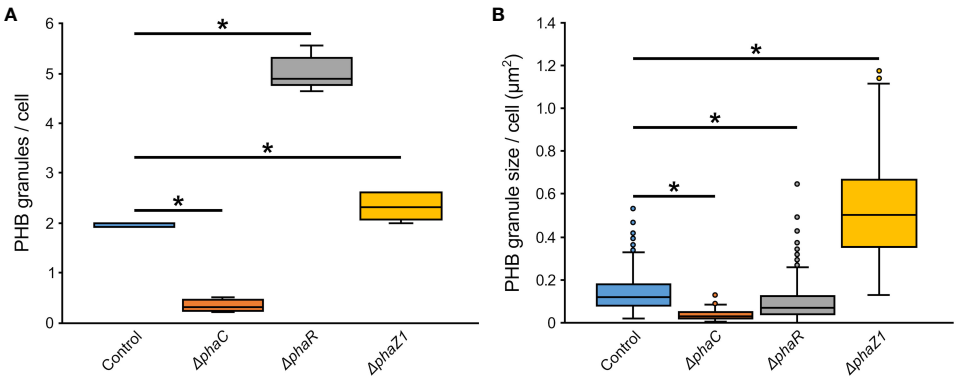

FIGURE 2
The number and size of PHB granules in *ΔphaR*, *ΔphaC*, and *ΔphaZ1* and control. **(A)** The number of PHB granules per cell of bacteria; **(B)** The size of PHB granules per cell in µm^2. The analysis was made with 5 biological replicates (TEM images), and the values were quantified from the TEM images using the program ImageJ. The minimum and maximum values are denoted by whiskers; and the median is denoted by the black line inside each box, respectively. *=p<0.05 (Student's *t*-test).

10.3389/fpls.2024.1302705

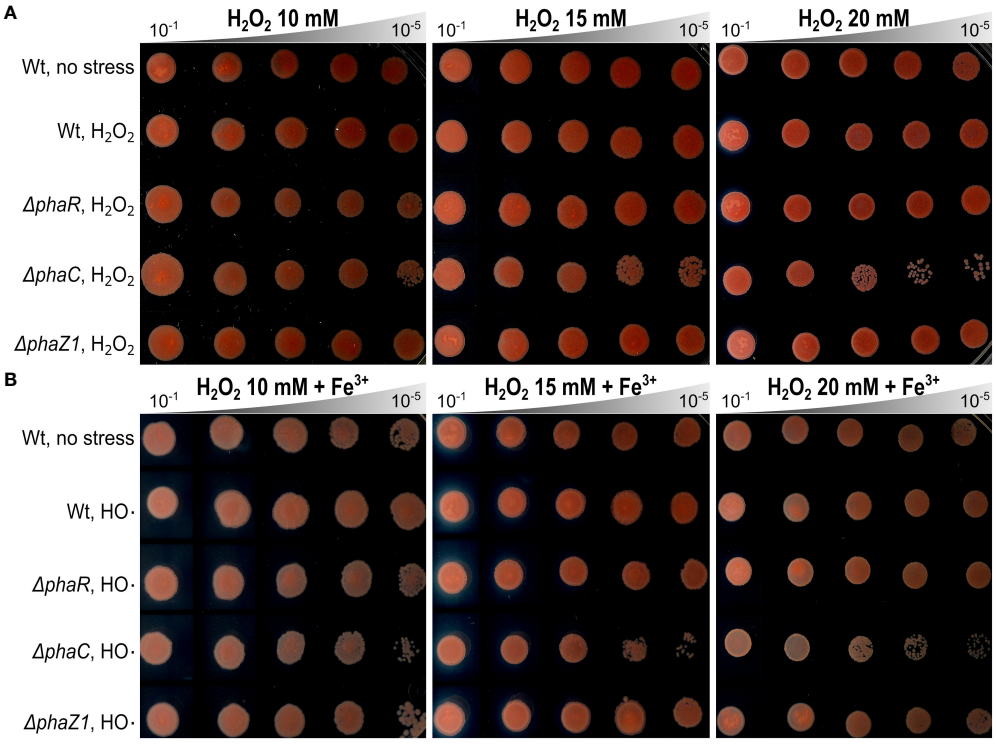

FIGURE 3
Oxidative stress assays. **(A)** Effect of hydrogen peroxide (H_2O_2) on the growth of *ΔphaR, ΔphaC, ΔphaZ1*, and the control 13061. **(B)** Effect of hydroxyl radicals (HO·), generated by Fenton reaction using H_2O_2 (as above) supplemented with $FeCl_3$ (Fe^{3+}). Data are representative of ten-fold serial dilutions of bacterial cells (10^{-1} to 10^{-5}, gray triangle) from three independent experiments. Separately scanned images were combined, and the contrast adjustment was applied equally across the images. Wt refers to *M. extorquens* 13061.

Effect of HO· stress on gene expression

To study whether another depolymerase gene of *M. extorquens* DSM13060, *phaZ2*, compensates for the loss of *phaZ1* in the deletion strain, the expression of *phaZ1* and *phaZ2* was studied by ddPCR in comparison to the control under HO· stress (15 mM H_2O_2, supplemented with 0.39 mM $FeCl_3$). The expression of *phaZ2* gene was slightly but not statistically significantly induced in the *ΔphaZ1* strain at one hour post-induction (hpi) of stress compared to the control (Figure 4). However, at 3 hpi, the gene *phaZ2* had a significantly higher expression in the control than in *ΔphaZ1* ($p<0.01$) (Figure 4). The *phaZ1* gene had a high expression in the control in the beginning of the experiment and under stress after 3 hours, but the differences were not statistically significant (Figure 4).

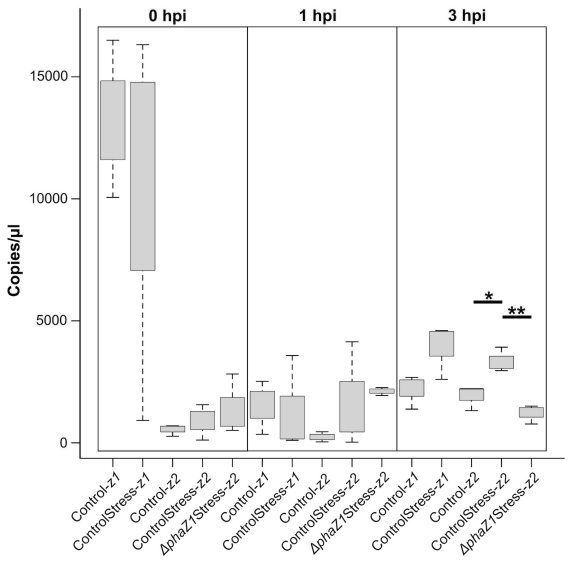

FIGURE 4
Gene expression of *phaZ1* and *phaZ2* under HO· stress in the control and *ΔphaZ1*. The average of three biological replicates at 0, 1 and 3 hpi, maximum and minimum values are denoted by whiskers and the median by the black line inside each box. The data was analyzed by one-way ANOVA and Tukey's test, *=p<0.05, **=p<0.01.

Colonization of plant tissue by the deletion strains

When confocal laser scanning microscopy (CLSM) was performed on the strains *ΔphaC*, *ΔphaR*, and *ΔphaZ1*, we observed differences in the infection, colonization, and the intracellular establishment in the plant tissues by the bacteria. The control *M. extorquens* 13061 abundantly colonized the epidermal layer, the cortex (Figure 5A), and in the parenchymal cells of vascular tissue (Figure 5B) of pine roots

10.3389/fpls.2024.1302705

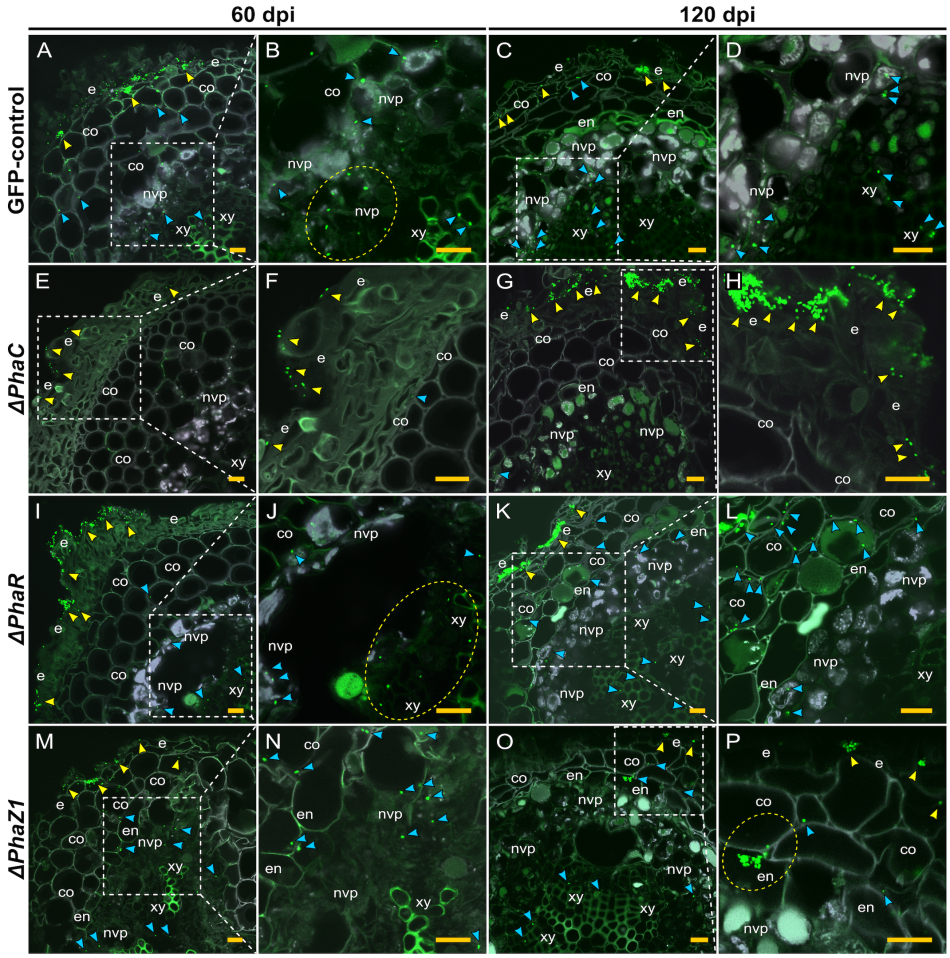

FIGURE 5
CLSM of pine roots colonized by the strains *ΔphaC*, *ΔphaR*, *ΔphaZ1*, and the control, *M. extorquens* 13061, 60 **(A, B, E, F, I, J, M, N)** and 120 **(C, D, G, H, K, L, O, P)** dpi. Bacterial cells labeled with a fluorescent GFP reporter under the control of a constitutive promoter are visualized in bright green, whereas the structures of plant tissue are visible mainly in grey color with the exception of lignified tissues of the endodermis and xylem, and cells of non-vascular parenchyma. Representatives of approximately 50-60 CLSM images are shown for each strain. **(A–D)** A cross-section of root inoculated with the control. Arrowheads indicate bacterial infection pockets (yellow) in the epidermis, and single bacterial cells (blue) in the plant cortical cells and **(B)** non-vascular parenchyma (encircled in the magnification). **(C)** Arrowheads show control bacteria (blue) colonizing further in the cells of the cortex and vascular tissue, and fewer cells are found in the infection pockets at the epidermis (yellow). **(D)** A magnification of **(C)**. **(E–H)** A cross-section of root inoculated with *ΔphaC*. **(E)** A low number of single *ΔphaC* cells (yellow arrowhead) is visible outside of the epidermis and, in the magnification **(F)**, a sporadic *ΔphaC* cell (blue) is found in the cortex. **(G)** The interior of pine root rarely hosts *ΔphaC* cells (blue arrowhead), but the quantity of *ΔphaC* cells outside of the epidermis has increased (yellow arrowhead), magnified in **(H)**. **(I–L)** A cross-section of root inoculated with *ΔphaR*. **(I)** Yellow arrowheads indicate numerous bacterial cells outside of the epidermis, and a number of *ΔphaR*. cells (blue) have reached the xylem (encircled), magnified in **(J)**. **(K)** Large infection pockets (yellow arrowhead) are present in the epidermis, and numerous *ΔphaR* cells (blue) are present between the cortical cells, magnified in **(L)**. **(M–P)** A cross-section of root inoculated with *ΔphaZ1*. **(M)** Small infection pockets (yellow arrowhead) are present in the epidermis, and several *ΔphaZ1* cells (blue) have colonized the cortex and vascular tissues, magnified in **(N)**. **(O)** Few *ΔphaZ1* cells are visible in the epidermis (yellow arrowhead), and a number of cells (blue) have reached the xylem tissue. **(P)** A magnification of **(O)**, where an infection pocket is formed by *ΔphaZ1* in the endodermis (encircled), and single *ΔphaZ1* cells (blue) are found in the cortex and xylem. Co, cortex; e, epidermis; en, endodermis; nvp, non-vascular parenchyma; xy, xylem. Dashed square=magnified area. Scale bars, 5 µm. Original CLSM images are shown as Supplementary Material 2.

at 60 days post-inoculation (dpi), as observed before (Koskimäki et al., 2015). At 120 dpi, the control had progressively advanced towards the vascular bundles (Figure 5C), where numerous cells were present in the xylem vessels (Figure 5D). In contrast, cells of the *ΔphaC* strain were unable to colonize the roots as rigorously (Figures 5E–H). At 60 dpi, single cells, instead of the microcolonies observed for the control, were found on the epidermis (Figure 5E). Sporadically, a cell or two were observed in the cortex, and no cells were observed in the endodermis or the xylem layers (Figure 5F). At 120 dpi, the *ΔphaC* strain formed large microcolonies and infection pockets on and in the epidermis (Figures 5G, H), but the number of bacteria was equally low in the cortex as at 60 dpi (Figure 5H) and still completely negligible in the endodermis and xylem (Figure 5G).

The deletion strains *ΔphaR* and *ΔphaZ1* had more similar patterns of pine root colonization as the control (Figures 5I–P). The cells of *ΔphaR* formed smaller infection pockets than the control in the epidermis at 60 dpi (Figure 5I), and individual cells were found in the xylem (Figure 5J). At 120 dpi, the *ΔphaR* had formed dense

10.3389/fpls.2024.1302705

infection pockets in the epidermis (Figure 5K), and several singular cells were present in the intercellular spaces of cortical cells (Figure 5L). Although *ΔphaZ1* showed roughly a similar colonization pattern as the control within 60 days, the density of cells inside the tissues was lower (Figures 5M, N). There were infection pockets formed in the epidermis less frequently than in the control (Figure 5M). At 120 dpi, the *ΔphaZ1* cells had reached the xylem vessels (Figure 5O), and small infection pockets were visible in the epidermis, similar to the control (Figure 5P).

The colonization of pine shoots by *ΔphaR*, *ΔphaC*, and *ΔphaZ1* followed roughly the same patterns as in roots (Figure 6). However, the colonization of *ΔphaC* and *ΔphaZ1* was slower compared to the control, as they were not present in the samples of 60 dpi, hence the data are not shown. At 120 dpi, the control colonized throughout the shoot system (Figures 6A–D). The bacteria were present in the epidermis, the cortex, and in the vascular tissues (Figures 6A, C). The *ΔphaC* strain was found at very small quantities in the shoots at 120 dpi (Figures 6E–H). There were a few clusters of bacteria on the epidermal tissues (Figures 6E, F), and occasionally one or two individual cells were observed in the cortex (Figures 6G, H). The *ΔphaR* strain was present in the epidermis and cortex (Figures 6I–L), mainly intercellularly (Figures 6I, L). Individual bacterial cells were

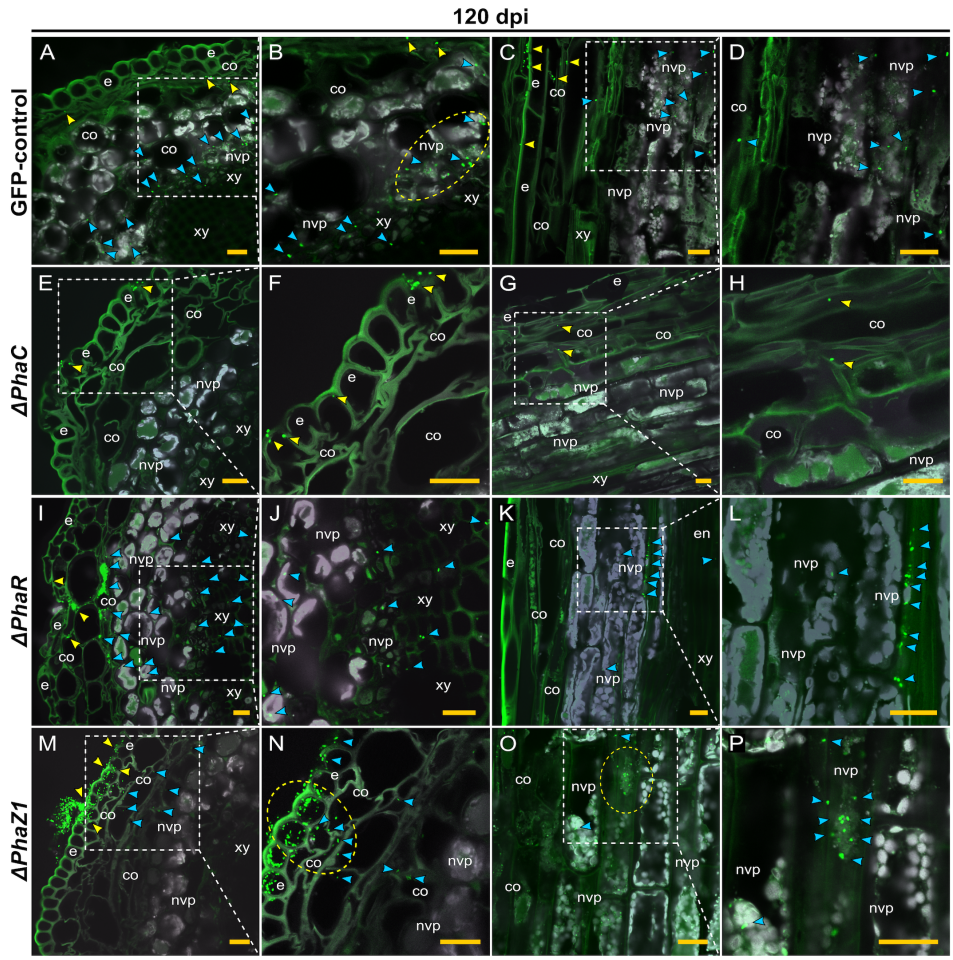

FIGURE 6
CLSM of pine shoots colonized by the strains *ΔphaC*, *ΔphaR*, *ΔphaZ1* and control, *M. extorquens* 13061, 120 dpi. Bacterial cells labeled with a fluorescent GFP reporter under the control of a constitutive promoter are visualized in bright green, whereas the structures of plant tissue are visible mainly in grey color with the exception of cuticula and lignified tissues of the epidermis. Representatives of 50-60 CLSM images are shown for each strain. Cross **(A, B)** and lateral **(C, D)** sections of pine shoot inoculated with the control. **(A)** Single control cells are found in the cortex (yellow arrowheads), and clusters of bacteria (blue) are visible in the non-vascular parenchyma, magnified in **(B)**. The bacterial cells of control (encircled) have aggregated around the plant non-vascular parenchyma. **(C)** Single bacterial cells of the control are visible inside the cortical cells (yellow arrowhead) and bacterial clusters are found in the cells of non-vascular parenchyma (blue), magnified in **(D)**. Cross **(E, F)** and lateral **(G, H)** sections of the shoot inoculated with the *ΔphaC* strain. **(E)** A low number of *ΔphaC* cells (yellow arrowhead) is visible in and on the epidermal cells, magnified in **(F)**. **(G)** Sporadic *ΔphaC* cells (yellow arrowhead) are present in the cortex, magnified in **(H)**. Cross **(I, J)** and lateral **(K, L)** sections of the shoot inoculated with the *ΔphaR* strain. **(I)** Infection pockets and individual cells of *ΔphaR* (yellow arrowhead) are visible between cortical cells, and a number of *ΔphaR* cells (blue) have reached the non-vascular parenchyma, magnified in **(J)**. **(K)** Blue arrowheads point out the mainly intercellular location of the *ΔphaR* cells, magnified in **(L)**. Cross **(M, N)** and lateral **(O, P)** sections of shoot inoculated with the *ΔphaZ1* strain. **(M)** The *ΔphaZ1* cells (yellow arrowhead) have breached the epidermis in numbers and colonize further (blue) the cells of cortex. **(N)** A magnification of **(M)**, where a cluster of *ΔphaZ1* cells penetrating through plant epidermis is encircled. **(O)** The *ΔphaZ1* cells have reached the non-vascular parenchyma (blue arrowhead), and several *ΔphaZ1*cells are aggregating around the plant nucleus (encircled), magnified in **(P)**. Co, cortex; e, epidermis; en, endodermis; nvp, non-vascular parenchyma; xy, xylem. Dashed square=magnified area. Scale bars, 5 µm. Original CLSM images are shown as Supplementary Material 2.

detected in the non-vascular parenchyma and xylem (Figures 6J, L). The *ΔphaZ1* strain showed an equal colonization in the shoots as the control (Figures 6M–P). The bacterial cells actively penetrated from microcolonies through the epidermal layer (Figures 6M, N) and accumulated in the non-vascular parenchyma cells (Figures 6O, P).

To evaluate the presence of hydroxyl radicals in the pine tissue during infection, the Fenton reagents, H_2O_2 and iron (Fe^{2+} and Fe^{3+}), were localized in the pine root tissues at 60 dpi (Figure 7). The quantities of H_2O_2 and iron were low and uniformly distributed throughout the tissues of water-inoculated roots (Figures 7A–C, E). In the root tissues of *M. extorquens* DSM13060-inoculated seedlings, H_2O_2 and Fe^{2+} accumulated at specific sites of epidermis and cortex (Figure 7D), indicating the occurrence of oxidative burst and generation of hydroxyl radicals. The Fe^{3+} was co-localized with H_2O_2 to the same tissues as Fe^{2+}, in the epidermal or cortical cells of the root tissue (Figure 7F).

Discussion

Our previous results have shown that during the infection of the plant host, the endosymbiont *M. extorquens* DSM13060 utilizes polyhydroxybutyrate-derived compounds, ME-3HB oligomers, for protection against host-generated oxidative stress (Koskimäki et al., 2016). Therefore, we hypothesized that the deletion of the genes responsible for PHB synthesis and degradation, *phaC* and *phaZ1*, respectively, could affect the colonization of the host. We assumed that another gene potentially affecting the host colonization is *phaR*, which is a transcription factor that plays a key role in coordinating the other PHB-associated genes (Nishihata et al., 2018).

When the phenotypes of the deletion strains *ΔphaR*, *ΔphaC*, and *ΔphaZ1* of the endosymbiont *M. extorquens* DSM13060 were studied, their cellular morphologies varied to a degree. The cells of *ΔphaC* had very few or no PHB granules, which is in line with previous findings. For example, in *Azorhizobium caulinodans*,

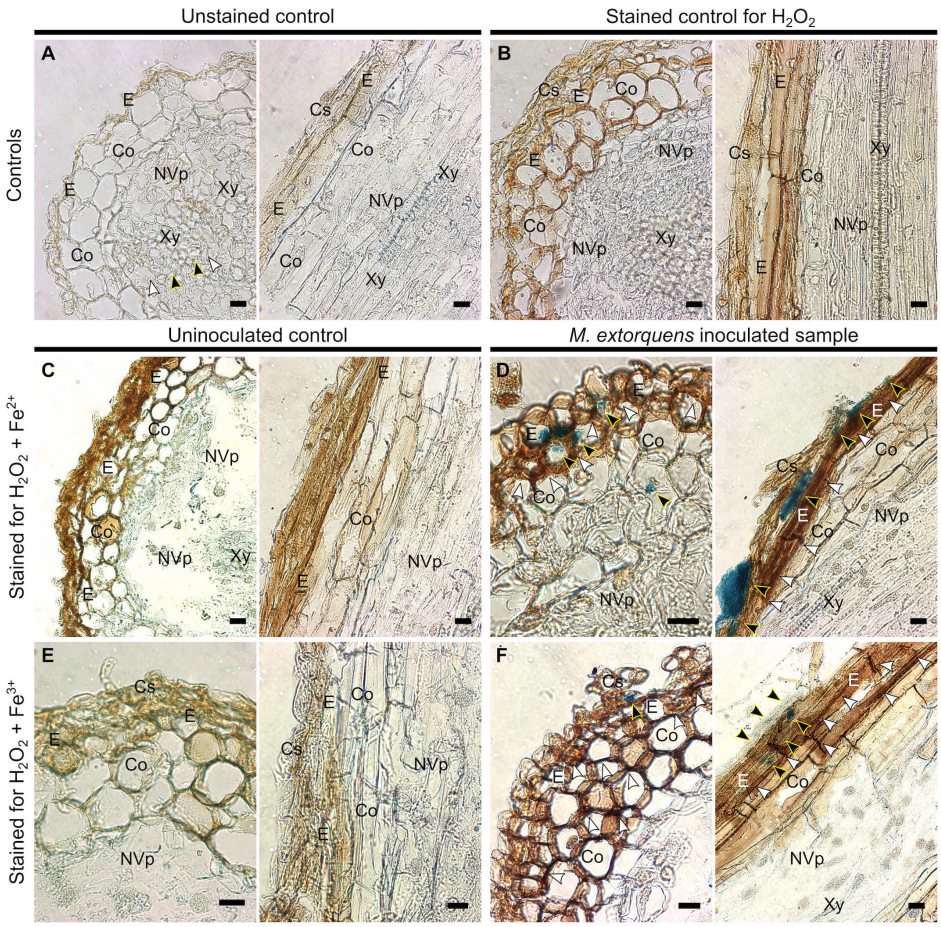

FIGURE 7
Light microscopy of Scots pine roots without inoculation (controls, **A-C, E**) or 60 dpi with *M. extorquens* DSM13060 (samples, **D, F**) stained for detection of H_2O_2 (brown), Fe^{2+}, or Fe^{3+} (blue). **(A)** Cross and lateral sections of pine root of unstained control **(B)** and control stained for H_2O_2 **(C)** or Fe^{2+} and H_2O_2. **(D)** Cross and lateral sections of root inoculated with *M. extorquens* showing local deposits of Fe^{2+} in cortex and epidermis (black arrowheads) and local accumulation of H_2O_2 (white arrowheads) predominantly in the epidermis. **(E)** Cross and lateral sections of pine root of control stained for Fe^{3+} and H_2O_2. **(F)** Cross and lateral sections of inoculated root stained for Fe^{3+} and H_2O_2 showing colocalization of Fe^{3+} (black arrowheads) and H_2O_2 in cells of epidermis and cortex; black arrowheads indicate Fe^{2+} and Fe^{3+}; white arrowheads indicate H_2O_2. Cs, cylindrical sheath; Co, cortex; E, epidermis; En, endoderm; NVp, nonvascular parenchyma; Xy, xylem. Scale bars, 20 µm.

ΔphaC was unable to produce PHB granules, resulting in decreased growth rates and the loss of capacity for nitrogen fixation in the host (Crang et al., 2021). Although the draft genome of *M. extorquens* DSM13060 harbors only one known PHB synthase gene (Koskimäki et al., 2015), *ΔphaC* was able to occasionally produce low numbers of small PHB granules, which suggests that an additional copy exists within the unsequenced region. The cells of *ΔphaR* had numerous small PHB granules in the polar regions of the cells, and the cell shape was irregular. Deletion of *phaR* in the closely related *M. extorquens* AM1 has resulted in slow growth in the culture medium and a subsequent decrease in PHB synthesis (Korotkova et al., 2002), but the morphology of the cells has not been previously analyzed. Similarly, although the *phaZ* genes have often been deleted to enhance accumulation of medium chain-length polyhydroxyalkanoates in many bacterial species (Cai et al., 2009), the morphology of the deletion mutants has rarely been studied. The *ΔphaZ1* of *M. extorquens* DSM13060 accumulated PHB granules significantly greater in size and higher in number than the control granules, occasionally encompassing almost the entire volume of the cell. The *phaZ1* is an intracellular depolymerase with homology to the *phaZ2* of *R. eutropha* (York et al., 2003). Similar to *M. extorquens* DSM13060, the deletion of the *phaZ2* of *R. eutropha* leads to an increased granule volume and a higher number of granules per cell than in the wild type (Brigham et al., 2012).

When the deletion strains *ΔphaC, ΔphaR*, and *ΔphaZ1* were subjected to abiotic stress, similar growth patterns were observed, except that *ΔphaC* survived the heat shock in contrast to *ΔphaR* and *ΔphaZ1*, which arrested their growth. The better survival of *ΔphaC* under heat stress has been explained by the fact that hydroxybutyrate, the monomer of PHB, accumulates in the mutant and protects proteins from aggregation (Soto et al., 2012; Alves et al., 2020). However, in the oxidative stress assay, the deletion strain *ΔphaC* exhibited reduced growth rates compared to the control strain under 20 mM H_2O_2, and 10 mM HO·. In contrast, no significant differences between the control, *ΔphaR*, and *ΔphaZ1* were observed in the oxidative stress tolerance. To analyze if another *phaZ* gene, *phaZ2* of *M. extorquens* DSM13060 (Koskimäki et al., 2016) compensates for the loss of *phaZ1*, we studied the gene expression of *phaZ1* and *phaZ2* under oxidative stress. However, there was no significant difference in the *phaZ2* gene expression between *ΔphaZ1* and the control one hour after the HO· stress application, and after three hours, the *phaZ2* expression was significantly the highest in the stressed control. This suggests that *phaZ1* is the main gene responsible for PHB degradation in *M. extorquens* DSM13060 under oxidative stress. Generation of multiple deletions of *phaZ* genes would complete our understanding of the role of PHB depolymerases in stress tolerance of *M. extorquens* DSM13060.

Our previous results (Koskimäki et al., 2015; Koskimäki et al., 2016) have shown that the endosymbiont *M. extorquens* DSM13060 invades the host plant by similar mechanisms as the stem-colonizing rhizobia. It enters the plant actively through the epidermis in roots and through epidermis or stomatal apertures in stem, and forms infection pockets upon entry. The bacterial cells invade intracellularly through the endoderm further into the vascular tissues, leading to systemic colonization of the *in vitro*-grown Scots pine seedling within three months (Koskimäki et al., manuscript). In the current study, the control strain showed a successful colonization of pine seedlings as described. However, the deletion strains, *ΔphaC, ΔphaR*, and *ΔphaZ1* demonstrated mixed levels of colonization in the pine roots and shoots compared to the control. The *ΔphaZ1* of *M. extorquens* DSM13060 was a poorer colonizer in pine seedlings than the control, as no bacteria were identified in the shoots after 60 days. The infection and colonization process of *ΔphaR* differed from the control. Whereas the same tissues were colonized by *ΔphaR* as by the control, at an equal quantity and pace, the colonization was mainly intercellular instead of intracellular. The PhaR is responsible for regulating PHB biogenesis (Nishihata et al., 2018), and therefore we propose that the coordination of PHB degradation upon host cell infection was disrupted by the *phaR* deletion in *M. extorquens* DSM13060, preventing intracellular entry. The pine colonization by the deletion strain *ΔphaC* was strikingly different from the control. The *ΔphaC* basically lacked the potential for plant colonization in both root and shoot tissues. Majority of the bacteria resided epiphytically on the epidermis, and only sporadic single cells were observed in the deeper tissues.

In earlier studies, the biosynthesis and degradation of PHB has mainly been studied from the point of view of carbon metabolism (Trainer and Charles, 2006) due to the traditionally recognized role of PHB as a bacterial carbon storage (Lemoigne, 1926). Therefore, the plant colonization potential of the deletion strains has been linked with the availability of host carbon and the stringency of the plant defense system (Müller-Santos et al., 2021). In general, the extent of host colonization by the deletion strains has greatly depended on the type of symbionts and their hosts. For example, in the endophyte *Azospirillum brasilense*, an impaired *phaC* gene resulted in reduced colonization on both wheat and maize plants (Kadouri et al., 2003a; Kadouri et al., 2003b). In the rhizobial strain *Sinorhizobium meliloti*, the *phaC* deletion mutant was able to colonize and nodulate the host plant *Medicago* sp., but the symbiotic properties, such as nodule development and the number of nodules formed, were reduced (Aneja et al., 2005). In contrast, the *ΔphaR* deletion strain of *Bradyrhizobium diazoefficiens* was more competitive than the wild type for nodule formation, and performed better in symbiosis with soybean plants, although the bacteria were unable to produce PHB granules (Quelas et al., 2016).

Considering intracellular plant colonization, deletions within the PHB metabolism pathway have a minor effect on the colonization by rhizobia, such as *ΔphaC* or *ΔphaZ* of *S. meliloti, Rhizobium etli*, or *R. leguminosarum* bv. *phaseoli* (Trainer and Charles, 2006; Trainer et al., 2010) and *ΔphaR* of *B. diazoefficiens* (Quelas et al., 2016). In our study on *M. extorquens* DSM13060, the deletion strains *ΔphaZ1* and *ΔphaR* had an impaired capacity for plant colonization and, specifically, the deletion of the *phaC* gene had a drastic effect on the colonization potential by this intracellular symbiont. Besides losing the capacity for plant colonization, the *ΔphaC* deletion strain had a poor tolerance of oxidative stress. We have previously linked the generation of ME-3HB oligomers from PHB by the PhaC and PhaZ1 enzymes with the ability to alleviate oxidative stress during host infection by *M. extorquens* DSM13060

(Koskimäki et al., 2016). In our current study, the colonization by *ΔphaC* was halted at the epidermis, which also accumulated the hydroxyl-radical generating Fenton reagents H_2O_2, Fe^{2+}, and Fe^{3+} upon bacterial infection. Based on our results, the PHB metabolism is more important in endosymbiotic interactions than in rhizobial ones, potentially due to the lack of a finely tuned cellular recognition machinery that exists in the rhizobial symbiosis. Therefore, endosymbiotic strains, such as *M. extorquens* DSM13060, need to alleviate the host-induced oxidative stress through PHB metabolism for a successful entry in the plant host. Altogether, our findings demonstrate that the metabolism of PHB is an important trait in the intracellular plant-microbe interaction due to the high antioxidative power of this molecule (Koskimäki et al., 2016).

Data availability statement

The original contributions presented in the study are included in the article/Supplementary Material. Further inquiries can be directed to the corresponding author.

Author contributions

NB: Software, Writing – review & editing, Data curation, Formal analysis, Investigation, Methodology, Visualization, Writing – original draft. RH: Formal analysis, Investigation, Methodology, Data curation, Writing – original draft. MR: Methodology, Software, Writing – review & editing. AMP: Conceptualization, Funding acquisition, Project administration, Resources, Software, Supervision, Validation, Writing – review & editing. JJK: Methodology, Software, Writing – review & editing, Conceptualization, Formal analysis, Investigation, Resources, Supervision, Visualization.

Funding

The author(s) declare financial support was received for the research, authorship, and/or publication of this article. This work was supported by research grants 343565 and 308766 to NB, JK, and AP from the Academy of Finland.

Acknowledgments

We are most grateful to Dr. J. Vorholt and Dr. M. Bortfeld-Miller (ETH Zürich, Switzerland) for the advice on generating deletion mutants of *M. extorquens* and the gift of *E. coli* S17-1 λpir. Transmission Electron Microscopy (TEM) was performed at the Biocenter Oulu Electron Microscopy Core Facility. We wish to thank Dr. I. Miinalainen and the Core Facility staff for their assistance and expertise.

Conflict of interest

The authors declare that the research was conducted in the absence of any commercial or financial relationships that could be construed as a potential conflict of interest.

The author(s) declared that they were an editorial board member of Frontiers, at the time of submission. This had no impact on the peer review process and the final decision

Publisher's note

Supplementary material

The Supplementary Material for this article can be found online at: https://www.frontiersin.org/articles/10.3389/fpls.2024.1302705/full#supplementary-material

References

Alves, L. P. S., Santana-Filho, A. P., Sassaki, G. L., de Oliveira Pedrosa, F., Maltempi de Souza, E., Chubatsu, L. S., et al. (2020). 3-Hydroxybutyrate derived from poly-3-hydroxybutyrate mobilization alleviates protein aggregation in heat-stressed Herbaspirillum seropedicae SmR1. *Appl. Environ. Microbiol.* 86, e01265–e01220. doi: 10.1128/AEM.01265-20

Aneja, P., Zachertowska, A., and Charles, T. C. (2005). Comparison of the symbiotic and competition phenotypes of Sinorhizobium meliloti PHB synthesis and degradation pathway mutants. *Can. J. Microbiol.* 51, 599–604. doi: 10.1139/w05-042

Boyer, H. W., and Roulland-dussoix, D. (1969). A complementation analysis of the restriction and modification of DNA in Escherichia coli. *J. Mol. Biol.* 41, 459–472. doi: 10.1016/0022-2836(69)90288-5

Brigham, C. J., Reimer, E. N., Rha, C., and Sinskey, A. J. (2012). Examination of PHB depolymerases in Ralstonia eutropha: further elucidation of the roles of enzymes in PHB homeostasis. *AMB Express* 2, 1–13. doi: 10.1186/2191-0855-2-26

Cai, L., Yuan, M.-Q., Liu, F., Jian, J., and Chen, G.-Q. (2009). Enhanced production of medium-chain-length polyhydroxyalkanoates (PHA) by PHA depolymerase knockout mutant of Pseudomonas putida KT2442. *Bioresour Technol.* 100, 2265–2270. doi: 10.1016/j.biortech.2008.11.020

Choi, Y. J., Bourque, D., Morel, L., Groleau, D., and Míguez, C. B. (2006). Multicopy integration and expression of heterologous genes in *methylobacterium extorquens* ATCC 55366. *Appl. Environ. Microbiol.* 72, 753–759. doi: 10.1128/AEM.72.1.753-759.2006

Compant, S., Reiter, B., Sessitsch, A., Nowak, J., Clément, C., and Ait Barka, E. (2005). Endophytic colonization of Vitis vinifera L. by plant growth-promoting bacterium Burkholderia sp. strain PsJN. *Appl. Environ. Microbiol.* 71, 1685–1693. doi: 10.1128/AEM.71.4.1685-1693.2005

Crang, N., Borah, K., James, E. K., Jorrín, B., Green, P., Tkacz, A., et al. (2021). Role and regulation of poly-3-hydroxybutyrate in nitrogen fixation in azorhizobium

caulinodans. *Mol. Plant-Microbe Interact.* 34, 1390–1398. doi: 10.1094/MPMI-06-21-0138-R

Fall, R. (1996). "Cycling of methanol between plants, methylotrophs and the atmosphere," in *Microbial Growth on C1 Compounds*, eds. M. E. Lidstrom, F. R. Tabita (Dordrecht: Springer). doi: 10.1007/978-94-009-0213-8_45

Figurski, D. H., and Helinski, D. R. (1979). Replication of an origin-containing derivative of plasmid RK2 dependent on a plasmid function provided in *trans*. *Proc. Natl. Acad. Sci.* 76, 1648–1652. doi: 10.1073/pnas.76.4.1648

Hardoim, P. R., van Overbeek, L. S., Berg, G., Pirttilä, A. M., Compant, S., Campisano, A., et al. (2015). The hidden world within plants: ecological and evolutionary considerations for defining functioning of microbial endophytes. *Microbiol. Mol. Biol. Rev.* 79, 293–320. doi: 10.1128/MMBR.00050-14

Heinze, S., Kornberger, P., Grätz, C., Schwarz, W. H., Zverlov, V. V., and Liebl, W. (2018). Transmating: conjugative transfer of a new broad host range expression vector to various Bacillus species using a single protocol. *BMC Microbiol.* 18, 56. doi: 10.1186/s12866-018-1198-4

Izumi, H. (2011). "Diversity of endophytic bacteria in forest trees," in *Endophytes of Forest Trees. Forestry Sciences*, vol 80, eds. A. Pirttilä, A. Frank (Dordrecht: Springer). doi: 10.1007/978-94-007-1599-8_6

James, E. K., and Olivares, F. L. (1998). Infection and colonization of sugar cane and other graminaceous plants by endophytic diazotrophs. *CRC Crit. Rev. Plant Sci.* 17, 77–119. doi: 10.1080/07352689891304195

James, E. K., Reis, V. M., Olivares, F. L., Baldani, J. I., and Döbereiner, J. (1994). Infection of sugar cane by the nitrogen-fixing bacterium Acetobacter diazotrophicus. *J. Exp. Bot.* 45, 757–766. doi: 10.1093/jxb/45.6.757

Kadouri, D., Jurkevitch, E., and Okon, Y. (2003a). Involvement of the reserve material poly-β-Hydroxybutyrate in azospirillum brasilense stress endurance and root colonization. *Appl. Environ. Microbiol.* 69, 3244–3250. doi: 10.1128/AEM.69.6.3244-3250.2003

Kadouri, D., Jurkevitch, E., and Okon, Y. (2003b). Poly β-hydroxybutyrate depolymerase (PhaZ) in Azospirillum brasilense and characterization of a phaZ mutant. *Arch. Microbiol.* 180, 309–318. doi: 10.1007/s00203-003-0590-z

Knief, C., Frances, L., Cantet, F., and Vorholt, J. A. (2008). Cultivation-independent characterization of Methylobacterium populations in the plant phyllosphere by automated ribosomal intergenic spacer analysis. *Appl. Environ. Microbiol.* 74, 2218–2228. doi: 10.1128/AEM.02532-07

Korotkova, N., Chistoserdova, L., and Lidstrom, M. E. (2002). Poly-β-hydroxybutyrate biosynthesis in the facultative methylotroph Methylobacterium extorquens AM1: identification and mutation of gap11, gap20, and phaR. *J. Bacteriol.* 184, 6174–6181. doi: 10.1128/JB.184.22.6174-6181.2002

Koskimäki, J. J., Kajula, M., Hokkanen, J., Ihantola, E.-L., Kim, J. H., Hautajärvi, H., et al. (2016). Methyl-esterified 3-hydroxybutyrate oligomers protect bacteria from hydroxyl radicals. *Nat. Chem. Biol.* 12, 332–338. doi: 10.1038/nchembio.2043

Koskimäki, J. J., Pirttilä, A. M., Ihantola, E.-L., Halonen, O., and Frank, A. C. (2015). The intracellular scots pine shoot symbiont Methylobacterium extorquens DSM13060 aggregates around the host nucleus and encodes eukaryote-like proteins. *mBio* 6, e00039–e00015. doi: 10.1128/mBio.00039-15

Koskimäki, J. J., Pohjanen, J., Kvist, J., Fester, T., Härtig, C., Podolich, O., et al. (2022). The meristem-associated endosymbiont *Methylorubrum extorquens* DSM13060 reprograms development and stress responses of pine seedlings. *Tree Physiol.* 42, 391–410. doi: 10.1093/treephys/tpab102

Lam, J., Katti, P., Biete, M., Mungai, M., Ashshareef, S., Neikirk, K., et al. (2021). A universal approach to analyzing transmission electron microscopy with imagej. *Cells* 10 (9), 2177. doi: 10.3390/cells10092177

Lemoigne, M. (1926). Produit de déshydratation et de polymérisation de l'acide b-oxybutyrique. *Bull. Soc. Chim. Biol. (Paris)* 8, 770–782.

Liu, G., Greenshields, D. L., Sammynaiken, R., Hirji, R. N., Selvaraj, G., and Wei, Y. (2007). Targeted alterations in iron homeostasis underlie plant defense responses. *J. Cell Sci.* 120, 596–605. doi: 10.1242/jcs.001362

Marx, C. J. (2008). Development of a broad-host-range sacB-based vector for unmarked allelic exchange. *BMC Res. Notes* 1 (1), 1–8. doi: 10.1186/1756-0500-1-1

Moore, J., Yin, J.-J., and Yu, L. (2006). Novel fluorometric assay for hydroxyl radical scavenging capacity (HOSC) estimation. *J. Agric. Food Chem.* 54, 617–626. doi: 10.1021/jf052555p

Mucha, J., Guzicka, M., Łakomy, P., and Zadworny, M. (2012). Iron and reactive oxygen responses in Pinus sylvestris root cortical cells infected with different species of Heterobasidion annosum sensu lato. *Planta* 236, 975–988. doi: 10.1007/s00425-012-1646-6

Müller-Santos, M., Koskimäki, J. J., Alves, L. P. S., de Souza, E. M., Jendrossek, D., and Pirttilä, A. M. (2021). The protective role of PHB and its degradation products against stress situations in bacteria. *FEMS Microbiol. Rev.* 45, fuaa058. doi: 10.1093/femsre/fuaa058

Nemecek-Marshall, M., MacDonald, R. C., Franzen, J. J., Wojciechowski, C. L., and Fall, R. (1995). Methanol emission from leaves (enzymatic detection of gas-phase methanol and relation of methanol fluxes to stomatal conductance and leaf development). *Plant Physiol.* 108, 1359–1368. doi: 10.1104/pp.108.4.1359

Nishihata, S., Kondo, T., Tanaka, K., Ishikawa, S., Takenaka, S., Kang, C.-M., et al. (2018). Bradyrhizobium diazoefficiens USDA110 PhaR functions for pleiotropic regulation of cellular processes besides PHB accumulation. *BMC Microbiol.* 18, 1–17. doi: 10.1186/s12866-018-1317-2

Obruca, S., Marova, I., Stankova, M., Mravcova, L., and Svoboda, Z. (2010). Effect of ethanol and hydrogen peroxide on poly(3-hydroxybutyrate) biosynthetic pathway in Cupriavidus necator H16. *World J. Microbiol. Biotechnol.* 26, 1261–1267. doi: 10.1007/s11274-009-0296-8

Pirttilä, A. M., Laukkanen, H., Pospiech, H., Myllylä, R., and Hohtola, A. (2000). Detection of intracellular bacteria in the buds of Scotch pine (Pinus sylvestris L.) by in *situ* hybridization. *Appl. Environ. Microbiol.* 66, 3073–3077. doi: 10.1128/AEM.66.7.3073-3077.2000

Pohjanen, J., Koskimäki, J. J., Sutela, S., Ardanov, P., Suorsa, M., Niemi, K., et al. (2014). Interaction with ectomycorrhizal fungi and endophytic Methylobacterium affects nutrient uptake and growth of pine seedlings in *vitro*. *Tree Physiol.* 34, 993–1005. doi: 10.1093/treephys/tpu062

Quelas, J. I., Mesa, S., Mongiardini, E. J., Jendrossek, D., and Lodeiro, A. R. (2016). Regulation of polyhydroxybutyrate synthesis in the soil bacterium bradyrhizobium diazoefficiens. *Appl. Environ. Microbiol.* 82, 4299–4308. doi: 10.1128/AEM.00757-16

Quelas, J. I., Mongiardini, E. J., Pérez-Giménez, J., Parisi, G., and Lodeiro, A. R. (2013). Analysis of two polyhydroxyalkanoate synthases in Bradyrhizobium japonicum USDA 110. *J. Bacteriol.* 195, 3145–3155. doi: 10.1128/JB.02203-12

Ryan, R. P., Germaine, K., Franks, A., Ryan, D. J., and Dowling, D. N. (2008). Bacterial endophytes: recent developments and applications. *FEMS Microbiol. Lett.* 278, 1–9. doi: 10.1111/j.1574-6968.2007.00918.x

Schäfer, A., Tauch, A., Jäger, W., Kalinowski, J., Thierbach, G., and Pühler, A. (1994). Small mobilizable multi-purpose cloning vectors derived from the Escherichia coli plasmids pK18 and pK19: selection of defined deletions in the chromosome of Corynebacterium glutamicum. *Gene* 145, 69–73. doi: 10.1016/0378-1119(94)90324-7

Soto, G., Setten, L., Lisi, C., Maurelis, C., Mozzicafreddo, M., Cuccioloni, M., et al. (2012). Hydroxybutyrate prevents protein aggregation in the halotolerant bacterium Pseudomonas sp. CT13 under abiotic stress. *Extremophiles* 16, 455–462. doi: 10.1007/s00792-012-0445-0

Sy, A., Timmers, A. C. J., Knief, C., and Vorholt, J. A. (2005). Methylotrophic metabolism is advantageous for Methylobacterium extorquens during colonization of Medicago truncatula under competitive conditions. *Appl. Environ. Microbiol.* 71, 7245–7252. doi: 10.1128/AEM.71.11.7245-7252.2005

Tian, J., He, A., Lawrence, A. G., Liu, P., Watson, N., Sinskey, A. J., et al. (2005a). Analysis of transient polyhydroxybutyrate production in Wautersia eutropha H16 by quantitative Western analysis and transmission electron microscopy. *J. Bacteriol.* 187, 3825–3832. doi: 10.1128/JB.187.11.3825-3832.2005

Tian, J., Sinskey, A. J., and Stubbe, J. (2005b). Kinetic studies of polyhydroxybutyrate granule formation in Wautersia eutropha H16 by transmission electron microscopy. *J. Bacteriol.* 187, 3814–3824. doi: 10.1128/JB.187.11.3814-3824.2005

Trainer, M. A., Capstick, D., Zachertowska, A., Lam, K. N., Clark, S. R., and Charles, T. C. (2010). Identification and characterization of the intracellular poly-3-hydroxybutyrate depolymerase enzyme PhaZ of Sinorhizobium meliloti. *BMC Microbiol.* 10, 92. doi: 10.1186/1471-2180-10-92

Trainer, M. A., and Charles, T. C. (2006). The role of PHB metabolism in the symbiosis of rhizobia with legumes. *Appl. Microbiol. Biotechnol.* 71, 377–386. doi: 10.1007/s00253-006-0354-1

Wei, H. L., Chakravarthy, S., Worley, J. N., and Collmer, A. (2013). Consequences of flagellin export through the type III secretion system of Pseudomonas syringae reveal a major difference in the innate immune systems of mammals and the model plant Nicotiana benthamiana. *Cell. Microbiol.* 15 (4), 601–618.

White, J. F. Jr., Torres, M. S., Somu, M. P., Johnson, H., Irizarry, I., Chen, Q., et al. (2014). Hydrogen peroxide staining to visualize intracellular bacterial infections of seedling root cells. *Microsc Res. Tech* 77, 566–573. doi: 10.1002/jemt.22375

Xi, C., Lambrecht, M., Vanderleyden, J., and Michiels, J. (1999). Bi-functional gfp- and gusA-containing mini-Tn5 transposon derivatives for combined gene expression and bacterial localization studies. *J. Microbiol. Methods* 35, 85–92. doi: 10.1016/S0167-7012(98)00103-1

York, G. M., Lupberger, J., Tian, J., Lawrence, A. G., Stubbe, J., and Sinskey, A. J. (2003). *Ralstonia eutropha* H16 Encodes Two and Possibly Three Intracellular Poly[d -(–)-3-Hydroxybutyrate] Depolymerase Genes. *J. Bacteriol.* 185, 3788–3794. doi: 10.1128/JB.185.13.3788-3794.2003

frontiers | Frontiers in Plant Science

TYPE Original Research
PUBLISHED 13 March 2024
DOI 10.3389/fpls.2024.1346523

OPEN ACCESS

EDITED BY
Marcia Soares Vidal,
Brazilian Agricultural Research Corporation (EMBRAPA), Brazil

REVIEWED BY
Sowmyalakshmi Subramanian,
McGill University, Canada
Niraj Agarwala,
Gauhati University, India
José Luis Aguirre-Noyola,
National Autonomous University of Mexico, Mexico

*CORRESPONDENCE
Adriana Silva Hemerly
hemerly.adriana@gmail.com

†PRESENT ADDRESS
Flávia Thiebaut,
Departamento de Biologia Celular e Molecular, Instituto de Biologia, Universidade Federal Fluminense, Niterói, RJ, Brazil

‡These authors have contributed equally to this work and share first authorship

RECEIVED 29 November 2023
ACCEPTED 28 February 2024
PUBLISHED 13 March 2024

CITATION
Rosman AC, Urquiaga MCO, Thiebaut F, Ballesteros HGF, de Oliveira EAG and Hemerly AS (2024) Dual RNA-seq of maize and *H. seropedicae* ZAE94 association, in different doses of nitrate, reveals novel insights into Plant-PGPB-environment relationship. *Front. Plant Sci.* 15:1346523. doi: 10.3389/fpls.2024.1346523

Dual RNA-seq of maize and *H. seropedicae* ZAE94 association, in different doses of nitrate, reveals novel insights into Plant-PGPB-environment relationship

Aline Cardozo Rosman‡, Maria Clara de Oliveira Urquiaga‡, Flávia Thiebaut†, Helkin Giovani Forero Ballesteros, Eduardo Alves Gamosa de Oliveira and Adriana Silva Hemerly*

Laboratório de Biologia Molecular de Plantas, Instituto de Bioquímica Médica Leopoldo de Meis, Universidade Federal do Rio de Janeiro, Rio de Janeiro, RJ, Brazil

The interactions between plants, beneficial bacteria and their environment are profoundly shaped by various environmental factors, including light, temperature, water availability, and soil quality. Despite efforts to elucidate the molecular mechanisms involved in the association between plants and beneficial bacteria, like Plant Growth-Promoting Bacteria (PGPB), with many studies focusing on the transcriptional reprogramming in the plant, there is no report on the modulation of genetic controls from both plant and associated bacteria standpoints, in response to environment. The main goal of this study was to investigate the relationship between plant-bacteria-environment signaling, using as a model maize plants inoculated with *H. seropedicae* ZAE94 and cultivated with different doses of N (0.3 and 3 mM). For this purpose, we performed rRNA-depleted RNA-seq to determine the global gene expression of both maize roots and associated *H. seropedicae* ZAE94. Our results revealed a differential modulation of maize nitrogen metabolism, phytohormone and cell wall responses when associated with *H. seropedicae* ZAE94 at different N concentrations. In parallel, a modulation of the bacterial metabolism could be observed, by regulating genes involved in transport, secretion system, cell mobility, oxidoreductases, and chemotaxis, when bacteria were associated with maize roots and cultivated at different doses of N. The molecular and phenotypic data of maize plantlets suggested that different doses of N fertilization differentially regulated the beneficial effects of bacterial inoculation, as higher doses (3 mM) favored shoot elongation and lower doses (0.3 mM) favored increase in plant biomass. Our results provide a valuable integrated overview of differentially expressed genes in both maize and associated *H. seropedicae* ZAE94 in response to different N availability, revealing new insights into pathways involved in grass-PGPB associations.

KEYWORDS

***Zea mays* sp., beneficial bacteria, beneficial association, differentially expressed genes, transcriptome, hormone metabolism, cell wall metabolism, nitrogen metabolism**

1 Introduction

The world production and productivity of maize (*Zea mays* L.) has doubled in the last two decades, resulting in a production of 1.2 billion tons of grains in 2022 (FAOSTAT, 2024a). This significant increase in productivity is mainly attributed to chemical inputs, crop management and genetic improvement (Ladha et al., 2016; Mueller et al., 2019). Agricultural use of inorganic fertilizers in 2021 was just above 195 million tons of nutrients, of which 56% was nitrogen (N) (FAOSTAT, 2024b). However, recent results have demonstrated that the indiscriminate use of nitrogenous chemical fertilizers has caused serious environmental problems (Keeler et al., 2016; Mateo-Sagasta et al., 2017; Kanter, 2018), raising severe concerns about the dependence of modern agriculture on these inputs. In addition to the negative environmental impact, N fertilizers also account for about 20% of maize production costs (Richetti and Ceccon, 2020).

Although maize is highly dependent on N fertilization, N use efficiency (NUE) is estimated to be less than 50% (Mueller et al., 2019). According to Sheoran et al. (2021), a promising alternative strategy to reduce dependence on N fertilization in plant cultivation is the inoculation with plant growth-promoting bacteria (PGPB). These bacteria can enhance NUE in plants through various mechanisms. Nitrogen-fixing PGPB can directly contribute N to plants, while PGPB in general can benefit plants by improving assimilation of nitrogen, solubilizing nutrients like phosphate, producing hormones, enhancing root architecture, providing biocontrol against pests and diseases, and improving stress tolerance (Di Benedetto et al., 2017; Zeffa et al., 2019; Pankievicz et al., 2021; Gaspareto et al., 2023). These actions collectively lead to increased NUE by enhancing nutrient uptake and overall plant health, reducing the reliance on synthetic N fertilizers.

Among the genera of PGPB that establish efficient associations with different crop species, *Herbaspirillum* stands out as a model to study the processes of bacterial recognition, colonization, and growth promotion in grasses, being recommended as maize inoculant (Reis et al., 2010). *Herbaspirillum seropedicae* is an endophytic β-proteobacteria found naturally associating with several economically important grasses such as sugarcane, wheat, rice, and maize, increasing crop productivity (Baldani et al., 1986; Olivares et al., 1996; Gyaneshwar et al., 2002; Monteiro et al., 2008). Despite being frequently found in the rhizosphere, endophytic colonization by *H. seropedicae* is based on the attachment of the bacteria to root surfaces and the subsequent colonization of the emergence points of lateral roots (Monteiro et al., 2012). In particular, *H. seropedicae* strain ZAE94, originally isolated from rice roots, has been extensively tested in maize showing great potential as PGPB (Alves et al., 2015; Breda et al., 2019; Alves et al., 2021).

The inoculation of *H. seropedicae* in maize can alter the N metabolism and plant development, increasing length and volume of roots, promoting leaf growth, as well as the accumulation of N, P and K in the aerial part, and ensuring better stress tolerance (Alves et al., 2015; Breda et al., 2016; Curá et al., 2017; Hardoim et al., 2019; Alves et al., 2021; Nunes et al., 2021). Furthermore, foliar inoculation of *H. seropedicae* in maize can also increase grain yield by up to 65% (Canellas et al., 2013). At gene expression level, a previous work by our research group showed that the expression pattern of N metabolism genes was modulated in whole maize seedlings inoculated with *Azospirillum brasilense* Sp245 and *H. seropedicae* HRC54, suggesting that some responses are common to both beneficial bacteria, while others are specific for each bacterial species (Hardoim et al., 2019). In addition to modulation of genes related to N, the expression of gene clusters that might be related to plant-microbe interaction, cell wall, hormones and of several transcription factors allow the bacteria to recognize plant signals and modulate plant gene expression for endophytic colonization and plant growth promotion (de Carvalho et al., 2011; Thiebaut et al., 2014; de Azevedo et al., 2019; Hardoim et al., 2019).

The interactions between plants, beneficial bacteria and their environment are profoundly shaped by various environmental factors, including light, temperature, water availability, and soil quality (Vargas et al., 2014; Li et al., 2019; Thiebaut et al., 2022; Leisner et al., 2023). These factors dictate a plant's ability to thrive, affecting growth, resilience, and overall health. Simultaneously, the environment plays a pivotal role in determining the efficacy of PGPB. PGPB thrive in specific environmental conditions that support their growth and activity, and their ability to enhance plant growth is intricately tied to the soil quality and nutrient availability in the ecosystem (Berthrong et al., 2014; Zhou et al., 2015; Wang et al., 2016a; Ding et al., 2017; Wang et al., 2017; Fan et al., 2019; Zhou et al., 2021). When plants, PGPB and the environment function synergistically, they create a harmonious ecosystem where plants are well-adapted to their surroundings, and PGPB optimize nutrient uptake and bolster defense mechanisms. This integrated relationship between plant-bacteria-environment not only benefits agriculture through increased yields and reduced chemical inputs but also supports biodiversity and environmental health. Recognizing and managing these intricate relationships is crucial for sustainable agriculture and the preservation of natural ecosystems.

Despite efforts to elucidate the molecular mechanisms involved in the interaction between maize and PGPB, with many studies focusing on the transcriptional reprogramming in maize (Alves et al., 2015; Breda et al., 2016; Curá et al., 2017; Hardoim et al., 2019; Alves et al., 2021; Nunes et al., 2021) or *H. seropedicae* ZAE94 (Tadra-Sfeir et al., 2015; Balsanelli et al., 2016; Pankievicz et al., 2016; Brusamarello-Santos et al., 2019; Grillo-Puertas et al., 2021; Pessoa et al., 2021), there is no report on the modulation of genetic controls in response to plant-bacteria-environment interactions, from both plant and associated bacteria standpoints. In the present work, we investigated the integration between plant-bacteria-environment signaling, based on the association of maize plants inoculated with *H. seropedicae* ZAE94 and cultivated with different doses of N. The investigation used different approaches, such as: (i) phenotypic analysis of plant growth; (ii) quantification of bacterial colonization; (iii) ribosomal RNA-depleted (rRNA-depleted) RNA sequencing (RNA-seq) to determine the global gene expression of both maize and *H. seropedicae* ZAE94, when associated and cultivated under different doses of N; (iv) validation of gene expression profiles by qRT-PCR. Our results provide the first integrated overview of differentially expressed genes in both maize and associated *H. seropedicae* ZAE94 in response to

10.3389/fpls.2024.1346523

different N availability, revealing new insights into pathways involved in grass-PGPB associations, potentially offering sustainable alternatives to reduce chemical fertilizers dependence in agriculture.

2 Materials and methods

2.1 Plant material and PGPB inoculation

For RNA-seq library construction, the maize (*Zea mays* L.) inbred line Santa Helena SHS 5050, which is a triple hybrid responsive to *H. seropedicae* ZAE94 (BR 11417) (Alves et al., 2015, 2021), was used. The hydroponic experiment set up and performed analyses are described in Figure 1 and Table 1. Briefly, maize seeds were pre-washed with sterile ddH_2O and then surface-sterilized using a solution of 0.5% (v/v) sodium hypochlorite and 0.01% (v/v) Tween 20 for 5 minutes under constant smooth agitation. After that, the seeds were washed 3 times (5 minutes each) with sterile phosphate buffer (KH_2PO_4, 50 mmol L^{-1} pH 7.0) under the same conditions as described above. Seeds were sown into phenolic foam and incubated in a growth chamber for 4 days at 30°C for germination and initial growth. After the first growth period, the seedlings were inoculated with 10^9 cells mL^{-1} for 1 hour and then transferred to 5 L hydroponic containers where the experiment was performed. Briefly, for inoculation, the strain ZAE94 was used after it had been grown in DYGS medium (2 g/L malic acid; 2 g/L glucose; 1.5 g/L bacteriological peptone; 2 g/L yeast extract; 0.5 g/L K_2HPO_4; 0.5 g/L $MgSO_4.7H_2O$ and 1.5 g/L glutamic acid, pH 6.0). Control seedlings were mock-inoculated with sterile DYGS. Each hydroponic container

TABLE 1 Abbreviations used for the sample types and dataset comparisons.

Conditions	Description of experimental conditions
CTN+	Mock-inoculated plants cultivated in 3 mM of Nitrate
CTN-	Mock-inoculated plants cultivated in 0.3 mM of Nitrate
INN+	Inoculated plants cultivated in 3 mM of Nitrate
INN-	Inoculated plants cultivated in 0.3 mM of Nitrate
Dataset comparisons (plant)	**Dataset comparisons (bacteria)**
CTN+ vs CTN-	–
INN+ vs CTN+	INN+ vs CTN+
INN- vs CTN-	INN- vs CTN-

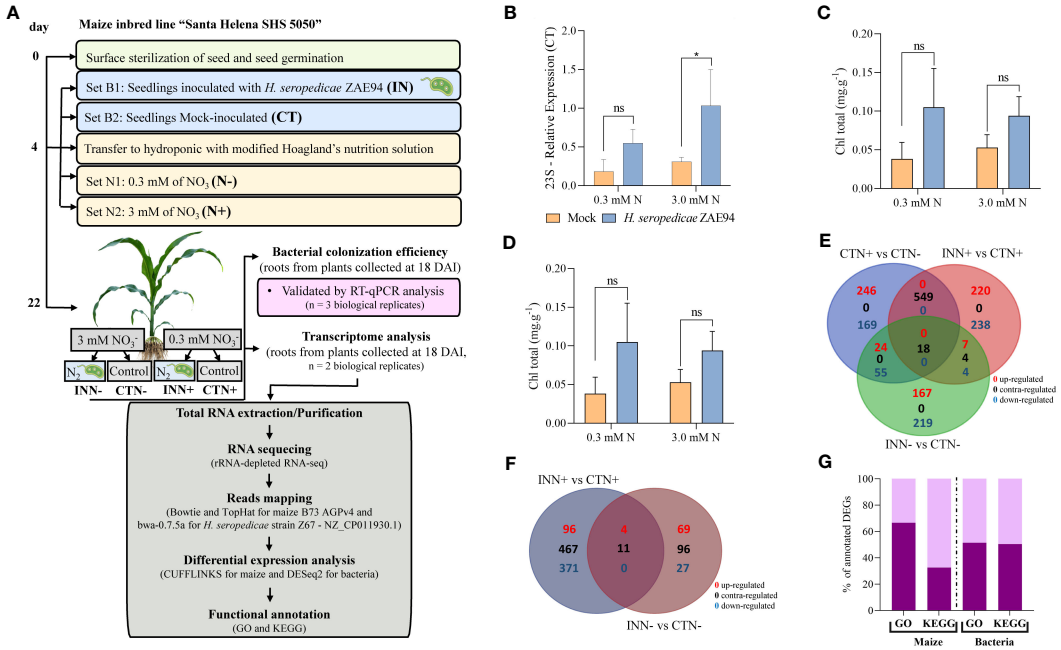

FIGURE 1
Nitrogen assay of maize colonized with beneficial diazotrophic bacteria. **(A)** Experimental design for the transcriptome analyses of maize inbred line Santa Helena SHS 5050 with diazotrophic bacteria *H. seropedicae* ZAE94 (IN) or mock-inoculated (CT). Four-day-old maize seedlings were inoculated with or without bacteria and transferred to a hydroponic system with modified Hoagland's nutrition solution containing 0.3 mM (N-) or 3 mM (N+) of nitrate. Maize root samples were collected at eighteen days after inoculation (DAI) for transcriptome analysis. **(B)** qRT-PCR quantification of maize colonization by *H. seropedicae* 18 DAI. Bacterial *23S rRNA* levels are presented relative to *28S* levels in each sample. Bars represent mean ± standard deviation of the relative mRNA expression in three biological replicates and each biological replicate analyzed with three technical replicates. Means with asterisk are significantly different at 5% level of confidence (One-way ANOVA test with Tukey's post-test) **(C, D)** Total chlorophyll (Chl) content. Total carotenoids (Car) content, respectively. Bars represent mean ± standard deviation of three biological replicates. Means with asterisk are significantly different at 5% level of confidence and means with ns were not significant (One-way ANOVA test with Tukey's post-test) **(E, F)** Venn diagrams of DEGs in maize and in the bacteria, respectively. **(G)** Functional annotation of DEGs in GO and KEGG.

received 5 L modified half-strength Hoagland nutrient solution (Hoagland and Arnon 1950) (Supplementary Table S1) and was kept under constant aeration. Two N concentrations (0.3 and 3 mM) were set up as low and high concentrations, respectively, and were applied after 6 days of acclimatization period. The experiment was performed in blocks in a completely randomized fashion, with five biological replicates for each treatment, and the plants were harvested 18 days after inoculation (DAI). Three biological replicates were used for the phenotypic analysis of the experiment and for molecular analyses to validate the RNA-seq experiment. Two biological replicates were sent for RNA sequencing.

In order to phenotypically and molecularly evaluate the responses of maize to inoculation under different doses of N, an experiment very similar to the one performed for RNA-seq library construction was carried out, using 10 biological replicates for phenotype analysis and three biological replicates for molecular analysis. Maize seeds were superficially sterilized by immersion in a disinfestation solution (0.5% NaOCl and 0.01% Tween 20) under agitation at 65 rpm, for 5 min at 30°C. Then, three washes of 5 min each were performed with a phosphate buffer solution (50 mM; pH 7), under the same conditions. Subsequently, the seeds were pre-germinated on germitest paper in growth chambers at 26/27°C with a photoperiod of 16/8 hours, for 4 days. After this period, maize seedlings were selected, choosing those with a root length of approximately 5 cm. The inoculant was prepared as in the prior experiment, and maize seedlings were inoculated with 10^9 cells mL^{-1} for 1 hour. Following inoculation, the seedlings were transferred to test tubes containing 25 mL of modified Hoagland nutrient solution with 1.5 mM of N concentration. After a 6-days acclimatization period, the plants were transferred to modified Hoagland solution at 1/2 ionic force containing two different concentrations of N (0.3 and 3 mM), using $Mg(NO_3)_2$, $(NH_4)_2SO_4$ and $Ca(NO_3)_2$ as a source of N (Dias et al., 2021). The plants were harvested 18 DAI.

2.2 Phenotypic analyses of maize plants

After separating the plants into shoots and roots, both parts were initially weighed in order to obtain fresh matter values. In addition, shoot length was measured from the end that continued the root to the end of the longest leaf. Subsequently, each shoot and root replica was placed in paper bags and left in an oven at 50°C for three days, when they were weighed again to obtain dry matter values. The values of shoot length and fresh and dry matter obtained were statistically analyzed using GraphPad Prism software version 8.0.0. Statistical analysis was performed using the Two-way ANOVA test with Tukey's post-test. Statistical significance was defined in all cases as p-value < 0.05.

For analyses of root development, the harvested roots were immersed in 70% ethanol for 7 days. Then, roots were laid out in an acrylic container (30 × 40 cm), with water at an approximate depth of 1 cm, and placed onto the scanner. They were scanned and characterized by image analyses using WinRHIZO Pro® software (Regent Instruments, QC, Quebec, Canada) coupled to an Epson Expression 11000XL LA2400 image scanner, as described in previous works (Bauhus and Messier, 1999; Bouma et al., 2000; Dias et al., 2021). In total, 10 plants per treatment were analyzed. The surface area (m^2) of the roots was evaluated. All analyzes used the ANOVA test with Tukey's post-test, with a bilateral analysis. Statistical significance was defined as p-value < 0.05.

2.3 Photosynthetic pigments

Chlorophyll a (chl a [12.74 A665 – 3.62 A649]), chlorophyll b (chl b [25.06 A649 – 6.5 A665]), total chlorophyll (total chl [chl a + chl b]) and total carotenoid (total car [1000 A480 -1.29 Ca – 53.78 Cb)/220]) contents were determined in the complete third fully expanded leaves. The leaves were immersed in 5 mL of dimethyl sulfoxide (DMSO) and then incubated in the dark for 72 hours. Pigment concentrations were quantified using the spectrophotometric method at wavelengths of 649 and 665 nm for chlorophyll a, b and 480 nm for carotenoids. The pigment concentrations were determined as proposed by Wellburn (1994). Statistical analysis was based on the Two-way ANOVA test with Tukey's post-test. Statistical significance was defined in all cases as p-value < 0.05.

2.4 RNA extraction and RNA-seq library construction

For all molecular analyses, plant roots were collected at 18 DAI and flash-frozen in liquid nitrogen. Samples of each treatment, i.e. maize seedlings inoculated with *H. seropedicae* ZAE94 and their respective mock-inoculated seedlings, were used for Illumina sequencing (Table 1). In addition, these samples were used for plant or bacteria transcriptome expression and bacterial colonization qRT-PCR validations. Total RNA was isolated from root plants using Trizol home-made as described by Valach (2014). RNA concentration was measured with a Nano-Drop™ 2000c spectrophotometer (Thermo Scientific, USA), and integrity was evaluated with an Agilent-2100 Bioanalyzer (Agilent Technologies; RNA 6000 NanoChips). Plant samples with a 10 ug total RNA were sent to Fasteris Life Sciences SA (Plan-les-Ouates, Switzerland) for RNA-seq library constructions and subsequent sequencing by Illumina technology. To prepare the eight libraries two protocols were combined. Total RNA samples were depleted using the module for rRNA depletion from the Illumina TruSeq Stranded total RNA Library Prep kit Plant. Depleted RNA was then used as input for library preparation with the Ovation Complete Prokaryotic RNA-seq DR Multiplex System 1-8 from Nugen. Briefly, cDNA sequencing library was prepared from the rRNA-depleted using the mRNA-seq HiSeq SBS Kit V4 (Illumina, San Diego, CA). Sequencing of paired-end RNA-seq libraries was performed using an Illumina HiSeq 2500 instrument at Fasteris Life Sciences SA (Plan-les-Ouates, Switzerland), following the manufacturer's protocol. To ensure the reliability of our molecular analyses, we prioritized sequencing quality in this study. More than 93% of bases had a base quality ≥Q30, and the real-time error rate of spiked PhiX was 0.13%, indicating high

sequencing quality. The datasets generated can be found at SRA/NCBI https://www.ncbi.nlm.nih.gov/sra/PRJNA1047090.

2.5 Transcriptome analysis

Sequence and primary analysis of the Illumina RNA-seq libraries of maize roots generated 495 million paired-end reads (see Supplementary Table S2). High quality reads for each sample were analyzed using the "Tuxedo Suite" package (Trapnell et al., 2012) against the reference maize B73 genome (Emsenbl AGPv4, from iGenome database). Briefly, the alignment of reads was performed with Bowtie and Tophat v2.0.9 (Kim et al., 2013). The transcript abundance, estimated with Cufflinks v2.1.1 (Trapnell et al., 2012), was reported as Fragments Per Kilobase of exon per Million fragments mapped (FPKM), serving as a normalized measure. The entire process, including normalization and comparison, was conducted using Cufflinks v2.1.1 software (Trapnell et al., 2012). Quality filtered RNA-seq reads were also mapped to reference genome sequences of *H. seropedicae* Z67 (NZ_CP011930.1) with Burrows-Wheeler Alignment (BWA) Tool v0.7.5a (Li and Durbin, 2010). The quantification was performed using bedtools, and for normalization and comparison, DESeq2 was used (Anders and Huber 2010). The FPKM values from maize plants inoculated with *H. seropedicae* and cultivated in 0.3 mM or 3 mM of N were compared to FPKM values obtained from mock-inoculated maize plants. Differentially expressed genes (DEGs) were considered when showing significantly (p-value < 0.05) different transcript levels between treatments, using tuxedo protocol for maize and DESeq2 R package for bacteria.

2.6 Functional assignment and metabolic pathway analysis

To assign putative functions to DEGs in this study, the functional annotation of maize genome (*Zea mays* B73 AGPv4) was retrieved from Phytozome v. 12.1.6 (Goodstein et al., 2012) and Maize Genomics Resource (Hoopes et al., 2019), and the functional annotation of *H. seropedicae* was retrieved from KEGG and UNIPROT database. The DEGs of maize and *H. seropedicae* were annotated in the KEGG and GO database. Genes encoding proteins involved in hormone biosynthesis, receptor, signaling, and response were identified using the Arabidopsis Hormone Database v.2 (Jiang et al., 2011). Genes involved in cell wall pathways were identified using the cell wall genomics (https://cellwall.genomics.purdue.edu/) and CAZy (http://www.cazy.org/) databases. Genes encoding proteins involved in N transporter and metabolism were identified using the Arabidopsis homologs present in the list of (Wang et al., 2019) and also those that were annotated in KEGG. For the enrichment analysis of functional categories, DEGs were classified according to Gene Ontology (GO) terms and KEGG pathway using OmicShare tools (http://www.omicshare.com/tools). A GO term or KEGG pathway was considered significantly enriched if the p-value < 0.05.

2.7 Real-time quantitative PCR

Total RNA samples were treated with DNAse I (Biolabs), including both those utilized for RNA-seq (two replicates) and an additional third replicate intended for validating the gene expression observed in the RNA-seq. Additionally, these samples encompass those from the complementary experiment conducted. Reverse transcription was conducted, according to the manufacturer's instructions, using superscript reverse transcriptase III (Invitrogen) with random hexamers as primer. The expression of maize individual genes was measured with gene-specific primers by real time PCR analysis with a 7500 Real-Time PCR System (Thermo Fisher Scientific) and SYBR Green PCR Master Mix (Thermo Fisher Scientific). For plant samples the relative expression was quantitated with the $2^{-\Delta\Delta Ct}$ calculation as previously described (Livak and Schmittgen, 2001) by using the average of expression from *28S rRNA*. The quantification of bacterial cells inside maize plants was also evaluated by molecular approach. Primer pairs designed specifically to detect *23S rRNA* genes of *H. seropedicae* ZAE94 were used (Supplementary Table S3). Total RNA from inoculated and mock-inoculated plants was used to compare the efficiency of inoculation. All primers used in the quantitative reverse transcription-polymerase chain reaction (qRT-PCR) are described in Supplementary Table S3.

3 Results

3.1 Interaction between maize and *H. seropedicae* strain ZAE94, cultivated under different N concentrations

To understand the plant-bacteria-environment relationship, we used the maize-*Herbaspirillum*-different doses of nitrogen as a model. First, a hydroponic model was established to investigate the interaction between maize and *H. seropedicae*, cultivated under different N concentrations of 0.3 mM and 3 mM (Figure 1A). Initially, pre-germinated maize plantlets were inoculated with the *H. seropedicae* strain ZAE94. Subsequently, these plantlets were transferred to hydroponic cultivations with either i) 0.3 mM of N or ii) 3 mM of N (Figure 1A).

To validate the association between maize and PGPB under our experimental conditions, root colonization by *H. seropedicae* ZAE94 was assessed 18 DAI. This was achieved by quantifying the relative expression of ribosomal RNA 23S using qRT-PCR (Figure 1B and Supplementary Table S3). Mock plants in both treatments (0.3 mM or 3 mM of N) showed low amounts of expression, indicating that maize seeds were inherently colonized by endophytic bacteria. Thus, the source of bacterial transcripts in the CTN treatments, not inoculated with *Herbaspirillum*, comes from the natural colonization of maize seeds by *H. seropedicae*. However, relative expression of *H. seropedicae* 23S was higher in inoculated plants, indicating that greater numbers of this bacteria colonized maize roots 18 DAI, compared to mock control plants, at both N concentrations (Figure 1B). These results confirmed that maize plants were associated with *H. seropedicae* after 18 DAI.

Since beneficial plant associations with PGPB are known to enhance leaf chlorophyll and carotenoid content (Hamid et al., 2021), these parameters were quantified in maize plants at 18 DAI (Figures 1C, D). There was no significant difference in chlorophyll and carotenoid contents observed between inoculated and mock plants for both N doses. However, there was a strong tendency for inoculated plants to have higher contents of photosynthetic pigments compared to non-inoculated controls (Figures 1C, D).

3.2 RNA-seq profiling of roots of maize seedlings interacting with *H. seropedicae* in two different doses of nitrogen

To investigate how maize and associated *H. seropedicae* respond to cultivation of different doses of N, we next assessed the co-expression responses of maize seedlings and *H. seropedicae* in the presence of N. Gene expression profiles of both organisms were analyzed using RNA-seq with ribosomal RNA depletion methodology. mRNA libraries of maize roots were generated and sequenced using Illumina RNA-seq. In total, eight RNA-seq libraries were sequenced: maize tissues inoculated with *H. seropedicae* (IN) and grown in either 0.3 mM (N+) or 3 mM (N-) of N, as well as mock-inoculated plants (CT) grown under the same N concentrations. The transcript abundance of maize genes was quantified through Cufflinks and calculated as FPKM. A total of 35.198 maize genes were expressed in our samples out of 41.942 genes annotated in the iGenome database. For the transcript abundance of *H. seropedicae* genes, it was used bedtools and all genes (4.840) annotated in the NCBI were expressed in our samples.

To identify differentially expressed genes (DEGs) in maize, three comparisons were analyzed: **(1)** CTN+ vs CTN-, revealing a total of 1061 DEGs (285 down-regulated and 776 up-regulated); **(2)** INN+ vs CTN+, which showed 1040 DEGs (749 down-regulated and 291 up-regulated); and **(3)** INN- vs CTN-, resulting in a total of 498 DEGs (293 down-regulated and 205 up-regulated) (Figure 1E and Supplementary Table S4). Notably, when inoculated plants were grown in the presence of a higher N concentration, a greater number of genes exhibited differential regulation compared to those grown in a lower N concentration. In the INN+ vs CTN+ comparison, 72% of genes were down-regulated, in contrast to 58.8% in INN- vs CTN- comparison. These results suggest that the inoculation with higher doses of N can lead to a down-regulation of a greater number of genes, when compared to inoculation at lower doses. In contrast, maize plants grown at higher doses of N and without inoculation showed 73% of DEGs being up-regulated. Among the three comparisons, only 18 DEGs were found to be common, and the majority of these genes exhibited the same expression pattern in both CTN+ vs CTN- and INN- vs CTN- comparisons, while the INN+ vs CTN+ comparison showed DEGs with contrasting expression patterns (Figure 1E). It is noteworthy that the same DEGs identified in both CTN+ vs CTN- and INN- vs CTN- comparisons share the same expression pattern, suggesting that *H. seropedicae* inoculation in lower doses of N could share some similar responses as N fertilization in maize. Conversely, the equal DEGs in CTN+ vs CTN- and INN+ vs CTN+ comparisons demonstrate contrasting expression patterns, suggesting that plants would be less responsive to *H. seropedicae* inoculation in higher doses of N, and the predominant expression profile reflected plant responses to higher N fertilization (Figure 1E).

To analyze the global changes in *H. seropedicae* ZAE94 generated in response to two different doses of N, two comparisons were analyzed: (1) INN+ vs CTN+: a total of 482 (382 down-regulated and 100 up-regulated) DEGs were found; and (2) INN- vs CTN-: a total of 111 DEGs (38 down-regulated and 73 up-regulated) were found (Figure 1F). Notably, *H. seropedicae* ZAE94 associated with maize plants grown in the presence of a higher N concentration, a greater number of genes exhibited differential regulation compared to those grown in a lower N concentration. In the INN+ vs CTN+ comparison, 79.2% of genes were down-regulated, in contrast to 34.2% in INN- vs CTN- comparison. These results suggest that higher doses of N can lead to a down-regulation of a greater number of *H. seropedicae* ZAE94 genes associated with maize plants, when compared to lower doses. Additionally, the limited overlap of only 15 DEGs between the two comparisons (Figure 1F) suggests that *H. seropedicae* ZAE94 shows specific responses to different N doses, with many genes exhibiting contrasting expression patterns.

To better understand the influence of different N doses in the plant-bacteria interactions, from both plant and bacterial standpoints, a functional annotation of DEGs in the GO and KEGG databases was performed. Our findings revealed that within the GO database, 66.5% of the total maize DEGs and 60.4% of the *H. seropedicae* ZAE94 DEGs were categorized into functional groups. Additionally, the KEGG database revealed that 32.6% of maize DEGs and 48.8% of bacteria DEGs were mapped to specific pathways (Figure 1G and Supplementary Table S4). This analysis provides valuable information on the specific biological processes and pathways affected by both N availability and the presence of PGPB, further enhancing our understanding of the intricate interactions between maize and *H. seropedicae* ZAE94. In addition, it also brings valuable information about the genetic response of bacteria associated with maize cultivated at different doses of N.

The GO classification was employed to categorize the function of DEGs into three main categories: cellular component, molecular function and biological processes. In maize, the comparisons yielded the following results: (1) For the CTN+ vs CTN- comparison a total of 704 (66.4%) DEGs were classified into 36 functional subcategories (Supplementary Table S5); (2) INN+ vs CTN+ a total of 714 (68.7%) DEGs were classified into 37 functional subcategories (Supplementary Table S5); (3) INN- vs CTN- a total of 321 (64.5%) DEGs were classified into 36 functional subcategories (Supplementary Table S5). The GO analysis revealed that most DEGs from the CTN+ vs CTN- and INN+ vs CTN+ were annotated with the same GO terms. However, when the gene set from CTN+ vs CTN- is up-regulated for a specific GO term, the one from the INN+ vs CTN+ comparison is down-regulated, and vice versa. This suggests a suppression of crucial pathways in plants inoculated with diazotrophic bacteria and cultivated with higher doses of N (Supplementary Figure S1 and Supplementary Table S5). For *H. seropedicae*, the comparisons

10.3389/fpls.2024.1346523

yielded the following results: (1) INN+ vs CTN+: a total of 322 (66.8%) DEGs were classified into 31 functional subcategories (Supplementary Figure S2 and Supplementary Table S6); (2) INN- vs CTN-: a total of 60 (54%) DEGs were classified into 23 functional subcategories (Supplementary Figure S2 and Supplementary Table S6). Most genes were categorized under identical GO terms in the two comparisons analyzed. However, in nine GO terms, the majority of annotated genes exhibited an up-regulated expression pattern in one comparison, while the other comparison showed a down-regulated pattern. This suggests that higher N concentration can differently regulate important *H. seropedicae* genes and possibly interfere with the success of the plant-bacteria association.

3.3 Nitrogen metabolism in maize associated with *H. seropedicae* when fertilized with two different doses of nitrogen

Nitrogen (N) is crucial for maize, acquired as nitrate (NO_3^-) or ammonium (NH_4^+). Our investigation highlights the significant impact of *H. seropedicae* on N metabolism in maize plants, especially in the presence of different doses of N. The expression patterns of several genes related to N assimilation, transport, and utilization were found to be differentially regulated in response to both the presence of *H. seropedicae* and varying N availability. Among the 20 DEGs identified within the N metabolism, most are associated with the *NRT/PTF* family (NPF) (Figure 2 and Supplementary Table S7).

For instance, in the comparison between non-inoculated control plants grown under different N concentrations (CTN+ vs CTN-), most of the identified DEGs were up-regulated (Figure 2 and Supplementary Table S7). Notably, genes encoding high-affinity transporters, *NRT3.1* and *NRT2.4*, were down-regulated in the presence of higher N concentrations, whereas low-affinity transporters, *NPF2.13* and *NPF5.10*, were up-regulated. In addition to N transporters, several other genes exhibited differential regulation and greater expression in CTN+, including glutamine synthase (*GS)* (encodes a key enzyme in N assimilation and remobilization) (Li et al., 2017), aspartate aminotransferase (*AspAT*) (a marker of N use efficiency) (Cañas et al., 2010), GATA TRANSCRIPTION FACTOR 21 (*GATA21*) (involved in chlorophyll biosynthesis modulation), glutamate synthase (*GLU1/Fd-GOGAT*) (Hudson et al., 2011), and alpha and beta carbonic anhydrases (*ACA/BCA)*. The increased expression of genes like *NRT2.13*, *NPF5.10*, *GS*, *AspAT* and *GATA21* suggests enhanced N utilization and chlorophyll biosynthesis in plants cultivated with higher N availability. To confirm the overall expression pattern observed by RNA-seq data, the *GS* gene was selected and validated by qRT-PCR (Figure 3).

A higher number of DEGs involved in N metabolism were found in inoculated plants growing in higher N (INN+ vs CTN+) and most of them were down-regulated (Figure 2 and Supplementary Table S7). Intriguingly, contrasting profiles were observed in the comparison of INN+ vs CTN+ compared to CTN+ vs CTN-, in which DEGs such as *NPF5.10*, *NPF2.13*, *GS* and *AspAT* exhibited a negative regulation in INN+ vs CTN+ and positive regulation in CTN+ vs CTN-. These results indicate that the presence of *H. seropedicae* induces unique responses compared to

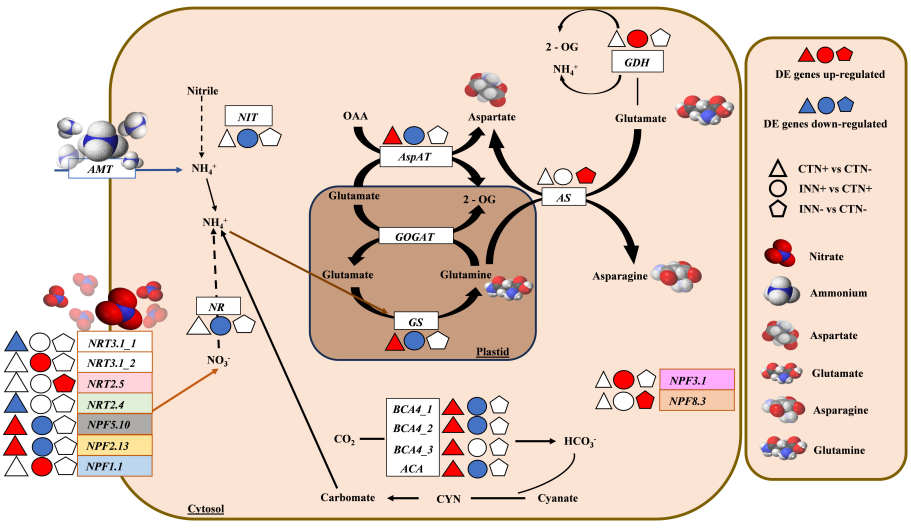

FIGURE 2
Overview of a scheme showing the regulation of nitrogen metabolism. This model presents the differentially expressed genes of maize plants inoculated with *H. seropedicae* ZAE94 (IN) or mock-inoculated (CT), and cultivated in 0.3 mM (N-) or 3 mM (N+) of nitrate. Up-regulated (red colors) or down-regulated (blue colors). White Symbol represents expressed genes, but not differentially regulated. *NIT*, nitrilase; *NRT*, nitrate transporter protein; *NPF*, nitrate transporter 1/peptide transporter family; *AMT*, ammonium transporter; *GOGAT*, glutamate synthase; *GS*, glutamine synthetase; *NR*, nitrate reductase; *BCA*, beta carbonic anhydrase; *ACA*, alpha carbonic anhydrase; *AspAT*, aspartate aminotransferase; *AS*, asparagine synthase; *GDH*, glutamate dehydrogenase; *CYN*, cyanate hydratase; *2-OG*, 2-oxoglutarate; *OAA*, oxaloacetate.

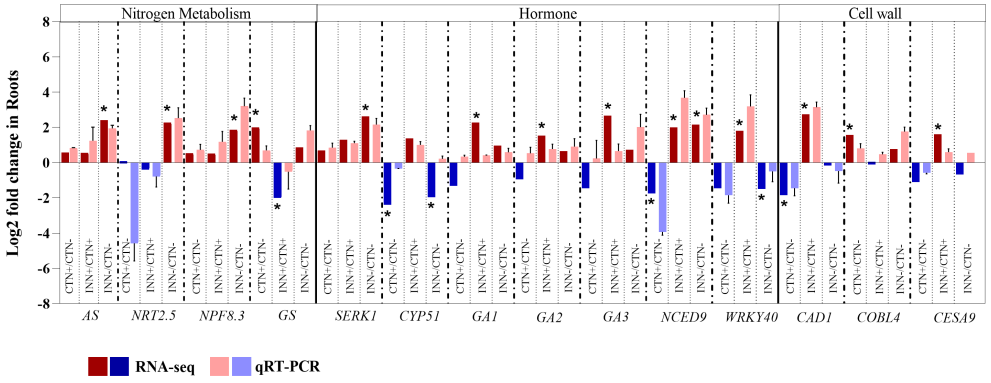

FIGURE 3
Validation of RNA-seq results by qRT-PCR analysis for maize roots. Transcript abundance pattern of selected differentially expressed genes within nitrogen metabolism, hormone synthesis and response and cell wall metabolism categories are shown for RNA-seq and qRT-PCR analyses. qRT-PCR results are presented as the ratio of expression of each gene relative to the constitutive expression of *28S rRNA* gene in each treatment when compared to mock-inoculated plants. Values are transformed into log2 fold change. Bars represent mean ± standard deviation of the relative mRNA expression in three biological replicates and each biological replicate analyzed with three technical replicates. Means with asterisk are significantly different at 5% level of confidence (Bengamini-Hochberg correction for multiple-test3).

uninoculated plants, especially when higher N doses are present. Also, genes such as *NRT3.1*, which encodes a nitrate transporter that acts in low-N concentrations, and *NPF3.1*, which is involved in the transport of GAs in plants under conditions of low-N content (David et al., 2016), were more expressed in INN+. The *NR* gene encoding a cytosolic isoform of nitrate reductase, which is involved in the first step of N assimilation, was less expressed in INN+. Carbonic anhydrase genes, *ACA* and *BCA*, known for their role in legume roots with a potential role in biological nitrogen fixation (BNF) (Wang et al., 2021), were also less expressed in INN+. Nevertheless, their function in grasses with BNF remains relatively unexplored. Together, these data indicate that N metabolism can be differentially regulated, being less active in plants inoculated and grown in N+ compared to control plants grown in N+.

Lastly, in the comparison of inoculated plants with low-N levels (INN- vs CTN-) all DEGs were more expressed in inoculated plants (Figure 2 and Supplementary Table S7). *NRT2.5*, which encodes a low-affinity nitrate transporter, has been shown to play a role in the plant responses independent of N uptake. Furthermore, it has been demonstrated that *NRT2.5* is essential in promoting plant growth by beneficial bacteria in *A. thaliana* (Kechid et al., 2013). *NPF8.3* encodes a di- and tri-peptide transporter that recognizes a variety of different amino acid combinations (Rentsch et al., 1995; Chiang et al., 2004), suggesting a possible active role in the N assimilation pathway, which generates amino acids. Additionally, *AS* encodes the enzyme asparagine synthetase, a key enzyme in the production of the amino acid asparagine, which is crucial for primary N metabolism (Hwang et al., 2011). *AS* was also induced in plants inoculated with low-N levels (INN-). These findings suggest that the presence of *H. seropedicae* can enhance N assimilation even in N-limited environments. qRT-PCR demonstrated greater expression of *AS*, *NRT2.5* and *NPF8.3* (Figure 3), validating the expression pattern described in the RNA-seq analysis.

3.4 Modulation of plant hormonal signaling by nitrogen fertilization and association with *H. seropedicae*

In addition to promoting plant-growth, some PGPB can produce essential phytohormones for plant development, as well as modulate endogenous plant hormonal signaling. In order to understand whether the difference in N availability and the presence of *H. seropedicae* regulate maize genes involved in phytohormone signaling, we categorized DEGs related to different phytohormones pathways. In the three comparisons studied, 115 DEGs related to eight groups of plant hormones auxin (AUX), gibberellic acid (GA), brassinosteroid (BR), abscisic acid (ABA), jasmonic acid (JA) and salicylic acid (SA) were found (Figure 4 and Supplementary Table S8).

Auxins and gibberellins, plant growth hormones produced by *H. seropedicae* (Irineu et al., 2022), influence the regulation of plant genes involved in various pathways. Remarkably, these two hormonal pathways showed higher numbers of DEGs in the comparison INN+ vs CTN+. Auxin is a phytohormone regulating key plant developmental processes. The auxin-regulating gene SUPERROOT2 (*SUR2*), encoding a Cytochrome P450 monooxygenase (CYP83B1), was repressed in INN+ vs CTN+. In Arabidopsis, the mutant of *SUR2* showed a block in the synthesis of glucosinolates leading to accumulation of the metabolic intermediate indole-3-acetaloxime (IAOx), which can be converted into indole-3-acetic acid (IAA), being an alternative route for auxin synthesis (Zhao, 2014). This data suggests that the repression of *SUR2* could contribute to activating the auxin biosynthesis pathway in maize roots inoculated with bacteria, cultivated under 3 mM of N. On the other hand, some members of the auxin response factors (ARFs) (*ARF2*, *ARF3* and *ARF6*), a family of transcription factors that regulate expression of early auxin responsive genes, were repressed in inoculated plants.

10.3389/fpls.2024.1346523

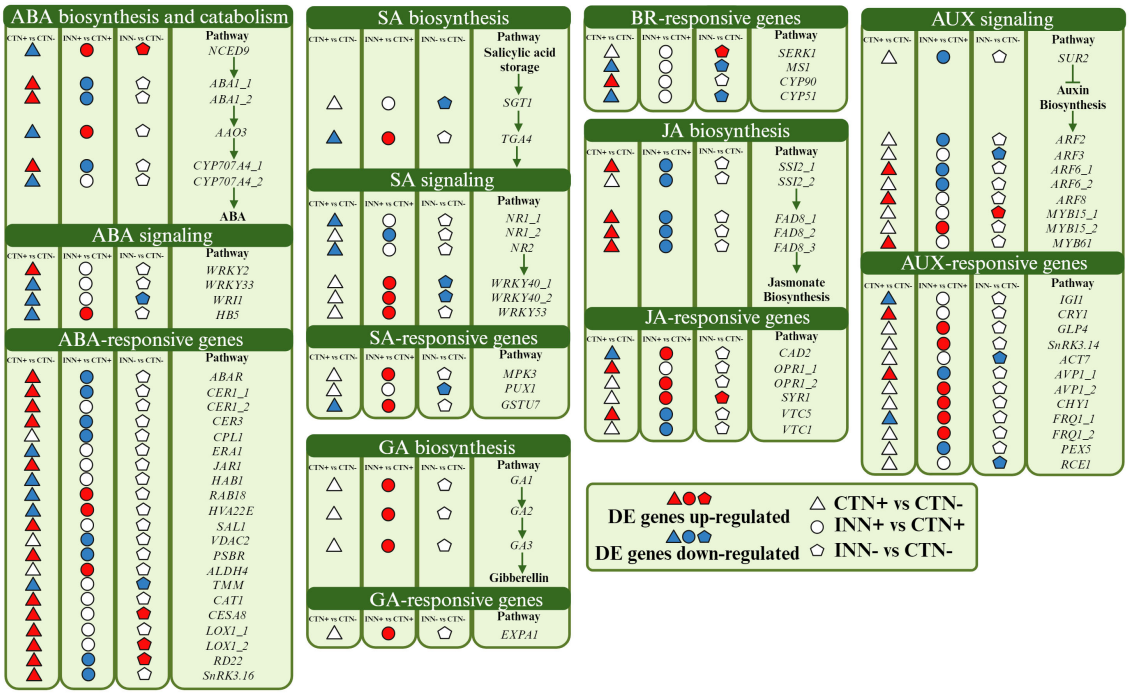

FIGURE 4
Overview of a scheme showing the regulation of hormone pathways. This model presents the differentially expressed genes of maize plants inoculated with *H. seropedicae* ZAE94 (IN) or mock-inoculated (CT) and cultivated in 0.3 mM (N-) or 3 mM (N+) of N. Up-regulated (red colors) or down-regulated (blue colors). White Symbol represents expressed genes, but not differentially regulated. ABA, abscisic acid; GA, gibberellin; AUX, auxin; JA, jasmonic acid; SA, salicylic acid; BR, brassinosteroid. Created with bioRender.com accessed on 01 December 2023.

Accordingly, a global activation of the auxin-responsive genes was identified in the transcriptome for the INN+ vs CTN+ suggesting that, under high N conditions, the bacteria may be promoting maize growth. It is worth highlighting the positive regulation of Arabidopsis Vacuolar H^+-Pyrophosphatase 1 (*AVP1*), which encodes a vacuolar H^+-pyrophosphatase that pumps H^+ into the vacuole. Gibberellin (GA) is another phytohormone promoting plant growth (Zou et al., 2019; Qin et al., 2022). All DEGs related to the gibberellin biosynthesis pathway were up-regulated in INN+ vs CTN+ comparison, including *GA1*, *GA2* and *GA3*. These three genes are involved in the initial step of gibberellin synthesis: *GA1* encodes ent-copalyl diphosphate synthase (CPS), *GA2* encodes ent-kaurene synthase (KS) and *GA3* encodes ent-kaurene oxidase (KO) (Sun, 2008), suggesting that the levels of this hormone were elevated in plants inoculated in higher levels of N (3 mM). The RNA-seq expression profiles for *GA1*, *GA2* and *GA3* were confirmed by qRT-PCR (Figure 3). The GA-responsive gene, Expansin 1 (*EXPA1)*, was also up-regulated in INN+ vs CTN+. Expansin proteins are known for their multifaceted roles in plant growth, especially cell walls. Overexpression of *EXPA1* was accompanied by changes in the chemical composition of the cell wall leading to changes in root development in Arabidopsis seedlings (Samalova et al., 2023), suggesting that *EXPA*, together with several genes encoding enzymes involved in cell wall remodeling, may be part of the regulatory network involved in elongation/cell expansion, regulated by GA.

Brassinosteroids participate in the regulation of various developmental processes, including root and shoot growth, vascular differentiation, and seed germination, as well as in responding to environmental stresses (Bajguz et al., 2020). Notably, DEGs in the BR pathway were not observed in the INN + vs CTN+ comparison. Although the regulation of a specific BR pathway was not observed, SOMATIC EMBRYOGENESIS RECEPTOR KINASE 1 (*SERK1)*, a BR-responsive gene, was induced in INN- vs CTN- and the RNA-seq expression profile for *SERK1* was confirmed by qRT-PCR (Figure 3). *SERK* has been proposed to mediate the interaction between BR and PAMP signaling, with evidence that the growth inhibitory effect of PAMP perception does not operate through BR signaling antagonism (Albrecht et al., 2012). Thus, *SERK1* could be also associated with the regulation of root and shoot growth, acting as a positive regulator. In the INN- vs CTN- comparison it was observed a down-regulation of a cytochrome P450, the *CYP51*, which catalyzes a step of BR-dependent sterol biosynthesis, acting decisively in the activation of defense against pathogens (Nelson and Werck-Reichhart, 2011).

ABA, recognized as a growth inhibitor, accumulates under a variety of stress conditions (Brookbank et al., 2021). Interestingly, ABA-related DEGs were predominantly found in the CTN+ vs CTN- comparison. 9-cis-epoxycarotenoid dioxygenase (*NCED*), a DEG in all comparisons, catalyzes xantoxin production, the first regulatory step in ABA biosynthesis. The xantoxin is converted to

abscisic aldehyde, which is oxidized to ABA (Seo and Koshiba, 2002). *NCED* was repressed in the control situation, and it was induced in the presence of the bacteria, both in 3 mM and in 0.3 mM of N supplementation, suggesting a possible increase in ABA levels in response to inoculation. The RNA-seq expression profiles for *NCED* were confirmed by qRT-PCR (Figure 3). In addition, Abscisic Aldehyde Oxidase 3 (*AAO3*) is a key enzyme in the ABA biosynthesis pathway, described as up-regulated after treatment with phytohormones (ABA, auxin and GA), abiotic stress (such as saline, osmotic and cold) and biotic stress in Arabidopsis (Chan, 2012). Here, we observed a down-regulation of this gene in the CTN + vs CTN- comparison, however it was induced in INN+ vs CTN+, which may suggest an increase in ABA biosynthesis in plants inoculated in higher levels of N (3 mM). The negative regulation of the ABA biosynthesis pathway verified in the CTN+ vs CTN- comparison reinforces the need for N availability to ensure healthy plant growth. Repression of the transcription factor *HB5* expression, a positive regulator of the ABA signaling pathway, in this comparison also suggests a decrease in the inhibitory effect of ABA on growth during seedling development. On the other hand, the positive regulation of this pathway in INN+ vs CTN+ could indicate that the presence of the bacteria constitutes a stress for the plant by increasing ABA levels. However, Cohen et al. (2015) reported that, during association with maize, PGPB such as *Azospirillum* spp., can promote plant growth through several mechanisms, including stimulating the production of phytohormones such as ABA, IAA and GA, not necessarily inducing a defense response.

JA is another hormone related to plant development and plant response to stresses (Bari and Jones, 2009). Genes associated with the JA biosynthesis pathway, *FAD8* and *SSI2*, were induced only in the CTN+ vs CTN- comparison, and showed a repressed expression pattern comparing INN+ vs CTN+. Fatty acid desaturases (FADs) introduce a double bond in the acyl chain of fatty acids, resulting in unsaturated fatty acids participating in the first steps of JA synthesis and playing essential roles in response to biotic and abiotic stresses (Hajiahmadi et al., 2020). Previous work in Arabidopsis showed that *fad3–2 fad7–2 fad8* plants showed reduced defense response to root rot caused by the root pathogen *Pythium mastophorum*, while wild-type plants were not affected by this fungus (Reymond and Farmer, 1998). As a result of this regulation, we verified the down-regulation of JA-responsive genes in INN+ vs CTN+, such as *VITAMIN C DEFECTIVE 1 (VTC1)* and *VTC5*. These genes are important to maintain the cellular reduction/oxidation (redox) homeostasis by detoxifying the cellular excessive reactive oxygen species (ROS) beyond modulates the plant development and cell growth (Song et al., 2019). In our results, the JA biosynthesis pathway was entirely repressed in INN+ vs CTN+ and not regulated in INN- vs CTN-.

The other important phytohormone that shows DEGs is the SA. SA signaling is differentially regulated by members of the WRKY family of transcription factors (Eulgem and Somssich, 2007). *WRKY40* is a pathogen-induced transcription factor that was repressed in INN- vs CTN- and induced in INN+ vs CTN+. *WRKY40* had the expression profile confirmed by qRT-PCR (Figure 3). Overall, these results underscore the diverse hormonal responses triggered by maize when associating with PGPB under different N concentrations, emphasizing the potential activation of the defense system, especially in higher N conditions.

3.5 Modulation of plant cell wall metabolism by nitrogen fertilization and association with *H. seropedicae*

The cell wall plays a fundamental role in the plant perception of bacterial and other microorganisms, in addition to its involvement in growth and development (Cosgrove, 2005; Engelsdorf et al., 2018). The plant cell wall structure consists of different molecules and components, such as proteins and polysaccharides, cellulose, hemicelluloses, pectins and lignin (Höfte and Voxeur, 2017), that can be modulated during plant-bacteria interaction (Ballesteros et al., 2021). In this study we analyzed DEGs related to pathways of cell wall synthesis and assembly in maize plants inoculated with the bacteria *H. seropedicae* ZAE94, and growing in two different doses of N. A total of 124 DEGs were annotated in the different maize gene families involved in cell wall formation, differentiation and signaling (Supplementary Table S9).

Differentially expressed genes from the Cellulose synthase (*CESA*) family showed induction and repression profiles depending on N concentration or association with bacteria (Figure 5). CESA proteins are divided into two subclasses, CESA1, 2, 3, 5, 6, and 9, and CESA4, 7, and 8, which are involved in the synthesis of primary and secondary cell walls, respectively (Li et al., 2020). The comparisons CTN+ vs CTN- and INN- vs CTN- showed up-regulated DEGs involved in secondary cell wall, while INN+ vs CTN+ comparison showed one DEG down-regulated (*CESA3*) and one DEG up-regulated (*CESA9*), that are involved in the synthesis of primary cell wall (Figure 5). These results suggest that a beneficial maize – diazotrophic bacteria association, in soils with lower levels of N, could favor the synthesis of cell wall components such as cellulose. The increase in cellulose accumulation could thicken the cell wall, making it more resistant in response to possible stressful situations such as pathogen attack and drought.

The cell wall architecture and growth pathway, important for the extension of the cell wall, showed several DEGs in the CTN+ vs CTN- comparison (Figure 5). The N doses can positively regulate wall extensibility since some genes, such as Expansin B2 (*EXPB2_1*), (*EXPB2_2*) Expansin B4 (*EXPB4*), FASCICLIN-like Arabinogalactan-protein 10 (*FLA10*) and FASCICLIN-like arabinogalactan-protein 11 (*FLA11*), were induced. On the other hand, in inoculated plants, the expression pattern of some genes involved in this pathway were repressed in N+ condition, such as the ones that were positively regulated in the control condition, as well as in low-N condition as Xiloglucan endotransglycosylase 22 and 25 (*XTH22* and *XTH25*) (Figure 5). This result suggests that bacterial association could modulate cell wall composition, leading to less enzymatic activity in some processes involved in extending and loosening the wall.

The substrate generation pathway showed several DEGs up-regulated or down-regulated in the CTN+ vs CTN- and INN+ vs

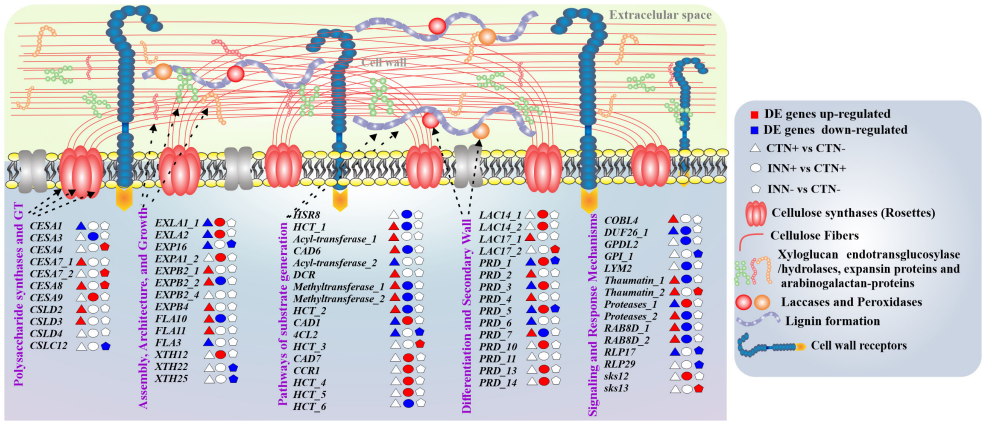

FIGURE 5
Overview of a scheme showing the regulation of cell wall components. This model presents the differentially expressed genes of maize plants inoculated with *H. seropedicae* ZAE94 (IN) or mock-inoculated (CT) and cultivated in 0.3 mM (N-) or 3 mM (N+) of N. Up-regulated (red colors) or down-regulated (blue colors). White Symbol represents expressed genes, but not differentially regulated. *CESA*, cellulose synthase, *EXLA*, expansin-like A; *EXP*, expansin; *EXPA*, expansin A; *EXPB*, expansin B; *FLA*, fasciclin-like arabinogalactan; *XTH*, xyloglucan endo-transglycosylase; *HSR8*, NAD(P)-binding Rossmann-fold superfamily protein; *HCT*, hydroxycinnamoyl-CoA shikimate/quinate hydroxycinnamoyl transferase; *CAD*, cinnamyl alcohol dehydrogenase; *DCR*, HXXXD-type acyl-transferase family protein; 4CL2, 4-coumarate-CoA ligase 2; *CCR1*, cinnamoyl-CoA reductase 1; *LAC*, laccase; *PRD*, peroxidase; *COBL4*, COBRA-like extracellular glycosyl-phosphatidyl inositol-anchored protein family; *DUF26*, Domain of unknown function; *GPDL2*, PLC-like phosphodiesterase family protein; *GPI*, Carbohydrate-binding X8 domain superfamily protein; *LYM2*, Lysm domain GPI-anchored protein 2 precursor; *RAB8D*, RAB GTPase homolog E1B; *RLP*, Leucine-rich repeat (LRR) family protein; *SKS*, SKU5 similar.

CTN+ comparisons, showing contrasting expression profiles between the two comparisons. On the other hand, some genes such as cinnamyl-alcohol dehydrogenase 1 (*CAD1*) (Figure 3), cinnamyl-alcohol dehydrogenase 7 (*CAD7*), cinnamoyl coa reductase 1 (*CCR1*) and hydroxycinnamoyl-CoA shikimate/quinate hydroxycinnamoyl transferase (*HCT*) were induced only on INN+ vs CTN+ comparison (Figure 5). The induction of this group of genes may indicate greater lignification in root cells that have a secondary wall, since they are related to the synthesis and production of lignin. This lignification profile can be confirmed with the expression profile of laccase and peroxidase enzymes that are part of the secondary cell wall differentiation and synthesis pathway (Figure 5). Several DEGs were induced in the INN+ vs CTN+ comparison, suggesting that a high concentration of N applied to plants that were inoculated with PGPB, has a greater expression of enzymes that act in oxidation and formation of lignified compounds. On the other hand, in plants inoculated and treated with low-N, few laccases and peroxidase DEGs were regulated, and in most of them, the expression was reduced (Figure 5). This result may suggest that INN- vs CTN- plants could have more permeable and less rigid walls, but with more cellulose content, as previously discussed based on the expression profile of cellulose synthase genes (Figures 3 and 5).

In the signaling and response pathways related to cell wall, several DEGs were induced in CTN+ vs CTN- comparison, including Cobra like 4 gene (*COBL4*) Domain of unknown function (*DUF26*), *Thaumatin 1* and *2* (Figure 3), suggesting that plants in high N concentrations may have a more active immune system, considering that these genes are related to plant protection against biotic and abiotic stresses. On the other hand, several repressed DEGs were observed in the INN+ vs CTN+ comparison, and only the Proteases_1 and SKU5 similar 12 (*SKS12*) genes related to homeostasis of reactive oxygen species were induced (Figure 5) (Van der Hoorn and Klemenčič, 2021; Chen et al., 2023). In the comparison of INN- vs CTN-, only a few genes were DEGs and most showed a repression expression profile, such as glycosylphosphatidylinositol-anchored protein 1 (*GPI_1*) and two Receptor like protein (*RLPI 17* and *29*) (Figure 5). Possibly the repression of these genes attenuates the immune system, making the plant's association with PGPB more efficient in conditions where plant nutrients are scarce.

3.6 Reprogramming of *H. seropedicae* ZAE94 metabolic subsystems in response to N availability

After wide identification of the functional categories of genes differentially expressed in *H. seropedicae* identified by RNA-seq, a more detailed analysis of a possible involvement of DEGs in physiological and metabolic processes of the bacteria was performed. A schematic representation of the results found is shown in Figure 6. In addition to checking the gene expression profile, we also analyzed the regulation of CDS, indicated based on Hsero_XXXX codes.

The association process of *H. seropedicae* with poaceous species begins with the attraction of bacteria to the host roots, subsequently the bacteria attachment on the root surfaces occurs and finally the emergence points of the lateral roots are colonized (Monteiro et al., 2012; Thiebaut et al., 2022). The RNA-seq analyses revealed that genes related to adhesion were down-regulated in the INN+ vs CTN + comparison, including three genes coding for lipopolysaccharides (LPS) biosynthesis proteins (*rfaC*, *waaA* and *htrB*). In addition, Hsero_0756, coding for membrane porin of the OmpA family, was

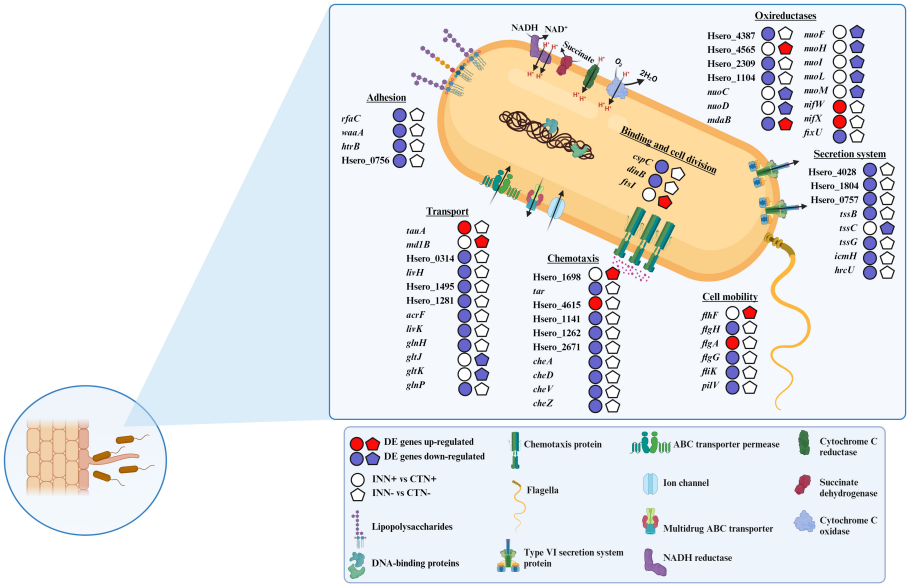

FIGURE 6
Overview of the major *H. seropedicae* strain ZAE94 metabolic pathways and functions differentially expressed in two different doses of nitrate. Pathways involved in relevant aspects of *H. seropedicae* ZAE94 as PGPB are represented, including adhesion, transport, chemotaxis, cell mobility, secretion system and oxireductases. Up-regulated (red colors) or down-regulated (blue colors). White Symbol represents expressed genes, but not differentially regulated. Created with bioRender.com accessed on 01 December 2023.

also repressed in INN+ treatment when compared to CTN+ (Figure 6). These results suggest that the adhesion process is being repressed in inoculated plants growing at higher N levels.

Regarding genes related to bacterial chemotaxis, two DEGs, Hsero_1698 and Hsero_2164, were up-regulated in INN- vs CTN- comparison. The RNA-seq expression profiles for Hsero_1698 was confirmed by qRT-PCR (Figure 7). The INN+ vs CTN+ comparison revealed that four *MCP* genes were significantly repressed (Hsero_4615, Hsero_1141, Hsero_1262 and Hsero_2671). The RNA-seq expression profiles for Hsero_2671 was confirmed by qRT-PCR (Figure 7). Moreover, several genes that encode chemotaxis-related proteins were down-regulated in this comparison: *cheA, cheD, cheV* and *cheZ* (Figure 6). Bacterial cell mobility has also a crucial implication in plant colonization by the plant growth promoter, since bacteria chemotactic movement in response to various stimuli and environmental changes depends on flagella-driven motility

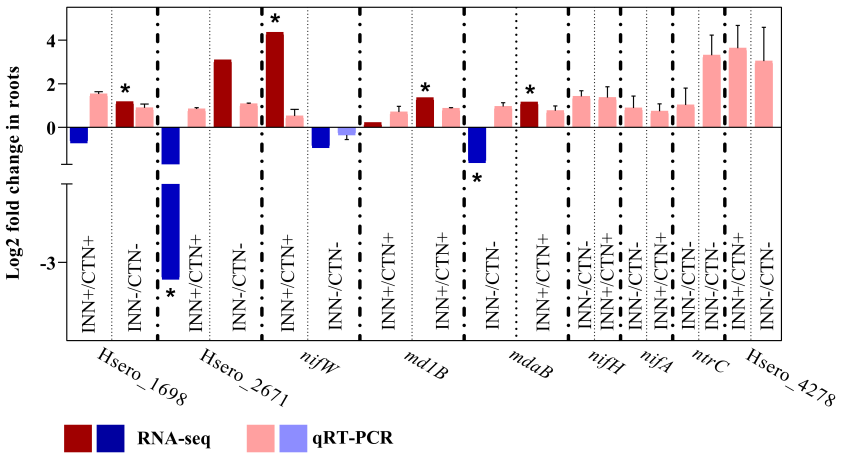

FIGURE 7
Validation of RNA-seq results by qRT-PCR analysis for *H. seropedicae* associated with maize roots and expression quantification of *nif* and *auxin* production genes in *H. seropedicae* ZAE94 colonizing maize roots by qRT-PCR. Transcript abundance patterns of selected differentially expressed genes are shown for RNA-seq and qRT-PCR analyses. qRT-PCR results are presented as the ratio of expression of each gene relative to the constitutive expression of *28S rRNA* gene in each treatment when compared to mock-inoculated plants. Bars represent mean ± standard deviation of the relative mRNA expression in three biological replicates and each biological replicate analyzed with three technical replicates. Values are transformed into log2 fold change. Means with asterisk are significantly different at 5% level of confidence (Bengamini-Hochberg correction for multiple-test3).

(Tadra-Sfeir et al., 2015). Regarding the INN+ vs CTN+ comparison, the flagellin gene *fliK* was significantly repressed. Moreover, two genes involved in the formation of the flagellar basal body, *flgH* and *flgG*, showed reduced expression levels (Figure 6). In this context, the gene *pilV*, coding for a putative type IV *pilus* assembly protein, was also repressed (Figure 6). However, in the condition of low availability of N, the comparison INN- vs CTN- revealed the up-regulation of *flhF* gene, coding for transcription activator protein (Figure 6). Taken together, the results indicate that, under low-N conditions, there is an increase in the expression of genes involved in chemotaxis and flagellar biosynthesis in *H. seropedicae* when compared to the mock group, suggesting that this condition may have positive effects on motility processes that are important for establishing association with the plant. On the other hand, a large number of genes involved in chemotaxis and motility were repressed in *H. seropedicae* under high-N conditions, suggesting that this condition is not favorable for processes important for plant-interaction.

In pathogenic bacteria, T3SS and T6SS are key secretion systems acting to transport effector proteins to host plants. Therefore, these two types of secretory systems are commonly absent or present in low abundance in beneficial endophytic bacteria (Dudeja et al., 2021). In this study, *T3SS* secretion system genes were not differentially expressed in any of the comparisons analyzed. Some *T6SS* genes were significantly down-regulated in INN+ vs CTN+ comparison: *icmH*, *hrcU, tssB, tssG*, Hsero_1804, Hsero_0757 and Hsero_4028; meanwhile only *tssC* showed a decreased expression pattern in INN- vs CTN- (Figure 6). Down-regulation of *tssC* and other *T6SS* genes in inoculated plants may indicate that this protein secretion system is present with reduced abundance during the colonization of maize plants by *H. seropedicae* ZAE94, reinforcing the beneficial aspect of this association for the plant.

The transcriptomic analysis revealed a large number of differently expressed transport related genes among the highlighted comparisons, including transporters of the resistance-nodulation-division (RND) family, the major facilitator superfamily (MFS) and the ATP-binding cassette (ABC) (Supplementary Table S10). Hsero_3390, coding for a putative nitrate ABC transporter, was induced in *H. seropedicae* ZAE94 in response to high N availability (Figure 6). However, several ABC transporter genes involved in amino acid transport were significantly repressed in INN+ vs CTN+ comparison, including *glnP*, *glnH*, *livK*, Hsero_4012, Hsero_1495 and Hsero_1281 (Figure 6). In addition, two multidrug ABC transporter genes, *acrF* and Hsero_0314, also had the expression decreased (Figure 6). On the other hand, just four ABC transporters were regulated in the comparison INN- vs CTN-, two glutamate/aspartate ABC transporters, *gltK* and *gltJ*, and a urea ABC transporter, *urt* were down-regulated, and the multidrug ABC transporter gene *md1B* was up-regulated (Figure 6). *md1B* expression levels were validated by qRT-PCR analyzes (Figure 7). The data shows that a large number of genes involved in transport were repressed in *H. seropedicae* under high-N conditions.

RNA-seq analyzes showed that an expressive number of genes involved in oxidoreductase activity were differentially expressed in the comparisons analyzed (Supplementary Table S10). *nifW* and *nifX* were significantly up-regulated, while *fixU* was down-regulated in INN+ vs CTN+ (Figure 6). The expression level of the *nifW* gene was also evaluated, which was up-regulated in INN+ vs CTN+ and down-regulated in INN- vs CTN- (Figure 6). Considering that the ability of *H. seropedicae* to promote plant growth might depend on many genes involved in N_2 fixation (Pedrosa et al., 2011), our results suggest that, under our experimental conditions, the presence of N would be favorable to bacterial N_2 fixation in *H. seropedicae* ZAE94. Among the DEGs with differential expression profiles in the INN+ vs CTN+ and INN- vs INN+ comparisons are 11 contra-regulated genes, including genes involved in oxidoreductase activity (Figure 1F and Supplementary Table S10). Interestingly, *mdaB* had its expression down-regulated in INN+ vs CTN+, and was up-regulated in INN- vs INN. *mdaB* expression pattern was validated in qRT-PCR analyzes (Figure 7). Among the genes with repressed expression in INN+ vs CTN+ comparison, there are three genes involved in the cytochrome C enzymatic chain, which is associated to bacterial microaerobic respiration: Hsero_4387, Hsero_2309 and Hsero_1104 (Figure 6). In particular, seven genes encoding NADH ubiquinone oxidoreductase were significantly down-regulated in INN- vs CTN- comparison, *nuoC*, *nuoD*, *nuoF*, *nuoH*, *nuoI*, *nuoL* and *nuoM* (Figure 6).

Among the regulated genes that have functions involved in cell division, we verified the induction of *ftsI* expression in the INN- vs CTN- comparison (Figure 6), which encodes an essential transpeptidase that introduces peptide cross-linking into the peptidoglycan cell wall in the division septum during cell division (Weiss et al., 1999). Meanwhile, *dinB* (Hsero_4328) had expression decreased in INN+ vs CTN+, coding a DNA polymerase (pol) IV, which is highly expressed to help bacterial cells tolerate certain types of DNA damage (Friedberg et al., 1995) (Figure 6). In addition, *cspC* (Hsero_0505), coding for a cold shock protein, was also down-regulated in *H. seropedicae* ZAE94 in comparison to the mock-inoculated group, under high N levels (Figure 6).

3.7 Nitrogen control of the beneficial effects of maize inoculation with *H. seropedicae*

A global view of the integrated modulation of gene expression in the maize and *H. seropedicae* association, occurring with different doses of N fertilization, was generated by the RNA-seq data. To further characterize the influence of N fertilization to the benefits to the plant, a new experiment was carried out to investigate the beneficial effects of maize inoculation with *H. seropedicae* ZAE94, cultivated in two different doses of N (0.3 mM and 3 mM).

First, to confirm that maize and *H. seropedicae* were associated under the experimental conditions performed, root colonization by *H. seropedicae* ZAE94 was assessed by quantifying the relative expression of *23S rRNA* (Figure 8). The data validated the inoculation and suggested a better bacterial colonization in plants growing with lower dose of N.

The effects of fertilization with two doses of N were analyzed in plants 18 DAI (Supplementary Figure S3). Several phenotypic parameters were evaluated to quantify the benefits of inoculation

10.3389/fpls.2024.1346523

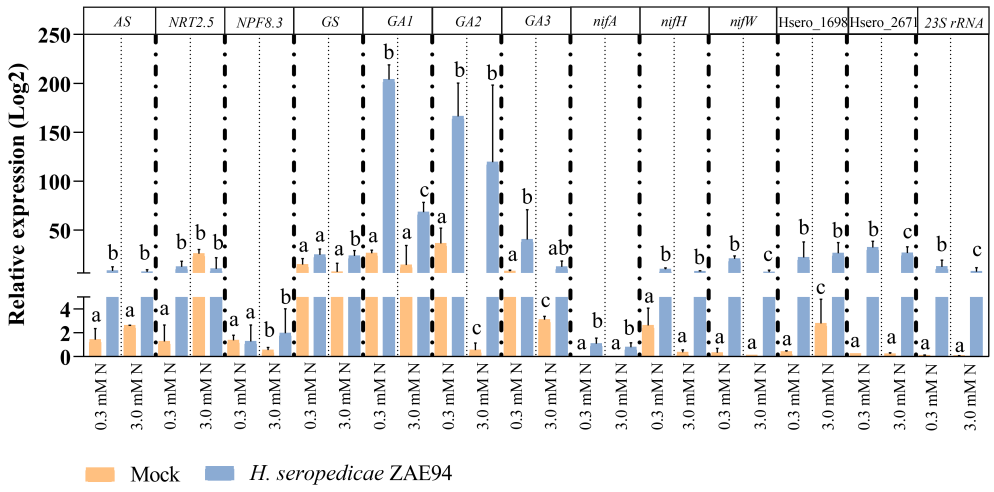

FIGURE 8
qRT-PCR analysis for genes of *H. seropedicae* associated with maize roots. Transcript abundance patterns of selected differentially expressed genes are shown for RNA-seq and qRT-PCR analyses. qRT-PCR results are presented as the ratio of expression of each gene relative to the constitutive expression of *28S rRNA* gene in each treatment when compared to mock-inoculated plants. Values are transformed into log2 fold change. Bars represent mean ± standard deviation of the relative mRNA expression in three biological replicates and each biological replicate analyzed with three technical replicates. Means with different letters are significantly different at 5% level of confidence (Two-way ANOVA test with Tukey's post-test).

in promoting shoot and root growth, such as shoot length, fresh and dry matter, as well as the root fresh matter, in addition to the analysis of the roots surface (Figure 9). The parameters were measured 18 DAI, according to the harvest performed for RNA-seq analysis. Remarkably, different beneficial effects were observed in inoculated plants growing with 0.3 mM or 3 mM of N. At 18 DAI, shoots were longer in inoculated plants compared to mock plants at 3 mM of N (Figure 9A). Furthermore, the association with *H. seropedicae* increased total root surface area in the high-N treatment (Figure 9B). On the other hand, the shoot and root dry matter of inoculated plants were higher than that observed for the mock plants only in response to 0.3 mM of N (Figures 9C, D). Interestingly, these results suggest that the effect of inoculation in promoting biomass was greater in plants subjected to lower N concentrations, statistically equating the biomass of these plants to those observed in plants grown under higher doses of N. The inoculation had no effect on the fresh matter of the root, at all N doses evaluated (Figures 9E, F). Also, chlorophyll and carotenoid contents were not significantly different in response to inoculation, regardless of the N doses used (Figures 9G, H). Taken together, the results obtained in the new experiment validate the data obtained in RNA-seq at the level of plant development. Also, the results suggest that the reduction of doses of N fertilization commonly applied in maize crops, from 3 mM of N to 0.3 mM, allows inoculation with *H. seropedicae* to produce more significant effects in promoting plant biomass, both in aerial part and roots, probably due to an improvement in the efficiency of the plant-bacteria association.

In addition to plant growth validation, mRNA expression in genes that participate in key biological processes involved in a beneficial association for the plant were analyzed. The expression profile of four genes associated with N metabolism (*AS*, *NRT2.5*, *NPF8.3* and *GS*) was analyzed revealing higher expression levels of *NPF8.3* and *GS* in inoculated plants cultivated with 0.3 mM N (Figure 8). In general, the increased expression of these genes in inoculated plants, compared to control plants, suggests an improvement in N utilization, especially in plants cultivated with lower N availability. As observed in the transcriptome analyses, these results reinforce that the presence of *H. seropedicae* can promote N assimilation in N-limited environments, leading to increases in plant biomass. Furthermore, three genes involved in GA metabolism (*GA1*, *GA2* and *GA3*) were also verified, showing higher mRNA levels in inoculated plants cultivated with 3 mM N, compared to mock-inoculated seedlings, as verified in RNA-seq (Figure 8).

From the bacterial side, the expression patterns of five *H. seropedicae* genes, associated with chemotaxis and N_2-fixation (*nifA*, *nifH*, *nifW*, Hsero_2671 and Hsero_1698), were evaluated in response to different doses of N, by qRT-PCR (Figure 8). Expression analysis of the N_2-fixation genes, *nifA* and *nifH*, demonstrated a strong trend towards higher expression in samples cultivated under 0.3 mM N when compared to the 3.0 mM N treatment, being significantly higher in this condition for *nifW* expression (Figure 8). The same expression patterns were verified for the Hsero_2671 gene (Figure 8). These results suggest that the lowest dose of N can stimulate the bacterial metabolism, promoting the expression of *nif* genes, as well as host adhesion and recognition, in accordance to the RNA-seq data.

4 Discussion

Plants are remarkably sensitive organisms that respond dynamically to the environment in which they grow. Plant associations with beneficial bacteria are combined to components

10.3389/fpls.2024.1346523

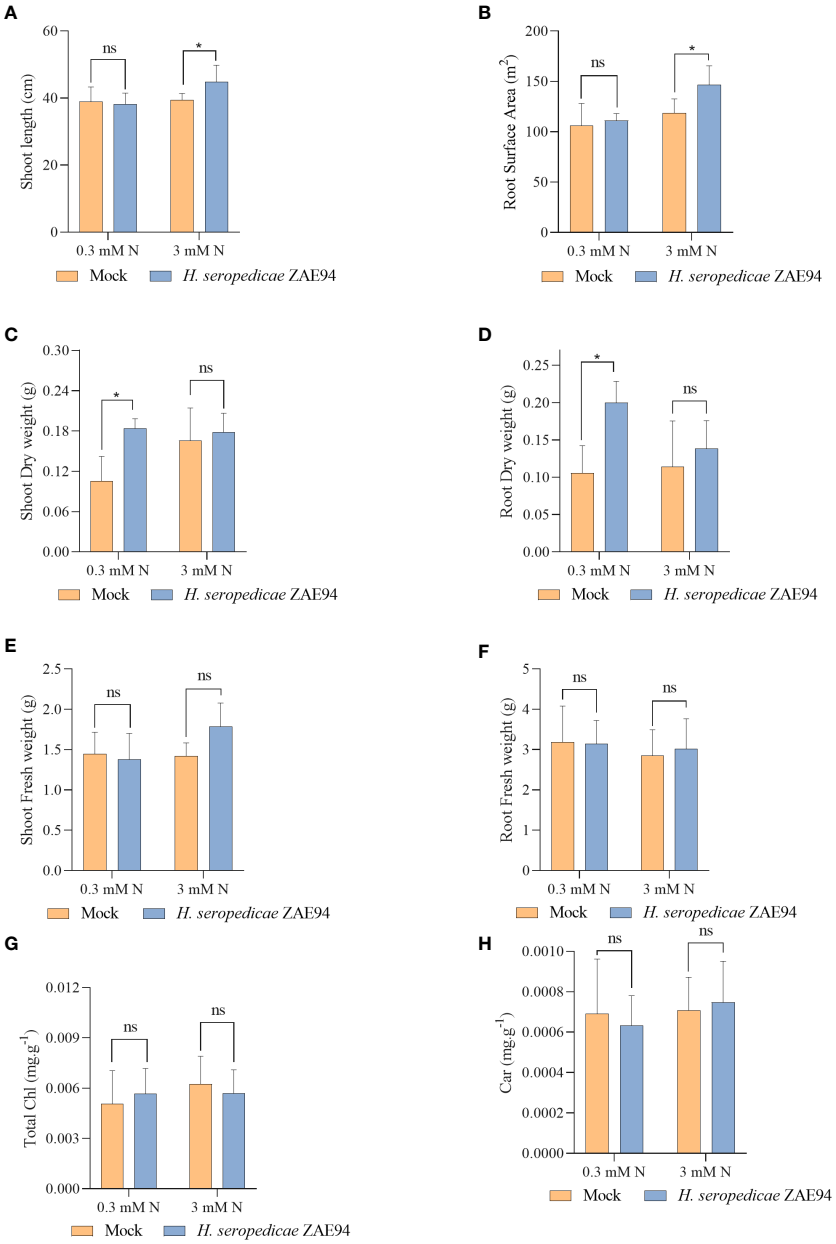

FIGURE 9
Effects of inoculation with *H. seropedicae* ZAE94 on maize plants grown in two different doses of N (0.3 mM and 3 mM of nitrate), 18 days after inoculation. **(A)** Shoot length; **(B)** Root surface area; **(C)** Shoot dry weight; **(D)** Root dry weight; **(E)** Shoot fresh weight; **(F)** Root fresh weight; **(G)** Total chlorophyll content; **(H)** Carotenoid content. Columns represent the mean value and bars represent the standard error of 10 replicates. Means with asterisk are significantly different at 5% level of confidence and means with ns were not significant (Two-way ANOVA test with Tukey's post-test).

of the environment such as soil, water or the atmosphere, functioning as a coordinated unit to generate plant adaptive responses, improving growth (Carvalho et al., 2016). Many studies have shown that the efficiency of the plant association with PGPB is dependent on external factors, such as the plant genotype, the bacterial genotype, and the soil nutritional status (Ballesteros et al., 2021; Carvalho et al., 2022; Thiebaut et al., 2022). Among the environmental factors, the nutritional composition of the soil plays a pivotal role in shaping the growth and development of plants. The presence of essential nutrients and micronutrients profoundly impact the health and productivity of plants (Nadeem et al., 2018). Deficiencies or imbalances in these nutrients can hinder vital processes like photosynthesis, root development and overall growth (Nadeem et al., 2018). Therefore, to advance the understanding of the mechanisms involved in a beneficial association for the plant, it is important to investigate, in an integrated way, the genetic, physiological and biochemical factors in response to multiple stimuli. To address that, in this work, we

studied the relationship between plant-bacteria-environment signaling, using as a model the association of maize plants with *H. seropedicae* ZAE94 and cultivated with different doses of N. Ribosomal RNA-depleted RNA sequencing was performed to generate a global view of the integrated modulation of gene expression of both maize and *H. seropedicae* ZAE94, when associated and cultivated under different doses of N. In parallel, N control of the beneficial effects of maize inoculation with *H. seropedicae* was investigated by phenotyping the development of maize inoculated plants. Taken together, our results revealed new insights into pathways involved in grass-PGPB associations, potentially offering sustainable alternatives to reduce chemical fertilizers dependence in agriculture.

To enhance our comprehension of the overall benefits arising from different doses of N, plant growth-promoting bacteria, or their combined application, we have crafted a representative figure encapsulating the comprehensive results of our study. This figure illustrates the co-regulation of specific plant and bacterial pathways when associated under different N doses (Figure 10).

4.1 The relationship between nitrogen nutritional status with maize and bacteria nitrogen metabolism

In this study, the acquisition of N seems to be induced in maize plants grown in higher doses of N or inoculated with PGPB and cultivated in low-N, since most of the genes involved in N metabolism were induced in the RNA-seq and qRT-PCR analysis. Corroborating our data, studies involving plant inoculation with PGPB have consistently shown the transcriptional induction of genes related to nitrate transporters and N metabolism enzymes. For instance, Hardoim et al. (2019) demonstrated that *A. brasilense* and *H. seropedicae* inoculation induced the expression of genes encoding nitrate transporter proteins (NRT1.11 and NRT3.1), NR, and NiR in maize. Similarly, Li et al. (2019) observed increased expression of *NRT2.1*, *NR* and *GS* in maize, along with several genes (*NRT1.1, NRT2.1, NRT2.3, NR, GS1, GOGAT*) in wheat, and others (*NRT1.3, NRT2.2, NR1, NiR, GS1, GOGAT*) in cucumber upon inoculation with *Paenibacillus beijingensis* BJ-18. *NRT* genes that were also significantly up-regulated in tomato grown in low-N and inoculated with diazotrophic *Enterobacter radicincitans* (Berger et al., 2013). Similar data was also reported in plant inoculation with beneficial fungi. Sherameti et al. (2005) showed that the inoculation of the endophytic fungus *Piriformospora indica* lead to up-regulation of *NR* gene expression, resulting in increased N accumulation in Arabidopsis and tobacco seedlings. It was also reported that the expression levels of *GS* and *NRT* genes were significantly higher in plants inoculated with the endophytic fungus *Phomopsis liquidambari* compared to uninoculated plants, under low-N (Yang et al., 2014). Notably, the enhanced expression of the genes involved in N metabolism was predominantly observed in plants inoculated and cultivated under low-N conditions rather than in those grown under high-N conditions, in accordance with the data obtained in our work.

Remarkably, functional analysis of homologs to the DEGs found in our studies, as well as other genes involved in N metabolism, lead to benefits to the plant similar to the ones provided by the PGPB. Studies on the overexpression of *AS* showed its positive impact on N uptake and assimilation, improving tolerance to N deficiency in rice (Lee et al., 2020) and greater tolerance to N limitation, accompanied by an increase in total free amino acids in *A. thaliana* (Lam et al., 2003). Ravazzolo et al. (2020) reported increased expression of genes like *GS* and

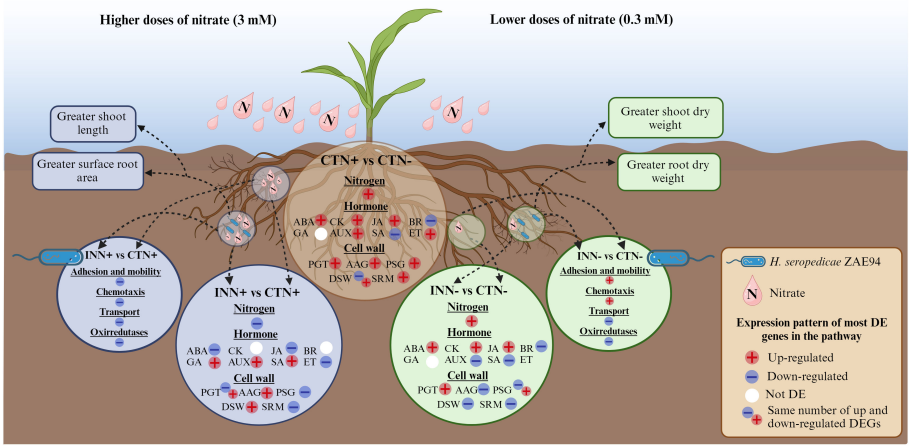

FIGURE 10
Schematic model for genetic controls modulated in response to maize - *H. seropedicae* – nitrogen interactions. This model presents a summary of the most relevant results for the differentially expressed pathways of maize plants inoculated with *H. seropedicae* ZAE94 (IN) or mock-inoculated (CT) and cultivated in 0.3 mM (N-) or 3 mM (N+) of N and promoting plant growth in each condition. See text for detailed discussion. Up-regulated (red colors) or down-regulated (blue colors). White Symbol represents that there were expressed genes in the pathway, but not differentially regulated. DE, differentially expressed; ABA, abscisic acid; GA, gibberellin; AUX, auxin; JA, jasmonic acid; SA, salicylic acid; BR, brassinosteroid; PGT, polysaccharide synthases and GT; AAG, assembly, architecture, and growth; PSG, pathways of substrate generation; DSW, differentiation and secondary wall; SRM, signaling and response mechanisms. Created with bioRender.com accessed on 01 December 2023.

BCA4 in maize roots when grown in the presence of N, contrasting with those grown without a N source. Transgenic maize constitutively overexpressing *GLN1-3*, which encodes a cytosolic GS, showed a 30% increase in grain number (Martin et al., 2006), while GS-deficient maize mutants showed a reduction in grain yield (Cañas et al., 2010). Additionally, overexpressing *DvGS1* improved growth and N utilization in *A. thaliana* (Zhu et al., 2014). Furthermore, overexpression of *AspAT* genes in rice led to altered N metabolism and increased amino acid and protein content in seeds. Our results, combined with data from the literature, demonstrate that the positive regulation of plant N metabolism genes can contribute to plant growth benefits. Given that inoculation of PGPB under low-N conditions positively regulated the expression of crucial genes in the N pathway, it can be inferred that reducing N doses for cultivation may lead to environmentally sustainable and economically viable agriculture.

Previous studies confirmed that inoculation of *H. seropedicae* promotes higher accumulation of N in the biomass of maize (de Araujo et al., 2013; Alves et al., 2015; Breda et al., 2019; Dias et al., 2021). Interestingly, the greatest effects of the inoculation of this diazotrophic bacteria, especially in the metabolism of N, are reported under conditions of low availability of N. In addition, the application of the ZAE94 strain in maize seeds using peat as a carrier modified the plant response to N fertilization in a hybrid genotype, significantly increasing grain yield, mainly at the lowest tested dose of 0.8 mM of N (Alves et al., 2015). Similarly, our results corroborate these previous studies, as they demonstrate a beneficial effect of inoculation at a low-N dose of 0.3 mM, by increasing maize root and shoot biomass (Figure 10).

From the bacterial side, genes related to N fixation were also regulated in *H. seropedicae* during association with maize. In the INN+ vs CTN+ comparison, three *nif genes* were identified, encoding proteins involved in the synthesis, maturation and assembly of the nitrogenase complex (Chubatsu et al., 2012). *nifW* and *nifX* were significantly induced, while *fixU* had the expression repressed. Although the transcriptional control of N fixation and assimilation are well described in *H. seropedicae* (Chubatsu et al., 2012), N fixation during grass-bacteria associations is still poorly understood. The *nifH* and *nifA* gene expression profiles were up-regulated in both doses of N (0.3 mM and 3 mM) in the inoculated samples compared to the control, suggesting that the bacteria fixes N_2 when associated with the plant. In addition, the expression levels of one of the components of the most studied two-component systems, the response regulators NtrC, and one of the main actors in the regulatory cascade that controls N metabolism in Proteobacteria, were up-regulated in plants inoculated under both doses of N.

The gene expression data showed that maize inoculation with the diazotrophic PGPB, *H. seropedicae*, reprogram both the plant and the bacteria N metabolism, with better responses in plants cultivated in low-N. It remains to be determined if the benefits observed to the plant are, at least in part, mediated by the direct transfer by the bacteria of the fixed N to the plant, or if it results from the ability of the PGPB to make N compounds available in the soil, to be assimilated by the plant.

4.2 Nitrogen-driven dynamics: orchestrating bacterial colonization and regulating plant defense hormonal pathways

Our findings may suggest that conditions of high N can have a negative effect on the stages of establishment and colonization by the bacteria, since the plant is in ideal growth conditions, developing independently of the beneficial association. In contrast, few DEGs were identified under low-N conditions, a regulatory profile that may be associated with a phase shift from bacterial colonization to an already well-established interaction (Figure 10).

During the establishment of the plant-bacteria interaction, the adhesion and host recognition stages are based on the release of signaling root exudates by the plants, which direct the free-swimming bacteria towards the roots (Balsanelli et al., 2016). In this study, three genes that encode LPS biosynthesis proteins had their expression reduced in INN+ vs CTN+. Previous studies have report that the attachment step of bacteria to the host roots is mediated by molecules of the bacterial cell envelope such as LPS, which actively contribute to early stages of the plant colonization process, being the first structures that contact the roots (Serrato et al., 2012; Balsanelli et al., 2016). In case of *H. seropedicae*, several studies reported that intact LPS is required for attachment and endophytic colonization of maize roots, since they are the outermost component of the outer membrane in Gram-negative bacteria (Balsanelli et al., 2010, 2013). The chemotaxis system acts through MCPs (Pereira et al., 2004). Two genes coding for MCPs, Hsero_1698 and Hsero_2164, had the expression increased in INN- vs CTN- comparison. Similar expression profiles of *MCP* genes were also observed in *H. seropedicae* SmR1 during the early stages of association with wheat roots (Pankievicz et al., 2016). The expression of several *MCPs* in *H. seropedicae* during maize colonization suggests that this endophytic bacterium could adapt its motility towards the host roots in response to different environmental signals, such as carbon sources, pH gradients and N availability (Balsanelli et al., 2016). Also, a gene involved in the flagellar formation, *flhF* was up-regulated in low N condition. Thus, our results indicate that, under low-N conditions, there is an increase in *MCP* gene expression in *H. seropedicae* ZAE94, suggesting that this induction has positive effects in bacterial motility and in the biosynthesis of flagella (Figure 10). In contrast, analysis of the INN+ vs CTN+ comparison revealed that *MCPs* genes were significantly repressed, and several genes that encode chemotaxis-related proteins were also down-regulated, suggesting that these experimental conditions may have a negative effect on the steps of establishment and colonization by bacteria (Figure 10). Similarly, repression of genes related to flagellar motility was also observed in INN+ vs CTN+ comparison, including down-regulation of flagellin gene *fliK*, as well as two genes involved in the formation of the flagellar basal body, *flgH* and *flgG*. The contrasting expression profile observed in response to the low-N and high-N conditions, could suggest that low N availability can generate a differential regulation, which

induces the occurrence of colonization at an early stage in this case. The same expression profile was also described in *H. seropedicae* associated with several crops such as maize, wheat and sugarcane, a few days after inoculation (Balsanelli et al., 2016; Pankievicz et al., 2016; Pessoa et al., 2021).

Our results provided a complete panorama of gene expression of *H. seropedicae* during colonization of maize roots and revealed insights into pathways involved in a plant-bacteria interaction at later stages after inoculation (18 DAI). Notably, few DEGs involved in adhesion, chemotaxis, mobility, transport and secretion systems were identified under 0.3 mM of N conditions, a regulatory profile that may be associated with a change from initial bacterial colonization for an already well-established interaction (Figure 10). Our results corroborate the idea that the set of adhesion genes expressed depends possibly on the stage of colonization. Considering Roncato-Maccari et al. (2003) reported the presence of *H. seropedicae* occupying a xylem vessel of a maize stem by light microscopy, 15 DAI, it can be assumed that at this stage of later colonization, the bacteria have passed the adhesion phase and are located in host intercellular spaces. Moreover, although initial bacteria-plant communication may involve bacterial chemotaxis for root exudates, genes of the chemotaxis system were down-regulated under low-N conditions and at a later stage of colonization, indicating that this function became dispensable in the presence of plant fluid. Repression of genes related to chemotaxis and flagellar assembly were also reported in *H. seropedicae* HRC54 (Pessoa et al., 2021) and *Nitrospirillum amazonense* CBAmC (Terra et al., 2020) in response to sugarcane apoplastic fluid, suggesting that this plant fluid provides the nutrients necessary for bacteria metabolism, avoiding energy expenditure on bacterial motility. In addition, data obtained here suggest a transition from a mobile to a sessile lifestyle since genes associated with cell motility were not differentially regulated. Flavonoids can also influence the bacterial colonization process, and may modulate motility of *H. seropedicae* in maize rhizosphere (Tadra-Sfeir et al., 2011, 2015). Tadra-Sfeir et al. (2015) reported that, in the presence of the flavonoid naringerin in maize roots, flagella biosynthesis genes were highly repressed in *H. seropedicae* SmR1, in addition to regulating the expression of genes involved in the synthesis of the bacterial cell wall during the early stages of association with maize roots (Tadra-Sfeir et al., 2011). Since flavonoids represent a large fraction of root exudates involved in root colonization, the down-regulation of flagellar genes might also represent a phase shift in the colonization process, from free-swimming to sessile lifestyle by adhering to the maize roots (Pankievicz et al., 2016). These results corroborate data from scanning electron microscopy that report the detection of mucilage halos surrounding *H. seropedicae* in several areas on maize and sorghum roots, indicating heavy colonization 12 DAI (Roncato-Maccari et al., 2003). Our results suggest that at 18 DAI, at later stages of colonization, bacteria would have developed changes in their motility system to adapt to endophytic life by reducing flagella gene expression (Figure 10).

From the plant side, a differential regulation was observed in the expression of some genes involved in the biosynthesis and signaling pathways of SA, BR and ABA, phytohormones known to be involved in responses to biotic stresses, in response to the inoculation depending on the dose of N (Figure 10). An induction on the expression of some genes involved in the SA pathway in comparison INN+ vs CTN+, and a repression of these genes in other comparisons, suggested a better plant-bacteria association at low-N. SA is derived from phenolic compounds and is involved in the response to pathogen attacks (Vlot et al., 2009; An and Mou, 2011). *WRKY40* is a pathogen-induced transcription factor that was repressed in INN- vs CTN- and induced in INN+ vs CTN+. Several studies have described an important participation of salicylic acid in the regulation of endophytic colonization and diversity of endophytic bacterial populations (Pinski et al., 2019), as well as its essential role in the recruitment of specific rhizosphere microbiomes has been reported (Zhu et al., 2022). BR participates in the regulation of plant developmental processes, but also triggers responses to environmental stresses (Bajguz et al., 2020). Although the regulation of a specific pathway was not observed, we observed the negative regulation of CYP51, which acts decisively in the activation of defense against pathogens (Nelson and Werck-Reichhart, 2011), both in INN- vs CTN- and in CTN+ vs CTN-. Thus, we could infer an impairment of the plant's basal defense response to beneficial inoculation. Some works have also demonstrated that the ABA pathway can be modulated by PGPB (Hardoim et al., 2019). Two genes involved in ABA biosynthesis were repressed CTN+ vs CTN-, but induced in the INN+ vs CTN+ comparison, *NCED9* and *AAO3* (Wang et al., 2016b), probably increasing ABA concentration in these plants. The repression of the ABA biosynthesis pathway observed in the CTN+ vs CTN- comparison demonstrates the need for N supplementation to ensure the growth of maize plants. Thus, the induction of this pathway observed in INN+ vs CTN+ may indicate that the combination of factors, inoculation and high dose of N, constitutes a stress for the plant by increasing ABA accumulation. In addition, *CYP707A* gene family plays a major regulatory role in controlling the level of ABA in plants, being involved in ABA catabolism (Kushiro et al., 2004). This gene was repressed in INN+ vs CTN+, suggesting an increase of ABA content in maize plants inoculated with *H. seropedicae* in 3 mM of N.

Taken together, our results demonstrate that the success of the plant-bacteria association depends on several factors, such as the perception of the nutritional status of the environment, which can trigger a more attenuated plant defense response in favorable conditions for this association; but also changes in bacterial metabolism through the specific regulation of genes involved in the plant-bacteria perception step (Figure 10).

4.3 Differential modulation of plant growth: integrating nitrogen levels with hormonal metabolism in plant-bacteria interactions

The experimental and environmental conditions applied in this work suggested that different doses of N fertilization differentially regulated the beneficial effects of bacterial inoculation. Modulation of plant hormones by PGPB can increase plant nutrient uptake and regulate stress responses, promoting plant growth (Glick, 2012). Also, most PGPB synthetize plant growth hormones. *A. brasilense*

Ab-V5 produces IAA and has strong plant growth-promoting capacity, leading to increase in auxin concentration, which possibly favors plant biomass and a change in root architecture (Zeffa et al., 2019). *H. seropedicae* produces auxin (IAA) and gibberellin (GA), implicated in various processes of plant growth and development (Irineu et al., 2022). Our work identified that Hsero_4278, which encodes the enzyme indolepyruvate ferredoxin oxidoreductase responsible for the conversion of indolepyruvate into IAA, was up-regulated in both N doses, but showed more pronounced levels in the comparison INN+ vs CTN+, suggesting that, after 18 DAI, the bacteria may be producing IAA under both N availability, but mainly under conditions of increased N availability.

From the plant side, our results showed that most of the hormone pathways have the same regulation in both CTN+ vs CTN- and INN- vs CTN- comparisons and are opposite to the regulation observed for INN+ vs CTN+ (Figure 10). This result suggests that inoculation with the bacteria at low-N could share similar positive effects in promoting plant growth and modulating hormonal pathways to those observed with high N fertilization. Our analyses suggested that auxin biosynthesis could be up-regulated in inoculated maize roots, cultivated with 3 mM of N. In the auxin signaling, the *Arabidopsis* ARF2 and ARF3 transcription factors are repressors of expression of auxin responsive genes (Finet et al., 2013). In inoculated maize plants, *ARF2* was repressed in the comparison INN+ vs CTN+, while *ARF3* was down-regulated in low-N (INN- vs CTN-). *ARF2* has previously been reported to be also repressed in rice in response to inoculation by *H. seropedicae* (Brusamarello-Santos et al., 2012). Furthermore, a global induction of auxin-responsive genes such as *GLP4*, *FRQ1* and *AVP1* were identified in the INN+ vs CTN+ comparison, suggesting that under elevated N conditions bacteria could be contributing to promotion of maize growth. In *Arabidopsis*, overexpression of *AVP1* increased auxin transport, resulting in robust root development (Li et al., 2005). These results suggest that inoculation of *H. seropedicae* can affect the repression of specific genes of the auxin signaling pathway that could be involved in the promotion of root growth. In addition, genetic repression of members of the auxin pathway may also be important for the bacteria inside the plant, negatively regulating the defense system. Further studies are necessary to elucidate whether and how the auxin pathway participates in plant-bacteria interactions.

Gibberellins can also promote cell elongation and division (Sauter and Kende, 1992). It is important to highlight that the gibberellin produced by PGPB could also contribute to increasing root hair density (Bottini et al., 2004). Hormonal quantification showed a higher content of the GA1 and GA3 forms of gibberellin in inoculated maize roots, while the maize genes involved in the GA biosynthesis appear to be almost all repressed (Irineu et al., 2022). This result suggested that the production of gibberellin occurred through the bacterial activity of *H. seropedicae*. However, in our results, we observed that *GA1*, *GA2* and *GA3* were induced in the comparison INN+ vs CTN+, suggesting that bacterial inoculation activated plant GA synthesis. Remarkably, at higher N concentrations, *H. seropedicae* promoted other benefits to the plant, such as shoot length growth, without gain of dry mass (Figure 9). *EXPA1* was also up-regulated in INN+ vs CTN+, suggesting changes in the chemical composition of the cell wall that could be possibly modulating root development in response to inoculation under N+, as observed in the overexpression of *EXPA1* in Arabidopsis mutant seedlings (Samalova et al., 2023). Thus, our molecular and phenotypic results suggested that under conditions of high N availability, and in the presence of *H. seropedicae*, there is growth promotion in maize plants, without gain of dry mass. Further cellular and biochemical experiments in plants inoculated in high and low-N are necessary to elucidate mechanisms involved in the differential biomass acquisition by bacterial inoculation in these two conditions, at the stage of plant-bacteria association analyzed in our experiments.

Cell walls constitute more than 50% of the weight of dry biomass, which is largely dependent on cell wall components (López-Malvar et al., 2022), being candidates to be contributing, at least in part, to the different phenotypes observed in plants inoculated in low and high-N (Ballesteros et al., 2021). In contrast to the patterns observed in N metabolism and the hormonal pathway, the set of DE genes in the different cell wall-related families did not show a similar regulation of genes between CTN + vs CTN- and INN- vs CTN- comparisons (Figure 10). Cellulose synthase and cellulose-like synthase genes related to primary and secondary wall formation can be differentially expressed according to tissue type (Cosgrove, 2005). Isoforms of the genes *ZmCESA1* to *ZmCESA9* are involved in the primary cell wall synthesis, while the genes *ZmCESA10* to *ZmCESA12*, and their isoforms, are associated with secondary cell wall biosynthesis (Penning et al., 2019; Kozlova et al., 2020). Our study showed that the *CESA9* gene is induced in plants inoculated with *H. seropedicae* at N+ concentrations, suggesting that the presence of bacteria in this condition may regulate the expression of genes related to greater deposition of cellulose in the root cell walls. On the other hand, the *CESA* genes (*CESA4, CESA7* and *CESA8*), involved in the secondary wall formation, were mainly induced in plants inoculated with *H. seropedicae* cultivated under low-N. In *A. thaliana*, $cesa4^{irx5\text{-}4}$, $cesa7^{irx3\text{-}7}$, and $cesa8^{irx1\text{-}7}$ mutants exhibit dark green leaves and inflorescence stems; reduced plant height, lower cellulose content and collapsed xylem (Kumar et al., 2017). Thus, our data suggests that the presence of bacteria in low-N condition may promote a greater deposition of cellulose in the root primary cell walls, leading to increase in biomass gain. The regulation of *CESA* genes through the association with beneficial bacteria was also observed in contrasting genotypes for BNF in sugarcane plants (Ballesteros et al., 2021). The genotype best associated with the PGPB showed regulation of genes involved in primary and secondary cell walls, in response to bacterial association, increasing the cellulose contents and non-cellulolytic components in the cell walls of root cells.

In addition, several genes correlated with root growth and the vascular pattern of the cotyledons were differently regulated, including *SKU5* gene which encodes a family of multi-copper oxidase-like proteins with cupredoxin domains similar to laccase and ascorbate oxidase (Zhang et al., 2021). Our data showed that the *SKS12* and *SKS13* genes were up-regulated in plants inoculated with *H. seropedicae* cultivated in high and low-N conditions, respectively, indicating that the bacteria would have an effect on the regulation of these genes, and that it could induce the formation of lateral roots and root elongation as shown in other studies (Sedbrook et al., 2002). The *sku5* mutant exhibits a phenotype of skewed and looped roots, suggesting that *SKU5* is required for directional root growth,

possibly via an effect on cell expansion (Sedbrook et al., 2002). Therefore, our findings showed that the bacteria induce different forms of growth depending on the nutritional availability of the soil in relation to the N concentration, either lengthening as seen in high N or increasing biomass as seen in low-N.

Several evidences suggest that PGPB can regulate the N metabolism of grasses, or promote greater efficiency in the use of N, contributing to the status of this nutrient in the plant (Carvalho et al., 2014; Breda et al., 2019; Zeffa et al., 2019). Our results provided the first integrated overview of differentially expressed genes in both maize and associated *H. seropedicae* ZAE94 in response to different N availability, revealing intricate biochemical and physiological mechanisms governing beneficial plant-microbe interactions. While existing studies have focused on early plant recognition and colonization stages by *H. seropedicae*, our research sheds light on the transcriptional profile of *H. seropedicae* during the later stages of the association when the plant-bacteria interaction is well established. Taken together, our results demonstrate that the efficiency of a plant-bacteria association depends on several factors, such as the perception of the nutritional status of the environment and changes in plant and bacterial metabolism, which can form a combined response, leading to a more improved association and ensuring the promotion of plant growth and adaptation (Figure 10). The data provide a valuable contribution to how different N doses can alter the metabolism of maize and *H. seropedicae*. Our results corroborate several studies that propose that PGPB inoculation can lead to an increase in NUE, improving nutrient absorption and increasing dry matter, reducing dependence on synthetic N fertilizers. A further understanding of the relationship between plant-bacteria-environment signaling could potentially offer sustainable alternatives to reduce chemical fertilizers dependence in agriculture.

Data availability statement

The original contributions presented in the study are included in the article/Supplementary Files, further inquiries can be directed to the corresponding author/s.

Author contributions

AR: Data curation, Investigation, Methodology, Writing – original draft, Writing – review & editing. MU: Data curation, Methodology, Validation, Writing – original draft, Writing – review & editing. FT: Writing – original draft. HF: Writing – original draft. EO: Writing – original draft. AH: Funding acquisition, Supervision, Writing – review & editing.

Funding

The author(s) declare that financial support was received for the research, authorship, and/or publication of this article. The research was supported by Instituto Nacional de Ciência de Tecnologia (INCT) in Biological Nitrogen Fixation, Conselho Nacional de Desenvolvimento Científico e Tecnológico (CNPq), Fundação Carlos Chagas Filho de Amparo à Pesquisa do Estado do Rio de Janeiro (FAPERJ), Coordenação de Aperfeiçoamento de Pessoal de Nível Superior (CAPES) and Newton Fund grant (BB/N013476/1). AR and MU were supported by CNPq PhD fellowships. FT supported by CAPES posdoctoral fellowships. HF and EO were supported by FAPERJ posdoctoral fellowships. AH received support from a CNPq research grant.

Conflict of interest

The authors declare that the research was conducted in the absence of any commercial or financial relationships that could be construed as a potential conflict of interest.

Publisher's note

Supplementary material

The Supplementary Material for this article can be found online at: https://www.frontiersin.org/articles/10.3389/fpls.2024.1346523/full#supplementary-material

References

Albrecht, C., Boutrot, F., Segonzac, C., Schwessinger, B., Gimenez-Ibanez, S., Chinchilla, D., et al. (2012). Brassinosteroids inhibit pathogen-associated molecular pattern–triggered immune signaling independent of the receptor kinase BAK1. *Proc Natl Acad Sci USA*. 109 (1), 303–308. doi: 10.1073/pnas.1109921108

Alves, G. C., Dos Santos, C. L. R., Zilli, J. E., Dos Reis Junior, F. B., Marriel, I. E., da F. Breda, F. A., et al. (2021). Agronomic evaluation of Herbaspirillum seropedicae strain ZAE94 as an inoculant to improve maize yield in Brazil. *Pedosphere* 31, 583–595. doi: 10.1016/S1002-0160(21)60004-8

Alves, G. C., Videira, S. S., Urquiaga, S., and Reis, V. M. (2015). Differential plant growth promotion and nitrogen fixation in two genotypes of maize by several Herbaspirillum inoculants. *Plant Soil* 387, 307–321. doi: 10.1007/s11104-014-2295-2

An, C., and Mou, Z. (2011). Salicylic acid and its function in plant immunityF. *J. Integr. Plant Biol.* 53, 412–428. doi: 10.1111/j.1744-7909.2011.01043.x

Anders, S., and Huber, W. (2010). Differential expression analysis for sequence count data. *Nature Precedings*. doi: 10.1038/npre.2010.4282.2

Bajguz, A., Chmur, M., and Gruszka, D. (2020). Comprehensive overview of the brassinosteroid biosynthesis pathways: substrates, products, inhibitors, and connections 11. doi: 10.3389/fpls.2020.01034

Baldani, V. L. D., de B. Alvarez, M. A., Baldani, J. I., and Döbereiner, J. (1986). "Establishment of inoculated *Azospirillum* spp. in the rhizosphere and in roots of field grown wheat and sorghum," in *Nitrogen Fixation with Non-Legumes: The Third International Symposium on Nitrogen Fixation with Non-legumes, Helsinki, 2–8 September 1984*. Eds. F. A. Skinner and P. Uomala (Springer Netherlands, Dordrecht), 35–46.

Ballesteros, H. G. F., Rosman, A. C., Carvalho, T. L. G., Grativol, C., and Hemerly, A. S. (2021). Cell wall formation pathways are differentially regulated in sugarcane contrasting genotypes associated with endophytic diazotrophic bacteria. *Planta* 254, 109. doi: 10.1007/s00425-021-03768-0

Balsanelli, E., Serrato, R. V., de Baura, V. A., Sassaki, G., Yates, M. G., Rigo, L. U., et al. (2010). Herbaspirillum seropedicae rfbB and rfbC genes are required for maize colonization. *Environ. Microbiol.* 12, 2233–2244. doi: 10.1111/j.1462-2920.2010.02187.x

Balsanelli, E., Tadra-Sfeir, M. Z., Faoro, H., Pankievicz, V. C., de Baura, V. A., Pedrosa, F. O., et al. (2016). Molecular adaptations of Herbaspirillum seropedicae during colonization of the maize rhizosphere. *Environ. Microbiol.* 18, 2343–2356. doi: 10.1111/1462-2920.12887

Balsanelli, E., Tuleski, T. R., de Baura, V. A., Yates, M. G., Chubatsu, L. S., de Oliveira Pedrosa, F., et al. (2013). Maize Root Lectins Mediate the Interaction with Herbaspirillum seropedicae via N-Acetyl Glucosamine Residues of Lipopolysaccharides. *PloS One* 8, e77001. doi: 10.1371/journal.pone.0077001

Bari, R., and Jones, J. D. (2009). Role of plant hormones in plant defence responses. *Plant Mol. Biol.* 69, 473–488. doi: 10.1007/s11103-008-9435-0

Bauhus, J., and Messier, C. (1999). Evaluation of Fine Root Length and diameter measurements obtained using RHIZO image analysis. *Agron. J.* 91, 142–147. doi: 10.2134/agronj1999.00021962009100010022x

Berger, B., Brock, A. K., and Ruppel, S. (2013). Nitrogen supply influences plant growth and transcriptional responses induced by Enterobacter radicincitans in Solanum lycopersicum. *Plant Soil* 370, 641–652. doi: 10.1007/s11104-013-1633-0

Berthrong, S. T., Yeager, C. M., Gallegos-Graves, L., Steven, B., Eichorst, S. A., Jackson, R. B., et al. (2014). Nitrogen fertilization has a stronger effect on soil nitrogen-fixing bacterial communities than elevated atmospheric CO2. *Appl. Environ. Microbiol.* 80, 3103. doi: 10.1128/AEM.04034-13

Bottini, R., Cassán, F., and Piccoli, P. (2004). Gibberellin production by bacteria and its involvement in plant growth promotion and yield increase. *Appl. Microbiol. Biotechnol.* 65, 497–503. doi: 10.1007/s00253-004-1696-1

Bouma, T. J., Nielsen, K. L., and Koutstaal, B. (2000). Sample preparation and scanning protocol for computerised analysis of root length and diameter. *Plant Soil* 218, 185–196. doi: 10.1023/A:1014905104017

Breda, F., Alves, G., and Reis, V. (2016). Produtividade de milho na presença de doses de N e de inoculação de Herbaspirillum seropedicae. *Pesquisa. Agropecuaria. Bras.* 51, 45–52. doi: 10.1590/S0100-204X2016000100006

Breda, F., da Silva, T. F. R., dos Santos, S. G., Alves, G. C., and Reis, V. M. (2019). Modulation of nitrogen metabolism of maize plants inoculated with Azospirillum brasilense and Herbaspirillum seropedicae. *Arch. Microbiol.* 201, 547–558. doi: 10.1007/s00203-018-1594-z

Brookbank, B. P., Patel, J., Gazzarrini, S., and Nambara, E. (2021). Role of basal ABA in plant growth and development. *Genes (Basel).* 12, 1-22. doi: 10.3390/genes12121936

Brusamarello-Santos, L. C. C., Alberton, D., Valdameri, G., Camilios-Neto, D., Covre, R., Lopes, K., et al. (2019). Modulation of defence and iron homeostasis genes in rice roots by the diazotrophic endophyte Herbaspirillum seropedicae. *Sci. Rep.* 9, 10573. doi: 10.1038/s41598-019-45866-w

Brusamarello-Santos, L. C. C., Pacheco, F., Aljanabi, S. M. M., Monteiro, R. A., Cruz, L. M., Baura, V. A., et al. (2012). Differential gene expression of rice roots inoculated with the diazotroph Herbaspirillum seropedicae. *Plant Soil* 356, 113–125. doi: 10.1007/s11104-011-1044-z

Cañas, R. A., Quilleré, I., Lea, P. J., and Hirel, B. (2010). Analysis of amino acid metabolism in the ear of maize mutants deficient in two cytosolic glutamine synthetase isoenzymes highlights the importance of asparagine for nitrogen translocation within sink organs. *Plant Biotechnol. J.* 8, 966–978. doi: 10.1111/j.1467-7652.2010.00524.x

Canellas, L. P., Balmori, D. M., Médici, L. O., Aguiar, N. O., Campostrini, E., Rosa, R. C. C., et al. (2013). A combination of humic substances and Herbaspirillum seropedicae inoculation enhances the growth of maize (Zea mays L.). *Plant Soil* 366, 119–132. doi: 10.1007/s11104-012-1382-5

Carvalho, T. L. G., Ballesteros, H. G. F., Thiebaut, F., Ferreira, P. C. G., and Hemerly, A. S. (2016). Nice to meet you: genetic, epigenetic and metabolic controls of plant perception of beneficial associative and endophytic diazotrophic bacteria in non-leguminous plants. *Plant Mol. Biol.* 90, 561–574. doi: 10.1007/s11103-016-0435-1

Carvalho, T. L. G., Balsemão-Pires, E., Saraiva, R. M., Ferreira, P. C. G., and Hemerly, A. S. (2014). Nitrogen signalling in plant interactions with associative and endophytic diazotrophic bacteria. *J. Exp. Bot.* 65, 5631–5642. doi: 10.1093/jxb/eru319

Carvalho, T. L. G., Rosman, A. C., Grativol, C., de, M. N. E., Baldani, J. I., and Hemerly, A. S. (2022). Sugarcane genotypes with contrasting biological nitrogen fixation efficiencies differentially modulate nitrogen metabolism, auxin signaling, and microorganism perception pathways. *Plants (Basel).* 11, 1-31. doi: 10.3390/plants11151971

Chan, Z. (2012). Expression profiling of ABA pathway transcripts indicates crosstalk between abiotic and biotic stress responses in Arabidopsis. *Genomics* 100, 110–115. doi: 10.1016/j.ygeno.2012.06.004

Chen, C., Zhang, Y., Cai, J., Qiu, Y., Li, L., Gao, C., et al. (2023). Multi-copper oxidases SKU5 and SKS1 coordinate cell wall formation using apoplastic redox-based reactions in roots. *Plant Physiol.* 192, 2243–2260. doi: 10.1093/plphys/kiad207

Chiang, C. S., Stacey, G., and Tsay, Y. F. (2004). Mechanisms and functional properties of two peptide transporters, AtPTR2 and fPTR2. *J. Biol. Chem.* 279, 30150–30157. doi: 10.1074/jbc.M405192200

Chubatsu, L. S., Monteiro, R. A., de Souza, E. M., de Oliveira, M. A. S., Yates, M. G., Wassem, R., et al. (2012). Nitrogen fixation control in Herbaspirillum seropedicae. *Plant Soil* 356, 197–207. doi: 10.1007/s11104-011-0819-6

Cohen, A. C., Bottini, R., Pontin, M., Berli, F. J., Moreno, D., Boccanlandro, H., et al. (2015). Azospirillum brasilense ameliorates the response of Arabidopsis thaliana to drought mainly via enhancement of ABA levels. *Physiol. Plant* 153, 79–90. doi: 10.1111/ppl.12221

Cosgrove, D. J. (2005). Growth of the plant cell wall. *Nat. Rev. Mol. Cell Biol.* 6, 850–861. doi: 10.1038/nrm1746

Curá, J. A., Franz, D. R., Filosofía, J. E., Balestrasse, K. B., and Burgueño, L. E. (2017). Inoculation with Azospirillum sp. and Herbaspirillum sp. Bacteria Increases the Tolerance of Maize to Drought Stress. *Microorganisms*. 5 (3), 41. doi: 10.3390/microorganisms5030041

David, L. C., Berquin, P., Kanno, Y., Seo, M., Daniel-Vedele, F., and Ferrario-Méry, S. (2016). N availability modulates the role of NPF3.1, a gibberellin transporter, in GA-mediated phenotypes in Arabidopsis. *Planta* 244, 1315–1328. doi: 10.1007/s00425-016-2588-1

de Araujo, F. F., Simoneti Foloni, J. S., Wutzke, M., da Silva Melegari, A., and Rack, E. (2013). Híbridos e variedades de milho submetidos à inoculação de sementes com Herbaspirillum seropedicae. *Semina.: Ciências. Agrárias.* 34, 1043–1053. doi: 10.5433/1679-0359.2013v34n3p1043-1054

de Azevedo, I. G., Olivares, F. L., Ramos, A. C., Bertolazi, A. A., and Canellas, L. P. (2019). Humic acids and Herbaspirillum seropedicae change the extracellular H+ flux and gene expression in maize roots seedlings. *Chem. Biol. Technol. Agric.* 6, 8. doi: 10.1186/s40538-019-0149-0

de Carvalho, T. L. G., Ferreira, P. C. G., and Hemerly, A. S. (2011). Sugarcane genetic controls involved in the association with beneficial endophytic nitrogen fixing bacteria. *Trop. Plant Biol.* 4, 31–41. doi: 10.1007/s12042-011-9069-2

Dias, A. C., Alves, G. C., Da Silva, T. F. R., Alves, B. J. R., Santos, L. A., and Reis, V. M. (2021). Comparison of N uptake of maize inoculated with two diazotrophic bacterial species grown under two N levels. *Arch. Agron. Soil Sci.* 68 (6), 1–17. doi: 10.1080/03650340.2021.1922672

Di Benedetto, N. A., Corbo, M. R., Campaniello, D., Cataldi, M. P., Bevilacqua, A., Sinigaglia, M., et al. (2017). The role of Plant Growth Promoting Bacteria in improving nitrogen use efficiency for sustainable crop production: a focus on wheat. *AIMS. Microbiol.* 3, 413–434. doi: 10.3934/microbiol.2017.3.413

Ding, J., Jiang, X., Guan, D., Zhao, B., Ma, M., Zhou, B., et al. (2017). Influence of inorganic fertilizer and organic manure application on fungal communities in a long-term field experiment of Chinese Mollisols. *Appl. Soil Ecol.* 111, 114–122. doi: 10.1016/j.apsoil.2016.12.003

Dudeja, S. S., Suneja-Madan, P., Paul, M., Maheswari, R., and Kothe, E. (2021). Bacterial endophytes: Molecular interactions with their hosts. *J. Basic. Microbiol.* 61, 475–505. doi: 10.1002/jobm.202000657

Engelsdorf, T., Gigli-Bisceglia, N., Veerabagu, M., McKenna, J. F., Vaahtera, L., Augstein, F., et al. (2018). The plant cell wall integrity maintenance and immune signaling systems cooperate to control stress responses in Arabidopsis thaliana. *Sci. Signaling* 11, eaao3070. doi: 10.1126/scisignal.aao3070

Eulgem, T., and Somssich, I. E. (2007). Networks of WRKY transcription factors in defense signaling. *Curr. Opin. Plant Biol.* 10, 366–371. doi: 10.1016/j.pbi.2007.04.020

Fan, K., Delgado-Baquerizo, M., Guo, X., Wang, D., Wu, Y., Zhu, M., et al. (2019). Suppressed N fixation and diazotrophs after four decades of fertilization. *Microbiome* 7, 143. doi: 10.1186/s40168-019-0757-8

FAOSTAT (2024a). *Fertilizers by nutrients*. . Available at: https://www.fao.org/food-agriculture-statistics/en/.

FAOSTAT (2024b). *Food and agriculture organization of the united nations statistics division - Maize*. Available at: https://www.fao.org/food-agriculture-statistics/en/.

Finet, C., Berne-Dedieu, A., Scutt, C. P., and Marlétaz, F. (2013). Evolution of the ARF gene family in land plants: old domains, new tricks. *Mol. Biol. Evol.* 30, 45–56. doi: 10.1093/molbev/mss220

Friedberg, E. C., Walker, G. C., and Siede, W. (1995). DNA repair and mutagenesis. *Nature*. 421 (6921), 436–440. doi: 10.1038/nature01408

Gaspareto, R. N., Jalal, A., Ito, W. C. N., Oliveira, C., Garcia, C., Boleta, E. H. M., et al. (2023). Inoculation with plant growth-promoting bacteria and nitrogen doses improves wheat productivity and nitrogen use efficiency. *Microorganisms*. 11 (4), 1046. doi: 10.3390/microorganisms11041046

Glick, B. R. (2012). Plant growth-promoting bacteria: mechanisms and applications. *Scientifica* 2012, 963401. doi: 10.6064/2012/963401

Goodstein, D. M., Shu, S., Howson, R., Neupane, R., Hayes, R. D., Fazo, J., et al. (2012). Phytozome: a comparative platform for green plant genomics. *Nucleic Acids Res.* 40, D1178–D1186. doi: 10.1093/nar/gkr944

Grillo-Puertas, M., Villegas, J. M., Pankievicz, V. C. S., Tadra-Sfeir, M. Z., Teles Mota, F. J., Hebert, E. M., et al. (2021). Transcriptional responses of herbaspirillum seropedicae to environmental phosphate concentration 12. doi: 10.3389/fmicb.2021.666277

Gyaneshwar, P., James, E. K., Reddy, P. M., and Ladha, J. K. (2002). Herbaspirillum colonization increases growth and nitrogen accumulation in aluminium-tolerant rice varieties. *New Phytol.* 154, 131–145. doi: 10.1046/j.1469-8137.2002.00371.x

Hajiahmadi, Z., Abedi, A., Wei, H., Sun, W., Ruan, H., Zhuge, Q., et al. (2020). Identification, evolution, expression, and docking studies of fatty acid desaturase genes in wheat (Triticum aestivum L.). *BMC Genomics* 21, 778. doi: 10.1186/s12864-020-07199-1

Hamid, B., Zaman, M., Farooq, S., Fatima, S., Sayyed, R. Z., Baba, Z. A., et al. (2021). Bacterial plant biostimulants: A sustainable way towards improving growth, productivity, and health of crops. *Sustainability*. 13 (5), 2856. doi: 10.3390/su13052856

Hardoim, P., Carvalho, T., Ballesteros, H., Rabelo, D., Rojas, C., Venancio, T., et al. (2019). Genome-wide transcriptome profiling provides insights into the responses of maize (Zea mays L.) to diazotrophic bacteria. *Plant Soil.* 451, 121–143. doi: 10.1007/s11104-019-04193-9

Hoagland, D. R., and Arnon, D. I. (1950). *The water culture method for growing plants without soils*. Berkeley: California Agricultural Experimental Station.

Höfte, H., and Voxeur, A. (2017). Plant cell walls. *Curr. Biol.* 27, R865–r870. doi: 10.1016/j.cub.2017.05.025

Hoopes, G. M., Hamilton, J. P., Wood, J. C., Esteban, E., Pasha, A., Vaillancourt, B., et al. (2019). An updated gene atlas for maize reveals organ-specific and stress-induced genes. *Plant J.* 97, 1154–1167. doi: 10.1111/tpj.14184

Hudson, D., Guevara, D., Yaish, M. W., Hannam, C., Long, N., Clarke, J. D., et al. (2011). GNC and CGA1 modulate chlorophyll biosynthesis and glutamate synthase (GLU1/Fd-GOGAT) expression in Arabidopsis. *PloS One* 6, e26765. doi: 10.1371/journal.pone.0026765

Hwang, I. S., An, S. H., and Hwang, B. K. (2011). Pepper asparagine synthetase 1 (CaAS1) is required for plant nitrogen assimilation and defense responses to microbial pathogens. *Plant J.* 67, 749–762. doi: 10.1111/j.1365-313X.2011.04622.x

Irineu, L., Soares, C. P., Soares, T. S., Almeida, F. A., Almeida-Silva, F., Gazara, R. K., et al. (2022). Multiomic approaches reveal hormonal modulation and nitrogen uptake and assimilation in the initial growth of maize inoculated with herbaspirillum seropedicae. *Plants (Basel).* 12, 1–21. doi: 10.3390/plants12010048

Jiang, Z., Liu, X., Peng, Z., Wan, Y., Ji, Y., He, W., et al. (2011). AHD2.0: an update version of Arabidopsis Hormone Database for plant systematic studies. *Nucleic Acids Res.* 39, D1123–D1129. doi: 10.1093/nar/gkq1066

Kanter, D. R. (2018). Nitrogen pollution: a key building block for addressing climate change. *Climatic. Change* 147, 11–21. doi: 10.1007/s10584-017-2126-6

Kechid, M., Desbrosses, G., Rokhsi, W., Varoquaux, F., Djekoun, A., and Touraine, B. (2013). The NRT2.5 and NRT2.6 genes are involved in growth promotion of Arabidopsis by the plant growth-promoting rhizobacterium (PGPR) strain Phyllobacterium brassicacearum STM196. *New Phytol.* 198, 514–524. doi: 10.1111/nph.12158

Keeler, B. L., Gourevitch, J. D., Polasky, S., Isbell, F., Tessum, C. W., Hill, J. D., et al. (2016). The social costs of nitrogen. *Sci Adv.* 2, 10. doi: 10.1126/sciadv.1600219

Kim, D., Pertea, G., Trapnell, C., Pimentel, H., Kelley, R., and Salzberg, S. L. (2013). TopHat2: accurate alignment of transcriptomes in the presence of insertions, deletions and gene fusions. *Genome Biol.* 14, R36. doi: 10.1186/gb-2013-14-4-r36

Kozlova, L. V., Nazipova, A. R., Gorshkov, O. V., Petrova, A. A., and Gorshkova, T. A. (2020). Elongating maize root: zone-specific combinations of polysaccharides from type I and type II primary cell walls. *Sci. Rep.* 10, 10956. doi: 10.1038/s41598-020-67782-0

Kumar, M., Atanassov, I., and Turner, S. (2017). Functional analysis of cellulose synthase (CESA) protein class specificity. *Plant Physiol.* 173, 970–983. doi: 10.1104/pp.16.01642

Kushiro, T., Okamoto, M., Nakabayashi, K., Yamagishi, K., Kitamura, S., Asami, T., et al. (2004). The Arabidopsis cytochrome P450 CYP707A encodes ABA 8'-hydroxylases: key enzymes in ABA catabolism. *EMBO J.* 23, 1647–1656. doi: 10.1038/sj.emboj.7600121

Ladha, J. K., Tirol-Padre, A., Reddy, C. K., Cassman, K. G., Verma, S., Powlson, D. S., et al. (2016). Global nitrogen budgets in cereals: A 50-year assessment for maize, rice and wheat production systems. *Sci. Rep.* 6, 19355. doi: 10.1038/srep19355

Lam, H.-M., Wong, P., Chan, H.-K., Yam, K.-M., Chen, L., Chow, C.-M., et al. (2003). Overexpression of the ASN1 Gene enhances nitrogen status in seeds of arabidopsis. *Plant Physiol.* 132, 926. doi: 10.1104/pp.103.020123

Lee, S., Park, J., Lee, J., Shin, D., Marmagne, A., Lim, P. O., et al. (2020). OsASN1 overexpression in rice increases grain protein content and yield under nitrogen-limiting conditions. *Plant Cell Physiol.* 61, 1309–1320. doi: 10.1093/pcp/pcaa060

Leisner, C. P., Potnis, N., and Sanz-Saez, A. (2023). Crosstalk and trade-offs: Plant responses to climate change-associated abiotic and biotic stresses. *Plant Cell Environ.* 46, 2946–2963. doi: 10.1111/pce.14532

Li, H., and Durbin, R. (2010). Fast and accurate long-read alignment with Burrows-Wheeler transform. *Bioinformatics* 26, 589–595. doi: 10.1093/bioinformatics/btp698

Li, H., Hu, B., and Chu, C. (2017). Nitrogen use efficiency in crops: lessons from Arabidopsis and rice. *J. Exp. Bot.* 68, 2477–2488. doi: 10.1093/jxb/erx101

Li, Y., Li, Y., Zhang, H., Wang, M., and Chen, S. (2019). Diazotrophic paenibacillus beijingensis BJ-18 provides nitrogen for plant and promotes plant growth, nitrogen uptake and metabolism 10, 1119. doi: 10.3389/fmicb.2019.01119

Li, J., Wang, X., Wang, X., Ma, P., Yin, W., Wang, Y., et al. (2020). Hydrogen sulfide promotes hypocotyl elongation via increasing cellulose content and changing the arrangement of cellulose fibrils in alfalfa. *J. Exp. Bot.* 71, 5852–5864. doi: 10.1093/jxb/eraa318

Li, J., Yang, H., Peer, W. A., Richter, G., Blakeslee, J., Bandyopadhyay, A., et al. (2005). Arabidopsis H+-PPase AVP1 regulates auxin-mediated organ development. *Science* 310, 121–125. doi: 10.1126/science.1115711

Livak, K. J., and Schmittgen, T. D. (2001). Analysis of relative gene expression data using real-time quantitative PCR and the 2(-Delta Delta C(T)) Method. *Methods* 25, 402–408. doi: 10.1006/meth.2001.1262

López-Malvar, A., Santiago, R., Souto, X. C., et al. (2022). Cell Wall Composition Impacts Structural Characteristics of the Stems and Thereby Biomass Yield. *Journal of Agricultural and Food Chemistry*. doi: 10.1021/acs.jafc.1c06986

Martin, A., Lee, J., Kichey, T., Gerentes, D., Zivy, M., Tatout, C., et al. (2006). Two cytosolic glutamine synthetase isoforms of maize are specifically involved in the control of grain production. *Plant Cell* 18, 3252. doi: 10.1105/tpc.106.042689

Mateo-Sagasta, J., Zadeh, S. M., Turral, H., and Burke, J. (2017). *Water pollution from agriculture: a global review. Executive summary*. (Rome, Italy: FAO).

Monteiro, N. K., Aranda-Selverio, G., Exposti, D. T. D., Silva, M., Lemos, E. G. M., Campanharo, J. C., et al. (2012). Caracterização química dos géis produzidos pelas bactérias diazotróficas Rhizobium tropici e Mesorhizobium sp. *Química. Nova.* 35, 705–708. doi: 10.1590/S0100-40422012000400009

Monteiro, R. A., Schmidt, M. A., Baura, V., Balsanelli, E., Wassem, R., Yates, M. G., et al. (2008). Early colonization pattern of maize (Zea mays L. Poales, Poaceae) roots by Herbaspirillum seropedicae (Burkholderiales, Oxalobacteraceae). *Genet. Mol. Biol.* 31 (4), 932–937. doi: 10.1590/S1415-47572008005000007

Mueller, S. M., Messina, C. D., and Vyn, T. J. (2019). Simultaneous gains in grain yield and nitrogen efficiency over 70 years of maize genetic improvement. *Sci. Rep.* 9, 9095. doi: 10.1038/s41598-019-45485-5

Nadeem, M., Amjad Nawaz, M., Shahid, M. Q., Doğan, Y., comertpay, G., Yildiz, M., et al. (2018). DNA Molecular markers in plant breeding; Current status and recent advancements in genomic selection and genome editing. *Biotechnol. Biotechnol. Equip.* 32, 261–285. doi: 10.1080/13102818.2017.1400401

Nelson, D., and Werck-Reichhart, D. (2011). A P450-centric view of plant evolution. *Plant J.* 66, 194–211. doi: 10.1111/j.1365-313X.2011.04529.x

Nunes, R., Domiciano Abrahão, G., de Sousa Alves, W., Aparecida de Oliveira, J., César Sousa Nogueira, F., Pasqualoto Canellas, L., et al. (2021). Quantitative proteomic analysis reveals altered enzyme expression profile in Zea mays roots during the early stages of colonization by Herbaspirillum seropedicae. *Proteomics*. 21, 7-8, 2000129. doi: 10.1002/pmic.202000129

Olivares, F. L., Baldani, V. L. D., Reis, V. M., Baldani, J. I., and Döbereiner, J. (1996). Occurrence of the endophytic diazotrophs Herbaspirillum spp. in roots, stems, and leaves, predominantly of Gramineae. *Biol. Fertil. Soils.* 21, 197–200. doi: 10.1007/BF00335935

Pankievicz, V. C. S., Camilios-Neto, D., Bonato, P., Balsanelli, E., Tadra-Sfeir, M. Z., Faoro, H., et al. (2016). RNA-seq transcriptional profiling of Herbaspirillum seropedicae colonizing wheat (Triticum aestivum) roots. *Plant Mol. Biol.* 90, 589–603. doi: 10.1007/s11103-016-0430-6

Pankievicz, V. C. S., do Amaral, F. P., Ané, J.-M., and Stacey, G. (2021). Diazotrophic bacteria and their mechanisms to interact and benefit cereals. *Mol. Plant-Microbe Interactions®*. 34, 491–498. doi: 10.1094/MPMI-11-20-0316-FI. MPMI-11-20-0316-FI.

Pedrosa, F. O., Monteiro, R. A., Wassem, R., Cruz, L. M., Ayub, R. A., Colauto, N. B., et al. (2011). Genome of herbaspirillum seropedicae strain smR1, a specialized diazotrophic endophyte of tropical grasses. *PloS Genet.* 7, e1002064. doi: 10.1371/journal.pgen.1002064

Penning, B. W., McCann, M. C., and Carpita, N. C. (2019). Evolution of the cell wall gene families of grasses 10. doi: 10.3389/fpls.2019.01205

Pereira, M., Parente, J. A., Bataus, L. A., Cardoso, D., Soares, R. B., and Soares, C. M. (2004). Chemotaxis and flagellar genes of Chromobacterium violaceum. *Genet. Mol. Res.* 3, 92–101.

Pessoa, D. D. V., Dos-Santos, C. M., Vidal, M. S., Baldani, J. I., Tadra-Sfeir, M. Z., de Souza, E. M., et al. (2021). Herbaspirillum seropedicae strain HRC54 expression profile in response to sugarcane apoplastic fluid. *3 Biotech.* 11, 292. doi: 10.1007/s13205-021-02848-y

Pinski, A., Betekhtin, A., Hupert-Kocurek, K., Mur, L. A. J., and Hasterok, R. (2019). Defining the genetic basis of plant–endophytic bacteria interactions. *Int. J. Mol. Sci.* 20 (8), 1947. doi: 10.3390/ijms20081947

Qin, H., Pandey, B. K., Li, Y., Huang, G., Wang, J., Quan, R., et al. (2022). Orchestration of ethylene and gibberellin signals determines primary root elongation in rice. *Plant Cell* 34, 1273–1288. doi: 10.1093/plcell/koac008

Ravazzolo, L., Trevisan, S., Forestan, C., Varotto, S., Sut, S., Dall'Acqua, S., et al. (2020). Nitrate and ammonium affect the overall maize response to nitrogen availability by triggering specific and common transcriptional signatures in roots. *Int. J. Mol. Sci.* 21 (2), 686. doi: 10.3390/ijms21020686

Reis, V. M., Alves, G. C., Marriel, I. E., Júnior, F. B. R., and Zilli, J. E. (2010). *Recomendação de inoculante para cultura de milho utilizando a bactéria Herbaspirillum seropedicae, estirpe BR11417*. (Seropédica: Embrapa Agrobiologia. Comunicado Técnico 129).

Rentsch, D., Laloi, M., Rouhara, I., Schmelzer, E., Delrot, S., and Frommer, W. B. (1995). NTR1 encodes a high affinity oligopeptide transporter in Arabidopsis. *FEBS Lett.* 370, 264–268. doi: 10.1016/0014-5793(95)00853-2

Reymond, P., and Farmer, E. E. (1998). Jasmonate and salicylate as global signals for defense gene expression. *Curr. Opin. Plant Biol.* 1, 404–411. doi: 10.1016/S1369-5266(98)80264-1

Richetti, A., and Ceccon, G. (2020). Viabilidade econômica da cultura do milho safrinha 2021, em Mato Grosso do Sul. *EMBRAPA. - COMUNICADO. TÉCNICO.* 12, 1-12.

Roncato-Maccari, L. D., Ramos, H. J., Pedrosa, F. O., Alquini, Y., Chubatsu, L. S., Yates, M. G., et al. (2003). Endophytic *Herbaspirillum* seropedicae expresses nif genes in gramineous plants. *FEMS Microbiol. Ecol.* 45, 39–47. doi: 10.1016/S0168-6496(03)00108-9

Samalova, M., Melnikava, A., Elsayad, K., Peaucelle, A., Gahurova, E., Gumulec, J., et al. (2023). Hormone-regulated expansins: Expression, localization, and cell wall biomechanics in Arabidopsis root growth. *Plant Physiol.* 194 (1), 209–228. doi: 10.1093/plphys/kiad228

Sauter, M., and Kende, H. (1992). Gibberellin-induced growth and regulation of the cell division cycle in deepwater rice. *Planta* 188, 362–368. doi: 10.1007/BF00192803

Sedbrook, J. C., Carroll, K. L., Hung, K. F., Masson, P. H., and Somerville, C. R. (2002). The Arabidopsis SKU5 gene encodes an extracellular glycosyl phosphatidylinositol-anchored glycoprotein involved in directional root growth. *Plant Cell* 14, 1635–1648. doi: 10.1105/tpc.002360

Seo, M., and Koshiba, T. (2002). Complex regulation of ABA biosynthesis in plants. *Trends Plant Sci.* 7, 41–48. doi: 10.1016/s1360-1385(01)02187-2

Serrato, R. V., Balsanelli, E., Sassaki, G. L., Carlson, R. W., Muszynski, A., Monteiro, R. A., et al. (2012). Structural analysis of Herbaspirillum seropedicae lipid-A and of two mutants defective to colonize maize roots. *Int. J. Biol. Macromol.* 51, 384–391. doi: 10.1016/j.ijbiomac.2012.05.034

Sheoran, S., Kumar, S., Kumar, P., Meena, R. S., and Rakshit, S. (2021). Nitrogen fixation in maize: breeding opportunities. *Theor. Appl. Genet.* 134, 1263–1280. doi: 10.1007/s00122-021-03791-5

Sherameti, I., Shahollari, B., Venus, Y., Altschmied, L., Varma, A., and Oelmüller, R. (2005). The endophytic fungus Piriformospora indica stimulates the expression of nitrate reductase and the starch-degrading enzyme glucan-water dikinase in tobacco and Arabidopsis roots through a homeodomain transcription factor that binds to a conserved motif in their promoters. *J. Biol. Chem.* 280, 26241–26247. doi: 10.1074/jbc.M500447200

Song, W., Wang, F., Chen, L., Ma, R., Zuo, X., Cao, A., et al. (2019). GhVTC1, the Key Gene for Ascorbate Biosynthesis in Gossypium hirsutum, Involves in Cell Elongation under Control of Ethylene. *Cells.* 8 (9), 1039. doi: 10.3390/cells8091039

Sun, T. P. (2008). Gibberellin metabolism, perception and signaling pathways in Arabidopsis. *Arabidopsis. Book.* 6, e0103. doi: 10.1199/tab.0103

Tadra-Sfeir, M. Z., Faoro, H., Camilios-Neto, D., Brusamarello-Santos, L., Balsanelli, E., Weiss, V., et al. (2015). Genome wide transcriptional profiling of Herbaspirillum seropedicae SmR1 grown in the presence of naringenin. *Front. Microbiol.* 6. doi: 10.3389/fmicb.2015.00491

Tadra-Sfeir, M. Z., Souza, E. M., Faoro, H., Müller-Santos, M., Baura, V. A., Tuleski, T. R., et al. (2011). Naringenin regulates expression of genes involved in cell wall synthesis in Herbaspirillum seropedicae. *Appl. Environ. Microbiol.* 77, 2180–2183. doi: 10.1128/aem.02071-10

Terra, L. A., de Soares, C. P., Meneses, C. H. S. G., Tadra Sfeir, M. Z., de Souza, E. M., Silveira, V., et al. (2020). Transcriptome and proteome profiles of the diazotroph Nitrospirillum amazonense strain CBAmC in response to the sugarcane apoplast fluid. *Plant Soil* 451, 145–168. doi: 10.1007/s11104-019-04201-y

Thiebaut, F., Rojas, C. A., Grativol, C., Motta, M. R., Vieira, T., Regulski, M., et al. (2014). Genome-wide identification of microRNA and siRNA responsive to endophytic beneficial diazotrophic bacteria in maize. *BMC Genomics* 15, 766. doi: 10.1186/1471-2164-15-766

Thiebaut, F., Urquiaga, M. C. O., Rosman, A. C., da Silva, M. L., and Hemerly, A. S. (2022). The impact of non-nodulating diazotrophic bacteria in agriculture: understanding the molecular mechanisms that benefit crops. *Int. J. Mol. Sci.* 23, 1–22. doi: 10.3390/ijms231911301

Trapnell, C., Roberts, A., Goff, L., Pertea, G., Kim, D., Kelley, D. R., et al. (2012). Differential gene and transcript expression analysis of RNA-seq experiments with TopHat and Cufflinks. *Nat. Protoc.* 7, 562–578. doi: 10.1038/nprot.2012.016

Valach, M. (2014). *RNA extraction using the 'home-made' Trizol substitute. protocols.io*. doi: 10.17504/protocols.io.eiebcbe

Van der Hoorn, R. A. L., and Klemenčič, M. (2021). Plant proteases: from molecular mechanisms to functions in development and immunity. *J. Exp. Bot.* 72, 3337–3339. doi: 10.1093/jxb/erab129

Vargas, L., Santa Brígida, A. B., Mota Filho, J. P., de Carvalho, T. G., Rojas, C. A., Vaneechoutte, D., et al. (2014). Drought tolerance conferred to sugarcane by association with gluconacetobacter diazotrophicus: A transcriptomic view of hormone pathways. *PloS One* 9, e114744. doi: 10.1371/journal.pone.0114744

Vlot, A. C., Dempsey, D. M. A., and Klessig, D. F. (2009). Salicylic acid, a multifaceted hormone to combat disease. *Annu. Rev. Phytopathol.* 47, 177–206. doi: 10.1146/annurev.phyto.050908.135202

Wang, J., Li, Y., Zhu, F., Ming, R., and Chen, L.-Q. (2019). Genome-wide analysis of nitrate transporter (NRT/NPF) family in sugarcane saccharum spontaneum L. *Trop. Plant Biol.* 12, 133–149. doi: 10.1007/s12042-019-09220-8

Wang, L., Liang, J., Zhou, Y., Tian, T., Zhang, B., and Duanmu, D. (2021). Molecular characterization of carbonic anhydrase genes in lotus japonicus and their potential roles in symbiotic nitrogen fixation. *Int. J. Mol. Sci.* 22 (15), 7766. doi: 10.3390/ijms22157766

Wang, J., Zhang, P., Liu, S., Cong, B., and Chen, K. (2016b). A leucine-rich repeat receptor-like kinase from the antarctic moss pohlia nutans confers salinity and ABA stress tolerance. *Plant Mol. Biol. Rep.* 34, 1136–1145. doi: 10.1007/s11105-016-0994-y

Wang, J., Zhang, D., Zhang, L., Li, J., Raza, W., Huang, Q., et al. (2016a). Temporal variation of diazotrophic community abundance and structure in surface and subsoil under four fertilization regimes during a wheat growing season. *Agricult. Ecosyst. Environ.* 216, 116–124. doi: 10.1016/j.agee.2015.09.039

Wang, C., Zheng, M., Song, W., Wen, S., Wang, B., Zhu, C., et al. (2017). Impact of 25 years of inorganic fertilization on diazotrophic abundance and community structure in an acidic soil in southern China. *Soil Biol. Biochem.* 113, 240–249. doi: 10.1016/j.soilbio.2017.06.019

Weiss, D. S., Chen, J. C., Ghigo, J. M., Boyd, D., and Beckwith, J. (1999). Localization of FtsI (PBP3) to the septal ring requires its membrane anchor, the Z ring, FtsA, FtsQ, and FtsL. *J. Bacteriol.* 181, 508–520. doi: 10.1128/jb.181.2.508-520.1999

Wellburn, A. R. (1994). The Spectral Determination of Chlorophylls a and b, as well as Total Carotenoids, Using Various Solvents with Spectrophotometers of Different Resolution. *J. Plant Physiol.* 144, 307–313. doi: 10.1016/S0176-1617(11)81192-2

Yang, B., Wang, X.-M., Ma, H.-Y., Jia, Y., Li, X., and Dai, C.-C. (2014). Effects of the fungal endophyte Phomopsis liquidambari on nitrogen uptake and metabolism in rice. *Plant Growth Regul.* 73, 165–179. doi: 10.1007/s10725-013-9878-4

Zeffa, D. M., Perini, L. J., Silva, M. B., de Sousa, N. V., Scapim, C. A., Oliveira, A. L. M., et al. (2019). Azospirillum brasilense promotes increases in growth and nitrogen use efficiency of maize genotypes. *PloS One* 14, e0215332. doi: 10.1371/journal.pone.0215332

Zhang, K., Wang, F., Liu, B., Xu, C., He, Q., Cheng, W., et al. (2021). ZmSKS13, a cupredoxin domain-containing protein, is required for maize kernel development via modulation of redox homeostasis. *New Phytol.* 229 (4), 2163–2178. doi: 10.1111/nph.16988

Zhao, Y. (2014). Auxin biosynthesis. *Arabidopsis. Book.* 12, e0173. doi: 10.1199/tab.0173

Zhou, J., Guan, D., Zhou, B., Zhao, B., Ma, M., Qin, J., et al. (2015). Influence of 34-years of fertilization on bacterial communities in an intensively cultivated black soil in northeast China. *Soil Biol. Biochem.* 90, 42–51. doi: 10.1016/j.soilbio.2015.07.005

Zhou, J., Ma, M., Guan, D., Jiang, X., Zhang, N., Shu, F., et al. (2021). Nitrogen has a greater influence than phosphorus on the diazotrophic community in two successive crop seasons in Northeast China. *Sci. Rep.* 11, 6303. doi: 10.1038/s41598-021-85829-8

Zhu, C., Fan, Q., Wang, W., Shen, C., Wang, P., Meng, X., et al. (2014). Characterization of a glutamine synthetase gene DvGS1 from Dunaliella viridis and investigation of the impact on expression of DvGS1 in transgenic Arabidopsis thaliana. *Mol. Biol. Rep.* 41, 477–487. doi: 10.1007/s11033-013-2882-y

Zhu, F., Fang, Y., Wang, Z., Wang, P., Yang, K., Xiao, L., et al. (2022). Salicylic acid remodeling of the rhizosphere microbiome induces watermelon root resistance against Fusarium oxysporum f. sp. niveum infection 13. doi: 10.3389/fmicb.2022.1015038

Zou, X., Wang, Q., Chen, P., Yin, C., and Lin, Y. (2019). Strigolactones regulate shoot elongation by mediating gibberellin metabolism and signaling in rice (Oryza sativa L.). *J. Plant Physiol.* 237, 72–79. doi: 10.1016/j.jplph.2019.04.003

frontiers | Frontiers in Plant Science

TYPE Original Research
PUBLISHED 14 March 2024
DOI 10.3389/fpls.2024.1356545

OPEN ACCESS

EDITED BY
German Andres Estrada-Bonilla,
Colombian Corporation for Agricultural Research (AGROSAVIA), Colombia

REVIEWED BY
Arshad Jalal,
King Abdullah University of Science and Technology, Saudi Arabia
Waheed Ullah,
Kohat University of Science and Technology, Pakistan

*CORRESPONDENCE
Munawwar Ali Khan
Munawwar.Khan@zu.ac.ae
Sunil Mundra
sunilmundra@uaeu.ac.ae

†These authors have contributed equally to this work and share first authorship

RECEIVED 15 December 2023
ACCEPTED 15 February 2024
PUBLISHED 14 March 2024

CITATION
Tounsi-Hammami S, Khan MA, Zeb A, Anwar AR, Arora N, Naseem M and Mundra S (2024) Optimizing tomato seedling growth with indigenous mangrove bacterial inoculants and reduced NPK fertilization. *Front. Plant Sci.* 15:1356545. doi: 10.3389/fpls.2024.1356545

Optimizing tomato seedling growth with indigenous mangrove bacterial inoculants and reduced NPK fertilization

Soumaya Tounsi-Hammami[1†], Munawwar Ali Khan[1*†], Aroosa Zeb[1], Aneesa Rasheed Anwar[1], Naman Arora[1], Muhammad Naseem[2] and Sunil Mundra[3,4*]

[1]Department of Life and Environmental Sciences, College of Natural and Health Sciences at Zayed University, Dubai, United Arab Emirates, [2]Department of Life and Environmental Sciences, College of Natural and Health Sciences, Zayed University, Abu Dhabi, United Arab Emirates, [3]Department of Biology, College of Science, United Arab Emirates University, Abu-Dhabi, United Arab Emirates, [4]Khalifa Center for Genetic Engineering and Biotechnology (KCGEB), United Arab Emirates University, Al Ain, United Arab Emirates

The search for ecofriendly products to reduce crop dependence on synthetic chemical fertilizers presents a new challenge. The present study aims to isolate and select efficient native PGPB that can reduce reliance on synthetic NPK fertilizers. A total of 41 bacteria were isolated from the sediment and roots of mangrove trees (*Avicennia marina*) and assessed for their PGP traits under *in vitro* conditions. Of them, only two compatible strains of *Bacillus sp*ecies were selected to be used individually and in a mix to promote tomato seedling growth. The efficiency of three inoculants applied to the soil was assessed in a pot experiment at varying rates of synthetic NPK fertilization (0, 50, and 100% NPK). The experiment was set up in a completely randomized design with three replications. Results showed that the different inoculants significantly increased almost all the studied parameters. However, their effectiveness is strongly linked to the applied rate of synthetic fertilization. Applying bacterial inoculant with only 50% NPK significantly increased the plant height (44-51%), digital biomass (60-86%), leaf area (77-87%), greenness average (29-36%), normalized difference vegetation index (29%), shoot dry weight (82-92%) and root dry weight (160-205%) compared to control plants. Concerning the photosynthetic activity, this treatment showed a positive impact on the concentrations of chlorophyll a (25-31%), chlorophyll b (34-39%), and carotenoid (45-49%). Interestingly, these increases ensured the highest values significantly similar to or higher than those of control plants given 100% NPK. Furthermore, the highest accumulation of N, P, K, Cu, Fe, Zn, and Ca in tomato shoots was recorded in plants inoculated with the bacterial mix at 50% NPK. It was proven for the first time that the native PGP bacteria derived from mangrove plant species *A. marina* positively affects the quality of tomato seedlings while reducing 50% NPK.

KEYWORDS

Bacillus* sp., sustainable agriculture, biofertilization, nutrient management, *Avicennia marina

1 Introduction

The world's population is growing at an alarming rate and is expected to reach 9.1 billion by 2050. Consequently, the global food demand is expected to rise significantly, from 35% to 56% between 2010 and 2050 (Van Dijk et al., 2021). In the same period, the number of people at risk of hunger is projected to increase by 8% (Van Dijk et al., 2021), putting pressure on the agricultural sector to ensure food security. To achieve high crop production, synthetic fertilizers are commonly used in intensive agriculture and horticulture to correct soil nutrient deficiencies, particularly nitrogen, phosphorus, and potassium (Kong et al., 2018; Devi et al., 2022). Concerns over chemical residues in soil, water, and food have recently received significant attention due to their negative impact on environmental and human health (Akinnawo, 2023; Chataut et al., 2023). Furthermore, the consistent use of synthetic fertilizers presents a significant financial burden for farmers since fertilizer costs continue to rise (Majeed et al., 2015). Thus, agricultural and scientific communities are seeking innovative and sustainable management methods to improve crop yields and quality while safeguarding the environment and adapting to climate change.

Plant Growth Promoting bacteria (PGPB) are eco-friendly, low-cost natural resources that can be integrated to reduce the toxic effects of synthetic inputs and promote sustainable agriculture. PGP bacteria include different genera such as *Agrobacterium, Rhizobium, Azospirillum, Azotobacter, Bacillus*, and *Pseudomonas* (Boleta et al., 2020; Rosa et al., 2022; Tounsi-Hammami et al., 2022; Cirillo et al., 2023; Gen-Jiménez et al., 2023). These bacteria can act as biofertilizers through various mechanisms, including nitrogen fixation, nutrient solubilization, ammonium production, siderophore production and hormone production. Consequently, the use of PGPB can enhance plant nutrient uptake (Ijaz et al., 2021; Tsegaye et al., 2022) and increase the efficiency of synthetic fertilization (Mortinho et al., 2022; Asghar et al., 2023). The PGPB communities have great potential to reduce the dependency on synthetic fertilizers, such as nitrogen, phosphorus, and potassium, in both soil (Rosa et al., 2022; Tounsi-Hammami et al., 2022) and soilless conditions (Ikiz et al., 2024).

However, the success of PGPB inoculation depends on the efficiency of the selected strains, as well as its ability to adapt to environmental changes. Therefore, utilizing indigenous strains as biofertilizers has great potential, as they help maintain soil nutrient levels and can easily adapt to the local environment (Tounsi-Hammami et al., 2019). Given the lack of information on the impact of native PGP strains on reducing synthetic fertilizers in the United Arab Emirates, it was hypothesized that creating a consortium of indigenous PGPB could enhance plant nutrition and decrease farmers' reliance on synthetic fertilizers. In this context, the goal of the present research is to isolate and characterize indigenous bacteria and assess the potential of elite PGP strains to substitute or reduce NPK fertilization while improving the growth and quality of tomato seedlings.

2 Materials and methods

2.1 Isolation, characterization and identification of native bacteria

2.1.1 Sample collections

Samples of sediment and roots were collected in triplicates during March 2021 from Mangrove Beach in Umm Al Quwain, United Arabic Emirates (UAE) (25°32'06.0"N, 55°37'50.9"E), which is known as one of the UAE's largest natural A. marina ecosystems (Samara et al., 2020). Soil sediments and roots were collected manually, using a sterilized spatula, within 10–15 cm of the wet area (25°32' 07.8" N, 55°38 04.2" E) and dry area (25°32' 15.9" N, 55°37 20.7" E) and were immediately placed individually in sterile zip-lock plastic bags. All samples were stored in ice-cold conditions (4°C) away from heat and sunlight and transported to the laboratory within 3 hours. All samples were stored at 4 °C until use. The physicochemical properties of the wet and dry sediment samples were recorded using standard procedures (Table 1).

2.1.2 Bacterial isolation

Briefly, 10 grams of dry/wet sediments and rhizosphere soil samples were collected from 15 cm depth at plant vegetation sites. One gram of soil sediment from dry and wet areas was aseptically transferred to a tube containing 9 mL of sterile distilled water and then shaken for 30 minutes. Afterwards, a series of decimal dilutions (10^{-1} to 10^{-6}) of the soil suspensions were carried out in culture tubes. An aliquot of 100 µL of each dilution soil suspension was spread over a Jensen agar medium (HiMedia, Mumbai, India) and incubated at 28°C for 15 days for colony development. Single colonies were picked and repeatedly streaked on the same medium for purification. After isolation and purification, bacterial cultures were cultivated on LB media at 37°C for 48-72 hours.

For the isolation of root endophytes, about 1 gram of roots were surface sterilized with 70% ethanol for 1 minute, followed by soaking in a 25% sodium hypochlorite solution for three minutes to eliminate surface-contaminating microbes. Roots were rinsed in sterile distilled water to eliminate residual disinfectants and then air-dried in the laminar flow hood. The disinfected roots were excised and macerated in sterile distilled water using a mortar and pestle. About 1 ml of the sample was serially diluted in sterilized distilled water, and then 100 µL of each dilution aliquot was spread

TABLE 1 Dry and wet sediment characteristics at sampling locations.

	pH	EC (mS/cm)	OM (%)	N (mg/Kg)	P (mg/Kg)	K (mg/Kg)
Dry sediment	7.550	4.590	2.487	6792.493	288.867	735.367
Wet sediment	7.693	4.327	1.893	3593.267	458.833	808.890

Ec, Electric conductivity; OM, organic matter; N, total nitrogen; P, available phosphorous; K, potassium.

on Jensen agar medium. Plates were incubated at 28 °C for 15 days for colony development. Single colonies were picked and repeatedly streaked on the same medium for purification.

The pure bacteria isolated from wet and dry sediments and roots were maintained on nutrient broth agar slants, kept at 4°C, and −80 °C for long-term storage in nutrient broth adjusted with 20% (v/v) glycerol.

2.1.3 Morphological and biochemical characterization

The isolates were examined for their morphological features (Aneja, 2003). Gram staining and biochemical tests were performed, including oxidase and catalase tests (Cappuccino and Sherman, 1992). API-20E micro-test system was used for eight strains. Bacterial isolates were tested for their ability to metabolize the 20 metabolites in the API-20E test kit according to the manufacturer's instructions (BioMérieux, Marcy l'Etoile, France). The strips were incubated at 30°C, and the results were assessed after 24 and 48 h.

2.1.4 Plant growth promotion traits

2.1.4.1 Siderophore production

The secretion of siderophore was qualitatively analyzed using the Chrome Azurol S (CAS) method (Schwyn and Neilands, 1987). CAS agar plates were spot inoculated with each isolate, then incubated at 30°C for 7 days. After incubation, the appearance of an orange halo zone around bacterial isolates was considered positive (Louden et al., 2011). The experiment was performed in triplicate.

2.1.4.2 Ammonia production (NH_3)

Ammonia production was tested in peptone water following the Cappuccino and Sherman (1992) method. Ten ml of peptone water was inoculated with 100 µL (OD_{600nm} = 0.8) of a freshly cultured bacterial suspension, incubated at 30°C, and shaken at 150 rpm. An uninoculated medium served as the negative control. After 96 hours, 1 mL aliquots were taken and centrifuged at 10,000 rpm for 10 minutes. Then 0.5 ml of Nessler's reagent was added to each supernatant. The development of a brown-to-yellow color indicated positive ammonia production.

2.1.4.3 Indole acetic acid production

Quantitative estimation of IAA was performed on nutrient broth supplemented with tryptophan (0.2 mg ml^{-1}) as a precursor of IAA, according to Gordon and Weber (1951). After 72 hours of incubation at 30°C with shaking at 150 rpm, bacterial cells were removed by centrifugation at 10000 g for 10 minutes at 4°C. The supernatants were filtered through 0.22 µm sterile syringe filters. One ml of each filtrate was mixed vigorously with 2 ml of Salkowski's reagent consisting of 1 mL of 0.5 M $FeCl_3$ and 50 mL of 35% $HClO_4$ and allowed to stand at 30°C in the dark. After 20 minutes, the absorbance was recorded at 530 nm. The concentrations of IAA produced were estimated according to a standard curve using pure IAA (Sigma Aldrich, Overijse, Belgium) for concentrations in the 0–160 ppm range.

2.1.4.4 Hydrogen cyanide production

The secretion of HCN was qualitatively analyzed by adapting the method of Lorck (1948). TSA medium was amended with 0.44% glycine, and 100 µL (OD_{600nm} = 0.6) of each strain was flooded on poured agar plates using a sterilized glass spreader. A sterilized Whatman filter paper was soaked in an alkaline picrate solution (0.25% picric acid in 1.25% sodium carbonate) for 1 minute and then placed at the top of the plate. Plates were sealed with parafilm and incubated at 30°C for 4 days. The paper reacts with HCN gas, and its colour changes from yellow to orange or brown, indicating HCN production.

2.1.4.5 Potassium solubilization

The potassium solubilization was qualitatively evaluated on Alexandrov agar medium as described by Meena et al. (2015). Alexandrov agar plates were spot inoculated with each isolate and then incubated at 28°C for 7 days. The appearance of a clearing zone around the colonies indicated a positive potassium solubilization.

2.1.4.6 Phosphate solubilization

The phosphate (P) solubilization was qualitatively estimated on Pikovskaya's (PKV) agar medium (Pikovskaya, 1948). Plates were spot inoculated with each isolate and then incubated at 30°C for 7 days and observed for the development of the P solubilization zone around the colonies.

2.1.5 Molecular identification by 16S rRNA gene amplification

Out of the 41 strains, only 8 underwent molecular identification. To isolate DNA for 16S rRNA gene amplification, Qiagen's DNA extraction DNeasy® bacterial isolation kit was used. The concentration of the extracted DNA was measured using a Nanodrop spectrometer (Implen-NP80). Then, the extracts were stored at -20°C for further analysis. The 16S rDNA gene amplification was conducted with the forward and reverse primers 27F and 1492R primers, respectively, with sequences 5′-AGAGTTGATCMTGGCTCGAG-3′ and 5′-GGTTACCTTGTTACGACTT-3′ (Frank et al., 2008). Sequencing was performed by Beijing Genomic Institute China (China). Subsequently, sequence similarities were determined using the BLAST program (https://www.blast.ncbi.nlm.nih.gov/Blast.cgi). Finally, all new sequences were deposited in the NCBI database with accession numbers OP600564 to OP600571. (https://www.ncbi.nlm.nih.gov/nuccore/?term=OP600564:OP600571%5baccn).

2.1.6 Bacterial selection, compatibility test

Eight strains with multiple PGP traits were selected and tested for their compatibility with each other according to the methodology described by Prasad and Babu (2017). Two strains were grown in nutrient agar at 28°C for 3 days, then a first strain

was streaked in the center of freshly prepared agar plates, and a second strain was streaked on either side of the central strain. Then, the Petri plates were incubated at 28°C for 72 hours, and an inhibition zone around the central strain was observed daily. For each pair of strains, three replications were performed.

2.2 Pot experiment

2.2.1 Inoculum preparation

Only two strains were selected and used individually and in mix (M) to prepare the different inoculants. First, the selected strains were grown individually in glass tubes containing liquid nutrient broth medium on a rotating shaker (150 rpm) for 48 hours at 28°C to late exponential phase to obtain a final concentration of 10^9 CFU mL^{-1}. Then mix M was prepared by combining equal volumes of the individual bacterial suspensions before their application, corresponding to a final concentration of 10^9 CFU mL^{-1}.

2.2.2 Experimental set up

To experiment, a commercial variety of tomatoes, called Shourouq, was used. The tomato seeds were surface sterilized by immersing in 70% ethanol for 1 minute, followed by soaking in a 25% sodium hypochlorite solution for 1 minute, then rinsed ten times in sterile distilled water and soaked for an additional 10 minutes in sterile distilled water to remove any remaining traces of the disinfectant. The effectiveness of this disinfection was ascertained by incubating ten seeds on nutrient broth agar plates at 28°C for 72 hours and checking for the absence of bacterial contamination.

The sterilized tomato seeds were immediately sown in 500 ml pots filled with a sterilized mix of vermiculite and peat (1:1, v/v). Two seeds were sown in each pot, and seven days after sowing (DAS), only one seedling per pot was kept. At this stage, inoculants were applied directly to the soil close to the stem at a rate of 5 mL per seedling (Trabelsi et al., 2011). Uninoculated plants were inoculated with the same amount of sterile nutrient broth and served as controls (C). Three levels of NPK synthetic fertilization were applied: 0, 50, and 100% of the recommended dose. The full dose of NPK synthetic fertilization was carried out using the commercial fertilizer Macro Greenmix 20:20:20 (N:P: K) at the rate of 3 grams/l as recommended by the manufacturer (Moncada et al., 2020). In all, 12 treatments were set up in three replications arranged in a completely randomized design (Table 2).

The experiment was carried out under a growth room chamber at 25/22°C day/night temperature, 16/8 hours light/dark period, and an average of 250 µmol m^{-2} s^{-1} light intensity as measured with a handheld spectrometer (LICOR, USA, model LI-180). The pots were rotated thrice weekly to ensure uniform growth conditions in the growth chamber.

TABLE 2 Treatments used in the experiment, strain combinations, and levels of synthetic NPK fertilization.

T1: C-0%NPK	T5: C-50%NPK	T9: C-100%NPK
T2: S1-0%NPK	T6: S1-50%NPK	T10: S1-100%NPK
T3: S2-0%NPK	T7: S2-50%NPK	T11: S2-100%NPK
T4: M-0%NPK	T8: M-0%NPK	T12: M-100%NPK

C: uninoculated plants; S1: plants inoculated with strain S1=E1, S2: plants inoculated with Strain S2=E3, M, plants inoculated with the mix of the two strains: S1 and S2.

2.2.3 Plant and soil measurements

2.2.3.1 Morphological and vegetative indices

The effects of different inoculants and synthetic fertilization on the morphological and vegetative of tomato plants were evaluated at 42 DAS using the Phenospex Scan device (PlantEye F500, Phenospex, Heerlen, The Netherlands). Various traits were measured, such as the digital biomass (mm^3/plant) (DB), projected leaf area (mm^2/plant), greenness average of the leaves, the normalized difference vegetation index (NDVI), and the plant senescence reflectance index (PSRI).

On the same day, the plant height (PH) was measured from the soil's surface to the tip of the main stem for each treatment. The leaf numbers (LN) were determined for each plant. Then, tomato plants were harvested, and the stem diameter (SD) and root length (RL) were recorded. Then, plants were dried in an oven at 65°C until constant weight was achieved to determine their corresponding shoot and root dry weight (SDW, RDW).

2.2.3.2 Physiological parameters

Leaf chlorophyll concentration was analyzed by estimating the content of chlorophyll a (Chla), chlorophyll b (Chlb), and carotenoid (Car) by spectrophotometry at 645 nm, 663 nm, and 470 according to the method of Torrecillas et al. (1984). The leaf's relative water content (RWC) was determined as described by Turner (1986).

2.2.3.3 Micro and macro-nutrient content

Dry shoots of tomato plants were powdered using a blade mill and then passed through a 40-mesh sieve. Plant tissue samples were used for mineral analysis. Total nitrogen (N) was determined by the method of Kjeldahl (1883). The phosphorus concentration was determined by colorimetric method at 840 nm (Pauwels et al., 1992). Furthermore, the potassium (K), sodium (Na), Magnesium (Mg), Calcium (Ca), Copper (Cu), Iron (Fe), and Zinc (Zn) concentrations were analyzed by inductively coupled plasma-optical emission spectrometry – ICP-OES (Model no. 700 series, Agilent Technology, Santa Clara, CA, USA) (Toselli et al., 2009).

2.2.3.4 Soil microbial population

The soil microbial population was detected using the standard 10-fold dilution plating method. The data were expressed as the number of colony-forming units (CFU) per gram of soil (Somasegaran and Hoben, 1994).

2.3 Statistical analysis

The effect of bacterial inoculants, synthetic NPK fertilization, and their interactions on the various parameters measured in pot experiments was performed using the two-way analysis of variance (ANOVA) in accordance with the experimental design. The

treatment means were compared using LSD tests at a significance level of 5%. The ranking of each treatment was denoted by letters. Pearson correlation coefficient analysis heat map was used to assess the relationships between all the measured parameters. All statistical analyses were performed using R statistical software version 3.5.

3 Results

3.1 Isolation, morphological and biochemical characterization

A total of 41 strains, all fast-growing, with 3 originating from interior roots, 3 from rhizosphere, and 11 and 24 originating respectively from dry and wet sediments. The morphological and biochemical characteristics of isolates deduced from the colony and microscopic features are presented in Supplementary Table S1. Most bacteria showed circular, cream, flat, and undulate colonies with variable sizes on nutrient broth agar plates. All bacteria tested positive for Gram test and catalase. The strains mostly tested positive for oxidase except SD2, SD3, SD6, SW1, SW4, SW12, and SW20. The data obtained using the API 20E biochemical identification system are shown in Supplementary Table S2. The results showed that all eight tested bacterial strains could consume ortho-nitrophenyl-b-galactoside (ONPG) and arginine. They were also able to perform fermentation of gelatine, glucose, and mannitol, except strain R2. However, these strains could not ferment sorbitol, rhamnose, sucrose, and melibiose. Only strain SW14 was able to consume citrate.

3.2 *In vitro* Plant Growth–Promoting traits

The results pertaining to various plant growth-promoting traits conducted are shown in Table 3. In total, 78% of strains were identified as ammonium producers. The highest production was observed in strain SD7. Moreover, eight strains, namely SW3, SW4, SW10, SW19, SW24, E1, E3, and R2, demonstrated a strong ability to produce ammonium.

The quantitative estimation of the IAA production showed that only 24 strains (58%) could synthesize this phytohormone using tryptophane as a precursor. The amount of IAA production ranged from 1.51 to 8.55 ppm. The highest production was recorded by SW14, SD2, and SW2, producing 8.55 ppm, 7.36 ppm, and 5.63 of IAA, respectively. About 24 strains (58%) formed a visible halo, indicating a positive phosphate solubilizing activity, with a maximum recorded for SW22 (10 mm) and a minimum found for SW23 (5.83 mm). Only 15 strains were considered as potassium solubilizers, forming a visible halo around the colony. The highest values were found in SW14, with a diameter of 26 mm. In contrast, the smallest diameter was observed for strains SW2 (22 mm). Thirty-one strains were shown positive for siderophore production and formed an orange halo zone around the bacterial colony growing in CAS agar plate. The highest production was found in SW3, R1, and SW4, which showed the highest diameter, 12.63 mm, 10.33 mm, and 9.33 mm, respectively.

3.3 Molecular identification

A comparative sequence analysis of BLASTn search on NCBI revealed all the strains belonging to the phylum Firmicutes, class of Bacilli, and genus of *Bacillus* (Table 4). Three strains designated as SD7, SW7 and E3 were strongly related to *B. licheniformis* with a similarity compared to reference sequences ranging from 96.81% to 99.08. While three other strains designated as SD11, SW14, and SW22 could be affiliated respectively to *B. paralicheniformis*, *B. cabrialesii*, and *B. subtilis*. The remaining strains, designated as E1 and R2, shared 99.93 and 96.81% similarities with the most related strains, *B. wiedmannii* and *B. proteolyticus*, respectively.

3.4 Selection of compatible strains

According to the findings of the *in vitro* antagonistic assays (data not shown), it was determined that strains E3 and E1 are compatible and do not showcase any antagonistic effects toward each other. This was established by the absence of a growth inhibition zone at the intersection areas. As a result, it can be inferred that using these strains, either alone or in combination, is unlikely to cause any unwarranted interference.

3.5 Pot experiment

3.5.1 Morphological parameters and vegetative indices

The analysis of variance indicates that bacterial inoculation, synthetic fertilization and their interactions had a significant effect on all the studied parameters except for GA, which was not influenced by interactions between the two factors (Table 5 and Supplementary Table S3). It was found that the effectiveness of the bacterial inoculum varied depending on the level of NPK synthetic fertilization applied. Notably, tomato plant growth parameters showed significant improvement at 0% and 50% of synthetic fertilization compared to their respective controls C-0%NPK and C-50%NPK. Compared to control plants without NPK chemical fertilization, the inoculation with native strains S1, S2, and their mixture led to significant increases in DB (+159-162%), LA (+786-931%), GA (+47-66%) and NDVI (+41-50%). It is evident that these increases fell short of the expected maximum growth that can be attained with a complete dose of NPK fertilization. Indeed, the highest values were recorded for DB, LA, GA, and NDVI by applying the three inoculum and a half dose of NPK fertilization. Compared to the control plants at this treatment level, significant improvements amounting from 60 to 86% for DB, 77 to 87% for LA, 29 to 36% for GA and 29% for NDVI. Interestingly, at this treatment level, the growth parameters were statistically equivalent to, or higher than, those recorded in the control plants with 100% NPK fertilization. In contrast, at the full dose of NPK fertilization, inoculant application only had neutral effects on the growth parameters when compared to the application of synthetic NPK fertilizer alone.

10.3389/fpls.2024.1356545

TABLE 3 Plant growth–promoting abilities of the 42 native strains.

Strains	Ammonia production	IAA (mm)	P solubilization (mm)	K solubilization (mm)	Siderophore production (mm)	HCN
SD1	–	0.00	0.00	0.00	0.00	+
SD2	+	7.36ab ±0.03	7.00def ±0.00	0.00	0.00	+
SD3	+	3.10defgh ±0.04	7.00def ±0.00	0.00	4.667efgh ±1.15	+
SD4	–	0.00	0.00	0.00	0.00	+
SD5	++	2.51defgh ±0.12	8.83b ±0.29	0.00	1.67ghij ±0.58	+
SD6	+	0.00	0.00	0.00	2.00ghij ±1.00	+
SD7	++++	4.25cde ±0.42	7.00def ±0.00	25.00ab ±0.57	9.00bc ±2.00	+
SD8	+	1.96fgh ±0.51	7.33cdef ±0.59	22.50cd ±0.5	0.00	+
SD9	–	0.00	0.00	0.00	5.00defg ±2.00	+
SD10	+	2.34efgh ±0.13	7.67cd ±1.15	24.00abcd ±0.00	2.33fghij ±0.58	+
SD11	+	4.12cdefg ±0.18	7.50cde ±0.50	24.00abcd ±0.00	2.67fghij ±2.98	–
SW1	+	3.07defgh ±0.23	7.00def ±0.00	23.00bcd ±0.57	4.00fghij ±1.00	+
SW2	++	5.63bc ±0.03	7.00def ±0.00	22.00d ±0.57	9.00bc ±1.00	–
SW3	+++	3.61cdefgh ±0.13	9.00b ±0.00	0.00	12.67a ±3.06	+
SW4	+++	1.90cdefgh ±0.64	8.67b ±0.58	23.00bcd ±0.57	9.33ab ±0.58	+
SW5	–	0.00	0.00	0.00	1.33hij ±0.58	–
SW6	–	0.00	0.00	0.00	2.67fghij ±1.15	+
SW7	++	3.60cdefgh ±0.44	8.00c ±0.00	23.00bcd ±0.57	0.00	–
SW8	–	0.00	0.00	0.00	4.33efghi ±1.15	–
SW9	+	0.00	0.00	0.00	1.67ghij ±0.58	+
SW10	+++	0.00	0.00	0.00	3.67fghij ±2.08	+
SW11	–	0.00	0.00	0.00	3.67fghij ±1.15	–
SW12	++	3.34defgh ±0.26	7.00def ±0.00	0.00	8.33bcd ±1.15	–
SW13	++	2.83defgh ±0.41	7.33cdef ± 0.58	0.00	0.00	+
SW14	++	8.55a ±0.57	8.83d ±0.29	26.00a ±0.57	7.67bcde ±2.31	+
SW15	++	1.51h ±0.16	7.00def ±1.00	24.50abc ±0.00	0.00	+
SW16	+	4.14cdef ±0.00	6.67f ±1.15	0.00	0.00	+
SW17	++	0.00	0.00	0.00	1.67ghij ±0.58	+
SW18	+	0.00	0.00	0.00	0.00	+
SW19	+++	1.79h ±0.02	7.17def ±0.29	24.00abcd ±0.5	1.67ghij ±0.58	+
SW20	++	0.00	0.00	0.00	5.00defg ±1.00	+
SW21	+	0.00	0.00	0.00	1.00ij ±0.00	+
SW22	++	2.99defgh ±0.07	10.00a ±0.00	23.00bcd ±0.57	0.667j ±1.15	–
SW23	++	2.28efgh ±0.29	5.83g ±0.29	0.00	3.67fghij ±1.53	+
SW24	+++	0.00	0.00	0.00	9.00bc ±0.00	+
E1	+++	6.68cd ±0.11	7.00def ±0.00	25.00ab ±0.57	4.33efghi ±0.35	–
E2	++	0.00	0.00	0.00	3.33fghij ±1.53	+
E3	+++	1.87h ±0.12	7.17 def ± 0.29	23.00bcd ±0.57	5.67cdef ±0.58	+

(Continued)

TABLE 3 Continued

Strains	Ammonia production	IAA (mm)	P solubilization (mm)	K solubilization (mm)	Siderophore production (mm)	HCN
R1	+	0.00	0.00	0.00	10.33ab ±-.58	+
R2	+++	2.38efgh ±0.34	8.67b ±0.58	22.50cd ±0.00	0.00	+
R3	++	2.00fgh ±0.07	6.83ef ±0.29	0.00	4.00fghij ±1.00	+

Values are the mean of three separate experiments in triplicates: ammonia production (based on the intensity of color): absent (-), weak (+), moderate (++), strong (+++), and highly strong (++++). Each value is the mean of three replicates. Different letters indicate significant differences according to the LSD test.

The plant senescence reflectance index (PSRI) was adversely affected by bacterial and synthetic fertilization and their interactions (Table 5 and Supplementary Table S3). The highest PSRI readings were found in control plants not treated with synthetic fertilization, followed by inoculated plants at the same fertilizer level. Compared to control plants that received 50%NPK, bacterial inoculation caused a significant reduction in PSRI, with a reduction of 56% for S1, 55% for S2, and 66% for the bacterial mix M.

For their part, bacterial and synthetic fertilization positively affected the tomato plants' LN, PH, RL, SD, SDW, and RDW, quantified at harvest (Table 6 and Supplementary Table S4). The bacterial inoculants were more effective when the tomato plants received 50%NPK resulting in significant increases in the LN (+47-60%), PH (+44-51%), RL (+107-145%), SD (+79-84%), SDW (+82-92%), and RDW (+180-162%) compared to the control plants. Interestingly, at this treatment level, LN, RL, SD, SDW, and RDW were statistically higher than those recorded in the control plants with 100% N fertilization. It is important to highlight that for RL, the bacterial mix combined with 50% NPK reached an impressive length of 16.50 cm, which is significantly higher than that recorded for control plants receiving 100%NPK (10.99 cm).

3.5.2 Photosynthetic pigments and relative leaf water content

The photosynthetic pigments were affected by both bacterial inoculation and synthetic fertilization and the interactions between them (Supplementary Table S5). The results presented in Figure 1 indicate that the application of different inoculants (S1, S2 and M) led to significant increases in chlorophyll a (25-28%), chlorophyll b (34-39%), carotenoid (45-49%), and total chlorophyll (31-33%) concentration when compared to control plants receiving only 50% NPK. Interestingly, these increases resulted in values that were either similar to or higher than those observed in the control plants receiving a full rate of NPK fertilization.

The RWC was significantly influenced by the bacterial inoculants, the synthetic fertilization, and the interactions between the two factors ($P < 0.001$) (Figure 2, Supplementary Table S5). Compared to control plants, the RWC in leaves was significantly increased in response to bacterial inoculations at 0% NPK and 50%NPK. It was shown that the highest values were recorded in inoculated plants treated with 50%NPK.

3.5.3 Micro and macro-nutrient content tomato shoots

The micro and macronutrient content in tomato shoots, including N, P, K, Na, Ca, Mg, Fe, Cu, and Zn, were presented in Table 7. The analysis of variance showed that the bacterial inoculation, the synthetic fertilization, and their interactions significantly affected the accumulation of all the studied nutrients except for Na content, which remained unaffected by the interactions between the two factors (Supplementary Table S6). In most cases, inoculated plants' highest nutrient uptake was recorded, particularly with the bacterial mix treated with 50% NPK synthetic fertilization. At this level, the inoculation with native strains used individually and in mix significantly improved N (82-103%), P (90-101%), K (31-43%), Na (2-8%), Mg (4-13%), Ca (48-68%), Fe (62-70%), Cu (54-77%) and Zn (30-47%) compared with their respective control plants. Interestingly, these increases resulted in values statistically similar to or even higher than those observed in the control plants receiving a full dose of NPK synthetic fertilization.

TABLE 4 Taxonomic affiliation of selected eight strains based on nearly full-length 16S rRNA sequence analysis.

Strains	Sequence (bp)	Closest relative species	Phylum/class	Accession no.	Similarity (%)
SD7	1409	*Bacillus licheniformis*	Firmicuts/Bacilli	OP600567	99.08
SD11	1409	*Bacillus paralicheniformis*	Firmicuts/Bacilli	OP600568	100%
SW7	1409	*Bacillus licheniformis*	Firmicuts/Bacilli	OP600571	98%
SW14	1410	*Bacillus cabrialesii*	Firmicuts/Bacilli	OP600569	100%
SW22	1410	*Bacillus subtilis*	Firmicuts/Bacilli	OP600570	100%
E1	1395	*Bacillus wiedmannii*	Firmicuts/Bacilli	OP600564	99.93%
E3	1411	*Bacillus licheniformis*	Firmicuts/Bacilli	OP600565	96.81%
R2	1401	*Bacillus proteolyticus*	Firmicuts/Bacilli	OP600566	96.81%

10.3389/fpls.2024.1356545

TABLE 5 Effects of bacterial inoculation and synthetic fertilization on digital biomass (DB), leaf area (LA), greenness average (GA), the normalized difference vegetation index (NDVI), and plant senescence reflectance index (PSRI) of tomato plant at 42 DAS.

	DB (mm^3/plant)	LA (mm^2/plant)	GA	NDVI	PSRI
C-0%NPK	40.05c ±6.65	140.22f ±36	0.163d ±0.00	0.338e ±0.00	0.240a ±0.04
S1-0%NPK	104.81c ±11.82	2475.51e ±424	0.239c ±0.03	0.503d ±0.02	0.125bc ±0.04
S2-0%NPK	106.53c ±11.56	2153.84ef ±104	0.269bc ±0.04	0.508d ±0.04	0.133bc ±0.05
M-0%NPK	103.55c ±5.17	2129.21ef ±155	0.271dc ±0.07	0.478d ±0.06	0.155b ±0.01
C-50%NPK	849.93b ±94.96	8998.50d ±869	0.317b ±0.01	0.581c ±0.02	0.095cd ±0.01
S1-50%NPK	1517.69a ±187.67	15929.47ab ±1232	0.43a ±0.04	0.747ab ±0.01	0.042e ±0.02
S2-50%NPK	1361.64a ±295.06	16729.07a ±1195	0.41a ±0.03	0.749a ±0.01	0.043e ±0.02
M-50%NPK	1577.47a ±92.92	16792.07a ±2183	0.433a ±0.04	0.749a ±0.02	0.032e ±0.02
C-100%NPK	1439.63a ±194.13	13001.30c ±1482	0.393a ±0.01	0.699b ±0.03	0.051de ±0.02
S1-100%NPK	1426.45a ±155.94	13917.06bc ±1654	0.389a ±0.02	0.720ab ±0.02	0.036e ±0.02
S2-100%NPK	1584.69a ±318.59	12870.51c ±1357	0.418a ±0.05	0.730ab ±0.02	0.046e ±0.03
M-100%NPK	1541.07a ±256.68	13016.20c ±2477	0.399a ±0.04	0.727ab ±0.03	0.044e ±0.02
Bacterial inoculation (BI)	**	***	***	***	***
Synthetic fertilization (SF)	***	***	***	***	***
BI*SF	*	***	ns	***	*

C: uninoculated plants, S1: plants inoculated with strain E1, S2: plants inoculated with E3, M: plants inoculated with the mix of two strains, S1 and S2.
Each value is the mean of three replicates. Different letters indicate significant differences according to the LSD test.
Significance: ns = not significant; * significant at $p < 0.05$; ** significant at $p < 0.01$; *** significant at $p < 0.001$.

TABLE 6 Effects of bacterial inoculation and synthetic fertilization on leaf number (LN), plant height (PH), root length (RL), stem diameter (SD), shoot dry weight (SDW), and root dry weight (RDW) of tomato plant at 42 DAS.

	LN	PH (cm/plant)	RL (cm/plant)	SD (mm/plant)	SDW (g/plant)	RDW (g/plant)
C-0%NPK	2.00g ±0.00	6.03d ±0.55	3.56f ±0.55	1.50d ±0.50	0.007d ±0.00	0.012d ±0.01
S1-0%NPK	3.33f ±0.58	12.13c ±0.32	7.60e ±0.36	2.50c ±0.50	0.083d ±0.00	0.134c ±0.04
S2-0%NPK	3.00f ± 0.00	12.17c ±0.28	7.13e ± 0.32	2.50c ±0.50	0.067d ±0.01	0.107c ±0.04
M-0%NPK	3.33f ± 0.57	12.00c ±0.50	7.80e ±0.264	2.83c ±0.29	0.077d ± 0.01	0.146c ±0.06
C-50%NPK	5.00e ± 0.00	15.83b ±0.76	6.73e ±0.35	3.17c ±0.29	0.499c ±0.09	0.156c ±0.05
S1-50%NPK	8.00ab± 0.00	23.13a ±0.32	15.07b ± 0.66	5.83a ±0.29	0.907ab ± 0.07	0.405a ±0.03
S2-50%NPK	7.33 bc ± 0.57	23.83a ±0.76	13.93c ± 1.00	5.67a ±0.76	0.924ab ±0.02	0.408a ±0.09
M-50%NPK	8.33a± 0.57	22.83a ±0.28	16.50a ± 0.87	5.83a ±0.29	0.958a ±0.03	0.475a ±0.09
C-100%NPK	6.33d± 1.15	23.83a ±0.28	10.99d ±0.68	4.67b ±0.58	0.905ab ±0.00	0.270b ±0.03
S1-100%NPK	6.67cd ± 0.57	23.47a ±0.55	11.33d ± 0.57	4.83b ±0.29	0.855b ±0.11	0.303b ±0.02
S2-100%NPK	6.33d ± 0.57	23.67a ±0.76	11.33d ± 0.57	4.83b ±0.76	0.836b ±0.07	0.277b ±0.03
M-100%NPK	6.67cd± 0.57	23.30a ±1.12	11.00d ± 1.00	4.50b ±0.50	0.865ab ±0.10	0.267b ±0.05
Bacterial inoculation (BI)	***	***	***	***	***	***
Synthetic fertilization (SF)	***	***	***	***	***	***
BI*SF	**	***	***	***	***	**

C: uninoculated plants, S1: plants inoculated with strain E1, S2: plants inoculated with E3, M: plants inoculated with the mix of two strains, S1 and S2.
Each value is the average of three replicates. Different letters indicate significant differences according to the LSD test.
Significance: ** significant at $p < 0.01$; *** significant at $p < 0.001$.

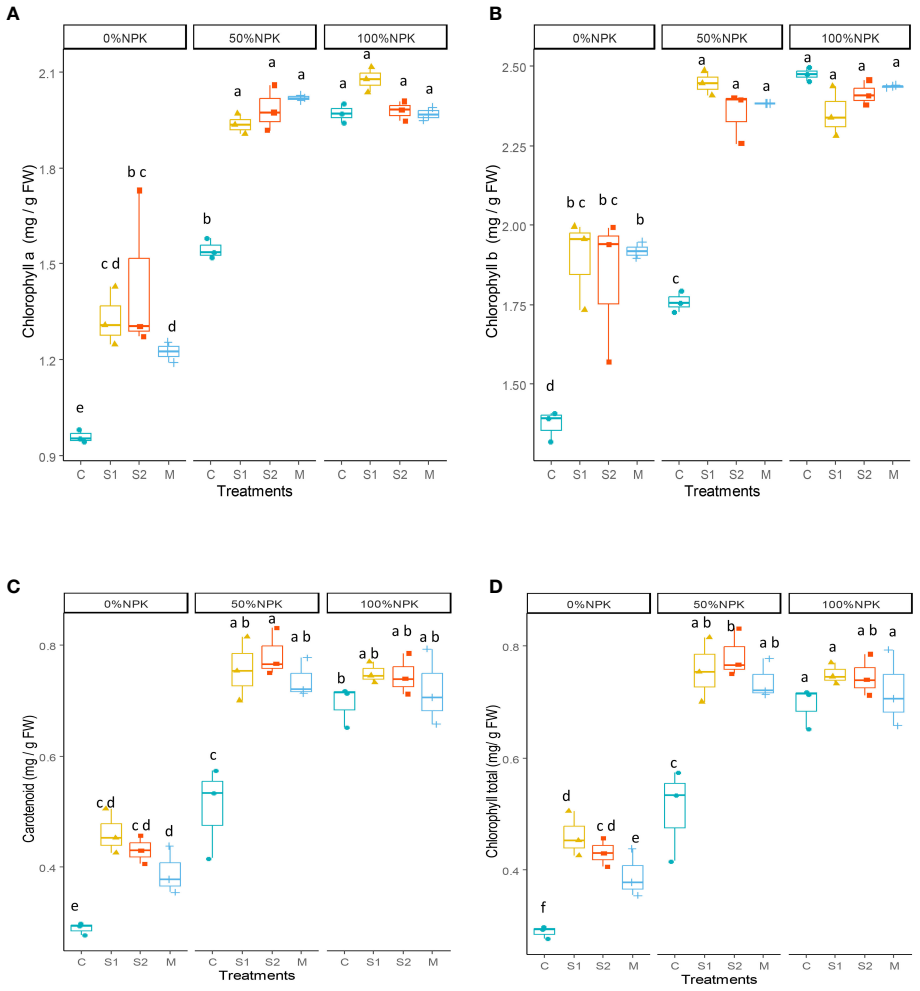

FIGURE 1
Effect of bacterial inoculation and synthetic fertilization on chlorophyll a **(A)**, chlorophyll b **(B)**, carotenoid **(C)**, total chlorophyll **(D)**. C: uninoculated plants, S1: plants inoculated with strain E1, S2: plants inoculated with E3, M: plants inoculated with the mix of two strains, S1 and S2. Each value is the mean of three replicates. Bars indicate the standard error of the mean. Different letters indicate significant differences according to the LSD test.

3.5.4 Rhizosphere soil bacterial population at harvest

The colony-forming units of culturable soil bacteria were transformed into their logarithms and presented in Figure 3. The analysis of variance indicated significant effects of bacterial inoculation, synthetic fertilization, and their interactions on bacterial populations in the rhizosphere (Supplementary Table S5). The results clearly indicated that using a full dose of synthetic fertilizers negatively affects the microbial population of the rhizospheric soil ($p < 0.001$), resulting in significant decreases. However, when a half dose of NPK chemical fertilizers was used along with a bacterial inoculum, the rhizospheric microbial population reached the highest levels with statistical significance.

3.5.5 Relationship between all the studied parameters

The Pearson correlation analysis between all the studied parameters is presented in Figure 4. Strong and positive correlations were found among almost all the morphological parameters (DB, LA, LN, PH, RL, SD, SDW, and RDW), physiological parameters (GA, NDVI, CHLA, CLHB, CHLTOT, CAR, and LRWC), and nutrient accumulation (N, P, K, Na, Mg, Ca, Cu, Fe, and Zn). In contrast, all the studied parameters showed a strong negative correlation with PSRI. Regarding the bacterial population at harvest, the neutral correlation was shown with all the morphological, physiological parameters and nutrient accumulation.

4 Discussion

It is becoming increasingly popular to develop microbial consortia using bacteria with various plant growth-promoting (PGP) traits as an eco-friendly alternative to traditional farming techniques (Kalozoumis et al., 2021; Tounsi-Hammami et al., 2022). This study was designed to isolate native PGP bacteria to select suitable strains as potential biofertilizers for reducing the dependency on NPK synthetic fertilization in the United Arab Emirates (UAE). A total of 41 gram-positive and fast-growing bacteria were isolated from the wet-dry sediments and roots of *A. marina* trees (Supplementary Table S1). Most strains exhibited multiple PGP

TABLE 7 Effect of bacterial inoculation (BI) and synthetic fertilization (SF) on nitrogen (N), phosphorus (P), potassium (K), sodium (Na), magnesium (Mg), calcium (Ca), copper (Cu), iron (Fe) and zinc (Zn) contents of tomato shoots.

	N (mg/g DM)	P (mg/g DM)	K (mg/g DM)	Na (mg/g DM)	Mg (mg/g DM)	Ca (mg/g DM)	Cu (µg/g DM)	Fe (µg/g DM)	Zn (µg/g DM)
C-0%NPK	1.803c ±0.195	1.762f ±0.158	30.608c ±1.587	10.167b ± 0.057	33.892cde ±0.303	22.051e ±0.780	10.501h ± 0.635	33.667f ±3.210	98.904d ±2.080
S1-0%NPK	2.437b ±0.130	2.300de ±0.030	41.813b ±3.020	11.223ab ± 0.979	32.634e ±1.357	25.675d ±0.669	12.227gh± 0.484	45.000e ± 4.000	113.486cd ±1.987
S2-0%NPK	2.477b ±0.108	2.253e ±0.117	42.540b ±1.821	11.740ab ± 1.547	34.764bcde ±0.511	23.598de ±0.375	13.560fg ± 0.951	56.000d ±1.000	113.061cd ±0.908
M-0%NPK	2.717b ±0.057	2.607de ±0.040	43.753b ±1.995	12.427ab ± 1.01	35.603abcd ±1.471	23.400de ±1.320	15.673e ± 0.623	53.667d ±2.080	118.575c ±0.636
C-50%NPK	2.467b ±0.153	2.733d ±0.321	47.490b ±7.464	11.683ab ± 0.616	33.175de ±2.025	21.475e ±0.534	15.170ef ± 1.32	52.667d ±2.520	122.097c ±3.467
S1-50%NPK	4.867a ±0.493	5.267ab ±0.208	65.596a ±0.874	11.981a ± 1.673	34.754bcde ±0.145	31.988c ±3.624	23.363bc ± 1.152	85.333ab ±4.040	159.191b ±18.773
S2-50%NPK	4.500a ±0.529	5.200ab ±0.361	62.475a ±1.804	12.47ab ± 0.869	37.138ab ±3.082	34.521ab ±0.937	24.159b ± 0.545	89.000a ±3.360	183.079a ±11.167
M-50%NPK	5.000a ±0.500	5.500a ±0.265	68.213a ±0.266	12.648a ± 0.895	37.577a ±0.499	36.181a ±0.581	26.910a ± 1.449	90.000a ±3.000	179.072a ±9.577
C-100%NPK	4.633a ±0.379	4.933bc ±0.100	63.063a ±5.603	11.894a ± 0.492	35.470abcd ±0.779	33.714bc ±1.696	22.177cd ± 0.789	69.000c ±3.610	151.588b ±15.684
S1-100%NPK	4.533a ±0.351	5.000bc ±0.208	63.597a ±5.229	12.258a ± 1.751	36.198abc ±1.882	33.460bc ±1.989	21.344d ±0.560	87.667ab ±2.520	146.195b ±7.429
S2-100%NPK	4.533a ±0.451	4.733c ±0.436	67.481a ±2.163	11.900a ± 0.869	35.883abc ±2.211	32.660bc ±0.214	22.117cd ± 1.201	82.667b ±2.520	153.010b ±14.327
M-100%NPK	4.633a ±0.153	4.700c ±0.404	67.482a ±2.196	12.984a ±0.671	36.002abc ±0.194	33.401bc ±0.422	22.548bcd ± 1.867	87.667ab ±2.080	153.307b ±5.876
Bacterial inoculation (BI)	***	***	***	*	*	***	***	***	***
Synthetic fertilization (SF)	***	***	***	ns	*	***	***	***	***
BI*SF	***	***	***	ns	ns	***	***	***	***

C: uninoculated plants, S1: plants inoculated with strain E1, S2: plants inoculated with E3, M: plants inoculated with the mix of two strains, S1 and S2.
Each value is the mean of three replicates. Bars indicate the standard error of the mean. Different letters indicate significant differences according to the LSD test. Significance: ns = not significant; * significant at $p < 0.05$; *** significant at $p < 0.001$.

10.3389/fpls.2024.1356545

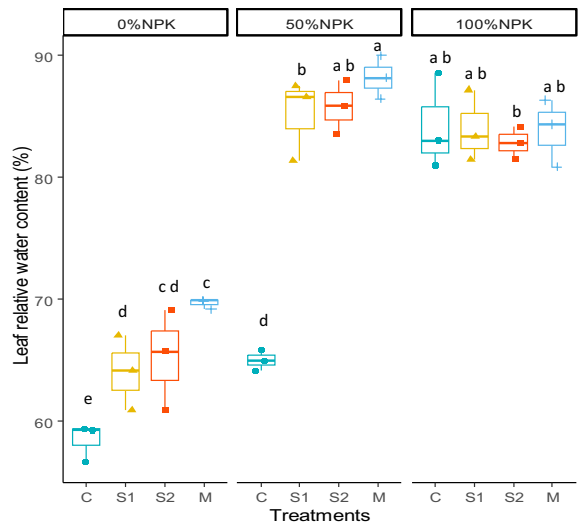

FIGURE 2
Effects of bacterial inoculation and synthetic fertilization on the leaf relative water content. C: uninoculated plants, S1: plants inoculated with strain E1, S2: plants inoculated with E3, M: plants inoculated with the mix of two strains, S1 and S2. Each value is the mean of three replicates. Bars indicate the standard error of the mean. Different letters indicate significant differences according to the LSD test.

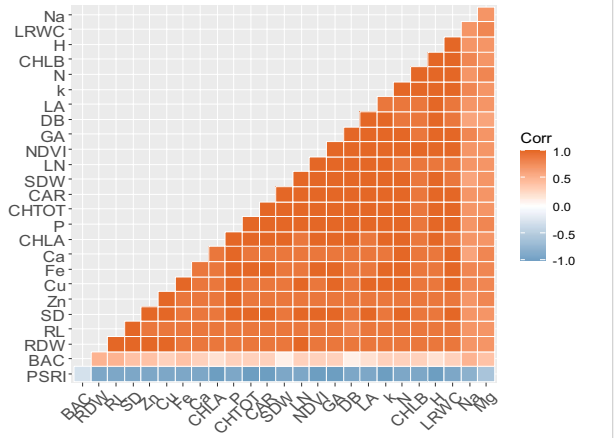

FIGURE 4
The Pearson correlation coefficient analysis heat map showing the correlation among all the studied parameters. DB, biomass; LA, leaf area; GA, greenness average; NDVI, the normalized difference vegetation index; PSRI, plant senescence reflectance index; LN, leaf number; PH, plant height; RL, root length; SD, stem diameter; SDW, shoot dry weight; RDW, root dry weight; CHLA, chlorophyll a; CHLB, chlorophyll b; CAR, carotenoid; CHLTOT, total chlorophyll; LRWC, leaf relative water content; BAC, bacterial population; N, nitrogen; P, phosphorus; K, potassium; Ca, calcium; Mg, magnesium; Fe, iron; Cu, copper; Zn, Zinc. Orange and blue gradients show positive and negative strength correlations; respectively.

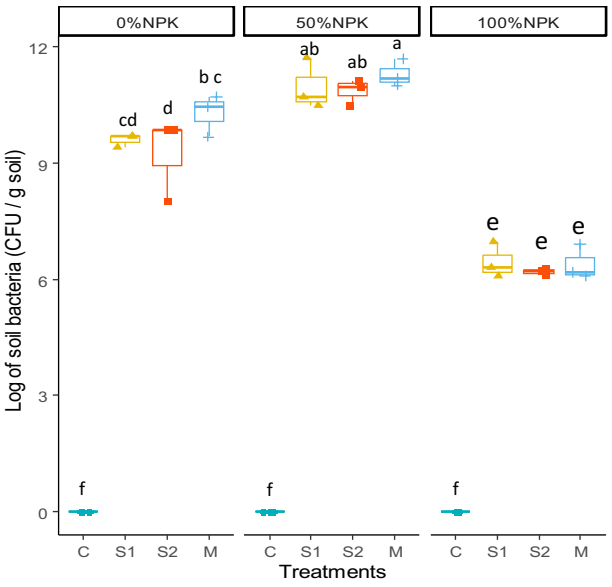

FIGURE 3
Effects of bacterial inoculation and synthetic fertilization on rhizosphere soil bacterial population at harvest. C: uninoculated plants, S1: plants inoculated with strain E1, S2: plants inoculated with E3, M: plants inoculated with the mix of two strains, S1 and S2. Each value is the mean of three replicates. Bars indicate the standard error of the mean. Different letters indicate significant differences according to the LSD test.

traits, including ammonia, IAA, siderophores production, P and K solubilization, and HCN production. Approximately 78% of native strains have been found to produce varying levels of ammonia, which acts as a nitrogen source for plant growth (Banik et al., 2019). Furthermore, excessive ammonia production can also prevent the colonization of pathogens on host plants and inhibit the germination of fungal spores (Singh and Parli, 2020). Considering the IAA production, the recorded amount ranged from 1.51 to 8.55 ppm with strains SW15 and SW14, respectively. The amounts of IAA detected in this study were similar to those reported by Barbaccia et al. (2022). The differences in the capacity of PGP bacteria to generate IAA, as presented in this study, may be due to a range of factors, such as the various biosynthetic pathways, the location of the involved genes, regulatory sequences, and the presence of enzymes that can convert active free IAA into conjugated forms (Patten and Glick, 1996). The IAA is widely recognized as the primary phytohormone that regulates many developmental processes. In low concentrations, IAA stimulates the elongation of primary roots. Conversely, elevated levels of IAA promote the growth of lateral and adventitious roots, facilitating water and nutrient absorption from the soil and indirectly promoting plant development (Naureen et al., 2017; Gowtham et al., 2022). Under *in vitro* conditions with iron limitation, 65% of the native strains were siderophore producers. It was reported that siderophores might help in the process of iron sequestration and solubilization, inhibiting the establishment of pathogenic (Sahu et al., 2021; Tripathi et al., 2022). Furthermore, our study discovered 24 and 15 native strains that effectively solubilize phosphate and potassium, respectively. These strains can convert insoluble P and K into plant-available forms, which is a crucial ability in areas where P and K are limiting factors for crop production (Bhat et al., 2022). Another mechanism of plant growth promotion, shown in our study, was the production of HCN, which is a volatile compound that plays a major role in the biocontrol process against phytopathogens (Sehrawat et al., 2022). Furthermore, Marques et al. (2010) reported a positive correlation between the

generation of HCN and nitrogen accumulation, root and shoot elongation, and biomass production. These results highlighted the richness of the mangrove ecosystem dominated by *A. marina* sp. associated native bacteria with multiple PGP traits that can, directly and indirectly, promote plant growth, making them potential biofertilizers for agricultural crops in the UAE and MENA region.

After analyzing the 16S rRNA profile of the eight selected strains, it was found that they all belonged to the *Bacillus* group, specifically related to *B. licheniformis, B. Paralicheniformis, B. cabrialesii, B. subtilis*, and *B. wiedmannii*. Our findings are consistent with previous research showing that *Bacillus* is the most common group found in the *A. marina* ecosystem around the world, including China (Tong et al., 2019; Liu et al., 2022), Oman (Ali et al., 2017), and India (Pallavi et al., 2023). Most of these bacteria are known as beneficial bacteria with growth promotion abilities under optimum as well as under different abiotic and biotic stress conditions (Akhtar et al., 2020; Tsotetsi et al., 2021; Rojas-Solis et al., 2023). Among the most promising PGP bacteria, the *Bacillus* group is gaining more attention in agriculture thanks to its long shelf life and stability in harsh environments (Luo et al., 2022).

Two compatible strains, E1 and E3, with multi-PGP traits, were selected to be tested as biofertilizers for tomato plants at varying levels of NPK fertilization (0, 50, and 100% of the recommended dose). Results revealed that using these native PGP bacteria, either alone or mixed, significantly improved all the studied morphological parameters and vegetative indices in tomato plants, Shourouq variety, compared to control plants (Tables 5, 6). However, strong interactions between bacterial inoculation and synthetic fertilization indicate that these PGP bacteria' effectiveness depended on the synthetic NPK rate. Compared to the control plants, applying bacterial inoculant alone did not match the efficiency of synthetic NPK fertilizer in achieving maximum growth. This is consistent with several previous studies on other crops worldwide such as wheat (*Triticum turgidum* spp. *durum* L.) in Tunisia (Tounsi-Hammami et al., 2022), maize (*Zea mays* L.) in Brazil (Bueno et al., 2022), and cucumber (*Cucumis sativus* L.) in Italy (Scagliola et al., 2021).

It is important to note that combining native PGP bacteria with 50%NPK resulted in the highest values of DB, LA, LN, PH, RL, SD, SDW, and RDW. These values were statistically similar or even greater than those observed in control plants that received 100% NPK (Tables 5, 6). This suggests that it's possible to replace 50% of NPK synthetic fertilizers with selected native bacteria without negatively affecting the plant's vegetative growth. The recorded improvement of morphological parameters is likely due to greater physiological activity compared to the control plants. Our findings show that applying native PGP bacteria along with 50%NPK resulted in significant increases in the relative leaf water content (Figure 2), indicating better water uptake and photosynthetic activity in plant tissues. Our findings supported the findings of a previous study by Yaghoubi Khanghahi et al. (2021) that bacterial inoculation can improve photosynthetic apparatus performance by positively impacting photosystem II functionality and chlorophyll pigment concentrations. This effect was reflected in the current study in higher GA, NDVI, and chlorophyll pigment concentrations, including the total chlorophyll, Chlorophyll a, Chlorophyll b, and carotenoids (Table 5; Figure 1). It may be suggested that inoculated plants could absorb more light energy to drive photosynthesis (Sahandi et al., 2019; Wu et al., 2019).

In contrast, when plants were given a full dose of synthetic NPK fertilization, the different bacterial inoculants showed no significant effect compared to control plants. According to Yan et al. (2019), synthetic fertilization did not affect the ability of beneficial bacteria to exhibit their PGP traits. However, the lack of any benefit from applying PGP bacteria in the present study may be explained by the significant decreases in the bacterial population recorded in the rhizospheric soil after applying 100%NPK (Figure 3). Our findings supported those of Yadav et al. (2009), who reported that the population of *G.diazotrophicus* in rhizospheric sugarcane was negatively affected by the addition of synthetic nitrogen. It was reported that high levels of synthetic inputs may enter the bacterial cells and disturb their metabolism, which decreases their abundance in rhizospheric soil (Reid et al., 2021), leading to significant reductions in root colonization (Bueno et al., 2022). It can be suggested that high levels of synthetic fertilizers lead to greater nutrient availability in rhizospheric soils, which may limit the plant's need to interact with beneficial microorganisms in the rhizosphere (Meena et al., 2017). Interestingly, a half rate of synthetic NPK positively affected the bacterial population in tomato roots' rhizosphere. It may be suggested that 50%NPK may support the growth of PGP bacteria and tomato plants equally (Zarei et al., 2012). Furthermore, the two selected native strains produced IAA, which induces significant increases in root development reflected in this study by increasing root length and biomass. It was reported previously that better root growth impacts soil microbiome via secreting more exudates, including sugars and organic acids. In response, soil microbes thrive and interact more frequently (Ye et al., 2020).

The boosting of plant growth observed in inoculated plants could be explained by the plants' greater absorption of several nutrients from the soil (Anli et al., 2020). In fact, strong and positive correlations were found between nutrient accumulation, physiological parameters, and morphological parameters (Figure 3). Our results revealed that plants treated with the mix of native PGP strains and 50%NPK had considerably higher contents of N, P, K, Ca, Fe, and Zn (Table 7). Our results aligned with several previous research (Ye et al., 2020; Scagliola et al., 2021; Sritongon et al., 2023). A theoretical relationship between the *in vitro* and *in vivo* results could explain these findings. The IAA produced by the strains promotes the growth of root cortical cells, leading to an increase in the number of root tips and branches, allowing greater exploration of the soil and higher absorption of nutrients. Additionally, the ability of these PGP strains to produce ammonia and solubilize P and K under *in vitro* conditions could explain the observed enhancement of N, P and K accumulation in the tomato shoots. Furthermore, tomato shoots' Fe, Zn, and Cu contents were significantly increased. This effect may be attributed to the ability of the two native strains to produce siderophores, known as iron-chelating compounds that enhance the uptake of various metals by plants (Scagliola et al., 2016; Prasad et al., 2019; Singh et al., 2022). Considering that crop productivity depends on early-stage seedling growth techniques, combining native PGP bacteria with 50% NPK should be adopted for farmers as well as for seedling nursery producers.

5 Conclusion

The present study demonstrates that using native PGP bacteria alone or in consortium as biofertilizers improves tomato seedling quality while reducing the global dependence on hazardous synthetic fertilizers. Although these results were obtained in partially controlled conditions, they suggest that bioinoculants could be used as a valid complement to synthetic fertilization for a more sustainable agricultural scenario. This simple approach can help farmers reduce cultivation costs while protecting the environment and human and soil health. However, further studies are required to evaluate the positive impact of these bacteria on the growth and productivity of other tomato varieties and different crops in large-scale field conditions and greenhouses.

Data availability statement

The datasets presented in this study can be found in online repositories. The names of the repository/repositories and accession number(s) can be found below: NCBI database with accession numbers OP600564 to OP600571.

Ethics statement

The manuscript presents research on animals that do not require ethical approval for their study.

Author contributions

ST-H: Data curation, Formal analysis, Investigation, Supervision, Writing – original draft, Software. MK: Conceptualization, Funding acquisition, Methodology, Project administration, Resources, Supervision, Writing – review & editing, Validation. AZ: Formal analysis, Methodology, Writing – review & editing. AA: Investigation, Methodology, Validation, Writing – review & editing. NA: Formal analysis, Investigation, Methodology, Validation, Writing – review & editing. MN: Data curation, Formal analysis, Methodology, Resources, Validation, Writing – review & editing. SM: Funding acquisition, Resources, Supervision, Visualization, Writing – review & editing.

Funding

The author(s) declare financial support was received for the research, authorship, and/or publication of this article. This work was financially supported by the UAEU-ZU Joint Research project (R22024; 12R139) and the Zayed University Research Incentive Fund (RIF) project-R21074.

Acknowledgments

We are grateful to former Zayed University undergraduate students Amna Alameri, Hawra Alfardan, Hamda Ahmad Rahimi, Fatma Abdulrahman and Fatma Mohamed Alraeesi for performing preliminary studies on the isolation and characterization of PGPB from Umm-Al Quwain mangrove forest. We thank Zayed University laboratory support staff Fatma Al Ali and Anil Menezes for logistics support for sample processing at Zayed University (Dubai) instrumentation and the hyperspectral lab (Abu Dhabi).

Conflict of interest

The authors declare that the research was conducted in the absence of any commercial or financial relationships that could be construed as a potential conflict of interest.

Publisher's note

Supplementary material

The Supplementary Material for this article can be found online at: https://www.frontiersin.org/articles/10.3389/fpls.2024.1356545/full#supplementary-material

References

Akhtar, S. S., Amby, D. B., Hegelund, J. N., Fimognari, L., Grobkinsky, D. K., Westergaard, J. C., et al. (2020). *Bacillus licheniformis* FMCH001 Increases water use efficiency via growth stimulation in both normal and drought conditions. *Front. Plant Sci.* 11. doi: 10.3389/fpls.2020.00297

Akinnawo, S. O. (2023). Eutrophication: causes, consequences, physical, chemical and biological techniques for mitigation strategies. *Environ. Chall* 12, 100733. doi: 10.1016/j.envc.2023.100733

Ali, A., Shahzad, R., Khan, A. L., Halo, B. A., Al-Yahyai, R., Al-Harrasi, A., et al. (2017). Endophytic bacterial diversity of *Avicennia marina* helps to confer resistance against salinity stress in *Solanum lycopersicum*. *J. Plant Interact.* 12, 312–322. doi: 10.1080/17429145.2017.1362051

Aneja, K. R. (2003). *Experiments in Microbiology, Plant Pathology and Biotechnology. 4th ed.* (New Delhi: New Age International Publishers, Daryaganj).

Anli, M., Symanczik, S., El Abbassi, A., Ait-El-Mokhtar, M., Boutasknit, A., Ben-Laouane, R., et al. (2020). Use of arbuscular mycorrhizal fungus Rhizoglomus irregulare and compost to improve growth and physiological responses of Phoenix dactylifera "Boufgouss". *Plant Biosyst.*, 1–14. doi: 10.1080/11263504.2020.1779848

Asghar, I., Ahmed, M., Farooq, M. A., Ishtiaq, M., Arshad, M., Akram, M., et al. (2023). Characterizing indigenous plant growth promoting bacteria and their synergistic effects with organic and chemical fertilizers on wheat (*Triticum aestivum*). *Front. Plant Sci.* 14. doi: 10.3389/fpls.2023.1232271

Banik, A., Dash, G. K., Swain, P., Kumar, U., Mukhopadhyay, S. K., and Dangar, T. K. (2019). Application of rice (*Oryza sativa* L.) root endophytic diazotrophic Azotobacter sp. strain Avi2 (MCC 3432) can increase rice yield under greenhouse and field condition. *Microbiol. Res.* 219, 56–65. doi: 10.1016/j.micres.2018.11.004

Barbaccia, P., Gaglio, R., Dazzi, C., Miceli, C., Bella, P., Papa, G. L., et al. (2022). Plant growth promoting activities of bacteria isolated from an anthropogenic soil located in Agrigento province. *Microorganisms* 10, 2167. doi: 10.3390/microorganisms10112167

Bhat, B. A., Tariq, L., Nissar, S., Islam, S. T., Islam, S. U., Mangral, Z., et al. (2022). The role of plant-associated rhizobacteria in plant growth, biocontrol and abiotic stress management. *J. Appl. Microbiol.* 133, 2717–2741. doi: 10.1111/jam.15796

Boleta, E. H. M., Shintate Galindo, F., Jalal, A., Santini, J. M. K., Rodrigues, W. L., Lima, B. H. D., et al. (2020). Inoculation with growth-promoting bacteria *Azospirillum brasilense* and its effects on productivity and nutritional accumulation of wheat cultivars. *Front. Sustain. Food Syst.* 4. doi: 10.3389/fsufs.2020.607262

Bueno, C. B., Dos Santos, R. M., De Souza Buzo, F., De Andrade Da Silva, M. S. R., and Rigobelo, E. C. (2022). Effects of chemical fertilization and microbial inoculum on *Bacillus subtilis* colonization in soybean and maize plants. *Front. Microbiol.* 13. doi: 10.3389/fmicb.2022.901157

Cappuccino, J. G., and Sherman, N. (1992). *Microbiology: A Laboratory Manual. 3rd ed* (New York, NY, USA: Benjamin-Cummings Pub Co (B.c.P).

Chataut, G., Bhatta., B., Joshi, D., Subedi, K., and Kafle, K. (2023). Greenhouse gases emission from agricultural soil: A review. *J. Agric. Food Res.* 11, 100533. doi: 10.1016/j.jafr.2023.100533

Cirillo, V., Romano, I., Woo, S. L., Di Stasio, E., Lombardi, N., Comite, E., et al. (2023). Inoculation with a microbial consortium increases soil microbial diversity and improves agronomic traits of tomato under water and nitrogen deficiency. *Front. Plant Sci.* 14. doi: 10.3389/fpls.2023.1304627

Devi, P. I., Manjula, M., and Bhavani, R. V. (2022). Agrochemicals, environment, and human health. *Annu. Rev. Environ. Resour.* 47, 399–421. doi: 10.1146/annurev-environ-120920-111015

Frank, J. A., Reich, C. I., Sharma, S., Weisbaum, J. S., Wilson, B. A., and Olsen, G. J. (2008). Critical evaluation of two primers commonly used for amplification of bacterial 16S rRNA Genes. *Appl. Environ. Microbiol.* 74, 2461–2470. doi: 10.1128/AEM.02272-07

Gen-Jiménez, A., Flores-Félix, J. D., Rincón-Molina, C. I., Manzano-Gomez, L. A., Rogel, M. A., Ruíz-Valdiviezo, V. M., et al. (2023). Enhance of tomato production and induction of changes on the organic profile mediated by Rhizobium biofortification. *Front. Microbiol.* 14. doi: 10.3389/fmicb.2023.1235930

Gordon, S. A., and Weber, R. P. (1951). Colorimetric estimation of indoleacetic acid. *Plant Physiol.* 26, 192. doi: 10.1104/pp.26.1.192

Gowtham, H. G., Singh, S. B., Shilpa, N., Aiyaz, M., Nataraj, K., Udayashankar, A. C., et al. (2022). Insight into recent progress and perspectives in improvement of antioxidant machinery upon PGPR augmentation in plants under drought stress: a review. *Antioxidants* 11, 1763. doi: 10.3390/antiox11091763

Ijaz, A., Mumtaz, M. Z., Wang, X., Ahmad, M., Saqib, M., Maqbool, H., et al. (2021). Insights into manganese solubilizing bacillus spp. for improving plant growth and manganese uptake in maize. *Front. Plant Sci.* 12. doi: 10.3389/fpls.2021.719504

Ikiz, B., Dasgan, H. Y., and Gruda, N. S. (2024). Utilizing the power of plant growth promoting rhizobacteria on reducing mineral fertilizer, improved yield, and nutritional quality of Batavia lettuce in a floating culture. *Sci. Rep.* 14, 1616. doi: 10.1038/s41598-024-51818-w

Kalozoumis, P., Savvas, D., Aliferis, K., Ntatsi, G., Marakis, E., Simou, G., et al. (2021). Impact of Plant Growth-Promoting Rhizobacteria inoculation and grafting on tolerance of Tomato to combined water and nutrient stress assessed via metabolomics analysis. *Front. Plant Sci.* 12. doi: 10.3389/fpls.2021.670236

Kjeldahl, C. (1883). A new method for the determination of nitrogen in organic matter. *Z Anal. Chem.* 22, 366. doi: 10.1007/BF01338151

Kong, X., Zhang, C., and Zhang, X. (2018). Change of factor endowment and improvement of agriculture capital organic composition: An explanation of China's agricultural development path since 1978. *Manage. World* 34, 147–160. doi: 10.3390/agriculture13091794

Liu, G. H., Liu, D. Q., Wang, P., Chen, Q. Q., Che, J. M., Wang, J. P., et al. (2022). Temperature drives the assembly of Bacillus community in mangrove ecosystem. *Sci. Total Environ.* 846, 157496. doi: 10.5897/AJB11.3194

Lorck, H. (1948). Production of hydrocyanic acid by bacteria. *Physiol. Plant* 1, 142–146. doi: 10.1111/j.1399-3054.1948.tb07118.x

Louden, B. C., Haarmann, D., and Lynne, A. M. (2011). Use of blue agar CAS assay for siderophore detection. *J. Microbiol. Biol. Educ.* 12, 51–53. doi: 10.1128/jmbe.v12i1.249

Luo, L., Zhao, C., Wang, E., Raza, A., and Yin, C. (2022). *Bacillus amyloliquefaciens* as an excellent agent for biofertilizer and biocontrol in agriculture: An overview for its mechanisms. *Microbial. Res.* 259, 127016. doi: 10.1016/j.micres.2022.127016

Majeed, A., Abbasi, M. K., Hameed, S., Imran, A., and Rahim, N. (2015). Isolation and characterization of plant growth-promoting rhizobacteria from wheat rhizosphere and their effect on plant growth promotion. *Front. Microbiol.* 6. doi: 10.3389/fmicb.2015.00198

Marques, A. P., Pires, C., Moreira, H., Rangel, A. O., and Castro, P. M. (2010). Assessment of the plant growth promotion abilities of six bacterial isolates using *Zea mays* as indicator plant. *Soil Biol. Biochem.* 42, 1229–1235. doi: 10.1016/j.soilbio.2010.04.014

Meena, V. S., Maurya, B. R., Verma, J. P., Aeron, A., Kumar, A., Kim, K., et al. (2015). Potassium solubilizing rhizobacteria (KSR): Isolation, identification, and K-release dynamics from waste mica. *Ecol. Eng.* 81, 340–347. doi: 10.1016/j.ecoleng.2015.04.065

Meena, V. S., Meena, S. K., Verma, J. P., Kumar, A., Aeron, A., Mishra, P. K., et al. (2017). Plant Beneficial Rhizospheric Microorganism (PBRM) strategies to improve nutrients use efficiency: a review. *Ecol. Eng.* 107, 8–32. doi: 10.1016/j.ecoleng.2017.06.058

Moncada, A., Vetrano, F., Esposito, A., and Miceli, A. (2020). Fertigation management and growth-promoting treatments affect tomato transplant production and plant growth after transplant. *Agronomy* 10, 1504. doi: 10.3390/agronomy10101504

Mortinho, E. S., Jalal, A., Da Silva Oliveira, C. E., Fernandes, G. C., Pereira, N. C. M., Rosa, P. A. L., et al. (2022). Co-inoculations with plant growth-promoting bacteria in the common bean to increase efficiency of NPK fertilization. *Agronomy* 12, 1325. doi: 10.3390/agronomy12061325

Naureen, Z., Rehman, N. U., Hussain, H., Hussain, J., Gilani, S. A., Al Housni, S. K., et al. (2017). Exploring the potentials of *Lysinibacillus sphaericus* ZA9 for plant growth promotion and biocontrol activities against phytopathogenic fungi. *Front. Microbiol.* 8. doi: 10.3389/fmicb.2017.01477

Pallavi,, Mishra, R. K., Sahu, P. K., Mishra, V., Jamal, H., Varma, A., et al. (2023). Isolation and characterization of halotolerant plant growth promoting rhizobacteria from mangrove region of Sundarbans, India for enhanced crop productivity. *Front. Plant Sci.* 14. doi: 10.3389/fpls.2023.1122347

Patten, C., and Glick, B. R. (1996). Bacterial biosynthesis of indole-3-acetic acid. *Can. J. Microbiol.* 42, 207–220. doi: 10.1139/m96-032

Pauwels, J. M., Van Ranst, E., Verloo, M., and Mvondoze, A. (1992). *Manuel de laboratoire de pédologie: Méthodes d'Analyses de sols et de plantes, Equipement, Gestion de stocks de Verrerie et de Produits chimiques* (Bruxelles, Belgique: Publications Agricoles, 28. Ministère de l'Enseignement Supérieur, de l'Informatique et de la Recherche Scientifique, Centre Universitaire de Dschang, Cameroun, Administration Générale de la Coopération au Développement), 265.

Pikovskaya, R. I. (1948). Mobilization of phosphorus in soil in connection with the vital activity of some microbial species. *Mikrobiologya* 17, 362–370.

Prasad, A. A., and Babu, S. (2017). Compatibility of *Azospirillum brasilense* and *Pseudomonas fluorescens* in growth promotion of Groundnut (*Arachis Hypogea* L.). *Anais Da Academia Bras. Ciências* 89, 1027–1040. doi: 10.1590/0001-3765201720160617

Prasad, M., Srinivasan, R., Chaudhary, M., Choudhary, M., and Jat., L. K. (2019). "Plant Growth Promoting Rhizobacteria (PGPR) for sustainable agriculture: Perspectives and challenges," in *PGPR Amelioration in Sustainable Agriculture*. Eds. A. K. Singh, A. Kumar and P. K. Singh (Elsevier, Amsterdam, The Netherland), 129–157.

Reid, T. E., Kavamura., V. N., Abadie, M., Torres-Ballesteros, A., Pawlett, M., Clark, M. I., et al. (2021). Inorganic chemical fertilizer application to wheat reduces the abundance of putative plant growth-promoting rhizobacteria. *Front. Microbiol.* 12. doi: 10.3389/fmicb.2021.642587

Rojas-Solis, D., García Rodríguez, Y. M., Larsen, J., Santoyo, G., and Lindig-Cisneros, R. (2023). Growth promotion traits and emission of volatile organic compounds of two bacterial strains stimulate growth of maize exposed to heavy metals. *Rhizosphere* 27, 100739. doi: 10.1016/j.rhisph.2023.100739

Rosa, P. A. L., Galindo, F. S., da Silva Oliveira, C. E., Jalal, A., Mortinho, E. S., Fernandes, G. C., et al. (2022). Inoculation with plant growth promoting bacteria to reduce phosphate fertilization requirement and enhance technological quality and yield of sugarcane. *Microorganisms* 10, 192. doi: 10.3390/microorganisms10010192

Sahandi, M. S., Mehrafarin, A., Badi, H. N., Khalighi-Sigaroodi, F., and Sharifi, M. (2019). Improving growth, phytochemical, and antioxidant characteristics of peppermint by phosphate-solubilizing bacteria along with reducing phosphorus fertilizer use. *Ind. Crops Prod.* 141, 111777. doi: 10.1016/j.indcrop.2019.111777

Sahu, P. K., Singh, S., Singh, U. B., Chakdar, H., Sharma, P. K., Sarma, B. K., et al. (2021). Inter-genera colonization of *Ocimum tenuiflorum* endophytes in tomato and their complementary effects on Na^+/K^+ balance, oxidative stress regulation, and root architecture under elevated soil salinity. *Front. Microbiol.* 12. doi: 10.3389/fmicb.2021.744733

Samara, F., Solovieva, N., Ghalayini, T., Nasrallah, Z. A., and Saburova, M. (2020). Assessment of the environmental status of the mangrove ecosystem in the United Arab Emirates. *Water* 12, 1623. doi: 10.3390/w12061623

Scagliola, M., Pii, Y., Mimmo, T., Cesco, S., Ricciuti, P., and Crecchio, C. (2016). Characterization of plant growth promoting traits of bacterial isolates from the rhizosphere of barley (*Hordeum vulgare* L.) and tomato (*Solanum lycopersicon* L.) grown under Fe sufficiency and deficiency. *Plant Physiol. Biochem.* 107, 187–196. doi: 10.1016/j.plaphy.2016.06.002

Scagliola, M., Valentinuzzi, F., Mimmo, T., Cesco, S., Crecchio, C., and Pii, Y. (2021). Bioinoculants as promising complement of chemical fertilizers for a more sustainable agricultural practice. *Front. Sustain. Food Syst.* 4. doi: 10.3389/fsufs.2020.622169

Schwyn, B., and Neilands, J. B. (1987). Universal chemical assay for the detection and determination of siderophores. *Anal. Biochem.* 160, 47–56. doi: 10.1016/0003-2697(87)90612-9

Sehrawat, A., Sindhu, S. S., and Glik, B. R. (2022). Hydrogen cyanide production by soil bacteria: Biological control of pests and promotion of plant growth in sustainable agriculture. *Pedosphere* 32, 15–38. doi: 10.1016/S1002-0160(21)60058-9

Singh, A. K., and Parli, B. V. (2020). Siderophore production by bacteria isolated from mangrove sediments: A microcosm study. *J. Exp. Mar. Biol. Ecol.* 524, 151290. doi: 10.1016/j.jembe.2019.151290

Singh, S. K., Wu, X., Shao, C., and Zhang, H. (2022). Microbial enhancement of plant nutrient acquisition. *Stress Biol.* 2, 3. doi: 10.1007/s44154-021-00027-w

Somasegaran, P., and Hoben, H. J. (1994). *Handbook for Rhizobia. Methods in Legume*–Rhizobium *Technology* (Heidelberg, NY: Springer). doi: 10.1007/978-1-4613-8375-8

Sritongon, N., Boonlue, S., Mongkolthanaruk, W., Jogloy, S., and Riddech, N. (2023). The combination of multiple plant growth promotion and hydrolytic enzyme producing rhizobacteria and their effect on Jerusalem artichoke growth improvement. *Sci. Rep.* 13, 5917. doi: 10.1038/s41598-023-33099-x

Tong, T., Li, R., Wu, S., and Xie, S. (2019). The distribution of sediment bacterial community in mangroves across China was governed by geographic location and eutrophication. *Mar. pollut. Bull.* 140, 198–203. doi: 10.1016/j.marpolbul.2019.01.046

Torrecillas, A., Leon, A., Del Amor, F., and Martinez-Mompean, M. C. (1984). Determinaciòn rápida de clorofla en discos foliares de limonero. *Fruits* 39, 617–622.

Toselli, M., Baldi, E., Marcolini, G., Malaguti, D., Quartieri, M., Sorrenti, G., et al. (2009). Response of potted grapevines to increasing soil copper concentration. *Aust. J. Grape. Wine. Res.* 15, 85–92. doi: 10.1111/j.1755-0238.2008.00040.x

Tounsi-Hammami, S., Hammami, Z., Dhane-Fitouri, S., Le Roux, C., and Ben Jeddi, F. (2022). A mix of *Agrobacterium* strains reduces nitrogen fertilization while enhancing economic returns in field trials with durum wheat in contrasting agroclimatic regions. *J. Soil. Sci. Plant Nutr.* 22, 4816–4833. doi: 10.1007/s42729-022-00962-1

Tounsi-Hammami, S., Le Roux, C., Dhane-Fitouri, S., De Lajudie, P., Duponnois, R., and Ben Jeddi, F. (2019). Genetic diversity of rhizobia associated with root nodules of white lupin (*Lupinus albus* L.) in Tunisian calcareous soils. *Syst. Appl. Microbiol.* 42, 448–456. doi: 10.1016/j.syapm.2019.04.002

Trabelsi, D., Mengoni, A., Ben Ammar, H., and Mhamdi, R. (2011). Effect of on-field inoculation of *Phaseolus vulgaris* with rhizobia on soil bacterial communities. *FEMS Microbiol. Ecol.* 77, 211–222. doi: 10.1111/j.1574-6941.2011.01102.x

Tripathi, S., Bahuguna, R., Shrivastava, N., Singh, S., Chatterjee, A., Varma, A., et al. (2022). Microbial biofortification: A sustainable route to grow nutrient-rich crops under changing climate. *Field Crops Res.* 287, 108662. doi: 10.1016/j.fcr.2022.108662

Tsegaye, Z., Alemu, T., Desta, A. F., and Assefa, F. (2022). Plant growth-promoting rhizobacterial inoculation to improve growth, yield, and grain nutrient uptake of teff varieties. *Front. Microbiol.* 13. doi: 10.3389/fmicb.2022.896770

Tsotetsi, T., Nephali, L., Malebe, M., and Tugizimana, F. (2021). *Bacillus* for plant growth promotion and stress resilience: What have we learned? *Plants* 11, 2482. doi: 10.3390/plants11192482

Turner, N. C. (1986). Crop water deficits: a decade of progress. *Adv. Agron.* 39, 1–51. doi: 10.1016/S0065-2113(08)60464-2

Van Dijk, M., Morley, T., Rau, M. L., and Saghai, Y. (2021). A meta-analysis of projected global food demand and population at risk of hunger for the period 2010–2050. *Nat. Food* 2, 494–501. doi: 10.1038/s43016-021-00322-9

Wu, F., Li, J., Chen, Y., Zhang, L., Zhang, Y., and Wang, S. (2019). Effects of phosphate solubilizing bacteria on the growth, photosynthesis, and nutrient uptake of Camellia oleifera Abel. *Forests* 10, 348. doi: 10.3390/f10040348

Yadav, R. L., Suman, A., Prasad, S. R., and Prakash, O. (2009). Effect of *Gluconacetobacter diazotrophicus* and *Trichoderma viride* on soil health, yield and N-economy of sugarcane cultivation under subtropical climatic conditions of India. *Eur. J. Agron.* 30, 296–303. doi: 10.1016/j.eja.2009.01.002

Yaghoubi Khanghahi, M., Leoni, B., and Crecchio, C. (2021). Photosynthetic responses of durum wheat to chemical/microbiological fertilization management under salt and drought stresses. *Acta Physiol. Plant* 43, 123. doi: 10.1007/s11738-021-03289-z

Yan, J., Han, X. Z., Chen, X., Lu, X. C., Chen, W. F., Wang, E. T., et al. (2019). Effects of long-term fertilization strategies on soil productivity and soybean rhizobial diversity in a Chinese Mollisol. *Pedosphere* 29, 784–793. doi: 10.1016/S1002-0160(17)60470-3

Ye, L., Zhao, X., Bao, B., Li, J., Zou, Z., and Cao, K. (2020). Bio-organic fertilizer with reduced rates of chemical fertilization improves soil fertility and enhances tomato yield and quality. *Sci. Rep.* 10, 177. doi: 10.1038/s41598-019-56954-2

Zarei, I., Sohrabi, Y., Heidari, G. R., Jalilian, A., and Mohammadi, K. (2012). Effects of biofertilizers on grain yield and protein content of two soybean (*Glycine max* L.) cultivars. *Af J. Biotechnol.* 11, 7028–7703. doi: 10.5897/AJB11.3194

frontiers | Frontiers in Plant Science

TYPE Original Research
PUBLISHED 22 March 2024
DOI 10.3389/fpls.2024.1324538

OPEN ACCESS

EDITED BY
Marcia Soares Vidal,
Brazilian Agricultural Research Corporation (EMBRAPA), Brazil

REVIEWED BY
Clarisse Brígido,
University of Evora, Portugal
Tianhao Liu,
Affiliated Hospital of Jiangnan University, China

*CORRESPONDENCE
Mostafa M. El-Sheekh
mostafaelsheikh@science.tanta.edu.eg

RECEIVED 19 October 2023
ACCEPTED 28 February 2024
PUBLISHED 22 March 2024

CITATION
Nagah A, El-Sheekh MM, Arief OM, Alqahtani MD, Alharbi BM and Dawwam GE (2024) Endophytic *Bacillus vallismortis* and *Bacillus tequilensis* bacteria isolated from medicinal plants enhance phosphorus acquisition and fortify *Brassica napus* L. vegetative growth and metabolic content. *Front. Plant Sci.* 15:1324538. doi: 10.3389/fpls.2024.1324538

Endophytic *Bacillus vallismortis* and *Bacillus tequilensis* bacteria isolated from medicinal plants enhance phosphorus acquisition and fortify *Brassica napus* L. vegetative growth and metabolic content

Aziza Nagah[1], Mostafa M. El-Sheekh[2]*, Omnia M. Arief[1], Mashael Daghash Alqahtani[3], Basmah M. Alharbi[4,5] and Ghada E. Dawwam[1]

[1]Botany and Microbiology Department, Faculty of Science, Benha University, Benha, Egypt, [2]Botany Department, Faculty of Science, Tanta University, Tanta, Egypt, [3]Department of Biology, College of Science, Princess Nourah bint Abdulrahman University, Riyadh, Saudi Arabia, [4]Biology Department, Faculty of Science, University of Tabuk, Tabuk, Saudi Arabia, [5]Biodiversity Genomics Unit, Faculty of Science, University of Tabuk, Tabuk, Saudi Arabia

Phosphorus fertilization imposes critical limitations on crop productivity and soil health. The aim of the present work is to explore the potential of two phosphate solubilizing bacteria (PSB) species in phosphorus supplementation of canola (*Brassica napus* L.). Out of 38 bacterial isolates obtained from nine medicinal plants, two bacterial strains (20P and 28P) were proved as the most potent for the *in-vitro* tricalcium phosphate solubilization test. These isolates verified their activity toward different enzymes as nitrogenase and alkaline phosphatase. Also, 20P and 28P gave a high amount of indole-3-acetic acid, 34.16 µg/ml and 35.20 µg/ml, respectively, and were positive for siderophores production as they detected moderate affinity for iron chelation. Molecular identification confirmed that strain 20P was *Bacillus vallismortis* and strain 28P was *Bacillus tequilensis*. A pot experiment was conducted to study the effect of four different phosphorus concentrations (0%, 50%, 75%, and 100% P) each alone and/or in combination with *B. vallismortis*, *B. tequilensis*, or both bacterial isolates on the vegetative growth and some physiological parameters of canola. The combined treatment of 50% phosphorus + (*B. vallismortis* + *B. tequilensis*) was generally the most effective with respect to shoot height, shoot dry mass, leaf area, photosynthetic pigment fractions, total sugar content, and accumulated NPK content. In contrast, the rhizosphere pH reached the minimum value under the same treatment. These findings highlighted the potential use of PSB (*B. vallismortis* and *B. tequilensis*) along with phosphorus fertilization as a safe sustainable tactic.

KEYWORDS

biofertilization, canola, phosphate solubilization, *Bacillus vallismortis*, *Bacillus tequilensis*, metabolic content

1 Introduction

In this contemporary epoch, cooking oils suffer an unprecedented leap in prices, which becomes one of the most critical challenges for consumers. Canola (*Brassica napus* L.) or oilseed rape as it is known elsewhere is a promising oilseed crop. Canola comes after soybean and palm oil in relation to oilseed crop production worldwide (Abdel Latef, 2011; Nobile et al., 2019). Above and beyond, canola is categorized as the first in terms to stress tolerance among the field oil crops (Lohani et al., 2020). The economic importance of canola seeds lies in their nutritional content represented by 25% protein and 40%–42% oil including 60% oleic acid and 8.8% linoleic acid (Milazzo et al., 2013; Carré and Pouzet, 2014).

Canola farming in Egypt offers a chance to overcome a number of manufacturing challenges with cooking oils. Furthermore, in order to avert opposition with other crops occupying the old cultivated lands, canola could be successfully grown in newly reclaimed land outside the old Nile Valley zones (ELSabagh et al., 2015). The nutritional status of the soil has a significant impact on the success of canola farming and any crop. Fertile soil is crucial for plants, because it contains vital nutrients as well as a diverse and influential biotic population that keeps the soil from ecological factors (Pereira and Da Gama, 2008). Enhancing the availability of soil nutrients to crop plants such as for oil and grain production is of great significance (Salimpour et al., 2010). Phosphorus (P) is an indispensable nutrient in the soil–plant nutrient cycling (Cheng et al., 2023). This macronutrient plays a pivotal role in plants at both physiological and biochemical levels during critical growth phases (Marschner, 2012; Malhotra et al., 2018). In addition to other metabolic pathways, P plays a role in the metabolism of phospholipids, adenosine triphosphate, and nucleic acids in plant cells (Poirier et al., 2022).

The productivity of several agroecosystems is hampered by soil P shortage (Reijnders, 2014). By means of root transporters, plants take up P from the soil; however, the accessible forms of P are restricted in rhizospheres (Bidondo et al., 2012). Thus, external amendment of chemical P fertilizers could satiate crop P demands during crucial growth phases (Fixen and Johnston, 2012; Cheng et al., 2023). The primary method of phosphorus amendment is the use of mineral fertilizer composed of phosphate rock (Reijnders, 2014). However, in soils that have insufficient P, certain microbes and plants can mobilize unavailable P along with organic waste (Richardson et al., 2011; Robles-Aguilar et al., 2019).

Khan (2020) revealed that there is a hesitation of the unjustified usage of synthetic fertilizers and pesticides in farming without ecological costs. This issue is under discussion due to ecological concerns and consumers' health fears. The excessive use of chemical fertilizers causes dramatic anxiety including changing soil pH resulting in its acidity, reduction in soil organic matter content, and contributes to the release of greenhouse gases (Kumar et al., 2019). Excessive consumption of P fertilizers leads to low-phosphorus acquisition efficiency. This has severe consequences for the environment and speeds up the exhaustion of this non-renewable P reserve by the end of the century (Fixen and Johnston, 2012; Cheng et al., 2023). The role of the researchers in increasing the life span of world phosphorus reserves lies in increasing the efficiency of P use in agriculture (Syers et al., 2008). This efficiency is around 10%–25% worldwide. In spite, the accessible P concentration in soil is 1 ppm, which is critically low (Khan et al., 2009). Precipitation reactions with the highly reactive Ca^{2+} in typical or calcareous soils cause significant amounts of P applied through fertilization to disperse to immobile pools (Gyaneshwar et al., 2002). Amorphous aluminum (Al), iron (Fe), or manganese (Mn)–bound P are other inorganic P forms (Xie et al., 2011). All of these phosphate-containing rock minerals frequently lack the solubility necessary to provide crops with adequate P requirements, so they must be converted into readily usable P forms (Houben et al., 2019).

From the previously mentioned and in light of the food crisis and climatic changes that strike the world everywhere, numerous researchers nominated green cultivation to encounter P shortage and sustain the dynamic biotic population. This strategy aims to offer more accessible P while restricting the excessive use of the mineral fertilizer (Faucon et al., 2015). The term bio-fertilization involves applying beneficial microorganisms or their metabolites in order to enhance soil biological and chemical properties, maintain soil fertility, and promote plant growth and productivity (Suleiman et al., 2020; Ammar et al., 2022). This application is a reliable alternative sustainable solution to displacing chemical fertilizers without ecological losses (Khan, 2020).

According to Hussain et al. (2016) and NAMLI et al. (2017), phosphate solubilizing bacteria (PSB) are used by the agro-industry in combination with applied phosphates to access more P and boost crop yields. For instance, PSB have the potential to convert insoluble phosphate into a more accessible form to plants through solubilization and mineralization processes (Cheng et al., 2023). For that, PSB became an alternative to chemical phosphatic fertilizer (Khan et al., 2007). Generally, colonization of beneficial microorganisms promotes root system expansion to enhance nutrient acquisition, thus enhancing the general performance of plants in terms of growth and productivity of crops (Kumar and Dara, 2021; Pirttilä et al., 2021). PSB not only carry out a crucial part in plant nutrition in agriculture but also make soluble phosphorus accessible to subsequent plants (Elhaissoufi et al., 2022). Bhattacharyya and Jha (2012) documented that several genera, including *Bacillus* species, contain the most promising PSB. These soil bacteria carry out a major task in the movement of soil P by secreting a number of organic acids, which dissolve P minerals, rendering P more accessible to roots (Sarker et al., 2014). According to Guang-Can et al. (2008), *Bacillus* species have the capacity to mineralize 8–18 g mL^{-1} of organic P and to solubilize 25–42 g mL^{-1} of inorganic P.

This investigation is constructed to evaluate the inspiration of seed presoaking and irrigation using PSB to facilitate the mobility of P for canola crops. To achieve this goal, we used liquid cultures of the two bacilli strains: *Bacillus vallismortis* strain 20P and *Bacillus tequilensis* strain 28P. Hence, canola species may increase both their own growth, as well as the subsequent crops, because of the increased P mobilization in the soil.

2 Materials and methods

2.1 Bacteriological assessments

2.1.1 Sample collection and bacterial isolation

Nine medicinal plants (Supplementary Table S1) were gathered from different farms at Qalyubiya Governorate (30°18'0"N/31° 15'0"E), Egypt. The healthy parts were chosen for the isolation of endophytic bacteria. The samples were separated into roots, stems, and leaves before being thoroughly rinsed with tap water to remove any clingy soil. The plant components were thoroughly cleaned and cut into 0.5–1 cm segments and subsequently sterilized with 70% ethanol and 2% sodium hypochlorite for 30 s and 5 min, respectively. The samples were then cleaned twice in a laminar flow hood with sterile distilled water (Elbeltagy et al., 2000). The sterilized components were ground in 0.8% saline solution and quartz sand, and they were then diluted decimally in 0.8% saline solution. Sterility tests were carried out to confirm that the isolated strains originated from endophytes (the inside of the plant). The final dilutions (10^{-4} and 10^{-5}) were applied to specific cultural medium, Pikovskaya's (PVK) agar medium (Pikovskaya, 1948). Bacterial plates were parafilm sealed and cultured at 37°C for 48h. Pure cultures were kept for future research after the incubation time on slants at 4°C.

2.1.2 Quantitative assessment of phosphate solubilization

For quantitative analysis of phosphate solubilization, bacterial isolates were transferred to the National Botanical Research Institute's phosphate (NBRIP) broth medium (Nautiyal, 1999) and then incubated for 7 days at 28°C. The cultures were subjected to centrifugation at 3885 RCF for 20 min, and the phosphorous concentration in the culture supernatant was detected by molybdenum blue colorimetric method (Olsen and Sommers, 1982). Using Spekol Spectrophotometer VEB Carl Zeiss set to 600 nm, the color was evaluated (Naik et al., 2009). For quantitative analysis, a standard curve was constructed using potassium dihydrogen phosphate (KH_2PO_4) solution. At the completion of the experiment, the ultimate pH of the media was determined by digital pH meter.

2.1.3 Screening for other plant growth-promoting traits

Different plant growth-promoting (PGP) traits as alkaline phosphatases, indole-3-acetic acid (IAA), siderophores production, HCN production, and nitrogenase activity were also detected. These traits were assessed for the most potent isolates (20P and 28P) that showed high efficiency for quantitative phosphate solubilization. According to Tabatabai and Bremner (1969) technique, alkaline phosphatases were measured using p-nitrophenyl phosphate, a colorless substrate that produces the yellow-colored end product p-nitrophenol. The absorbance at 420 nm was employed to quantify the concentration of p-nitrophenol in triplicates using a spectrophotometer. Values were estimated using a standard curve created using p-nitrophenol serially diluted solutions as the standard. The quantity of enzyme required to release 1 mol of p-nitrophenol/ml/min from di-Na p-nitrophenyl phosphate (tetrahydrate) under the test conditions was designated as one unit (U) of phosphatase activity.

Detection and quantification of IAA was implemented along with the technique outlined by Gordon and Weber (1951). The emergence of a pink–red color was used to detect IAA generation, and the absorbance at 530 nm was quantified using a spectrophotometer. In order to create a standard curve for quantitative analysis, color was produced in a standard solution of pure IAA (Sarwart et al., 1992).

Siderophores production was estimated by adding 8-hydroxyquinoline (50 mg/L) as iron chelators to tryptic soy agar (TSA) medium (Alexander and Zuberer, 1991). Freshly produced cultures were used to inoculate plates of TSA media, which were then incubated for 3–7 days at 28°C. Ability of isolates to grow on this medium was considered as a positive result for siderophores production.

In addition, the ability of isolates toward nitrogen fixation was evaluated by acetylene reduction assay (ARA) according to Hardy et al. (1973). Each bacterial isolate was inoculated in a 25-mL flask containing 10 mL of JNFb medium and incubated for 3 days at 30 ± 2°C. Inside air from the tubes is replaced with 5 mL of acetylene through a syringe and the tubes were incubated for 24h at 30 ± 2°C. The nitrogenase activity was assessed by ARA of mid-log phase broth cultures after 24h.

For assessing the antagonistic activity between bacterial isolates, a single bacterial isolate was inoculated in lines over the surface of the nutrient agar medium. Along lines perpendicular to the first inoculations, the second isolate was inserted. After an incubation period of 24h at 37°C, the growth inhibition zones were recorded (Seyfferth et al., 2021).

2.1.4 Molecular identification

2.1.4.1 DNA extraction and analysis of molecular phylogeny using the 16S rRNA gene sequence

According to the instructions provided by the GspinTM Total Extraction kits, the genomic DNA for 20P and 28P was obtained. Cells cultured on LB broth were used for the bacterial DNA extraction. Thermocycler was then used to amplify the new isolates' 16S rRNA genes (Biometra thermocycler, Germany) using the universal primers 27F 5' (AGA GTT TGA TCM TGG CTC AG) 3' and 1492R 5' (TAC GGY TAC CTT GTT ACG ACT T) 3' as designated by Pandey et al., (2002). The 20 µl of polymerase chain reaction (PCR) contained 0.2 µl of 2.5 U/µl Taq DNA polymerase, 2 µl of 10× buffer, 1.6 µl of 2.5 mM dNTPs, 1 µl Primer F, R (10 pmole/µl), 1 µl of template (20 ng/µl), and up to 20 µl of distilled water [High-performance liquid chromatography (HPLC) grade]. The PCR amplification condition includes an initial denaturation at 95°C for 5 min, subsequently 30 cycles (95° C denaturation for 30 s, 55°C annealing for 2 min, 68°C extension

for 1.5 min), and final extension at 68°C for 10 min. Purification of PCR products was performed using Montage PCR clean-up kit (Millipore). Purified PCR products were treated with BigDye Terminator Cycle Sequencing Kit v.3.1 (Applied Biosystems, USA), and the sequencing products were run on an Applied Biosystems Model 3730XL automated DNA sequencing system (Applied Biosystems, USA) at the Macrogen, Inc., Seoul, South Korea. The Sequence Similarity Search was disclosed for the 16S rDNA sequence using an online search tool (http://www.ncbi.nlm.nih.gov/blast/). The unknown organisms (20P and 28P) were identified using the maximum aligned sequence through BLAST search and deposited in GenBank under accession numbers (OM978276.1 and OM978277.1), respectively.

2.2 Plant experiment

2.2.1 Experiment design and growth conditions

A pot experiment was conducted on 26 September 2021 at the Benha University off-campus botanical garden, under natural conditions for canola growth. Canola seeds were surface sterilized with 0.01% mercuric chloride for 3 min and then thoroughly washed with distilled water. The sterilized seeds were classified into 16 groups as illustrated in Supplementary Figure 1. The experiment was set up under completely randomized block design with 160 bags. Each bag filled with 2 Kg washed and sterilized river clay: sand (2:1 V/V) soil. Plants received the recommended doses of phosphorus and potassium fertilizers by mixing with the soil three days before sowing. Superphosphate and potassium fertilizer (15.5% P_2O_5 and 48% K_2SO_4, respectively) were used. The optimum phosphorus concentrations for canola germination were determined by a preliminary germination experiment as 100%, 75%, and 50% P. These concentrations were achieved by the following recipes: 100% P (0.39 g superphosphate/2 Kg soil mixture), 75% P (0.225 g superphosphate/2 Kg soil mixture), and 50% P (0.195 g superphosphate/2 Kg soil mixture). In addition, urea fertilizer)46% N_2) was added 21 days after sowing (DAS) to the bags. The bags were maintained at the campus under normal day/night period and irrigated with tap water twice weekly or when needed. Canola seeds were applied to the selected endophytic bacterial inoculum (10^6 CFU/ml) carboxymethyl cellulose (CMC) solution (5%) in the range of 500 g seeds/125 ml of inoculum mixed with 25 ml of CMC. Regarding co-inoculation application, both bacterial strains were counted separately and then added to the soil. Uniform seeds were left to dryness before planting. Control treatment seeds were retained. After seedling growth, the plants were thinned to four plants per pot, and then each pot was inoculated with 10 ml of bacterial inoculum (10^6 CFU/ml) of endophytic bacterial strains (*B. vallismortis* and *B. tequilensis*) separately or in combination. Samples of canola plants representative for each treatment were collected 45 days old after sowing (45 DAS), when apparent variations in plant size could be seen between the various treatments. It should be mentioned that, for determination of the different growth parameters, five replicates were used, whereas triplicate samples were analyzed for the chemical analyses.

2.2.2 Evaluation of growth biomarkers

Representative plants from each treatment were taken out of their pots and dipped in a beaker of water to wash away any soil that had stuck to them. The plants were then wiped with tissue paper. A meter scale was used to measure the heights of the shoots. After that, the samples were weighed to determine their fresh masses, and they were then put in an oven that was set to 70°C. After cooling at room temperature, the samples were reweighed many times until we obtained their constant dry masses by the end of 72h. Root mass ratio was calculated as the ratio of root DM to total plant DM. Using a scanner and the ImageJ program, the depth of the roots and the total area of the plant's leaves were also measured.

2.2.3 Metabolic contents

2.2.3.1 Extraction and estimation of photosynthetic pigments

According to the recommendations of Arnon (1949) and Horvath et al. (1972) as well as the modifications of Kissimon (1999), the quantitative amounts of chlorophylls a and b and carotenoids were calculated. Estimation took place using a spectrophotometer. The extracts were measured in comparison to a blank of pure 80% aqueous acetone at three different wavelengths: 480 nm, 644 nm, and 663 nm. The concentration of each photosynthetic pigment was assessed as μg ml^{-1} according to the subsequent equations, taking into account the dilutions made:

$$\text{Chlorophyll a} = 10.3\ E663 - 0.918\ E644 = \mu g/ml$$

$$\text{Chlorophyll b} = 19.7\ E644 - 3.87\ E663 = \mu g/ml$$

$$\text{Carotenoids} = 5.02\ E480 = \mu g/ml$$

Then, the pigment fractions were expressed as mg g^{-1} dry weight of leaves.

2.2.3.2 Extraction and estimation of carbohydrate fractions

According to Prud'homme et al. (1992), known dried weights were digested. After that, soluble sugars were determined using the anthrone–sulfuric acid procedure as designated by Whistler and Wolfrom (1963). A blue–green color was formed, and it was determined spectrophotometrically at a wavelength of 620 nm in comparison to a blank made up only of water and anthrone reagent. For the purpose of measuring polysaccharides, the dry residue left over after the extraction of soluble sugars was used. The anthrone–sulfuric acid reagent technique was employed for polysaccharides estimation as in the case of soluble sugars. Triplicate samples were analyzed for carbohydrate analyses. Total carbohydrates were mathematically determined as the total of the sample's soluble sugar and polysaccharide concentrations. The calculations for all sugar fractions were calculated from a calibration curve created using only pure glucose, and the data were expressed as mg glucose g^{-1} dry weight. Triplicate samples were analyzed for the chemical analyses.

2.2.3.3 Extraction and estimation of the macronutrients NPK

By using the traditional semi-micro-modification of the Kjeldahl method (Chibnall et al., 1943), total nitrogen was digested. Following digestion, the Pregi (1945) method was employed to calculate the total nitrogen. The outcomes of the titration were expressed as mg nitrogen using

$$1\ \text{ml of } 0.0143\text{N} \quad H_2SO_4 = 0.28 \quad \text{mg} \quad \text{nitrogen}$$

The concentrations of total nitrogen were expressed as mg nitrogen 100 g^{-1} dry weight. Finally, the quantitative amounts of accumulated N were expressed by multiplying the nitrogen concentration (g) by DM (g) (Zhao et al., 2010).

A wet ashing procedure was employed to extract both potassium and phosphorus. The dried tissues were digested using the technique described in Chapman and Pratt (1962).

Utilizing the flame emission method, potassium was calculated (Ranganna, 1977). Whereas, phosphorus was measured with inductively coupled plasma optical emission spectrometry (Soltanpour, 1985). The quantitative amounts of accumulated PK were expressed as the case of accumulated N.

2.3 Statistical analysis

Data for quantitative phosphate solubilization (measurements were performed in triplicate) were analyzed on the premise Duncan's multiple range test at a probability level (P) ≤ 0.05 (IBM SPSS Statistics software version 21). Generalized least square models were used (Zuur et al., 2009) to test the response of canola using two bacteria (*Bacillus vallismortis* and *Bacillus tequilensis*) at four P levels and the interaction between these two factors. Normality of data was checked, and transformations of $\log_{10}$ were undertaken if required. If this interaction was significant (P< 0.05), then post-hoc *Tukey* tests were also performed (RStudio 2023.03.0). Pearson Correlation analysis was performed to determine the relationship between pH of culture media and the amount of solubilized phosphate (RStudio 2023.03.0). A principal component analysis (PCA) was performed on the logarithmic transformed data using factor extraction to rank the different variables affected by the different treatments. The eigenvalue remained greater than 1 after varimax rotation. Correlation matrix figure was fitted by the GraphPad Prism software 9.0 (GraphPad, USA).

3 Results

3.1 Bacterial isolation

Thirty-eight endophytic bacteria were obtained from nine medicinal plants on PVK media. The number of bacteria recovered from each plant is shown in the Supplementary Table S1. Stevia (*Stevia rebaudiana*) roots had the highest number of bacteria, while the least number of bacterial isolates was obtained from the leaves of Mint, Rosemary, Kalanchoe, Lemon, Nerium, and Roselle plants. We obtained 28 and 10 bacterial isolates from roots and leaves, respectively.

3.2 Quantitative phosphate solubilization

Endophytic bacterial isolates showed phosphate solubilization values that ranged between 2.09 and 28.14 µg/ml. Isolates code 28P and 20P recorded the highest phosphate solubilization value (28.42

TABLE 1 Screening of the 38 endophytic bacterial isolates for phosphate solubilization.

Isolate code	Phosphate concentration (µg/ml)	Final PH
1P	$2.66^{s} \pm 0.05$	6.25
2P	$9.44^{k} \pm 0.05$	5.09
3P	$18.26^{c} \pm 0.05$	5.2
4P	$18.24^{c} \pm 0.08$	5.03
5P	$3.20^{r} \pm 0.04$	5.7
6P	$12.79^{g} \pm 0.11$	4.63
7P	$2.29^{t} \pm 0.14$	5.55
8P	$3.14^{r} \pm 0.08$	5.29
9P	$8.37^{l} \pm 0.13$	4.87
10P	$7.68^{m} \pm 0.29$	5.7
11P	$8.61^{l} \pm 0.19$	4.79
12P	$9.35^{k} \pm 0.07$	5.4
13P	$11.72^{h} \pm 0.15$	4.55
14P	$10.41^{i} \pm 0.32$	4.74
15P	$10.17^{i} \pm 0.66$	4.46
16P	$13.62^{f} \pm 0.19$	4.73
17P	$4.18^{p} \pm 0.03$	5.02
18P	$16.35^{d} \pm 0.18$	4.67
19P	$3.24^{r} \pm 0.09$	5.19
20P	$20.43^{b} \pm 0.09$	4.41
21P	$14.19^{e} \pm 0.04$	4.74
22P	$6.72^{o} \pm 0.07$	4.91
23P	$10.37^{i} \pm 0.09$	4.68
24P	$7.16^{n} \pm 0.06$	5.18
25P	$10.44^{i} \pm 0.18$	5.25
26P	$3.62^{q} \pm 0.34$	6.17
27P	$9.77^{j} \pm 0.09$	5.51
28P	$28.42^{a} \pm 0.32$	4.32
29P	$8.44^{l} \pm 0.06$	5.55
30P	$2.49^{st} \pm 0.12$	5.71

(Continued)

10.3389/fpls.2024.1324538

TABLE 1 Continued

Isolate code	Phosphate concentration (µg/ml)	Final PH
31P	2.35^{st} ± 0.10	5.29
32P	3.67^{q} ± 0.11	5.67
33P	16.35^{d} ± 0.07	4.55
34P	3.62^{q} ± 0.26	5.76
35P	7.23^{n} ± 0.11	5.29
36P	3.19^{r} ± 0.04	5.44
37P	3.16^{r} ± 0.17	5.43
38P	3.20^{r} ± 0.06	5.41

*Results were expressed as mean ± standard deviation. No statistically significant difference between values in the same column marked by the same superscript lowercase letter ($p \leq 0.05$).

± 0.32 µg/ml and 20.43 ± 0.09 µg/ml), respectively. In addition, isolates code 7P and 31P gave the least values (2.29 ± 0.14 µg/ml and 2.35^{s} ± 0.10 µg/ml), respectively. The pH of the culture media was found to be dropping. The culture medium's pH was initially set at 7 and, as shown in Table 1, after the incubation time, the pH was reduced to a range of 4.32–4.41 for the media amended with isolates code 20P and 28P, respectively. A strong negative correlation was detected between culture pH and the amount of solubilized phosphate (−0.702, $P< 0.0001$).

The maximum alkaline phosphatase activity was measured at 1.7 ± 0.08 µmol and 2.4 ± 0.16 µmol p-NP mL^{-1} h^{-1} in isolates code 20P and 28P, respectively. For estimating nitrogenase activity, 20P and 28P isolates gave (9.6 ± 0.47 and 32.1 ± 0.60 n moles C_2H_4/ml/h) of ARA, respectively. In addition to phosphate solubilization, isolates 20P and 28P also produced a sizable quantity of IAA and siderophore. Endophytic bacterial isolates (20P and 28P) displayed an intense pink color and gave a high amount of IAA (34.16 ± 0.07 µg/ml and 35.20 ± 0.08 µg/ml), respectively. Furthermore, these isolates were positive for siderophores production and detected moderate affinity for iron chelation. The filter paper's transition from yellow to brown serves as a marker for the presence of HCN. As evidenced by the lack of any color change in the filter paper impregnated with picric acid, 20P and 28P did not exhibit HCN generation.

3.3 Molecular identification

A phylogenetic tree between the designated strains and other strains was exhibited by Figure 1. The most effective isolates were identified by molecular identification using 16S rRNA as *Bacillus vallismortis* strain 20P and *Bacillus tequilensis* strain 28P with 100% similarity and recorded in GenBank under accession numbers (OM978276.1 and OM978277.1), respectively.

About the antagonistic activity between the selected bacterial isolates, no antagonism was detected.

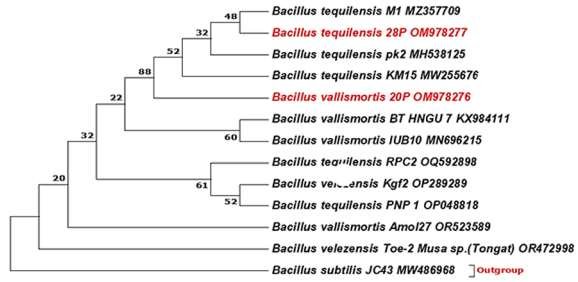

FIGURE 1
Phylogenetic tree was constructed using the neighbor-joining method. The bootstrap consensus tree inferred from 1,000 replicates is taken to represent the evolutionary history of the taxa analyzed. The percentage of replicate trees in which the associated taxa clustered together in the bootstrap test (1,000 replicates) is shown next to the branches. There was a total of 698 positions in the final dataset. Evolutionary analyses were conducted in MEGA7.

3.4 Effect of the different phosphorus concentrations and/or the phosphate solubilizing bacteria application on certain morphological parameters, rhizosphere pH, and physiological parameters of canola plant

As general speech, both the single and/or combined phosphorus and bacterial treatments significantly increased all the estimated vegetative and physiological parameters over the control plants. This finding is clearly illustrated by the data tabulated in Table 2.

3.5 Ranks of different variables as affected by the different treatments

In this study, PCA and computed eigenvalues had a substantial role in identifying and understanding the associations of different variables affected by the different concentrations of phosphorous combined by different bacterial isolates. Furthermore, the Varimax method was carried out to perform the rotation of the PCA, loadings greater than 0.60 are statistically significant and are marked in bold in Table 3 and Figure 2. The factor analysis included four factors that described 76.95% of total data variability. The first dominant factor accounted for 45.53% of the total variance with an eigenvalue of 9.11. This factor indicated that the shoot height, shoot FM, shoot DM, leaf area, total DM, pH, carotenoids, total pigments, soluble sugars, polysaccharides, total sugars, accumulated N, accumulated P, accumulated K were the major 14 variables affected by the different concentrations of phosphorous combined by different bacterial isolates. The second factor (13.93% of the total variance with eigenvalue = 2.79) revealed that both of root FM and root mass ratio were the second two variables affected by aforementioned different treatments. Just root DM was the third variable affected by the treatment (9.75% of the total variance with eigenvalue = 1.95). Meanwhile, root height,

10.3389/fpls.2024.1324538

TABLE 2 The effects of phosphorus (P) supplies (0%, 50%, 75%, and 100%) on vegetative growth and physiological characteristics of canola (*Brassica napus* L.) in the absence and/or presence of phosphate solubilizing bacteria PSB; *B. vallismortis*, *B. tequilensis* or both bacterial isolates.

Characteristic	Significance and F value						Marginal means for bacteria			
	P level		Bacteria		P level *Bacteria		B0	*B. vallismortis*	*B. tequilensis*	*B. vallismortis* + *B. tequilensis*
	P	F	*P*	F	*P*	F				
Shoot height (cm)	ns	1.085	**	5.862	ns	0.541	27.25	28.52	28.6	31.65
Shoot FM (g)	ns	1.9380	***	6.9603	ns	0.6943	13.90	14.75	14.55	19.6
Shoot DM (g)	ns	2.3636	***	7.2203	ns	0.8136	1.12	1.24	1.24	1.69
Leaf area (mm^2)	ns	1.8554	***	28.8209	*	2.0457				
Root height (cm)	*	2.929	***	7.5204	*	2.1087				
Root DM (g)	***	24.3937	***	16.2729	***	22.9774				
Root FM (g)	ns	4.38264	ns	4.24114	ns	1.78106				
Root mass ratio (g)	***	16.8236	***	6.5457	***	16.1989				
Total DM (g)	**	4.7021	***	8.166	ns	1.235	1.36	1.52	1.38	1.99
pH	***	3.600	***	21.103	***	3.511				
Chlorophyll a	*	3.849	***	4.867	**	3.849				
Chlorophyll b	*	2.266	ns	0.707	*	3.870				
Carotenoids	**	15.398	**	12.260	ns	0.814				
Total pigments	*	2.885	ns	1.403	ns	0.334				
Soluble sugars	***	16.453	***	26.589	***	1.405				
Polysaccharides	***	19.282	***	38.109	***	2.306				
Total sugars	***	21.891	***	42.193	***	2.453				
Accumulated N	***	0.751	**	5.749	ns	0.799				
Accumulated P	***	2.454	***	13.848	***	1.003				
Accumulated K	ns	1.014	**	6.158	ns	0.340				

*P< 0.05, ** P< 0.01, *** P< 0.001. DM, dry mass; FM: fresh mass; ns, nonsignificant difference. If there was no significant interaction of P level × bacteria, while bacteria or P level had a significant effect ($p \leq 0.05$), then the marginal means for bacteria are presented here. ***$p \leq 0.05$.

Chl.a, and Chl.b were the latest three variable affected by the treatments (8.27% of the total variance with eigenvalue = 1.65).

Figure 3 shows the vegetative growth of canola (*Brassica napus L.*) plant under the different concentrations of phosphorus (0%, 50%, 75%, and 100%) alone and/or in combination with *B. vallismortis*, *B. tequilensis* or both bacterial isolates. Shoot height and shoot dry mass ($P \leq 0.01$) differed significantly among the interaction bacteria × *P* levels ($P \leq 0.001$). The higher values were recorded for the combined treatment *B. vallismortis* + *B. tequilensis* under 50% P. These enhancements were evaluated by 31.37% and 140. 9% for shoot height and dry mass, respectively, over the control treatment; 0% P and 0 bacteria (Supplementary Table S2). In the same trend, the leaf area fluctuated significantly between P levels under the combined treatment *B. vallismortis* + *B. tequilensis*; that of 50% P was greater by 200.8% than the control treatment. The P level treatments brought about a slight modification in the total leaf area of all the other bacterial treatments (B0, *B. vallismortis*, and *B. tequilensis*), but there was no significant difference between P level treatments (Supplementary Table S2).

In contrast to the shoot system morphological parameters, root height, root dry mass, and root mass ratio exhibited the highest significant values under both 75 and 100% P + *B. tequilensis*, 50% P + *B. vallismortis*, and 75% +*B. vallismortis*, respectively (Supplementary Table S2). The use of the two bacterial strains, *B. vallismortis and B. tequilensis* had significantly improved the total dry mass under all P levels, especially 50% level. Under 50% P combined with (*B. vallismortis* + *B. tequilensis*), an augmented total dry mass estimated by 178.3% over the control plants was achieved (Supplementary Table S2).

The pH of rhizosheath soil varied significantly (Table 2 among all treatments and interaction between P level and bacterial treatments. The minimum soil pH of 6.11 was acquired for 50% P + (*B. vallismortis* + *B. tequilensis*) treatment. Whereas, the B0, *B. vallismortis*, and *B. tequilensis* treatments showed a bulk soil pH of

10.3389/fpls.2024.1324538

TABLE 3 Varimax rotated principle component analysis (PCA) for different morphological and physiological variables affected by the different concentrations of phosphors (0%, 50%, 75%, and 100% P) loaded by different bacterial isolates (B0, *B. vallismortis*, *B. tequilensis* and *B. vallismortis*+ *B. tequilensis*).

Variables	PC1	PC2	PC3	PC4
Shoot height	**0.809**	−0.408	0.153	−0.080
Shoot FM	**0.853**	−0.460	0.140	−0.054
Shoot DM	**0.878**	−0.429	0.150	0.007
Leaf area	**0.670**	0.188	−0.156	−0.083
Root height	0.378	−0.046	−0.087	**0.673**
Root FM	0.283	**0.679**	−0.044	−0.074
Root DM	0.188	0.471	**0.828**	0.035
Root mass ratio	−0.101	**0.626**	0.725	0.124
Total DM	**0.867**	−0.226	0.427	0.018
pH	**−0.601**	−0.125	0.278	0.338
Chl.a	0.389	0.418	0.160	**−0.602**
Chl.b	0.260	0.056	−0.129	**0.906**
Carotenoids	**0.671**	0.409	−0.232	0.289
Total pigments	**0.694**	0.268	0.110	0.315
Soluble sugars	**0.708**	0.440	−0.296	−0.130
Polysaccharides	**0.789**	0.460	−0.273	−0.030
Total sugars	**0.757**	0.498	−0.297	−0.028
Accumulated N	**0.924**	−0.345	0.120	0.000
Accumulated P	**0.924**	−0.134	0.014	−0.057
Accumulated K	**0.923**	−0.259	0.085	−0.020
Eigenvalue	9.11	2.79	1.95	1.65
Proportion of variance	45.53%	13.93%	9.75%	8.27%
Cumulative proportion of variance	45.53%	59.46%	69.21%	77.49%

*Bold loadings are statistically significant.

6.46, 6.50, and 6.30 under the same P level. The least pH value obtained at 50% P interacted with *B. vallismortis* + *B. tequilensis* was reduced by 6.1% less than the control in the acidic side (Figure 4).

With respect to photosynthetically active pigments content, Table 2 exposed that all the PSB inoculation treatments could significantly improve the pigment content. The co-inoculation of the two potent PSB *strains B. vallismortis* and *B. tequilensis* and their synergistic interaction caused a positive effect on the pigments' synthesis. In this connection, chlorophyll a and chlorophyll b, under the bacterial treatment (*B. vallismortis* + *B. tequilensis*), exhibited the greatest amount alongside with 50% P and 75% P in the same order (Figures 5A, B). This treatment brought about a significant increase (Table 2) reaching more than two and 10-folds above the control for Chl.a and Chl.b, respectively. The proportion of the carotenoids differed significantly among P level and bacterial treatments, with values ranging from 0.56 to 0.66 mg/g F.wt of canola leaves under 50% P for both B0 and *B. vallismortis* + *B. tequilensis* passing by B. *tequilensis*. Furthermore, carotenoids augmented dramatically under the same P level combined with the single treatment of *B. vallismortis* treatment to record 0.82 mg/g D. wt of canola leaves (Table 2 and Figure 5C). The fluctuated responses of the pigment fractions reflected on the total pigments content. The later exhibited the maximum level under 100% p level shared with the inoculation by *B. tequilensis* to achieve 196.4% rise over the control plants. (Table 2 and Figure 5D).

Similar to leaf photosynthetic pigments, soluble sugars differed significantly among P level, bacteria, and interaction between P level × bacteria treatments (Table 2). Under 50% P level treatments, soluble sugars varied greatly and an increase was obtained by 68.95% for *B. vallismortis* and 71.5 for *B. tequilens*is and by 102.6% for *B. vallismortis* + *B. tequilensis* treatments (Figure 6A). Polysaccharides also differed significantly among P level, bacteria, and the interaction between P level × bacteria treatments (Table 2). Under 50% level treatment, it showed a rise by 88.1% for *B. vallismortis*, 95.2 for *B. tequilensis*, and 130.4 for *B. vallismortis* + *B. tequilensis* treatment (Figure 6B). Under 75% P-level treatment, a similar trend was obtained for *B. vallismortis* and *B. vallismortis* + *B. tequilensis* (Figure 6B). Consequently, total sugars varied greatly

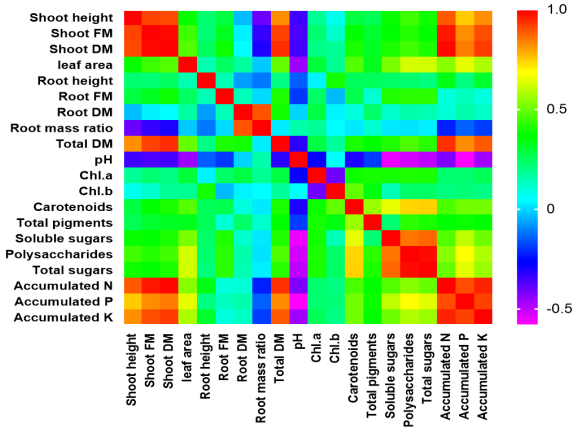

FIGURE 2
Person correlation matrix of different studied morphological and physiological variables affected by the different concentrations of phosphors (0%, 50%, 75%, and 100% P) loaded by different bacterial isolates (B0, *B. vallismortis*, *B. tequilensis* and *B. vallismortis+ B. tequilensis*).

among P level, bacteria, and interaction between P level × bacteria treatments (Table 2). Under 50% P level treatment, a surge was increased by 85.6% for *B. tequilensis* treatment and a maximum increment by 119.3% for *B. vallismortis* + *B. tequilensis* treatment. A similar propensity with a 106.6% increment was observed under 75% in combination with *B. vallismortis* + *B. tequilensis*) treatment (Figure 6C). With regard to the accumulated NPK (nitrogen, phosphorus, and potassium) content, the synergistic phosphorus-bacterial interaction greatly enriched the mineral content. The treatment 50% P combined with *B. vallismortis* + *B. tequilensis* intensified the accumulated NPK to 0.065 g, 0.013 g, and 0.050 g DM against 0.021 g, 0.002 g, and 0.013 g DM of the corresponding control treatments, respectively (Figures 7A–C).

4 Discussion

According to our study, 38 endophytic bacteria were isolated on PVK media from nine medicinal plants. The bacteria can grow on this medium and form a clear zone around the colonies (Amri et al., 2023) due to converting tricalcium phosphate in the medium from insoluble to soluble forms (Zuluaga et al., 2023). The pH of the culture medium used for phosphate solubilization decreased, which may be a sign of organic acids indirectly present. According to some reports, the PSB produces organic acids that cause the culture medium to become more acidic (Benbrik et al., 2020; Sanchez-Gonzalez et al., 2022), which is the primary microbial mechanism by which inorganic P is solubilized (Prabhu et al., 2019).

According to Richardson (2001), the activity of the enzyme phosphatase helps to dissolve the organic phosphates in the soil. Phosphatase activities showed comparable results to those of Bayisa (2023) who recorded alkaline phosphatase activity of *Bacillus Velezensis*. It is significant to note that when inorganic P levels in the growth medium are limited, the innovative production of these enzymes is triggered (Dick et al., 2011). Another advantageous function of several groups of microorganisms is to enable the enzyme nitrogenase to convert molecular nitrogen (N_2) into ammonia (NH_3) (Miljaković et al., 2020). The amino acids that are formed from ammonia are then absorbed by plant roots. Radhakrishnan et al. (2017) reported the nitrogenase activities of a number of *Bacillus* species, such as *B. megaterium*, *B. cereus*, *B. pumilus*, *B. circulans*, *B. licheniformis*, *B. subtilis*, *B. brevis*, and *B. firmus*. The nitrogen fixation ability of endophytic *Bacillus* spp. was

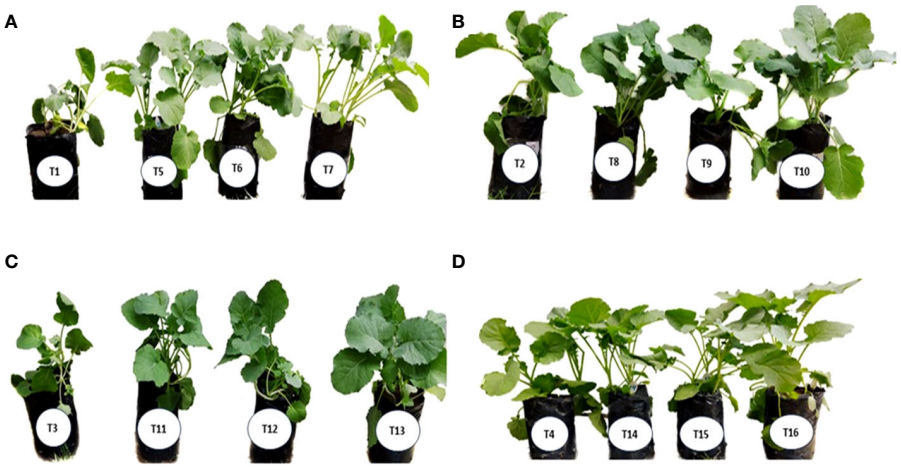

FIGURE 3
The effect of different concentrations of phosphorus (0%, 50%, 75%, and 100% P) alone and/or in combination with *B. vallismortis*, *B. tequilensis* or both bacterial isolates. on the vegetative growth of canola (*Brassica napus L.*) plant: **(A)** 0% P, (T1): B0, (T5): *B. vallismortis*, (T6): *B. tequilensis* and (T7): *B. vallismortis* + *B. tequilensis*; **(B)** 50% P, (T2): B0, (T8): *B. vallismortis*, (T9): *B. tequilensis* and (T10): *B. vallismortis* + *B. tequilensis*; **(C)** 75% P, (T3): B0, (T11): *B. vallismortis*, (T12): *B. tequilensis* and (T13): *B. vallismortis* + *B. tequilensis*; and **(D)** 100% P, (T4): B0, (T14): *B. vallismortis*, (T15): *B. tequilensis*, and (T16): *B. vallismortis* + *B. tequilen*.

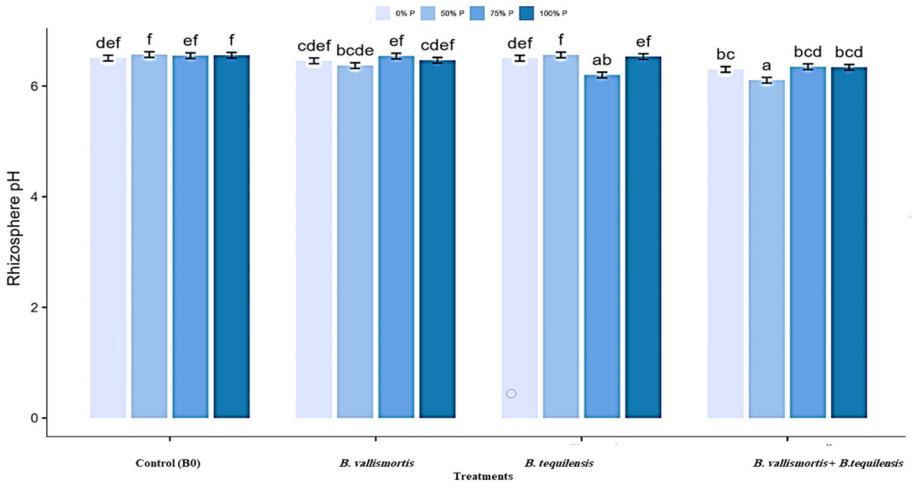

FIGURE 4
Rhizosphere pH of Canola inoculated with PSB (*B. vallismortis* and/or *B. tequilensis*) shown at (x-axis) under four levels of P (0%, 50%, 75%, and 100% P) shown at *y*-axis. Bars are the means, and error bars are the standard errors of the mean, derived from generalized least square models. Different letters among treatments indicate significant difference within each panel (post-hoc Tukey test, $P \leq 0.05$). The mean of three replicates ($n = 3$), See Table 2 for details of the statistical analysis.

determined using the ARA, according to Szilagyi-Zecchin et al. (2014). Furthermore, Ikeda et al. (2015) revealed that among the environmental factors, low nitrogen strongly affected the community structures of leaf blade-associated bacteria in rice by increasing the relative abundance of *Bacilli*. Thus, suggesting the potential contribution of their biological nitrogen fixation.

In addition to phosphate solubilization, isolates code 20P and 28P gave a high amount of IAA and were positive for siderophores production, as they exihibited moderate affinity for iron chelation. The IAA phytohormone induces cell elongation, lateral root development, cell division, and differentiation (Goswami et al., 2016). On the other side, siderophore performs a major role in the chelation of micronutrients like iron even in unfavorable conditions (Arora and Verma, 2017). According to previous researches, *Bacillus* spp. have been proven as producers of IAA and siderophores which are crucial for nutrient uptake and plant growth (Walpola and Yoon, 2013; Ribeiro et al., 2018). Additionally, *B. safensis* has been confirmed to produce siderophore and IAA efficiently according to Mukhtar et al. (2017) and Chakraborty et al. (2013), respectively. Producing siderophores, by *Bacillus* spp., helps chelate iron from precipitated forms ($FePO_4$) and increases the supply of phosphate ions in the rhizosphere and hence to the plant (Sharma et al., 2013). These characteristics qualified *B. safensis* to promoting plant growth

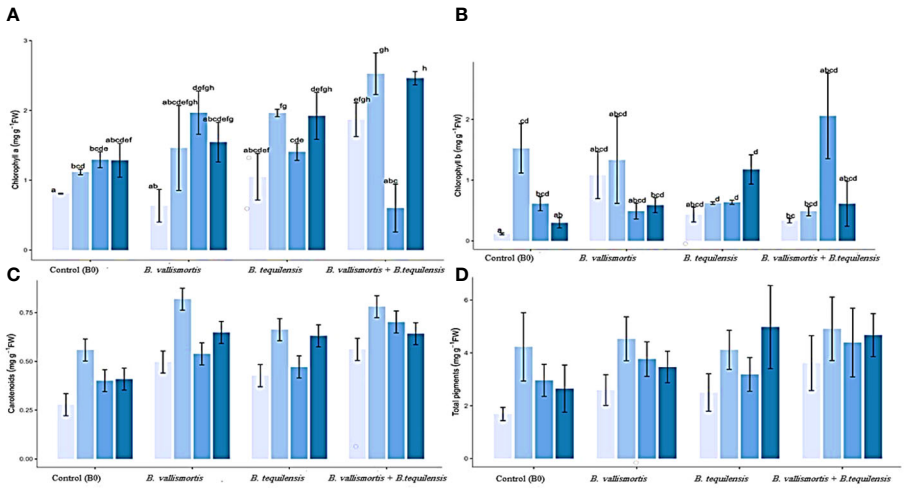

FIGURE 5
Effect of inoculation with PSB under four levels of P (0%, 50%, 75%, and 100% P) on photosynthetic pigments (mg/g leaves F.wt) of Canola inoculated with PGR shown at (x-axis) under four levels of P Shown at (y-axis). Bars are the means, and error bars are the standard errors of the mean, derived from generalized least square models **(A)** chlorophyll a; **(B)** chlorophyll b; **(C)** carotenoids; and **(D)** total pigments. The mean of three replicates ($n = 3$). See Table 2 for details of the statistical analysis.

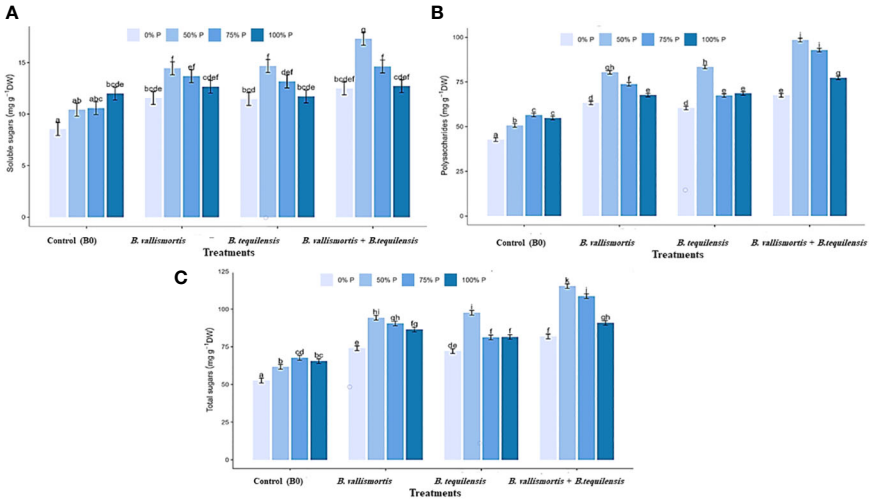

FIGURE 6
Effect of inoculation with PSB under four levels of P (0%, 50%, 75%, and 100% P) on sugar content of Canola Sp., **(A)** soluble sugars, **(B)** polysaccharides, and **(C)** total sugars. Values are expressed as mg glucose/g DW bars are the means, and error bars are the standard error of the means, derived from generalized least square models the mean is of three replicates (n = 3). See Table 2 for details of the statistical analysis.

and productivity in both biotic and abiotic environments (Lateef et al., 2015).

In our investigation, the two most potent isolates have been molecularly identified using 16S rRNA as *Bacillus vallismortis* strain 20P and *Bacillus tequilensis* strain 28P with 100% similarity respectively. *Bacillus* spp. are the most prevalent PGPR in nature and are frequently utilized to improve plant growth, development, and yield via secreting bioactive extra-metabolites and nutrients in addition to possessing the capacity to solubilize phosphate in soil.

The present study showed that co-inoculation with PSB; *B. varllismortis* strain 20P and *B. tequilensis* strain 28P generally improved the nutritional canola status, with the consequent significant increase in the development of the plant biomass. Plants co-inoculated with *B. varllismortis* + *B. tequilensis* under 50% P showed significantly higher shoot and root heights, dry masses, leaf area, total dry mass, low rhizosphere pH, higher chlorophyll a, carotenoids, higher soluble sugars, polysaccharides, and total sugars and higher accumulated NPK contents. These results represent a mean of promoting plant growth by increasing the P availability under this P concentration (50% P).

Our findings are consistent with those of Salimpour et al. (2012) who reported enhanced growth, physiological attributes and nutrient uptake of canola as result of applying *Bacillus* sp. and *Thiobacillus* sp. Siddikee et al. (2010) also recorded increased root elongation and dry weight for canola seedlings inoculated with *B. aryabhattai* strain RS341 than un-treated plants.

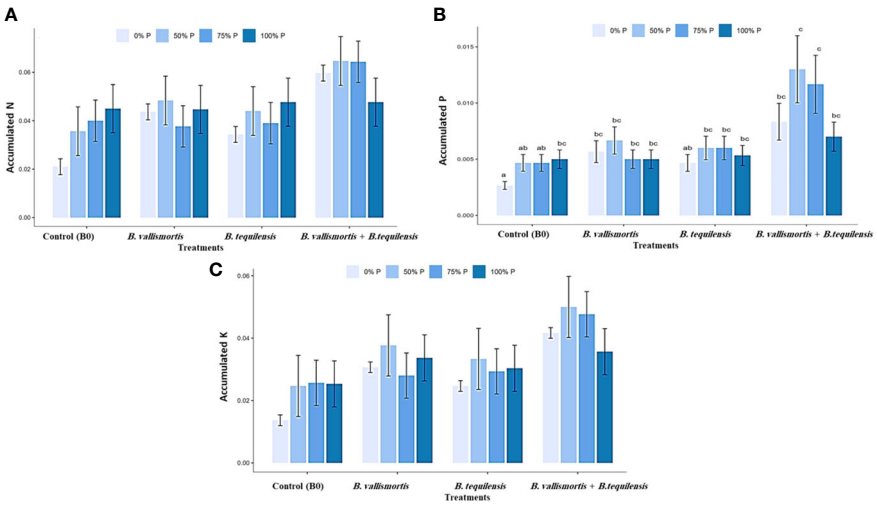

FIGURE 7
Effect of inoculation with PSB under four levels of P (0%, 50%, 75%, and 100% P) on the accumulated NPK content in plant mature leaf of Canola Sp. **(A)** accumulated N (g) **(B)** accumulated P (g) and **(C)** accumulated K(g). Bars are the means, and error bars are the standard error of the means, derived from generalized least square models, the mean is of three replicates (n = 5). See Table 2 for details of the statistical analysis.

In support, Park et al. (2015) reported that inoculation of *Kalanchoe daigremontiana* plants with plant growth-promoting rhizobacteria enhanced the plant height, shoot weight, and stem width as well as plant development in terms of increasing number of leaves per plant. Similar consequences were observed in oil palms; the multi-microbial biofertilizer application increased height, chlorophyll, and the number of leaves per plant as compared to the sole chemical fertilizer application (Adiprasetyo et al., 2014). Another valuable explanation of the PSB role is that these bacteria colonize root and rhizosphere soil, which improves microbial and root respiration and root exudation. Finally, this colonization definitely led to enhanced plant height, stem diameter, number of branches, and plant biomass (Khan et al., 2020; Iqbal et al., 2023). Several studies reported that PSB excrete organic acids, which definitely reduces the soil pH that facilitates the P intake (Vazquez et al., 2000; Mehnaz and Lazarovits, 2006; Ali et al., 2017). This fact was a strong proof of our findings which demonstrated the lower pH as the fate of the most effective treatment.

Moreover, Hawkesford et al. (2012) and Youssef et al. (2017) documented that phosphorus enhances the number and mass of roots, the formation of lateral roots, and the root/shoot ratio of plants. As a result, the soil's ability to absorb nutrients is improved, which in turn promotes plant growth, total chlorophyll, total carbohydrates, and carbon metabolism (Mohamed et al., 2021).

On the contrary, the total dry mass and chl.b showed the maximum level under 75% P combined with *B. varllismortis* +*B. tequilensis*. Accordingly, some studies have documented a reduction in chlorophyll content in combination with PGPR such as (Ajeng et al., 2020). This is most likely due to the non-suitable N needs, as N is a crucial component for chlorophyll content enhancement (Naher et al., 2018). This leads us to hypothesize that the elevated level of Chl.a under 50%P+ *B. varllismortis* + *B. tequilensis*) simultaneously with the depressed levels of Chl.b under the same treatment, because more N is exhausted in Chl.a formation on the expense of Chl.b.

It has been frequently recorded that enhancing phosphorus supplies has varying effects on carbohydrates content in relation to a source/sink equilibrium in roots and aerial tissues. The accessibility of phosphorus is generally correlated with the metabolism of sugars (Garcia-Caparros et al., 2021). PSB stimulate several metabolic pathways that lead to the synthesis of sucrose, glucose, and fructose. According to results published by Kang et al. (2014), the phosphate-solubilizing *B. megaterium* mj1212 improved photosynthetic pigments and subsequent processes like carbohydrate synthesis, which led to better growth. They also stated that plant-bacterial interactions determine how plants metabolize carbohydrates.

One of the principal roles of PSB is the enhancement of root morphological traits, causing improved nutrient uptake and N fixation (Khan, 2020; de Andrade et al., 2023). In synchronization, Hassan et al. (2017) stated that *Bacillus subtilis* enhanced Pegaga growth by enhancing nutrient intake in the treated plants. An increased N, P, and K contents were observed in black lentils and chickpea plants inoculated with *P. indica* (Nautiyal et al., 2010; Iqbal et al., 2023). PSB converts P from insoluble to soluble available form readily for plant absorption (Reddy, 2014; Gupta et al., 2015). Thus, we can hypothesize that the higher P under co-inoculation of both *Bacillus* strains is most likely due to the optimum P availability specially when being under 50% P treatment.

Generally, these bacillus strains may have the ability to enhance the availability of nutrients such as phosphorus and the production of siderophores and phytohormones (Viruel et al., 2011). In addition, these strains may also be able to colonize the root system and have a positive interaction with the plant, these bacterial characteristics could contribute to growth-promoting effect. The increased nutrient uptake could be ascribed to two main machineries: the first is the synthesis of auxin as IAA, which has a cascading impact on root growth and nutrient intake and, second, to the bacterial propensity to solubilize phosphate, which raises soil P availability. This in turn resulted in enhanced crop yield by promoting plant growth and development (Richardson et al., 2009).

5 Conclusion

Overall, co-inoculation of canola with PSB, *Bacillus varllismortis* strain 20P and *Bacillus tequilensis* strain 28P under 50%P showed an upsurge in the yield contributing traits than sole inoculation and the combined inoculation under higher P supply (75 and 1005 P). Our results are a valuable addition to the core of sustainable agricultural practices knowledge and represent one of many steps taken toward the sustainability and maintenance of our planet. It provides information for future field studies of these PSB candidates for development of bioinoculants to improve nutrient availability in soil, reduce chemical fertilizer application, and minimize environmental pollution.

Data availability statement

The original contributions presented in the study are included in the article/Supplementary Material, further inquiries can be directed to the corresponding author/s.

Author contributions

AN: Data curation, Formal analysis, Investigation, Methodology, Resources, Software, Writing – original draft. ME: Supervision, Validation, Writing – review & editing. OA: Formal analysis, Investigation, Methodology, Software, Writing – original draft. MA: Funding acquisition, Resources, Software, Validation, Formal analysis, Writing – original draft. BA: Funding acquisition, Resources, Software, Validation, Supervision, Writing – original draft. GD: Data curation, Formal Analysis, Investigation, Methodology, Resources, Software, Writing – original draft.

Funding

The author(s) declare that no financial support was received for the research, authorship, and/or publication of this article.

Acknowledgments

We gratefully acknowledge the Faculty of Science, Benha University, Egypt for all the facilities throughout the whole work and the Agricultural Research Center, Giza, Egypt for supplying pure strains of Canola (*Brassica napus L.*) seeds. We extend our thanks to Princess Nourah bint Abdulrahman University Researchers Supporting Project number (PNURSP2024R355), Princess Nourah bint Abdulrahman University, Riyadh, Saudi Arabia.

Conflict of interest

The authors declare that the research was conducted in the absence of any commercial or financial relationships that could be construed as a potential conflict of interest.

Publisher's note

Supplementary material

The Supplementary Material for this article can be found online at: https://www.frontiersin.org/articles/10.3389/fpls.2024.1324538/full#supplementary-material

References

Abdel Latef, A. A. H. (2011). Ameliorative effect of calcium chloride on growth, antioxidant enzymes, protein patterns and some metabolic activities of canola (*Brassica napus* L.) under seawater stress. *J. Plant Nutr.* 34, 1303–1320. doi: 10.1080/01904167.2011.580817

Adiprasetyo, T., Purnomo, B., Handajaningsih, M., and Hidayat, H. (2014). The usage of BIOM3G-Biofertilizer to improve and support sustainability of land system of independent oil palm smallholders. *Int. J. Adv. Sci. Eng. Inf Technol.* 4, 345–348. doi: 10.18517/ijaseit.4.5.431

Ajeng, A. A., Abdullah, R., Malek, M. A., Chew, K. W., Ho, Y.-C., Ling, T. C., et al. (2020). The effects of biofertilizers on growth, soil fertility, and nutrients uptake of oil palm (*Elaeis guineensis*) under greenhouse conditions. *Processes* 8, 1681. doi: 10.3390/pr8121681

Alexander, D. B., and Zuberer, D. A. (1991). Use of chrome azurol S reagents to evaluate siderophore production by rhizosphere bacteria. *Biol. Fertil Soils* 12, 39–45. doi: 10.1007/BF00369386

Ali, M. A., Naveed, M., Mustafa, A., and Abbas, A. (2017). The good, the bad, and the ugly of rhizosphere microbiome. *Probiotics Plant Health*, 253–290. doi: 10.1007/978-981-10-3473-2

Ammar, E., Aioub, A., Elesawy, A., M. Karkour, A., Mouhamed, M., Amer, A., et al. (2022). Algae as Bio-fertilizers: Between Current situation and Future prospective. *Saudi J. Biol. Sci.* 29 (5), 3083-3096. doi: 10.1016/j.sjbs.2022.03.020

Amri, M., Rjeibi, M. R., Gatrouni, M., Mateus, D. M., Asses, N., Pinho, H. J., et al. (2023). Isolation, identification, and characterization of phosphate-solubilizing bacteria from Tunisian Soils. *Microorganisms* 11, 783. doi: 10.3390/microorganisms11030783

Arnon, D. I. (1949). Copper enzymes in isolated chloroplasts. Polyphenoloxidase in Beta vulgaris. *Plant Physiol.* 24, 1. doi: 10.1104/pp.24.1.1

Arora, N. K., and Verma, M. (2017). Modified microplate method for rapid and efficient estimation of siderophore produced by bacteria. *Biotech.* 7, 381. doi: 10.1007/s13205-017-1008-y

Bayisa, R. A. (2023). *Bacillus velezensis* AR1 mediated plant nourishing through solubilization of hardly soluble phosphorus nutrient sources. *Cogent Food Agric.* 9, 2276561. doi: 10.1080/23311932.2023.2276561

Benbrik, B., Elabed, A., El Modafar, C., Douira, A., Amir, S., Filali-Maltouf, A., et al. (2020). Reusing phosphate sludge enriched by phosphate solubilizing bacteria as biofertilizer: Growth promotion of *Zea Mays*. *Biocatal Agric. Biotechnol.* 30, 101825. doi: 10.1016/j.bcab.2020.101825

Bhattacharyya, P. N., and Jha, D. K. (2012). Plant growth-promoting rhizobacteria (PGPR): emergence in agriculture. *World J. Microbiol. Biotechnol.* 28, 1327–1350. doi: 10.1007/s11274-011-0979-9

Bidondo, L. F., Bompadre, J., Pergola, M., Silvani, V., Colombo, R., Bracamonte, F., et al. (2012). Differential interaction between two *Glomus intraradices* strains and a phosphate solubilizing bacterium in maize rhizosphere. *Pedobiol. (Jena)* 55, 227–232. doi: 10.1016/j.pedobi.2012.04.001

Carré, P., and Pouzet, A. (2014). Rapeseed market, worldwide and in Europe. *Ocl* 21, D102. doi: 10.1051/ocl/2013054

Chakraborty, U., Chakraborty, B. N., Chakraborty, A. P., and Dey, P. L. (2013). Water stress amelioration and plant growth promotion in wheat plants by osmotic stress tolerant bacteria. *World J. Microbiol. Biotechnol.* 29, 789–803. doi: 10.1007/s11274-012-1234-8

Chapman, H. D., and Pratt, P. F. (1962). Methods of analysis for soils, plants and waters. *Soil Sci.* 93, 68. doi: 10.1097/00010694-196201000-00015

Cheng, Y., Narayanan, M., Shi, X., Chen, X., Li, Z., and Ma, Y. (2023). Phosphate-solubilizing bacteria: Their agroecological function and optimistic application for enhancing agro-productivity. *Sci. Total Environ.* 166468. doi: 10.1016/j.scitotenv.2023.166468

Chibnall, A. C., Rees, M. W., and Williams, E. F. (1943). Quoted vogel in organic chemistry. *Biochemi. J.* 37, 54.

de Andrade, L. A., Santos, C. H. B., Frezarin, E. T., Sales, L. R., and Rigobelo, E. C. (2023). Plant growth-promoting rhizobacteria for sustainable agricultural production. *Microorganisms* 11, 1088. doi: 10.3390/microorganisms11041088

Dick, C. F., Dos-Santos, A. L. A., and Meyer-Fernandes, J. R. (2011). Inorganic phosphate as an important regulator of phosphatases. *Enzyme Res.* 2011. doi: 10.4061/2011/103980

Elbeltagy, A., Nishioka, K., Suzuki, H., Sato, T., Sato, Y.-I., Morisaki, H., et al. (2000). Isolation and characterization of endophytic bacteria from wild and traditionally cultivated rice varieties. *Soil Sci. Plant Nutr.* 46, 617–629. doi: 10.1080/00380768.2000.10409127

Elhaissoufi, W., Ghoulam, C., Barakat, A., Zeroual, Y., and Bargaz, A. (2022). Phosphate bacterial solubilization: A key rhizosphere driving force enabling higher P use efficiency and crop productivity. *J. Adv. Res.* 38, 13–28. doi: 10.1016/j.jare.2021.08.014

ELSabagh, A., Abd Elhamid, O., SANEOKA, H., and Barutçular, C. (2015). Evaluation agronomic traits of canola (*Brassica napus* L.) under organic, bio-and chemical fertilizers. *Dicle Üniversitesi Fen Bilimleri Enstitüsü Dergisi* 4, 59–67. doi: 10.1016/S1002-0160(08)60042-9

Faucon, M.-P., Houben, D., Reynoird, J.-P., Mercadal-Dulaurent, A.-M., Armand, R., and Lambers, H. (2015). Advances and perspectives to improve the phosphorus availability in cropping systems for agroecological phosphorus management. *Adv. Agron.* 134, 51–79. doi: 10.1016/bs.agron.2015.06.003

Fixen, P. E., and Johnston, A. M. (2012). World fertilizer nutrient reserves: a view to the future. *J. Sci. Food Agric.* 92, 1001–1005. doi: 10.1002/jsfa.4532

Garcia-Caparros, P., Lao, M. T., Preciado-Rangel, P., and Sanchez, E. (2021). Phosphorus and carbohydrate metabolism in green bean plants subjected to increasing phosphorus concentration in the nutrient solution. *Agronomy* 11, 245. doi: 10.3390/agronomy11020245

Gordon, S. A., and Weber, R. P. (1951). Colorimetric estimation of indoleacetic acid. *Plant Physiol.* 26, 192. doi: 10.1104/pp.26.1.192

Goswami, D., Thakker, J. N., and Dhandhukia, P. C. (2016). Portraying mechanics of plant growth promoting rhizobacteria (PGPR): A review. *Cogent Food Agric.* 2, 1127500. doi: 10.1080/23311932.2015.1127500

Guang-Can, T. A. O., Shu-Jun, T., Miao-Ying, C. A. I., and Guang-Hui, X. I. E. (2008). Phosphate-solubilizing and-mineralizing abilities of bacteria isolated from soils. *Pedosphere* 18, 515–523.

Gupta, G., Parihar, S. S., Ahirwar, N. K., Snehi, S. K., and Singh, V. (2015). Plant growth promoting rhizobacteria (PGPR): current and future prospects for development of sustainable agriculture. *J. Microb. Biochem. Technol.* 7, 96–102. doi: 10.4172/1948-5948.1000188

Gyaneshwar, P., Naresh Kumar, G., Parekh, L. J., and Poole, P. S. (2002). Role of soil microorganisms in improving P nutrition of plants. *Plant Soil* 245, 83–93. doi: 10.1023/A:1020663916259

Hardy, R., Burns, R. C., and Holsten, R. D. (1973). Applications of the acetylene-ethylene assay for measurement of nitrogen fixation. *Soil Biol. Biochem.* 5, 47–81. doi: 10.1016/0038-0717(73)90093-X

Hassan, M., Jaafar, N., and Mulana, K. (2017). Effect of *Bacillus subtilis* as plant beneficial bacteria on growth performance of Pegaga (*Centella asiatica*). *Biosci. Res.* 14, 1074–1079.

Hawkesford, M., Horst, W., Kichey, T., Lambers, H., Schjoerring, J., Møller, I. S., et al. (2012). "Functions of macronutrients," in *Marschner's mineral nutrition of higher plants* (525B street, Suite 1800. San Diego, CA 92101-4495, USA: Elsevier), 135–189. doi: 10.1016/B978-0-12-384905-2.00006-6

Horvath, G., Kissimon, J., and Faludi-Dániel, Á. (1972). Effect of light intensity on the formation of carotenoids in normal and mutant maize leaves. *Phytochemistry* 11, 183–187. doi: 10.1016/S0031-9422(00)89987-2

Houben, D., Michel, E., Nobile, C., Lambers, H., Kandeler, E., and Faucon, M.-P. (2019). Response of phosphorus dynamics to sewage sludge application in an agroecosystem in northern France. *Appl. Soil Ecol.* 137, 178–186. doi: 10.1016/j.apsoil.2019.02.017

Hussain, M., Asgher, Z., Tahir, M., Ijaz, M., Shahid, M., Ali, H., et al. (2016). Bacteria in combination with fertilizers improve growth, productivity and net returns of wheat (*Triticum aestivum* L.). *Pak J. Agric. Sci.* 53 (3). doi: 10.21162/PAKJAS/16.4901

Ikeda, S., Tokida, T., Nakamura, H., Sakai, H., Usui, Y., Okubo, T., et al. (2015). Characterization of leaf blade-and leaf sheath-associated bacterial communities and assessment of their responses to environmental changes in CO_2, temperature, and nitrogen levels under field conditions. *Microbes Environ.* 30, 51–62. doi: 10.1264/jsme2.ME14117

Iqbal, M., Naveed, M., Sanaullah, M., Brtnicky, M., Hussain, M. I., Kucerik, J., et al. (2023). Plant microbe mediated enhancement in growth and yield of canola (*Brassica napus* L.) plant through auxin production and increased nutrient acquisition. *J. Soils Sediments* 23, 1233–1249. doi: 10.1007/s11368-022-03386-7

Kang, S.-M., Radhakrishnan, R., You, Y.-H., Joo, G.-J., Lee, I.-J., Lee, K.-E., et al. (2014). Phosphate solubilizing *Bacillus megaterium* mj1212 regulates endogenous plant carbohydrates and amino acids contents to promote mustard plant growth. *Indian J. Microbiol.* 54, 427–433. doi: 10.1007/s12088-014-0476-6

Khan, N. (2020). Plant-microbial interactions and their role in sustainable agriculture and sustainability of agriculture soils. *Recent Pat. Food Nutr. Agric.* 11, 94–95. doi: 10.2174/2212798411022008061529 33

Khan, N., Bano, A., and Curá, J. A. (2020). Role of beneficial microorganisms and salicylic acid in improving rainfed agriculture and future food safety. *Microorganisms* 8, 1018. doi: 10.3390/microorganisms8071018

Khan, A. A., Jilani, G., Akhtar, M. S., Naqvi, S. M. S., and Rasheed, M. (2009). Phosphorus solubilizing bacteria: occurrence, mechanisms and their role in crop production. *J. Agric. Biol. Sci.* 1, 48–58.

Khan, M. S., Zaidi, A., and Wani, P. A. (2007). Role of phosphate-solubilizing microorganisms in sustainable agriculture — A review. *Agron. Sustain Dev.* 27, 29–43. doi: 10.1051/agro:2006011

Kissimon, J. (1999). "Analysis of the photosynthetic pigment composition," in *Proceedings of the International Workshop and Training Course on Microalgal Biol. and Biotech* (Mosonmagyar, Hungary), 13–26.

Kumar, K. K., and Dara, S. K. (2021). Fungal and bacterial endophytes as microbial control agents for plant-parasitic nematodes. *Int. J. Environ. Res. Public Health* 18, 4269. doi: 10.3390/ijerph18084269

Kumar, R., Kumar, R., and Prakash, O. (2019). Chapter-5 the impact of chemical fertilizers on our environment and ecosystem. *Chief Ed* 35, 69.

Lateef, A., Adelere, I. A., and Gueguim-Kana, E. B. (2015). The biology and potential biotechnological applications of *Bacillus safensis*. *Biol. (Bratisl) Biol.* 70, 411–419. doi: 10.1515/biolog-2015-0062

Lohani, N., Jain, D., Singh, M. B., and Bhalla, P. L. (2020). Engineering multiple abiotic stress tolerance in canola. *Brassica Napus Front. Plant Sci.* 11, 3. doi: 10.3389/fpls.2020.00003

Malhotra, H., Vandana, Sharma, S., and Pandey, R. (2018). Phosphorus nutrition: plant growth in response to deficiency and excess. *Plant Nutrients Abiotic Stress Tolerance*, 171–190. doi: 10.1007/978-981-10-9044-8_7

Marschner, P. (2012). *Mineral nutrition of higher plants*, *3rd ed.* (525B street, Suite 1800. San Diego, CA 92101-4495, USA: Academic press, Elsevier)

Mehnaz, S., and Lazarovits, G. (2006). Inoculation effects of *Pseudomonas putida*, *Gluconacetobacter azotocaptans*, and *Azospirillum lipoferum* on corn plant growth under greenhouse conditions. *Microb. Ecol.* 51, 326–335. doi: 10.1007/s00248-006-9039-7

Milazzo, M. F., Spina, F., Vinci, A., Espro, C., and Bart, J. C. J. (2013). Brassica biodiesels: Past, present and future. *Renewable Sustain. Energy Rev.* 18, 350–389. doi: 10.1016/j.rser.2012.09.033

Miljaković, D., Marinković, J., and Balešević-Tubić, S. (2020). The significance of *Bacillus* spp. in disease suppression and growth promotion of field and vegetable crops. *Microorganisms* 8, 1037. doi: 10.3390/microorganisms8071037

Mohamed, M. H. M., Ali, M., Eid, R. S. M., El-Desouky, H. S., Petropoulos, S. A., Sami, R., et al. (2021). Phosphorus and biofertilizer application effects on growth parameters, yield and chemical constituents of broccoli. *Agronomy* 11, 2210. doi: 10.3390/agronomy11112210

Mukhtar, S., Shahid, I., Mehnaz, S., and Malik, K. A. (2017). Assessment of two carrier materials for phosphate solubilizing biofertilizers and their effect on growth of wheat (*Triticum aestivum* L.). *Microbiol. Res.* 205, 107–117. doi: 10.1016/j.micres.2017.08.011

Naher, U. A., Panhwar, Q. A., Othman, R., Shamshuddin, J., Ismail, M. R., and Zhou, E. (2018). Proteomic study on growth promotion of PGPR inoculated aerobic rice (*Oryza sativa* L.) cultivar MR219-9. *Pak. J. Bot.* 50, 1843–1852.

Naik, B. S., Shashikala, J., and Krishnamurthy, Y. L. (2009). Study on the diversity of endophytic communities from rice (*Oryza sativa* L.) and their antagonistic activities in *vitro*. *Microbiol. Res.* 164, 290–296. doi: 10.1016/j.micres.2006.12.003

NAMLI, A., Mahmood, A., Sevilir, B., and ÖZKIR, E. (2017). Effect of phosphorus solubilizing bacteria on some soil properties, wheat yield and nutrient contents. *Eurasian J. Soil Sci.* 6, 249–258. doi: 10.18393/ejss.293157

Nautiyal, C. S. (1999). An efficient microbiological growth medium for screening phosphate solubilizing microorganisms. *FEMS Microbiol. Lett.* 170, 265–270. doi: 10.1111/fml.1999.170.issue-1

Nautiyal, C. S., Chauhan, P. S., DasGupta, S. M., Seem, K., Varma, A., and Staddon, W. J. (2010). Tripartite interactions among *Paenibacillus lentimorbus* NRRL B-30488, *Piriformospora indica* DSM 11827, and *Cicer arietinum* L. *World J. Microbiol. Biotechnol.* 26, 1393–1399. doi: 10.1007/s11274-010-0312-z

Nobile, C., Houben, D., Michel, E., Firmin, S., Lambers, H., Kandeler, E., et al. (2019). Phosphorus-acquisition strategies of canola, wheat and barley in soil amended with sewage sludges. *Sci. Rep.* 9, 14878. doi: 10.1038/s41598-019-51204-x

Olsen, S. R., and Sommers, L. E. (1982). "Phosphorus," in *Methods of Soil Analysis, Part 2. American Society of Agronomy*. Eds. A. L. Page, R. H. Miller and D. R. Weeny (Madison, Wisconsin), 403–430.

Pandey, R., MuÈller, A., Napoli, C. A., Selinger, D. A., Pikaard, C. S., Richards, E. J., et al. (2002). Analysis of histone acetyltransferase and histone deacetylase families of *Arabidopsis thaliana* suggests functional diversification of chromatin modification among multicellular eukaryotes. *Nucleic Acids Res.* 30, 5036–5055. doi: 10.1093/nar/gkf660

Park, Y.-S., Park, K., Kloepper, J. W., and Ryu, C.-M. (2015). Plant growth-promoting rhizobacteria stimulate vegetative growth and asexual reproduction of *Kalanchoe daigremontiana*. *Plant Pathol. J.* 31, 310. doi: 10.5423/PPJ.NT.01.2015.0006

Pereira, R. C., and Da Gama, B. A. P. (2008). "Macroalgal chemical defenses and their roles in structuring tropical marine communities," in *Algal chemical ecology* (Berlin Heidelberg: Springer), 25–55.

Pikovskaya, R. I. (1948). Mobilization of phosphorus in soil in connection with vital activity of some microbial species. *Mikrobiologiya* 17, 362–370.

Pirttilä, A. M., Mohammad Parast Tabas, H., Baruah, N., and Koskimäki, J. J. (2021). Biofertilizers and biocontrol agents for agriculture: How to identify and develop new potent microbial strains and traits. *Microorganisms* 9, 817. doi: 10.3390/microorganisms9040817

Poirier, Y., Jaskolowski, A., and Clúa, J. (2022). Phosphate acquisition and metabolism in plants. *Curr. Biol.* 32, R623–R629. doi: 10.1016/j.cub.2022.03.073

Prabhu, N., Borkar, S., and Garg, S. (2019). Phosphate solubilization by microorganisms: overview, mechanisms, applications and advances. *Adv. Biol. Sci. Res.*, 161–176. doi: 10.1016/B978-0-12-817497-5.00011-2

Pregi, F. (1945). *Quantitative organic micro analysis. 4th ed.* (Ltd London: Churchill), 126–129. doi: 10.1016/B978-0-12-817497-5.00011-2

Prud'homme, M.-P., Gonzalez, B., Billard, J.-P., and Boucaud, J. (1992). Carbohydrate content, fructan and sucrose enzyme activities in roots, stubble and leaves of ryegrass (*Lolium perenne* L.) as affected by source/sink modification after cutting. *J. Plant Physiol.* 140, 282–291. doi: 10.1016/S0176-1617(11)81080-1

Radhakrishnan, R., Hashem, A., and Abd_Allah, E. F. (2017). *Bacillus*: A biological tool for crop improvement through bio-molecular changes in adverse environments. *Front. Physiol.* 8, 667. doi: 10.3389/fphys.2017.00667

Ranganna, S. (1977). *Plant pigments. Manual of Analysis of Fruit and Vegetable Products* (New Delhi: Tata McGraw-Hill Publishing Co., Ltd), 72–93.

Reddy, P. (2014). *Potential role of PGPR in agriculture* (New Delhi: Springer), 17–34. doi: 10.1007/978-81-322-1973-6

Reijnders, L. (2014). Phosphorus resources, their depletion and conservation, a review. *Resour Conserv. Recycl* 93, 32–49. doi: 10.1016/j.resconrec.2014.09.006

Ribeiro, V. P., Marriel, I. E., de Sousa, S. M., de P. Lana, U. G., Mattos, B. B., de Oliveira, C. A., et al. (2018). Endophytic *Bacillus* strains enhance pearl millet growth and nutrient uptake under low-P. *Braz. J. Microbiol.* 49, 40–46. doi: 10.1016/j.bjm.2018.06.005

Richardson, A. E. (2001). Prospects for using soil microorganisms to improve the acquisition of phosphorus by plants. *Funct. Plant Biol.* 28, 897–906. doi: 10.1071/PP01093

Richardson, A. E., Hocking, P. J., Simpson, R. J., and George, T. S. (2009). Plant mechanisms to optimize access to soil phosphorus. *Crop Pasture Sci.* 60, 124–143. doi: 10.1071/CP07125

Richardson, A. E., Lynch, J. P., Ryan, P. R., Delhaize, E., Smith, F. A., Smith, S. E., et al. (2011). Plant and microbial strategies to improve the phosphorus efficiency of agriculture. *Plant Soil* 349, 121–156. doi: 10.1007/s11104-011-0950-4

Robles-Aguilar, A. A., Pang, J., Postma, J. A., Schrey, S. D., Lambers, H., and Jablonowski, N. D. (2019). The effect of pH on morphological and physiological root traits of *Lupinus angustifolius* treated with struvite as a recycled phosphorus source. *Plant Soil* 434, 65–78. doi: 10.1007/s11104-018-3787-2

Salimpour, S. I., Khavazi, K., Nadian, H., Besharati, H., and Miransari, M. (2010). Enhancing phosphorous availability to canola ("*Brassica napus*" L.) using P solubilizing and sulfur oxidizing bacteria. *Aust. J. Crop Sci.* 4, 330–334.

Salimpour, S., Khavazi, K., Nadian, H., Besharati, H., and Miransari, M. (2012). Canola oil production and nutrient uptake as affected by phosphate solubilizing and sulfur oxidizing bacteria. *J. Plant Nutr.* 35, 1997–2008. doi: 10.1080/01904167.2012.716892

Sanchez-Gonzalez, M. E., Mora-Herrera, M. E., Wong-Villarreal, A., de la Portilla-López, N., Sanchez-Paz, L., Lugo, J., et al. (2022). Effect of pH and carbon source on phosphate solubilization by bacterial strains in pikovskaya medium. *Microorganisms* 11, 49. doi: 10.3390/microorganisms11010049

Sarker, A., Talukder, N. M., and Islam, M. T. (2014). Phosphate solubilizing bacteria promote growth and enhance nutrient uptake by wheat. *Plant Sci. Today* 1, 86–93. doi: 10.14719/pst

Sarwart, M., Arshad, M., Martens, D. A., and Frankenberger, W. T. (1992). Tryptophan-dependent biosynthesis of auxins in soil. *Plant Soil* 147, 207–215. doi: 10.1007/BF00029072

Seyfferth, C., Renema, J., Wendrich, J. R., Eekhout, T., Seurinck, R., Vandamme, N., et al. (2021). Advances and opportunities in single-cell transcriptomics for plant research. *Annu. Rev. Plant Biol.* 72, 847–866. doi: 10.1146/annurev-arplant-081720-010120

Sharma, S. B., Sayyed, R. Z., Trivedi, M. H., and Gobi, T. A. (2013). Phosphate solubilizing microbes: sustainable approach for managing phosphorus deficiency in agricultural soils. *Springerplus* 2, 1–14. doi: 10.1186/2193-1801-2-587

Siddikee, M. A., Chauhan, P. S., Anandham, R., Han, G. H., and Sa, T. (2010). Isolation, characterization, and use for plant growth promotion under salt stress, of ACC deaminase-producing halotolerant bacteria derived from coastal soil. *J. Microbiol. Biotechnol.* 20, 1577–1584. doi: 10.4014/jmb.1007.07011

Soltanpour (1985). Use of ammonium bicarbonate DTPA soil test to evaluate elemental availability and toxicity. *Commun. Soil Sci. Plant Anal* 16 (3), 323–338.

Suleiman, A. K. A., Lourenço, K. S., Clark, C., Luz, R. L., da Silva, G. H. R., Vet, L. E. M., et al. (2020). From toilet to agriculture: Fertilization with microalgal biomass from wastewater impacts the soil and rhizosphere active microbiomes, greenhouse gas emissions and plant growth. *Resour Conserv. Recycl* 161, 104924. doi: 10.1016/j.resconrec.2020.104924

Syers, J. K., Johnston, A. E., and Curtin, D. (2008). Efficiency of soil and fertilizer phosphorus use. *FAO Fertilizer Plant Nutr. Bull.* 18, 5–50.

Szilagyi-Zecchin, V. J., Ikeda, A. C., Hungria, M., Adamoski, D., Kava-Cordeiro, V., Glienke, C., et al. (2014). Identification and characterization of endophytic bacteria from corn (*Zea mays* L.) roots with biotechnological potential in agriculture. *AMB Express* 4, 1–9. doi: 10.1186/s13568-014-0026-y

Tabatabai, M. A., and Bremner, J. M. (1969). Use of p-nitrophenyl phosphate for assay of soil phosphatase activity. *Soil Biol. Biochem.* 1, 301–307. doi: 10.1016/0038-0717(69)90012-1

Vazquez, P., Holguin, G., Puente, M. E., Lopez-Cortes, A., and Bashan, Y. (2000). Phosphate-solubilizing microorganisms associated with the rhizosphere of mangroves in a semiarid coastal lagoon. *Biol. Fertil Soils* 30, 460–468. doi: 10.1007/s003740050024

Viruel, E., Lucca, M. E., and Sineriz, F. (2011). Plant growth promotion traits of phosphobacteria isolated from Puna, Argentina. *Arch. Microbiol.* 193, 489–496. doi: 10.1007/s00203-011-0692-y

Walpola, B., and Yoon, M.-H. (2013). Isolation and characterization of phosphate solubilizing bacteria and their co-inoculation efficiency on tomato plant growth and phosphorous uptake. *Afr J. Microbiol. Res.* 7, 266–275. doi: 10.5897/AJMR12.2282

Whistler, R. L., and Wolfrom, M. L. (1963). *Methods in Carbohydrate Chemistry: Cellulose.* (New York: Academic Press).

Xie, C., Tang, J., Zhao, J., Wu, D., and Xu, X. (2011). Comparison of phosphorus fractions and alkaline phosphatase activity in sludge, soils, and sediments. *J. Soils Sediments* 11, 1432–1439. doi: 10.1007/s11368-011-0429-1

Youssef, S. M., Riad, G. S., and Abd Elhady, S. A. (2017). Effect of phosphorus sources and arbuscular mycorrhizal inoculation on growth and productivity of snap bean (*Phaseolus vulgaris* L.). *Gesunde Pflanzen* 69, 139–148. doi: 10.1007/s10343-017-0398-4

Zhao, D., Reddy, K. R., Kakani, V. G., and Read, J. J. (2010). Remote-sensing algorithms for estimating nitrogen uptake and nitrogen-use efficiency in cotton. *Acta Agriculturae Scandinavica Section B-Soil Plant Sci.* 60, 500–509. doi: 10.1080/09064710903233854

Zuluaga, M. Y. A., de Oliveira, A. L. M., Valentinuzzi, F., Jayme, N. S., Monterisi, S., Fattorini, R., et al. (2023). An insight into the role of the organic acids produced by Enterobacter sp. strain 15S in solubilizing tricalcium phosphate: in *situ* study on cucumber. *BMC Microbiol.* 23, 184. doi: 10.1186/s12866-023-02918-6

Zuur, A. F., Ieno, E. N., Walker, N. J., Saveliev, A. A., and Smith, G. M. (2009). *Mixed effects models and extensions in ecology with R* Vol. 574 (New York: Springer), 574. doi: 10.1007/978-0-387-87458-6

frontiers | Frontiers in Plant Science

TYPE Original Research
PUBLISHED 10 May 2024
DOI 10.3389/fpls.2024.1346154

OPEN ACCESS

EDITED BY
Carlos Henrique Meneses,
State University of Paraíba, Brazil

REVIEWED BY
Sharada Mallubhotla,
Shri Mata Vaishno Devi University, India
Paulo Ivan Fernandes-Júnior,
Embrapa Semiárido, Brazil

*CORRESPONDENCE
Quanren Cui
540791346@qq.com
Fuzhao Nian
nianfzh@ynau.edu.cn

†These authors have contributed equally to this work

RECEIVED 29 November 2023
ACCEPTED 19 April 2024
PUBLISHED 10 May 2024

CITATION
Shi Y, He Y, Zheng Y, Liu X, Wang S, Xiong T, Wen T, Duan H, Liao X, Cui Q and Nian F (2024) Characteristics of the phyllosphere microbial community and its relationship with major aroma precursors during the tobacco maturation process.
Front. Plant Sci. 15:1346154.
doi: 10.3389/fpls.2024.1346154

Characteristics of the phyllosphere microbial community and its relationship with major aroma precursors during the tobacco maturation process

Yixuan Shi[1†], Yuansheng He[2†], Yuanxian Zheng[2], Xixi Liu[1], Shuzhong Wang[2], Tian'e Xiong[2], Tao Wen[2], Hong Duan[2], Xiaolin Liao[3], Quanren Cui[4*] and Fuzhao Nian[1*]

[1]College of Tobacco Science, Yunnan Agricultural University, Kunming, Yunnan, China, [2]Technology and Research Center, Lincang Branch Company of Yunnan Tobacco Company, Lincang Yunnan, China, [3]College of Food Science and Technology, Yunnan Agricultural University, Kunming, Yunnan, China, [4]Tobacco Research Institute, Anhui Academy of Agricultural Sciences, Hefei, Anhui, China

Numerous bacteria, fungi and other microorganisms in the tobacco phyllosphere interstellar area participate in the physiological metabolism of plants by interacting with the host. However, there is currently little research on the characteristics of tobacco phyllosphere microbial communities, and the correlation between tobacco phyllosphere microbial communities and phyllosphere factor indicators is still unknown. Therefore, high-throughput sequencing technology based on the 16S rRNA/ITS1 gene was used to explore the diversity and composition characteristics of tobacco phyllosphere bacterial and fungal communities from different maturation processes, and to identify marker genera that distinguish phyllosphere microbial communities. In this study, the correlations between tobacco phyllosphere bacterial and fungal communities and the precursors of major aroma compounds were explored. The results showed that as the tobacco plants matured, the density of glandular trichomes on the tobacco leaves gradually decreased. The surface physicochemical properties of tobacco leaves also undergo significant changes. In addition, the overall bacterial alpha diversity in the tobacco phyllosphere area increased with maturation, while the overall fungal alpha diversity decreased. The beta diversity of bacteria and fungi in the tobacco phyllosphere area also showed significant differences. Specifically, with later top pruning time, the relative abundances of *Acidisoma*, *Ralstonia*, *Bradyrhizobium*, *Alternaria* and *Talaromyces* gradually increased, while the relative abundances of *Pseudomonas*, *Filobassidium*, and *Tausonia* gradually decreased. In the bacterial community, *Acidisoma*, *Ralstonia*, *Bradyrhizobium*, and *Alternaria* were significantly positively correlated with tobacco aroma precursors, with significant negative correlations with tobacco phyllosphere trichome morphology, while *Pseudomonas* showed the opposite pattern; In the fungal community, *Filobasidium* and *Tausonia* were significantly negatively correlated with tobacco aroma precursors, and significantly positively correlated with

tobacco phyllosphere trichome morphology, while *Alternaria* showed the opposite pattern. In conclusion, the microbiota (bacteria and fungi) and aroma precursors of the tobacco phyllosphere change significantly as tobacco matures. The presence of *Acidisoma*, *Ralstonia*, *Bradyrhizobium* and *Alternaria* in the phyllosphere microbiota of tobacco may be related to the aroma precursors of tobacco.

KEYWORDS

tobacco, phyllosphere microbiota, ecological zone, top pruning, aroma precursors

Introduction

The phyllosphere mainly refers to the environment formed by leaves, including the surface and internal environment (Ruinen, 1961). Phyllosphere microorganisms refer to the collective term for epiphytic bacteria on the surface and endophytic bacteria inside (Marie-Agnès and Morris, 1995; Mina et al., 2020). The phyllosphere of plants is rich in biodiversity, and includes various bacteria, archaea, fungi, oomycetes, nematodes, and viruses (Wallace et al., 2018; Bashir et al., 2022).Archaea, viruses, and other microbes in the phyllosphere are poorly characterized due to the lack of related research. Therefore, bacteria and fungi are the most studied groups in plant tissues. Phyllosphere microorganisms play a very important role in the phyllosphere, as they can promote plant growth by promoting nutrient absorption, synthesizing plant hormones, and assisting plants in adapting to abiotic stress (Vorholt, 2012). Phyllosphere microorganisms can also induce systemic resistance in plants to maintain plant health through nutrient or spatial competition, the production of antibacterial metabolites, and interference with plant pathogen quorum sensing (Berg and Koskella, 2018). Chen et al. reported that when the balance of the leaf microbiota is disrupted, microbial diversity decreases, and *Proteobacteria* proliferate and inhibit *Bacillota* growth, leading to symptoms such as leaf tissue yellowing or necrosis in plants (Chen et al., 2020). In addition, leaf microorganisms can produce alkaloids, terpenes, esters, and other compounds, which affect the diversity of plant metabolites. Mucciarelli et al. reported that endophytic bacteria are beneficial for increasing terpenoids levels in the leaves of Mentha canadensis (Mucciarelli et al., 2007). Due to their long-term symbiosis and coevolution with the host plant, some endophytic fungi can produce secondary metabolites that are the same or similar to those of the host. For example, Stierle et al. isolated the endophytic fungus Taxomyces andreanae from Taxus wallichiana var. chenensis, which can produce paclitaxel (Stierle et al., 1993). Phyllosphere microorganisms have high biodiversity, complex community structures, and large biomasses (Vorholt, 2012; Laforest-Lapointe and Whitaker, 2019; Bashir et al., 2022; Sohrabi et al., 2023). The interaction between plants and their potential functions is a new research field in the interdisciplinary research of botany and microbiology (Berg et al., 2016; Das et al., 2022; Pathak et al., 2022). However, there are currently few related studies, far behind the research on rhizosphere microorganisms (Mendes et al., 2013; Qu et al., 2020; Ling et al., 2022; Liu et al., 2023). Only a few studies have focused on the stimulation of plant resistance, the control of plant pathogens, and the regulation of plant respiration by phyllosphere microorganisms, which is insufficient for understanding the interactions between phyllosphere microorganisms and plants and understanding the functions of phyllosphere microorganisms (Cappelletti et al., 2016; Gharaie et al., 2017; Zhang et al., 2023). Therefore, it is important to understand the differences in the community structure of different plant phyllosphere microorganisms and their driving mechanisms from multiple perspectives in order to understand the interactions between plants and phyllosphere microorganisms.

Tobacco aroma components are mostly generated by the degradation and conversion of aroma precursors, especially some important aroma components of tobacco (Banožić et al., 2020). Each aroma component can have one or several precursors (Wu et al., 2014). Therefore, the content of aroma precursors in tobacco is closely related to the content of aroma substances and the aroma of tobacco (Deng et al., 2010; Banožić et al., 2020). Aroma precursors generally have a relatively large molecular weight, are nonvolatile or have low volatility, and do not have obvious aromas. However, they often generate specific types of aroma components after degradation and conversion. The important and extensively studied aroma precursors of tobacco include high molecular weight terpenols, fatty acids, phenols, sugar-amino acids, and alkaloids (Yinju et al., 2018). Among them, high molecular weight terpenols

Abbreviations: EP, Eppendorf; SD, Standard deviation; ITS, Internal Transcribed Spacer; QIIME, Quantitative Insights Into Microbial Ecology; ASVs, Amplicon Sequence Variants; PCoA, Principal Co-ordinates Analysis; ada_, adaxial; aba_, abaxial; GTD, glandular trichomes density; LGTD, long glandular trichomes density; SGTD, short glandular trichomes density; DADA2, Divisive Amplicon Denoising Algorithm2; PICRUST2, Phylogenetic Investigation of Communities by Reconstruction of Unobserved States 2.

are the main components of tobacco glandular trichomes and are important precursors of tobacco aroma and flavor. There are two main types of terpenols cembrenediol and labdane diterpenoids. Researchers have demonstrated that fresh tobacco leaves have a relatively high content of α-cembratrienedio, which accounts for 0.7% of the fresh weight of the leaves and 50% of the total lipid content on the leaf surface (Chang and Grunwald, 1976). Moreover, all types of cembrenediol are present in ordinary burley tobacco. Labdane compounds mainly include (+)-cis-abienol and labdane diterpenes, which are abundant in menthol cigarettes but less common in flue-cured and burley tobacco (Vontimitta et al., 2010). During the curing period of tobacco leaves, (+)-cis-abienol oxidizes and decomposes, generating a large amount of aroma substances, giving the smoke a pleasant aroma and flavor similar to those of pine wood (Guo et al., 1994; Vontimitta et al., 2010). (+)-cis-abienol is the main labdane compound in the fresh tobacco leaves of menthol cigarettes, and it is also a plant growth regulator. Fatty acids, which can be esterified with alcohols or exist in a free form, are also important aroma precursors in tobacco (Liu et al., 2022a). Higher fatty acids (palmitic acid, stearic acid, etc.) do not have a direct effect on the aroma of tobacco, but they can regulate the acidity of tobacco, make the smoke mellow, and indirectly affect the aroma of the smoke, playing a balancing role in the smoke (Kawasaki et al., 1998). Although polyphenolic compounds have very low volatility and very few directly enter smoke during combustion and inhalation, they participate in important reactions during the curing period, increasing the complexity of the aroma and improving the balance of the smoke, making them important aroma precursors in tobacco (Liu et al., 2022b). Although previous research has studied microbes in tobacco leaves and aroma precursors, there is little research on the changes and differences in the microbial community and the relationships between the microbial community and aroma precursors in the intercellular space of tobacco leaves (English et al., 1967).

Therefore, this study focused on fresh tobacco leaves and used high-throughput sequencing technology based on the 16S rRNA/ITS1 gene to sequence bacteria and fungi on the tobacco phyllosphere surface. The characteristics of the tobacco phyllosphere microbial community are elucidated from changes in the phyllosphere microbial community during the maturation process. On this basis, the correlation between the characteristics of phyllosphere bacterial and fungal communities and aroma precursors was explored. The research results not only provide a theoretical basis for subsequent related research, but also fill the gap in knowledge on the correlation between the tobacco phyllosphere microbiota and aroma precursors.

Materials and methods

Experimental design and sample collection

To study the changes in the microbial community of tobacco leaves during the maturation process and their relationship with tobacco aroma precursors, the representative tobacco variety Zhongyan 100 from Yiyang County, Luoyang City, Henan Province, was sampled and analyzed. In terms of botanical classification, Zhongyan 100 is a member of the Nicotiana tabacum (Solanaceae). Zhongyan 100 is a high-quality multi-resistance flue-cured tobacco variety developed by the China Tobacco Genetic and Breeding Research (Northern) Center, which hybridizes the high-quality variety NC82 with the multi-resistance complementary parent 9201. After 5 generations of backcrossing with NC82, the variety was selectively selected and cultivated using the pedigree method. This study was approved by the China Tobacco Variety Approval Committee in December 2022). The soil type of the tested field was sandy loam, and the previous season planting model was winter fallow stubble. The agronomic characteristics of the soil were as follows: pH, 7.76; organic matter, 6.03 g/kg; alkali-hydrolyzed nitrogen, 80.71 mg/kg; available phosphorus, 5.88 mg/kg; and available potassium, 123.24 mg/kg. Cultivation management followed the local quality tobacco leaf management standards. Fresh tobacco leaf samples were collected 20 d (BD20), 40 d (BD40), and 60 d (BD60) after top pruning (on days without rain or fog). In each sampling field, 5 points were selected, 5 healthy plants were chosen at each point using the five-point sampling method, and then the samples from these 5 points were merged into one sample. Fifteen 5-point sampling methods were used at each time point, and a total of 15 samples were collected.

Tobacco phyllosphere sample processing

To preserve and restore the characteristics of fresh tobacco leaves to the greatest extent possible, a portion of the tobacco leaves collected from the field were quickly placed in 50 mL sterile centrifuge tubes, wrapped in tin foil, and flash-frozen in liquid nitrogen. The fully frozen tobacco leaf samples were then transferred to the laboratory and buried in dry ice for the extraction of phyllosphere microbial DNA. After removing the stems, another portion of the leaves was placed in self-sealing bags and transported to the laboratory using dry ice for the determination of surface secretions and leaf chemical indicators. Portions of the leaves were punched at symmetrical positions on both sides of the main vein at the widest part of the leaf using a hole puncher. Two to three circular pieces were taken from the same variety, mixed together, and fixed in Eppendorf (EP) tubes containing 2.5% glutaraldehyde for observation under a scanning electron microscope.

Morphology of glandular trichomes in the tobacco phyllosphere

The fresh tobacco leaf samples were fixed in EP tubes containing 2.5% glutaraldehyde for 4 h, followed by fixation in 1% osmic acid for 1 h. The circular pieces were then washed three times with 0.1 mol/L phosphate buffer solution, with each wash lasting 10 min. Then, a gradient dehydration process was conducted using a solvent mixture of tert-butanol and ethanol at concentrations of 30%, 50%, 70%, and 90%, with each

dehydration step lasting 5 min. After that, the samples were dehydrated twice in 100% tert-butanol, with each dehydration step lasting 5 min. Finally, the tert-butanol was placed in a refrigerator at 4°C until it solidified, and the samples were freeze-dried under vacuum. The dried samples were then glued onto sample holders using conductive adhesive and coated with gold using a HITACHI E-1010 ion sputter. The treated samples were observed and photographed for the morphology and density of glandular trichomes on the surface tobacco leaves at different varieties and for different time periods using a HITACHI SU3500 scanning electron microscope.

Determination of aroma precursors in the tobacco phyllosphere

(1) Polyphenols: First, 0.5 g of vacuum freeze-dried tobacco leaf powder, was accurately weighed, 25 mL of 80% acetone was added, and the sample was treated with 100 Hz ultrasound at room temperature for 30 min. After centrifugation, the supernatant was collected, the residue was extracted twice via the same method, and the three supernatants. were combined. The mixture at 45°C under reduced pressure, and the precipitate was diluted with methanol to 10 mL. Filter through a 0.45 μm organic membrane to obtain the tobacco polyphenol test solution. The Folin-phenol method was used with gallic acid as a standard to create a standard curve, and the absorbance was used as the ordinate for determination (Vázquez et al., 2015).

(2) Flavonoids: First, 0.5 g of vacuum freeze-dried tobacco leaf powder was accurately weighed, 30 mL of 30% ethanol was added, and the mixture was extracted in a constant-temperature water bath at 65°C for 2 h. The hot solution was filtered through qualitative filter paper, and the filtrate was transferred to a 50 mL volumetric flask. The filter paper and residue were rinsed with 30% ethanol, and the combined filtrate was diluted with 30% ethanol to the same volume as the test solution. The aluminum nitrate colorimetric method was used with rutin as a standard to create a standard curve, and absorbance was used as the ordinate for determination (Chang et al., 2012).

(3) Alkaloids: The visible spectrophotometry method in the ELISA kit (Shanghai Lianmai Biotechnology, Double antibody sandwich method) was used for determination. Briefly, the tissue was washed with precooled PBS (0.01 M, pH=7.4), weighed, cut into small pieces, and ground with the corresponding volume of PBS (1:9) on ice. Finally, the homogenate was centrifuged at 4 °C and 5000 rpm for 10 min, and the supernatant was collected for detection according to the instructions of the ELISA kit.

(4) Soluble total sugars: First, 20 mg of vacuum freeze-dried tobacco leaf was placed in a 10 mL centrifuge tube, 4 mL of 80% ethanol was added, and the mixture was heated in a water bath at 80°C for approximately 30 min and shaken a few times during the process. The mixture was centrifuged at 5000 rpm for 10 min, and the supernatant was collected. This step was repeated three times. Subsequently, the supernatant was combined and diluted to 10 mL to determine the total soluble sugars (Zhu et al., 2012).

(5) Starch: After transferring the supernatant from the precipitate for soluble sugar determination, 2 mL of distilled water was added, and the mixture was boiled in a water bath for 15 min. Then, 1 mL of 9.2 mol/L perchloric acid solution was added, the mixture was shaken for 15 min, 2 mL of distilled water was added, and the mixture was mixed well. The mixture was centrifuged at 5000 rpm for 10 min, and the supernatant was collected. This step was repeated three times. Subsequently, the supernatant was combined and diluted to 10 mL to determine the total soluble sugars (Lustinec et al., 1983).

(6) Amino acids: First, 1 g of vacuum freeze-dried tobacco leaf powder sample was accurately weighed in a 100 mL grinding mouth triangular flask. Then, 50 mL of hydrochloric acid solution was added, and the mixture was sealed with a stopper, ultrasonicated, and filtered. Two milliliters of the filtrate was accurately removed, concentrated, and evaporated (the temperature did not exceed 60°C). One milliliter of sample diluent was added, and the mixture was shaken well. The solution was filtered through a 0.45 μm filter membrane, and the sample was measured by RP-HPLC (Lei et al., 2006).

(7) The extraction and determination of leaf surface secretions (α-cembratrienedio and β-cembrenediol) from tobacco leaves were carried out according to the methods of Marija et al (Banožić et al., 2021). Twenty circular leaf pieces with a diameter of 10 cm were cut on both sides of the main vein of the tobacco leaves. The leaf circular pieces were extracted in 500 mL of dichloromethane, each for 2 seconds, for a total of 8 times. After filtration, 1 mL of internal standard containing N-17-alkanols was added. The extract was concentrated to 50 mL using a rotary evaporator, and after derivatization, it was analyzed by GC/MS in combination with a computer. The composition of various substances in the leaf surface secretions was determined by retrieving the NIST12 spectral library. The retention time of each peak was obtained based on the peak elution time on the chromatographic flow curve of different substances, and the substances were quantified using the internal standard method.

Phyllosphere microbiota (bacterial and fungal communities) of the tobacco plants

Extraction of genomic DNA from the tobacco phyllosphere microbiota

Microbial cells were collected from the leaves following the extraction method proposed by Kembel (Kembelsteven and Muellerrebecca, 2013). Briefly, 10 g of tobacco leaf tip sample was weighed and placed in a sterile triangular flask to collect microorganisms on the surface of tobacco leaves. Total DNA was extracted from the filter membrane using a Fast DNA Spin Kit (Qbiogene, Irvine, CA). The instructions of the kit were followed to dissolve the extracted DNA in 100 μL of ddH2O and store it at -20°C.

16S rRNA and ITS PCR amplification of the tobacco phyllosphere microbiota

The bacterial 16S rRNA gene V4-V5 region and the fungal ITS1 region were sequenced for 45 samples using the Illumina MiSeq sequencing platform. A total of 90 sequences were obtained for bacteria and fungi. The bacterial primers used for amplification were 515F: (5'-AACMGGATTAGATACCCKG-3') and 907R: (5'-

ACGTCATCCCCACCTTCC-3'). The fungal primers used were ITS5F: GGAAGTAAAAGTCGTAACAAGG and ITS1R: GCTGCGTTCTTCATCGATGC. The amplification program was as follows: predenaturation at 98 °C for 5 min, followed by 25 cycles (denaturation at 98 °C for 30 s, annealing at 53 °C for 30 s, and extension at 72 °C for 45 s), extension at 72 °C for 10 min, and storage at 4 °C. The PCR mixture was 5× Trans Start Fast Pfu Buffer (5 μL), 2.5 mmol/L dNTPs (2 μL), forward primer (10 μMol/L) (1 μL), reverse primer (10 μMol/L) (1 μL), fast PFU DNA polymerase (5 U/μL) (0.25 μL), template DNA (1 μL), and ddH2O (14.75 μL). The quality of the library was evaluated on a Qubit@2.0 fluorometer (Thermo Scientific) and an Agilent Bioanalyzer 2100 system. The PCR products were detected by 2% agarose gel electrophoresis, and the PCR amplification recovery products were quantified using fluorescence. According to the fluorescence quantification results and the sequencing volume requirements of each sample, the purified products of each sample were mixed in the corresponding proportions for purification before loading and analysis by a sequencer (Redford et al., 2010). The sequencing procedure for this study was completed by Shanghai Paisenno Biotechnology Co., Ltd.

Bioinformatics analysis

After using the Illumina MiSeq sequencing platform for paired-end sequencing, the obtained raw reads were subjected to quality control, and low-quality sequences (average quality of 50 consecutive bases <25, sequence length <50 bp, and 1 or more ambiguous bases) were discarded. The DADA2 (divisive amplicon denoising algorithm 2) method (DADA2: high-resolution sample inference from Illumina amplicon data) was used to perform primer trimming, quality filtering, denoising, merging, and chimera removal on the paired-end data to obtain clean reads.

First, QIIME2 software (Bolyen et al., 2019) (Quantitative Insights Into Microbial Ecology, v1.8.0) was used to identify ambiguous sequences. Then, the DADA2 method in the QIIME2 software was used to quality control, denoising, stitching, and de chimeric sequences. Sequences derived from chloroplast and mitochondria sources were also excluded to obtain high-quality sequences for analysis in this study. The UCLUST sequence alignment tool in QIIME2 software was used to cluster and assign ASVs based on 100% sequence similarity. The representative sequence of each ASV was compared with the template sequence in the corresponding database to determine its taxonomic status and obtain taxonomic information. The Greengenes and Silva databases were used for bacterial analysis, while the UNITE and Silva databases were used for fungal analysis. The QIIME2 software was used to calculate alpha diversity indices. Canoco software was used to perform principal coordinate analysis (PCoA) to investigate the impact of environmental factors on community structure. The random forest algorithm in QIIME2 software, along with nested cross-validation, was used to identify indicator species of phyllosphere microbial communities. The GeneCloud platform was used to analyze the correlations between phyllosphere microbial community structure, phyllosphere physicochemical properties, and major aroma precursors using the Spearman algorithm. Microsoft Excel 2016 and SPSS 26.0 software were used to perform ANOVA and Duncan's *post hoc* analysis to assess the significance of differences among phyllosphere microbial diversity indices, major aroma precursors in tobacco leaves, leaf surface exudates, and phyllosphere physicochemical properties. A histogram was used to determine whether the data follows a normal distribution. If the data follows a normal distribution, perform a parametric test (one-way ANOVA analysis), with data represented as mean ± standard deviation (SD). If the data does not follow a normal distribution, use a non-parametric test (Friedman test analysis), with data presented as median [25% quantile (Q1), 75% quantile (Q3)]. Differences with $P < 0.05$ were considered to indicate statistical significance.

Correlation analysis

Correlation analysis between the indicator bacteria and fungi and the morphology of tobacco phyllosphere trichomes and aroma precursors was conducted using GeneCloud tools, which are free online platforms for data analysis (https://www.genescloud.cn).

Functional potential prediction

The Phylogenetic Investigation of Communities by Reconstruction of Unobserved States (PICRUSt2) (Douglas et al., 2020), available at https://github.com/picrust/picrust2/wiki, was used to predict the functional abundance of bacterial or fungal samples (Gavin M. Douglas, et al., print). In short, based on the full-length sequence of the 16S rRNA gene in the tested microbial genome, infer the gene functional profile of their common ancestor. Infer gene function profiles of other untested species in the Greengenes database and construct gene function prediction profiles for the entire lineage of archaea and bacteria domains. Finally, the composition of the microbial community obtained from sequencing is mapped to the database to predict the metabolic function of the microbial community.

Statistical analysis

All the data were analyzed with GraphPad Prism 8.0 (GraphPad Software, San Diego, Canada). A histogram and Shapiro-Wilk analysis were used to determine whether the data follows a normal distribution. If the data follows a normal distribution, perform a parametric test (one-way ANOVA analysis), with data represented as mean ± standard deviation (SD). If the data does not follow a normal distribution, use a non-parametric test (Friedman test analysis), with data presented as median [25% quantile (Q1), 75% quantile (Q3)]. * indicates a significant difference, $P < 0.05$; ** indicates a very significant difference, $P < 0.01$; *** indicates an

extremely significant difference, $P < 0.001$; NS indicates that there is no significant difference between the data, $P > 0.05$.

Results

Morphology of tobacco phyllosphere glandular trichomes during the ripening process

Since tobacco glandular trichomes occur on more primitive epidermal cells, the overall density of glandular trichomes on tobacco leaves is greater. As the leaves develop and the leaf area expands, the density of glandular trichomes on the tobacco leaf surface decreases ($P < 0.05$) (Figures 1A–C, F). Specifically, the density of long-stalked glandular trichomes on the upper epidermis of tobacco leaves increased and then decreased with increasing top pruning time, while the density of long-stalked glandular trichomes on the lower epidermis gradually decreased with increasing top pruning time ($P < 0.05$) (Figures 1D, G). The density of short-stalked glandular trichomes on the upper epidermis of tobacco leaves gradually decreased with later top pruning times, while the density of short-stalked glandular trichomes on the lower epidermis increased and then decreased with later top pruning times ($P < 0.05$) (Figures 1E, H).

Aroma precursors in the tobacco phyllosphere during the ripening process

The contents of polyphenols, flavonoids, α-cembratrienedio, alkaloids, and soluble sugars in tobacco leaf exudates peaked 60 d after top pruning and were significantly greater than those 20 and 40 d after top pruning ($P < 0.01$ or $P < 0.001$) (Figures 2A–E). The contents of amino acids and β-cembrenediol in tobacco leaf exudates significantly decreased with increasing pruning time ($P < 0.05$, $P < 0.01$ or $P < 0.001$) (Figures 2G, H). The starch content in tobacco leaf exudates gradually decreased with increasing top pruning time and reached its lowest level 60 d after top pruning ($P < 0.001$) (Figure 2F).

Alpha diversity of bacterial and fungal communities in the phyllosphere area during the ripening process of tobacco

The alpha diversity of the bacterial community in the tobacco phyllosphere gradually increased according to Simpson's index, Shannon's index, and Pielou's evenness index with the number of top pruned tobacco leaves ($P < 0.05$, $P < 0.01$ or $P < 0.001$, respectively) (Figures 3B–D). The Chao1 index and Observed_species index first decreased and then increased with

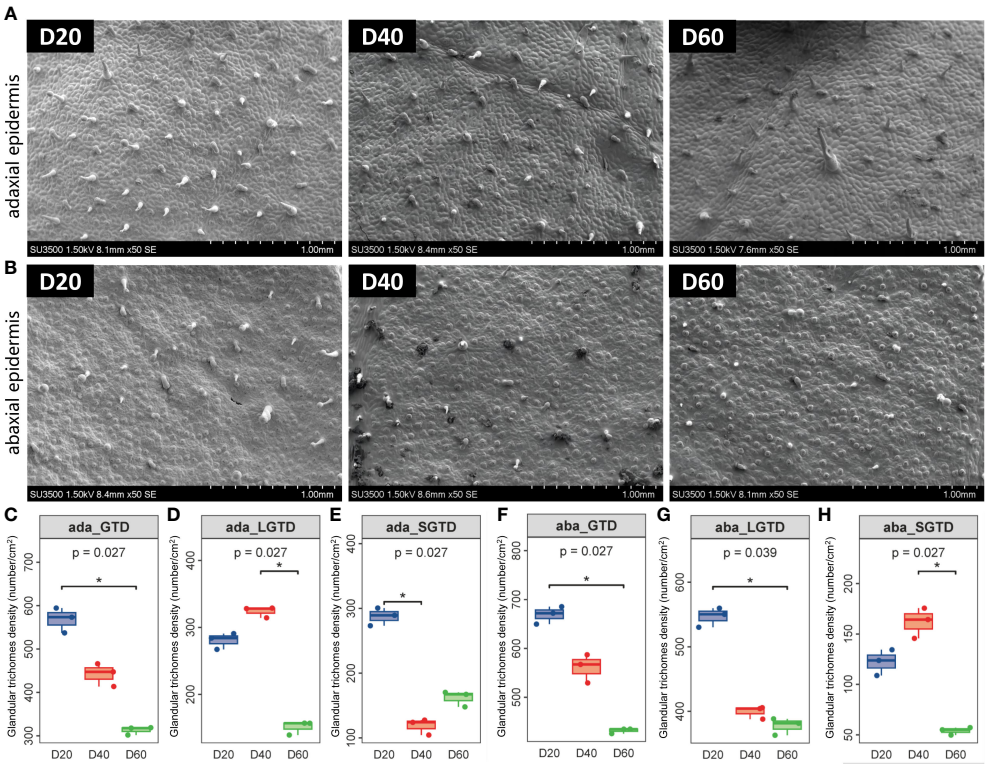

FIGURE 1
Morphology of tobacco phyllosphere glandular trichomes. **(A)** Morphological structure of glandular trichomes on the upper epidermis of the tobacco phyllosphere. **(B)** Morphological structure of glandular trichomes on the upper epidermis of the tobacco phyllosphere. **(C–E)** Statistical analysis of the morphology and structure of glandular trichomes on the upper epidermis of tobacco phyllosphere. **(F–H)** Statistical analysis of the morphology and structure of glandular trichomes on the under epidermis of tobacco phyllosphere. * represents $P<0.05$, indicating a significant difference.

10.3389/fpls.2024.1346154

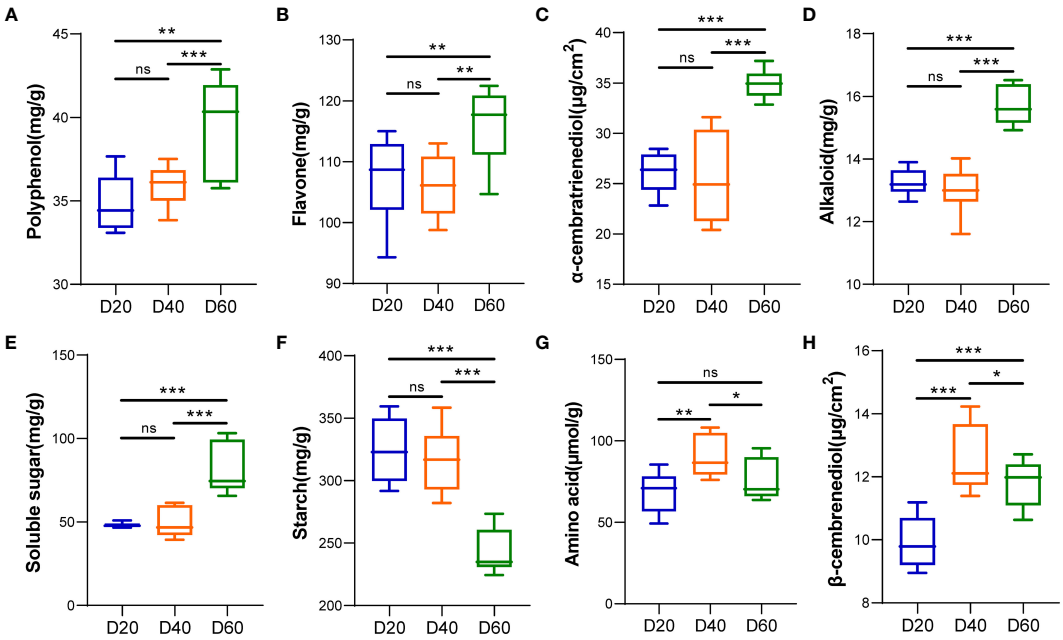

FIGURE 2
Analysis of tobacco phyllosphere surface secretions (aroma precursor substances). **(A)** Polyphenols. **(B)** Flavonoids. **(C)** α-cembratrienedio. **(D)** Alkaloids. **(E)** Soluble sugars. **(F)** Starch. **(G)** Amino acids. **(H)** β-cembrenediol. * represents $P < 0.05$, indicating a significant difference. ** represents $P < 0.01$, indicating an very significant difference. *** represents $P < 0.001$, indicating an extremely significant difference. ns represents $P > 0.05$, indicating a no significant difference.

increasing top pruning time ($P < 0.05$, $P < 0.01$ or $P < 0.001$) (Figures 3A, F), while Good's coverage index tended to first increase and then decrease with increasing top pruning time on tobacco leaves ($P < 0.01$ or $P < 0.001$) (Figure 3E). The alpha diversity of the fungal community in the tobacco phyllosphere did not significantly differ between 20 and 40 d after top pruning ($P > 0.05$), while the Chao1 and Observed_species indices of the fungal communities were significantly greater at 60 d after top pruning than at 20 and 40 d after top pruning ($P < 0.001$) (Figures 3G, L). The Simpson's index, Shannon's index, Pielou's evenness index, and Good's coverage index of the fungal community were also significantly greater at 60 d after top pruning than at 20 and 40 d after top pruning ($P < 0.01$ or $P < 0.001$) (Figures 3H–K).

Beta diversity of bacterial and fungal communities in the phyllosphere area during the ripening process of tobacco

The PCoA results of the bacterial community in the tobacco phyllosphere showed that there were significant differences within the community at 20 and 40 d after top pruning, while the differences within the community were relatively small at 60 d after top pruning. Moreover, as the time after top pruning increased, the differences between the groups also increased (Figures 4A–C). The PCoA results of the fungal community in the tobacco phyllosphere showed that there were significant differences within the community at 20 and 40 d after top pruning, while the differences within the community were relatively small at 60 d after top pruning. At the same time, the differences between the groups were relatively small at 20 and 40 d after top pruning, but they increased compared to those at 60 d after top pruning (Figures 4D–F).

Composition of bacterial and fungal communities in the phyllosphere area during the ripening process of tobacco

The results of the composition of phyllosphere bacterial communities in tobacco leaves showed that at the phylum level, the relative abundance of *Bacillota* increased 40 d after top pruning, while the relative abundance of *Proteobacteria* decreased at 20 and 60 d after top pruning. However, the relative abundances of *Bacillota* and *Proteobacteria* returned to 20 d after top pruning 60 d later (Figure 5A). At the genus level, the relative abundance of *Pseudomonas* gradually decreased with increasing top pruning time, while the relative abundances of *Acidisoma*, *Ralstonia*, and *Bradyrhizobium* did not change at 20 and 40 days after top pruning but did increase at 60 days after top pruning (Figure 5B). Moreover, the results of random forest analysis further revealed that *Bradyrhizobium*, *Streptacidiphilus*, *Acidisoma*, *Polaromonas* and *Ralstonia* were the genera associated with differences among the three groups (Figure 5C). Furthermore, Venn analysis of the 15 most important genera and the 15 most abundant genera revealed that *Mitochondria*, *Acidisoma*, *Ralstonia*, *Bradyrhizobium*, *Cutibacterium*, *Caulobacter*, and *Corynebacterium_1* were common genera (Figure 5D). Moreover, the relative abundances

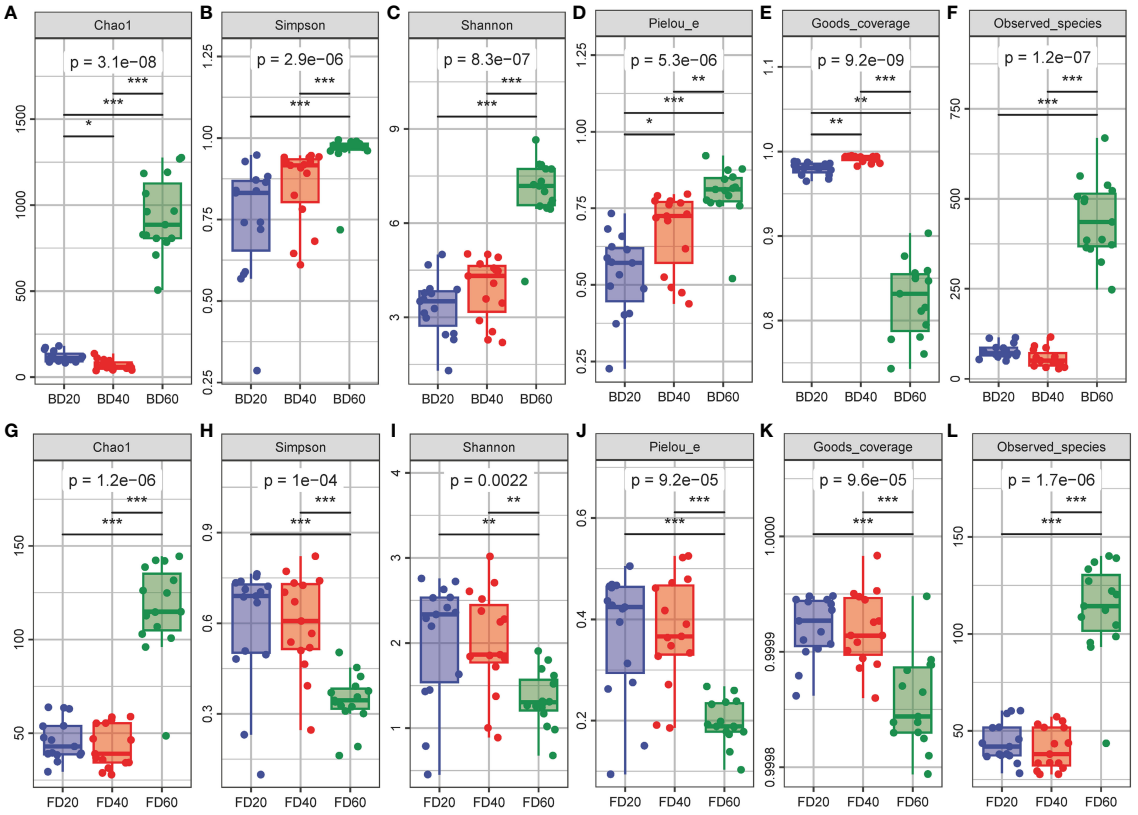

FIGURE 3
Alpha diversity of microbial community in tobacco phyllosphere. **(A–F)** Alpha diversity of bacterial community in tobacco phyllosphere. **(G–L)** Alpha diversity of fungal community in tobacco phyllosphere. * represents $P < 0.05$, indicating a significant difference. ** represents $P < 0.01$, indicating an very significant difference. *** represents $P < 0.001$, indicating an extremely significant difference.

of *Acidisoma*, *Ralstonia* and *Bradyrhizobium* in the intercellular space of tobacco leaves were significantly greater at 60 d after top pruning than at 20 d and 40 d after top pruning ($P < 0.01$ or $P < 0.001$). On the other hand, the relative abundance of *Pseudomonas* was significantly lower at 60 d after top pruning than at 20 d and 40 d after top pruning ($P < 0.001$) (Figure 5E).

The analysis of the composition of the intercellular fungal communities in tobacco leaves revealed that at the phylum level, there was no significant change in the fungal composition at 20 and 40 d after top pruning, while the relative abundance of Ascomycota was greater than that at 20 and 40 d after top pruning at 60 d after top pruning, and the relative abundance of Basidiomycota was less than that at 20 and 40 d after top pruning. At 60 d after top pruning, the relative abundance of *Bacillota* and Proteobacteria returned to the level observed at 20 d after top pruning (Figure 5F). At the genus level, there was no significant change in the fungal composition at 20 and 40 d after top pruning, while the relative abundance of *Alternaria* was greater than that at 20 and 40 d after top pruning at 60 d after top pruning, and the relative abundances of *Filobasidium*, *Nigrospora*, and *Tausonia* were less than those at 20 and 40 d after top pruning (Figure 5G). Moreover, the results of random forest analysis further revealed that *Tausonia*, *Neosetophoma*, *Talaromyces*, *Periconia*, and *Exserohilum* were marker genera of differences among the three groups (Figure 5H). Furthermore, Venn analysis of the 15 most important genera and the 15 most abundant genera revealed that *Alternaria*, *Mycosphaerella*, *Filobasidium*, *Didymella*, *Talaromyces*, *Septoria*, *Selenophoma*, and *Periconia* were common genera (Figure 5I). Moreover, the relative abundances of *Alternaria* and *Talaromyces* in the intercellular space of tobacco leaves were significantly greater than those at 20 and 40 d after top pruning at 60 d after top pruning ($P < 0.01$ or $P < 0.001$), while the relative abundances of *Filobasidium* and *Tausonia* were significantly lower than those at 20 and 40 d after top pruning ($P < 0.001$) (Figure 5J).

Correlation analysis

The association analysis results showed that the bacterial communities *Acidisoma*, *Ralstonia* and *Bradyrhizobium* were significantly positively correlated with tobacco aroma precursors (polyphenols, flavonoids, alkaloids, soluble sugars, and α-cembratrienedio), with significant negative correlations with tobacco leaf glandular trichome morphology (ada_GTD, aba_GTD, ada_LGTD, aba_SGTD, and aba_LGTD) ($P < 0.05$ or $P < 0.01$ or $P < 0.001$), while *Pseudomonas* showed the opposite pattern. In the fungal communities, Filobasidium and Tausonia were significantly negatively correlated with tobacco aroma precursors (polyphenols, flavonoids, alkaloids, soluble sugars, and α-cembratrienedio) and significantly positively correlated with

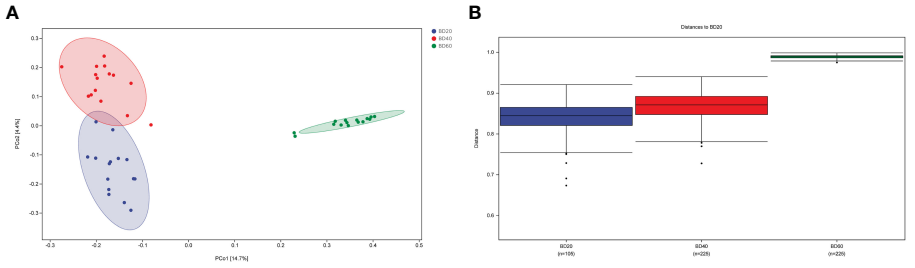

Group1	Group2	Sample size	Permutations	Pseudo F	*P* value	Q value
all	-	45	999	4.698507	0.001	-
BD20	BD40	30	999	2.120883	0.001	0.001
BD20	BD60	30	999	5.766278	0.001	0.001
BD40	BD60	30	999	6.07813	0.001	0.001

Group1	Group2	Sample size	Permutations	Pseudo F	*P* value	Q value
all	-	45	999	4.138689	0.001	-
FD20	FD40	30	999	1.491571	0.018	0.018
FD20	FD60	30	999	5.559166	0.001	0.0015
FD40	FD60	30	999	5.392738	0.001	0.0015

FIGURE 4
Beta diversity of microbial community in tobacco phyllosphere. **(A)** PCoA analysis of bacterial communities. **(B)** Analysis of differences between groups of bacterial communities (Figure). **(C)** Analysis of differences between groups of bacterial communities (Table). **(D)** PCoA analysis of fungal communities. **(E)** Analysis of differences between groups of fungal communities (Figure). **(F)** Analysis of differences between groups of fungal communities (Table).

tobacco leaf glandular trichome morphology (ada_GTD, aba_GTD, ada_LGTD, aba_SGTD, and aba_LGTD) ($P < 0.05$ or $P < 0.01$ or $P < 0.001$), while Alternaria showed the opposite pattern (Figure 6). Correlation analysis between other nonsignificantly different microorganisms and tobacco glandular trichomes and aroma precursors revealed that *Caulobacter* was negatively correlated with tobacco glandular trichome density but positively correlated with aroma precursors (Supplementary Figure S1). *Nigrospora* was positively correlated with the density of tobacco glandular trichomes and negatively correlated with aroma precursors. In addition, the correlation analysis between bacteria and fungi revealed a negative overall correlation trend (Supplementary Figure S2).

Functional potential prediction results

The PICRUSt2 analysis results showed that bacteria mainly participated in amino acid biosynthesis, cofactor, repair group, electron carrier, and vitamin biosynthesis, as well as metabolic pathways such as fatty acid and lipid biosynthesis (Figure 7A). Fungi mainly participated in metabolic pathways such as nucleoside and nucleotide biosynthesis, electron transfer, and respiration, as well as some amino acid biosynthesis cofactors, repair groups, electron carriers, vitamin biosynthesis, and fatty acid and lipid biosynthesis (Figure 7B).

Discussion

During the ripening process of tobacco, colloidal secretions, which are precursors of many aroma substances and are closely related to the production of aroma substances in tobacco leaves, are produced on the surface of leaves (Yue et al., 2002). The tobacco phyllosphere microbiota coexists in the same growth environment as tobacco leaf surface glandular trichomes and tobacco leaf surface aroma precursors. However, there is currently little research on the characteristics of the tobacco phyllosphere microbiota community during the maturation process, and the phyllosphere factor indicators that affect changes in the tobacco phyllosphere microbiota community are not yet known.

Tobacco leaf glandular trichomes are specialized structures of leaf epidermal cells that can specifically synthesize and secrete various bioactive substances such as diterpenoids, sucrose esters, and aroma precursors, which have a positive impact on tobacco leaf quality (Keene and Wagner, 1985; Tooker et al., 2010; Huchelmann et al., 2017). Twenty days after top pruning, the cytoplasm of tobacco leaves is rich, with more contents, and the stem cells are

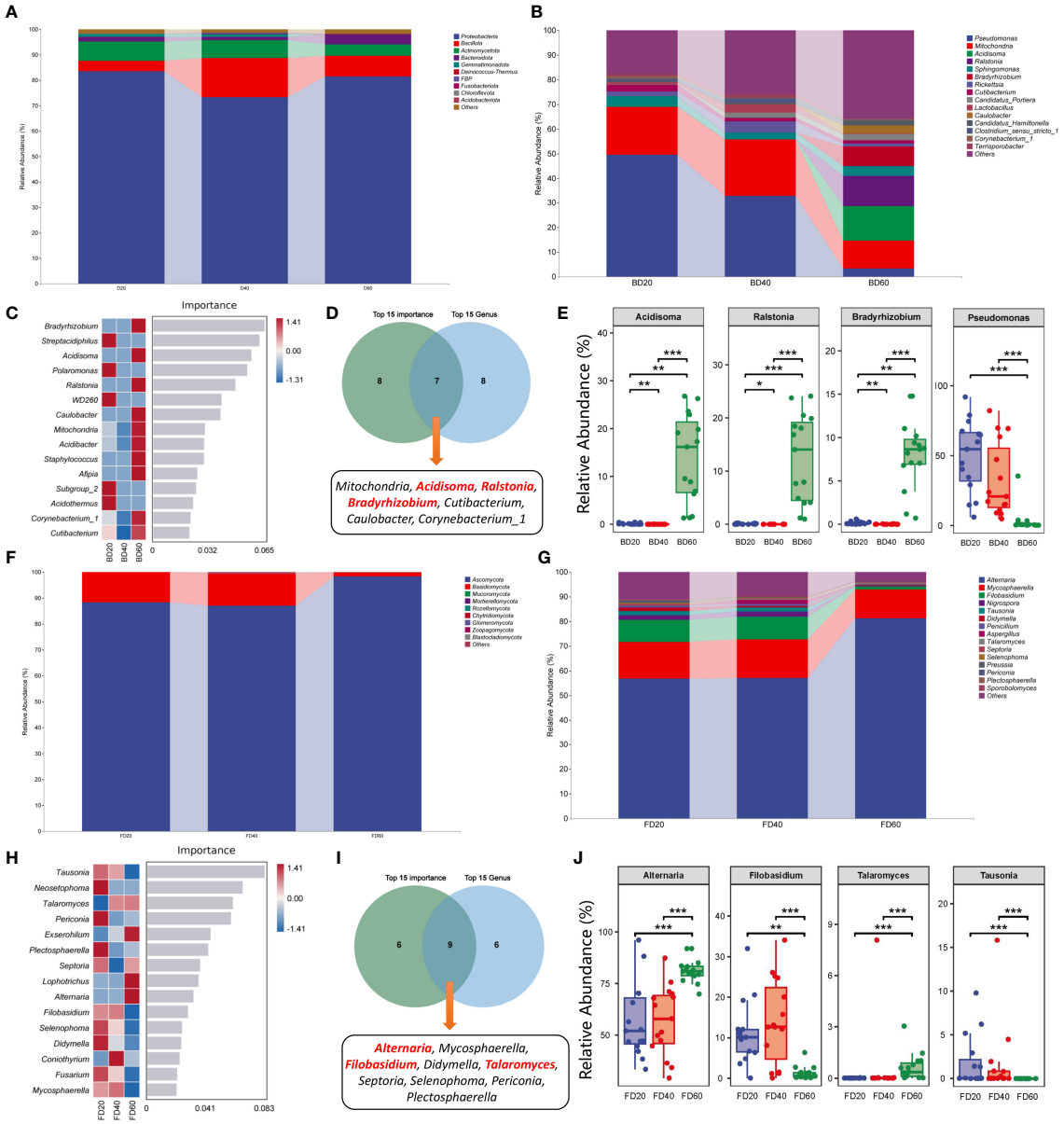

FIGURE 5
Species composition of microbial community in tobacco phyllosphere. **(A)** Species composition of bacterial communities at the phylum level. **(B)** Species composition of bacterial communities at the genus level. **(C)** Top 15 important genera of bacterial communities. **(D)** Interaction analysis of the top 15 bacteria in relative abundance and the top 15 bacteria in importance. **(E)** Differences in core bacteria during the maturation process of tobacco. **(F)** Species composition of fungal communities at the phylum level. **(G)** Species composition of fungal communities at the genus level. **(H)** Top 15 important genera of fungal communities. **(I)** Interaction analysis of the top 15 fungi in relative abundance and the top 15 fungi in importance. **(J)** Differences in core fungi during the maturation process of tobacco. * represents $P < 0.05$, indicating a significant difference. ** represents $P < 0.01$, indicating an very significant difference. *** represents $P < 0.001$, indicating an extremely significant difference.

full and plump, with robust glandular trichomes, indicating a strong secretion function of glandular trichomes at this time. Forty days after top pruning, the long-stalked glandular trichomes on the tobacco leaves exhibited significant shedding, and some of the cells became dry and shriveled, with the stem cells exhibiting a concave shape. At this time, the secretion function of glandular trichomes is weakened. At 60 d after top pruning, long-stalked glandular trichomes had shed significantly, while short-stalked glandular trichomes were more prominent and had a more complete morphology. The overall number of glandular trichomes in tobacco leaves showed a decreasing trend in the three stages after top pruning. Long-stalked glandular trichomes first appear in the juvenile stage, and at the mature stage, the glandular head breaks and releases secretions. In terms of quantity, long-stalked glandular trichomes are the main type of glandular trichome, which is consistent with the results of this study. Court suggested that varieties with high glandular trichome density also have greater glandular trichome secretion content (Shishehian et al., 2023). However, Nielsen et al. suggested that the extent of glandular trichome secretion may depend more strongly on the secretion

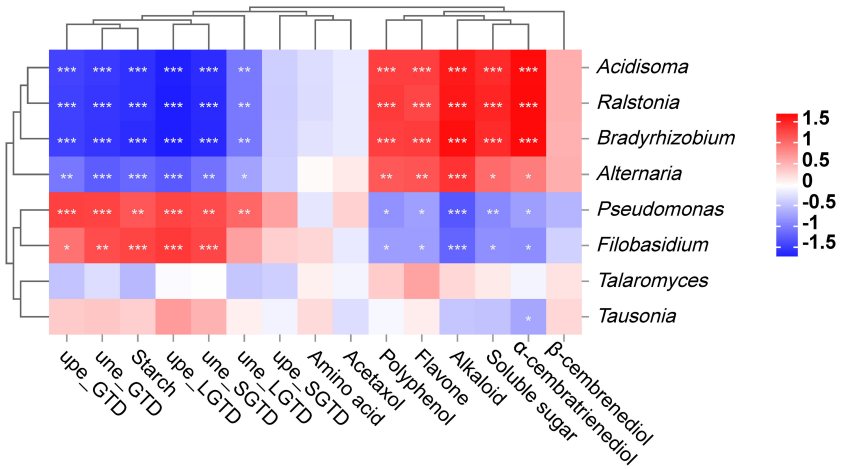

FIGURE 6
Correlation analysis between the core microbiota of tobacco phyllosphere and the morphology and secretion (aroma precursors) of tobacco phyllosphere. * represents $P < 0.05$, indicating a significant difference. ** represents $P < 0.01$, indicating an very significant difference. *** represents $P < 0.001$, indicating an extremely significant difference.

ability of glandular trichomes and is not closely related to glandular trichome density (Nielsen and Severson, 1990). The secretion content of glandular trichomes may be influenced by multiple factors, and glandular trichome density is likely the main factor affecting the secretion content of leaf glandular trichomes. Research has shown that the density of long-stalked glandular trichomes in tobacco first increases and then decreases with increasing growth period. This may be due to differences in fertility conditions during the planting process. The mechanism by which insufficient fertility affects the development of tobacco glandular trichomes in the later stage of tobacco growth needs further research (Lin et al., 2014; Yajie et al., 2015). In addition, β-cembrenediol is not only the main product of tobacco glandular trichomes but also a precursor to the aroma of tobacco. The higher its content is, the richer the aroma of tobacco leaves (Han et al., 2013). This study showed that under the climatic conditions of the experimental area, the content of cyclodextrin in tobacco tended to first increase and then decrease with time, which is consistent with the results of Lu et al. (Leng and Lu, 2014). Moreover, the change in the content of β-cembrenediol in flue-cured tobacco is consistent with the change in the density of long-stalked glandular trichomes, and the surface cypermethritol may be closely related to the long-stalked glandular trichomes of flue-cured tobacco.

The physical and chemical properties of tobacco leaves are different, and the type and environment of the phyllosphere microbiota can lead to differences in the density of glandular trichomes on tobacco leaves. Therefore, this study further analyzed the relationships among the phyllosphere microbiota, phyllosphere physical and chemical properties, and glandular trichome traits in tobacco leaves. The results of the microbial diversity analysis showed that there was a diversity of microorganisms in the phyllosphere area during the ripening process of tobacco. Overall, the diversity of bacteria in the phyllosphere area was greater than that of fungi, which is consistent with the findings of previous study (Pugh et al., 1978). Gao et al. indicated that in the early stages of nutrient growth, bacterial α and β diversity often decreases, and these findings may explain to some extent why the initial phyllosphere microbiota had difficulty capturing new host plants during colonization, which subsequently modified them. As tobacco leaves grow, the increase in diversity and species richness may play a role in the high functional redundancy within the microbiome, enabling it to cope with complex environmental changes and quickly recover from stress (Gao et al., 2023). The opposite trend was observed for the Pielou, Shannon, and Simpson indices for the fungal and bacterial communities over time. The reason for trend may be that, as tobacco grows and develops, more nutrients are utilized by bacteria. Moreover, bacteria may have a greater ability to compete with fungi for nutrients. The association analysis between bacteria and fungi also supports this point. In addition, with increasing top pruning time, the relative abundances of *Acidisoma*, *Ralstonia*, and *Bradyrhizobium* in the bacterial community gradually increased, while the relative abundance of *Pseudomonas* gradually decreased. Similarly, the relative abundances of *Alternaria* and *Talaromyces* in the fungal community gradually increased, while the relative abundances of *Filobassidium* and *Tausonia* gradually decreased. Studies have shown that the abundance of *Pseudomonas* in susceptible tobacco leaves increases abnormally, which in turn affects the diversity of the microbial community in tobacco leaves. In this study, as the top pruning time progressed, the tobacco gradually matured, and its ability to resist pathogens gradually increased, which may be the reason for the decrease in *Pseudomonas* colonization.

Furthermore, by analyzing the correlations between phyllosphere boundary bacteria and fungi during the ripening process of tobacco and phyllosphere physiological indicators, it was found that there was a strong correlation between bacteria or fungi such as *Acidisoma*, *Ralstonia*, *Bradyrhizobium*, *Alternaria*, *Pseudomonas*, *Talaromyces*, *Filobassidium*, and *Tausonia* and the physicochemical properties of tobacco leaves. Plant phyllosphere fungi are closely related to plants, and their community structure

FIGURE 7
Functional prediction of microbial communities. **(A)** Functional prediction of MetaCyc metabolic pathway in bacterial community. **(B)** Functional prediction of MetaCyc metabolic pathways in fungal communities.

and diversity are the result of interactions among plants, microorganisms, and other environmental factors (Chao-Jiang and Shi-Qing, 2017). The functional prediction results of PICRUST2 showed that microorganisms are mainly involved in the biosynthesis of amino acids, vitamins, and fatty acids. English et al. reported that tobacco leaves inoculated with a mixture of Bacillus subtilis and Bacillus ring-shaped bacteria can quickly produce a pleasant aroma. Further analysis revealed that with the growth of microorganisms, the total sugar and reducing sugar contents in tobacco leaves decrease (English et al., 1967). Microbial degradation of macromolecular substances in tobacco, such as starch, protein, pectin, etc., can reduce the production of harmful substances, such as nicotine and tar, which is beneficial for improving the quality of tobacco by producing small molecular substances, increasing the content of aroma components in tobacco, and improving the quality of tobacco (Chen et al., 2008). These findings indicate that microorganisms are the main factor driving the aroma precursors of tobacco. Hunter et al. reported that differences in the phyllosphere bacterial community in lettuce are closely related to phyllosphere morphological parameters, soluble carbohydrates, water content, and phyllosphere exposure, while the sugar and organic acid contents in tomato fruits are greater than those in stems and leaves. *Bacteroides thetaiotaomicron* is mainly present in the flesh, while *Rosenbergiella nectaria* is abundant in the peel (Hunter et al., 2010). These bacteria can promote the degradation of carbohydrates during tomato fruit development and maturation (Zhao et al., 2016). The differences in physiological indices among different plant parts and in the nutritional preferences of phyllosphere microorganisms may be one of the reasons for the differences in correlations between phyllosphere microorganisms and physiological indicators. Yadav et al. evaluated the impact of different phyllosphere characteristics on the size of phyllosphere bacterial communities in 8 perennial trees (Yadav et al., 2005). The results showed that the size of

phyllosphere bacterial populations was positively correlated with the density of secretory and non-secretory glandular trichomes, and negatively correlated with leaf thickness, mesophyll thickness, and phyllosphere dorsal epidermis thickness. The surface exudates of fresh tobacco leaves are positively correlated with the density of secretory and non-secretory glandular trichomes (Yadav et al., 2005), and there is a certain correlation between the phyllosphere microbiota and tobacco surface exudates.

Conclusion

In this study, as tobacco matured, the bacterial richness in the phyllosphere of tobacco gradually increased, and the fungal richness gradually decreased, with a main, negative correlation between the two parameters. Both bacteria and fungi are involved in the biosynthesis of amino acids, vitamins, and lipids, which may be important factors driving the precursor substances of tobacco aroma. The presence of *Acidisoma*, *Ralstonia*, *Bradyrhizobium* and *Alternaria* in the phyllosphere microbiota of tobacco may be related to the aroma precursors of tobacco. The abundances of *Pseudomonas* and *Filobassidium* may be correlated with the density of tobacco glandular trichomes. These microorganisms may have important potential in improving the quality of tobacco.

Data availability statement

The datasets presented in this study can be found in online repositories. The names of the repository/repositories and accession number(s) can be found below: https://www.ncbi.nlm.nih.gov/genbank/, PRJNA1036814, https://www.ncbi.nlm.nih.gov/genbank/, PRJNA1036808.

Author contributions

YS: Writing – original draft. YH: Writing – original draft. YZ: Methodology, Writing – review & editing. XXL: Visualization, Writing – review & editing. SW: Writing – review & editing. T'EX: Writing – review & editing. TW: Data curation, Writing – review & editing. HD: Data curation, Writing – review & editing. XLL: Writing – review & editing. QC: Writing – review & editing. FN: Funding acquisition, Resources, Supervision, Writing – review & editing.

Funding

The author(s) declare financial support was received for the research, authorship, and/or publication of this article. This research was funded by the science and technology projects of Yunnan Branch of China Tobacco Corporation (2022530900242002). The funders had no role in the study design, data collection and interpretation or the decision to submit the work for publication.

Conflict of interest

Author YH, YZ, SW, T'EX, TW, and HD were employed by the company Technology and Research Center, Lincang Branch Company of Yunnan Tobacco Company.

The remaining authors declare that the research was conducted in the absence of any commercial or financial relationships that could be construed as a potential conflict of interest.

Publisher's note

Supplementary material

The Supplementary Material for this article can be found online at: https://www.frontiersin.org/articles/10.3389/fpls.2024.1346154/full#supplementary-material

References

Banožić, M., Aladić, K., Jerković, I., and Jokić, S. (2021). Volatile organic compounds of tobacco leaves versus waste (scrap, dust, and midrib): extraction and optimization. *J. Sci. Food Agric.* 101, 1822–1832. doi: 10.1002/jsfa.10796

Banožić, M., Jokić, S., Ačkar, Đ., Blažić, M., and Šubarić, D. (2020). Carbohydrates-key players in tobacco aroma formation and quality determination. *Molecules* 25, 1734. doi: 10.3390/molecules25071734

Bashir, I., War, A., Rafiq, I., Reshi, Z., Rashid, I., and Shouche, Y. (2022). Phyllosphere microbiome: Diversity and functions. *Microbiol. Res.* 254, 126888. doi: 10.1016/j.micres.2021.126888

Berg, G., Rybakova, D., Grube, M., and Köberl, M. (2016). The plant microbiome explored: implications for experimental botany. *J. Exp. Bot.* 67, 995–1002. doi: 10.1093/jxb/erv466

Berg, M., and Koskella, B. (2018). Nutrient- and dose-dependent microbiome-mediated protection against a plant pathogen. *Curr. Biol.* 28, 2487–2492.e2483. doi: 10.1016/j.cub.2018.05.085

Bolyen, E., Rideout, J. R., Dillon, M. R., Bokulich, N. A., Abnet, C. C., Al-Ghalith, G. A., et al. (2019). Reproducible, interactive, scalable and extensible microbiome data science using QIIME 2. *Nat. Biotechnol.* 37, 852–857. doi: 10.1038/s41587-019-0209-9

Cappelletti, M., Perazzolli, M., Antonielli, L., Nesler, A., Torboli, E., Bianchedi, P. L., et al. (2016). Leaf treatments with a protein-based resistance inducer partially modify phyllosphere microbial communities of grapevine. *Front. Plant Sci.* 7, 1053. doi: 10.3389/fpls.2016.01053

Chang, K. M., Choi, S. I., and Kim, G. H. (2012). Anti-oxidant activity of saussurea lappa C.B. Clarke roots. *Prev. Nutr. Food Sci.* 17, 306–309. doi: 10.3746/pnf.2012.17.4.306

Chang, S. Y., and Grunwald, C. (1976). Duvatrienediols in cuticular wax of Burley tobacco leaves. *J. Lipid Res.* 17, 7–11. doi: 10.1016/S0022-2275(20)37008-5

Chao-Jiang, W., and Shi-Qing, W. (2017). Analysis of bacterial diversity and community structure from three taisui based on high-throughput sequencing. *Hubei Agric. Sci.* 56, 2543–2547. doi: 10.14088/j.cnki.issn0439-8114.2017.13.037

Chen, C., Li, X., Yang, J., Gong, X., Li, B., and Zhang, K. Q. (2008). Isolation of nicotine-degrading bacterium Pseudomonas sp. Nic22, and its potential application in tobacco processing. *Int. Biodeterioration Biodegrad.* 62, 226–231. doi: 10.1016/j.ibiod.2008.01.012

Chen, T., Nomura, K., Wang, X., Sohrabi, R., Xu, J., Yao, L., et al. (2020). A plant genetic network for preventing dysbiosis in the phyllosphere. *Nature* 580, 653–657. doi: 10.1038/s41586-020-2185-0

Das, P. P., Singh, K. R., Nagpure, G., Mansoori, A., Singh, R. P., Ghazi, I. A., et al. (2022). Plant-soil-microbes: A tripartite interaction for nutrient acquisition and better plant growth for sustainable agricultural practices. *Environ. Res.* 214, 113821. doi: 10.1016/j.envres.2022.113821

Deng, X. H., Xie, P. F., Peng, X. H., Yi, J. H., Zhou, J. H., Zhou, Q. M., et al. (2010). [Effects of soil, climate, and their interaction on some neutral volatile aroma components in flue-cured tobacco leaves from high quality tobacco planting regions of Hunan Province]. *Ying Yong Sheng Tai Xue Bao* 21, 2063–2071. doi: 10.13287/j.1001-9332.2010.0296

Douglas, G. M., Maffei, V. J., Zaneveld, J. R., Yurgel, S. N., Brown, J. R., Taylor, C. M., et al. (2020). PICRUSt2 for prediction of metagenome functions. *Nat. Biotechnol.* 38, 685–688. doi: 10.1038/s41587-020-0548-6

English, C. F., Bell, E. J., and Berger, A. J. (1967). Isolation of thermophiles from broadleaf tobacco and effect of pure culture inoculation on cigar aroma and mildness. *Appl. Microbiol.* 15, 117–119. doi: 10.1128/am.15.1.117-119.1967

Gao, J., Uwiringiyimana, E., and Zhang, D. (2023). Microbial composition and diversity of the tobacco leaf phyllosphere during plant development. *Front. Microbiol.* 14, 1199241. doi: 10.3389/fmicb.2023.1199241

Gharaie, S., Vaas, L., Rosberg, A. K., Windstam, S. T., Karlsson, M. E., Bergstrand, K. J., et al. (2017). Light spectrum modifies the utilization pattern of energy sources in Pseudomonas sp. DR 5-09. *PloS One* 12, e0189862. doi: 10.1371/journal.pone.0189862

Guo, Z., Severson, R. F., and Wagner, G. J. (1994). Biosynthesis of the diterpene cis-abienol in cell-free extracts of tobacco trichomes. *Arch. Biochem. Biophys.* 308, 103–108. doi: 10.1006/abbi.1994.1015

Han, J., Zhang, Z., Liu, H., Wang, X., and Mao, G. (2013). Research advance in tobacco glandular trichomes and their secretion substance cembranoids. *Acta Tabacaria Sin.* 19, 118–124.

Huchelmann, A., Boutry, M., and Hachez, C. (2017). Plant glandular trichomes: natural cell factories of high biotechnological interest. *Plant Physiol.* 175, 6–22. doi: 10.1104/pp.17.00727

Hunter, P. J., Hand, P., Pink, D., Whipps, J. M., and Bending, G. D. (2010). Both leaf properties and microbe-microbe interactions influence within-species variation in bacterial population diversity and structure in the lettuce (Lactuca Species) phyllosphere. *Appl. Environ. Microbiol.* 76, 8117–8125. doi: 10.1128/AEM.01321-10

Kawasaki, W., Matsui, K., Akakabe, Y., Itai, N., and Kajiwara, T. (1998). Long-chain aldehyde-forming activity in tobacco leaves. *Phytochemistry* 49, 1565–1568. doi: 10.1016/S0031-9422(98)00236-2

Keene, C. K., and Wagner, G. J. (1985). Direct demonstration of duvatrienediol biosynthesis in glandular heads of tobacco trichomes. *Plant Physiol.* 79, 1026–1032. doi: 10.1104/pp.79.4.1026

Kembelsteven, W., and Muellerrebecca, C. (2013). Plant traits and taxonomy drive host associations in tropical phyllosp. *Botany-botanique* 92, 159. doi: 10.1139/cjb-2013-0194

Laforest-Lapointe, I., and Whitaker, B. K. (2019). Decrypting the phyllosphere microbiota: progress and challenges. *Am. J. Bot.* 106, 171–173. doi: 10.1002/ajb2.1229

Lei, W., Guang-Yu, M., Rui-Guo, Y. U., Xu-Dong, L., Jie-Feng, H., and Rong, L. I. (2006). Determinaton of free amino acids in tobacco of different technological processes by reversed phase high performance liquid chromatography. *J. Instrument. Anal.* 3, 46–49.

Leng, L., and Lu, Y. G. (2014). Analysis of trichome density and the content of glandular secretion on different flue-cured tobacco leaves. *Appl. Mech. Mater.* 651-653, 200–206. doi: 10.4028/www.scientific.net/AMM.651-653

Lin, C., Guo-Xiang, B., Peng, G., Ding-Yuan, T., and University, G. (2014). Observation analysis of glandular hairs morphology and density on different tobacco varieties by scanning electron microscopy. *Modern Agric. Sci. Technol.* 15, 10–12.

Ling, N., Wang, T., and Kuzyakov, Y. (2022). Rhizosphere bacteriome structure and functions. *Nat. Commun.* 13, 836. doi: 10.1038/s41467-022-28448-9

Liu, A., Yuan, K., Li, Q., Liu, S., Li, Y., Tao, M., et al. (2022a). Metabolomics and proteomics revealed the synthesis difference of aroma precursors in tobacco leaves at various growth stages. *Plant Physiol. Biochem.* 192, 308–319. doi: 10.1016/j.plaphy.2022.10.016

Liu, A., Yuan, K., Xu, H., Zhang, Y., Tian, J., Li, Q., et al. (2022b). Proteomic and metabolomic revealed differences in the distribution and synthesis mechanism of aroma precursors in Yunyan 87 tobacco leaf, stem, and root at the seedling stage. *ACS Omega* 7, 33295–33306. doi: 10.1021/acsomega.2c03877

Liu, S., Gao, J., Wang, S., Li, W., and Wang, A. (2023). Community differentiation of rhizosphere microorganisms and their responses to environmental factors at different development stages of medicinal plant Glehnia littoralis. *PeerJ* 11, e14988. doi: 10.7717/peerj.14988

Lustinec, J., Hadacová, V., Kamínek, M., and Procházka, Z. (1983). Quantitative determination of starch, amylose, and amylopectin in plant tissues using glass fiber paper. *Anal. Biochem.* 132, 265–271. doi: 10.1016/0003-2697(83)90006-4

Marie-Agnès, J., and Morris, C. E. (1995). A review of issues related to the quantification of bacteria from the phyllosphere. *FEMS Microbiol. Ecol.* 1, 1–14.

Mendes, R., Garbeva, P., and Raaijmakers, J. M. (2013). The rhizosphere microbiome: significance of plant beneficial, plant pathogenic, and human pathogenic microorganisms. *FEMS Microbiol. Rev.* 37, 634–663. doi: 10.1111/1574-6976.12028

Mina, D., Pereira, J. A., Lino-Neto, T., and Baptista, P. (2020). Epiphytic and endophytic bacteria on olive tree phyllosphere: exploring tissue and cultivar effect. *Microbial. Ecol.* 80, 145–157. doi: 10.1007/s00248-020-01488-8

Mucciarelli, M., Camusso, W., Maffei, M., Panicco, P., and Bicchi, C. (2007). Volatile terpenoids of endophyte-free and infected peppermint (Mentha piperita L.): chemical partitioning of a symbiosis. *Microb. Ecol.* 54, 685–696. doi: 10.1007/s00248-007-9227-0

Nielsen, M. T., and Severson, R. F. (1990). Variation of flavor components on leaf surfaces of tobacco genotypes differing in trichome density. *J. Agric. Food Chem.* 38, 467–471. doi: 10.1021/jf00092a030

Pathak, P., Rai, V. K., Can, H., Singh, S. K., Kumar, D., Bhardwaj, N., et al. (2022). Plant-endophyte interaction during biotic stress management. *Plants (Basel)* 11, 2203. doi: 10.3390/plants11172203

Pugh, G. J. F., Dickinson, C. H., and Preece, T. F. (1978). Microbial ecology of aerial plant surfaces. *J. Ecol.* 66, 328. doi: 10.2307/2259200

Qu, Q., Zhang, Z., Peijnenburg, W., Liu, W., Lu, T., Hu, B., et al. (2020). Rhizosphere microbiome assembly and its impact on plant growth. *J. Agric. Food Chem.* 68, 5024–5038. doi: 10.1021/acs.jafc.0c00073

Redford, A. J., Bowers, R. M., Knight, R., Linhart, Y., and Fierer, N. (2010). The ecology of the phyllosphere:geographic and phylogenetic variability in the distribution of bacteria on tree leaves. *Environ. Microbiol.* 12, 2885–2893. doi: 10.1111/j.1462-2920.2010.02258.x

Ruinen, J. (1961). The phyllosphere. *Plant Soil* 15, 81–109. doi: 10.1007/BF01347221

Shishehian, A., Firouz, F., Khazaee, S., Rajabi, H., Farhadian, M., and Niaghiha, F. (2023). Evaluating the color stability of 3D-printed resins against various solutions. *Eur. J. Transl. Myol.* 33, 11493. doi: 10.4081/ejtm.2023.11493

Sohrabi, R., Paasch, B. C., Liber, J. A., and He, S. Y. (2023). Phyllosphere microbiome. *Annu. Rev. Plant Biol.* 74, 539–568. doi: 10.1146/annurev-arplant-102820-032704

Stierle, A., Strobel, G., and Stierle, D. (1993). Taxol and taxane production by Taxomyces andreanae, an endophytic fungus of Pacific yew. *Science* 260, 214–216. doi: 10.1126/science.8097061

Tooker, J. F., Peiffer, M., Luthe, D. S., and Felton, G. W. (2010). Trichomes as sensors: detecting activity on the leaf surface. *Plant Signal Behav.* 5, 73–75. doi: 10.4161/psb.5.1.10234

Vázquez, C. V., Rojas, M. G., Ramírez, C. A., Chávez-Servín, J. L., García-Gasca, T., Ferriz Martínez, R. A., et al. (2015). Total phenolic compounds in milk from different species. Design of an extraction technique for quantification using the Folin-Ciocalteu method. *Food Chem.* 176, 480–486. doi: 10.1016/j.foodchem.2014.12.050

Vontimitta, V., Danehower, D. A., Steede, T., Moon, H. S., and Lewis, R. S. (2010). Analysis of a Nicotiana tabacum L. genomic region controlling two leaf surface chemistry traits. *J. Agric. Food Chem.* 58, 294–300. doi: 10.1021/jf903256h

Vorholt, J. A. (2012). Microbial life in the phyllosphere. *Nat. Rev. Microbiol.* 10, 828–840. doi: 10.1038/nrmicro2910

Wallace, J., Laforest-Lapointe, I., and Kembel, S. W. (2018). Variation in the leaf and root microbiome of sugar maple (Acer saccharum) at an elevational range limit. *PeerJ* 6, e5293. doi: 10.7717/peerj.5293

Wu, L., Li, Q., Li, C., Cao, J., Lai, Y., Qiu, K., et al. (2014). Determination of aroma components in Chinese southwest tobacco by directly suspended droplet microextraction combined with GC-MS. *J. Chromatogr. Sci.* 52, 1317–1325. doi: 10.1093/chromsci/bmt170

Yadav, R. K., Karamanoli, K., and Vokou, D. (2005). Bacterial colonization of the phyllosphere of mediterranean perennial species as influenced by leaf structural and chemical features. *Microb. Ecol.* 50, 185–196. doi: 10.1007/s00248-004-0171-y

Yajie, Z., Qionghua, X. U., Zichao, M., Weiqiong, P. U., Junying, L. I., and Yanping, C. (2015). Comparison of density and morphology of glandular trichome of tobacco leaves of four species at different collection periods. *J. Yunnan Agric. University(Natural Science).* 30, 35–43. doi: 10.16211/j.issn.1004-390X(n).2015.01.007

Yinju, Y., Yan, Z., Shusheng, W., Guangliang, L., Na, X. U., Chengdong, W., et al. (2018). Effect of topping on polyphenols metabolism and key enzymes in tobacco leaves. *Acta Tabacaria Sinica*. 24, 60–67. doi: 10.16472/j.chinatobacco.2017.263

Yue, L. I., Chao, C., Hao, J., Huo, L. I., and Feng, W. (2002). Studies on leaf maturity of Yunyan 85, a variety of flue-cured tobacco I. Relationship between the maturity and the tissue, color and chemical compositions in leaves. *J. Fujian Agric. University.* 1, 16–21.

Zhang, L., Meng, F., Ge, W., Ren, Y., Bao, H., and Tian, C. (2023). Effects of colletotrichum gloeosporioides and poplar secondary metabolites on the composition of poplar phyllosphere microbial communities. *Microbiol. Spectr.* 11, e0460322. doi: 10.1128/spectrum.04603-22

Zhao, J., Xu, Y., Ding, Q., Huang, X., Zhang, Y., Zou, Z., et al. (2016). Association mapping of main tomato fruit sugars and organic acids. *Front. Plant Sci.* 7, 1286. doi: 10.3389/fpls.2016.01286

Zhu, H., Sheng, K., Yan, E., Qiao, J., and Lv, F. (2012). Extraction, purification and antibacterial activities of a polysaccharide from spent mushroom substrate. *Int. J. Biol. Macromol.* 50, 840–843. doi: 10.1016/j.ijbiomac.2011.11.016

Frontiers in
Plant Science

Cultivates the science of plant biology and its applications

The most cited plant science journal, which advances our understanding of plant biology for sustainable food security, functional ecosystems and human health.

Discover the latest Research Topics

See more →

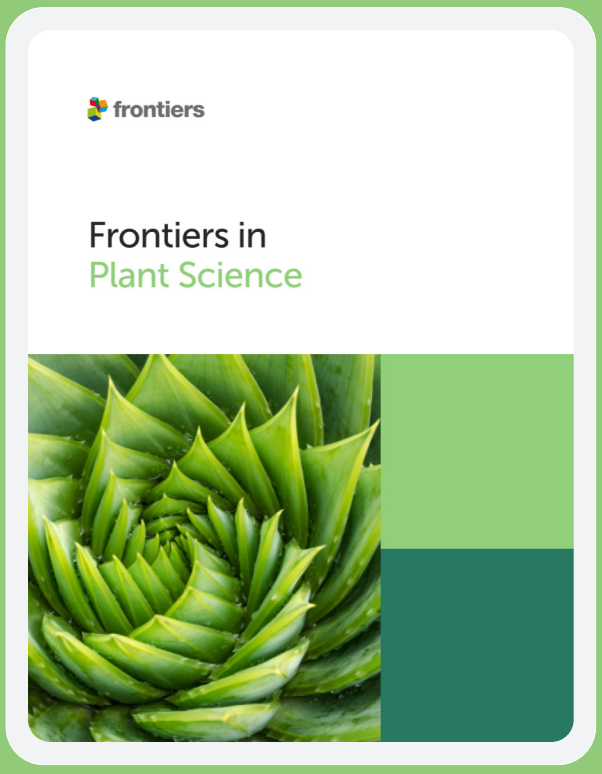

Frontiers

Avenue du Tribunal-Fédéral 34
1005 Lausanne, Switzerland
frontiersin.org

Contact us

+41 (0)21 510 17 00
frontiersin.org/about/contact